NONLINEAR ANALYSIS AND DESIGN OF R/C COUPLED WALL SYSTEMS SUBJECTED TO EARTHQUAKE

Thesis submitted in accordance with the requirements of
the University of Liverpool for the Degree of
Doctor in Philosophy

by

Omar CHAALLAL

November, 1983

A THOUGHT

Scientists believe they know why earthquakes happen. They believe they can estimate where and roughly when they will occur. There is however nothing anyone can do to prevent them.
In November 1980, more than 3000 people died (from whom I personally knew a few) and most of the city was destroyed as an earthquake struck Al-Asnam (Algeria).
If nobody can prevent the occurence of earthquakes, it is my belief and conviction that something can and must be done to minimise and ultimately avoid the catastrophical loss of human life and property that we have witnessed so far. It is my profound wish that the present work represents a small contribution in this respect.
This thesis is dedicated to all those who died or lost their homes and roots following Al-Asnam Earthquake.

UNE PENSEE

Les hommes de science croient savoir pourquoi, où, et approximativement quand un tremblement de terre aurait lieu. Il semble cependant qu'il n'y ait rien à faire pour le stopper.
En novembre 1980, plus de 3000 personnes ont disparu et la majeure partie de la ville detruite suite au tremblement de terre qui frappa Al-Asnam.
Si personne ne peut stopper un tremblement de terre d'avoir lieu, je suis convaincu quant à moi que les ressources humaines sont immenses et je suis certain qu'elles peuvent, si réunies, orientées et surtout utilisées à bon escient, contribuer à minimiser, voire eviter, les pertes catastrophiques humaines et materielles dont nous avons été temoins à maintes reprises.
Je souhaite que cette thèse, que je dédis humblement aux victimes d'Al-Asnam, represente une petite contribution dans ce sens.

SUMMARY

In this thesis the nonlinear analysis of coupled shear walls subjected to earthquake forces is investigated and nonlinear methods of design are suggested.

Inelastic spectrum analysis (ISA) as applied to coupled shear walls was first investigated. Using a finite element (F.E) method of analysis, coupled shear walls with a wide variety of geometries are investigated. The formulation and procedure of the method has been given in detail. A design method for coupled shear walls built in seismic areas is suggested and an example is carried out. The method is seen to be very practical as it gives a good approximate dimensioning of the coupled shear walls. Furthermore, it has a great potential future as it can easily be incorporated into a design code of practice.

A comprehensive nonlinear step-by-step dynamic analysis is then carried out. A dynamic finite element computer program which takes into account the nonlinearities that stem from the very nature of reinforced concrete, is developed. Allowances are made for phenomena such as cracking, yielding and crushing of concrete, yielding of steel, bond deterioration and stiffness degradation in the coupling beams and aggregate-interlock. To test the validity of the assumptions made concerning the material behaviour, the analytical results are compared with experimental results and existing data.

It is usually a human instinct to fight back with force even in case of defence against " Nature ". The consequent philosophy of stronger and stiffer buildings to counter earthquake forces has been with us for quite some time, but the experience of many catastrophical events has taught us to reconsider our way of thinking. Energy absorbing capacity and ductility have been the

emphasis and the key for structural survival for the last few years. While it is relatively easy to assess the available ductility or ductility supply of a member, ductility demand however, seems to depend on so many factors that it cannot be estimated without preliminary parametric studies. Energy absorbing philosophy and factors which might influence ductility demand are investigated in this study and an optimal nonlinear analysis which balances strength and ductility is suggested.

Even though only coupled shear walls are dealt with in this investigation, the computer program is capable of dealing with plane frame and plane frame - shear wall systems as well. Both the walls and the coupling beams can be either idealised as finite elements or as line elements. Nonlinearities in line elements are confined to preset hinges at the element's ends and monitored by a moment-rotation relationship. When using the FEM approach however, nonlinearities are confined to Gaussian integration points (4 in this study) over the element and monitored by the stress - strain curves of steel and concrete.

ACKNOWLEDGEMENTS

It has been a great privilege for the author to have had the opportunity to carry the research described in this thesis under Mr. C. Thomas, Msc., lecturer in civil engineeering, supervision. His active interest , valuable suggestions and stimulating questions are gratefully acknowledged.

The author wishes to express his gratitude to Professeur Sawko and Mr. Bungey, both from the Civil Engineering Departement, for indulging the inconvenience he might have caused at the beginning of this study.

The author wishes to thank all the staff members of the Civil Engineering Departement for their support, help and encouragement. Special thanks are due to Miss O'Brien, J., for her efficient help in typing and the staff of the computer laboratory for the facilities provided and the always present kindness. Thanks are also due to the Bibby Award for enabling me to cover the travel expenses to Italy.

The financial support from the Algerian Ministry of Higher Education and Scientific Research is gratefully acknowledged.

Finally the author is especially indebted to his family in general and his mother in particular for her forbearance and moral support despite all the difficulties.

CONTENTS

TERMINOLOGY

Certain terms are used in this thesis and are generally defined when first used, however it was thought useful to list them below for convenient reference.

Aseismic = Earthquake resistant.

Critical Damping = Viscous damping that will cause a displaced system to return to its initial position without oscillation.

Damping = dissipation of energy during vibration due to internal and external friction.

Design Earthquake = The ground motion that is taken as basis of design of a structure.

Ductility = The ability of a member or a structure to deform beyond its elastic limit without significant loss of strength.

Ductility Factor = Ratio of maximum deformation response to yield deformation.

Dynamic = Varying with time.

Earthquake Input motion (Ground motion) = Time history of the ground acceleration due to earthquake excitation used as input loading for response history analysis.

Elastic = Indicates a return to initial state on unloading without residual deformation.

Energy Dissipating = Specific phenomenon by which earthquake energy input is dissipated (e.g. inelastic deformations).

Energy Dissipation = Dissipation of the energy input by an earthquake into a structure by hysteresis, damping or other mechanisms.

First Mode = Phase relationship in which three level signals oscillate in the same phase.

Flexural Strength = Ultimate bending moment that can be carried by a section.

Frequency = Number of cycles of a periodical oscillation occuring in a unit time.

Fundamental Mode = The mode of vibration with the largest period, i.e., the shortest frequency.

Higher Modes = Modes of vibration except first mode.

Hinging Region = The length of a member over which yielding accurs due to bending moment exceeding yield moment.

Hysteresis = Nonlinear force-displacement relationship of a member under reversal of loadings.

Inelastic = Indicates an incomplete return to initial state on unloading and hence residual deformations.

Linear = Indicates proportionality between force and displacement.

Lumped Mass = Idealisation of the distribution of mass in which concentrated masses are assigned to nodal points.

Nonlinear = Indicates lack of proportionality between force and displacement.

Response History Analysis = Response analysis based on direct numerical integration of the eqn. of motion by a step-by-step procedure.

Rigid Joint = Joint with infinite flexural rigidity.

R M S (root mean square) = Response value calculated as the square root of the sum of the squares of the maximum modal components.

Rotational Spring = A spring at the ends of a beam element which simulates its nonlinearities.

Second Mode = Phase relationship in which only two adjacent level signals oscillate in the same phase.

Seismic = Caused by or subject to ground motion such as earthquake.

Sequence of Plastification = The sequence in which yielding spreads to the various structural members.

Spectra Based or Modal Analysis = Response analysis based on modal response spectra.

Spectral Acc. (disp. or Vel.) = The maximum absolute acceleration (displacement or velocity) response of a sdof system having a given period.

Spectrum Intensity = Index defining the intensity of base motion. It is based on the area under a velocity response spectrum in a specified frequency range as defined by Housner [23].

Third Mode = Phase relationship in which the first and the third level signals are in phase.

Viscous Damping = A type of damping represented by a force that resists the motion and is proportional to velocity. It is often expressed as a fraction of critical damping.

Yielding = A stage of response at which a section reaches its yield moment.

NOTATIONS

CHAPTER II

C = Damping matrix of the structure.

f_i = Eathquake force distribution at mode i.

Fmax = Maximum earthquake force distribution for all modes.

I = Structure importance factor used by the code.

K = Stiffness matrix of the structure.

K^*_i = Modal stiffness = $\phi j\ K\ \phi i$ for i=j .

M = Mass matrix of the structure.

M^*_i = Modal mass = $\phi j\ M\ \phi i$ for i=j .

ϕ = Mode shape vector

S = Foundation condition factor as used by the code

Sa_i = i^{th} modal spectral acceleration

Ti = Period at mode i

Umax = Maximum displacement distribution for all modes

Vo_i = Base shear for mode i

Vo_{max} = maximum base shear for all modes

W = Total weight of the structure

w_i = Frequency at mode i

y" = Ground acceleration vector

Z = Seismic zoning factor (code)

z_i = Damping ratio for mode i

CHAPTER III

[B] = Strain-displacement matrix

[D] = Property or elasticity matrix

Det[J] = Determinant of the Jacobian matrix [J]

δ_e = Element displacement vector

f = Displacement function vector

[J] = Jacobian matrix

K = Global stiffness matrix of a structure

[Ke] = Element stiffness matrix

[N] = Shape function matrix

Qe = Element total potential energy

R = Overall load vector

Re = Nodal load vector

s, t = Local coordinate for isoparametric elements

U = Displacement vector in x direction

Us = Element strain energy

V = Displacement vector in y direction

x, y = Global coordinates of an element

W = Element potential energy

W_j, W_k = Weight factors at Gaussian points j and k

ϵ = Strain vector = $[\epsilon x \ \epsilon y \ \epsilon xy]^T$

θ = Principal stress direction with respect to the element axis

σ = Stress vector = $[\sigma x \ \sigma y \ \sigma xy]^T$

$\sigma_{1,2}$ = Major and minor principal stresses

τ_{max} = Maximum shearing stress

CHAPTER IV

c = Damping ratio of a sdof system

c_c = Critical damping

Dy = Maximum yield drift indice

F = Resistance

Fmax = Maximum force distribution

K = Stiffness matrix of a mdof structure

Kud = Neutral axis depth of a section

Ln = Modal participation factor

lp = Hinging zone, i.e., zone where plasticity spreads

M = Mass matrix of a mdof system

m = Mass of a sdof system

My = Yield moment of a section

Pn = Maximum modal forces

Ry = Yield resistance force

Sa = Spectral acceleration

T = Period

u u' u" = Displacement response and derivatives

Umax = Maximum displacement

Uy = Displacement at yield

Un = Modal displacement

w = Frequency

x" = Base acceleration

z = Damping factor = c/c_c

δ_n = Modal drift

δ_{ymax} = Maximum yield drift

ϕ_n = n^{th} modal shape vector

φ_y = Curvature at yield

Θ_{max} = Maximum rotation of a section or a member

Θ_p = Plastic rotation of a section or a member

Θ_y = Yield rotation of a section or a member

μ = Structural ductility factor

μ_b = Rotational ductility of a beam

CHAPTER V

Cw = Qualitative "crack width"

d, d' = Depth of tensile and compressive reinforcement respectively

Dc, Dcr, D'cr = Elastic & cracked property matrices of concrete at different stages

Dep = Elasto-plastic property matrix

$D\Theta_i$ = Incremental rotation at beam's end i

DM_i = Incremental moment at beam's end i

DL = Elongation of reinforcing steel due to bond slip

Ds = Property matrix of steel

Ec = Elastic Young's modulus of concrete

Es = Elastic Young's modulus of steel

EI_a = Actual rigidity of a beam element

EI_e = Elastic rigidity of a beam element

F = Flexibility matrix of a beam element

Fs = Stress in reinforcement due to bond slip

$f_s(M)$ = Flexibility due to bond slip

G = Elastic shear modulus

G_{eq} = Shear modulus after cracking has occured

My = Yield moment of a section or a member

p = Reinforcement ratio

R(M) = Rotation due to slippage of steel at applied moment M

α = Global shear reduction factor = $\alpha_s + \alpha_d$

α_s = Shear reduction factor due to aggregate interlock

α_d = Shear reduction factor due to dowel action

ϵ_c = Strain vector of concrete

ϵ_{cr} = Strain when cracking first accurs

ϵ_{max} = Maximum strain at which interlocking becomes ineffective

ϵ_{min} = Minimum strain at which concrete is assumed crushed

μ = Poisson's ratio of concrete

σ_c = Stress vector in concrete

CHAPTER VI

C = Damping matrix of the structure.

DPs = Pseudo-load vector

Dv, Dv'

Dv" = Incremental nodal displacement and derivatives

Dy"(t) = Incremental ground acceleration

Dt = Time step

K = Stiffness matrix of a mdof structure

K* = Dynamic stiffness matrix

M = Mass matrix of a mdof system

Me = Element mass matrix

Mext = External mass matrix

R = Overall load vector

w_n = Frequency of the structure at mode n

z_n = Damping factor for mode n

β = Newmark's constant indicating the variation of acceleration in a time interval

ϵ = Convergence tolerance

CHAPTER VII & VIII

θ_{max} = Maximum rotation of a section or a member

θ_p = Plastic rotation of a section or a member

θ_y = Yield rotation of a section or a member

μ = Ductility demand

μ_r = Rotational ductility

dM = Moment increment

Es = Young's modulus of steel

f'_c = Compressive strength of concrete

f_y = Yield stress of steel

Lb = Length of the coupling beams

My = Yield moment of a section

My_{min} = Minimum yield miment capacity (as stipulated by code)

CHAPTER ONE

INTRODUCTION

1.1 General

The use of reinforced concrete as a structural building material has become more and more a standard feature of modern construction. This was possible mainly as a consequence of extensive experimental and analytical investigations on reinforced concrete models. The results of these investigations allowed a set of design guidelines and rules that survived the test of time successfully for quasi-static loading conditions. However experience has shown that these rules were not suitable when it came to dynamic loading conditions such as earthquakes.

Few of the buildings constructed in seismic areas are designed on the basis of the results of dynamic analysis. The code of practice allows for earthquake loads to be approximated by so called equivalent static loads. The magnitude of the latter depends on the seismic zone and the fundamental period of the structure in hand. An approximate formula is suggested for estimating the fundamental period. Furthermore, the code load requirements are very small compared with those experienced during a significant earthquake. As a result of these limitations, enormous property damage and loss of human life have been caused by destructive earthquakes during the last decades. The primary objective of a structural engineer should therefore be to design any structure rationally in such a way that it will resist moderate earthquakes without damage and not collapse and cause loss of lives , even in the case of severe ground motion. To achieve this,

the need to conduct a more comprehensive earthquake analysis and a better understanding of the behaviour of structures seems to be more than necessary.

Since the very rapid increase of high rise buildings all over the world, reinforced concrete wall systems have for many years been a very common means of resisting lateral forces due to wind and earthquake. Usually the so-called shear walls are built over the whole height of the building and are laid out either as a series of walls connected by beams and/or slabs, or as a central core structure with openings to accomodate doors, windows or corridors. A good approximation of the interaction between shear walls and connecting beams, as well as their proportioning and design under severe ground motions, would be a great help towards improving the behaviour and avoiding "the unexpected" in the case of a major eathquake.

1.2 General Review

It was Rosman [1] who, in 1964 , broke the tradition of treating coupled shear walls as deep columns acting as separate cantilever beams. He proposed a solution in which the coupling system is replaced by a continuous medium (laminae) of equivalent stiffness. Later Coull and Choudhury [2 & 3] and Coull and Irwin [4] extended the laminae method. They took into account shear deformation effects and presented very convenient graphical charts to determine the stresses and deflections of coupled shear walls of different geometric characteristics and subjected to various lateral static load cases. Tso and Chan [5] and Coull et al. [6 & 7] used the method to determine approximate natural frequencies of coupled shear walls which can be used with the response spectrum approach.

Although these methods were a good improvement with respect to the unduly conservative approach by which no credit was given to the coupling

effect, they are still limited by various simplifications on loading and boundary conditions and fail to produce accurate results and details on the distribution of stresses over the entire structure if need be. The emergence of finite element method (FEM) [8] as applied to elastic continuum and the growing popularity of computer facilities bridged the gap. Indeed the FEM has been used succefully for static as well as dynamic problems [9]. Some of the advantages of FEM in solving shear wall problems are its ability to treat:

a) variation in thickness of the shear walls

b) irregularities of loading

c) irregularities in the geometry of the openings

d) variation in material properties.

The observed nonlinear behaviour of reinforced concrete structures also had to be simulated analytically. Shear walls were first idealised as deep columns based on the modified " EI " procedure. Nonlinearities in frames and walls were generally monitored by the nonlinear force -displacement relationship of preset hinges generally located at the element's ends [10]. The first basic moment - rotation relationship used to monitor nonlinear behaviour was the bilinear elastic perfectly plastic idealisation. Shepherd et al. [11] used the latter for nonlinear dynamic analysis and reported a good correlation between analytical and experimental predictions.

The need for an inelastic approach to earthquake response problems simple enough to be introduced into a code of practice and capable of taking nonlinearities into account gave rise to many investigations from which the ductility factor method [12] and the inelastic spectrum approach [14 - 16] emerged. The difference between the inelastic spectrum and the usual elastic modal analysis is that the former uses an inelastic spectra, that is derived from a nonlinear force - deformation relationship of a single degree of freedom (sdof) system, instead of the usual elastic spectra.

Shibata and Sozen [17] developed a design method for reinforced concrete frames in which a softer and more damped " substitute structure " is analysed by elastic modal analysis. This general category of methods which uses an elastic spectra as the loading has been applied by many investigators [18 -20] to sdof systems. Gerra & Esteva [13] used the same procedure but accounted for the inelastic behaviour by using a frequency shift and an increased value of damping.

Newmark & Hall [14] proposed a method in which elastic modal analysis was used along with a reduced design spectra. The reduction in the elastic design spectra was derived from observed sdof inelastic spectra for various damping and frequency combinations. Lai & Biggs [16] assessed the method and applied it to inelastic response of plane frame for 2 % and 5 % damping respectively. They concluded that the method was unconservative for 2% damping and conservative for 5% damping but led to satisfactory design. Anagnotopoulos et al. [15] also used the method to examine the response of a multistorey building and concluded that the approach could be unconservative. He believed this was due to the variations in the input motions which can never match a smooth spectra exactly.

As far as nonlinear dynamic history response behaviour of structures subjected to ground motions is concerned several inelastic models were used extensively. They range from one component model [21] in which each member is represented by an elastic beam element with inelastic springs (hinges) at its two ends, to multicomponent model [22 & 23], in which the idealised beam has an elastic member and several elasto - plastic members in parallel. Otani [24] modelled a beam element as two cantilever beams whose free ends coincide with the inflection point. He assumed the inflection point of a deformed member was at the middle and the member deformed in antisymmetric bending. This model was believed to match better the

hysteresis data based on test results. This was particularly true when the effects of vertical loads were negligeable or nonexistent. Based on the same general principle and in order to obtain a better prediction and accuracy, some researchers [25 to 27] attempted either a finer idealisation by subdividing a beam element into yet more beam elements or by introducing more rotational springs in the regions where non linearities are likely to occur. Fibre or layering model was also introduced [28]. Each section was subdivided into many layers and the moment-curvature relationship was derived from steel and concrete constitutive laws. Member stiffness was then determined by integrating along the member length. This model, though leading to a better insight, was very time consuming and tedious and hence unpopular.

Takeda et al. [29] developed their very popular hysteretic model which was modified to take stiffness degradation and strain hardening into account by Kannan & Powell [30]. Because it was based on several experimental studies, this model was found to be successful in simulating both static and dynamic behaviour of reinforced concrete joints of cantilever beams. Later Takeda's model coupled with the assumptions made by Otani [24] concerning the inflection point and the antisymmetric bending deformation shape, has been used extensively by many investigators to simulate nonlinear response of frame structures (i.e., assembly of beam elements) subjected to earthquake forces.

Ngo and Scordelis [31] followed by Nilson [32] were the first to demonstrate the capability of the finite element method of analysis to cope with reinforced concrete nonlinearities. They analysed simple beams as two - dimensional systems with predefined crack pattern and introduced the concept of link element in order to model the bond between concrete and steel. However their approach fell short because of the inconvenience and impracticality of their redefinition of the structure topology after cracking

had occured. Finite element method as applied to plane stress problems has been applied successfully to nonlinear analysis of reinforced concrete by Suidan & Schnobrich [33], Agrawal et al. [34] and Schnobrich [35]. Such two dimensional analysis has been satisfactory for the response of isolated walls subjected mainly to monotonically increased loads.

Darwin and Pecknold [36], using the concept of equivalent uniaxial strain, analysed reinforced concrete shear panels under cyclic loading and reported a good correlation with experimental results. Rashid [37] was the first to introduce the most popular approach by which cracked concrete was treated as an orthotropic material. In his representation, the elastic modulus of concrete in the direction normal to the crack was reduced to zero, giving rise to a cracked element rather than a sharp crack and avoiding in this way the need for updating the topology of the structure after cracking had occured. This approach has been used successfully by many investigators [40-41 & 33]. Cevenka and Gerslte [38-39] investigated panels under cyclic loading assuming an elastic-perfectly plastic behaviour for concrete in compression. Recently Agrawal et al. [42] claimed to present the first successful application of the plane stress finite element method in determining the nonlinear behaviour of an isolated reinforced concrete wall subjected to simulated earthquake motions. They used a biaxial constitutive law and orthotropic material properties for cracked elements.

In most of these applications coupled shear walls have been idealised either by the " equivalent EI " procedure or by a two - dimensionnal plane stress approach for both wall and beam members. In view of the energy absorbing philosophy, that is strong wall - weak beam, necessary for the design of concrete structures in seismic areas there is a need for a more realistic model of coupled shear walls. This can be achieved by idealising

the walls as plane stress elements and the coupling beams, much slender, as line elements.

It is well accepted that during earthquake excitation, part of the energy released [43] is absorbed by the structure elastically, the other part is either absorbed by purposedly designed damping devices or through structural damage beyond repair or even complete collapse. As far as coupled shear walls are concerned it is generally accepted that energy dissipation by hysteretic damping is the most viable. Paulay has investigated ways by which available ductility in a member, that is energy absorbing capacity without loss of strength, could be improved. He suggested diagonal reinforcement for deep beams where shear is predominant [44-45] and squat shear walls [46]. Allen et al. [47] tested the behaviour and investigated the design of ductile walls. They found that concentrating tension steel at each end of the wall, as recommended by most aseismic codes [48-51], improved its ductile behaviour. They concluded that available ductility remains almost constant with changes in main tension steel areas and generally decreases with increasing axial load. The use of barbell cross section walls has also been recommended by some investigators and most codes of practice. A good review of the state - of - art of seismic resistant design of shear walls is given by Bertero [52].

Due to the instability problems that the yielding of the walls might cause, their use as the first line of defence against earthquakes has been discouraged in favour of ductile girders and coupling beams. To ensure this happens the coupling beams are intentionally made moderately strong to allow them to yield ahead of the walls. Coull and Choo [53] proposed an approximate inelastic method based on the continuum approach. They divided the structure into elastic and plastic zones and determined the positions of these zones by making assumptions and simplifications on the

form of shear distribution in the coupling beams as the load increases. Fintel and Ghosh [54] investigated the nonlinear dynamic response of a 31 storey coupled shear wall - frame system. Keeping columns and walls elastic, they attempted to balance the ductility enforced upon the beams, or ductility demand, and their available ductility or ductility supply. They used a trial and error process and repetitive nonlinear dynamic history analysis. Later Fintel and Ghosh [55] used the same technique, this time however they allowed the columns and the walls to yield ahead of the beams. They concluded that the walls, if ductile, can dissipate the majority of the energy input through inelastic deformations. Deretcho et al. [56] studied the effect of axial force -flexural interaction on the nonlinear response of coupled shear walls and concluded that substantial axial force in the walls may affect available ductility in individual members.

1.3 Objective and Scope

In case of severe earthquakes, structures will deform well beyond their elastic range. Some elements will be more overstressed than others giving rise to successive adjustments of load distribution and hence to a different behaviour than one might expect if no specific nonlinear analysis had been made to permit such prediction. When designing a structure one may wish to counter most of the energy demand upon the structure through inelastic deformations confined to desired members, or through a predetermined sequence of degradation or plastification. Therefore the need to perform a comprehensive nonlinear dynamic analysis appears to be desirable.

Although reinforced concrete is very complex to model, the emergence of computer facilities has made nonlinear dynamic analysis possible by allowing for phenomena such as cracking, yielding, bond deterioration, stiffness degradation and aggregate - interlock. Our first objective will therefore be to

develop a dynamic finite element computer program to take into account the nonlinearities that stem from the very nature of reinforced concrete. To test the validity of the assumptions made concerning material behaviour, the analytical results are compared with existing experimental tests and data.

Confining inelastic deformations to certain members of the structure requires nonlinear analysis to be performed repetitively and proportioning and design changed consequently until desired behaviour is achieved. This is a time consuming and tedious process, therefore an alternative needs to be found which yields, either a good approximate dimensioning of the coupled shear wall structures in the case where the computer facilities are not available, or an advantageous starting point if nonlinear dynamic analysis can be performed. The development of inelastic spectrum approach (ISA) as applied to coupled shear walls seems to be appropriate and is the subject of the second objective of this research.

It is usually a human instinct to fight back with force even in case of defence against " Nature ". The consequent philosophy of stronger and stiffer buildings to counter earthquake forces has been with us for quite some time, but the experience of many catastrophical events has taught us to reconsider our way of thinking. Energy absorbing capacity and ductility have been the emphasis and the key for structural survival for the last few years. While it is relatively easy to assess the available ductility or ductility supply of a member, ductility demand however, seems to depend on so many factors that it cannot be estimated without preliminary parametric studies. Energy absorbing philosophy and factors which might influence ductility demand constitute the final objective of this study.

Even though only coupled shear walls are dealt with in this investigation, the computer program is capable of dealing with plane frame and plane frame - shear wall systems as well. Both the walls and the coupling beams can be

either idealised as finite elements or as line elements. Nonlinearities in line elements are confined to preset hinges at the element's ends and monitored by a moment-rotation relationship. When using the FEM approach however, nonlinearities are confined to Gaussian integration points (4 in this study) over the element and monitored by the stress - strain curves of steel and concrete. The computer program is an extention of the program developed by Wee [57] for elastic dynamic analysis and is also capable of dealing with statically applied loads in the elastic range. The step-by-step procedure can be applicable to any dynamic force in addition to earthquake excitations for both elastic and inelastic systems.

1-4 Outline of the Thesis

Many approaches are currently available for the aseismic design of reinforced concrete structures. Similarities and limitations of these approaches are the subject of Chapter II of this thesis. Chapter III is dedicated to the description of the theory of finite element method.

As previously stated the first objective of this study is dedicated to the inelastic spectrum approach (ISA) as applied to coupled shear wall structures, and is covered in chapter IV. In this chapter the free vibration analysis of a wide variety of coupled shear walls with a range of geometries is carried out. The natural frequencies are computed for different typical floor weights and related to the corresponding stiffnesses. Then an inelastic design spectra is developed and applied to coupled shear walls.

The second major part of the thesis is devoted to the nonlinear step-by-step analysis. This is covered in three chapters. The first, Chapter V, deals with the nonlinear behaviour of reinforced concrete and the mathematical models assumed in this investigation to simulate nonlinearities. The step - by - step numerical solution of the equations of motion and the overall analytical

procedure are described in chapter VI. To check the validity of the assumed models, analytical results are compared with either experimental data or other existing models. This is discussed in chapter VII and ends the second part of this investigation.

The capacity of coupled shear walls to absorb the energy input by earthquake ground motions is limited by the available ductilily of their coupling beams which should be greater than the ductility demand at any time interval. In chapter VIII the various factors which influence ductility demand are discussed and an optimal nonlinear procedure is proposed.

Finally a description of the computer program and its use are given in the appendices along with a Fortran IV listing.

CHAPTER TWO

CURRENT SEISMIC APPROACHES

2-1 General

This chapter gives a description of the different approaches which may be used for the analysis of a structure such as coupled shear wall when subjected to earthquake ground motions. There are three types of approaches when designing aseismic structures:

a) 'Code of practice requirements' approach in which the effect of the earthquake loads are simulated by so-called equivalent lateral forces.

b) Elastic dynamic analysis approach which takes the dynamic aspect of the problem into account.

c) Nonlinear method of analysis approach which, in addition to the dynamic aspect of the problem, considers the changes in structure properties and the effects of the energy absorbing capacity of the structure.

The first part of this chapter is dedicated to the mathematical formulation of the elastic dynamic analysis. Most of the codes [48-51] being practically similar, the second part of this chapter is devoted to a brief presentation of the most advanced and widely used code of practice and the philosophy behind it. This is followed by a very brief presentation of the existing nonlinear approaches. These are presented more in detail in chapters 4, 5 and 6.

2-2 Elastic Dynamic Approach

The equations of motion of a structure subjected to a ground motion can be written in terms of the relative displacements of the mass points as

$$M\ U'' + C\ U' + K\ U = -M\ y'' \qquad 2.1$$

where M = mass matrix

C = damping matrix

K = stiffness matrix

U'' , U' , U = relative acc., vel. and displ. vector respectively

y'' = base acceleration vector

The solution of these equations can be achieved using the direct integration method or the less computer time consuming mode superposition method.

2-2-1 Direct Integration Approach: In this technique, eqns. 2.1 is solved directly using numerical integration with respect to time, that is a finite difference technique. Several methods are commonly used, the most popular being the Newmark-beta [102] and the Wilson-theta [103] methods. In all these schemes the nodal displacements and their derivatives are evaluated at time interval Dt and various assumptions are made as to the variations of these quantities within this time interval. A major problem of such schemes is ensuring that they are stable with respect to time. The advantage of these methods is their capability to deal with nonlinearities. In this thesis, the well known Newmark-beta method is used for nonlinear analysis and is therefore developed and discussed in detail in chapter VI.

2-2-2 Mode Superposition Technique: An alternative approach to the direct integration is the modal analysis technique. In this method the nodal displacements U are transformed to new set of displacements x through the generalised coordinates as:

$$U = [\phi]\ x \qquad 2.2$$

where $[\phi]$ is the matrix of all the mode shapes and x is the vector of modal amplitudes.

i) Mode Shapes and Natural Frequencies The mode shapes are obtained by solving the undamped, unforced behaviour of a structural system, i.e.,

$$M\ U'' + K\ U = 0 \qquad 2.3$$

by analogy to single degree of freedom (sdof) systems, the solution may be written as

$$U = q \sin(wt + \theta) \qquad 2.4$$

substituting eqn. 2.4 into 2.3 leads to

$$(K - w^2 M)\ [\phi] = 0 \qquad 2.5$$

for a non-trivial solution it follows

$$\det(K - w^2 M) = 0 \qquad 2.6$$

which is an n-degree polynomial in terms of w^2 which has n positive or zero roots called eigenvalues w_n^2. These roots are called natural frequencies and have periods $Tn=2\pi /w_n$. For each w_n, there exists a corresponding ϕ_n vector i.e., the mode shape or eigenvector. ϕ_n is obtained by back substitution of w_n in eqn. 2.5.

ii) Orthogonality: One of the most attractive and important properties of eigenvectors is their orthogonality with respect to the matrices M and K. It can be demonstrated [12] that

$$\phi_j^T M \phi_i = 0 \qquad \text{for } i \neq j \qquad 2.7$$

$$\phi_j^T K \phi_i = 0 \qquad \text{for } i \neq j \qquad 2.8$$

and

$$\phi_j^T M \phi_i = M^*_i \qquad \text{for } i = j \qquad 2.9$$

$$\phi_j^T K \phi_i = K^*_i \qquad \text{for } i = j \qquad 2.10$$

where M^*_i and K^*_i are scalar quantities called modal mass and modal stiffness respectively.

When damping is present and the damping matrix is arbitrary, the mode shapes are not orthogonal with respect to it. If however the mode shapes are to be orthogonal with respect to the damping matrix, it can be shown [12] that the latter must be expressed as a linear combination of the mass and the stiffness matrices as

$$C = a_1 M + a_2 K \qquad 2.11$$

in which a_1 and a_2 are proportionality factors. Then,

$$\phi_j^T C \phi_i = 0 \qquad \text{for } i \neq j \qquad 2.12$$

$$\phi_j^T C \phi_i = C^*_i \qquad \text{for } i = j \qquad 2.13$$

where C^*_i is the modal danping coefficient for the i^{th} mode.

iii) Maximum Modal Response: Substituting eqn. (2.2) and its derivatives into eqn. (2.1) yields

$$M \phi x'' + C \phi x' + K \phi x = - M y'' \qquad 2.14$$

Premultiplying eqn. (2.14) by ϕ_i^T gives

$$\phi_i^T M \phi x'' + \phi_i^T C \phi x' + \phi_i^T K \phi x = -\phi_i^T M y'' \qquad 2.15$$

Applying the orthogonality properties expressed in eqns. (2.9), (2.10) and (2.11), eqn. (2.15) then becomes

$$M^*_i x'' + C^*_i x' + K^*_i x = - \phi_i^T M y'' \qquad 2.16$$

which is the sdof equation for the i^{th} mode. Dividing eqn. (2.16) by M^*_i yields

$$x'' + (C^*_i/M^*_i) x' + (K^*_i/M^*_i) x = -(P^*_i/M^*_i) y'' \qquad 2.17$$

in which $$P^*_i = \phi_i^T M \qquad 2.18$$

Eqn. (2.5) can be written as

$$K \phi_i = w_i^2 M \phi_i \qquad 2.19$$

premultipying eqn. (2.19) by ϕ_i^T produces

$$\phi_i^T K \phi_i = w_i^2 \phi_i^T M o_i \qquad 2.20$$

or

$$K^*_i = M^*_i w_i^2 \qquad 2.21$$

and hence

$$\frac{K^*_i}{M^*_i} = w_i^2 \qquad 2.22$$

It can be shown also [12] that

$$\frac{C^*_i}{M^*_i} = 2z_i w_i \qquad 2.23$$

where z_i is the damping ratio in the i^{th} mode.

Substituting eqns. (2.22) and (2.23) into eqn. (2.17) one can obtain

$$x_i'' + 2z_i w_i x_i' + w_i^2 x_i = - (P^*_i/M^*_i) y'' \qquad 2.24$$

Eqn. (2.24) is a sdof equation. Its solution yields the maximum modal amplitude x_{imax} for specific ground motion, damping factor and frequency. If the frequency is varied then displacement, velocity or acceleration spectra can be plotted using the maximum values x_{max}, wx_{max}, w^2x_{max}. These are often designated as Sd, Sv, and Sa respectively. Using these curves, the maximum spectra based response can be evaluated. For instance the maximum displacement for mode i may be expressed as:

$$x_{i_{max}} = \frac{P^*_i \cdot Sa_i}{M^*_i \cdot w_i^2} \qquad 2.25$$

The relative displacements or the distribution of maximum displacement in mode i can then be computed using eqn. (2.2) as:

$$U_i = \phi_i x_{max} \qquad 2.26$$

or using eqn. (2.25)

$$U_i = \phi_i \cdot \frac{P^*_i \quad Sa_i}{M^*_i \quad w_i^2} \qquad 2.27$$

Similarly the distribution of maximum accelerations in mode i is given by

$$U''_i = \phi_i x''_{max} = \phi_i w_i^2 x_{max} \qquad 2.28$$

and hence the distribution of maximum earthquake forces

$$f_i = M U''_i \qquad 2.29$$

$$f_i = M \phi_i \cdot \frac{P^*_i \quad Sa_i}{M^*_i} \qquad 2.30$$

from these elastic distributed forces, any desired force quantity can be obtained using any standard method of statics. For instance the maximum base shear V_o as

$$V_o = \int_o^H f_i (x)\, dx \qquad 2.31$$

where H is the total height of the structure. Eqn. 2.31 can be written as

$$V_o = \int_0^H \frac{P^*_i \quad Sa_i}{M^*_i} \quad M \phi_i \, x \, dx \qquad 2.32$$

$$V_o = \frac{P^{*2}_i \quad Sa_i}{M^*_i} \qquad 2.33$$

It must be emphasized that the quantities derived so far have been for individual modes, however the total maximum quantities can be obtained using an approximate combination of the modal contributions. If the root-mean-square (RMS) procedure is used then,

$$U_{max} = (U_1^{\,2} + U_2^{\,2} + \ldots U_n^{\,2})^{\frac{1}{2}} \qquad 2.34$$

similarly,

$$F_{max} = (\sum_{1}^{n} f_i^{\,2})^{\frac{1}{2}} \qquad 2.35$$

$$V_{o_{max}} = (\sum_{1}^{n} V_o^{\,2})^{\frac{1}{2}} \qquad 2.36$$

It is apparent from eqn. 2.34 that only some of the modes will make significant contribution to the total nodal displacements. A very good approximation of the exact response can be obtained by including only the first few terms of the RHS of eqn. 2.34. This fact is one of the major advantages of the mode superposition technique over the direct integration formulation. The other important advantage is that the equations are uncoupled and hence no simoultaneous equation solution need be performed.

2-3 Code of Practice Requirements

The seismic design code provisions are given by a set of equivalent lateral forces which simulate inertial loads generated by the earthquake motion. It must be borne in mind however that these prescribed forces are generally far too small to be similar to those induced in case of a real severe earthquake. The relatively low equivalent forces specified by the code are justified for two main reasons

i) It is economically unwarranted to design buildings to resist major earthquakes elastically.

ii) It is recognised that structures with adequate strength and ductility have

the capability to withstand earthquake through inelastic deformations.

2-3-1 Recommended Lateral Forces: In this section the Californian code of practice SEAOC [49] is chosen for the illustration. In this code, the principal seismic provisions defines the effective intensity of the design earthquake in terms of the maximum base shear V_{max} as:

$$V_{max} = Z\ I\ K\ C\ S\ W \qquad 2.37$$

in which

Z = seismic zoning factor. The value of 1 corresponds to the areas of highest seismicity

I = structure importance factor (e.g for hospitals I=1.5)

K = factor depending on the structure framing system. It is intended to count for energy dissipation capacity of the structure

C = seismic response factor. It is expressed in terms of the fundamental period as $C = 1/(15T^{\frac{1}{2}})$

S = foundation conditions factor

W = total weight of the structure

if eqn. (2.37) is written in the form of

$$V_{max} = K^*\ C\ W \qquad 2.38$$

an analytical expression corresponding to the code formula can be derived from eqn. 2.33 by considering only the fundamental mode as:

$$V_o = \frac{P^*_1{}^2\ Sa_1}{M^*_1} \qquad 2.39$$

comparing eqn. 2.38 and eqn. 2.39 reveals the folowing correspondance

$$C = \frac{Sa_1}{g} \qquad W = \frac{P^*_1{}^2}{M^*_1}\ g \qquad 2.40$$

Thus, C is the spectral acceleration expressed in g units and the total weight W is considered to be equivalent to the effective weight in the first mode.

2-3-2 Distribution of Recommended Lateral Forces: The other provision of the SEAOC code defines how the total base shear force is distributed over the height of the structure ,i.e.,

$$f_i = \frac{W_i x_i}{\sum_1^n W_i x_i} V^*_{max} \qquad 2.41$$

in which f_i = lateral force at floor level

W_i = weight at level i

x_i = height of level i above the base

$V^*_{max} = V_{max} - F_{tp}$

F_{tp} = force to be applied additionally at the top and accounts for higher modes if significant.

a corresponding analytical expression can be derived from eqn. 2.30 by considering the fundamental mode, i.e.,

$$f_i = M \phi_1 \frac{P^*_1 \; Sa_1}{M^*_1} \qquad 2.42$$

or by substituting eqn. 2.39 into eqn. 2.42,

$$f_i = \frac{M \phi_1}{P^*_1} V_{o_{max}} \qquad 2.43$$

writing the excitation factor P^*_1 in the form $\sum_1^n M_i \phi_{1_i}$ yields

$$f_i = \frac{M \phi_1}{\sum_1^n M_i o_{1_i}} V_{o_{max}} \qquad 2.44$$

It can be seen by comparing eqn. 2.41 and eqn. 2.44 that the code expression represents the response of a lumped mass system deflecting with a straight line shape, i.e., $\phi_{1i} = x_i/H$. This assumption stems from observations that the first mode shape is generally close to a straight line.

2-4 Nonlinear Methods of Analysis

In section 2-2 of this chapter the description of elastic dynamic analysis has been attempted. It has been assumed then, that the structure is a linear system i.e., its properties do not change during the earthquake motion. It is accepted however that during ground motions of even moderate intensity, displacements well in excess of the yield displacement are induced. The inertial forces generated by earthquakes are so large that it is not economically feasible to design for them. Instead the designer relies on the energy absorbing capabilities of yielding structures to absorb a large portion of the energy input by the earthquake through inelastic deformations. Therefore allowance for nonlinearity in the analysis procedure to assess these inelastic deformations is a major design consideration. This gave rise to approximate methods such as the inelastic spectrum approach and ductility factor method approach in addition to the rigorous step-by-step nonlinear dynamic analysis.

The step-by-step procedure and the Inelastic Response Spectrum method of analysis, used in this dissertion, will be developed later in this study. Therefore this section is confined to describing the approximate ductility factor method of analysis.

2-4-1 Approximate Ductility Factor Method: The Ductility factor method [12] is the first approximate method developed to obtain a reasonable measure of the nonlinear behaviour without carrying out a complete nonlinear analysis. Its procedure stems directly from its basic assumption, that the deflection produced by any earthquake input is essentially the same whether the structure behaves

elastically or inelastically. Consequently the forces (moments, shear and axial forces) obtained from an elastic analysis are reduced by a factor μ, which accounts for the fact that the structure is ductile and will respond inelastically. The value of the ductility factor varies from case to case, however, the value of 4 has been popular because dynamic analyses of structures subjected to El Centro earthquake have shown that the elastic forces generated in typical structures are about 4 times as large as the yield level that the equivalent lateral static forces computed according to the SAEOC code [49] would prescribe.

CHAPTER THREE

THE FINITE ELEMENT THEORY

3.1 General

The finite element method (FEM) of analysis which started as an extention of the stiffness or displacement method is probably the most powerful tool for structural analysis. Since the growing development of computer facilities, the method has widely spread its application and is nowadays used to solve in addition to structural problems, different kinds of physical problems such as fluid mechanics, soil mechanics, thermodynamics, electrodynamics, ... etc. Detailed presentations and description of the method are widely published [58 - 61].

In the stiffness method for skeletal structure the elements are connected together at discrete joints and equations of equilibrium involving external loads and member end forces are established to solve for end joint displacements. Similarly, when dealing with a two or three - dimensional continuum, the structure is subdivided into "elements" of some geometrical shape (triangle, quadrilateral, cubic :...) connected at a finite number of points or "nodes" at their boundaries and stiffness relationships between nodal displacements and nodal forces are derived in the same manner as for skeletal structure using various energy theorems. In this way a continuum with an infinite number of degrees of freedom (dof) can be discretisized as an equivalent system with finite dof. As can be expected the number of finite elements considered, as well as the size of the elements given by their aspect ratio, play a big role in the accuracy and the converging properties of the analysis. These however are beyond the scope of this study.

The finite element method is based on assumed patterns or functions. These functions can define the variation for either the element displacements (displacement method) or the stress patterns (equilibrium method) or both (hybrid method). In this study, the displacement method is used and the derivation of the stiffness properties is based on the principle of minimum potential energy.

3.2 General Finite Element Procedure

3.2.1 Displacement Function: The basic philosophy of the FEM is piecewise approximation. That is, we approximate a solution of a complicated problem by representing the solution within each subdivision by a relatively simple function. Therefore the choice of suitable displacement functions is of paramount importance. For plane stress consideration the nodal displacement δ_i is represented by two translational displacements U_i and V_i. If the displacements of an element are represented by f , they may be expressed as:

$$f = [\, N1 \,,\, N2 \,,\, \ldots\ldots \,,\, Nn \,] \quad . \quad \begin{bmatrix} \delta_1 \\ \delta_2 \\ \ldots \\ \delta_4 \end{bmatrix} \qquad 3.1$$

i.e.,

$$f = [\, N \,] \,.\, \delta_e \qquad 3.2$$

where n is the number of element nodes and Ni are the interpolation polynomials or shape functions which should be chosen with care to satisfy the following convergence criteria

i) continuity of displacements at the interelement boundaries

ii) all rigid body diplacements should be included

iii) as the element area is reduced, a constant strain condition should result

3.2.2 Strain - Displacement Relationship: The strains are obtained through appropriate differentiation of the displacement function f with respect to the relevant coordinate x or y. For plane stress conditions, these can be written as:

$$\epsilon = \begin{Bmatrix} \epsilon_x \\ \epsilon_y \\ \epsilon_{xy} \end{Bmatrix} = \begin{Bmatrix} \frac{\partial U}{\partial x} \\ \frac{\partial V}{\partial y} \\ \frac{\partial U}{\partial y} + \frac{\partial V}{\partial x} \end{Bmatrix} \qquad 3.3$$

$$= \left\{ \begin{bmatrix} \sum_{i=1}^{n} \frac{\partial N_i}{\partial x} \cdot U_i \\ \sum_{i=1}^{n} \frac{\partial N_i}{\partial y} \cdot V_i \\ \sum_{i=1}^{n} \frac{\partial N_i}{\partial y} \cdot U_i + \frac{\partial N_i}{\partial x} \cdot V_i \end{bmatrix} \right\} \qquad 3.4$$

i.e.,

$$\epsilon = [B]\, \delta_e \qquad 3.5$$

where [B] is the strain - displacement matrix and is given in detail in the next section for isoparametric elements.

3.2.3 Strain - Stress Relationship: The element stresses σ are related to the corresponding strain ϵ using the generalised Hooke's law as:

$$\sigma = [D].\epsilon \qquad 3.6$$

where the stress vector σ is defined as

$$\sigma^T = [\sigma x , \sigma y , \tau xy] \qquad 3.7$$

and the matrix [D] is referred to as elasticity or property matrix. For a plane stress element with isotropic property [D] is given by [62]

$$[D] = E/(1-\mu^2) \begin{bmatrix} 1 & \mu & 0 \\ \mu & 1 & 0 \\ 0 & 0 & (1-\mu)/2 \end{bmatrix} \qquad 3.8$$

where E is the elastic Young's modulus and μ is the Poisson's ratio. Substituting eqn. 3.5 into eqn. 3.6 yields

$$\sigma = [D][B]\ \delta_e \qquad 3.9$$

3.2.4 Minimization of Total Potential Energy: The element strain energy U_s is given by

$$U_s = \tfrac{1}{2} \int_{vol} \epsilon^T . \sigma \ d(vol) \qquad 3.10$$

which after substituting for ϵ and σ from eqns. 3.5 and 3.6 becomes

$$U_s = \tfrac{1}{2} \int_{vol} \delta_e^T . B^T . D . B . \delta_e \ d(vol) \qquad 3.11$$

The potential energy due to nodal loads Re is given by

$$W = - \delta_e^T . Re \qquad 3.12$$

and the total element potential energy is given by

$$Q_e = U_s + W \qquad 3.13$$

or, using eqn. 3.11 and eqn. 3.12

$$Q_e = \frac{1}{2}\int_{vol} \delta_e^{\,T} B^T D B \, \delta_e \, d(vol) - \delta_e^{\,T} Re \qquad 3.14$$

The minimization procedure [3.2 - 3.5] requires that

$$\frac{\partial Q_e}{\partial \delta} = 0 \qquad 3.15$$

which yields

$$\int_{vol} B^T D B \, \delta_e \, d(vol) = Re \qquad 3.16$$

i.e.,

$$[K_e]\,\delta_e = Re \qquad 3.17$$

in which the stiffness matrix $[K_e]$ is given by

$$[K_e] = \int_{vol} B^T D B \, d(vol) \qquad 3.18$$

Once the displacement vector δ_e has been determined, it is possible to compute the stress distribution at any point within the element using eqn. 3.6. If however, the principal stresses and maximum shear stresses are desired, they can be calculated from the following expressions [62]:

$$\sigma_{1,2} = \frac{\sigma x + \sigma y}{2} \pm \sqrt{\frac{(\sigma x - \sigma y)^2}{(2)^2} + \tau xy^2} \qquad 3.19$$

$$\tau_{max} = \frac{\sigma_1 - \sigma_2}{2} \qquad 3.20$$

$$\tan 2\Theta = - \frac{2\tau xy}{\sigma x - \sigma y} \qquad 3.21$$

where σ_1 and σ_2 are the major and minor principal stresses, τ_{max} is the maximum shearing stress and θ defines the principal stresses direction with respect to the element axis.

3.3 Coupled Shear Wall Discretisation

A suitable representatiom of a structure such as coupled walls requires the use of two types of elements

i) quadrilateral plane stress elements for the walls

ii) line element for the coupling beams.

3.3.1 Isoparametric Quadrilateral Elements: The stiffness formulation of this family of elements is well documented and can be found in many references [58-61]. The formulation is carried out using localised coordinates (s , t). These coordinates are chosen to have values +1 and -1 along the sides of the element and hence vary from -1 to +1. The element may have 4, 8, or 12 nodes depending on whether a linear , quadratic or cubic function is assumed respectively. As far as this study is concerned , linear four noded elements are assumed. Each node i has two degrees of freedom Ux_i and Vy_i (fig. 3.1). The local and global coordinates are related by

$$x = \sum_{i=1}^{4} N_i x_i \qquad 3.22$$

$$y = \sum_{i=1}^{4} N_i y_i$$

where the interpolation functions N_i are defined as

$$\begin{aligned} N_1 &= \tfrac{1}{4}(1-s)(1-t) \\ N_2 &= \tfrac{1}{4}(1+s)(1-t) \\ N_3 &= \tfrac{1}{4}(1+s)(1+t) \\ N_4 &= \tfrac{1}{4}(1-s)(1+t) \end{aligned} \qquad 3.23$$

From the basic definition of isoparametric elements, the same interpolation function relates displacements within the element to nodal displacements, i.e.,

$$Ux = \sum_{i=1}^{4} N_i \, Ux_i$$

3.24

$$Vy = \sum_{i=1}^{4} N_i \, Vy_i$$

In view of its poor behaviour under bending, the linear isoparametric quadrilateral element has been improved by the introduction of so-called incompatible modes (fig. 3.3) suggested by Wilson [63]. This involves the addition of corrective displacements to the displacement fields defined by eqn. 3.24. Following Wilson's procedure equation 3.24 becomes

$$Ux = \sum_{i=1}^{4} N_i \, Ux_i + c_1(1-s^2) + c_2(1-t^2)$$

3.25

$$Vx = \sum_{i=1}^{4} N_i \, Vy_i + c_3(1-s^2) + c_4(1-t^2)$$

The constants c_1, ..., c_4 are additional degrees of freedom and therefore increase the element stiffness matrix to (12 x 12). However these constants being relative to the corner nodal displacements, they can be condensed by minimisation of the strain energy at element level.

As the shape functions are given in local coordinates (s , t), the relationships between local coordinates and global derivatives must be found to determine the strain matrix [B] given by eqn. 3.3. Using the usual chain rules of partial differentiation, the general transformations for function N_i may be written as

$$\begin{Bmatrix} \frac{\partial N_i}{\partial s} \\ \\ \frac{\partial N_i}{\partial t} \end{Bmatrix} = \begin{bmatrix} \frac{\partial N_i}{\partial x} \cdot \frac{\partial x}{\partial s} & \frac{\partial N_i}{\partial y} \cdot \frac{\partial y}{\partial s} \\ \\ \frac{\partial N_i}{\partial x} \cdot \frac{\partial x}{\partial t} & \frac{\partial N_i}{\partial y} \cdot \frac{\partial y}{\partial t} \end{bmatrix} \qquad 3.26$$

or in matrix form as:

$$\begin{Bmatrix} \frac{\partial N_i}{\partial s} \\ \\ \frac{\partial N_i}{\partial t} \end{Bmatrix} = \begin{bmatrix} \frac{\partial x}{\partial s} & \frac{\partial y}{\partial s} \\ \\ \frac{\partial x}{\partial t} & \frac{\partial y}{\partial t} \end{bmatrix} \cdot \begin{bmatrix} \frac{\partial N_i}{\partial x} \\ \\ \frac{\partial N_i}{\partial y} \end{bmatrix} \qquad 3.27$$

$$\begin{Bmatrix} \frac{\partial N_i}{\partial s} \\ \\ \frac{\partial N_i}{\partial t} \end{Bmatrix} = [\,J\,] \cdot \begin{Bmatrix} \frac{\partial N_i}{\partial x} \\ \\ \frac{\partial N_i}{\partial y} \end{Bmatrix} \qquad 3.28$$

where [J] is known as the Jacobian matrix. It can be computed explicitly in terms of local coordinates as

$$[\,J\,] = \begin{bmatrix} \frac{\partial N_1}{\partial s} & \frac{\partial N_4}{\partial s} \\ \\ \frac{\partial N_1}{\partial t} & \frac{\partial N_4}{\partial t} \end{bmatrix} \cdot \begin{bmatrix} x_1 & y_1 \\ .. & .. \\ .. & .. \\ .. & .. \\ x_4 & y_4 \end{bmatrix} \qquad 3.29$$

and hence the required derivatives

$$\begin{Bmatrix} \frac{\partial N}{\partial x} \\ \\ \frac{\partial N}{\partial y} \end{Bmatrix} = [\,J\,]^{-1} \cdot \begin{Bmatrix} \frac{\partial N}{\partial s} \\ \\ \frac{\partial N}{\partial t} \end{Bmatrix} \qquad 3.30$$

The strain matrix (eqn. 3.3) can now be written as:

$$\epsilon = [B] \cdot \begin{Bmatrix} U_1 \\ V_1 \\ .. \\ U_4 \\ V_4 \end{Bmatrix} \qquad 3.31$$

where

$$[B] = [B_1, B_2, B_3, B_4]$$

in which

$$[B_i] = \begin{bmatrix} \frac{\partial N_i}{\partial x} & 0 \\ 0 & \frac{\partial N_i}{\partial x} \\ \frac{\partial N_i}{\partial y} & \frac{\partial N_i}{\partial x} \end{bmatrix} \qquad 3.32$$

The element stiffness matrix (eqn. 3.18) can now be written in local coordinates (s,t) as

$$[K_e] = h \int_{-1}^{+1}\int_{-1}^{+1} B^T D B \ \det[J] \, ds \, dt \qquad 3.33$$

where h is the element thickness and det[J] the determinant of matrix [J]. Using G aussian quadrature [59] for the numerical integration, the element stiffness matrix (eqn. 3.33) can be written as:

$$[K_e] = h \sum_j \sum_k W_j \, W_k \det[J] \, B^T_{(s_j,t_k)} \, D \, B_{(s_j,t_k)} \qquad 3.33$$

in which j and k are the Gaussian integration points and W_j and W_k their corresponding weight factors. Table 3.1 shows the local coordinates of the Gaussian points and their weight factors.

3.3.2 Line Element: The elastic stiffness matrix for this element is given in its general form with respect to the reference axis as

$$[Ke] = \begin{bmatrix} S1 & 0 & 0 & -S1 & 0 & 0 \\ & S2 & S4 & 0 & -S2 & S4 \\ & & S3 & 0 & -S4 & S5 \\ \text{symmetric} & & & S1 & 0 & 0 \\ & & & & S2 & -S4 \\ & & & & & S3 \end{bmatrix} \qquad 3.35$$

in which

$$S2 = \frac{12EI}{L^3(1+2g)} \qquad S3 = \frac{4EI(1+g/2)}{L(1+2g)}$$

$$S4 = \frac{6EI}{L^2(1+2g)} \qquad S5 = \frac{2EI(1-g)}{L(1+2g)}$$

where $g = (6fEI)/GAL^2$

G = Shear modulus

f = Shape form factor

A = Area of cross section

I = Moment of inertia of the section

L = Length of the beam element

If the element is inclined at an angle α with respect to the global coordinates (fig. 3.2), then the stiffness matrix (eqn. 3.38) must be transformed to the global coordinates system before the overall assembly. In the particular case where the element is vertical (e.g column), then [K] specialises as:

$$[Ke] = \begin{bmatrix} S2 & 0 & -S4 & -S2 & 0 & -S4 \\ & S1 & 0 & 0 & -S1 & 0 \\ & & S3 & S4 & 0 & S5 \\ & & & S2 & 0 & S4 \\ & \text{symmetric} & & & S1 & 0 \\ & & & & & S3 \end{bmatrix}$$

Assuming that the displacements of the reference axis are related to the displacements of the corner of the element (fig. 3.2) by the following relation:

$$U_r = [A_{rc}].U_c \qquad 3.38$$

where

$$[A_{rc}] = \begin{bmatrix} 0.5 & 0 & 0 & 0 & 0 & 0 & 0 & 0 \\ 0 & 0.5 & 0 & 0 & 0 & 0 & 0 & 0.5 \\ 1/D & 0 & 0 & 0 & 0 & 0 & -1/D & 0 \\ 0 & 0 & 0.5 & 0 & 0.5 & 0 & 0 & 0 \\ 0 & 0 & 0 & 0.5 & 0 & 0.5 & 0 & 0 \\ 0 & 0 & 1/D & 0 & -1/D & 0 & 0 & 0 \end{bmatrix} \qquad 3.39$$

D = Depth of the beam element

Uc = Displacement vector of the corners of the beam element.

Ur = Displacement vector at the reference axis of the beam.

by the application of the principle of virtual work one can arrive at the stiffness matrix of a new line element with 8 degrees of freedom, i.e.,

$$[Ke,c] = [A_{rc}]^T [Ke] [A_{rc}] \qquad 3.40$$

In the computation of the 8 x 8 stiffness matrix of the beam element, it was assumed that the displacements 2, 4, 6, and 8 are independent which implies a possible change in the cross-section depth. If the displacements in the directions 2 and 8 and similarly 4 and 6 (fig. 3.2b) can be made equal, the cross-section will remain unchanged across its depth. A very simple method of ensuring that is by adding large stiffness terms to the positions K22, K28, K82, K88. Physically this can be visualized as if a fictitious, very rigid bar exists between node i and l and j and k respectively. The moment, shear and axial forces acting at the reference axis can be computed using the following relation:

$$F_r = [B_{rc}]^T . F_c \qquad 3.41$$

where

F_r = vector of forces acting at reference axis

F_c = vector of forces acting at element corners

$[B_{rc}] = [A_{rc}]^{-1}$, i.e.,

$$[B_{rc}] = \begin{bmatrix} 1 & 0 & D/2 & 0 & 0 & 0 \\ 0 & 1 & 0 & 0 & 0 & 0 \\ 0 & 0 & 0 & 1 & 0 & D/2 \\ 0 & 0 & 0 & 0 & 1 & 0 \\ 0 & 0 & 0 & 1 & 0 & -D/2 \\ 0 & 0 & 0 & 0 & 1 & 0 \\ 1 & 0 & -D/2 & 0 & 0 & 0 \\ 0 & 1 & 0 & 0 & 0 & 0 \end{bmatrix} \qquad 3.42$$

3.4 Overall Solution

The stiffness matrix of the whole structure is constructed from the individual element matrices by using the direct stiffness matrix method [8], i.e., by summing up the individual element stiffnesses as

$$[K] = \sum_{1}^{n} [K_e] \qquad 3.43$$

where $[K]$ = overall stiffness matrix

$[K_e]$ = element stiffness matrix

n = number of elements in structure

Similarly, the overall load vector R is given by

$$R = \sum_{1}^{n} R_e \qquad 3.44$$

and the potential energy of the structure Q is the sum of the element potentials as given by eqn. 3.14, i.e.,

$$Q = \sum_{1}^{n} Q_e \qquad 3.45$$

substituting eqns. (3.40) and (3.42) into eqn. 3.44 yields

$$Q = \delta^T \left(\tfrac{1}{2} \sum_{1}^{n} [K_e]\, \delta - \sum_{1}^{n} R_e \right) \qquad 3.46$$

i.e.,

$$Q = \delta_o^T \left([K]\, \delta_o - R \right) \qquad 3.47$$

where δ is the overall displacement vector. Minimizing the potential energy requires

$$\frac{\partial Q}{\partial \delta} = 0 \qquad 3.48$$

i.e.,

$$[K]\, \delta_o = R \qquad 3.49$$

By introducing the structural forces R and the known boundary conditions, the unknown structural displacement vector δ_o is obtained by solving the system of simultaneous equations given by

$$\delta_o = [K]^{-1} R \qquad 3.50$$

In this study, Gaussian elimination procedure [8] is employed for the solution of equation 3.50. Eqn. 3.50 is general and is applicable to static as well as dynamic problems. In a dynamic history analysis, the equation of motion is generally solved using step-by-step numerical integration method. In each time interval, the equations of motion can be transformed to the above general form (eqn. 3.50) as demonstrated in chapter five.

TABLE 3.1 GAUSSIAN QUADRATURE CONSTANTS

± a			H		
		n = 2			
0.57735	02691	89626	1.00000	00000	00000
		n = 3			
0.77459	66692	41483	0.55555	55555	55556
0.00000	000000	00000	0.88888	88888	88889

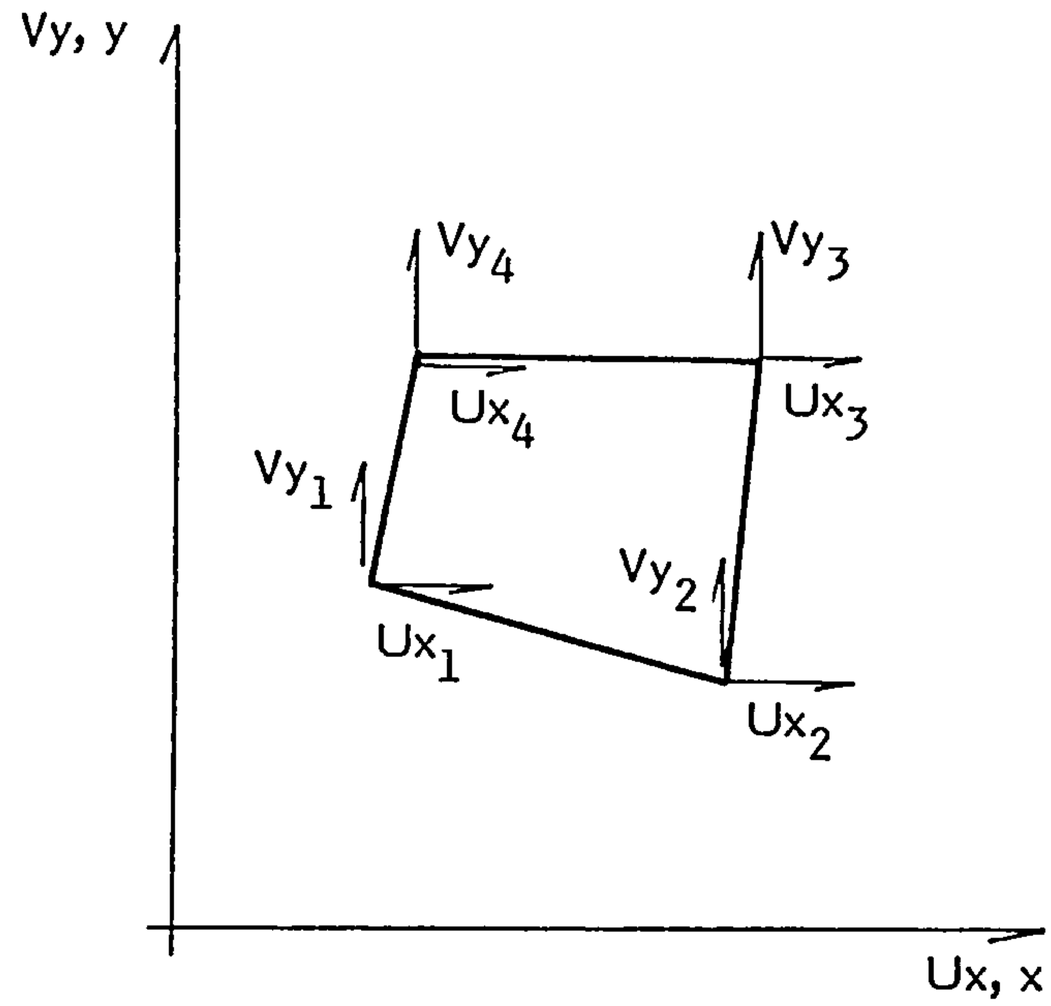

a) Cartesian Coordinates b) Local Coordinates

FIG. 3.1 TWO-DIMENSIONAL ISOPARAMETRIC ELEMENT

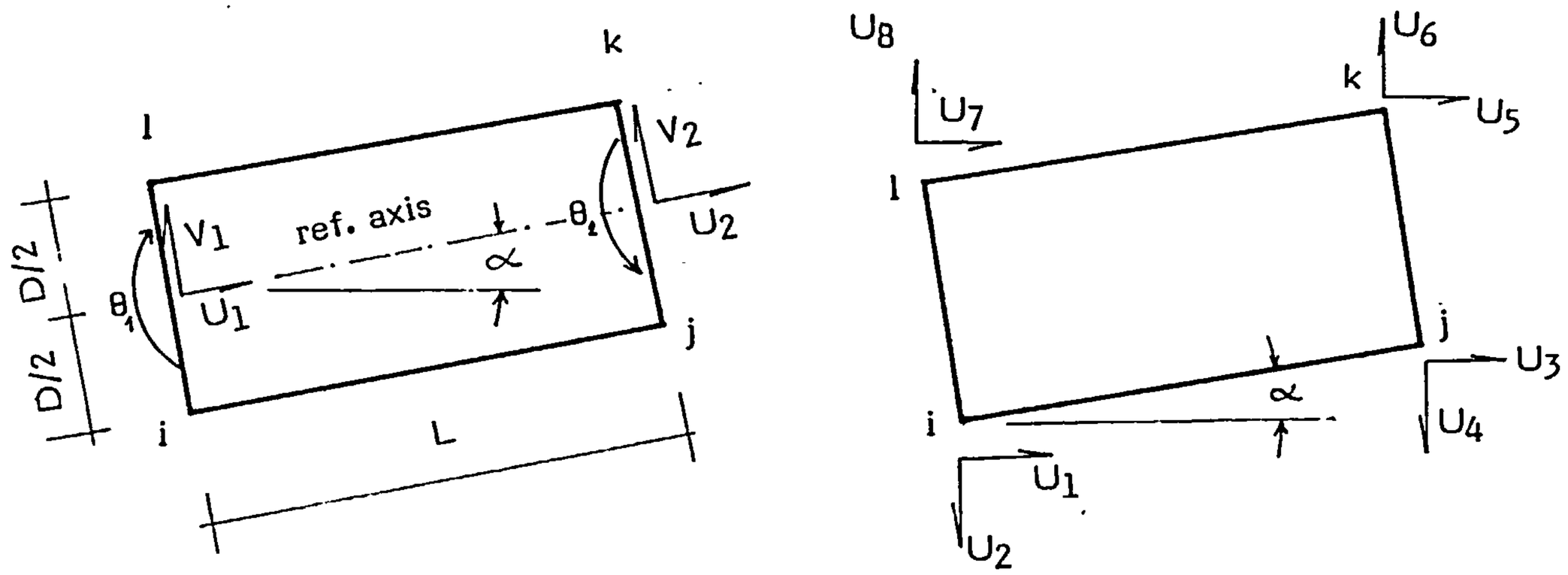

a) Displacements at reference axis b) Displacements at corners

FIG. 3.2 LINE ELEMENT IDEALISATION

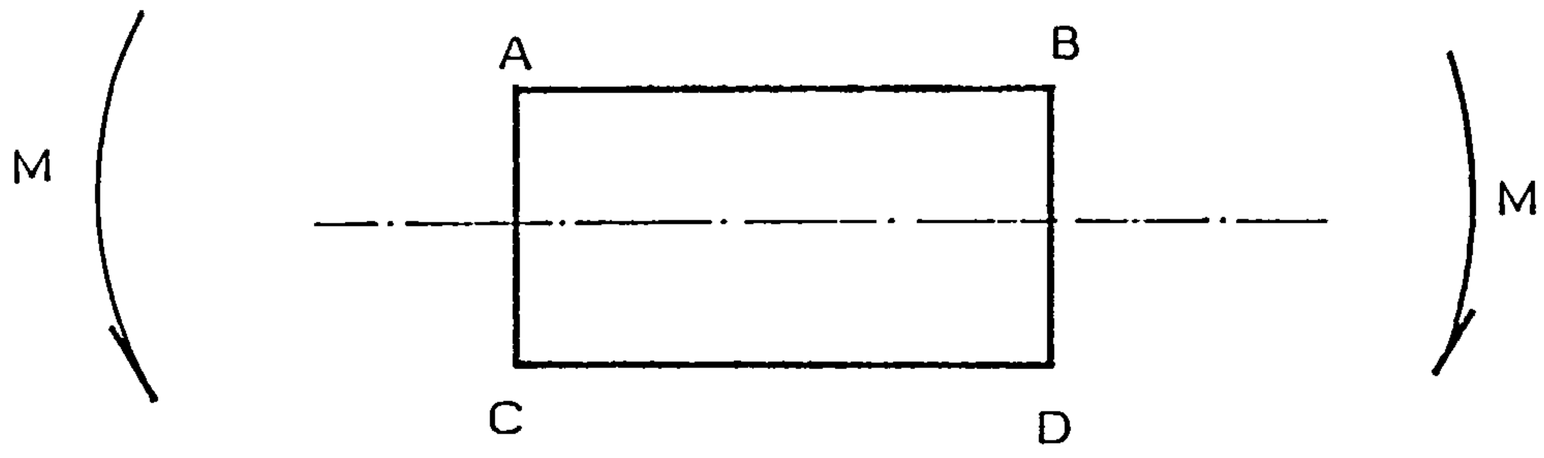

A) Flexural Element

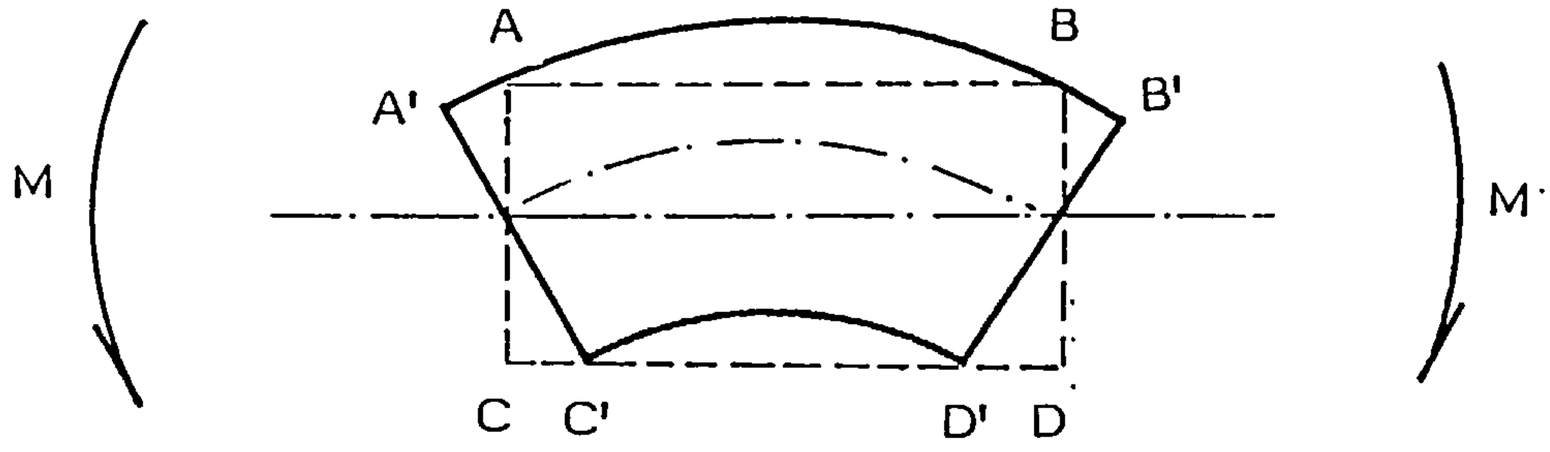

B) Deformed Shape of the Flexural Element

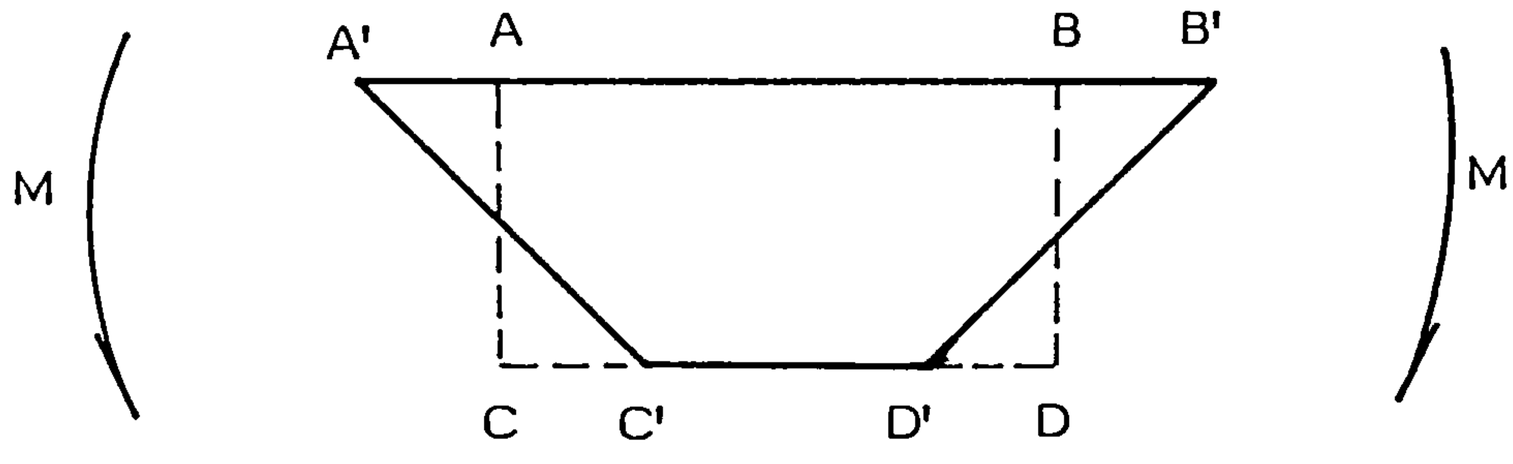

C) Deformed Shape of the Quadrilateral Element

FIG. 3.3 BENDING BEHAVIOUR OF A QUADRILATERAL ELEMENT

CHAPTER FOUR

INELASTIC SPECTRUM PROCEDURE

4-1 General

In carrying out a dynamic analysis to obtain the response of a structure subjected to earthquake forces, one can use the response spectrum analysis or the more sophisticated and computer time consuming, time history analysis. Time history analysis involves step-by-step integration of the equations of motion for a ground motion accelerogram and is applicable to both linear and nonlinear systems. In recent years many researchers [26, 27, 29, 36, 64-68] have focused their work on improving the nonlinear mathematical models to be used along with the step-by-step method of analysis. Despite that, however, the corresponding improvements in the ability of structures to withstand earthquake is far behind. This is because, first analysis has far outstripped practical use of the results for design purpose and second, the step-by-step method of analysis is too expensive to be attractive for practical purposes and need be performed repeatedly to meet an acceptable behaviour and to take the randomness of ground motion [12] into account, i.e., because of the sensivity of the structural response to the details of ground motion input.

The response spectra-based analysis however, although limited so far to elastic systems, may be a potential practical method for inelastic structure design. Eventhough the inelastic spectrum analysis [11, 16, 69, 70] is not strictly correct, the simplicity required by a code of practice on one hand, and the complexity and questionable reliability of the step-by-step integration procedure on the other, makes the method most attractive for the future. Therefore this chapter is intended to develop this method and to investigate its application for a practical design of coupled shear wall structures.

The general approach and its limitations are discussed first then the procedure of the method is presented and the different influencing parameters are investigated in section 4.3. The response spectrum analysis is based on a response spectra as loading data, therefore the development of an inelastic design spectra is also presented in section 4.3. Section 4.4 is devoted to the application of the inelastic spectrum analysis to coupled shear wall structures.

4-2 Approach and Limitations

Although the term response spectrum was originally used with reference to linear single degree of freedom (sdof) systems, its use has been extended to mdof systems by modeling each vibration mode by the response of a sdof system. For a particular linear sdof system defined by its frequency and damping, a point on a response spectrum curve is obtained by subjecting the system to a specific ground motion record. The maximum value of the response parameter of interest (acceleration, velocity or displacement) during the excitation and associated frequency or period for a specific damping ratio defines a point of the spectrum. Other points are obtained by varying the frequency (or period). Fig. (4.1) shows an example of such a spectrum for different damping ratios.

The response spectrum analysis consists of the superposition of the modal responses obtained from . specific spectra. In using such an elastic spectrum, the only source of inaccuracy in the method lies in the way the modal contributions are combined. When subjected to a ground motion, an inelastic single degree of freedom system may respond as shown in fig. (4.2). If a ductility factor defined as (fig. 4.2b)

$$\mu = \frac{U_{max}}{U_y} \qquad 4.1$$

Umax and Uy being the maximum displacement and the displacement at yield respectively, is chosen and if the yield value Ry is selected by trial and error so that the computed ductility is equal to that preset, then an inelastic spectrum can be generated in the same way described above for elastic analysis. Fig. (4.3) shows an example of such spectrum for different ductilities.

If the structure to be designed is a sdof system, the use of an inelastic spectrum is theoretically correctly applicable. In the case of a mdof system however, the modal analysis used in the inelastic spectrum analysis is not rigorously valid because of its principle of superposition which does not hold beyond the elastic range [12, 71] unless all plastic hinges associated with the assumed failure mechanism form simultaneously [72].

4.3 Procedure of the Method

Apart from the development of the inelastic spectra which is an iterative process for a preset ductility factor, the rest of the procedure is very much the same as the elastic modal analysis and involves the following steps:

i) Design Earthquake Ground Motion: The choice of an earthquake input as a basis for design is one of the most difficult and uncertain features in the overall procedure of seismic analysis. This is because, first, the determination of any earthquake record depends to a large extent on the disciplines of geology and seismology [73] and therefore may differ from one site to another and second, the response of a structure depends not only on the intensity of the earthquake but also on such factors as frequency content, duration, etc... Therefore two different records of the same intensity are most likely to excite a given structure quite differently. Researchers [74, 75, 12] have dealt with the problem of selection of design earthquakes and most of them agreed that the use of a single record to define a design earthquake

leaves considerable uncertainty as to the significance of the response it produces.

While averaging the maximum responses of each of the record considered to produce design spectra to be used along with modal analysis is quite usual, the procedure seems to be impractical for the step-by-step integration method and one is confined to perform the analysis for each of the record seperately. This shows yet again the advantage and practicality of inelastic spectrum analysis over the time history analysis. In this dissertation four earthquake records of different characteristics have been considered. Their accelerogram time histories for the first 10 second duration are shown in fig. (4.5).

ii) Design Ductility: When subjected to a severe earthquake, the structure must have the capability of undergoing substantial inelastic deformation without collapse. These inelastic deformations are often referred to as ductility demand which is measured in terms of strains, displacements, curvatures or rotations, and is defined by the ratio of the ultimate to the yield value of the quantity considered, i.e.,

$$\mu = \frac{Du}{Dy} \qquad 4.2$$

For mdof systems the term ductility factor has been used with different meanings [55] adding confusion and ambiguity. Keeping in mind that the presented approach is intended to be integrated into a code and as far as shear walls are concerned, the displacement ductility seems to be the most suitable. This is so because the rotational ductility ($\theta u/\theta y$) can be very misleading when dealing with members of different depth, indeed because of the relatively smaller curvature associated with first yielding in a deep member such as shear wall, a rotational ductility factor of say 4, would represent a relatively lower lateral capacity than the same ratio would indicate when used for a

regular column. If one defines the storey drift as the relative displacement between two successive storeys, the ultimate drift Du would be the acceptable drift preset by the designer or the code of practice. It may be worth noting that the Applied Technology Council (ATC) [76] recommended a value of Du = 0.01h and the UBC code [50] a value of Du = 0.015h, h being the storey height.

iii) Developement of the Inelastic Response Spectrum: As explained in section 4.2, a spectrum is presented in terms of one of the parameters of interest. Throughout this dissertion spectral acceleration is considered. When subjected to a ground excitation x'', a single degree of freedom system (fig. 4.2) may be assumed to behave according to a preset hysteretic model. In this investigation , the Takeda hysteretic sdof model with degrading stiffness capability is assumed [29] (fig. 4.4). This experimentally based model is believed to comply better with the real behaviour of R/C structures and hence should lead to a better accuracy than elastic perfectly plastic model.

The model (fig. 4.2a) can be described by the sdof equation of motion as

$$mu'' + cu' + R = -mx'' \qquad 4.3$$

where m, c and R are the mass, damping and resistance respectively. u'' and u' are the derivatives of the displacement u. Note that the resistance R is equal to the product ku in the elastic range, k being the nominal stiffness and is represented by the slope of the elastic range of the load-deformation hysteretic model (fig. 4.4). In the case of a damped free vibration, one can define the critical damping [12] as:

$$c_c = 2mw \qquad 4.4$$

in which w is the circular frequency and is given by [12]

$$w = (k/m)^{\frac{1}{2}} \qquad 4.5$$

The natural frequency can be determined as

$$f = w/2\pi \qquad 4.6$$

and the period T as

$$T = 1/f = 2\pi/w = 2\pi(m/k)^{\frac{1}{2}} \qquad 4.7$$

It is useful to define the damping ratio z as the ratio between damping c and its critical value c_c, i.e.,

$$z = c/c_c = c/2mw = cT/4\pi m \qquad 4.8$$

The equation of motion (4.3) may be solved using any available method. In this dissertion the solution is carried out using the step-by-step numerical integration because of the nature of the exciting force (mx''). In order to obtain an acceleration spectrum for a specified ground motion x'', one needs to solve equation (4.3) as many times as the number of fundamental periods to be considered and plot the curve relating the spectral acceleration to the fundamental periods (or natural frequencies).

The structural model described by equation 4.3 is excited by one of the chosen design ground acceleration time histories (x''(t)). The solution of equation (4.3) is carried out by numerical integration. The yield level of the structure (fig. 4.4) given by

$$u_y = \frac{R_y}{k} \qquad 4.9$$

is then varied iteratively until the specified design ductility factor is obtained. The spectral acceleration Sa is the value of the acceleration which when multiplied by the mass of the model m, yields the yield resistance force Ry, i.e.,

$$R_y = m\, S_a \qquad 4.10a$$

$$S_a = \frac{R_y}{m} \qquad 4.10b$$

The different steps involved in the development of the inelastic spectra are summarized by the following computer orientated flow chart.

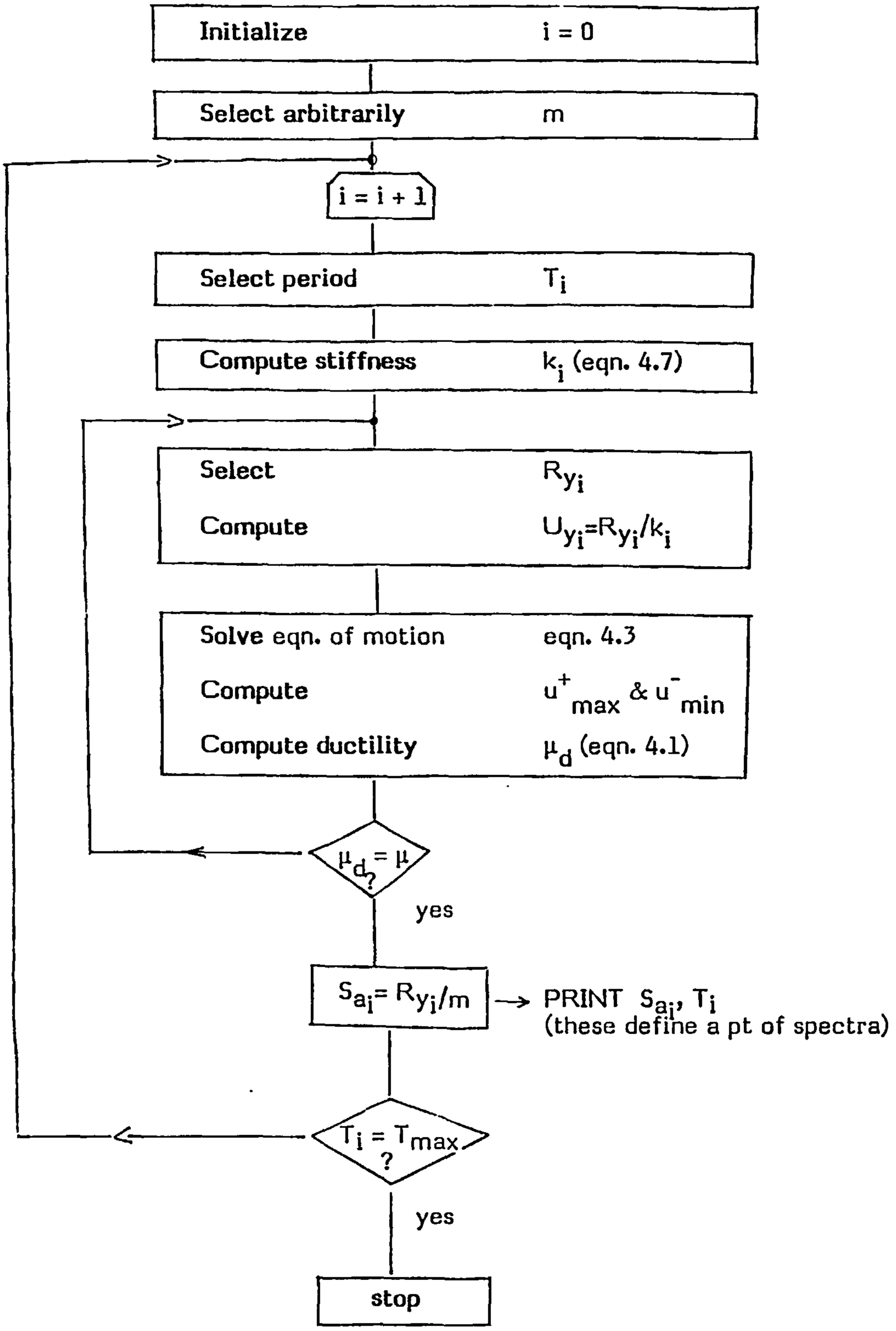
Initialize i = 0
Select arbitrarily m
i = i + 1
Select period T_i
Compute stiffness k_i (eqn. 4.7)
Select R_{y_i}
Compute $U_{y_i}=R_{y_i}/k_i$
Solve eqn. of motion eqn. 4.3
Compute u^+_{max} & u^-_{min}
Compute ductility μ_d (eqn. 4.1)
$\mu_d = \mu$?
yes
$S_{a_i}= R_{y_i}/m$
PRINT S_{a_i}, T_i
(these define a pt of spectra)
$T_i = T_{max}$?
yes
stop

The procedure is repeated for each of the records considered and for the different ductility factors. Fig. (4.6) shows the plot of the spectral acceleration versus the natural frequency for the four earthquake design records and for ductility factors of 1, 2, and 4 respectively.

iv) Average Design Spectra: Before averaging the spectra shown in fig. (4.6) and to achieve a consitent set of data for strong earthquake conditions, the records have been normalised to a standard intensity. Housner [111] proposed a measure of the intensity of ground motions. He defined the spectrum intensity as the area under a velocity response spectrum curve between periods of 0.1 and 2.5 seconds as

$$SI_p = \int_{0.1}^{2.5} S_v(p,T)\, dT$$

in which SI_p = Spectrum intensity at damping p

S_v = Velocity response spectrum

T = Period

The N/S component of 1940 El Centro earthquake, which had an approximate peak acceleration of 0.40 g, has long been considered as a typical strong motion, therefore a normalization corresponding to its intensity [111] has been chosen as a basis of the design spectra. Fig. (4.7) shows the normalized and the average design spectra.

4.4 Application of the Method to Coupled Walls

It has been years now that nonlinear methods of analysis have been used to solve structural problems and yet as far as coupled shear walls are concerned, no available systematic method exists to meet the practical need of structural engineers as concerning optimal selection of stiffness and strength of the walls and the coupling beams of coupled shear walls.

It is well accepted that energy demand by an earthquake is better contained by horizontal members if provided with appropriate and realistic ductility. This is because of different reasons, the most important being:

1) Stability problem if major yielding in vertical supporting members.

2) Beams (flexible) develop more ductility than walls (rigid and hence brittle).

3) Horizontal members generally easier to repair.

This trend of philosophy is even encouraged by most codes of practice [71, 77] by giving none or very little credit of any kind of ductility to shear walls.

Recently however, it has been shown by Paulay and Santhakumar [110], Bertero [52], Fintel and Ghosh [78, 79] and others [47, 80, 81] that, in fact, shear walls if well designed may develop substantial ductility. More experimental work is certainly needed for this to be fully accepted and made part of the code recommendations by lifting the severe burden on shear wall systems.

Recognising that shear walls can develop ductile behaviour, it is attempted in the following sections to describe a practical method of design of coupled shear walls. First free vibration analysis is carried out and results discussed. This is followed by the inelastic spectrum analysis and its direct application to the design of coupled shear walls.

4.4.1 Evaluation of Natural Frequencies and Mode Shapes: The evaluation of natural frequencies and mode shapes is a standard eigenvalue problem. They are derived from the solution of the equation:

$$(K - w_n^2 M) \phi_n = 0 \qquad 4.11$$

where K = stiffness matrix of the structure

M = structural mass matrix

w_n = circular frequency at mode n

ϕ_n = n^{th} modal shape vector

In this dissertation the bissection method [83] is used to solve equation 4.11. The stiffness matrix K is assembled using the direct method and the element stiffnes matrix was developed in chapter three.

As can be seen from equation 4.11 the natural frequency depends not only on the stiffness of the structure but also on its storey mass. In view of the substantial influence of the variation of storey mass upon the natural frequency (fig. 4.10) and hence storey drift, it has been decided to consider in addition to selfweight two typical extra storey masses namely 4 kips and 8 kips respectively. This is believed to cover a wide range of practical possibilities.

The first three natural frequencies where computed for a wide range of coupled shear walls ranging from 100ft to 400ft high (their general properties are shown in fig. (4.8)) and for 3 mass cases:

1) Selfweight only
2) Selfweight + extra storey mass = 4 kips
3) Selfweight + extra storey mass = 8 kips

These will be used later along with their related mode shapes for the modal response analysis. For convenience only the first natural frequencies are shown in fig. (4.9a), (4.9b), (4.9c), and (4.9d) for 100, 200, 300, and 400ft high structures respectively.

4.4.2 Discussion: At this point it may be worth noting the following points:

i) Generally as it can be expected, the natural frequency increases with the wall width Dw and the coupling beam depth and decreases with increasing beam length (L beam) or overall height.

ii) Contrary to what has been discussed in i), it was found sometimes that

from two structures having the same geometric characteristics, the one having the longest coupling beam length produces higher natural frequency. This somehow suprising result finds its explanation in the point iii) discussed below.

iii) As the ratio (beam depth/storey height) reaches a certain value which varies with the height of the structure and the beam length, the natural frequency tends very rapidly towards that of the solid wall without openings having the same overall dimensions.

iv) As the wall width (Dw) reaches a certain value, the fundamental period seems to depend no more on the beam depth. This is clearly shown by fig. (4.11).

v) The storey masses have a very big influence on the natural frequency (fig. 4.10) and therefore should be taken into account. For convenience the natural frequencies of structures with extra storey masses are shown in appendix B if needed. Their approximate values can also be derived as the product of the natural frequency of the structure with no extra storey mass and coefficient c_4 or c_8 derived from table 4.1 for extra storey mass of 4 and 8 kips respectively. The variation of c_i with respect to the beam length (Lbeam) and the beam depth (Hb) were found to be negligible and only the influence of the wall depth (Dw) on c_i was considered.

4.4.3 Modal Forces, Modal Drifts and Combinations: Based upon the inelastic acceleration response spectrum, the design ductility factor and the first three natural frequencies (these are believed enough for a good approximation), the maximum member forces and displacements are computed by modal analysis.

4.4.3.1 Maximum Modal Forces and Displacements: If one defines the so called participation factor [12] for mode n as

$$L_n = \frac{\phi_n^T M}{\phi_n^T M \phi_n} \qquad 4.12$$

where M = structural mass matrix

ϕ_n = shape vector at mode n

then the maximum modal forces in the n^{th} normal mode can be computed as

$$P_{n_{max}} = S_{a_n} L_n M \phi_n \qquad 4.13$$

in which S_{a_n} is the spectral acceleration read from the inelastic design spectrum for mode n. Modal shears, modal moments....etc may be obtained from modal forces using standard procedure of structural analysis.

Defining the storey drift as the relative deflection between two consecutive stories, the storey drift indice, i.e., the storey drift over the storey height, is certainly one of the very important quantities of structural response. This is because it reflects directly the distortion induced in that storey. The maximum displacement modal response for mode n, may be expressed as:

$$U_n = L_n S_{a_n} \phi_n / \omega_n^2 \qquad 4.14$$

hence the modal drifts between level y and y-1 is given by:

$$\delta_n = U_{n,y} - U_{n,y-1} \qquad 4.15$$

or

$$\delta_n = \frac{L_n S_{a_n}}{w_n^2} (\phi_{n,y} - \phi_{n,y-1}) \qquad 4.16$$

4.4.3.2 Maximum Response - Combinations: The maximum modal forces and displacements previously described are the maximum values attained during the response in the particular mode considered. Because these maxima do not

occur at the same time there is no exact way to determine precisely the maximum response and it would be generally unduly conservative to compute the latter by simply adding the maxima together. Therefore different probability based formulae have been proposed in order to obtain a reasonable estimate of the maximum response. In this research the usual procedure of combining the modal contributions using the square root of the sum of the squares, that is root-mean-square (RMS) procedure is utilised.

The maximum force distribution is then given by:

$$F_{max} = (\Sigma P_{n_{max}})^{\frac{1}{2}} \qquad 4.17$$

and the maximum yield drift by

$$\delta_{y_{max}} = (\Sigma \delta_{n,y})^{\frac{1}{2}} \qquad 4.18$$

As previously defined, the maximum yield drift indice can be computed as

$$Dy = \frac{\delta_{y_{max}}}{h} \qquad 4.19$$

in which h is the storey height. The value of the maximum drift indice δ_{ult} is related to the maximum yield drift $\delta_{y_{max}}$ by

$$\delta_{ult} = \mu \, \delta_{y_{max}} \qquad 4.20$$

4.4.4 Procedure: The direct relation between the dynamic characteristics (modal shape and natural frequency) of the structure and its interstorey drift has been demonstrated by Derecho et al [75], Machin and Bertero [82] and Fintel [77]. For any given coupled shear wall, one can attribute a natural frequency f_1. Plots of such a relation for different geometric characteristics of coupled shear walls are shown in figure (4.9). For the same coupled shear walls and for a chosen ductility factor and design spectra, one can compute

the maximum interstorey drift. The latter is then related to the natural frequency and plotted in figures (4.13), (4.14) and (4.15).

Having chosen the maximum acceptable drift, the designer may enter the charts of figures (4.13) to (4.15) which yield the required first natural frequency, which in turn is introduced in figure (4.9) to yield the required geometric parameter in terms of the known dimensions. Furthermore, the direct relation of storey drift and the plastic rotation in the storey coupling beam provides the necessary strength in the coupling beams. This and other features are discussed in the following sections of this chapter.

4.4.5 Results and Discussion: From the results the following observations can be made:

i) The maximum lateral displacement of three 20 storey coupled shear walls having different natural frequencies have been drawn in fig. (4.12). As can be seen clearly, the maximum lateral displacement increases almost in proportion to the fundamental period.

ii) The first fundamental periods of a variety of coupled shear walls have been related to the maximum yield storey drift indice. As can be expected the storey drift indice generally decreases almost in proportion to increasing fundamental period.

iii) Using the well known statistical least square method [84], the relationships of storey drift indice-period have been fitted into approximate curves for $\mu = 1$ (fig. 4.13), $\mu = 2$ (fig. 4.14), $\mu = 4$ (fig. 4.15). These curves are to be used for design as stipulated previously. Having selected the maximum tolerable storey drift indice and hence the maximum yield storey indice, the designer enters one of the charts (figs. 4.13 - 4.15), which yield the fundamental period of the required coupled shear wall. It may be worth noting that for convenience the period is that of the structure with no extra storey

masses. The period is then used to enter one of the diagrams of fig. (4.9) which in turn, yields one of the geometric parameters required.

4.4.6 Adequacy of the Design and Coupling Beam Strength: In performing a design according to the procedure described previously, it was assumed that the coupling beams undergo inelastic deformations with acceptable practical limit. Because of its paramount importance the ductile behaviour of the beams i.e., their ability to deform plastically without loss of strength, appears to be more than necessary and must therefore be checked by providing it with appropriate strength. In this section an attempt is made to relate the maximum drift to the plastic rotation demand on coupling beams, which in turn is related to the required yield moment of the beam.

Eventhough there are several ways of expressing inelastic demands on beams [85], the plastic hinge rotation is probably the most expressive because it can be directly relatable to the moment - curvature curve (m-φ) and the geometric properties of the beam cross-section. Figure (4.16) shows a beam-wall subassemblage in its displaced position at maximum drift. The deflections are exaggerated in order to clearly illustrate the geometric relationships. From the figure:

$$\Theta max = \Theta p + \Theta y \qquad 4.21$$

in which

Θmax = maximum rotation

Θy = rotation at yield

Θp = plastic rotation.

Assuming an acceptable rotational beam ductility factor μ_b, one may compute Θy as:

$$\Theta y = \frac{\theta_{max}}{\mu b} \qquad 4.22$$

For a plastic hinge length lp, i.e., the equivalent spread of plasticity [86], one may compute the yield curvature φ_y as:

$$\varphi_y = \frac{\theta_y}{lp} \qquad 4.23$$

The plastic hinge spread lp has been given empirically by Paulay [86] as:

$$lp = 0.5d + 0.05s \qquad 4.24$$

in which d is the effective depth of the section and s is the distance from the critical section to the inflection point.

Assuming a linear distribution of strain (fig. 4.17b) and if the yield steel strain ϵy and the effective depth of the cross section d are known, then the neutral axis depth K_{ud}, and hence ϵc and ϵ's can be computed. The equilibrium equation of the resultant forces (fig. 4.17c), i.e.,

$$Ts = Cc + Cs \qquad 4.25$$

yields the compressive and tensile steel sections A's and As respectively and hence the yield moment My required. (see design example appendix A).

4.5 Conclusion

A design tool has been presented for coupled shear wall systems built in zones where there is a high risk of strong earthquakes occuring. To illustrate the method a design example is carried out in appendix A. The importance of the structure can be taken into consideration through design ductility factor. The charts do not cover absolutely all the possible geometric characteristics, however interpolations can be made, bearing in mind what follows:

i) For coupled shear wall structures having the same total height (Ht) and the same beam length and depth (Lbeam, Hb), the fundamental period is almost inversely proportional to the wall depth (Dw) as shown by figure (4.11).

ii) For coupled shear wall structures having the same wall depth (Dw) and the same beam length and depth (Lbeam,Hb), the fundamental period can be assumed proportional to the square of the total height of the structure (Ht).

iii) The natural frequency of a structure having extra storey mass can be derived from fig. (4.9) struck by a factor c given in table 4.1 as explained in section 4.4.2.

iv) The yield drift is almost in proportion to the fundamental period. The error committed by assuming such a proportionality increases with increasing design ductility factor.

TABLE 4.1 COEFFICIENT c_4 and c_8 FOR MASS = 4 KIPS AND MASS = 8 KIPS RESPECTIVELY

	10 storey		20 storey		30 storey		40storey	
Dw	c_4	c_8	c_4	c_8	c_4	c_8	c_4	c_8
12	2.26	3.00	2.18	2.91	2.13	2.86	2.70	3.25
15	2.06	2.75	2.00	2.64	1.98	2.62	2.48	3.00
18	1.92	2.53	1.88	2.47	1.86	2.43	2.31	2.75
21	1.82	2.40	1.78	2.31	1.76	2.28	2.16	2.58

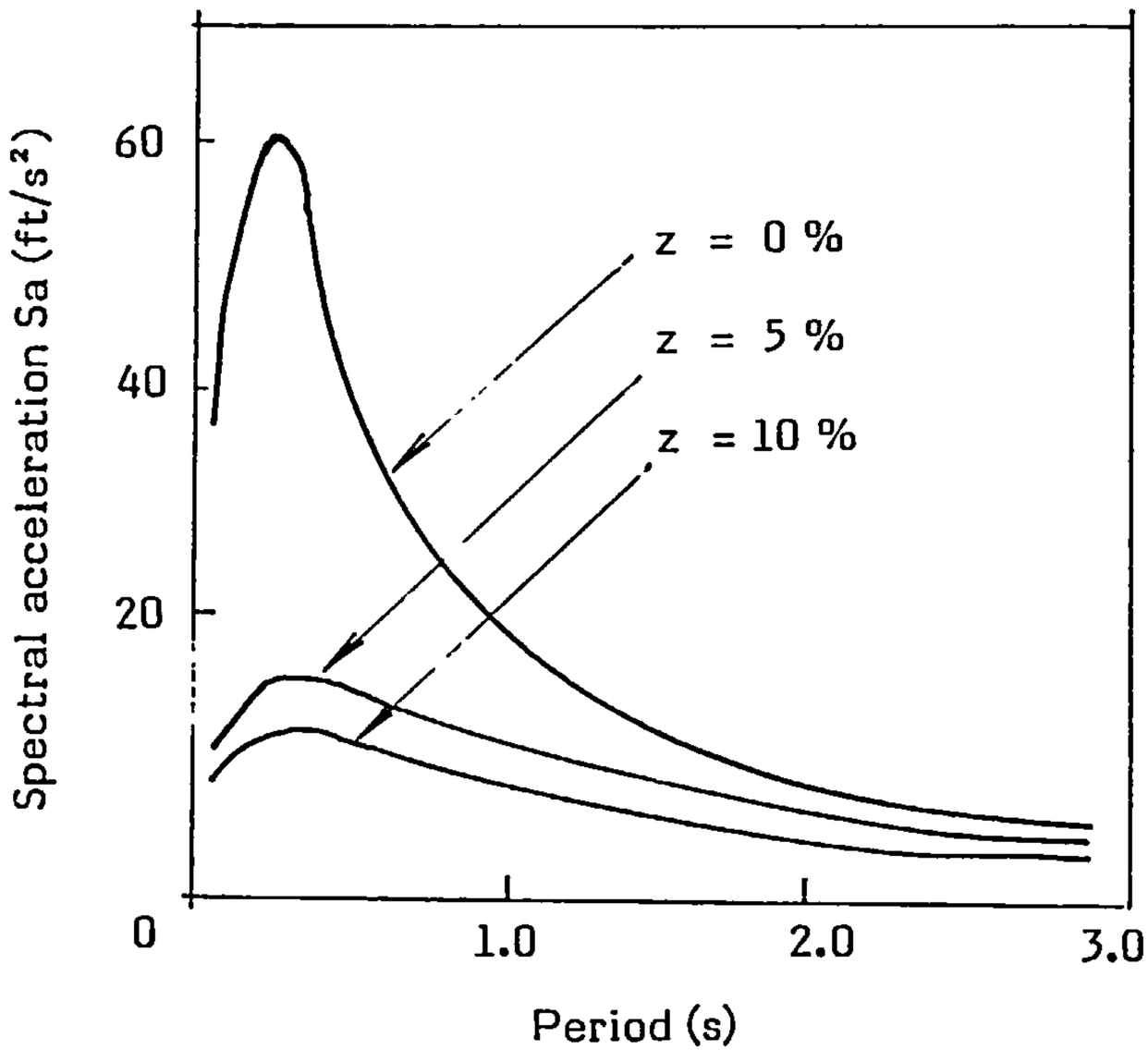

FIG. 4.1 TYPICAL ACCELERATION SPECTRUM FOR VARIOUS DAMPING RATIOS

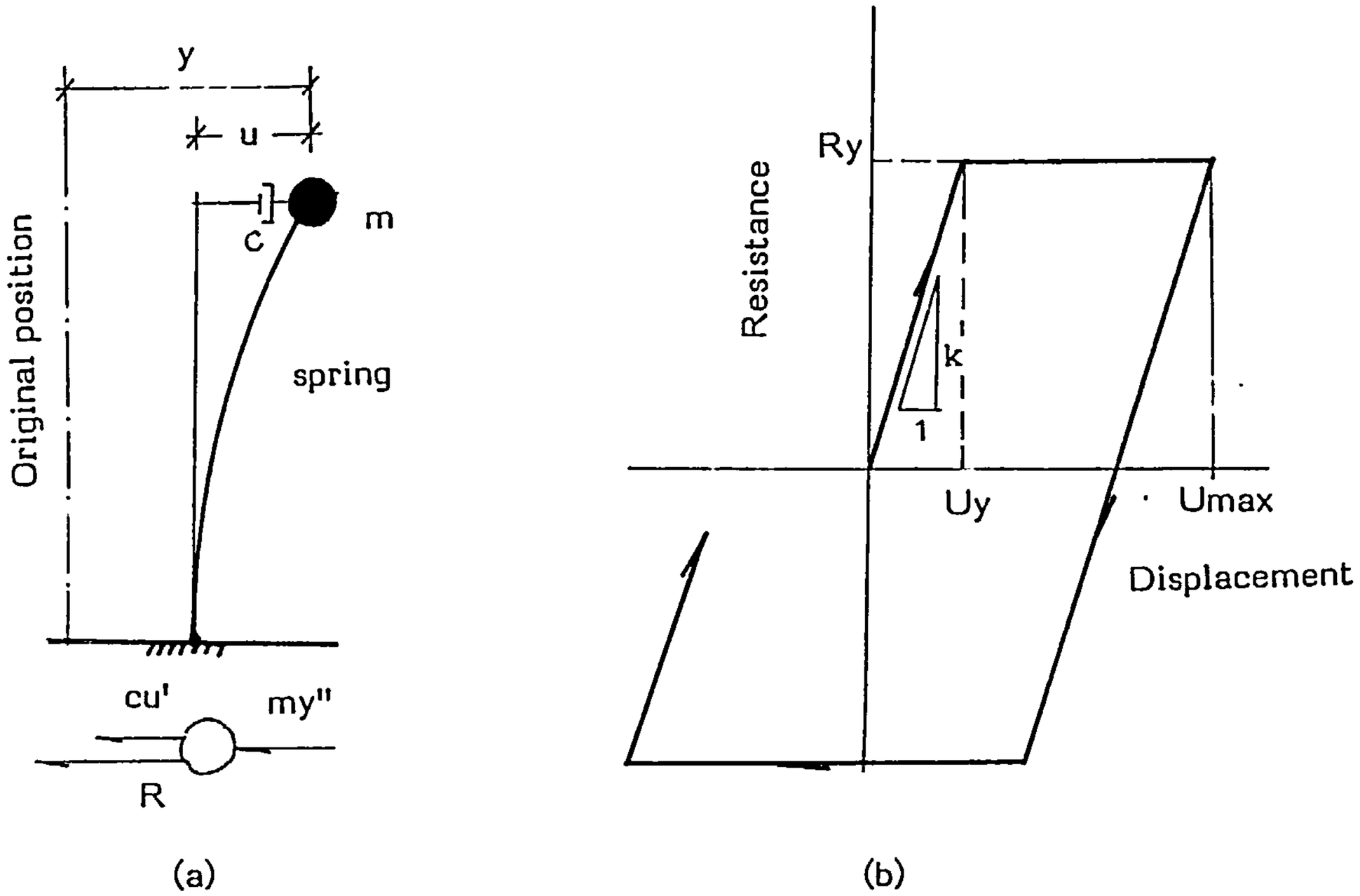

FIG. 4.2 a) SDOF SYSTEM SUBJECTED TO GROUND MOTION

b) LOAD-DEFORMATION RELATIONSHIP FOR THE SPRING

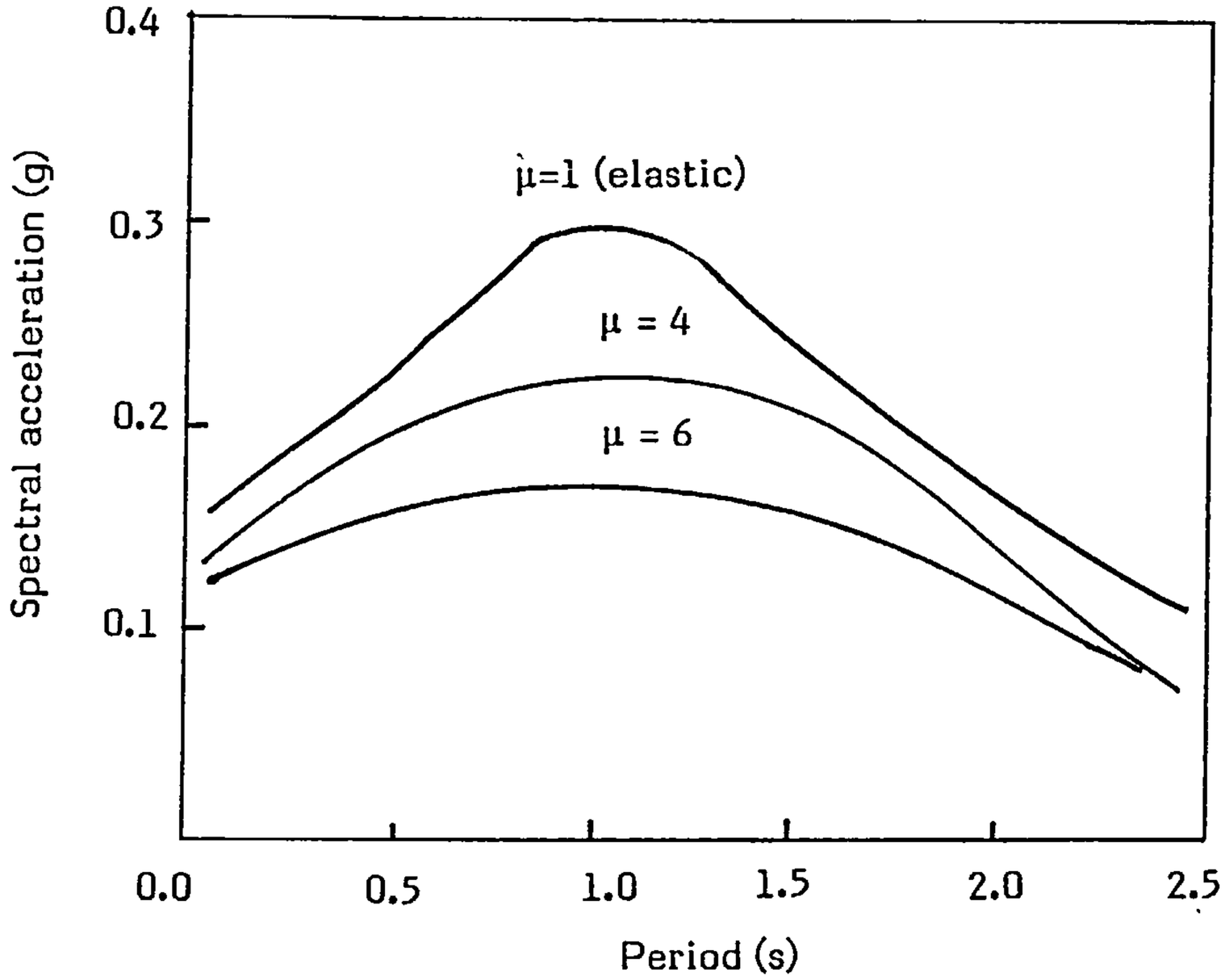

FIG. 4.3 ELASTIC AND INELASTIC SPECTRA FOR VARIOUS DUCTILITY FACTORS

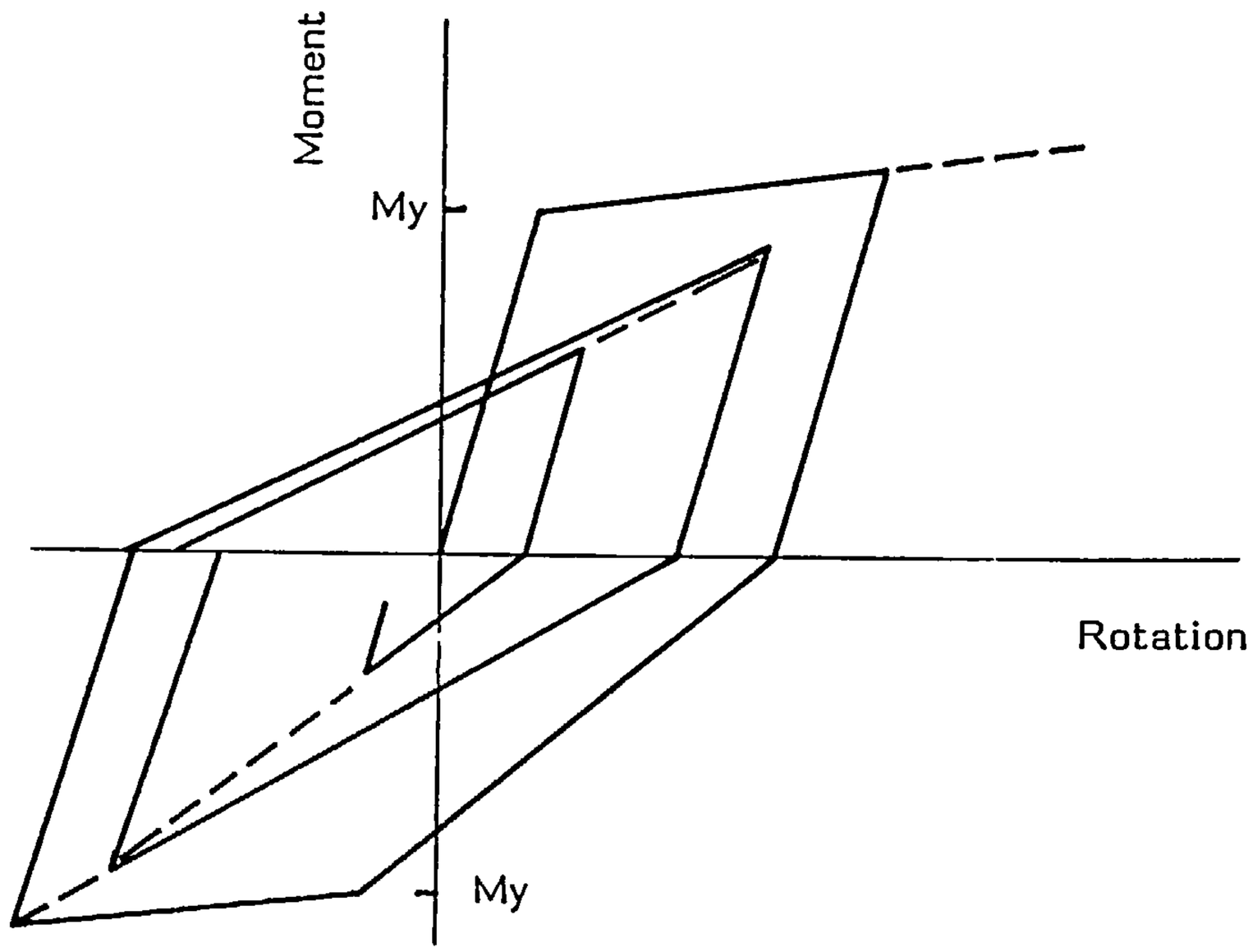

FIG. 4.4 HINGE MOMENT-ROTATION RELATIONSHIP FOR TAKEDA MODEL

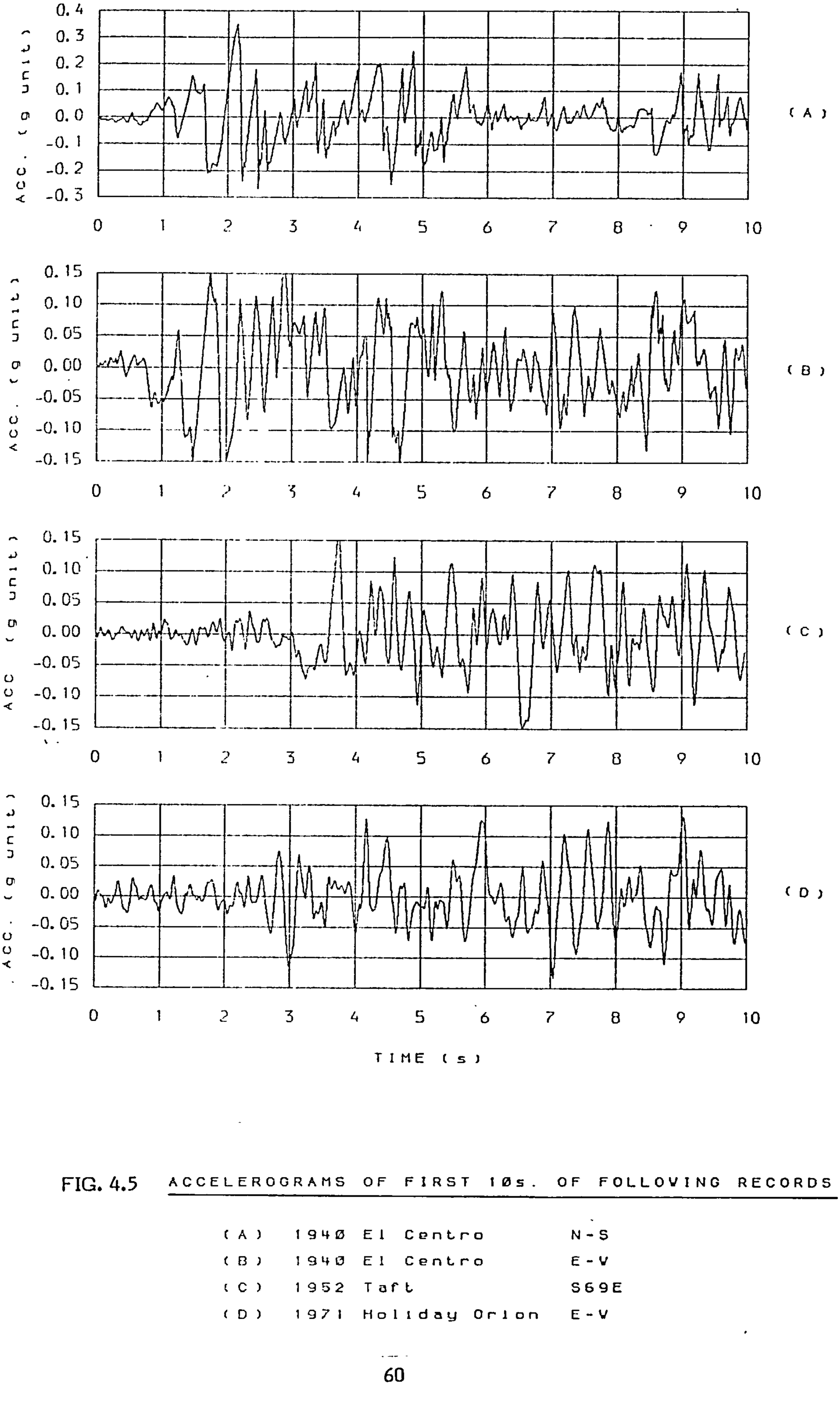

FIG. 4.5 ACCELEROGRAMS OF FIRST 10s. OF FOLLOVING RECORDS

(A)	1940	El Centro	N-S
(B)	1940	El Centro	E-V
(C)	1952	Taft	S69E
(D)	1971	Holiday Orion	E-V

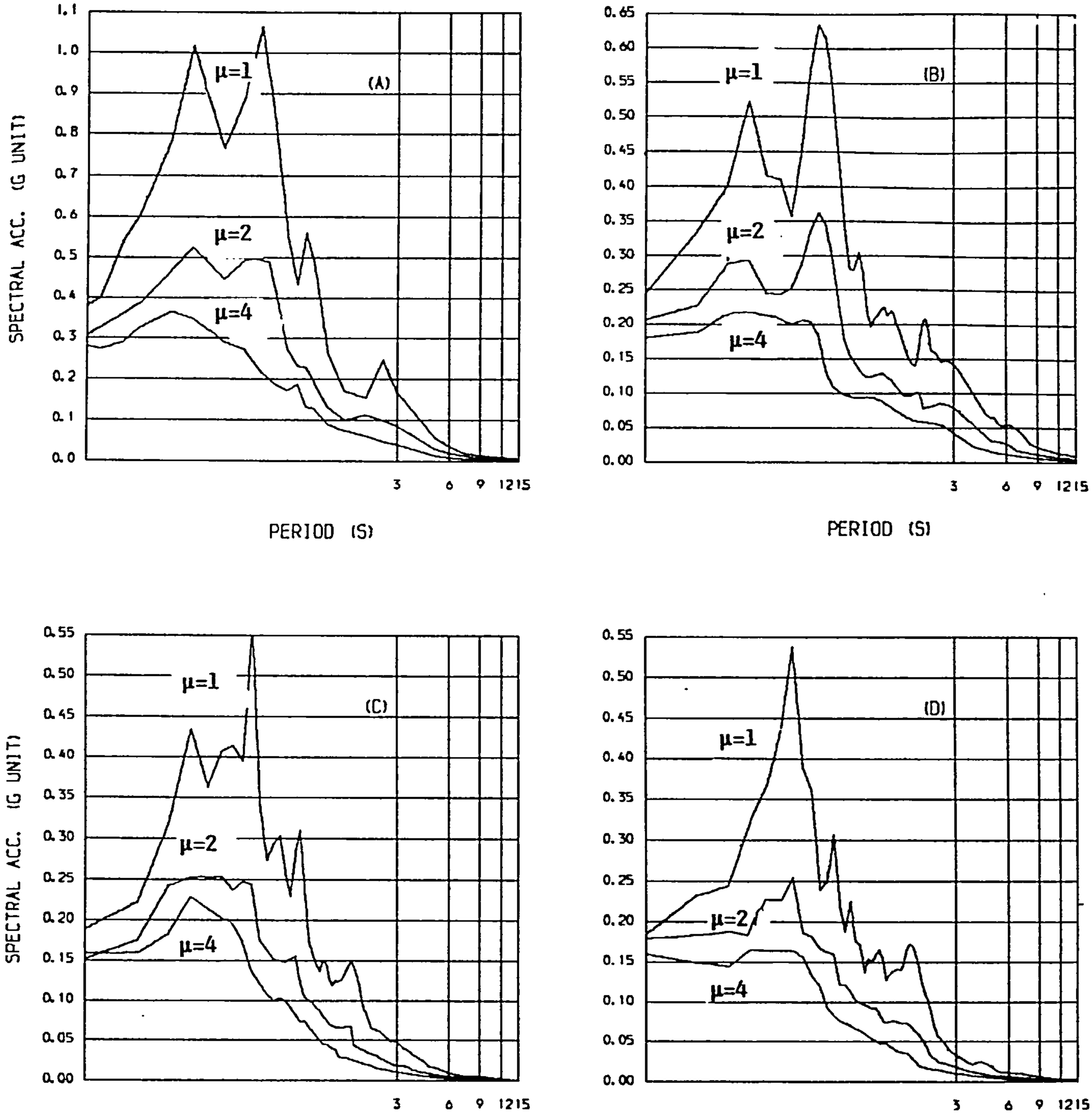

FIG. 4.6 ELASTIC AND INELASTIC SPECTRAS OF FOLLOVING RECORDS

(A)	1940 El Centro	N-S
(B)	1940 El Centro	E-V
(C)	1952 Taft	S69E
(D)	1971 Holliday Orion	E-V

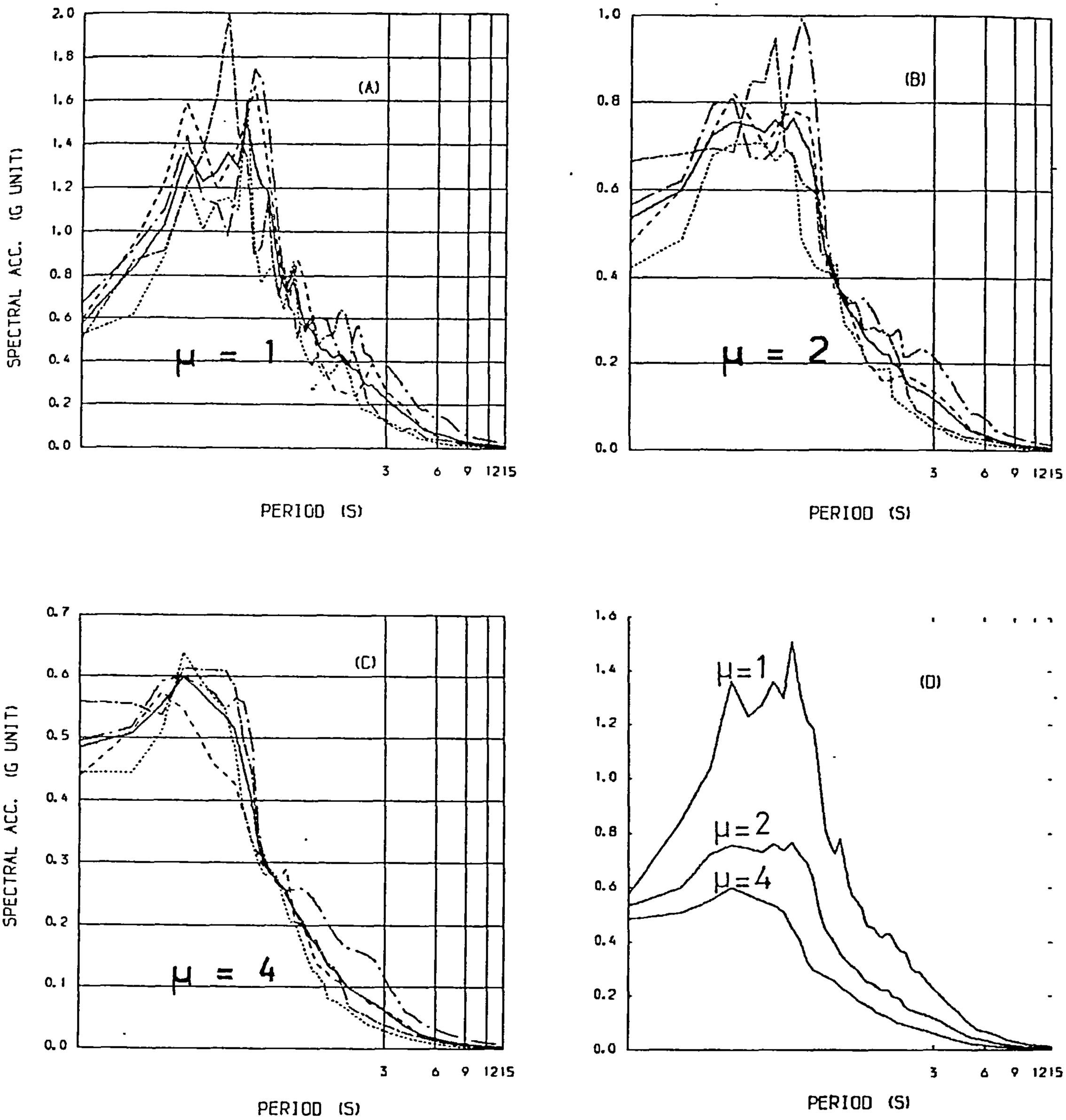

FIG. 4.7

DERIVATION OF DESIGN SPECTRA
FOR NORMALIZED 0.4g MAX ACC.

(A) elastic spectra	_____	1940 El Centro	N-S
(B) inelastic spectra	_._._.	1940 El Centro	E-W
(C) inelastic spectra	_ _ _ _ _	1952 Taft	S69E
(D) design spectra	_._._.	1971 Holiday Orion	E-W

FIG. 4.8 MATERIAL PROPERTIES AND GEOMETRIC CHARACTERISTICS

GEOMETRY	MATERIAL PROPERTIES	
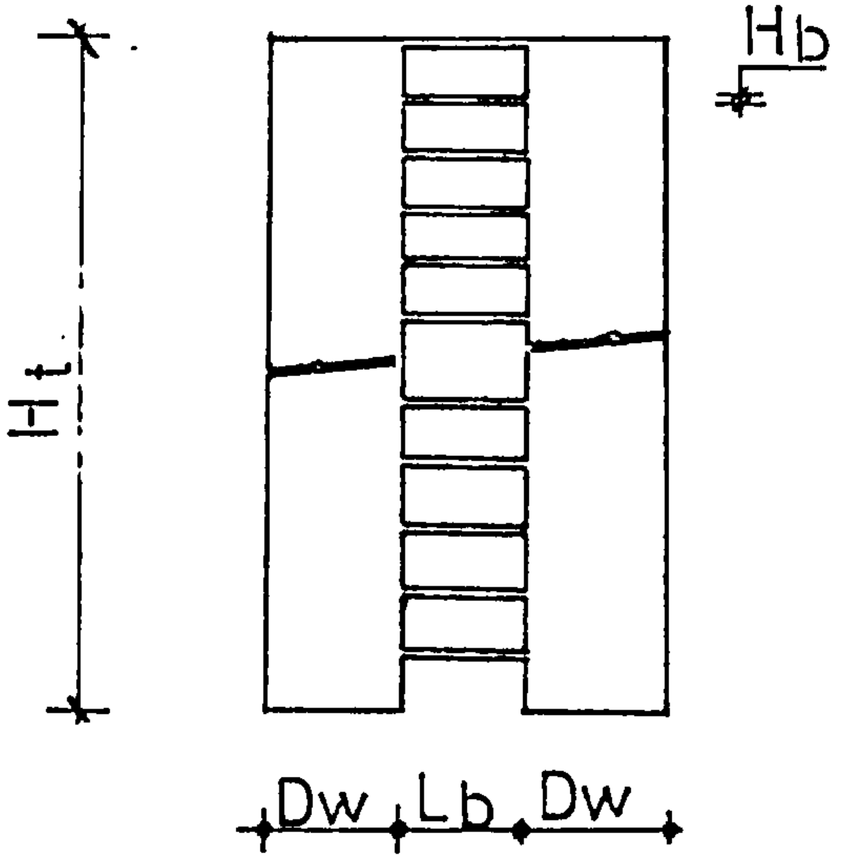	THICKNESS	t = 1.00 ft
	YOUNG'S MODULUS	$E = 464.10^3$ kip.ft^{-2}
	POISSON'S RATIO	$\mu = 0.20$
	WEIGHT DENSITY	$\rho = 0.149$ kip.ft^{-3}
	WALL DEPTH	Dw = variable
	BEAM DEPTH	Hb = variable
	TOTAL HEIGHT	Ht = variable
	BEAM LENGTH	Lbeam = variable

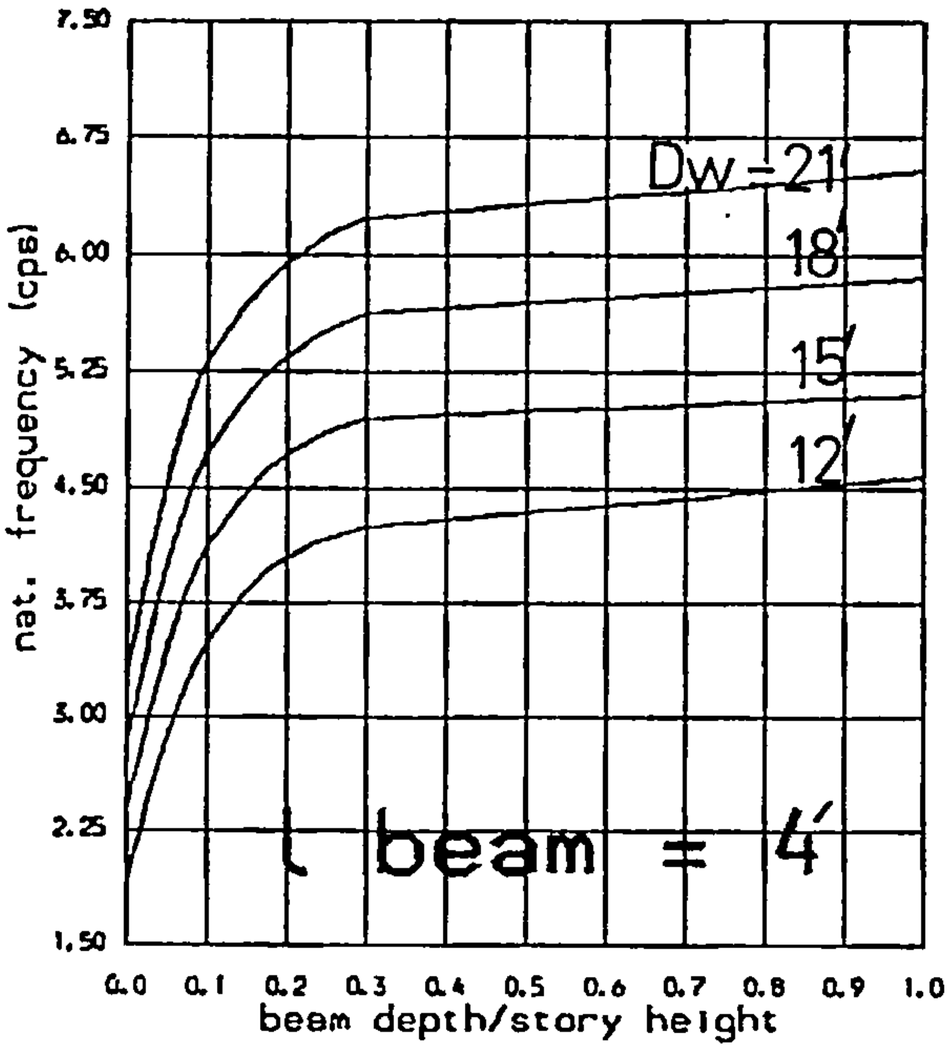

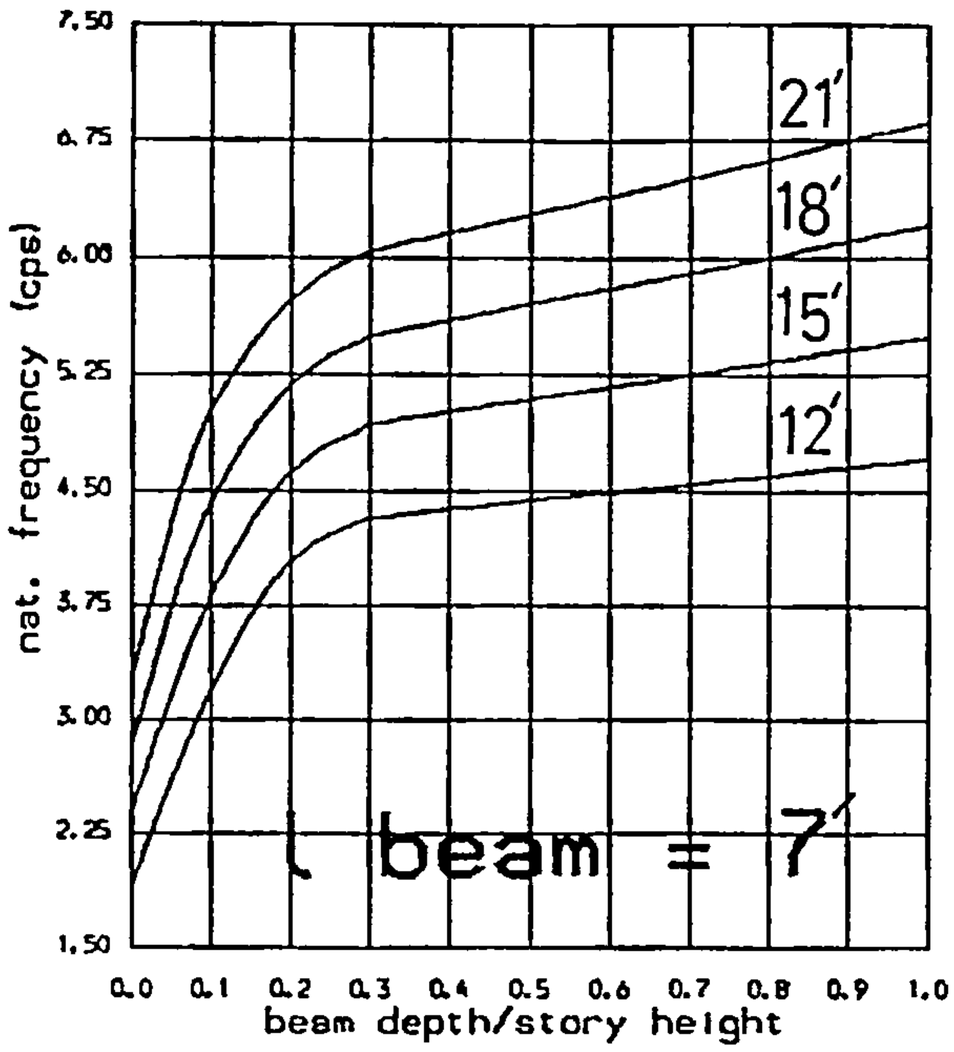

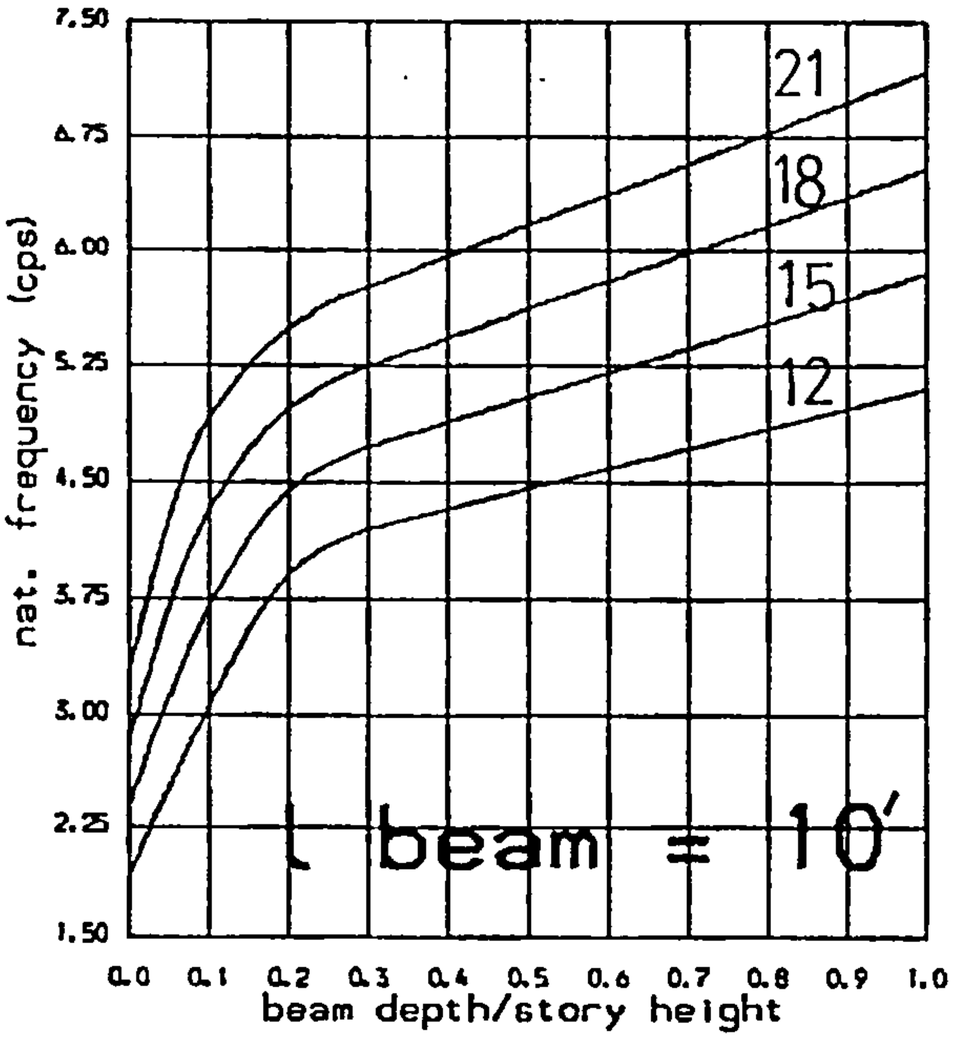

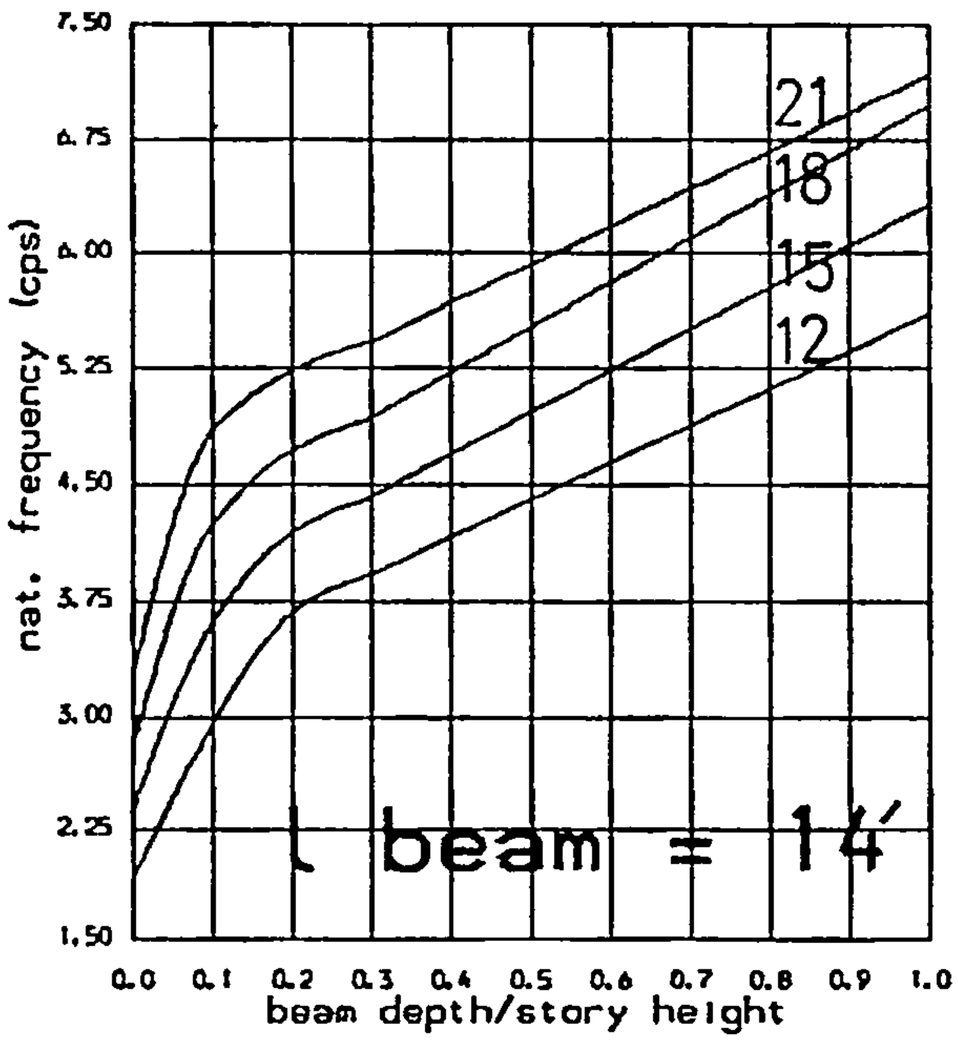

FIG. 4.9a
Variation of 1 st. natural freqency with beam depth and wall width (DV).

Total height : 100 ft
Nb of storeys : 10
Selfweight : yes
Extra story mass : none

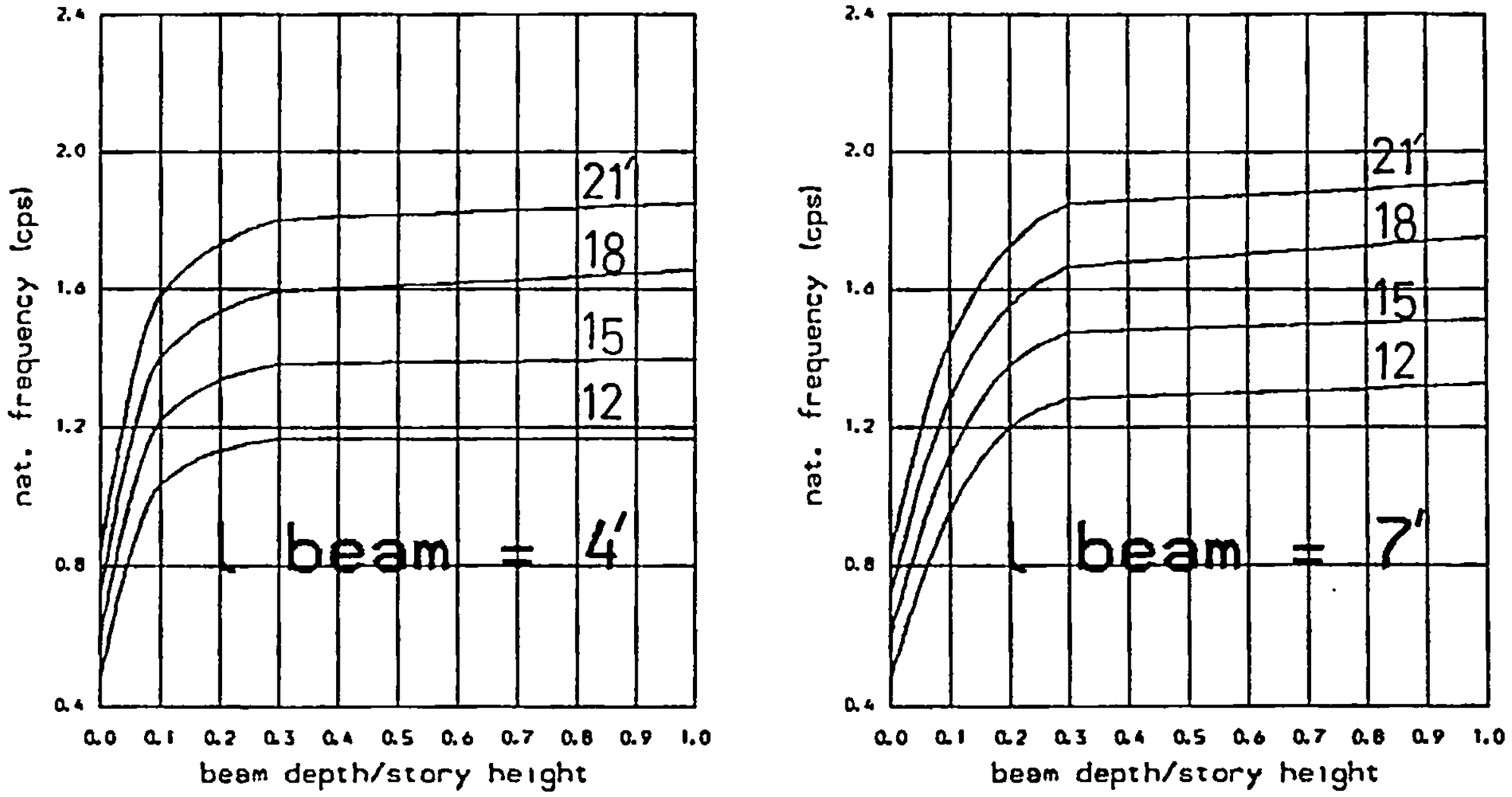

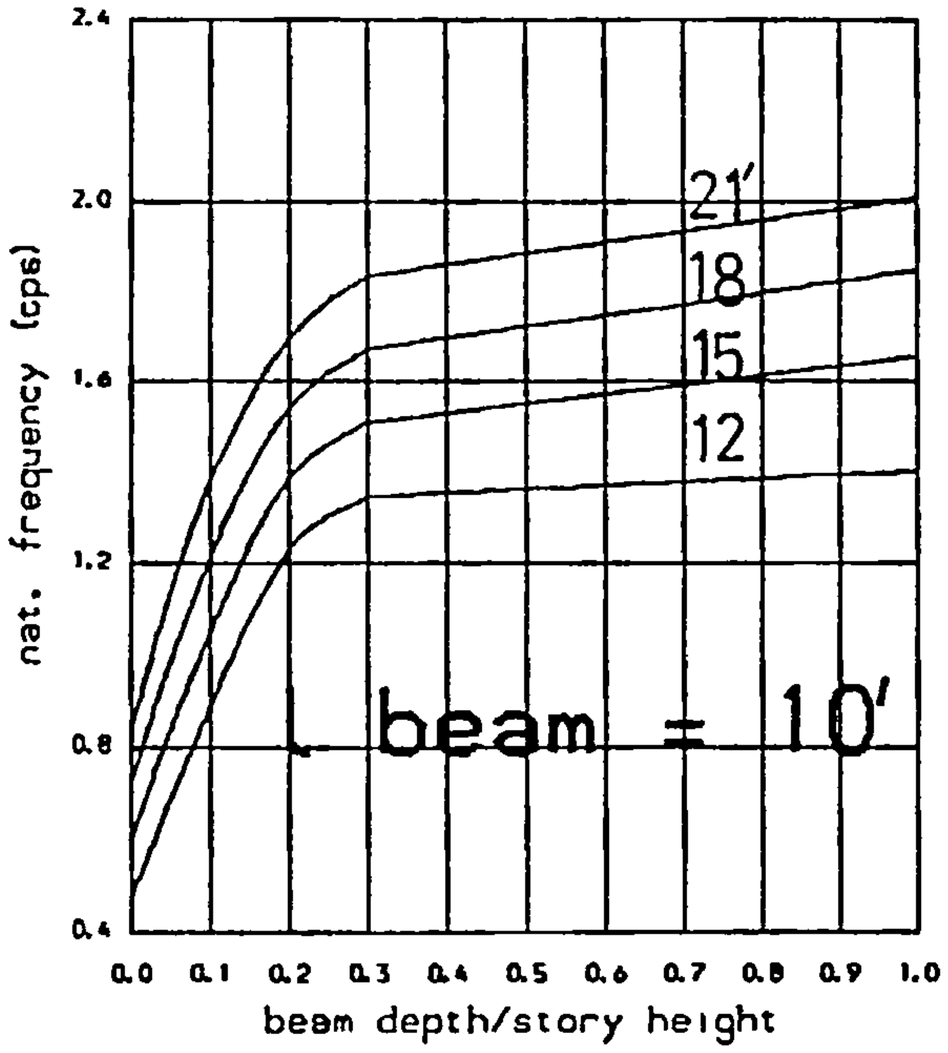

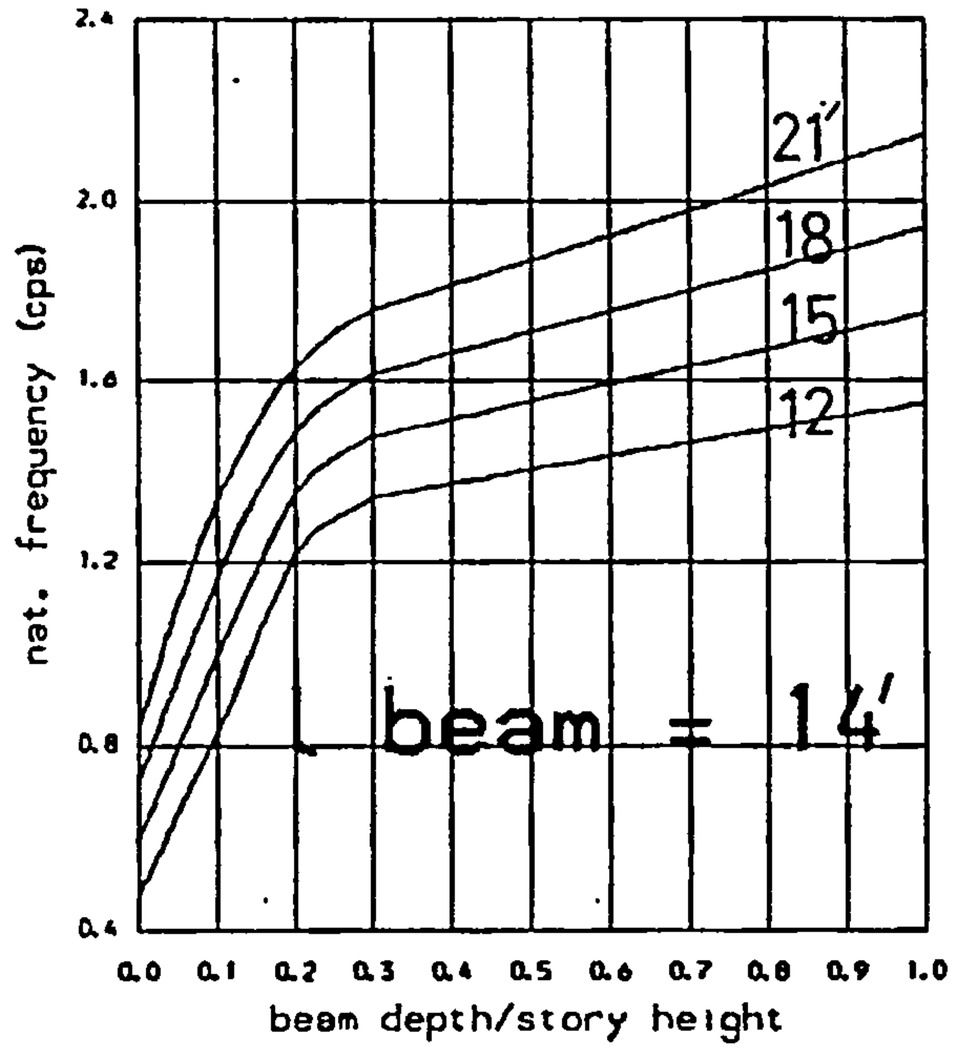

FIG. 4.9b	Total height	: 200 ft
Variation of 1 st. natural	Nb of storeys	: 20
freqency with beam depth	Selfweight	: yes
and wall width (DV) .	Extra story mass	: none

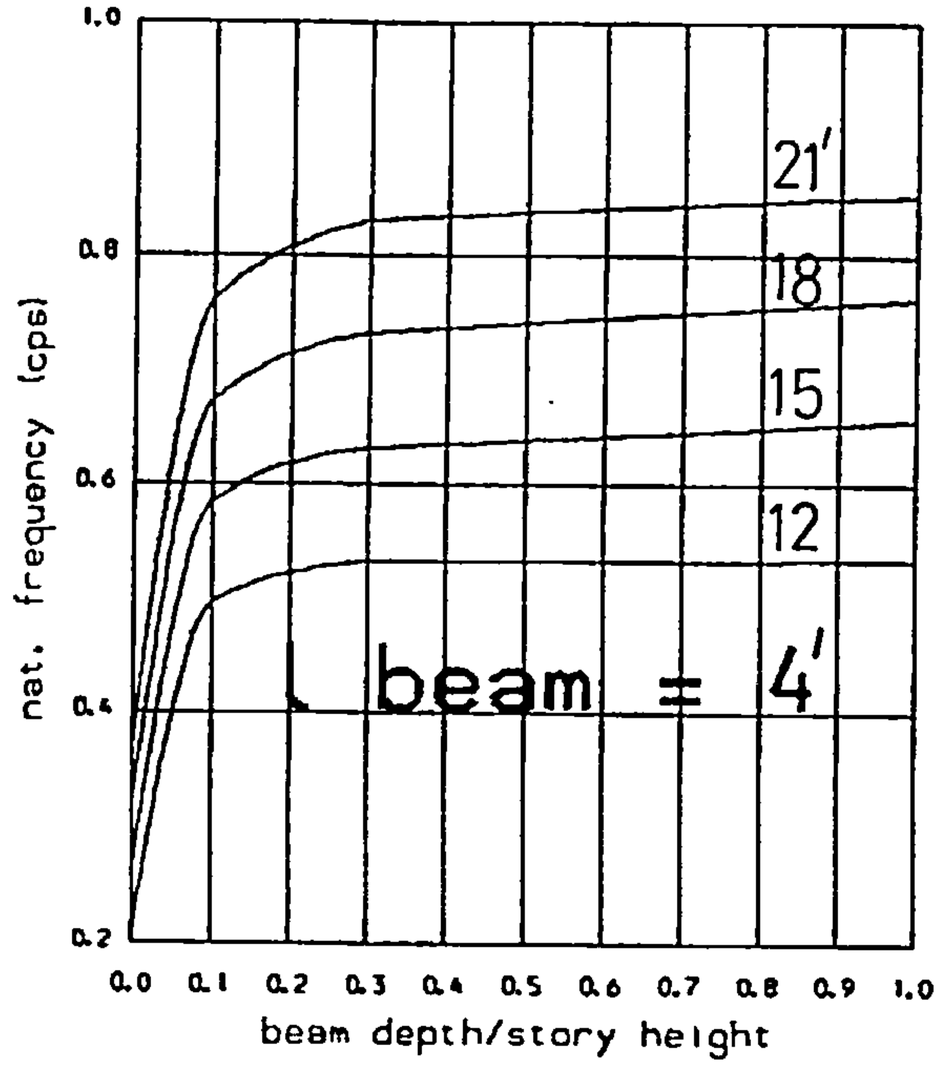

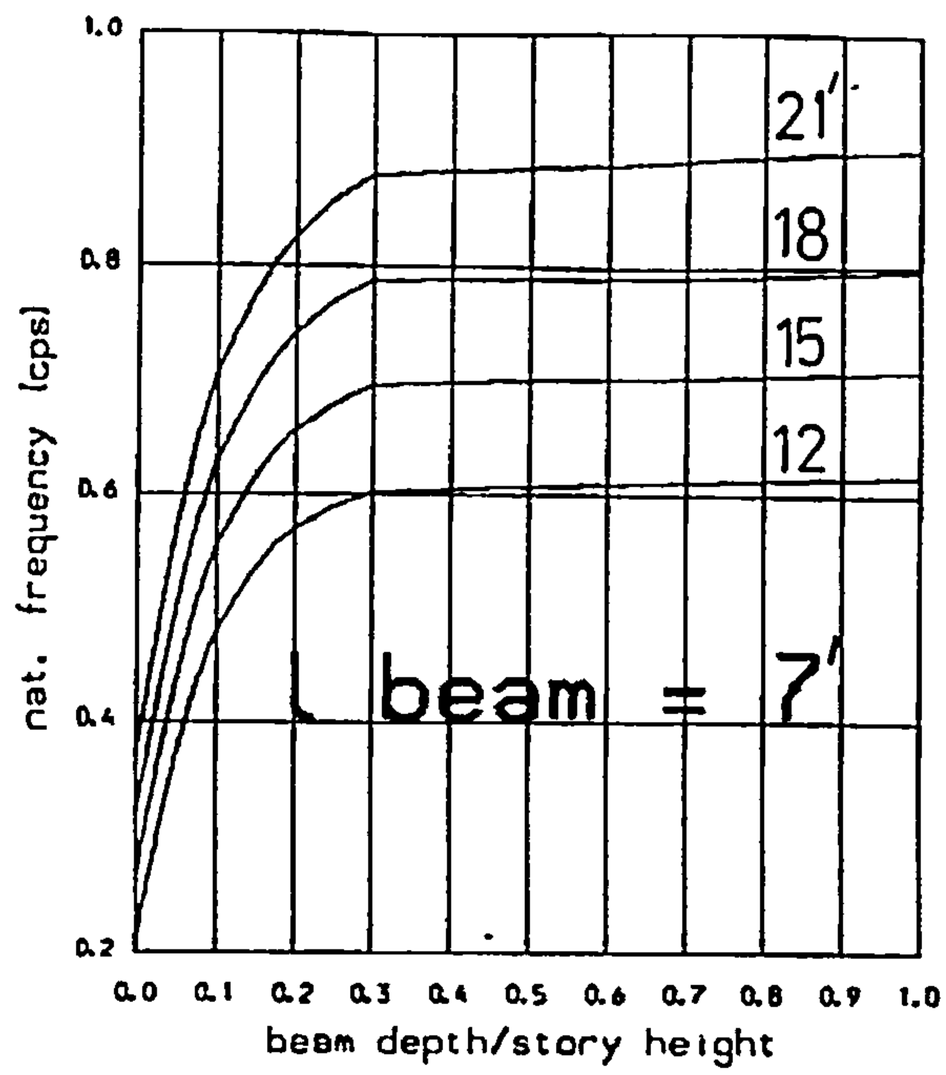

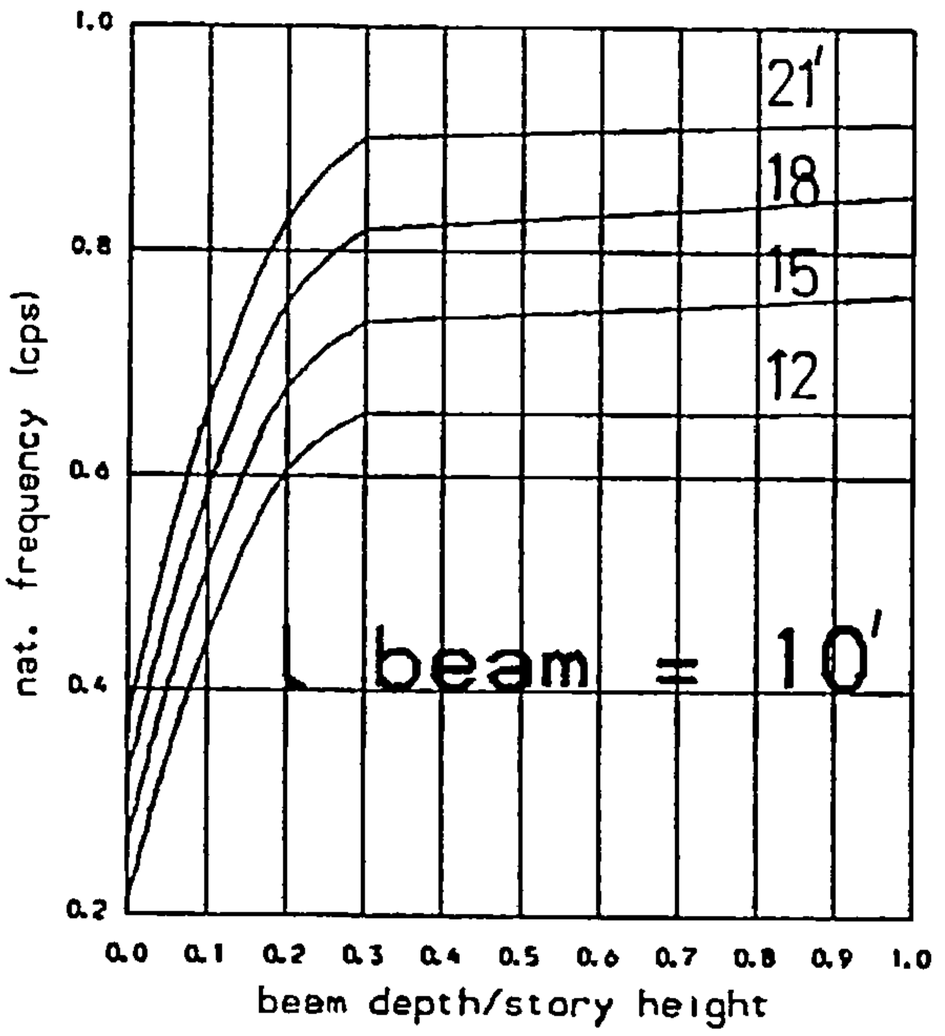

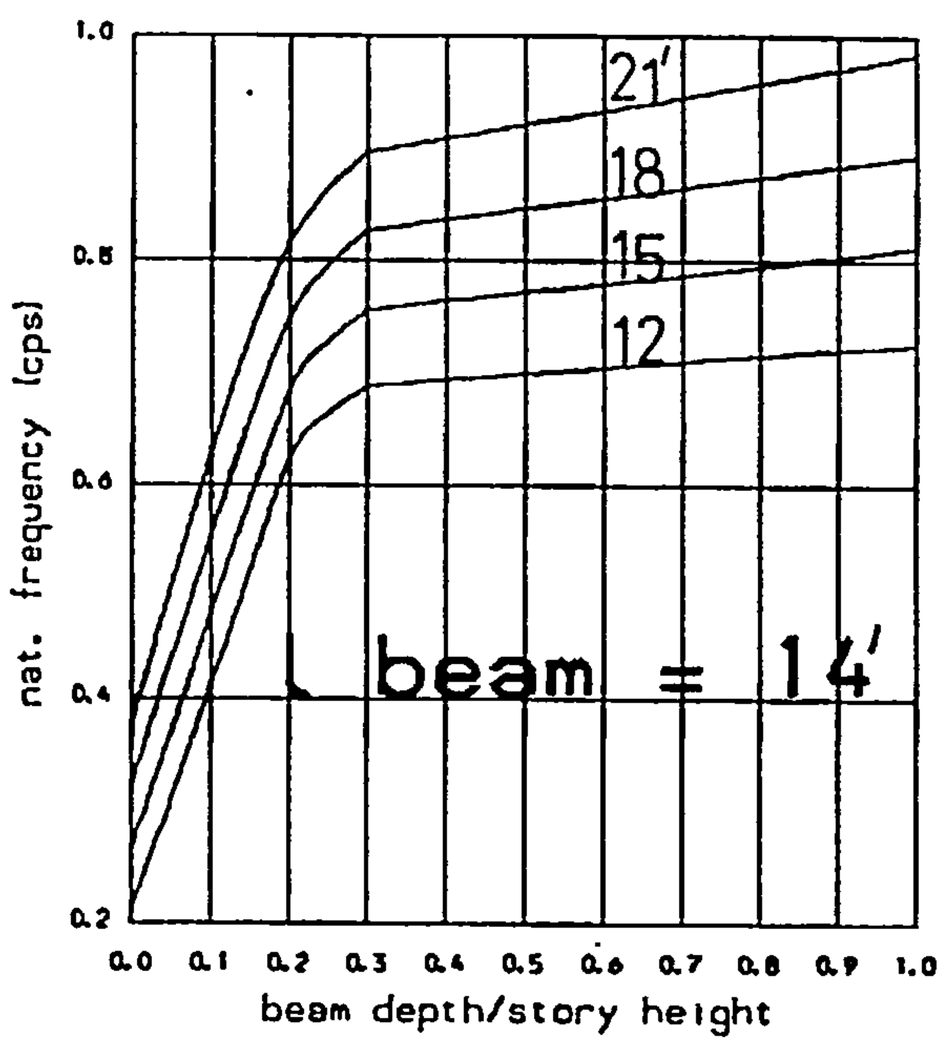

FIG. 4.9c	Total height	: 300 ft
Variation of 1 st. natural	Nb of storeys	: 30
freqency with beam depth	Selfweight	: yes
and wall width (DV) .	Extra story mass	: none

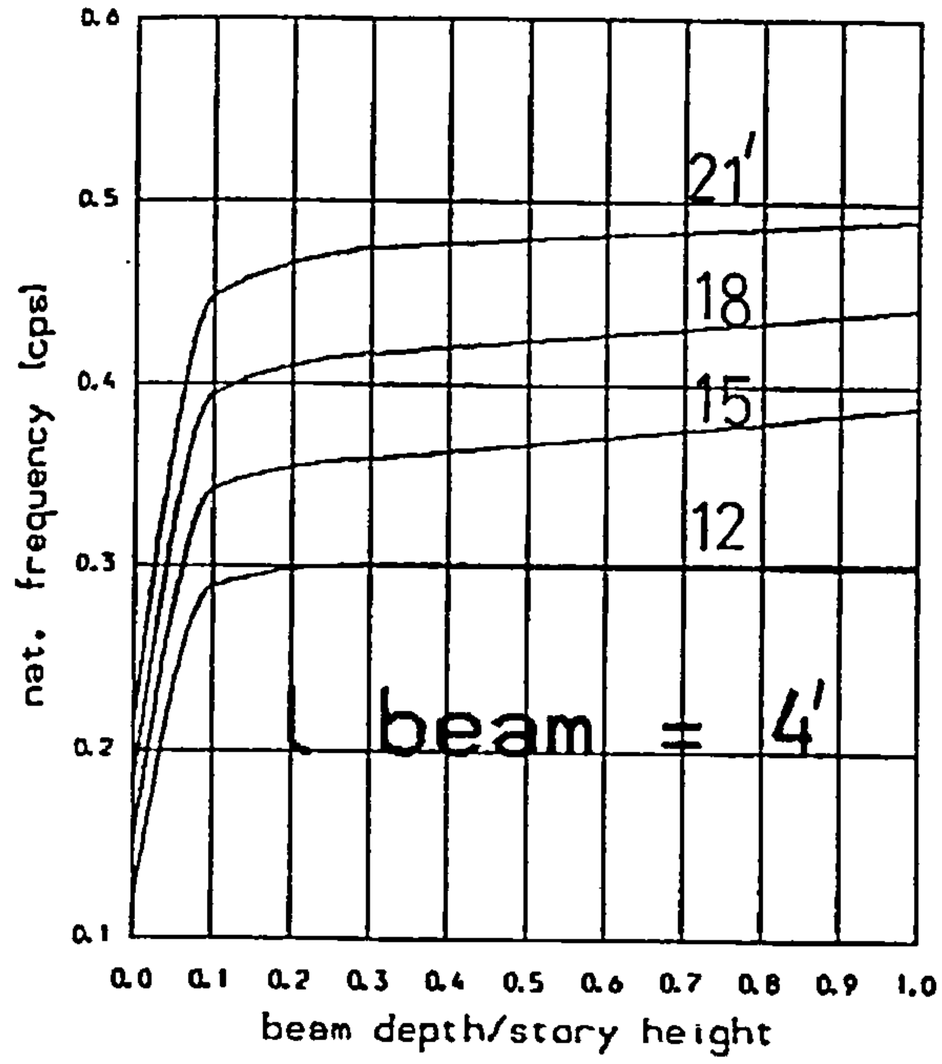

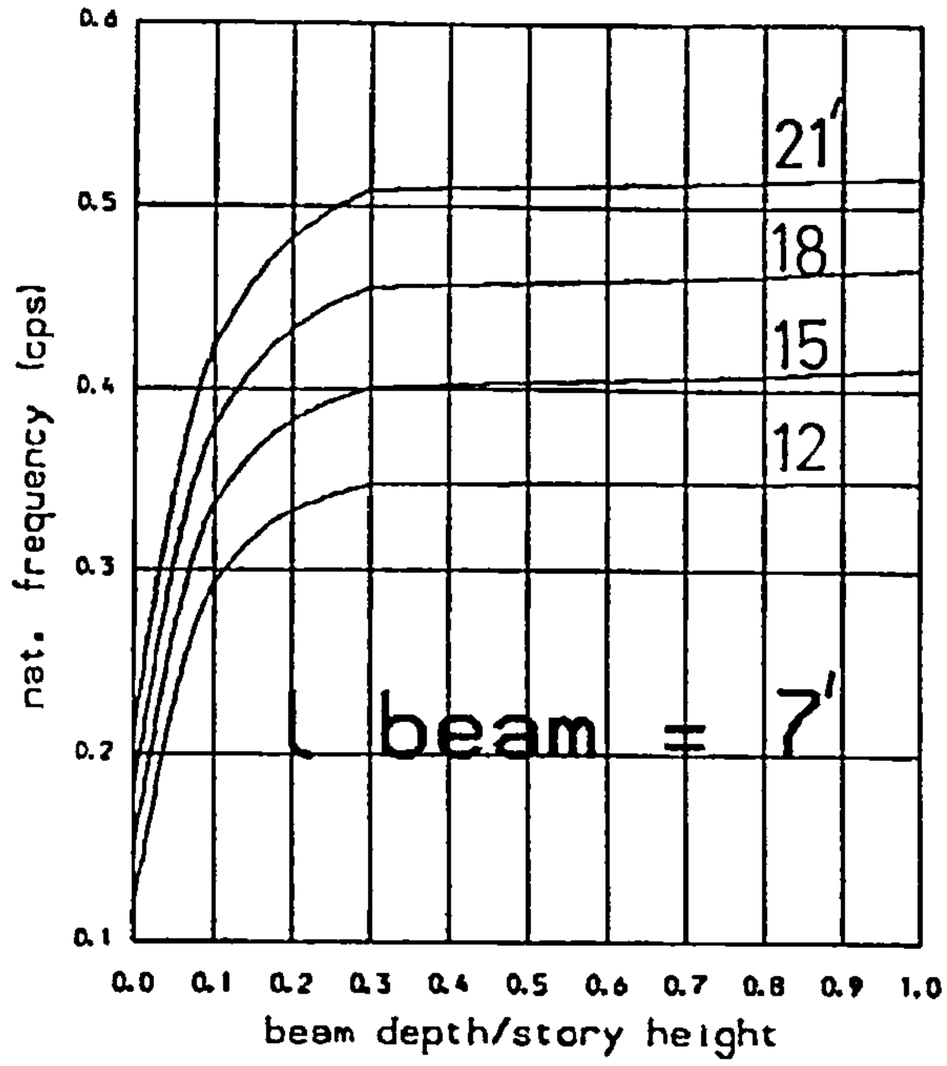

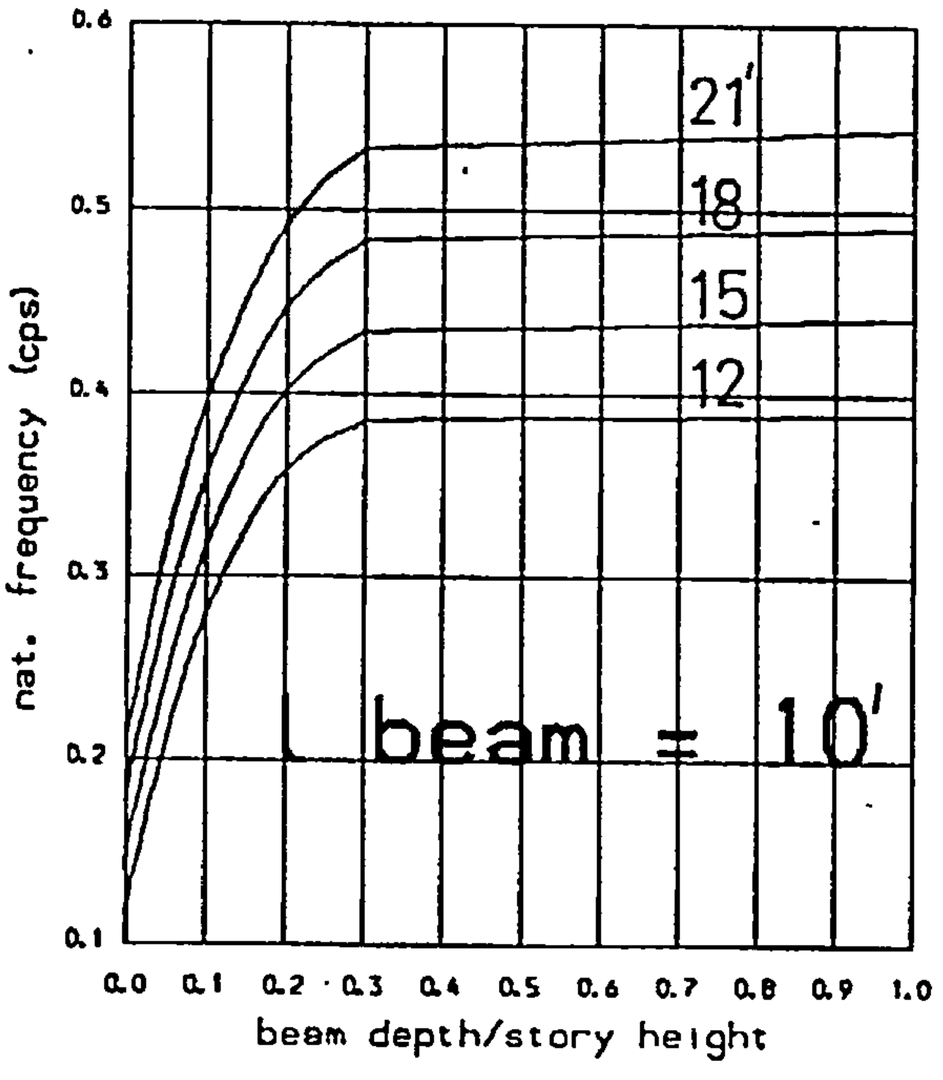

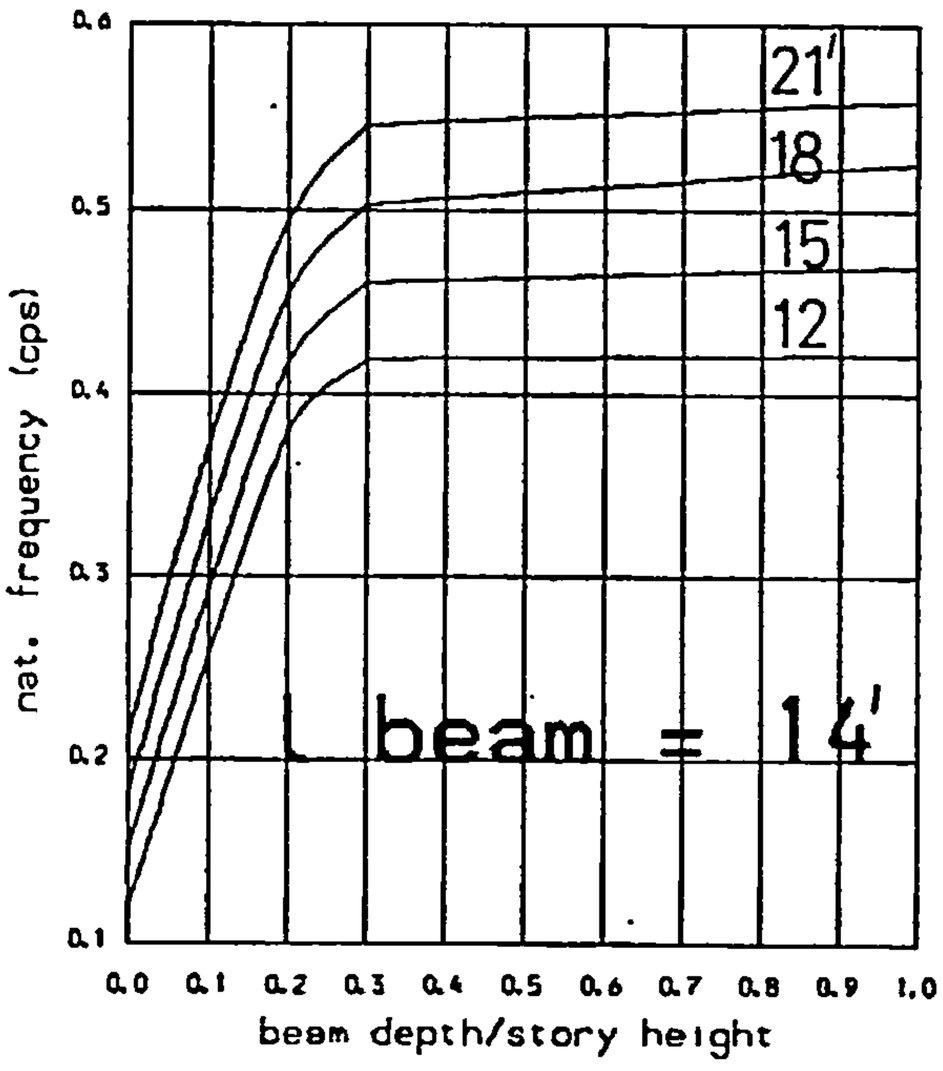

FIG. 4.9d	Total height : 400 ft
Variation of 1 st. natural	Nb of storeys : 40
freqency with beam depth	Selfweight : yes
and wall width (DV) .	Extra story mass : none

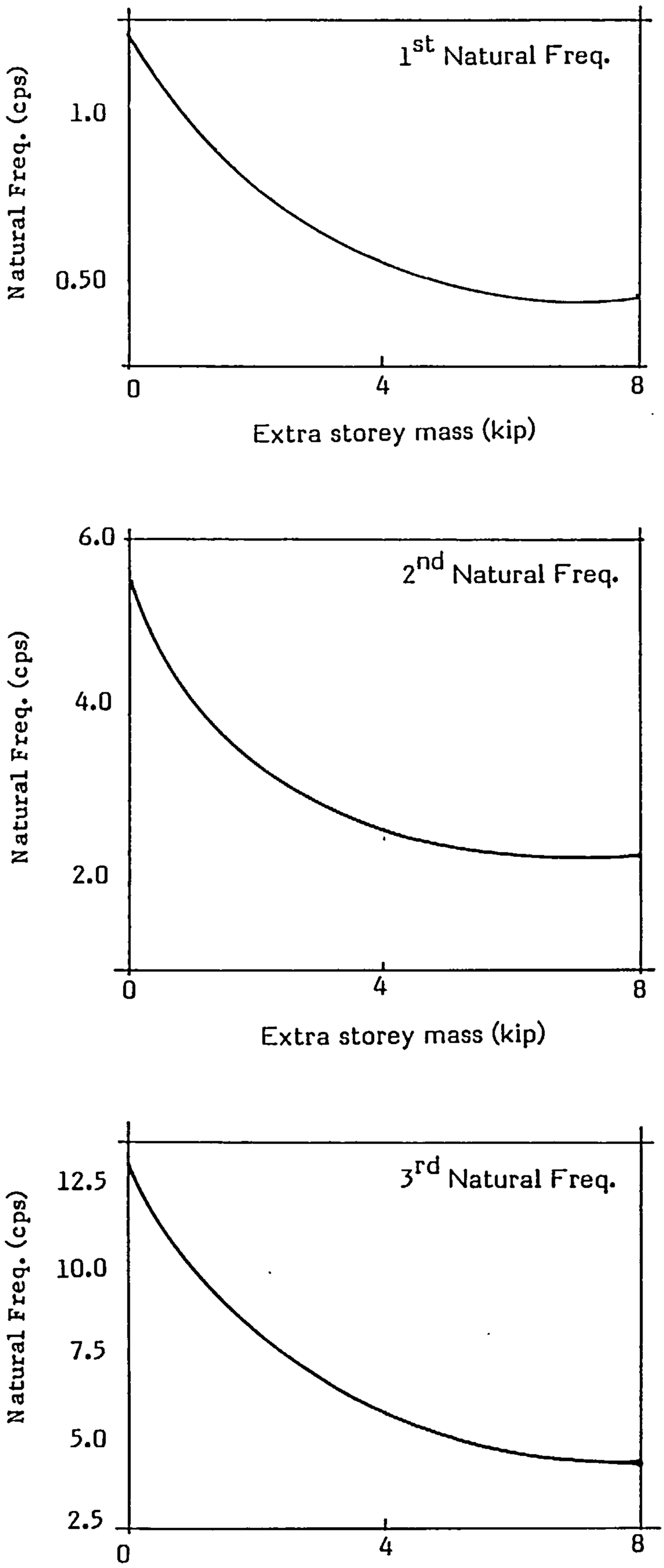

FIG. 4.10 INFLUENCE OF THE STOREY MASS ON THE NATURAL FREQUENCIES OF A 20 STOREY COUPLED SHEAR WALL

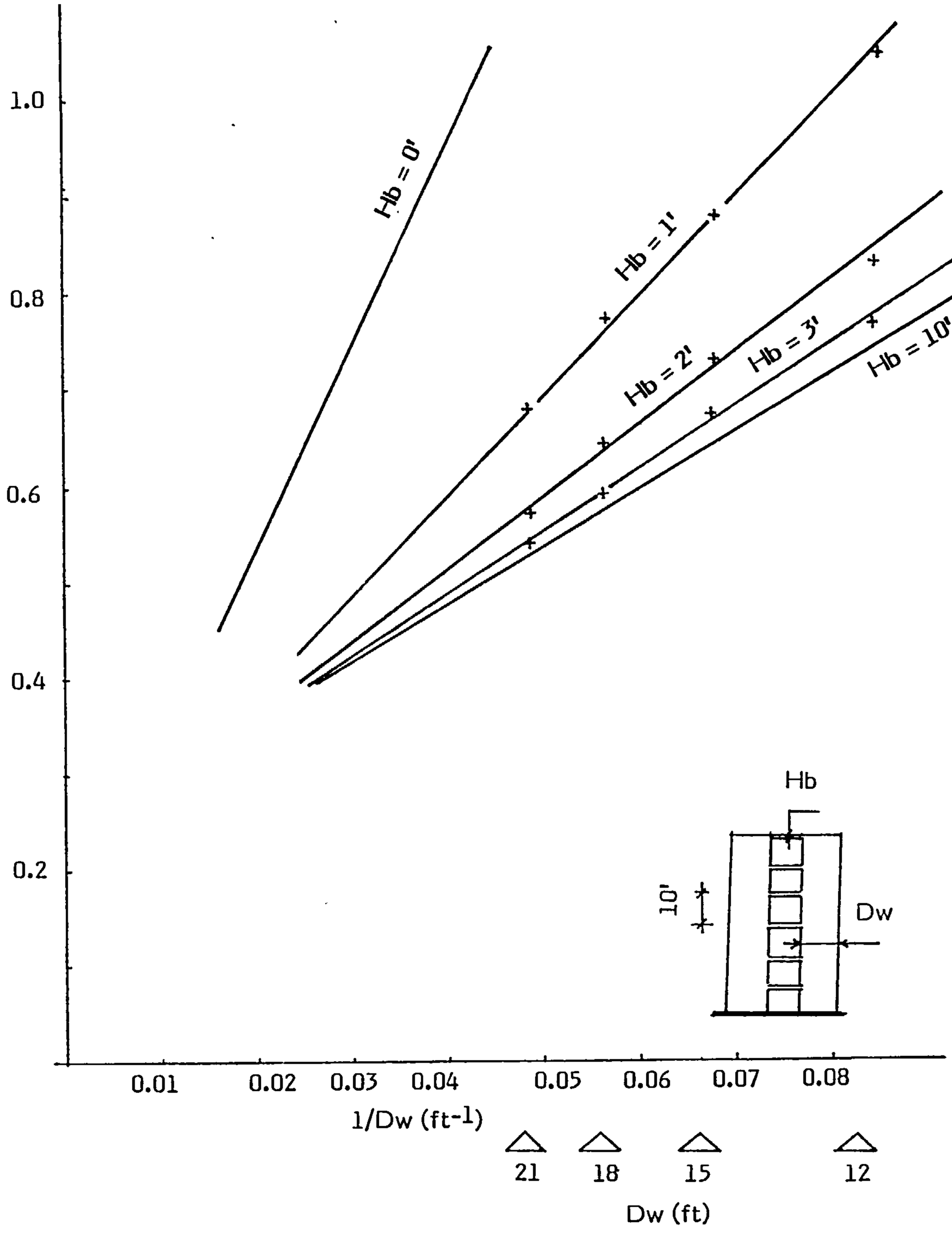

FIG. 4.11 VARIATION OF FUNDAMENTAL PERIOD IN TERMS OF WALL DEPTH Dw

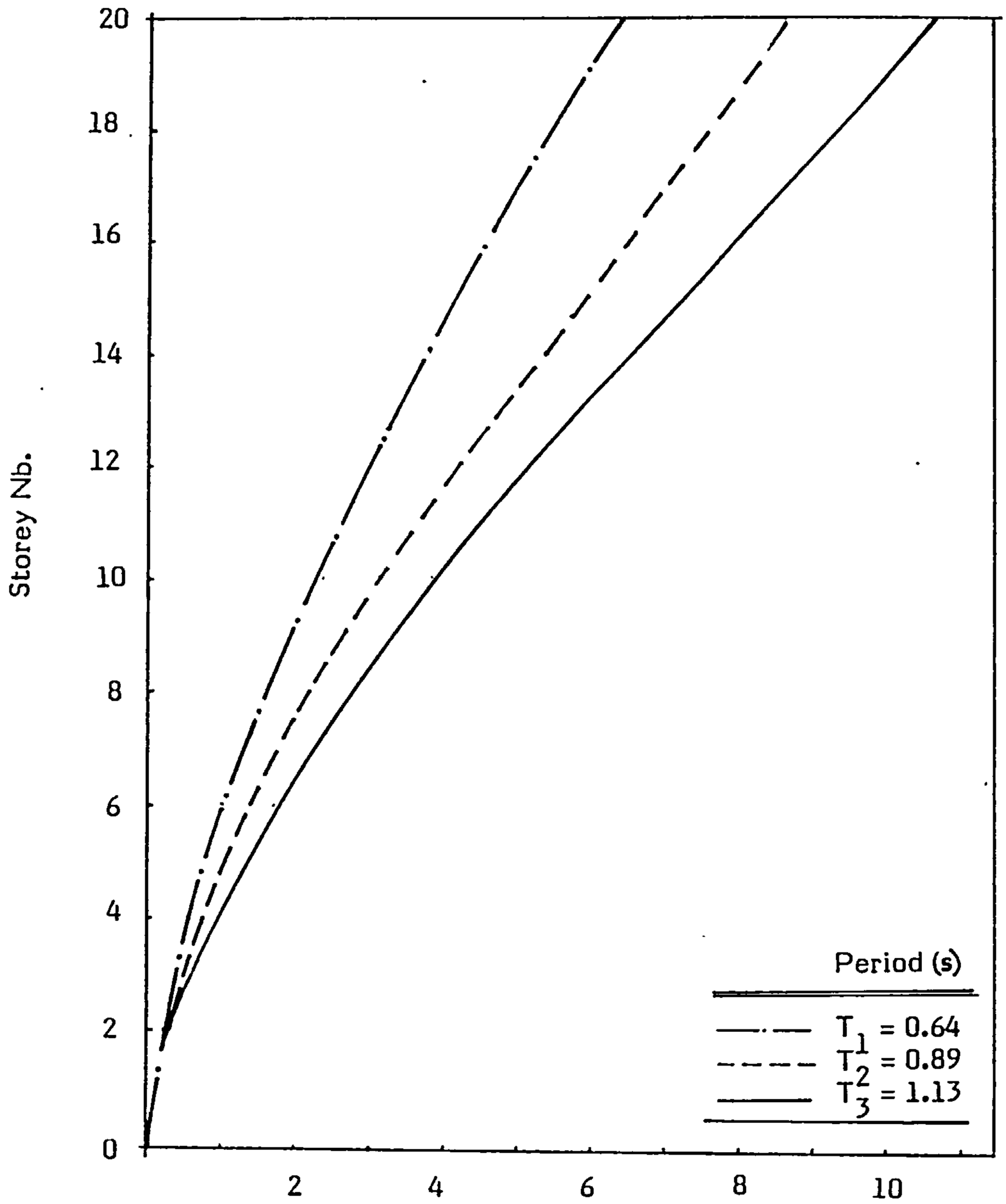

FIG. 4.12 VARIATION OF LATERAL DISPLACEMENT WITH NATURAL FREQUENCY OF A 20 STOREY COUPLED SHEAR WALL

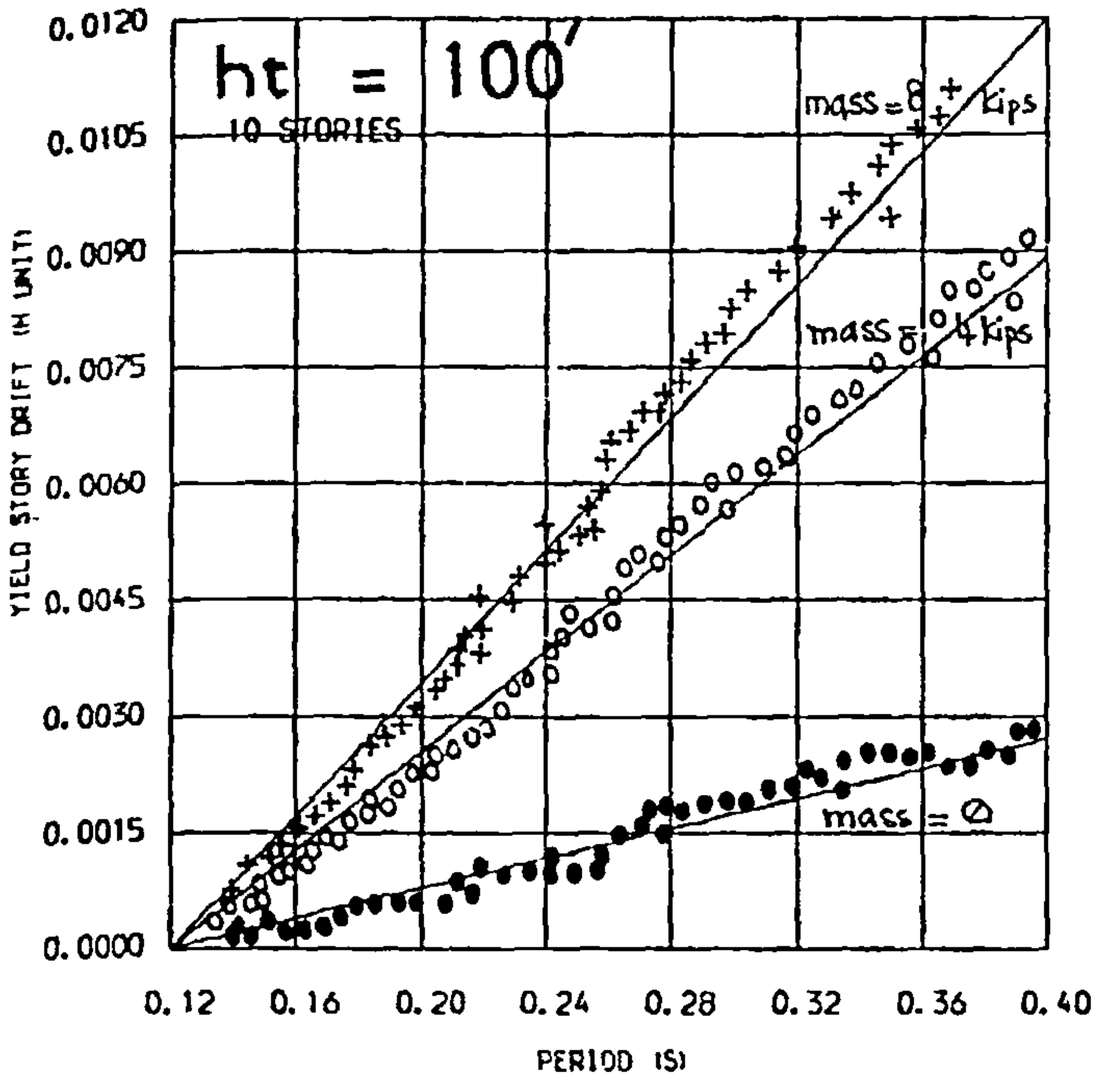

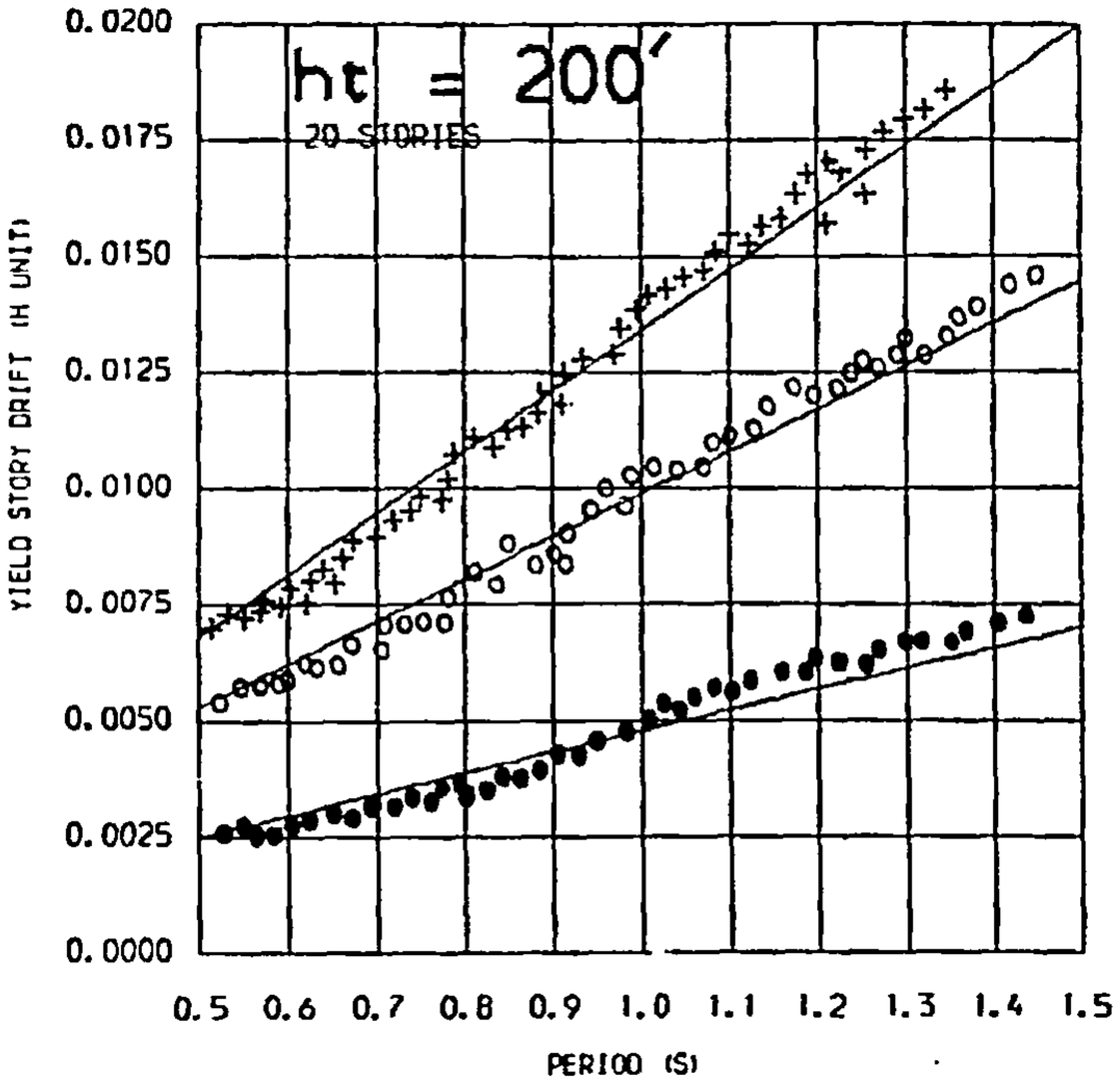

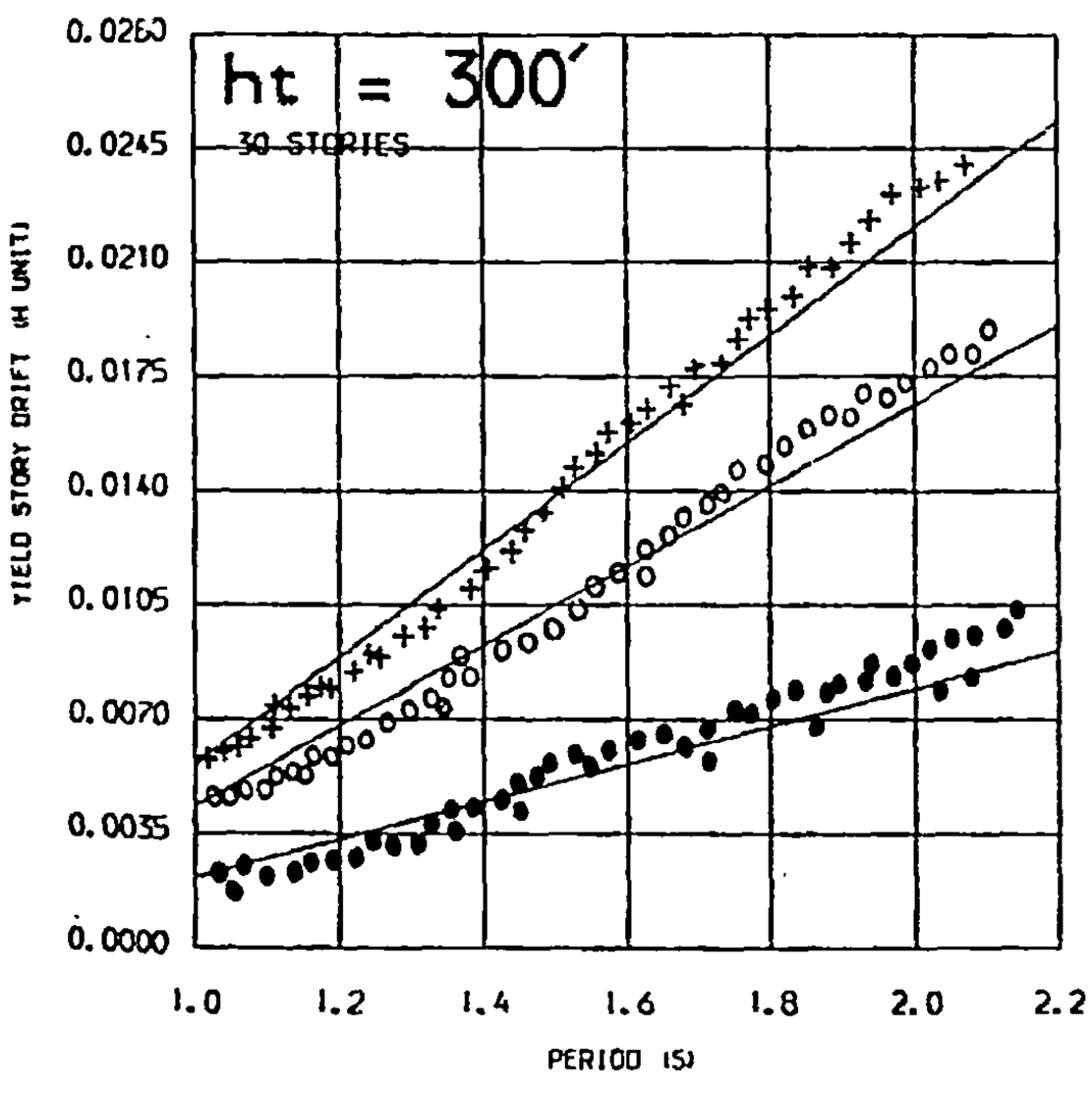

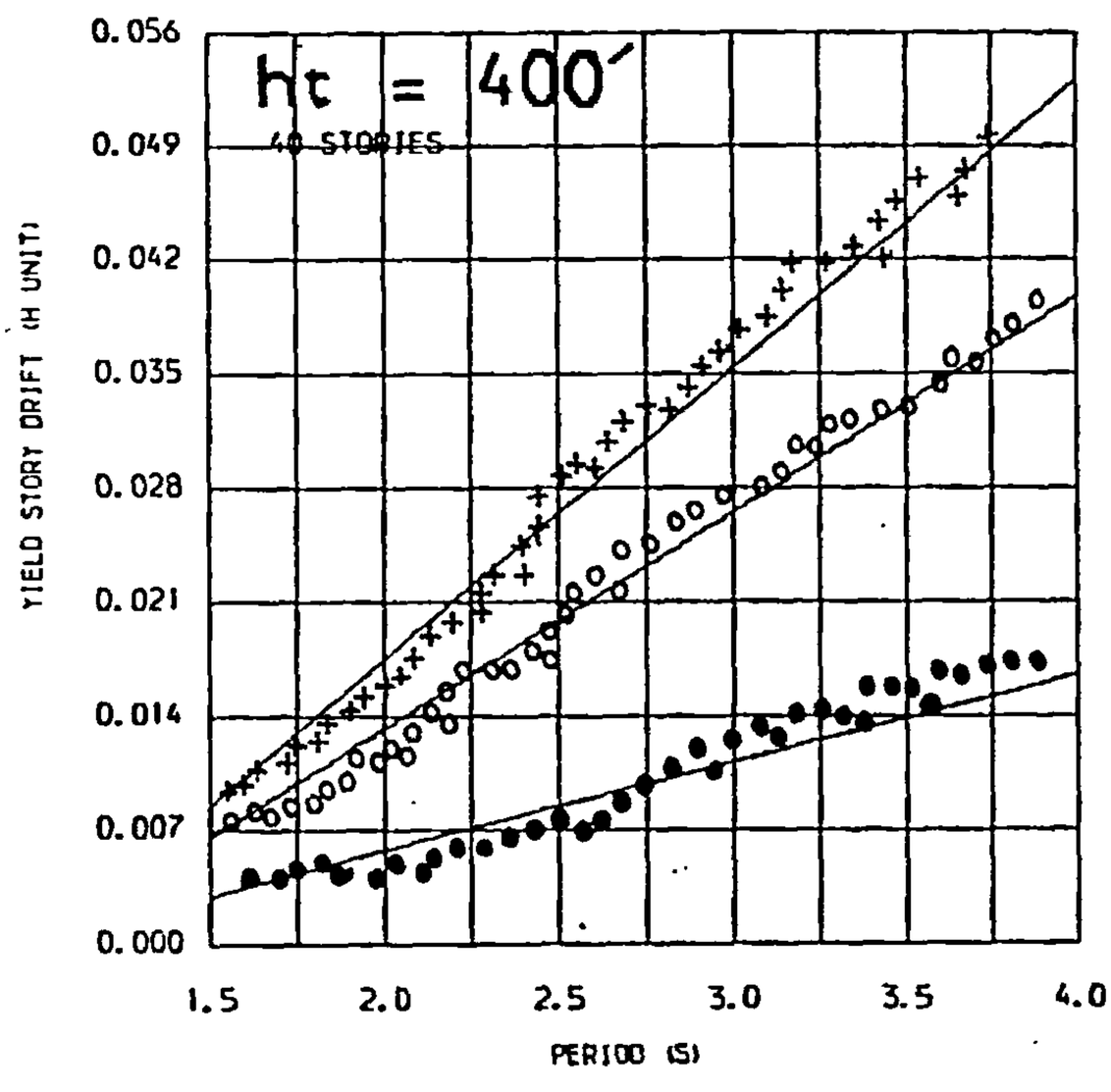

FIG. 4.13 MAXIMUM YIELD DRIFT INDICE VERSUS FUNDAMENTAL PERIOD FOR DUCTILITY FACTOR U=1. AND STORY MASS M=0 , 4 , 8 RESPECTIVELY

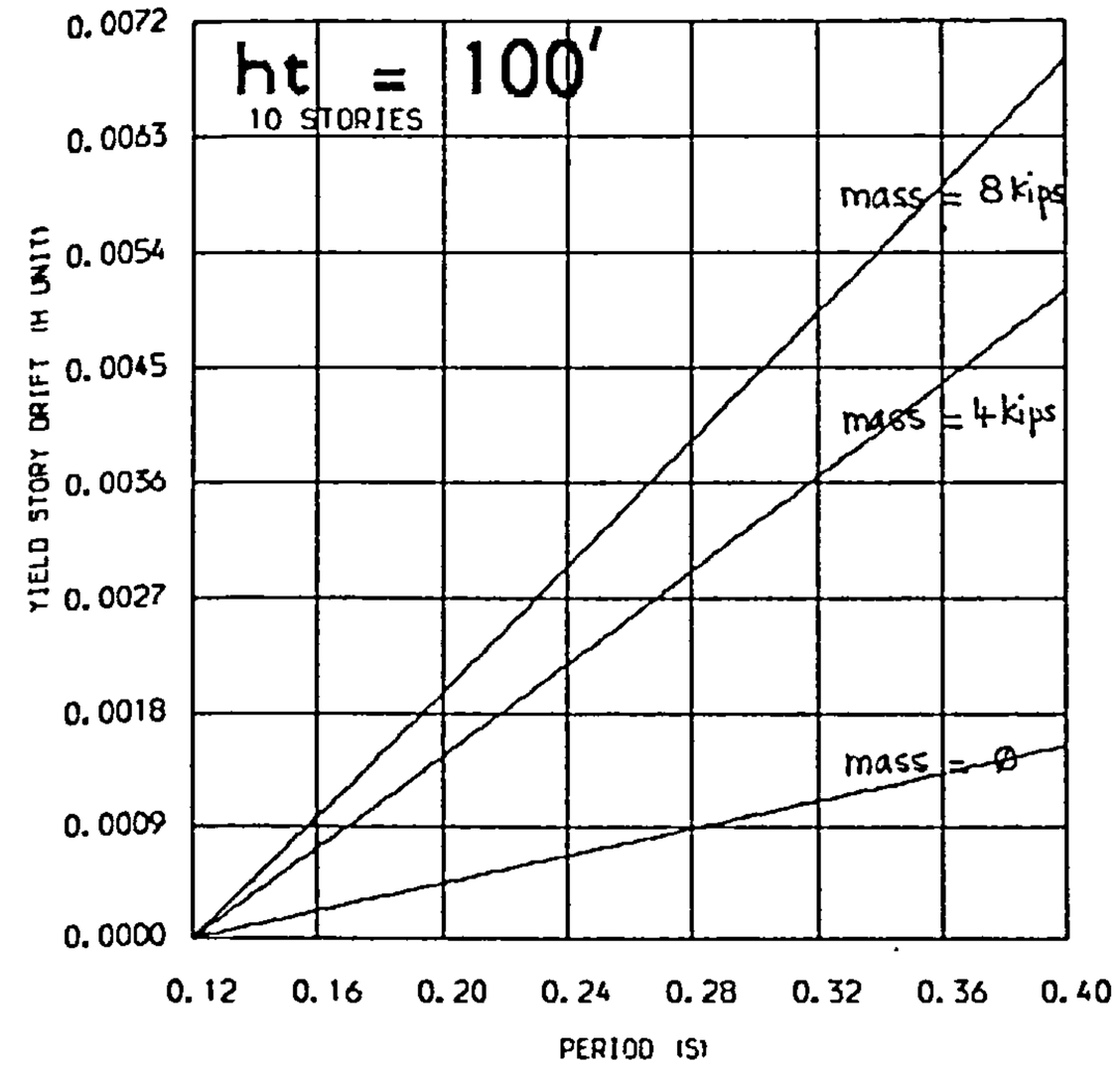

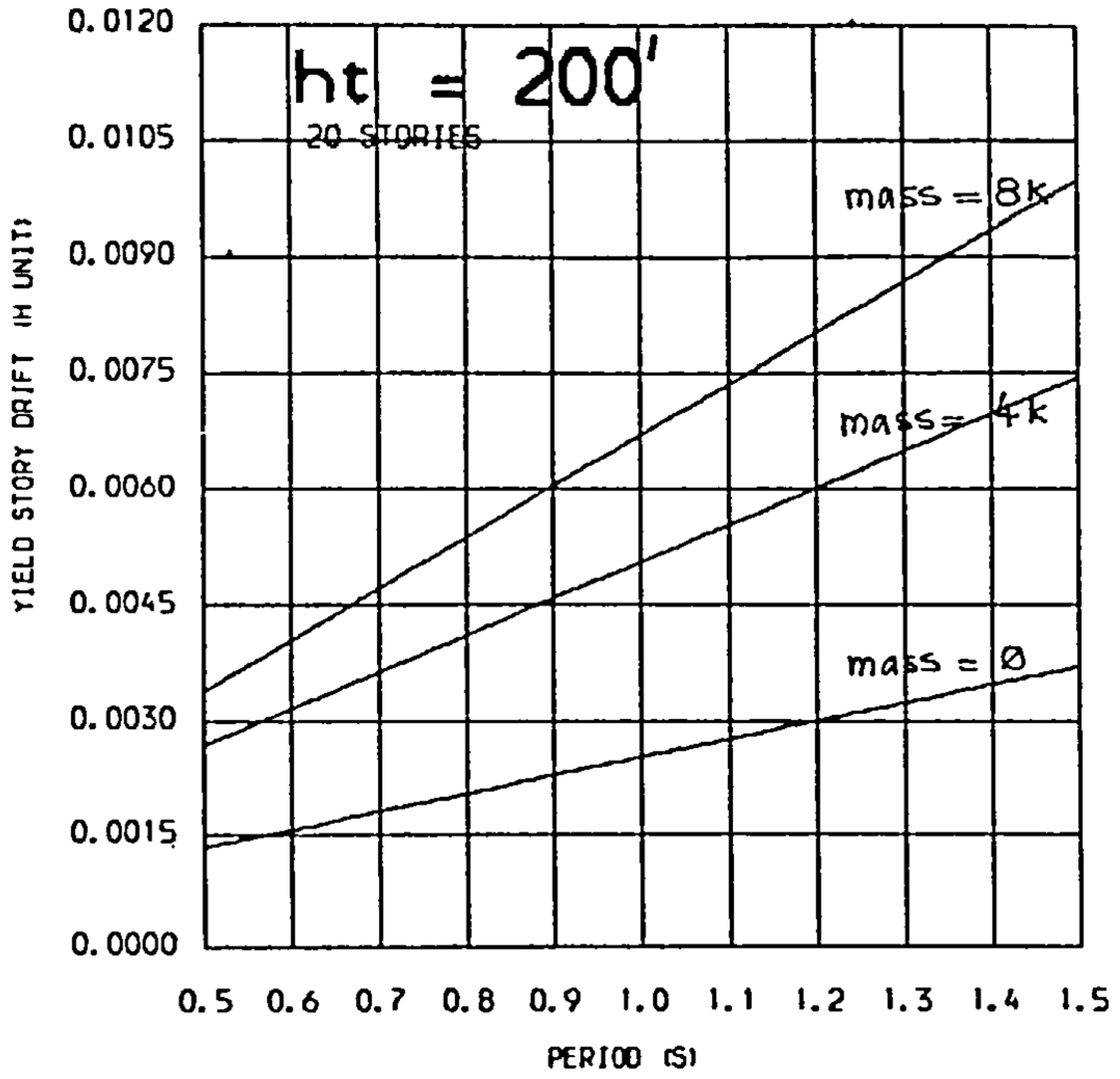

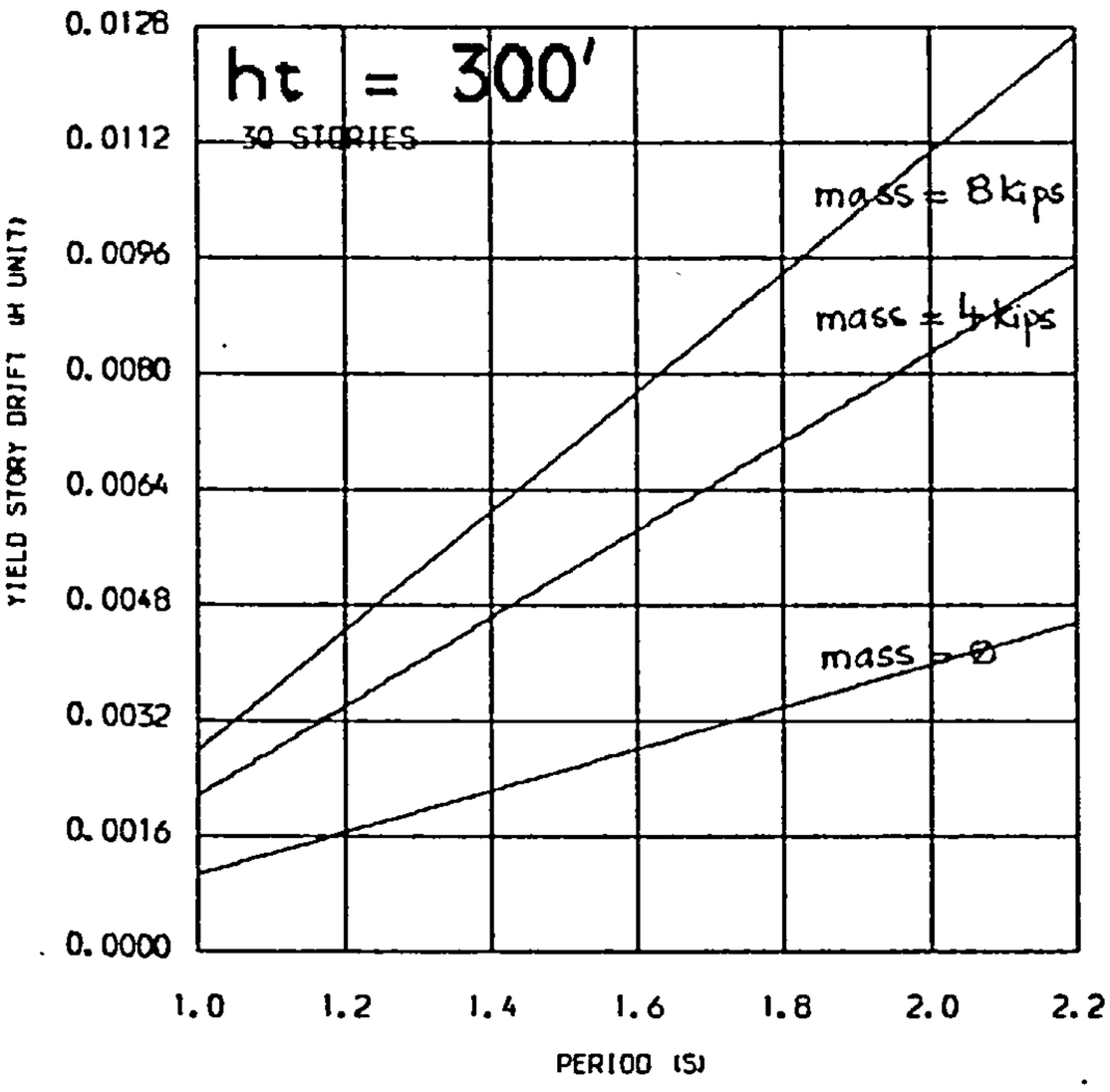

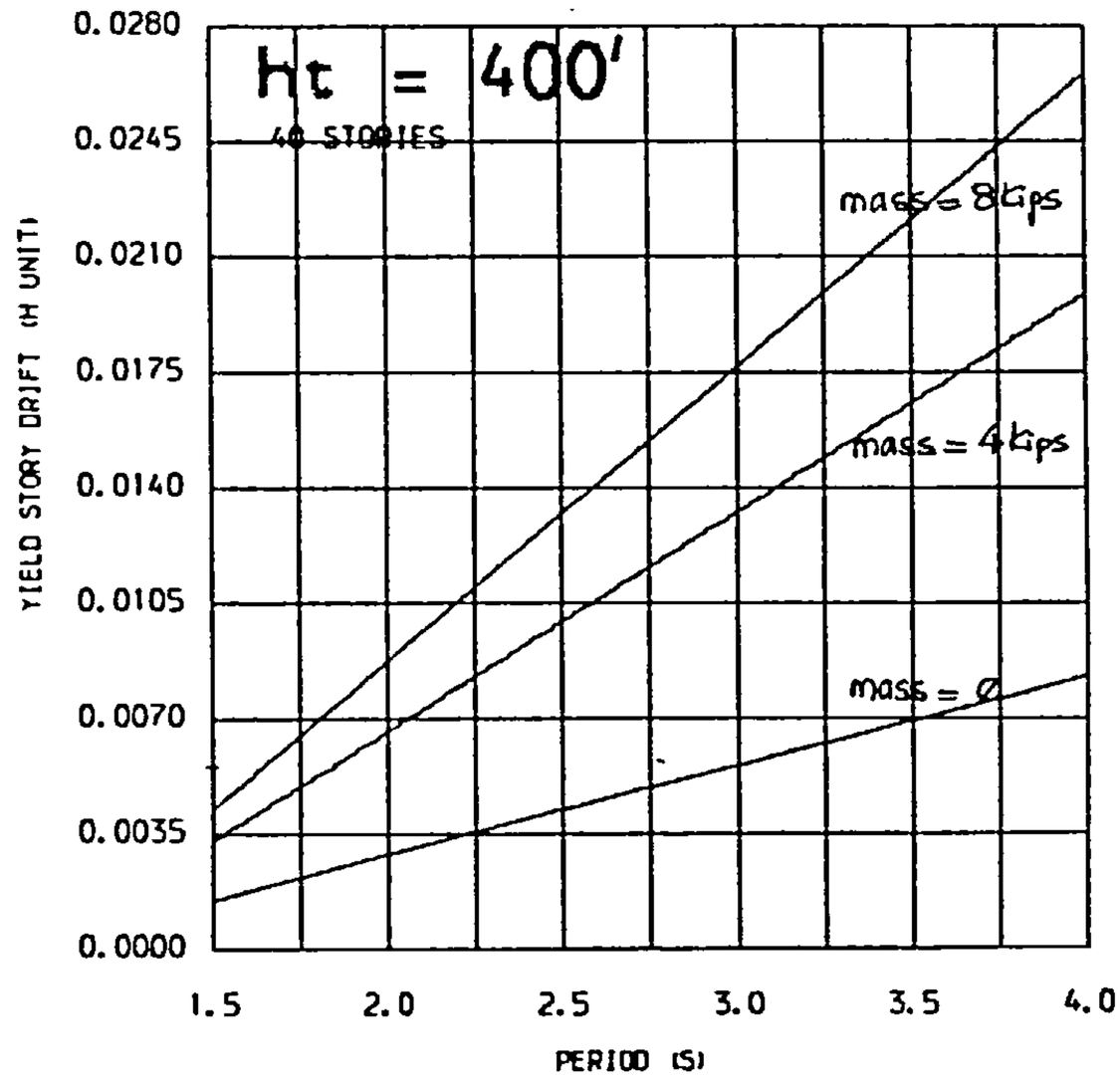

FIG. 4.14 MAXIMUM YIELD DRIFT INDICE VERSUS FUNDAMENTAL PERIOD FOR DUCTILITY FACTOR $\mu = 2$. AND STORY MASS M = Ø , 4 , 8 RESPECTIVELY

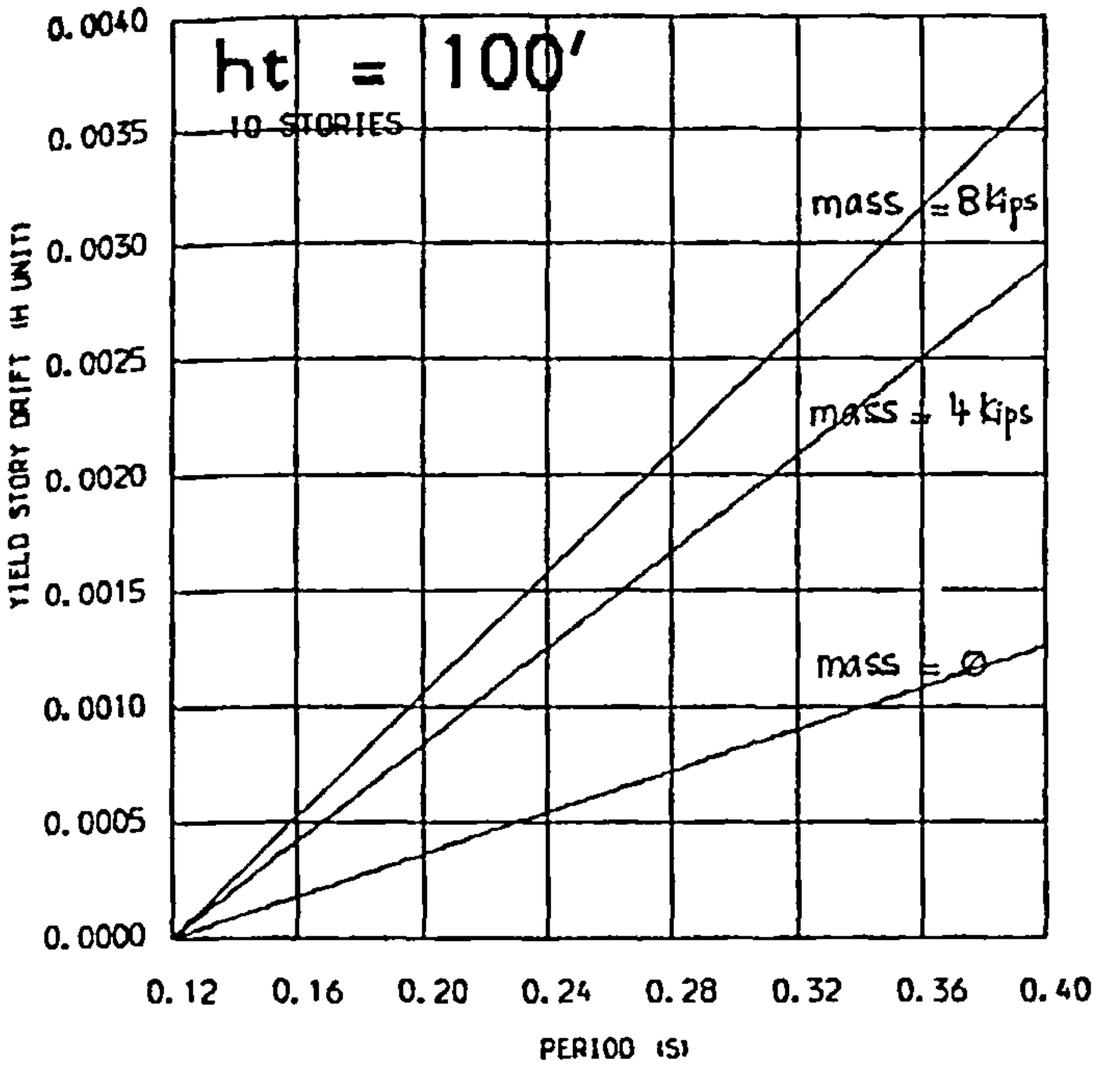

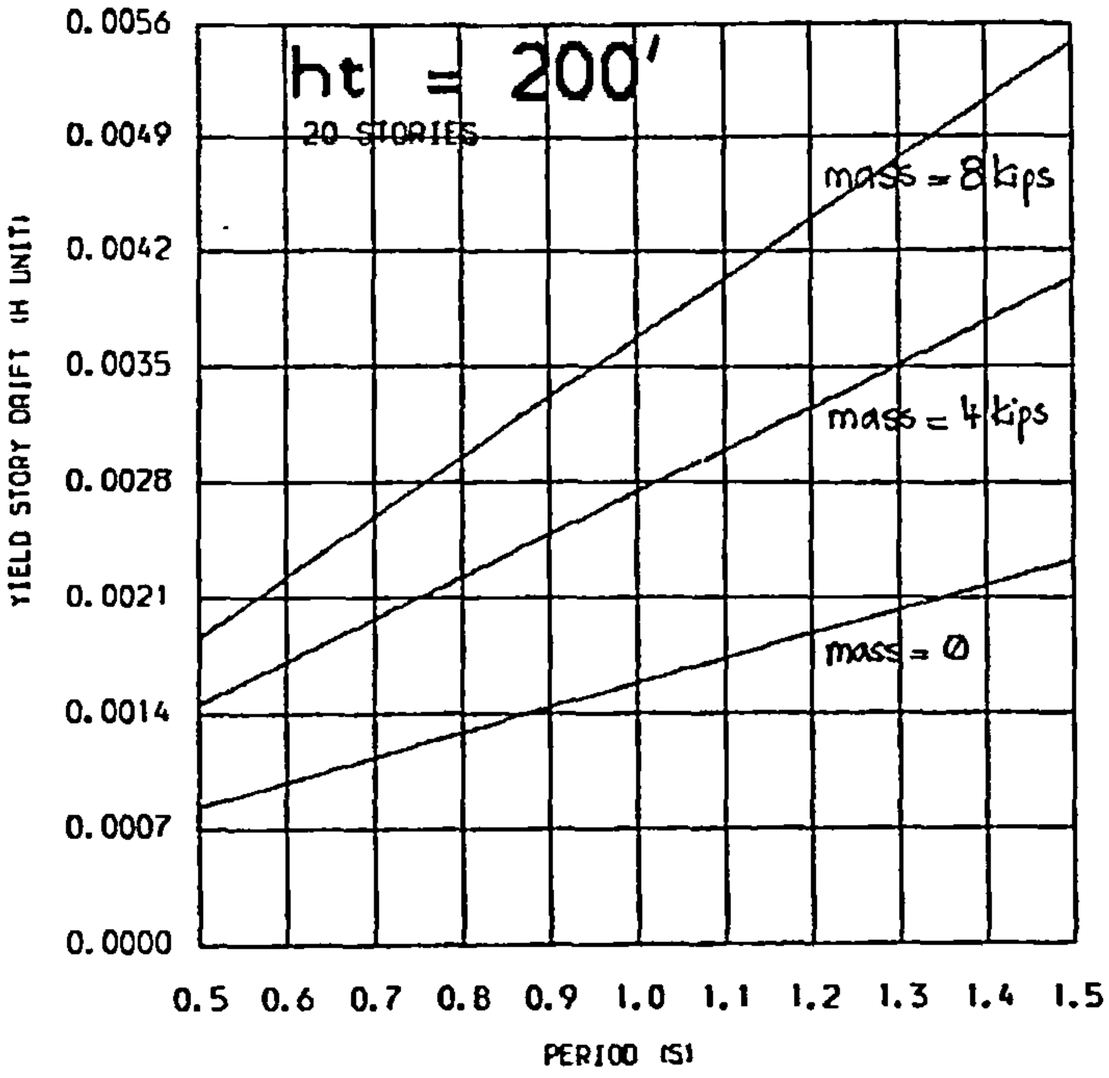

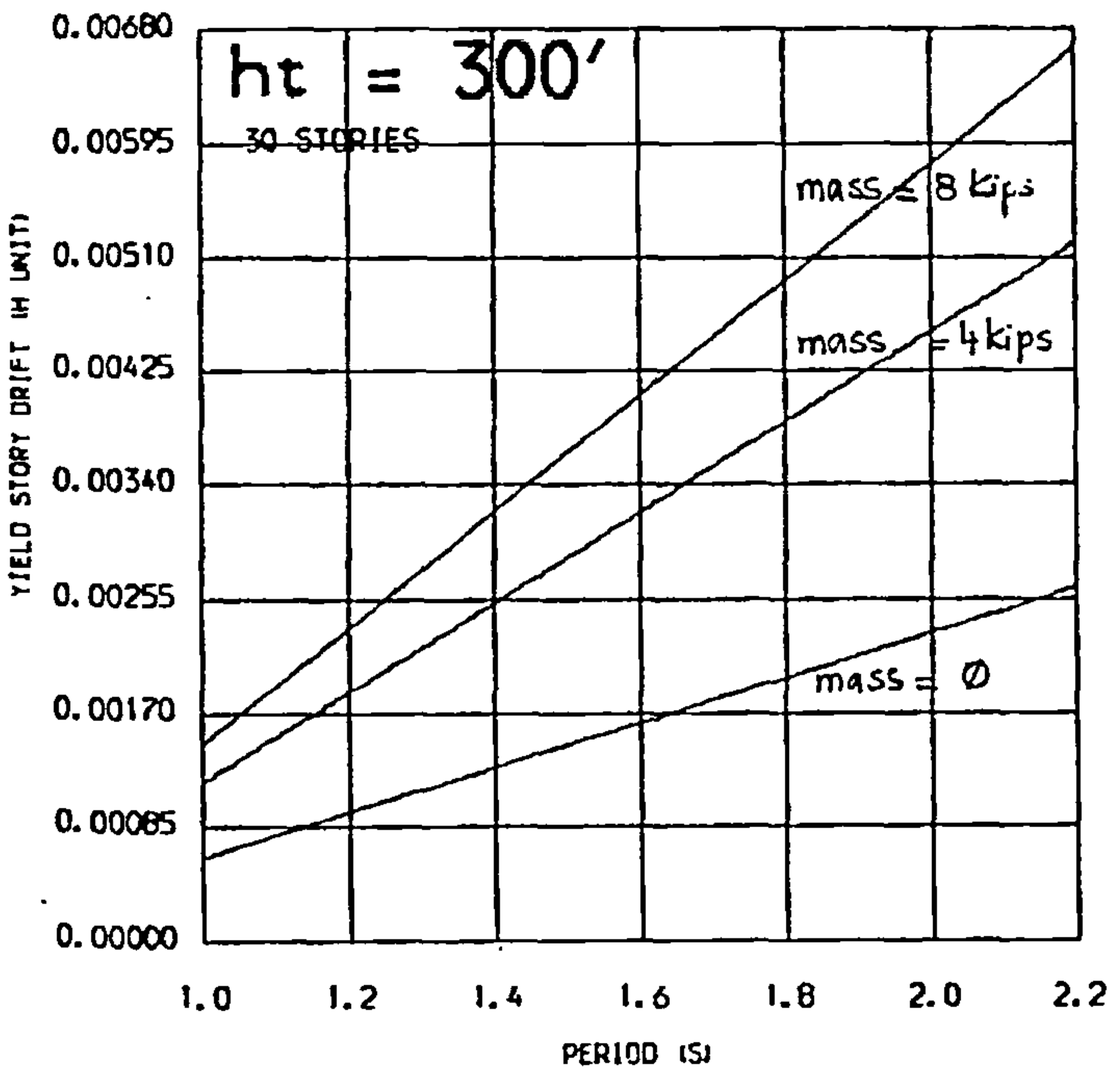

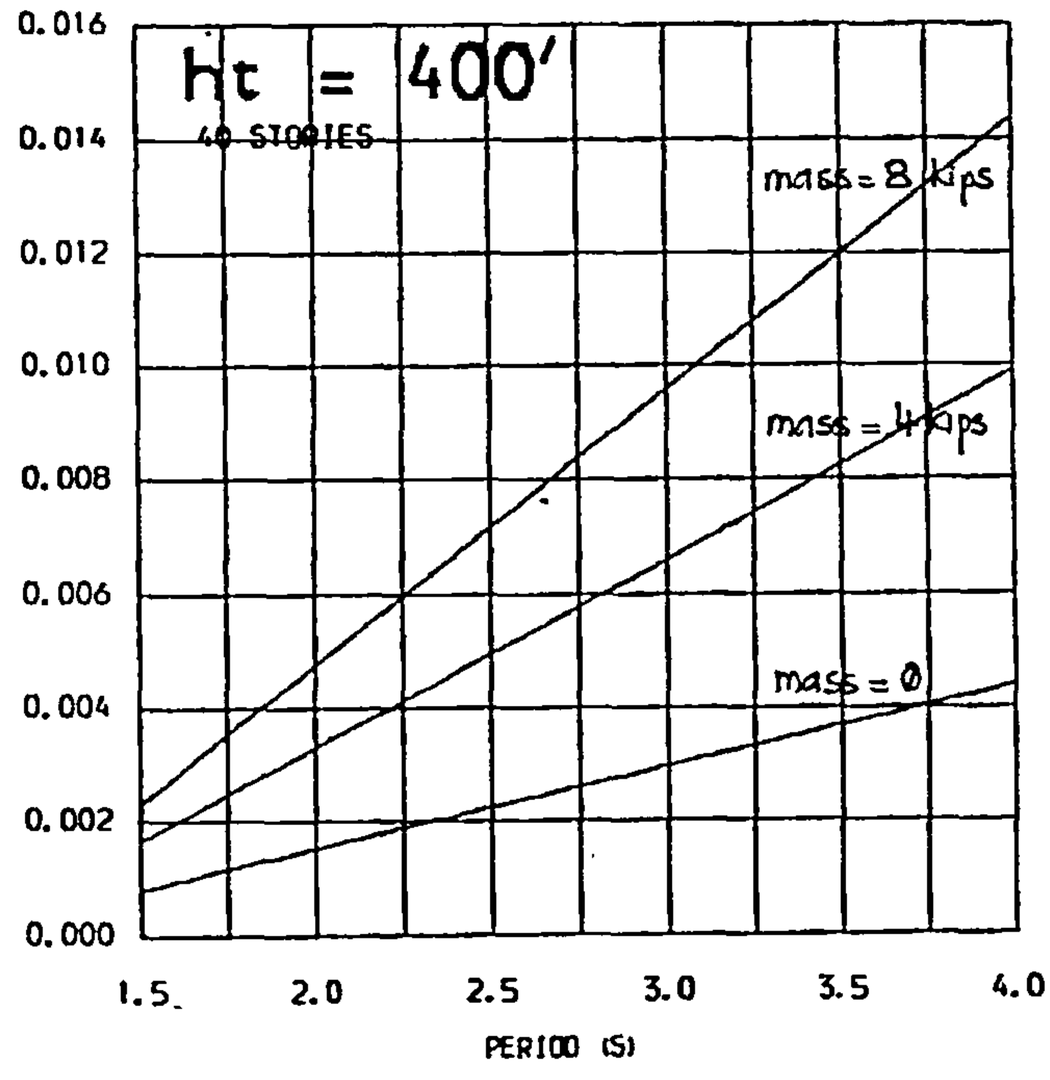

FIG. 4.15 MAXIMUM YIELD DRIFT INDICE VERSUS FUNDAMENTAL PERIOD FOR DUCTILITY FACTOR $\mu = 4$. AND STORY MASS M = Ø , 4 , 8 RESPECTIVELY

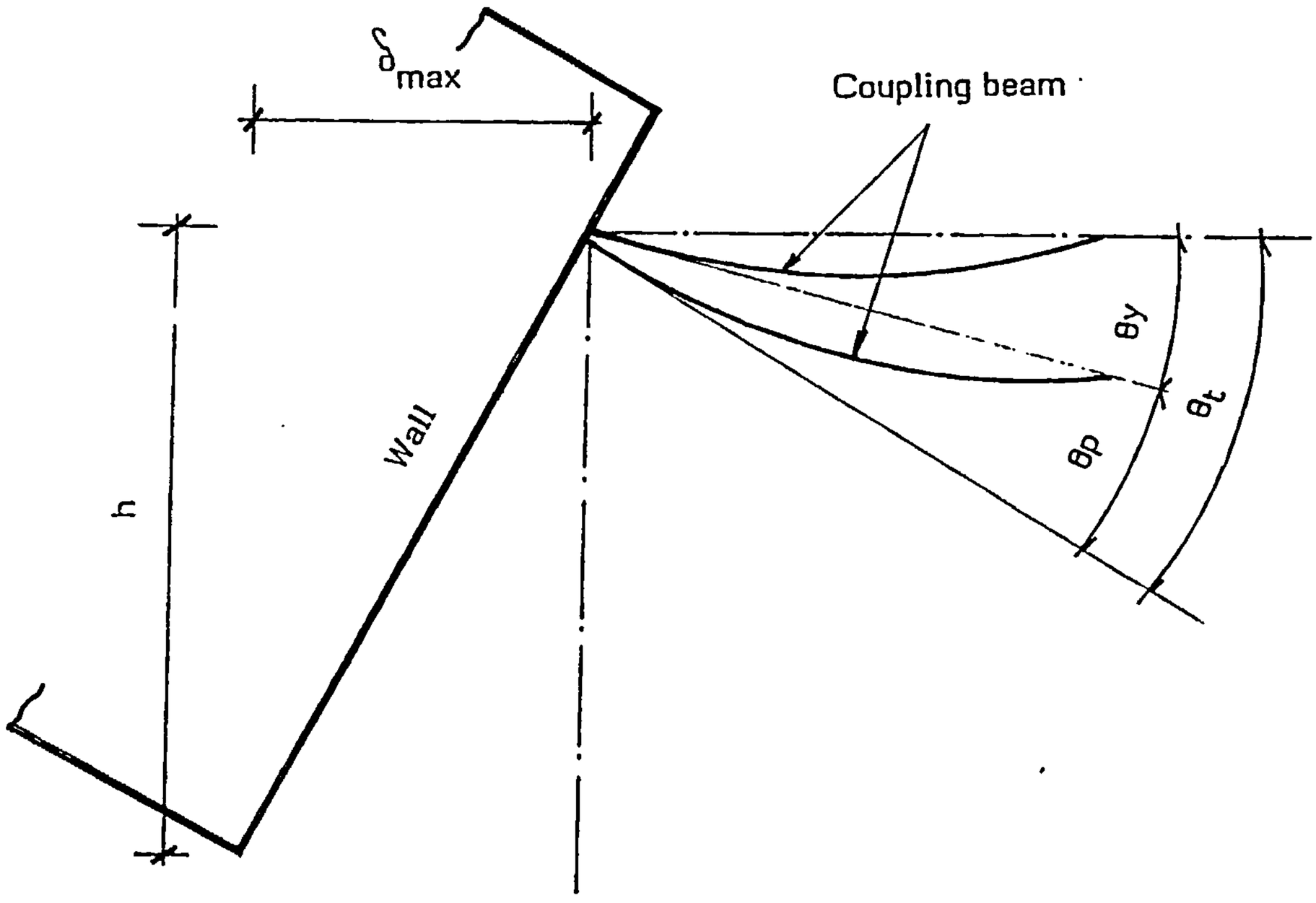

FIG. 4.16 BEAM - WALL CONNECTION

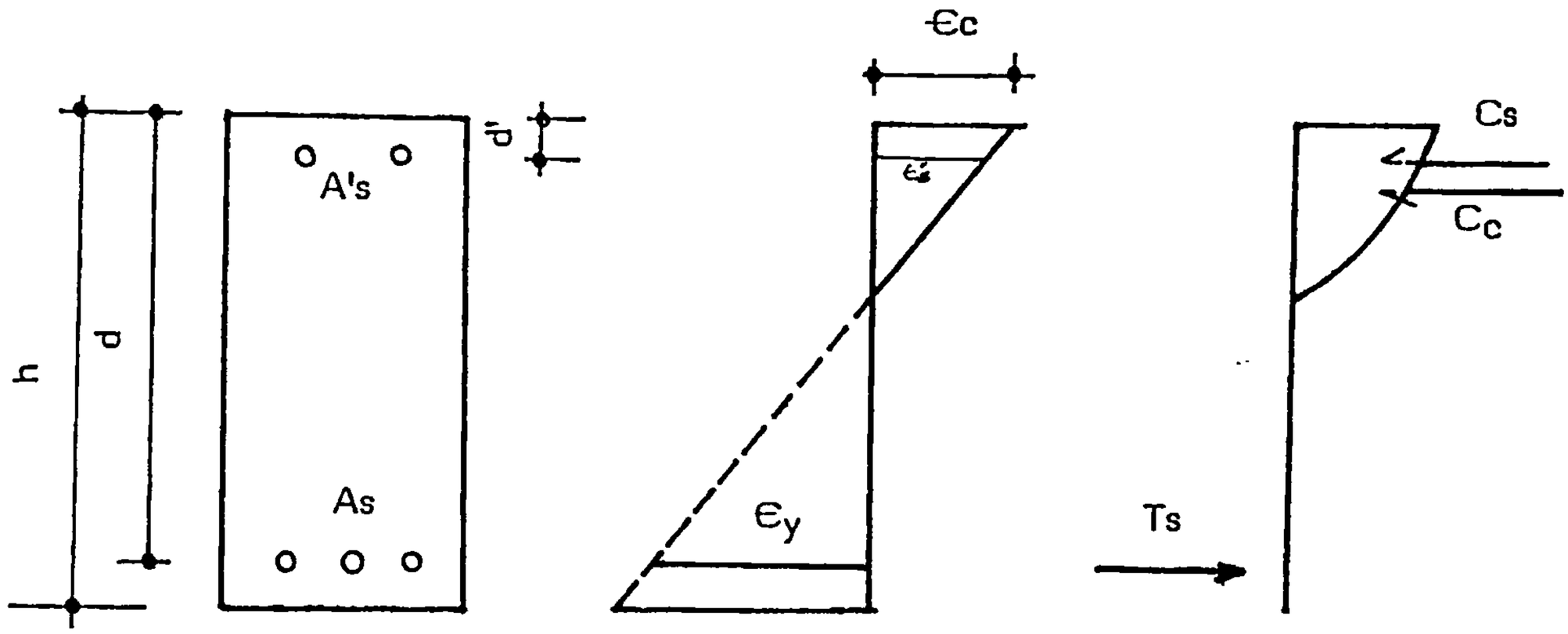

a) Cross Section b) Strain c) Stress Distribution

FIG. 4.17 DISTRIBUTION OF STRAIN AND STRESS OF A TYPICAL CROSS SECTION AT YIELD

CHAPTER FIVE

NONLINEAR BEHAVIOUR OF REINFORCED CONCRETE

5-1 General

When performing a nonlinear analysis, techniques have to be used that recognize material nonlinearities such as cracking and crushing of the concrete and the yielding of the steel. Most material nonlinearities are due to overstress, therefore a way must be found to postulate the critical combinations of stresses or yield criterion beyond which the elastic constitutive relationship does not hold any more. Also, the success of nonlinear analysis to trace the structural behaviour with time on one hand, update the stiffness matrix whenever necessary and predict nonlinearities and failures with good accuracy on the other hand, lies within the choice of suitable experimentally based models or idealisations. Before considering these criteria and models and the resulting modifications in element stiffness which are discussed in some detail in section 4, it was thought useful to give a brief general background on the behaviour of reinforced concrete material and its main components .

5-2 Behaviour of Reinforced Concrete

The finite element method of analysis has advanced considerably in the last decades to meet different problems in various complex fields. However further progress in the understanding and prediction of structural reinforced concrete behaviour is still needed. Indeed the complexity, nonhomogeinity, and anisotropy of the material all contribute to make this progress even slower because of lack of reliable experimental evidence. While relatively reliable experimental data is available on plain concrete and the steel reinforcement acting separately, the derivation of a reliable constitutive law for reinforced concrete is still under

investigation. This is because many of the phenomena influencing the composite material such as bond slip, dowel actions, shear deformations etc., are not fully understood. Before discussing the behaviour of the composite material, the available information on its basic components are presented in the following sections.

5-2-1 Concrete: It is well established that concrete may be idealized as a linear, elastic and brittle material in uniaxial tension. Because of its low and uncertain tensile strength, it is normal practice to ignore it altogether. Therefore most of the effort has been focused on the understanding of the behaviour of concrete under compression. It has been found that uniaxial compressive stress - strain relationship is nonlinear fig. (5.1). Karsan & Jirsa [88] investigated uniaxial concrete behaviour under reversal of loadings and a typical experimental stress-strain relationship is illustrated in fig. (5.3). A great deal of work has been done on uniaxial behaviour and a review of the existing data was given by Popovics [87].

Although an assumed uniaxial stress condition can be justified in many cases, it must be borne in mind that in most practical conditions, concrete is subjected to multiaxial stresses. One of the major experimental results on biaxial behaviour were produced by Kupfer et al. [89]. By conducting tests on plain concrete prisms subjected to different combinations of tension and compression, they defined a biaxial strength envelope as shown in fig. (5.2). They concluded that the strength of concrete under biaxial compression may be as much as 27% higher than under uniaxial compression. However the strength under biaxial tension was approximately equal to the uniaxial tensile strength.

5-2-2 Steel Reinforcement: The steel behaviour has been understood a long time before concrete. Steel behaves generally identically whether it is stressed in tension or in compression. A typical stress -strain curve relationship is illustrated by fig. (5.1b). Steel behaves elastically up to the yield point, after

that it can be idealised either as perfectly plastic or with strain hardening.

5-2-3 Reinforced Concrete: While the separate behaviour of the basic components of reinforced concrete are more or less understood, difficulties still remain in constructing a reliable analytical model for a reinforced concrete member. This stems from the difficulties in assessing phenomena such as dowel actions on steel reinforcement, bond between steel and concrete, aggregate - interlock and bond slip inherent to the material. Many researchers, aware that perfect bond between steel and concrete may only exist at early stage of loading, started investigating the phenomenon. One of the first to introduce bond into a finite element approach were Ngo & Scordelis [31] and Nilson [32]. The first modelled the bond as a linear relationship and used spring linkage elements between steel and concrete. The work was then extended by the second who considered a nonlinear relationship for bond - slip. The phenomenon of dowel action has also been investigated [64, 90, 91] but no reliable data has emerged to allow it to be taken into account with full confidence.

5-3 Description of the Models

5-3-1 Finite Element Idealisation: One of the most important and influencial steps of the overall analysis is certainly the choice of finite element idealisation. This depends on many features such as structural type, geometry, type of loading and general structural behaviour. As far as coupled shear walls are concerned the following idealisations have been adopted in this study :

i) Walls : The finite element idealisation of the walls used in this investigation is a four noded quadrilateral isoparametric plane stress element with two translational degrees of freedom (dof) at each node. However four extra dof corresponding to the nonconforming modes developed by Wilson et al. [63] are added to soften the element and to improve its behaviour in flexure. These extra dof have proven to be efficient in producing good agreements with various

elastic problems. The element stiffness matrix is calculated using the standard Gaussian numerical integration and its derivation is given in chapter III. It may be worth noting that the walls can also be idealised as vertical line elements if need be. Nonlinearities effect the element stiffness and are accounted for through the updating of the property matrix. These and other features are discussed in detail in section 5-4.

ii) Coupling Beams : Because of their likely behavioural response, the coupling beams are idealised as line elements in this study, although they can be idealised as plane stress elements if necessary. The depth of the element is taken into consideration by transforming the generalized displacements acting at the reference axis to eight degrees of freedom acting at the corners of the element. The line element stiffness matrix is also derived in chapter III. Nonlinearities are monitored by the moment - rotation relationship and are discussed in section 5-5.

5-4 Nonlinearities: Plane Stess Consideration

5-4-1 Cracking Phenomenon: In this study concrete is considered to behave elastically in tension. Concrete has very limited capacity to resist tension and is therefore allowed to crack when a principal stress exceeds the maximum permissible tensile stress σ_{ct}. In view of the dynamic character of the loading a crack can open and close again, and at each event the property matrix has to be updated to preset models. Therefore the rest of this section is devoted to the description of these models and the possible stages which can be experienced by a plane stress element during its response.

i) Elastic Element: Prior to cracking the concrete is assumed homogeneous, isotropic and elastic. The property matrix is therefore given by Hooke's law for plane stress elasticity as [92]:

$$\sigma c = D_c \epsilon_c \qquad 5.1$$

Where σc are element stresses, ϵ_c , element strains and D_c, the element elastic property matrix. Concrete property matrix D_c can be written as

$$D_c = Ec/(1-\mu^2) \begin{bmatrix} 1 & \mu & 0 \\ \mu & 1 & 0 \\ 0 & 0 & (1-\mu)/2 \end{bmatrix} \qquad 5.2$$

in which Ec = Young's modulus of elasticity of concrete

μ = Poisson's ratio of concrete

ii) Cracked Element: If one of the principal stresses σ_1 or σ_2 reaches the admissible tensile concrete stress σct, then concrete is assumed to have cracked perpendicularly to the considered principal stress direction and therefore can no longer carry any tensile stress perpendicular to the crack direction. However some shear resistance can still be transmitted through so called aggregate interlock and dowel action. These features can be expressed by updating the property matrix given in equation (5.2). For a section which was cracked due to $\sigma 1$ fig. (5.4) for instance the instantaneous property matrix is :

$$D'_{cr} = \begin{bmatrix} Ec & 0 & 0 \\ 0 & 0 & 0 \\ 0 & 0 & \alpha Ec/2(1+\mu) \end{bmatrix} \qquad 5.3$$

in which the shear transfer factor α is discussed in the next sections. Note that the matrix D'cr as expressed by equation 5.3 is given with respect to material coordinates (x', y') fig. (5.4) and can be transformed into element coordinates (x, y) by

$$D_{cr} = T^T D'_{cr} T \qquad 5.4$$

where T is the transformation matrix and is given by

$$T = \begin{bmatrix} c^2 & s^2 & cs \\ s^2 & c^2 & -cs \\ -2cs & 2cs & c^2-s^2 \end{bmatrix} \qquad 5.5$$

$s = \sin \beta$

$c = \cos \beta$

β = angle between x and x' fig. (5.4)

Similarly, if the cracking is due to σ 2, then D'cr becomes

$$D'_{cr} = \begin{bmatrix} 0 & 0 & 0 \\ 0 & Ec & 0 \\ 0 & 0 & \alpha Ec/2(1+\mu) \end{bmatrix} \qquad 5.6$$

If however two sets of cracks take place at the same time interval, then D'cr specializes as

$$D'_{cr} = \begin{bmatrix} 0 & 0 & 0 \\ 0 & 0 & 0 \\ 0 & 0 & \alpha Ec/2(1+\mu) \end{bmatrix} \qquad 5.7$$

iii) Tension Stiffening Effect: It is well accepted that the bond between the concrete and the reinforcing bars gives some resistance to the concrete after cracking has occured. This resistance is often referred to as tension stiffening effect. Its maximum value is equal to the tensile strength of concrete σ ct just after cracking and deteriorates rapidly with increasing strain. A typical relationship between this resistance stress σr and the strain is shown in fig. (5.7). As σr is in the direction of steel reinforcement, it is easy matter to convert it into equivalent stress vector in the global coordinates through a transformation matrix T. However, in view of the uncertainties involved on one hand and the lack of knowledge of the phenomenon under cyclic strains conditions on the other hand, the effect of tension stiffening is not considered in this study.

iv) Aggregate Interlock & Dowel Action: Shear can be transferred across cracks by interlocking of aggregate particles projecting from the cracked surfaces. In each region of contact across a crack, any tendency to relative movement of the two sides will introduce both direct and shear stresses. In order to evaluate the shear stresses induced, Paulay & Fenwick [91] conducted tests on aggregate interlock by considering concrete strength and crack width and proposed a shear stress - relative displacement relationship. Their relationship revealed that the shear stiffness is affected by both the strength of concrete and the opening of the cracks. Generally the shear stress-strain relationship can be expressed in the form

$$T = Geq.\epsilon xy = (Geq/G).G.\epsilon xy = \alpha_s.G.\epsilon xy \qquad 5.8$$

in which Geq= Shear modulus after cracking has occured

G = Elastic shear modulus

ϵxy= Shear strain

α_s= Shear reduction factor (=1 prior to cracking)

Many investigators beside Paulay et al. [91] have used different values for α_s. Some [33, 34] attributed constant values for α_s ranging from 0.25 to 0.50 regardless of the attained strain, some others used a linear [94] or a hyperbolic [95] shear factor-crack opening relationship. The summary of these relationships is illustrated in fig. (5.5) for comparison. As can be seen from the figure the discrepancy between them is considerable. This shows clearly that a great deal of research is needed in this respect.

Dulacska [90] was one of the first to conduct tests on dowel actions as influenced by concrete strength and diameter and angle of reinforcing bars. She proposed a displacement-dowel action relationship and concluded that dowel action is almost elastoplastic and depends to a large extent on whether or not bars have reached their dowel strength. Using Dulacska's relationship, the

relation between the ratio of equivalent shear stiffness due to dowel action and the elastic shear modulus G and the angle of reinforcing bars βs in the elastic dowel strength range, is plotted for different steel ratio (p) and diameters (ϕ) in fig. (5.6). This clearly shows that the influence of dowel action is very small in this range to compare with the effect of shear interlock. However this influence can be expected to be higher as plastic dowel strength is reached. Indeed Paulay et al. [91] conducted a number of tests and reported that dowel action could resist only 20 to 30% of the shear resisted by interlocking. He also introduced the notion of short dowel and long dowel by reporting that dowel action performance depended amongst other factors on the width of concrete at the level of the bars and suggested that the position of the reinforcing bars in the concrete had a marked influence on the capacity and performance of dowel action.

These factors make the modeling of dowel action very difficult to assess with reasonable confidence for simple cases yet alone to be introduced in a finite element procedure. It is clearly apparent that more research is highly desired and the consideration of the dynamic aspect of the problem of dowel action is certainly needed. However in view of what has previously been discussed, in this investigation the aggregate interlock and the dowel action are combined ie,

$$\alpha = \alpha_s + \alpha_d \qquad 5.9$$

in which α = combined shear reduction factor

α_s = Shear reduction factor due to aggragate interlock

α_d = Shear reduction factor due to dowel action

Furthermore, a variation of α decreasing with the crack width seems to be closer to the physical evidence, therefore in this study α is defined as follows

$$\begin{aligned} \alpha &= 0.4 \quad \text{if} \quad \epsilon < 3\epsilon_{cr} \\ \alpha &= 0.2 \quad \text{if} \quad \epsilon > 3\epsilon_{cr} \end{aligned} \qquad 5.10$$

where ϵ_{cr} is the strain at first crack. It must be borne in mind that the aggregate interlock reduction factor α_s becomes zero when interlocking becomes ineffective, ie, as the crack opening reaches a maximum value which can be interpolated from Paulay & Loeber's [93] experimental results as

$$\epsilon_{max} = 0.005 \qquad 5.11$$

However this is assumed not to affect the value of factor α given by eqn. 5.10.

v) Crack Width: The crack width is a very useful qualitative measure as it monitors the closing of an open crack during load reversals. The 'crack width' Cw is defined as the difference between the strain normal to the cracks ($\epsilon_{x'}$ referring to fig. (5.4)) and the strain arising from Poisson's ratio effect of stresses acting parallel to the cracks $\epsilon_{\mu,x'}$, i.e.,

$$C_w = \epsilon_{x'} - \epsilon_{\mu,x'} \qquad 5.12$$

in which (referring to fig. (5.4))

$$\epsilon_{x'} = \epsilon_x \cos^2\theta_{cr} + \epsilon_y \sin^2\theta_{cr} - \epsilon_{xy}\cos\theta_{cr}\sin\theta_{cr} \qquad 5.13$$

$$\epsilon_{\mu,x'} = -\mu\,\Theta_{y'}/E_c \qquad 5.14$$

where $\sigma_{y'}$,in the case of fig.(5.4), is given by

$$\sigma_{y'} = \sigma_y \cos^2\sigma_{cr} + \sigma_x \sin^2\sigma_{cr} - 2\tau_{xy}\cos\sigma_{cr}\sin\sigma_{cr} \qquad 5.15$$

Note that the ' crack width ' Cw expressed in eqn. 5.12 being in terms of strains, is to be seen rather as a descriptive quantity.

vi) Closing and Reopening Criteria: Obviously a crack closes as the 'crack width ' Cw defined by eqn. 5.12 for the situation described by fig. (5.4) is less or equal to zero. i.e.,

$$C_w \leq 0 \qquad 5.16$$

In this case the instantaneous property matrix is updated and becomes that of the uncracked element defined by eqn. 5.2. A closed crack reopens again as the stresses acting normal to the crack becomes tensile. An element having cracked on one direction can crack again in the direction perpendicular to the existing crack for similar reasons as the formation of the first crack, that is for the case of fig. (5.4) when $\sigma_2 > \sigma$ ct. In the case of closed cracks in both directions, normal procedure is then used to determine the new directions of the cracks if any. When open cracks occur at both directions, shear can still be transferred and the reduction factor α of eqn. 5.10 is reduced to $\alpha/2$ for each set of cracks. Because the cracks are formed at different angles, The updated property matrices are transformed separately to the element coordinate system and then summed up to yield the updated element property matrix Dcr.

vii) Crack Modes and Flow Chart: When performing a dynamic analysis, cracking conditions are likely to change with time. To follow the instantaneous changes throughout the entire response, a computer code has been allocated to each gaussian point to monitor the changes in cracking conditions. This code was designated by KODE and can take any integer value from 0 to 8. The interpretation of each of these values are given in table 5.1. To initiate the analysis, KODE is set equal to 0 (no cracking) for all elements. A computer directed flow chart of the cracking process is given in fig. (5.9).

viii) Pseudo Stresses Due to Cracking: During an interval of time, an element may crack leading sometimes to a substantial changes in its property matrix as explained through the previous sections. Consequently an element can only support a value of stress computed in terms of its property matrix Dcr, i.e.,

$$\sigma_{cr} = D_{cr}\, \epsilon \qquad 5.17$$

in which ϵ is the element strain vector defined as

$$\epsilon = \begin{Bmatrix} \epsilon_x \\ \epsilon_y \\ \epsilon_{xy} \end{Bmatrix} \qquad 5.18$$

The difference between the stresses previously attained and used for the state determination at the interval t, that is σ and the stresses which can actually be supported σ_{cr} called pseudo or initial stresses and are computed as

$$D\sigma = \sigma - \sigma_{cr} = (D - D_{cr}) \epsilon \qquad 5.19$$

5-4-2 Yielding and Crushing of Concrete in Compression:

i) Yielding: As explained in section 5-2 and as far as shear walls are concerned, concrete is assumed to behave biaxially. A typical biaxial behaviour of concrete was developed experimentally by Kupfer et al. [89] and is shown in fig. (5.2). The curve can be used as criterion to monitor concrete yielding. However, in this study the approximate Von Mises Yield criterion is assumed for the plasticity of concrete under biaxial stresses. The curve presenting this creterion is also shown in fig. (5.2) for comparison. The yield surface $F(\sigma)$ is defined by:

$$F(\sigma) = \sigma_x^2 + \sigma_y^2 - \sigma_x\sigma_y + 3\tau_{xy}^2 - \sigma_o^2 = 0 \qquad 5.20$$

in which σ_o is the uniaxial yield stress. The concrete is assumed to have started yielding if

$$F(\sigma) > 0 \qquad 5.21$$

Zienkiewich & al. [96] developed the so called initial stress method in which no updating of initial property matrix is needed as plasticity occurs. The method uses the initial elastic matrix repeatedly and making adjustment in the stresses by successive corrections to reproduce the actual stresses which would be obtained using the elasto-plastic property matrix. The corrections in stresses

are called initial stresses and are converted into nodal forces and applied to the structure during the next increment. This method is used in this investigation and is given in detail later in this section.

ii) Crushing of Concrete: Although very strong in compression, concrete crushes when its maximum admissible strain is reached. For normal weight concrete, a typical value for the maximum strain would be :

$$\epsilon_{min} = -0.0035 \qquad 5.22$$

Note that this typical value is determined by uniaxial compression tests and therefore can only be used in biaxial state for compression if an equivalent strain is defined. If Von Mises criterion is used, then the equivalent strain fig. (5.8) can be computed as

$$\epsilon_{eq} = (\epsilon_x^2 + \epsilon_y^2 - \epsilon_x\epsilon_y + 1.5\epsilon_{xy})^{\frac{1}{2}} \qquad 5.23$$

If

$$\epsilon_{eq} < \epsilon_{min} \qquad 5.24$$

then the concrete is assumed to have crushed and consequently can no longer sustain any further loading. Its stiffness is therefore disregarded for the rest of the increments.

iii) Yielding Code: Similarly to cracking conditions, a computer directed yielding code designated by IPEL is attributed to each Gaussian point within the element. IPEL can have any integer value ranging from 1 to 3 standing for

IPEL = 1 Elastic element

IPEL = 2 Yielding element

IPEL = 3 Crushed element

At initiation of analysis IPEL is set equal to unity for all elements.

iv) Pseudo - Stresses: The elasto-plastic property matrix developed in [96] and used for the computation of pseudo - stresses due to plasticity is of the general form:

$$D_{ep} = Dc - DcF'(\sigma)F'^{T}(\sigma)Dc\,[F'^{T}(\sigma)DcF'(\sigma)\,]^{-1} \qquad 5.25$$

in which Dc = Elastic property matrix given by eqn. 5.2

$$F'(\sigma) = dF(\sigma)/d\sigma$$

Equation 5.25 can also be written as [96]

$$D_{ep} = Dc - (\,Dc\Phi\Phi^{T}Dc \,/\, \Phi^{T}Dc\Phi\,) \qquad 5.26$$

in which Φ is given by

$$\Phi^{T} = [(\sigma_x - \sigma_y/2)\,(\sigma_y - \sigma_x/2)\,3\tau_{xy}\,] \,/\, \sigma_o \qquad 5.27$$

Within a typical load increment, steps should be taken to compute the initial stresses due to plasticity. These are given in ref. [96], modified to accomodate our study and repeated here for convenience.

Step 1. Apply the load increment and determine the elastic stress and strain increments (DELSIG & DELEPS) and hence the total stress and strain vectors (TAU & STRAIN).

Step 2. With TAU as state of stress, determine the value of the yield function F.

a) If F(tau)< 0, then elastic behaviour assumption holds and hence set STRESS=TAU and stop the process.

b) If F(TAU)≥ 0 and if the previous state of stress was plastic, set RATIO=0 and go to d) otherwise, there is a transition from elastic to plastic state and RATIO, which is the portion of incremental strain taken elastically, has to be determined so that

F(SIG + RATIO * DELSIG) = 0

where SIG is the previous stress vector.

c) Redefine TAU as the stress vector at start of yielding as

TAU = SIG + RATIO * DELSIG

d) Compute the elasto-plastic strain increment as

DESIG = Dep * DEPS

e) Evaluate the pseudo-stresses as

D = DELSIG - DESIG

5-4-3 <u>Yielding of Steel:</u> The steel reinforcement is treated as one dimensional and is stressed only along its axis. The behaviour of steel is assumed to be identical in tension and compression. The stress strain curve is assumed linear up to the initial yielding point and from then on it can be idealised as either perfectly plastic or as linearly strain hardening. Aktan & Sozen [25] investigated the behaviour of steel under reversal of strains. A typical stress-strain curve is shown in fig. (5.10). The assumed hysteresis is also indicated in the same figure. In this study the reinforcing bars are assumed uniformely laid over the element. Prior to yielding and for reinforcing bars inclined at an angle ψ to the element x-axis fig. (5.11), the property matrix of steel $D_{\psi s}$ can be written as

$$D_{\psi s} = (T^{-1}) \begin{bmatrix} pEs & 0 & 0 \\ 0 & 0 & 0 \\ 0 & 0 & 0 \end{bmatrix} (T^{-1})^T \qquad 5.28$$

where Es = elasic Young's modulus of steel

p = reinforcement ratio

T = Transformation matrix from material to element axes.

i) Yielding of Steel Reinforcement: As can be seen from eqn. 5.23, $D_{\psi s}$ is only in terms of Es and p. Through the response, p remains unchanged, however Es can take the value of Esh, that is the tangential modulus of steel in the strain hardening range as steel yields.

ii) Rupture of Steel: As steel bars reach their ultimate strain, they rupture and their property matrix $D_{\psi s}$ is disregarded

$$D_{\psi s} = 0 \qquad 5.29$$

iii) Hysteresis Modes and Flow Chart: A flag IBAR is chosen to monitor the changes in element reinforcement during the step-by-step analysis. To initiate analysis, IBAR is set equal to unity (elastic) for all elements. IBAR is allowed however to take any integer value from 1 to 6. The significance of each value is illustrated by fig. (5.12) and a computer directed flowchart of the hysteresis is given in fig. (5.13).

5-4-4 Composite Material: The composite material property matrix D of a reinforced concrete plane stress element can be obtained at any stage by adding the instantaneous material property matrix Dc or Dcr depending on whether concrete is uncracked or cracked respectively to the material property matrix of steel Ds which can be in terms of Es or Esh or null as discussed in section 5.4.3. Then,

$$D = D_C + D_{\psi s} \qquad 5.30$$

Obviously if another set of reinforcing bars is placed at an angle φ of the element axis , then

$$D = D_C + D_{\psi s} + D_{\varphi s} \qquad 5.31$$

Note that Dc may be equal to Dcr if concrete is cracked.

5-5 Beam Element Consideration

Because a relatively accurate prediction of plastic deformation and ductility demand is of paramount importance in the nonlinear response of coupled shear walls, the mechanical model simulating the coupling beams behaviour must be carefully chosen. The model should be experimentally tested and capable of taking into account the important features of reinforced concrete subjected to dynamic loading such as stiffness degradation or strain hardening if need be. The multicomponent model [22] is advantageous in two ways. First, the element stiffness matrix is easily formulated since the end rotations of all components are assumed the same, and secondly the yield condition at one end of the member depends on the conditions at both ends. However the incapability of this approach to simulate stiffness degradation [97] makes it unsuitable for this study. The advantages and drawbacks of the layering model [28] have already been discussed in chapter I.

In this investigation, the single component model developed by Giberson [21] is used. In this model each element is represented by an elastic beam element with inelastic rotational springs (hinges) at its two ends fig. (5.14a). These inelastic springs simulate the inelastic flexural deformations over the length of the member. The characteristics of the two hinges are derived from the assumptions made by Otani [24] that the beam deforms antisymmetrically in bending as shown in fig. (5.14b) and produces a point of contraflexure at the midpoint. These assumptions allow the beam behaviour to be approximated by two cantilever beams whose free ends coincide with the point of contraflexure. The moment-rotation hysteresis is assumed to follow an extended version of Takeda's model [29] and is shown in fig. (5.15). The numbers on the arms (fig. 5.15) stand for the rules which define the model and monitor each element at any stage of the response. The basic moment-rotation relationship assumed in this study is bilinear with an initial stiffness and subsequent strain hardening.

The degrading stiffness of the hinges is induced when reversal of loading is applied through the factors α and β (fig. 5.15).

The assessment of the actual initial stiffness is one of the most important steps of the analysis and special care should be exercised to ensure that a reasonable rigidity is used. The actual original stiffness of a reinforced concrete member is greatly influenced by the amount of cracking that has taken place. In the case of flexural stiffness, the cracking effect can be evaluated using the moment of inertia of the transformed cracked section ignoring tensile strength of concrete. The actual rigidity EIa can be written as

$$EI_a = (EI_e)\,\Theta_{cr} \qquad 5.32$$

in which EIa = actual rigidity

EIe = elastic rigidity

Θcr = factor representing the effect of cracking

The factor θ_{cr} varies with the amount of reinforcement. Its variation was conveniently given in reference [98]. A typical idealised moment - rotation relationship can be based on the elastic rigidity EIe or the cracked rigidity EI_{cr}. It may be worth noting however that tests performed by Abrams and Sozen [101] have shown that the actual rigidity can even be smaller than EIa fig. (5.17). This is explained by the additional rotation that bond slip enforces upon the member. The influence of this effect is considered separately and is discussed later in this section.

Initially the incremental moments DMi and DMj at the two ends i & j of a beam element are related to the incremental rotations Dθi and Dθj by

$$\begin{Bmatrix} D\Theta_i \\ D\Theta_j \end{Bmatrix} = F \cdot \begin{Bmatrix} DM_i \\ DM_j \end{Bmatrix} \qquad 5.33$$

where F is the flexibility matrix of the beam. For a uniform beam element

$$F = \begin{bmatrix} f11 & f12 \\ \text{symmetric} & f22 \end{bmatrix} \qquad 5.34$$

$f11 = f22 = L/3EI$

$f21 = f12 = -L/6EI$

EI = actual initial beam rigidity

L = beam length

5-5-1 Spring Nonlinearities Contribution: Prior to yielding, the spring stiffness Ki at end i is given a very big value to ensure it is essentially rigid. After the first yield, Ki takes its value according to the hysteresis rule. At any increment, the instantaneous hinge flexibility 1/Ki is added to the flexibility matrix given in eqn. 5.34. Similar procedure is followed for end j. Eqn. 5.34 can then be written as

$$F = \begin{bmatrix} f11+1/Ki & f12 \\ \text{symmetric} & f22+1/Kj \end{bmatrix} \qquad 5.35$$

5-5-2 Shear Deformation Contribution: Little work has been done to assess the inelastic shear deformations of reinforced concrete. The existing experimental data are very scattered [33, 34, 93-95]. Therefore it is usual practice to simply reduce the elastic shear stiffness. Taking shear deformations into account, the instantaneous flexibility matrix (eqn. 5.35) becomes

$$F = \begin{bmatrix} f11+1/Ki+1/k\alpha GAL & f12+1/k\alpha GAL \\ \text{symmetric} & f22+1/Kj+1/k\alpha GAL \end{bmatrix} \qquad 5.36$$

in which k = shape factor for shear deformation

AG = Shear rigidity

l = beam length

α = reduction factor (=1 in elastic range)

The shear modulus G can be computed in terms of elastic Young's modulus Ec and Poisson's ratio μ as

$$G = Ec/2(1+\mu) \qquad 5.37$$

5-5-3 Bond Slippage Contribution: The existence of cracks with finite width, spaced at finite distances in the tension zone of a beam subjected to flexure corresponds physically to a slip between steel and concrete. This phenomenon is usually referred to as ' bond slip '. The rotation due to bond slip of the tensile reinforcement of a coupling beam along its embedded length yields an additional flexibility factor for the nonlinear spring to be added to eqn. 5.36. Bond stress is assumed to be constant along the embedded length of the reinforcing bar and the steel stress to decrease linearly with distance in from the wall face fig. (5.16). It is also assumed that the reinforcement length of embedment is sufficient to provide the maximum tensile stress that occurs in the response. The relationship between steel stress and bond stress is given by the axial equilibrium condition as

$$\tau_b = (As\ Fs) / (\pi \phi L) \qquad 5.38$$

in which τ_b = average bond stress

As = cross sectional area of reinforcement

Fs = stress of reinforcement at the face of wall

L = development length

ϕ = diameter of reinforcing bar

Nilson [99] defined the slip as the relative longitudinal displacement between the concrete and the reinforcing steel, as indicated by DL in fig. (5.16). DL depends on the state of stress of reinforcement Fs. Therefore two cases need to be considered depending on whether or not Fs has exceeded the yield stress fy [100].

$$DL = \frac{L\,Fs}{2\,Es} \quad ; \qquad Fs \leq f_y \qquad 5.39a$$

$$DL = fy^2 L/2FsEs + (1-fy/Fs)\,(fy/Es+(fs-fy)/2Ey)\,L; \qquad Fs > f_y \qquad 5.39b$$

where Es = Young's modulus of steel

Ey = modulus of steel at yield

fy = yield stress of steel reinforcement

Replacing As by its value ($\pi\phi^2/4$) and substituting the value of L from eqn. 5.38 into eqns. 5.39, the latters become

$$DL = \phi Fs^2 / 8Es\tau b \; ; \qquad Fs \leq fy \qquad 5.40a$$

$$DL = (\phi/4\tau b)[(Fs-fy/2)(fy/Es)+(fs-fy)^2/2Ey); \qquad Fs > f_y \qquad 5.40b$$

however, because the stress of reinforcement at yield does not differ substantially of that at yield, the elongation DL defined by eqn. 5-40a is assumed for both cases in this study. Assuming that the rotation axis due to slippage of tensile reinforcement is at the level of compressive reinforcing steel fig. (5.16), it follows

$$R_{slip}(M) = \frac{DL}{(d-d')} \qquad 5.41$$

in which d = depth of tensile reinforcement

d'= depth of compressive reinforcement

Assuming the tensile reinforcement proportional to the applied moment M, one can write

$$\frac{Fs}{M} = \frac{f_y}{My} \qquad 5.42$$

in which My = moment at yield

M = applied moment

Substituting Fs from eqn. 5.42 and DL from eqn. 5.40a into eqn. 5.41 yields

$$R_{slip}(M) = (\Theta/8EsTb)\,(fy/My)^2\,(M^2/(d-d')) \qquad 5.43$$

For a bilinear idealisation for the moment - rotation relationship, the instantaneous flexibility due to slip rotation is then computed as

$$fs(M) = R_{slip}(My)/My \qquad M \leq My \qquad 5.44a$$

$$fs(M) = (R_{slip}(Mu) - R_{slip}(My)) \,/\, (Mu-My) \qquad M > My \qquad 5.44b$$

where $f_s(M)$ = flexibility due to bond slippage

My , Mu = moment at yield and ultimate moment respectively

then the incremental rotation of the spring due to bond slippage can be axpressed as

$$D\Theta_{slip} = fs(M).DM \qquad 5.45$$

and hence the overall flexibility matrix (eqn. 5.36) becomes

$$F = \begin{bmatrix} f11+1/Ki+1/k\alpha\,GAL+F(Mi) & f12+1/k\alpha\,GAL \\ \text{symmetric} & f22+1/Kj+1/k\alpha\,GAL+f(Mj) \end{bmatrix} \qquad 5.46$$

DESCRIPTION	KODE	DESIGNATION
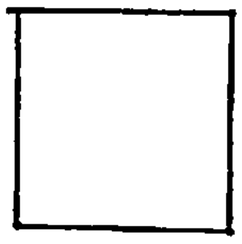	0	Uncracked concrete
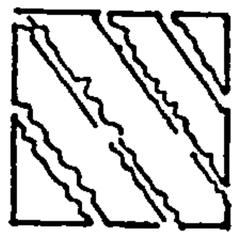	1	Crack 1 due to σ_1 opens
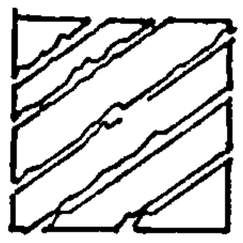	2	Crack 2 due to σ_2 opens
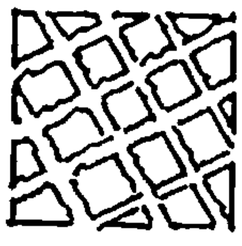	3	2 sets of cracks 1 & 2
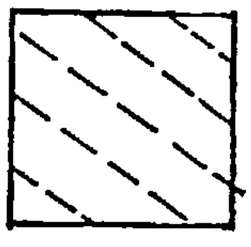	4	1 closes 2 still intact
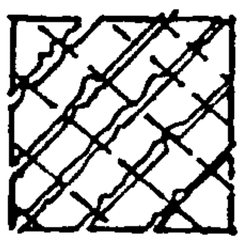	5	1 closes 2 still open
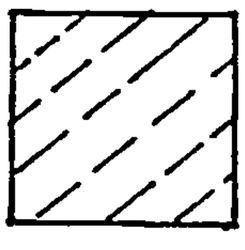	6	1 intact 2 closes
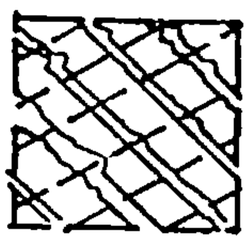	7	1 opens 2 still closed
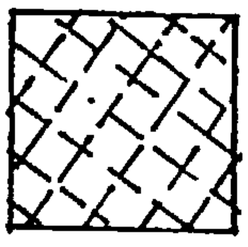	8	1 closed 2 closed

TABLE 5.1 CRACK MODES IN CONCRETE ELEMENTS

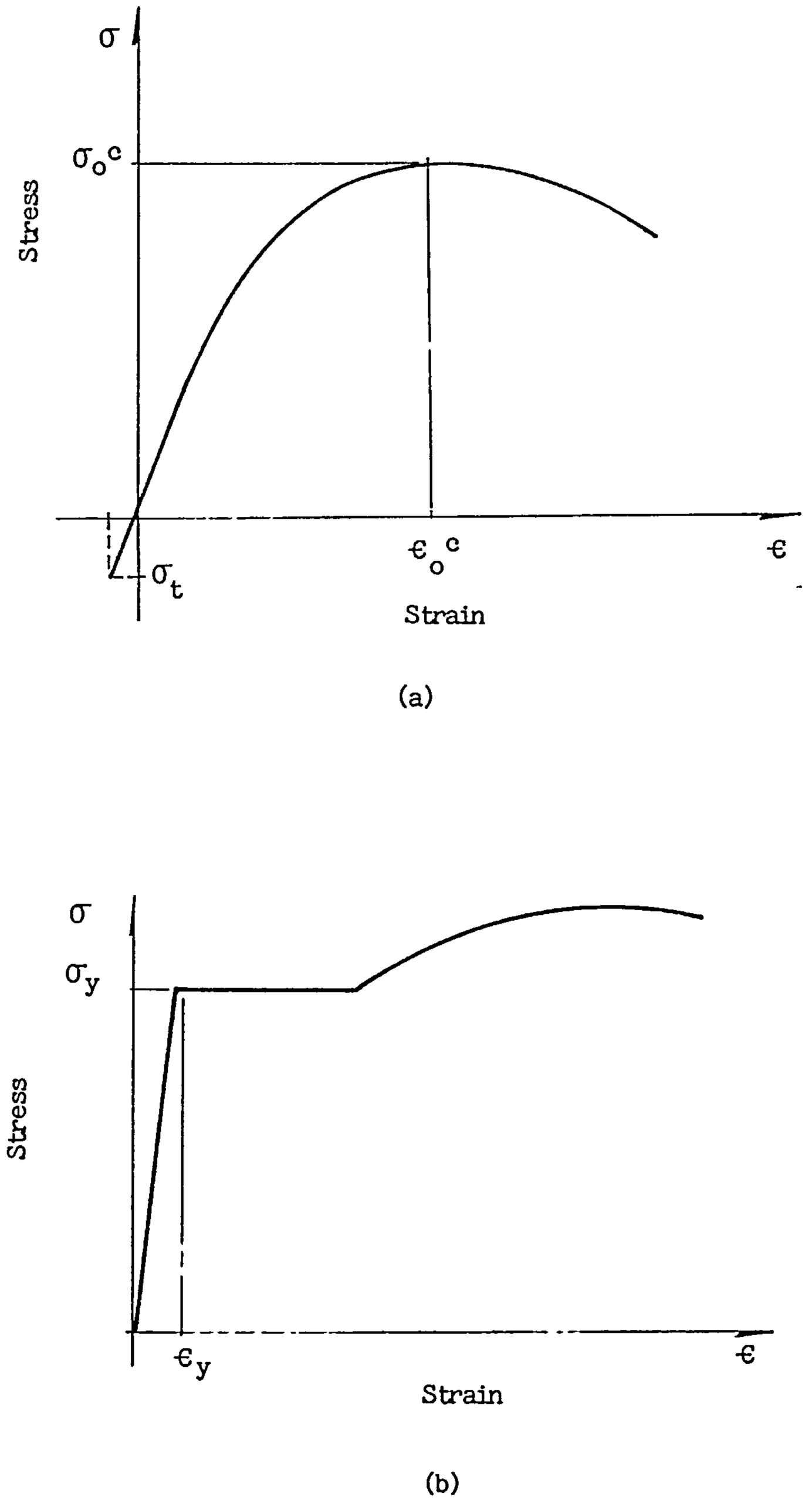

FIG. 5.1 a) TYPICAL UNIAXIAL STRESS-STRAIN FOR CONCRETE

b) TYPICAL STRESS-STRAIN FOR REINFORCEMENT

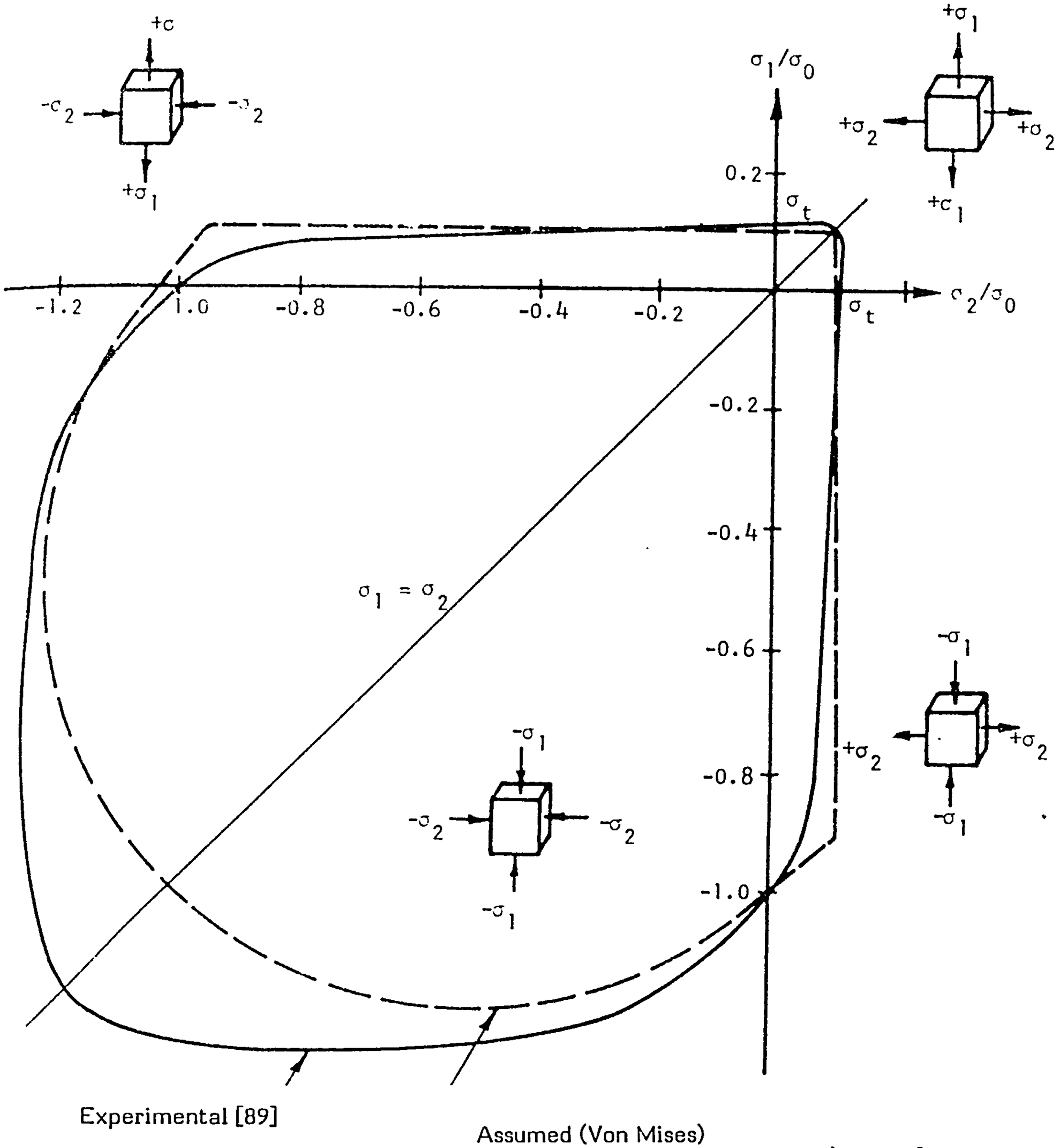

$$F(\sigma) = \sigma x^2 + \sigma y^2 - \sigma x\,\sigma y + 3\,\tau xy - \sigma o^2$$

FIG. 5.2 BIAXIAL STRENGTH OF CONCRETE

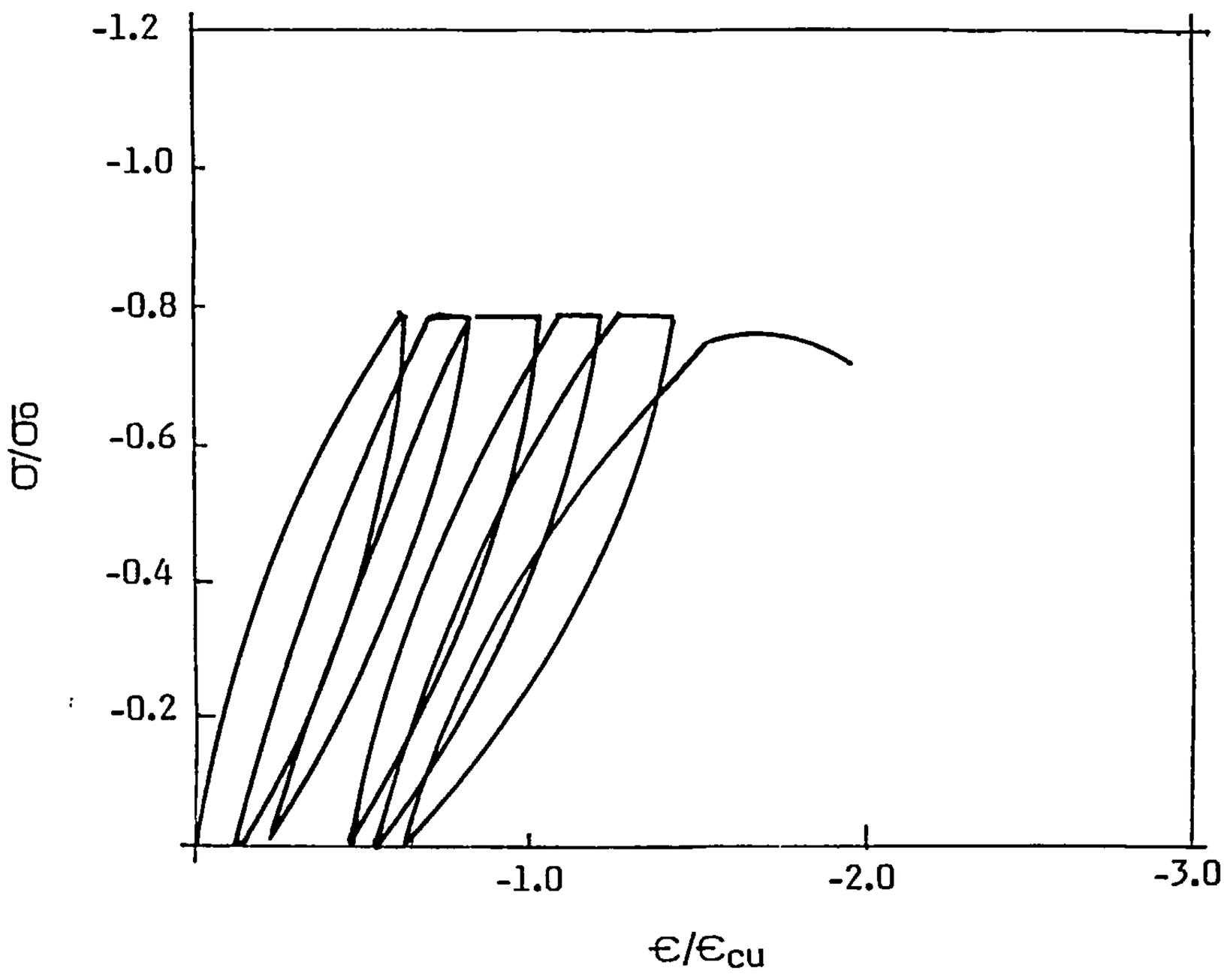

FIG. 5.3 TYPICAL CYCLIC UNIAXIAL STRESS-STRAIN FOR CONCRETE

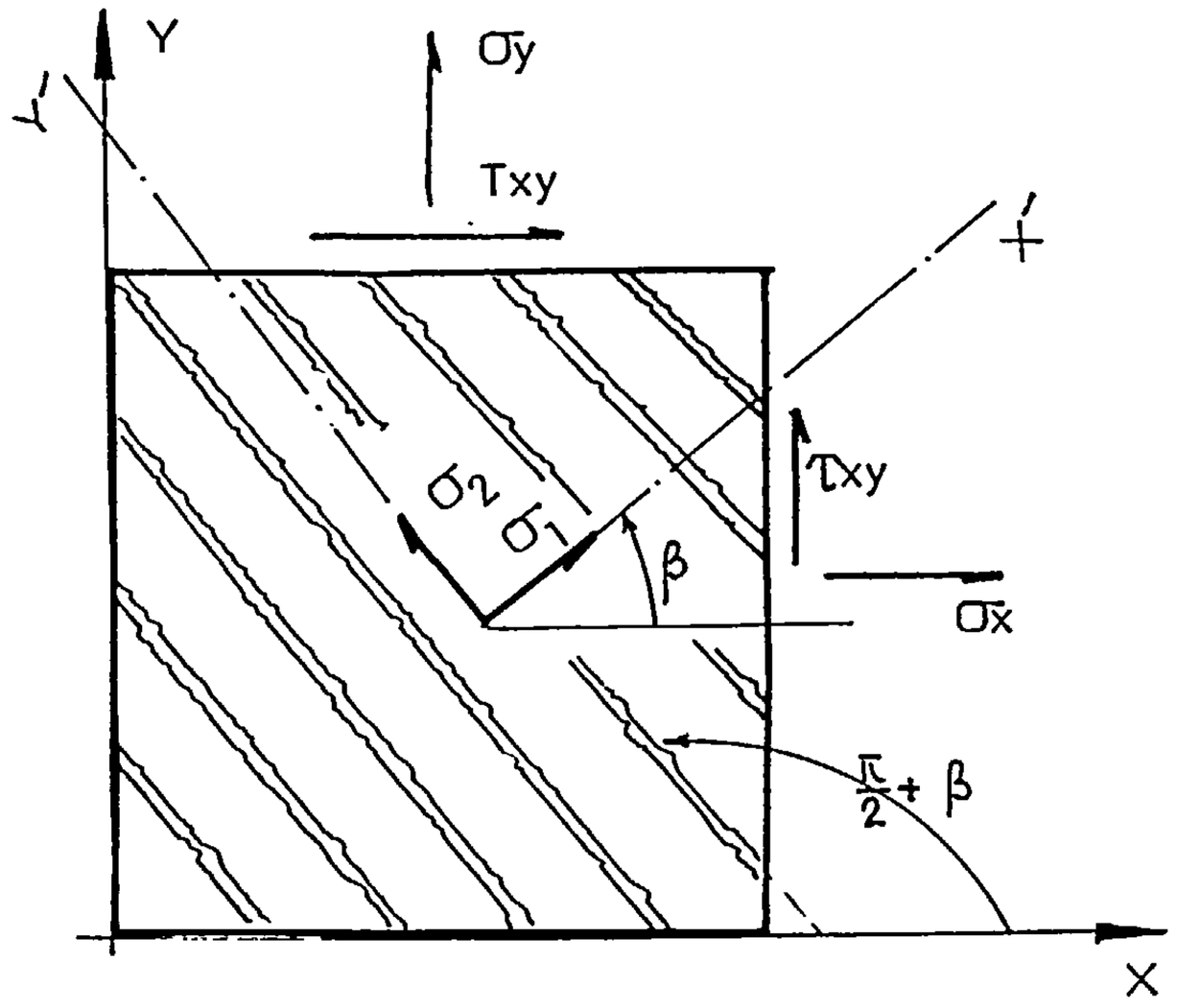

FIG. 5.4 CRACKING PHENOMENON AND PRINCIPAL STRESSES

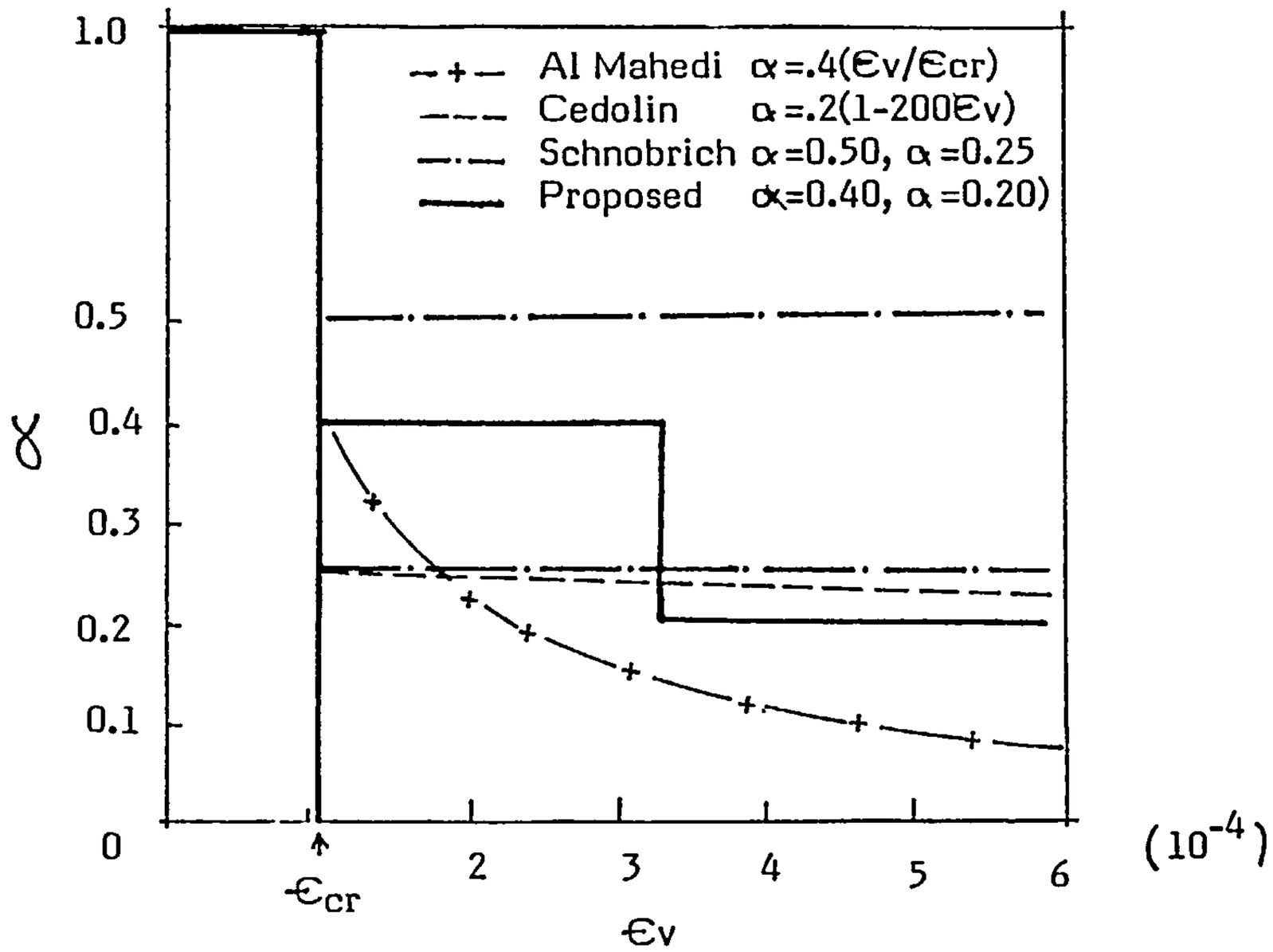

FIG. 5.5 SHEAR STIFFNESS REDUCTION IN CRACKED CONCRETE

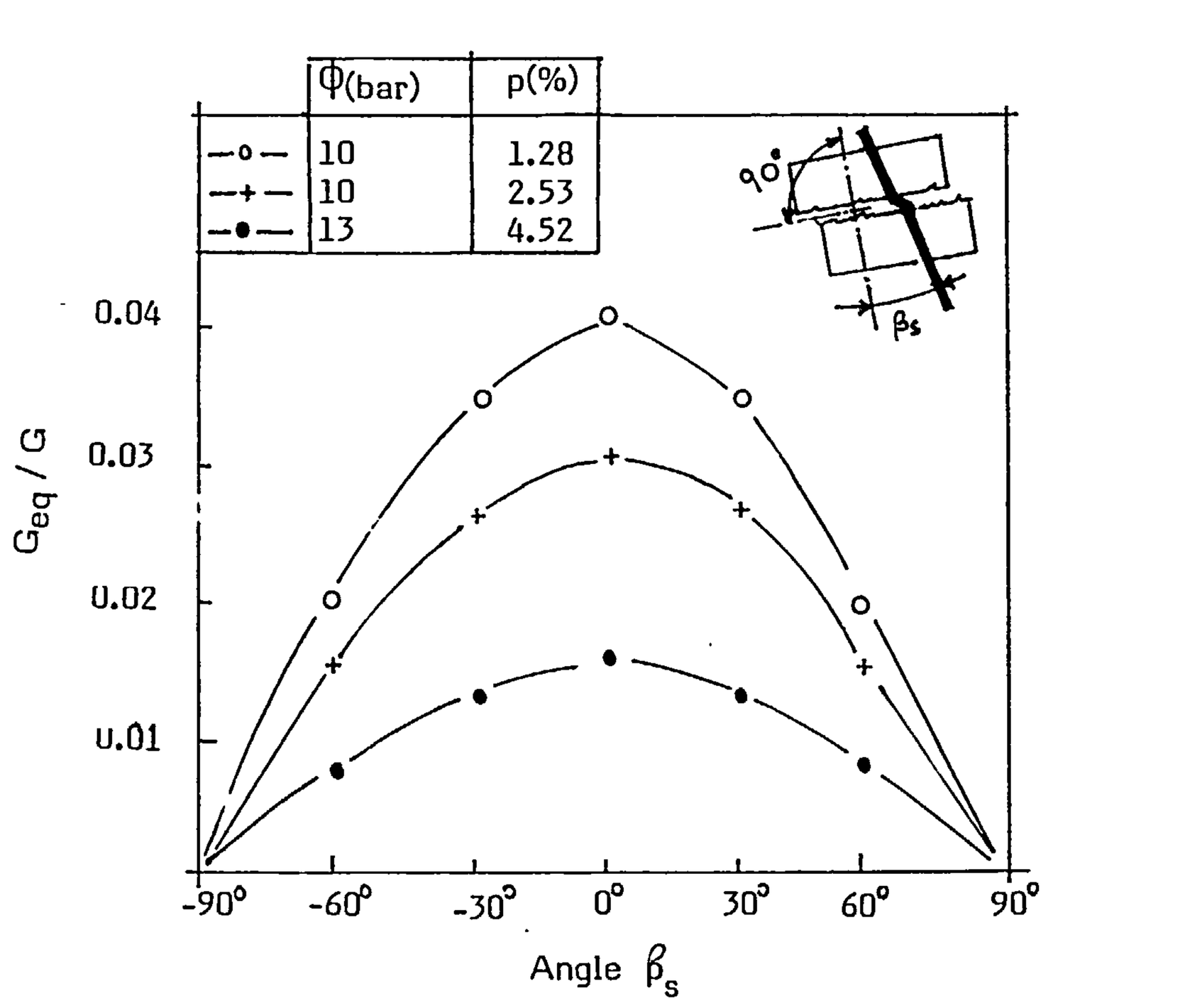

FIG. 5.6 SHEAR STIFFNESS DUE TO DOWEL ACTION

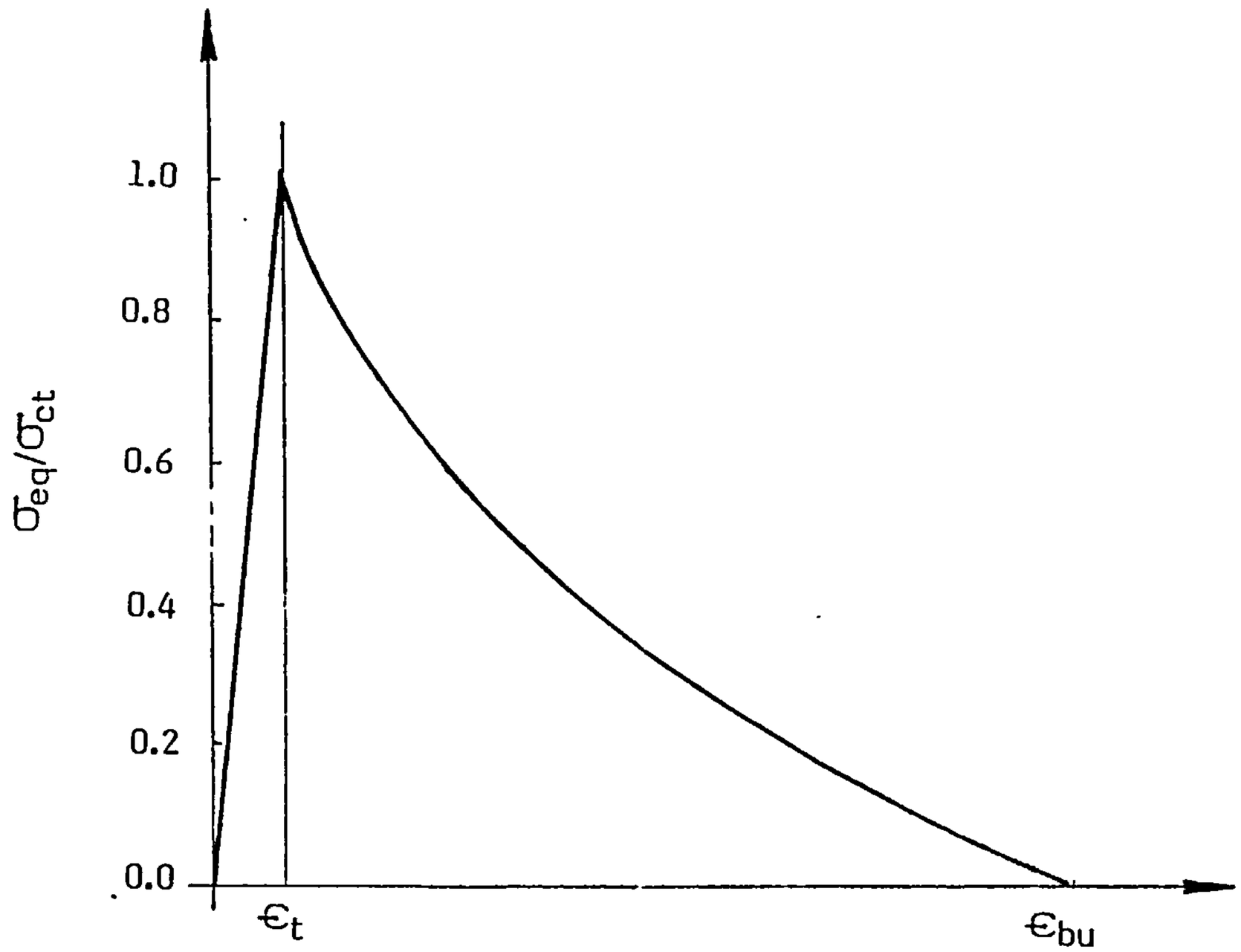

FIG. 5.7 TYPICAL TENSION STIFFENING EFFECT

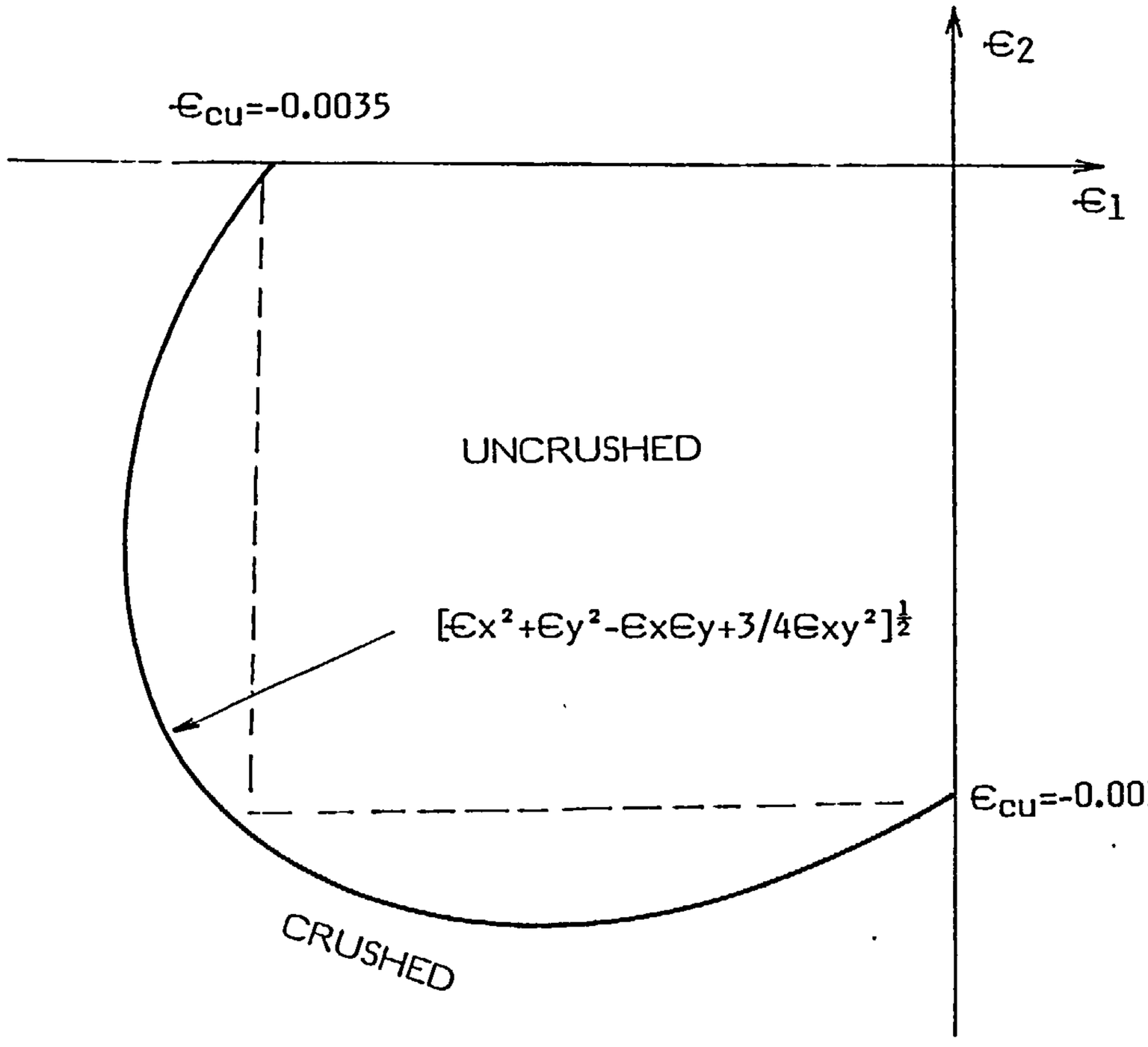

FIG. 5.8 ASSUMED BIAXIAL COMPRESSIVE STRAIN FOR CONCRETE

FIG. 5.9 FLOW CHART FOR OPENING AND CLOSING OF CRACKS IN CONCRETE

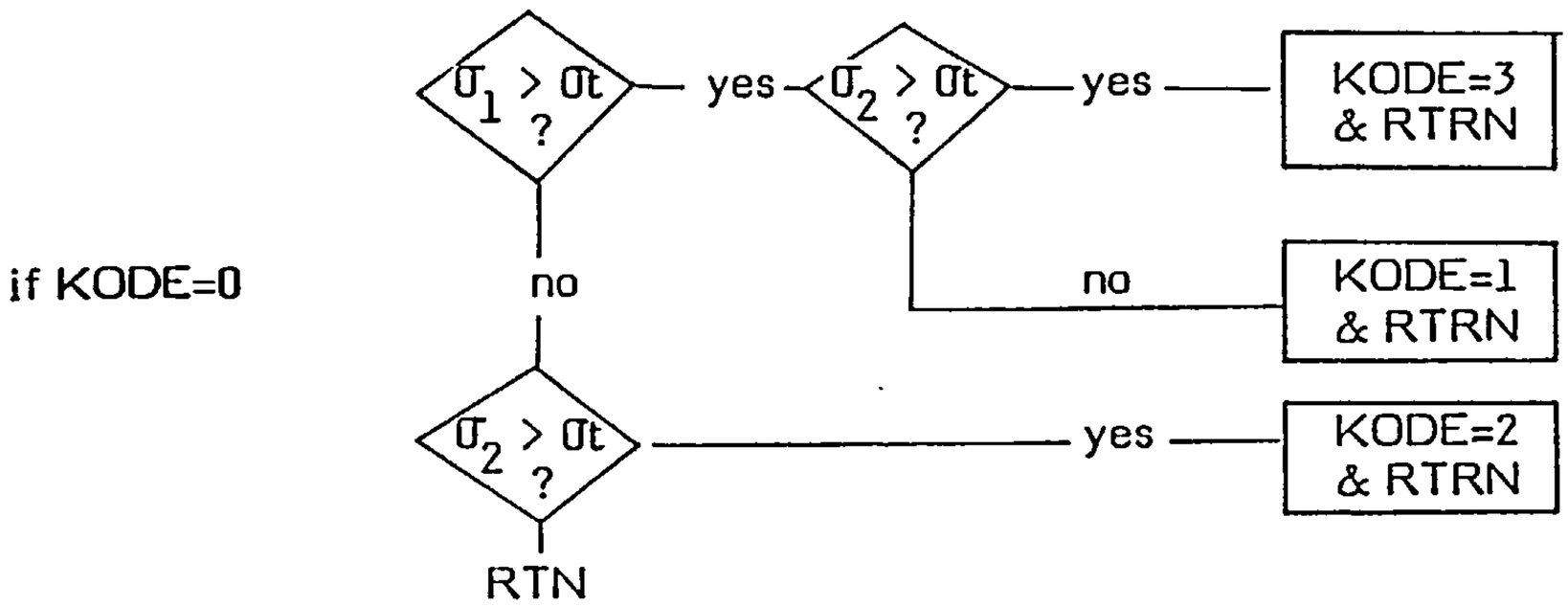

GO TO (1,2,3,4,5,6,7,8), KODE

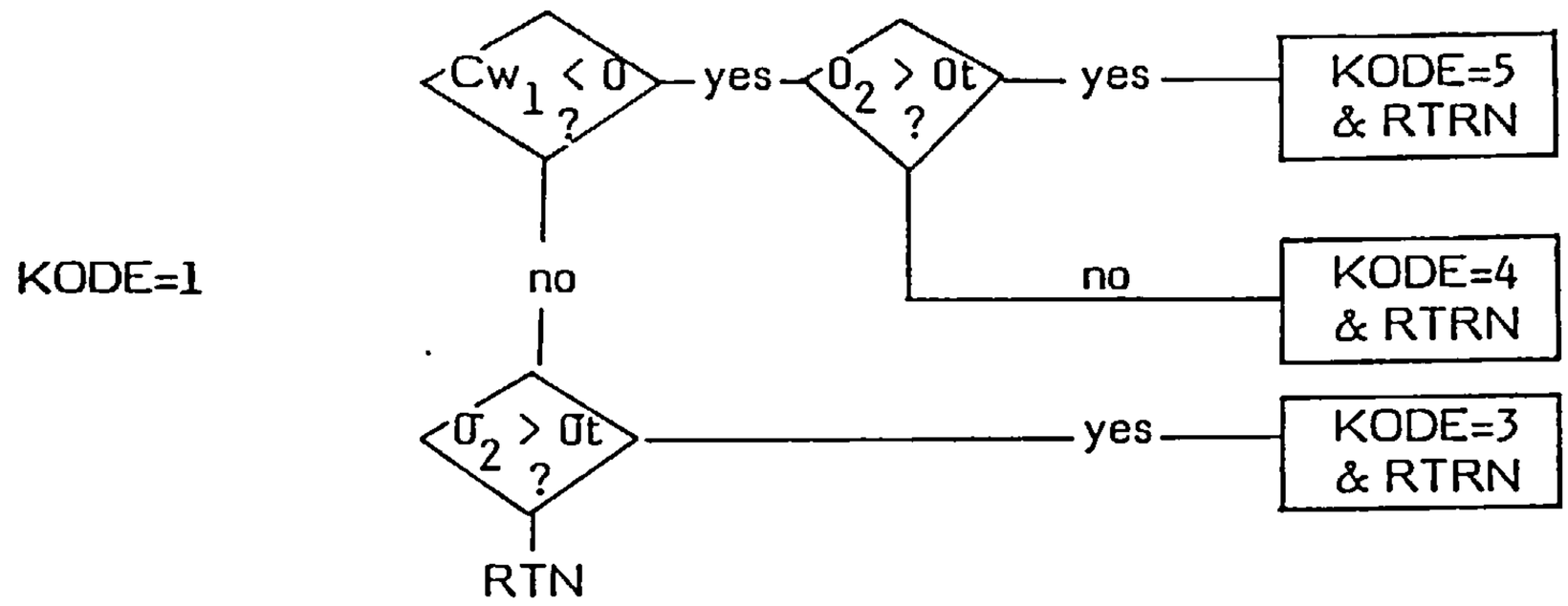

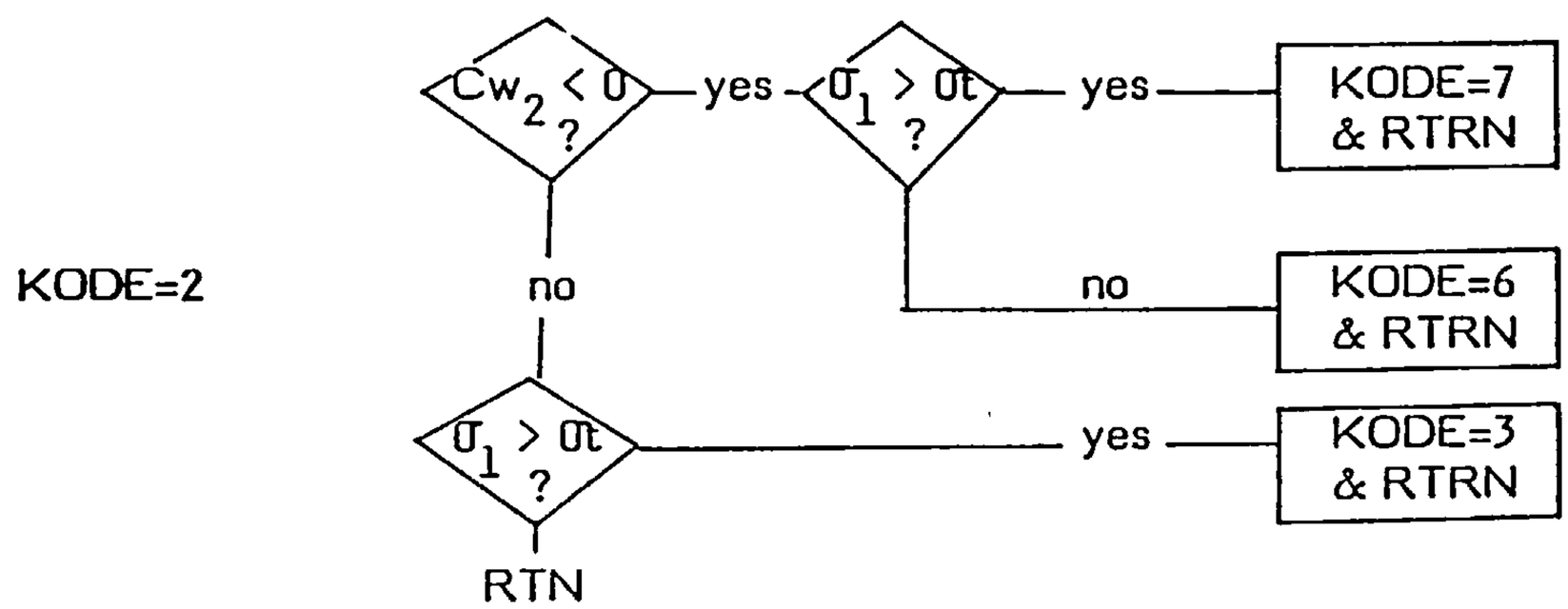

FIG. 5.9 (c'd) FLOW CHART FOR OPENING AND CLOSING OF CRACKS IN CONCRETE

KODE=3

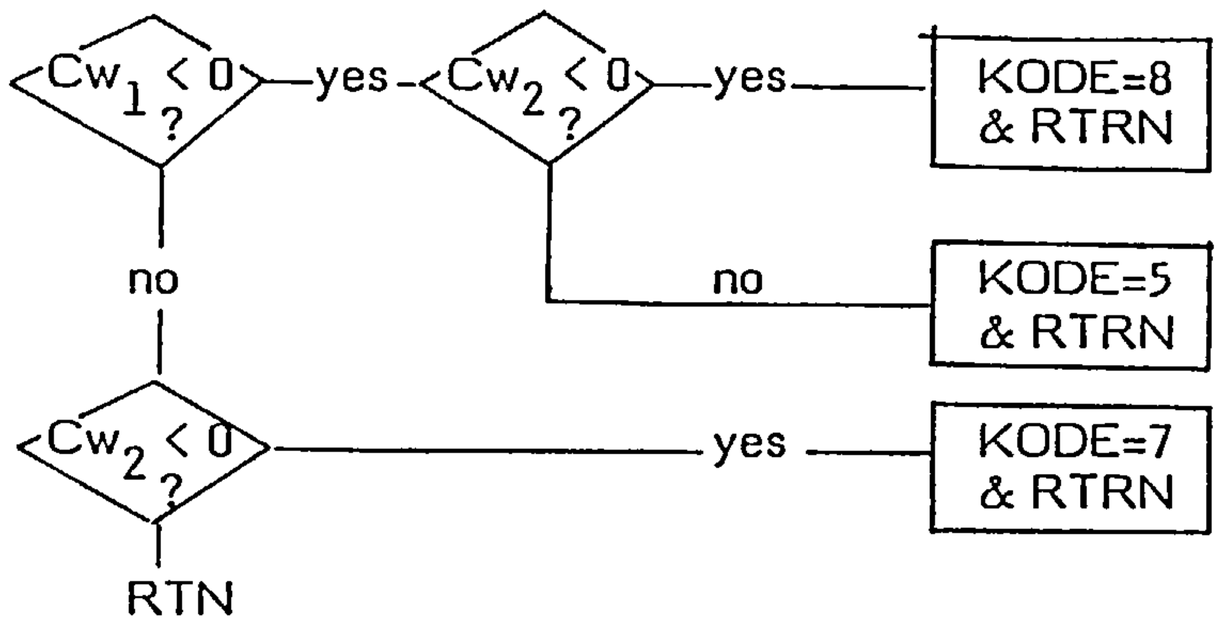

KODE=4

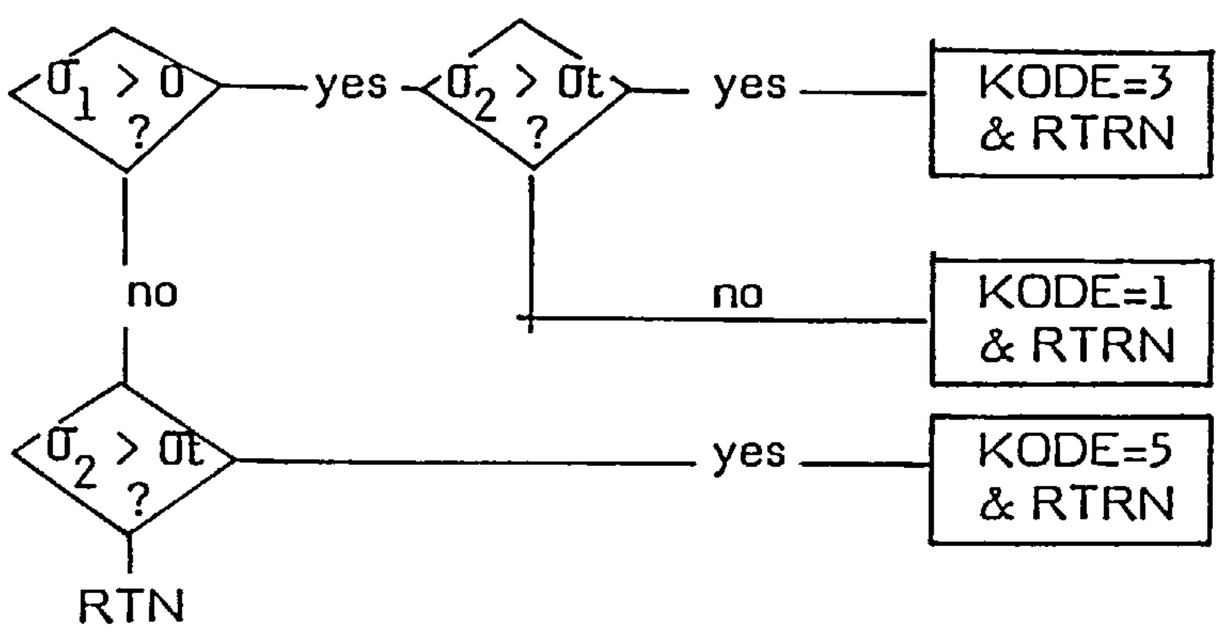

KODE=5

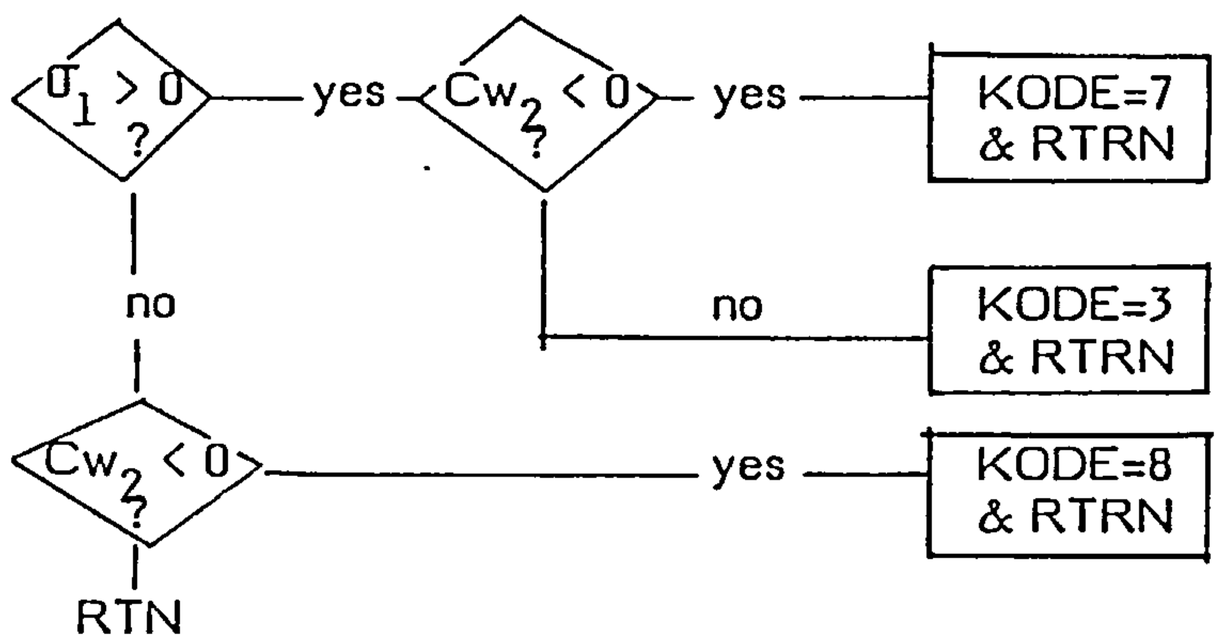

KODE=6

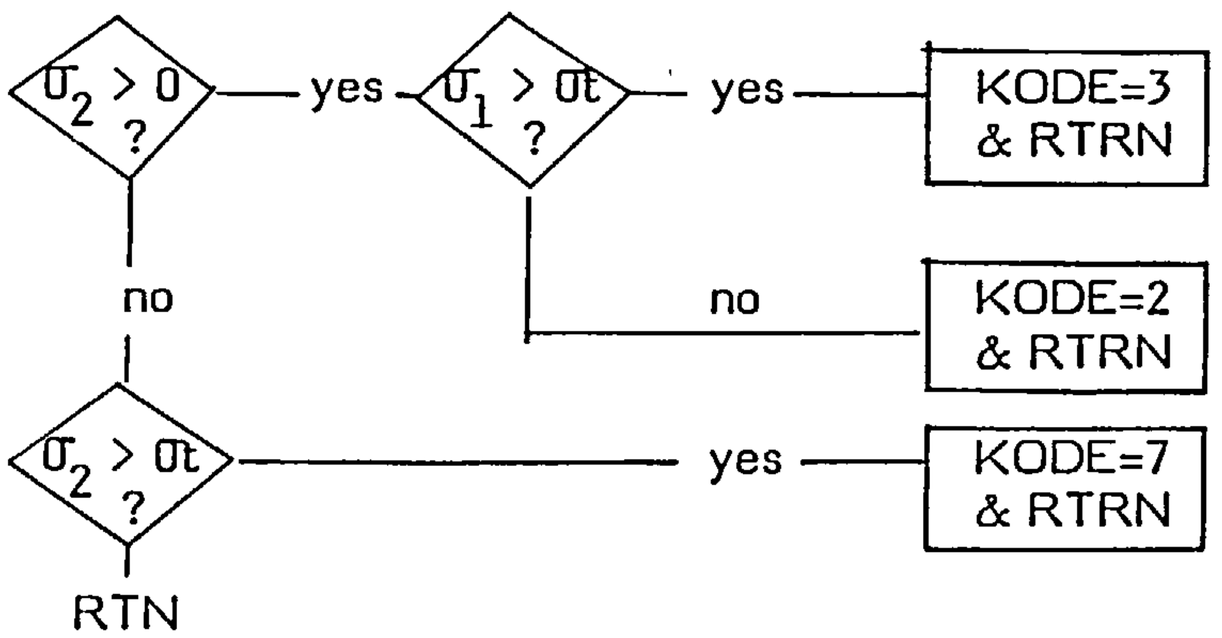

FIG. 5.9 (c'd) FLOW CHART FOR OPENING AND CLOSING OF CRACKS IN CONCRETE

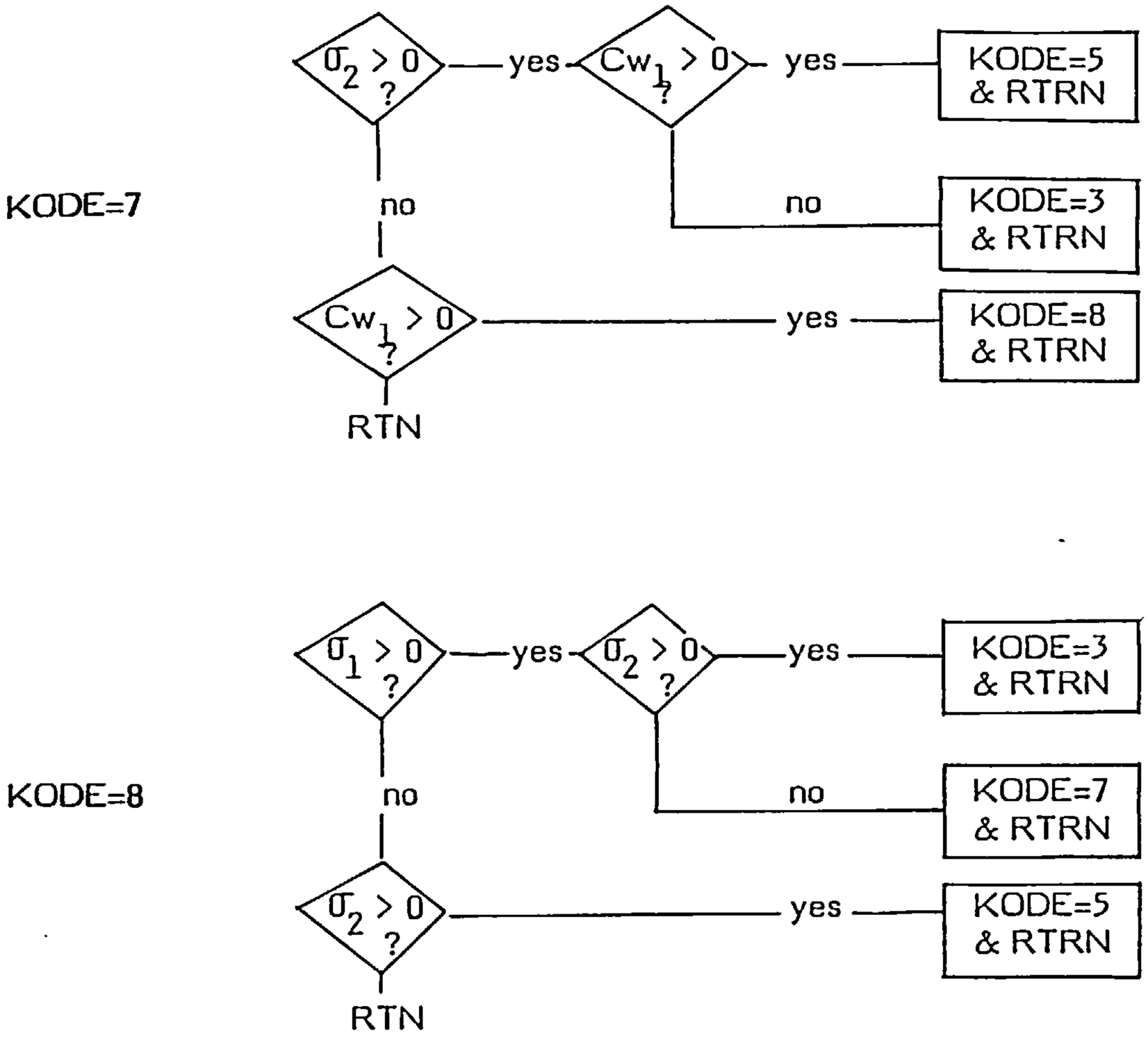

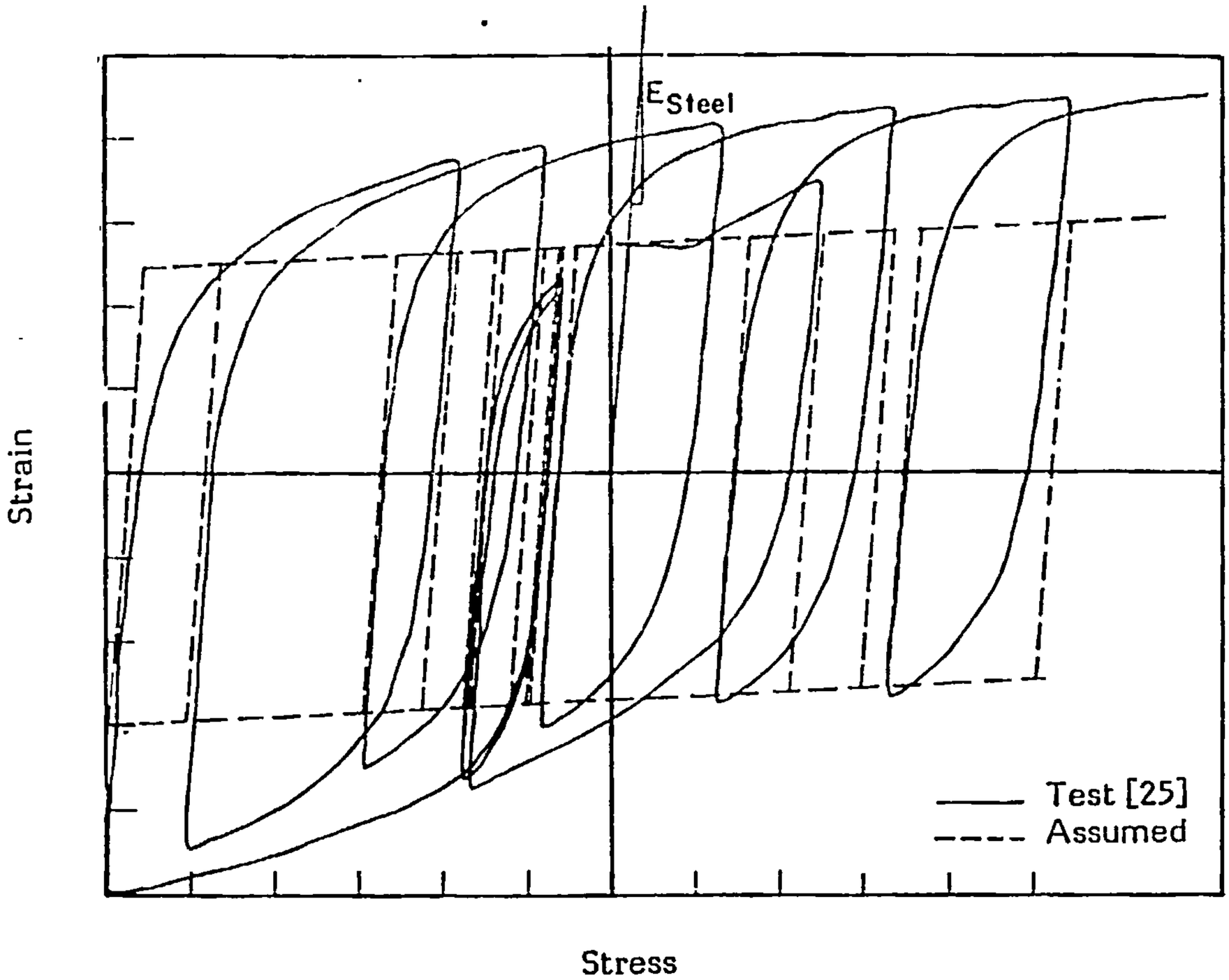

FIG. 5.10 TYPICAL HYSTERESIS STRAIN-STRESS FOR REINFORCEMENT

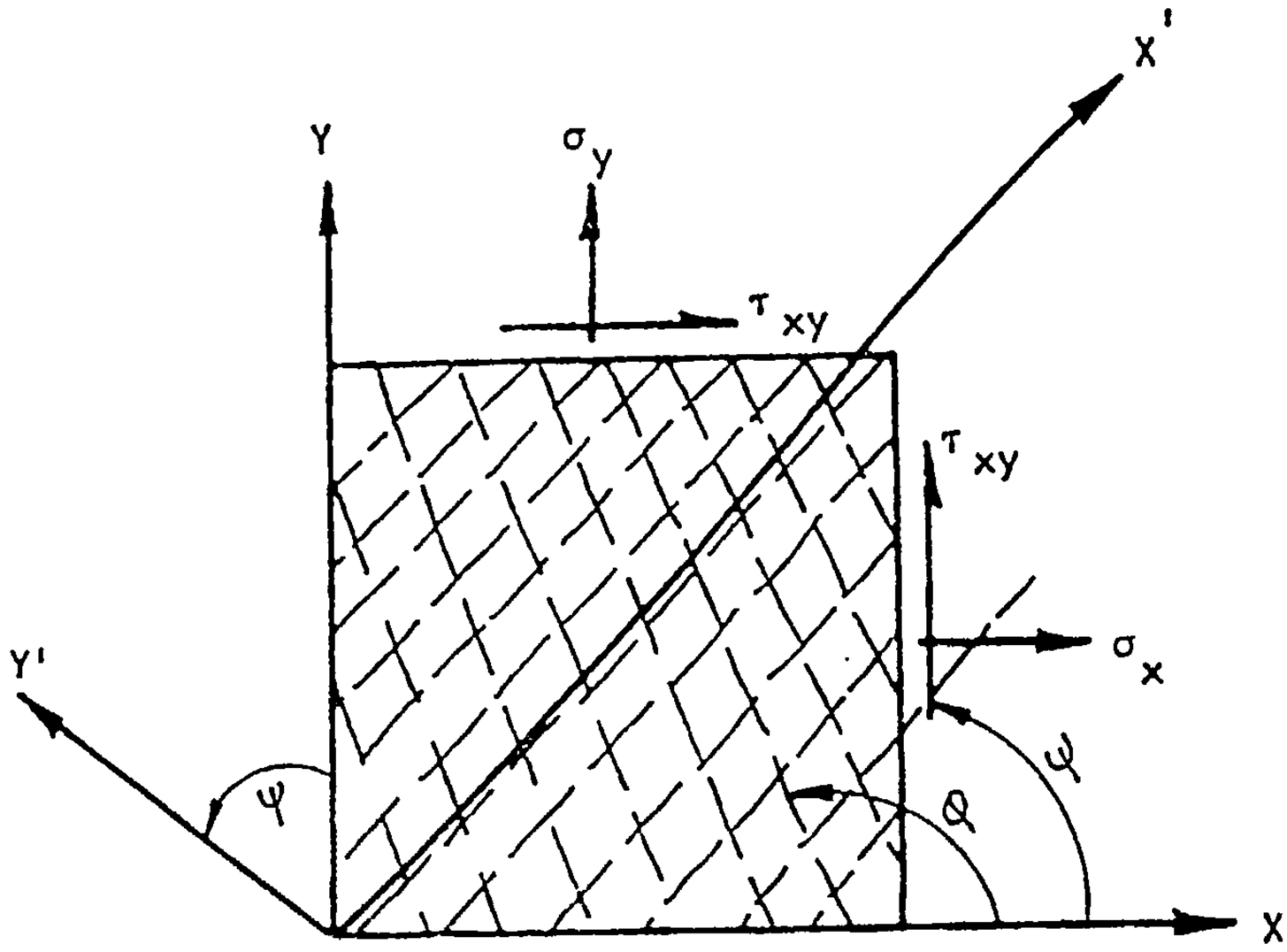

FIG. 5.11 DISTRIBUTION OF REINFORCING BARS

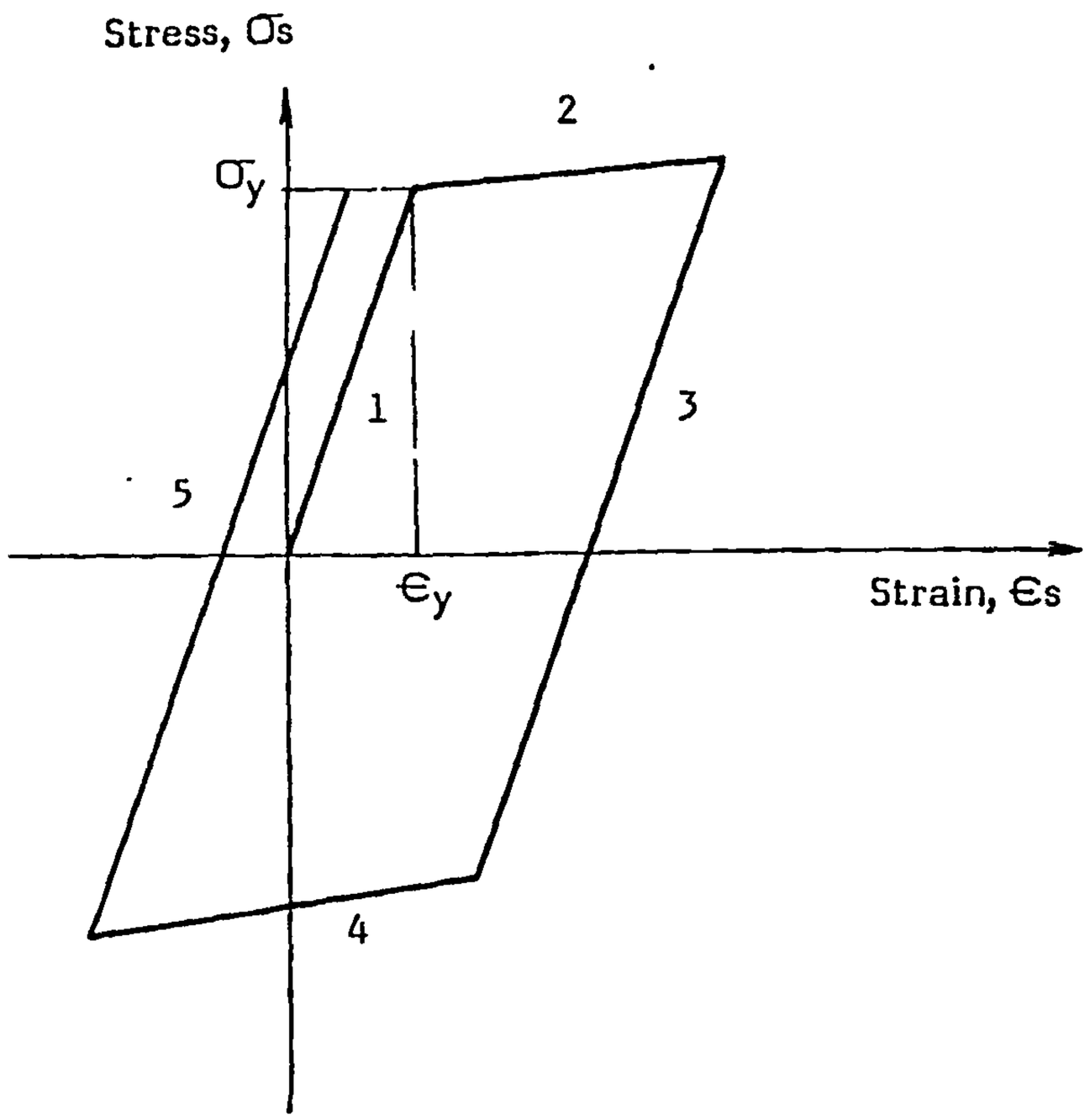

FIG. 5.12 HYSTERESIS OF REINFORCING BARS

FIG. 5.13 FLOW CHART FOR STRESS-STRAIN HYSTERESIS OF STEEL BARS

NOTATIONS:

ϵ_y= strain at yield
ϵ_t= strain at previous step
$\epsilon_{(t+dt)}$= current strain
Es= elastic Young's modulus of steel
Esh= Young's modulus of steel after yield

GO TO (1, 2, 3, 4, 5, 6), KBAR

KBAR=1

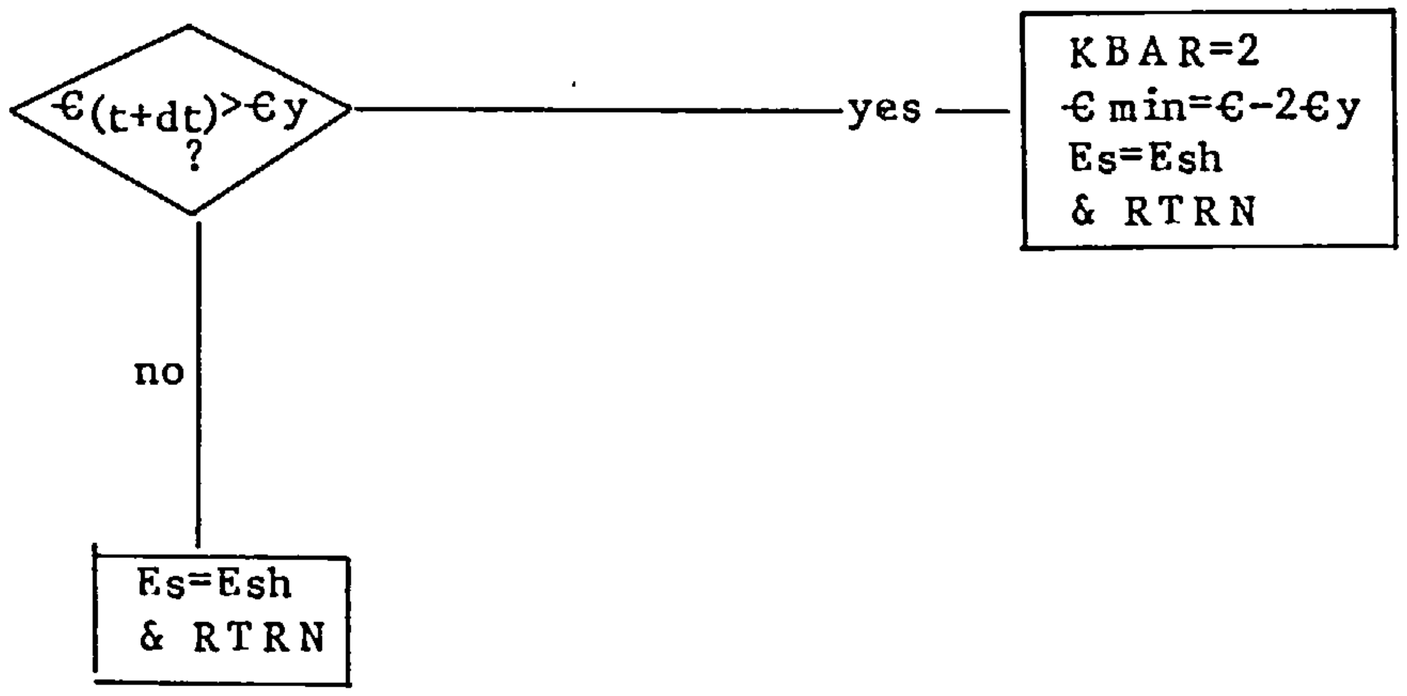

KBAR=2

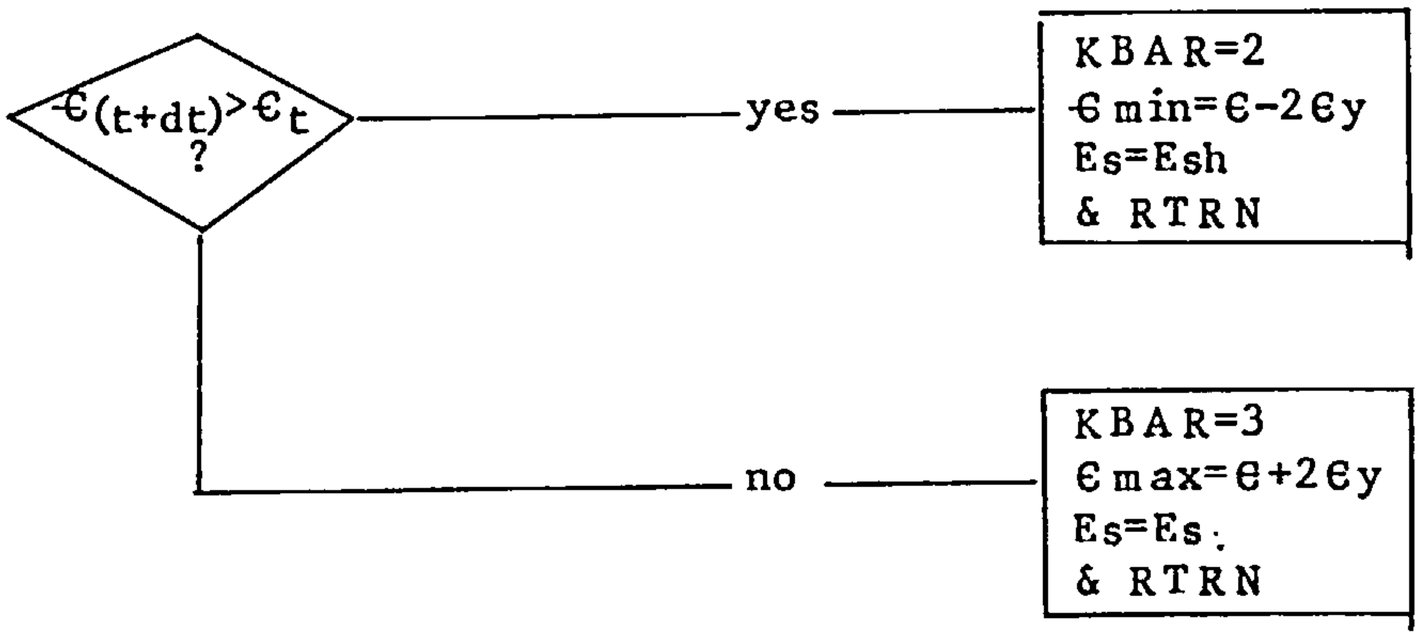

FIG. 5.13 (cont'd) FLOW CHART FOR STRESS-STRAIN HYSTERESIS OF STEEL BARS

KBAR=3

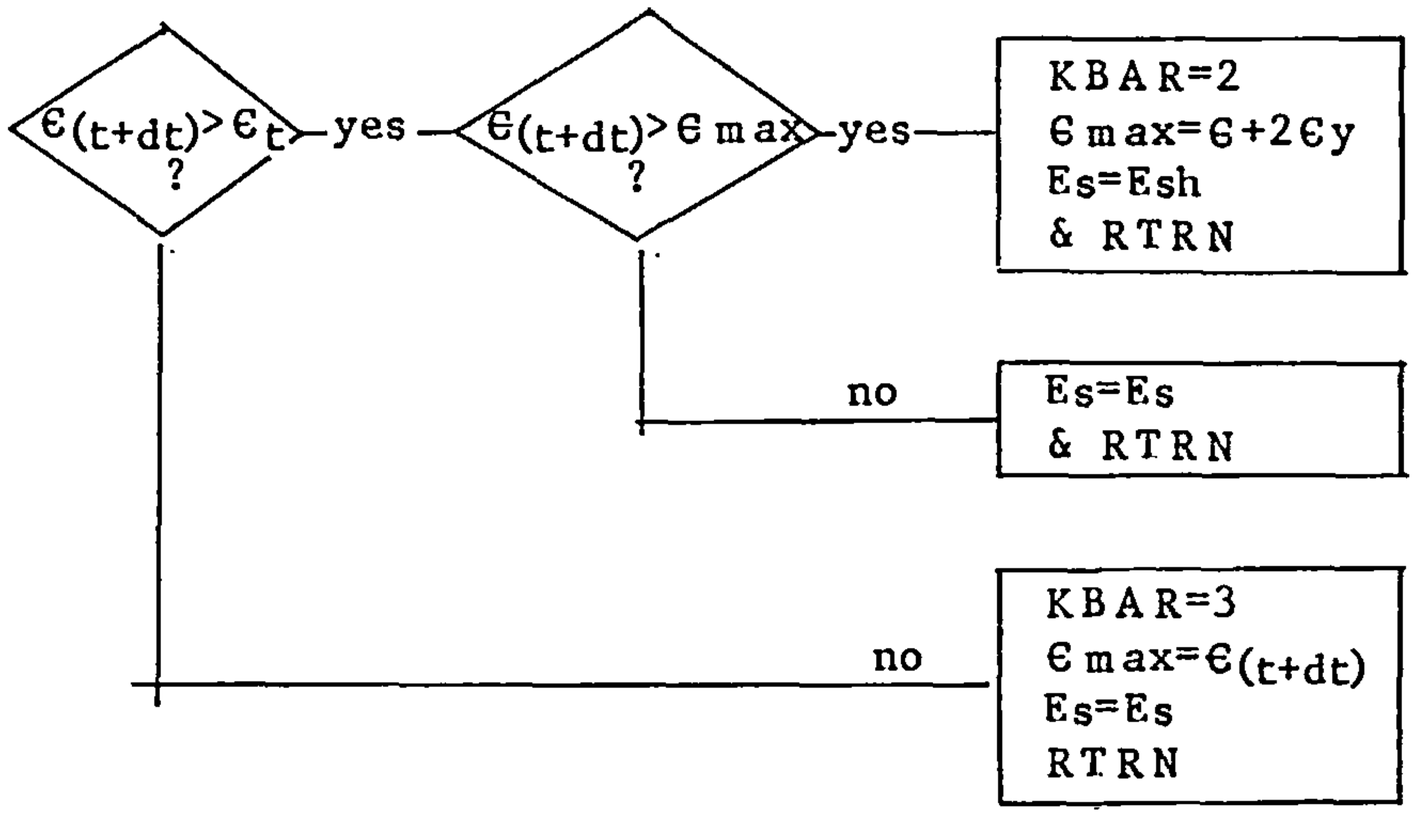

KBAR=4

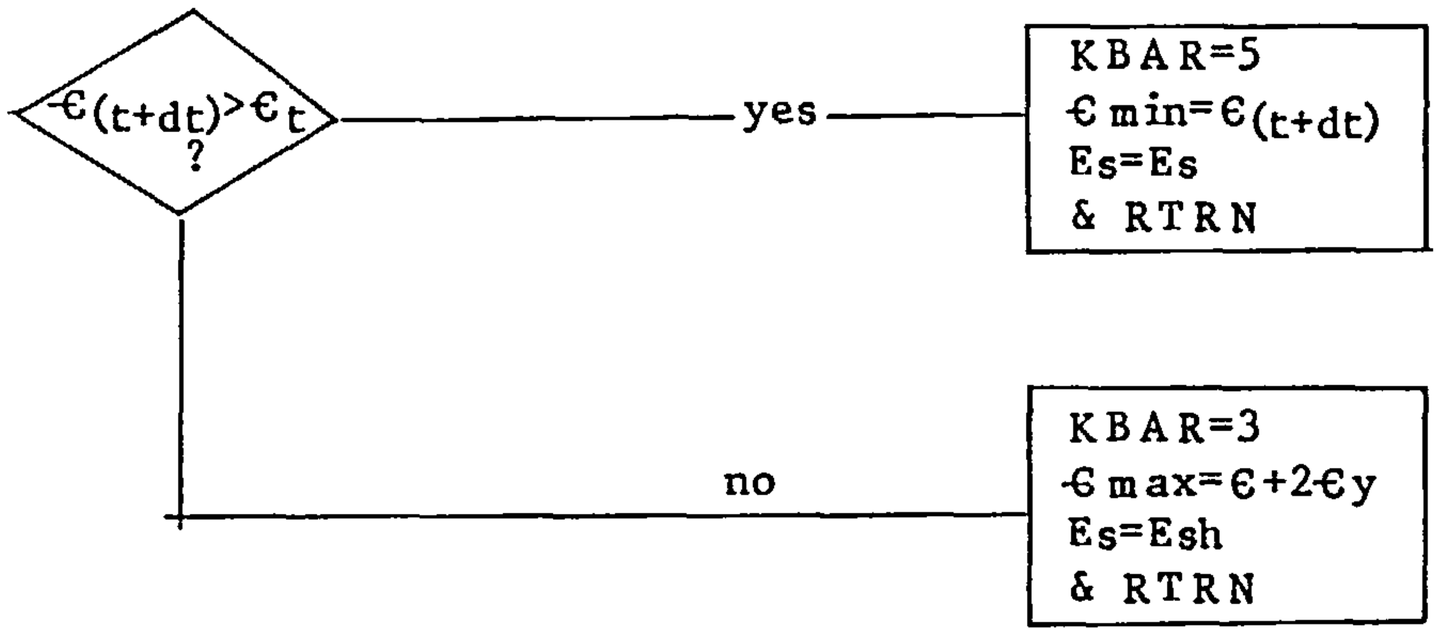

KBAR=5

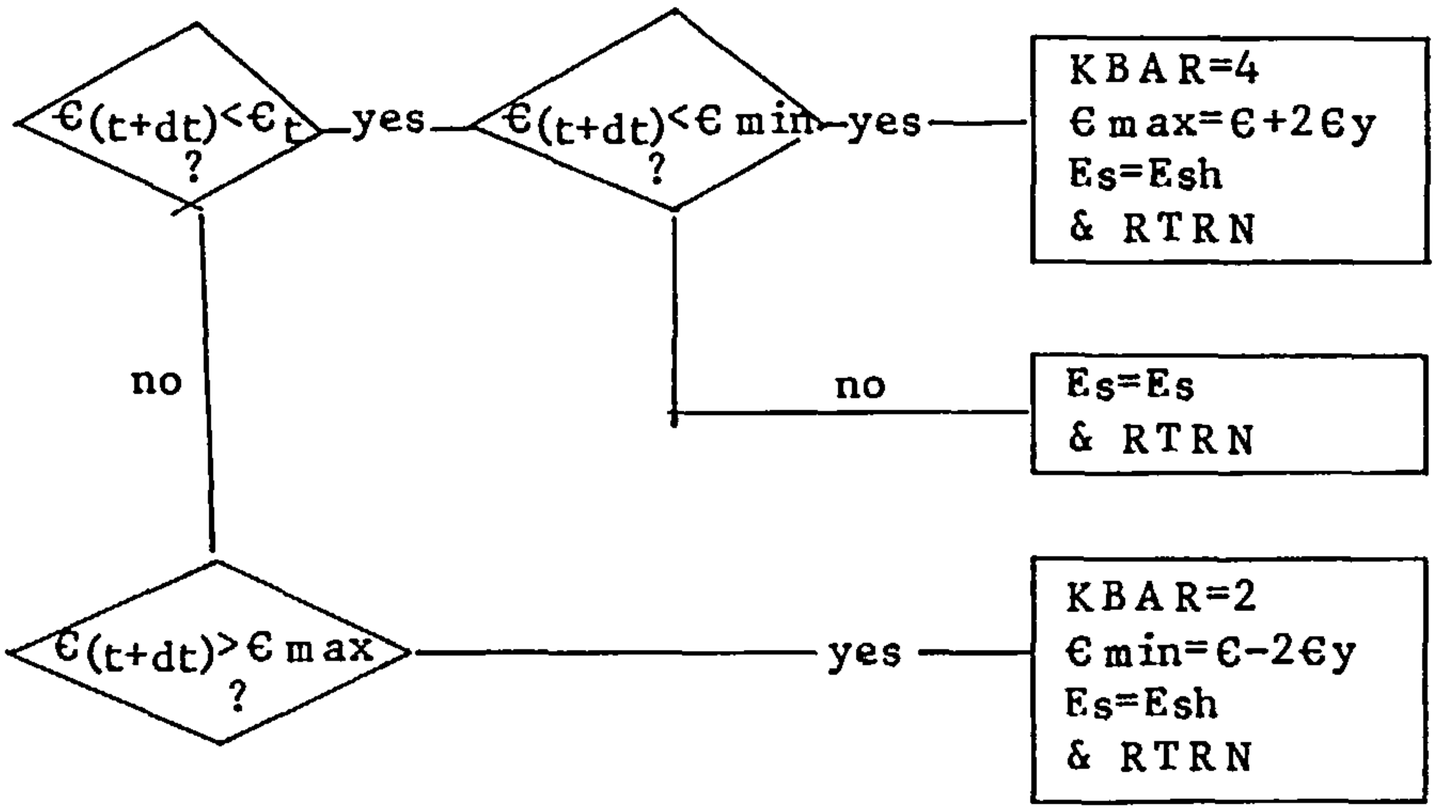

KBAR=6

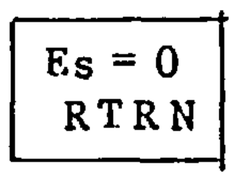

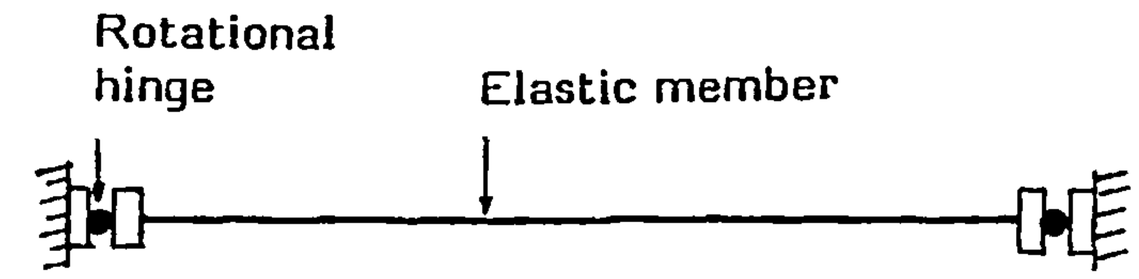

a) Idealisation

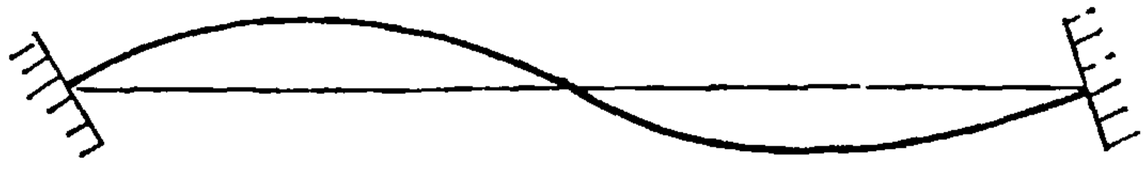

b) Beam behaviour

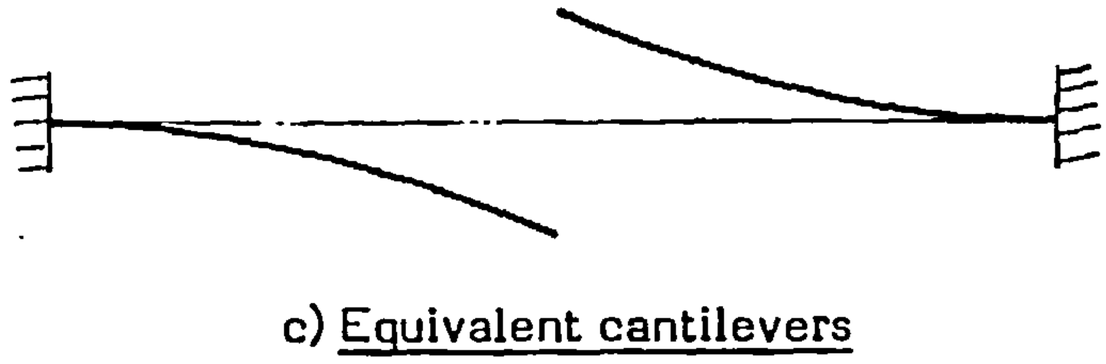

c) Equivalent cantilevers

FIG. 5.14 REPRESENTATION OF THE BEHAVIOUR OF LINE ELEMENTS

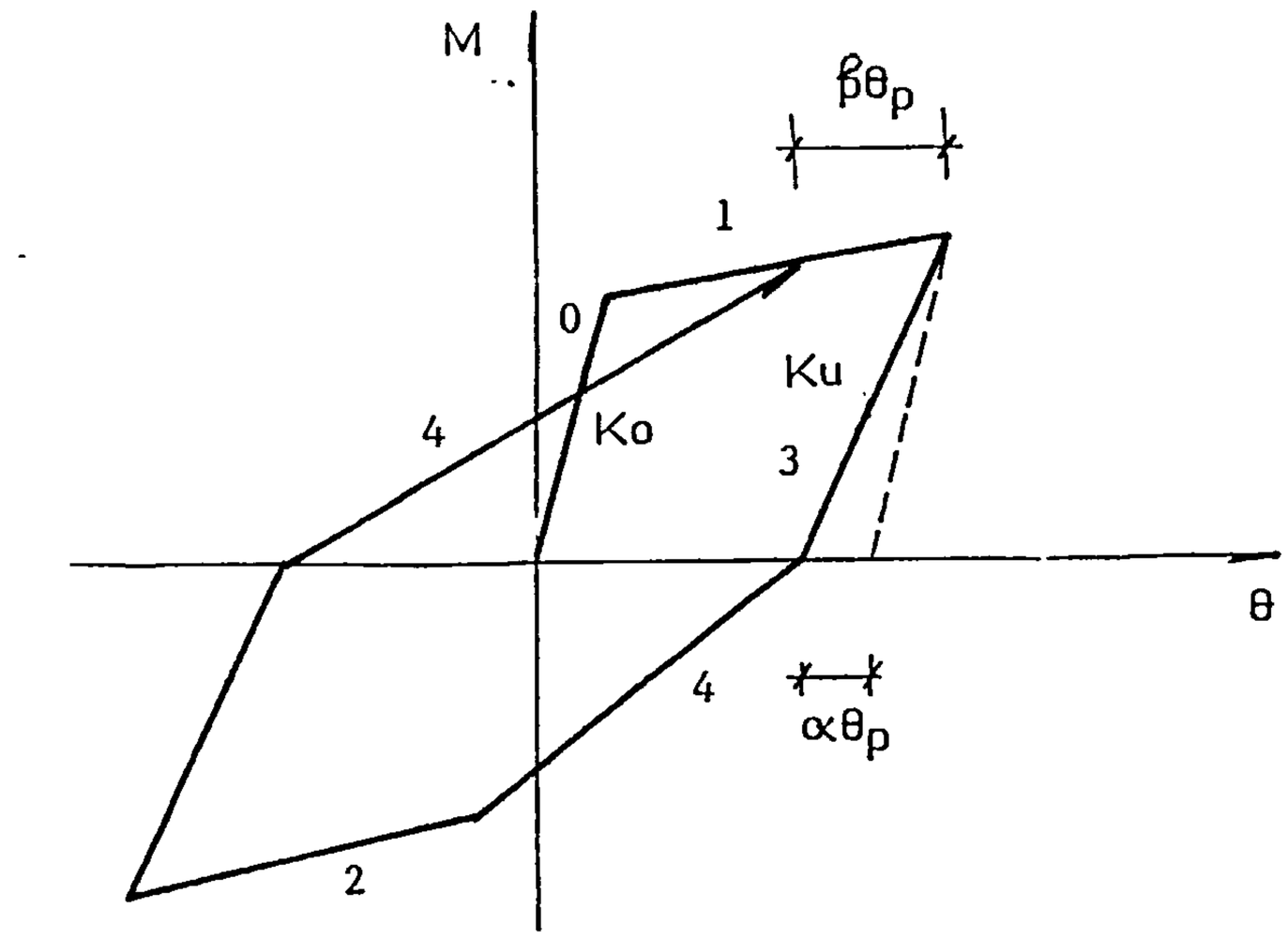

FIG. 5.15 MODIFIED TAKEDA MOMENT-ROTATION RELATIONSHIP

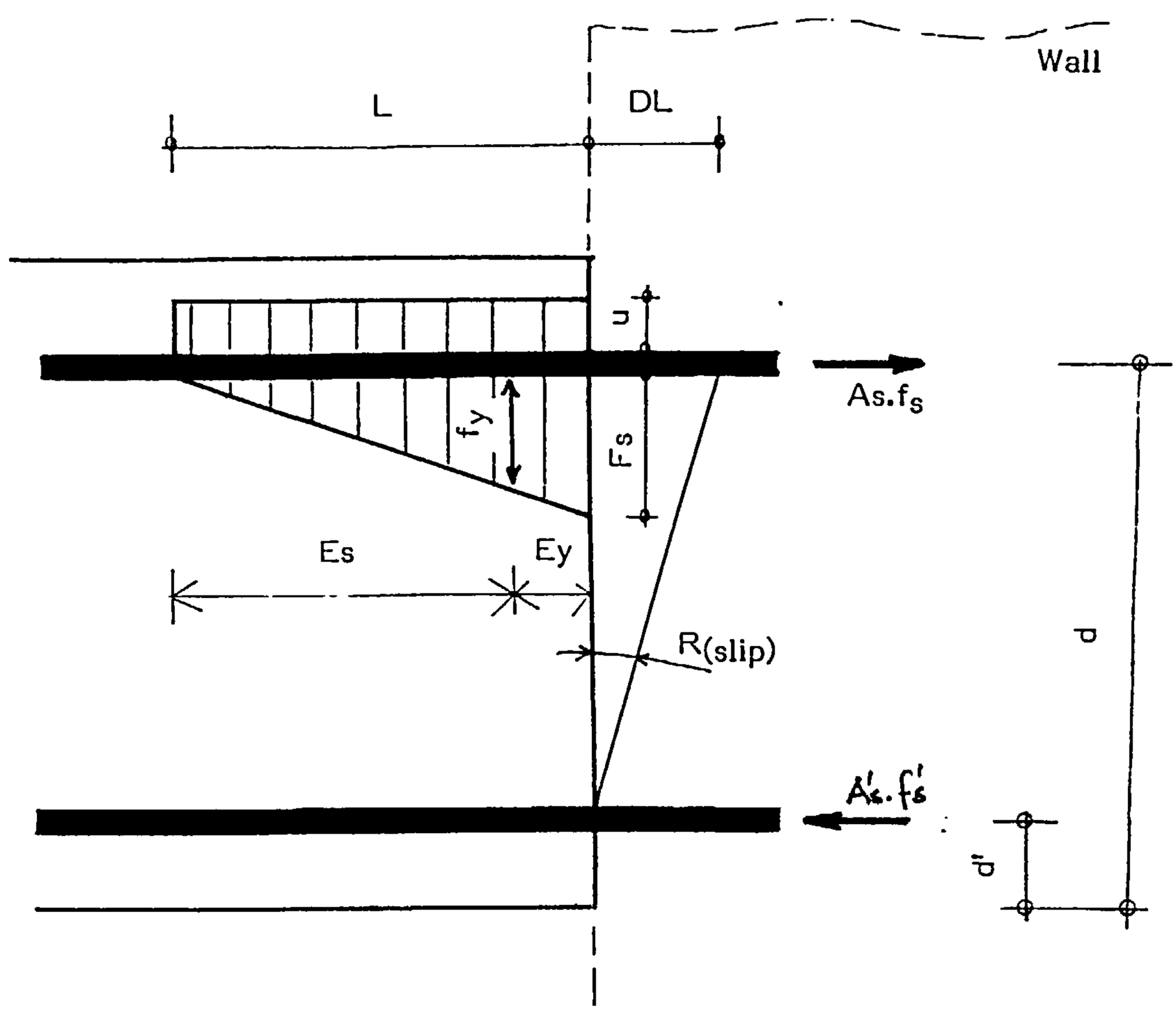

FIG. 5.16 ASSUMED BOND SLIP MECHANISM IN THE COUPLING BEAMS

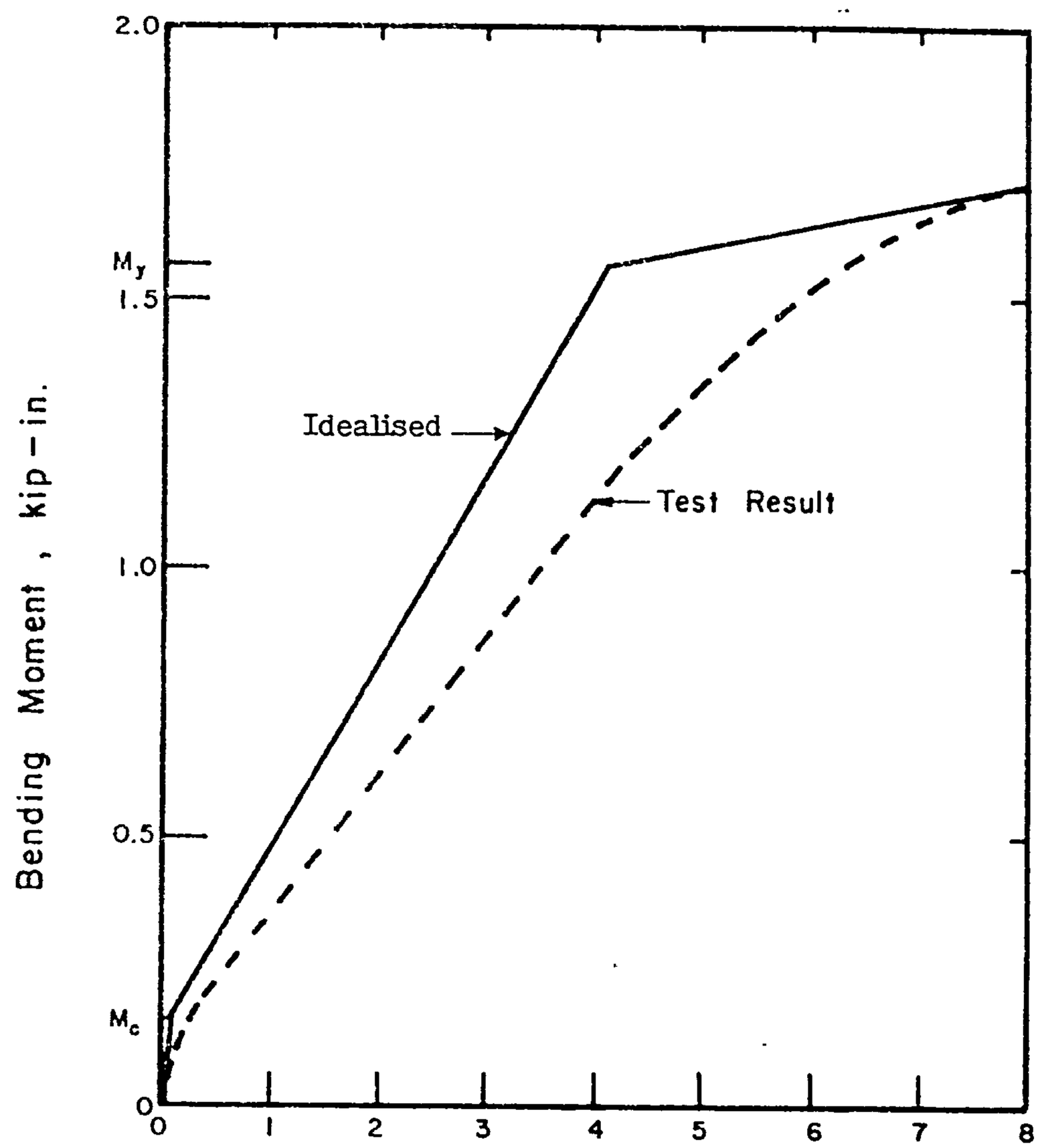

FIG. 5.17 MOMENT-ROTATION RELATIONSHIP OF A ROTATIONAL HINGE

CHAPTER SIX

NONLINEAR DYNAMIC PROCEDURE

6.1 Introduction and Assumptions

Probably the most powerful technique for nonlinear analysis is the step-by-step integration procedure. In this approach the response is evaluated for a series of short time increments. These are generally taken of equal length for computational convenience. The condition of dynamic equilibrium is established at the beginning and end of each interval, the response is calculated during each time increment for a linear system having the properties determined at the beginning of the interval. At the end of the increment the properties are modified to conform to its state of deformations and stress at that time. Thus the nonlinear analysis is approxi-mated as a sequence of analyses of successively changing linear systems. The most popular of the direct integration procedures are certainly the Newmark-Beta Method [102] and the Wilson-Theta Method [103]. In this study the Newmark-Beta Method is used and is discussed in some detail later in this chapter.

In any structural problem many assumptions are generally made in order to simplify the solution. As far as this investigation is concerned the basic assumptions are:

a) Only material nonlinearities are considered, geometric nonlinearities are assumed insignificant and hence neglected.

b) Torsional effects are not taken into consideration and the analysis is limited to planar coupled wall and wall systems.

c) The structure is assumed to be rigidly fixed at its base.

d) The mass of the structure can either be lumped at floor levels or distributed throughout the structure (consistent)

e) The stiffness of each element of the structure is assumed constant within an increment of time. Unbalanced loads are applied to the next step.

6.2 The Equations of Motion

The equations of dynamic equilibrium at any time t can be written in an incremental form as follows:

$$M\ Dv'' + C\ Dv' + K\ Dv = Dp(t) \qquad 6.1$$

where

M = Structure mass matrix

C = Damping matrix

K = Instantaneous Structure Stiffness matrix

Dv",Dv',Dv = Incremental nodal acc., vel. and disp. vector

Dp(t) = Incremental applied loading (= M Dy"(t))

Dy"(t) = Incremental base acceleration.

Equation 6.1 expresses the equilibrium conditions of the inertia forces, damping forces and resisting forces respectively. To calculate all these forces the mass matrix, damping matrix and instantaneous stiffness matrix must be evaluated.

6.3 Mass Matrix

Although the computer program is capable of dealing with a consistent mass element, in this study the lumped mass concept is used for convenience and economy. For a quadrilateral element the mass matrix is diagonal in the form of

$$M_e = \begin{bmatrix} 1.0 & & & & & & & \\ & 1.0 & & 0 & & & & \\ & & 1.0 & & & & & \\ & & & 1.0 & & & & \\ & & & & 1.0 & & & \\ & & & & & 1.0 & & \\ 0 & & & & & & 1.0 & \\ & & & & & & & 1.0 \end{bmatrix} . \; phA/4 \qquad 6.2$$

in which

p = mass density of reinforced concrete

h = depth of the element

A = area of the element

the great advantage of the lumped mass approach is that the mass matrix for the entire structure is diagonal and hence leads to a greater economy while consistent mass matrix has many off diagonal terms and hence requires more computational effort. The structure mass matrix is merely obtained as:

$$M = \Sigma M_e + M_{ext} \qquad 6.3$$

where M_e is the element mass matrix given in equation 6.2 and M_{ext} represents the external concentrated nodal masses. For nodes without concentrated masses, their position in M_{ext} is filled with zero.

6.4 Damping Matrix

It is well recognised that according to their material components, structures may show substantial damping effects when subjected to dynamic loadings. However the evaluation of such a phenomenon has been and is still quite vague and empirical and cannot therefore be assessed with absolute confidence. It is usual practice to use the viscous type of damping [104] for

convenience in the solution of dynamic response problems and for its mathematical simplicity. The damping matrix is expressed as either proportional to the stiffness matrix or to the mass matrix of the system, or as a linear combination of both as

$$C = a_1 M + a_2 K \qquad 6.4$$

where C is the viscous damping matrix and a_1 and a_2 are constants. The constant multipliers a_1 and a_2 can be related to the damping ratio for any mode n [104] by

$$z_n = (a_1 / 2w_n) + (a_2 w_n / 2) \qquad 6.5$$

where:

w_n = The circular frequency of the n^{th} mode

z_n = Damping factor for the n^{th} mode

In a direct integration solution a_1 and a_2 may be chosen to provide damping ratio at two selected frequencies [12]. If for instance the two first modes are selected then,

$$a_1 = \frac{2w_1 w_2 (z_2 w_1 - z_1 w_2)}{(w_1^2 - w_2^2)} \qquad 6.6a$$

$$a_2 = \frac{2w_1 w_2 (z_2 w_1 - z_1 w_2)}{(w_1^2 - w_2^2)} \qquad 6.6a$$

The damping factors are usually determined experimentally. However for concrete structures, it has been shown that they vary from 2% to 10% [105]. The circular frequency can be determined by free vibration analysis or can be extracted from the charts developed in chapter IV. If the damping matrix is considered to be proportional to only the stiffness matrix, the constant a_2 is then calculated using eqn. 6.5 assuming a_1 to be zero so that

$$a_2 = 2z_1/w_1 \quad \text{and} \quad C = a_2 K \tag{6.7}$$

Similarly, the constant a_1 is calculated by the following expression for the case where the damping matrix is assumed to be proportional to the mass matrix only

$$a_1 = 2z_1 w_1 \quad \text{and} \quad C = a_1 M \tag{6.8}$$

6-5 Numerical Solution

When solving the differential equations of motion (6.1) using step-by-step integration procedure, a way should be found to convert these equations to a set of simultaneous algebraic equations. This is accomplished by introducing simple relationships between displacement, velocity and acceleration which may be assumed to be valid for the increment of time chosen. On this basis, only one unknown vector (acc., vel. or displ.) remains in the equilibrium equations, the solution of which can be evaluated by any standard procedure. The most popular relationships between acceleration, velocity and displacement vectors are certainly those suggested by Newmark [102] and Wilson [103] as they have proven to be valid for elastic as well as for inelastic systems. In this study however, as said previously the Newmark's method is utilised.

The relationships between displacement, velocity and acceleration vectors are established by assuming the variation of the acceleration vector with time. Newmark associated two parameters α and β with this variation. Assuming $\alpha = 1/2$, he expressed incremental velocity and the incremental acceleration vectors as

$$Dv' = (1/2\beta Dt)\, Dv - (1/2\beta)\, V' - (1/4\beta - 1)Dt\, V'' \tag{6.9}$$

$$Dv'' = (1/\beta Dt^2)\, Dv - (1/\beta Dt)\, V' - (1/2\beta)\, V'' \tag{6.10}$$

where

Dt= Time increment

β= Constant indicating the variation of acc. in a time interval

Dv",Dv',Dv = Incremental nodal acc., vel. and disp. vector

V",V',V = Nodal acc., vel. and disp. vector

A linear acceleration assumption is known to be unstable in the presence of vibration modes with periods exceeding approxiamately one third of the time step regardless of whether the higher modes contribute significantly to the dynamic response or not [102]. Hence it is unsuitable as it requires a very short time increment. For this study the method based on constant acceleration within the time step was adopted ($\alpha = 1/2$, $\beta = 1/4$). The method is known to be unconditionally stable for linear systems.

There are two basic ways to solve the equations of motion with direct integration, the explicit approach and the implicit approach. Using the explicit method the accelerations are derived from the eqns of motion and then integrated to obtain the displacements and velocities. In case where implicit approach is used, the equations of motion along with approximate time integration operators yield the displacement vector directly. The advantages and drawbacks of both methods are discussed by Belytshko [108]. For this investigation however an implicit approach is assumed for convenience although the method is believed to be more sensitive to errors in case of big time increment. Table 6.1 illustrates the constant acceleration numerical method.

In any dynamic analysis greater accuracy can be expected as the integration time step is reduced. To minimise the computational effort, however, it is important to select as long a time step as possible. A great deal more research is required for the design of reliable time integration operators, including algorithms for the automatic selection of variable time step in order

to optimize the solution cost. Substituting equation 6.7 and equation 6.8 into the equations of motion (6.1) and replacing the damping matrix C by its assumed value (eqn. 6.4), yields the following resulting equation

$$K^* \, Dv_{(t+Dt)} = R \qquad 6.11$$

where

$$K^* = (1/b \, Dt^2)M + (1/2bDt)C + K \qquad 6.12$$

$$R = -Dp_{(t+Dt)} + A \, M + B \, C \qquad 6.13$$

$$A = (1/bDt) \, V' - (1/2b) \, V'' \qquad 6.14$$

$$B = (1/2b) \, V' - (1/4b-1)Dt \, V'' \qquad 6.15$$

and

t, t+Dt = previous and current time step

$Dv_{(t+Dt)}$ = incremental displacement vector at time t+Dt

Since the dynamic stiffness matrix K* and the load vector R can be avaluated at any time step t+Dt, eqn. (6.11) can now be solved for the displacement increment vector $Dv_{(t+Dt)}$ using any standard structural procedure. In this investigation however, the Gaussian elimination and back substitution method is used. As K* is banded, the method uses less computer time than the one in which K* is inverted. The incremental velocity vector can then be calculated using eqn. 6-7. The incremental acceleration vector however, is computed using the following equation which is a modified form of eqn. 6-1 and based on the current structural properties $K_{(t+Dt)}$.

$$Dv'' = -M^{-1} \left(C \, Dv' + K_{(t+Dt)} \, Dv + Dp_{(t+Dt)} \right) \qquad 6.16$$

Eqn. 6.16 was prefered to eqn. 6.9 for the evaluation of Dv" because the acceleration response is very sensitive to changes in the stiffness properties of

the structure. Therefore more accurate results can be expected by taking into account the updated stiffness matrix rather than the previous one.

6.6 Pseudo-Loads

At each time step the element constitutive law may change giving rise to pseudo-stresses. The way these pseudo-stresses are computed has been considered in detail in chapter V. These unsupported stresses are then converted into corrective or pseudo-loads and applied to the structure as a set of static loads in the next time increment. The pseudo-loads can be computed in two ways:

a) using the pseudo-stresses as

$$DP_s = B^T D\bar{\sigma}\, d(\text{area}) \qquad 6.16$$

in which DP_s = pseudo-loads

B = matrix relating nodal disp. to element strains (chapter III)

$D\bar{\sigma}$ = pseudo-stresses

b) using the previous and the updated stiffness matrix as

$$DP_s = (K_{(t+Dt)} - K_{(t)})\, Dv_{(t+Dt)} \qquad 6.17$$

where $K_{(t+Dt)}, K_{(t)}$ = stiffness matrix at time t+Dt & t respectively

In this study the second method (b) is used except when dealing with pseudo-stresses due to yielding of concrete in compression where the first method (a) is utilized for convenience.

6-7 Dynamic Equilibrium and Iterations

In nonlinear analysis, due to the approximations made with regard to acceleration velocity and displacement on one hand and the assumption of a

constant value of the stiffness in each time step on the other the dynamic equilibrium expressed by equation 6.1, may not necessarily be satisfied at the end of a time step and hence errors may be introduced. Depending on the nonlinearities in the system and the magnitude of the time interval Dt, the cumulation of these errors may lead the solution to diverge substantially from the exact solution. Obviously this phenomenon is much more serious in nonlinear dynamic analysis where the solution at any time is dependant on the previous history of solution, than in static analysis.

To prevent misleading errors occuring, after each time step or a preset number of steps, the portion of the total loading that is not balanced is calculated and used to compute an additional incremental diplacement. This process is repeated until equilibrium is approximated to within a certain tolerance. In this study the convergence tolerance used is the ratio of the Euclidean norms of incremental displacement and total displacement [106]. This ratio is defined as the square root of the sum of the squares (RSS) of the change in nodal displacements $dv^{(i)}$ over the RSS of the total nodal displacement V, i.e.,

$$\in = RSS(dv^{n}) / RSS(V) \qquad 6.17$$

where $$RSS(a) = (\Sigma a_i^{\,2})^{\frac{1}{2}} \qquad 6.18$$

If $\in$ is smaller than a prescribed tolerance value B , the solution is assumed to have converged and the process is terminated. Furthermore, if after a certain prescribed maximum number of iterations ITEMAX, convergence is not achieved, the process is also terminated and the analysis is performed all over again with a smaller time increment.

The need for equilibrium corrections could be avoided by subdividing time step whenever a change in stiffness properties occurs. The procedure was used by Porter & Powell [107]. However the method is complex and no substantial

improvement has been reported to justify the effort.

6.8 Analysis Procedure and Summary

The nonlinear response is traced by numerically solving the equations of motion for incremental displacements. The nonlinearity in the solution is introduced by changing the material properties of the effected elements and by releasing and distributing the unsupported stresses to adjacent elements which can sustain them. Taking the steel reinforcement to be elastic and concrete to be uncracked and elastic, material property and stiffness matrices are generated for individual elements. Whenever the material constitutive relationships are violated, the element material property and hence the stiffness matrices are updated. This is followed by adjustments of the stresses in the effected elements and calculation of the unsupported stresses. These are then converted into release or corrective loads and are applied to the structure as a set of static loads in the next time increment. For each time interval incremental displacements are produced due to two effects

a) the increment of input acceleration

b) the released loads from the previous time interval.

Finally the structural stiffness is reassembled because of the updating and the analysis procedure is continued for the remaining part of the record. A computer orientated summary of the step-by-step procedure is given in table 6.2 and a flow chart in fig. (6.1).

TABLE 6.1 SUMMARY OF THE STEP-BY-STEP NONLINEAR PROCEDURE

A. INITIAL CALCULATIONS

A1. Form linear stiffness matrix K, mass matrix M and damping matrix C

A2. Initialize acceleration, velocity and displacement vectors (V'', V', V)

B. FOR EACH STEP

B1. Form updated damping matrix if needed

$$C = a_1 M + a_2 K$$

B2. Form the effective dynamic stiffness K* using the updated value of K

$$K^* = (1/\beta Dt^2)M + (1/2\beta Dt)C + K$$

B3. Compute the following vectors

$$A = (1/\beta Dt)\, V' - (1/2\beta)\, V''$$

$$B = (1/2\beta)\, V' - (1/4\beta - 1)Dt\, V''$$

B4. Form the dynamic load vector R

$$R = -Dp_{(t+Dt)} + A\, M + B\, C$$

B5. Solve for incremental deformation vector $Dv_{(t+Dt)}$

$$K^*\, Dv_{(t+Dt)} = R$$

B6. Compute incremental velocity vector $Dv'_{(t+Dt)}$ as

$$Dv' = (1/2\beta Dt)\, Dv - (1/2\beta)\, V' - (1/4\beta - 1)Dt\, V''$$

B7. If iteration for dynamic equilibrium required, then initialize

o) $i = 0$ $\qquad \partial v^{(0)} = Dv_{(t+Dt)}$

i) $i = i + 1$

ii) calculate out-of-balance load vector as

$$DR = Dp_{(t+Dt)} - M\, V''^{i-1} - C V'^{i-1} - K V^{i-1}$$

iii) solve for the i^{th} correction to displacement increment

iv) calculate new displacement increment

$$Dv^i = Dv^{i-1} + \partial v^i$$

v) if convergence , go to B8, otherwise go to i)

B8. Compute stresses, strains and element forces and check compliance with constitutive laws

B9. Update the structural stiffness matrix K if necessary and compute the pseudo-loads

B10. Compute the acceleration increment vector as

$$Dv'' = -M^{-1} \left(C\, Dv' + K_{(t+Dt)}\, Dv + Dp_{(t+Dt)} \right)$$

B11. Compute new acceleration, velocity and displacement vector as

$$V''_{(t+Dt)} = V''_t + Dv''_{(t+Dt)}$$

$$V'_{(t+Dt)} = V'_t + Dv'_{(t+Dt)}$$

$$V_{(t+Dt)} = V_t + Dv_{(t+Dt)}$$

FIG. 6-1 FLOW CHART FOR NONLINEAR DYNAMIC ANALYSIS

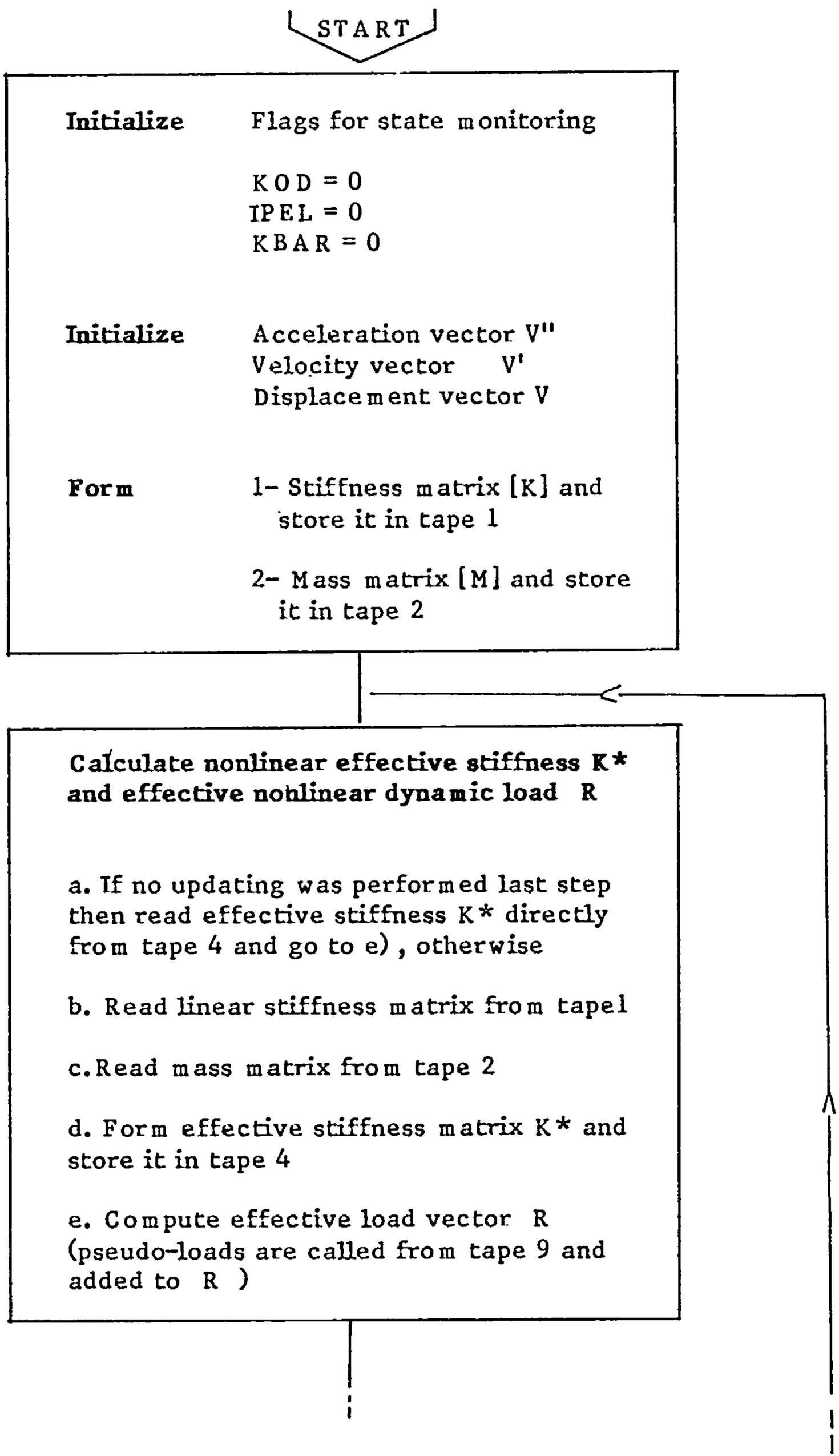

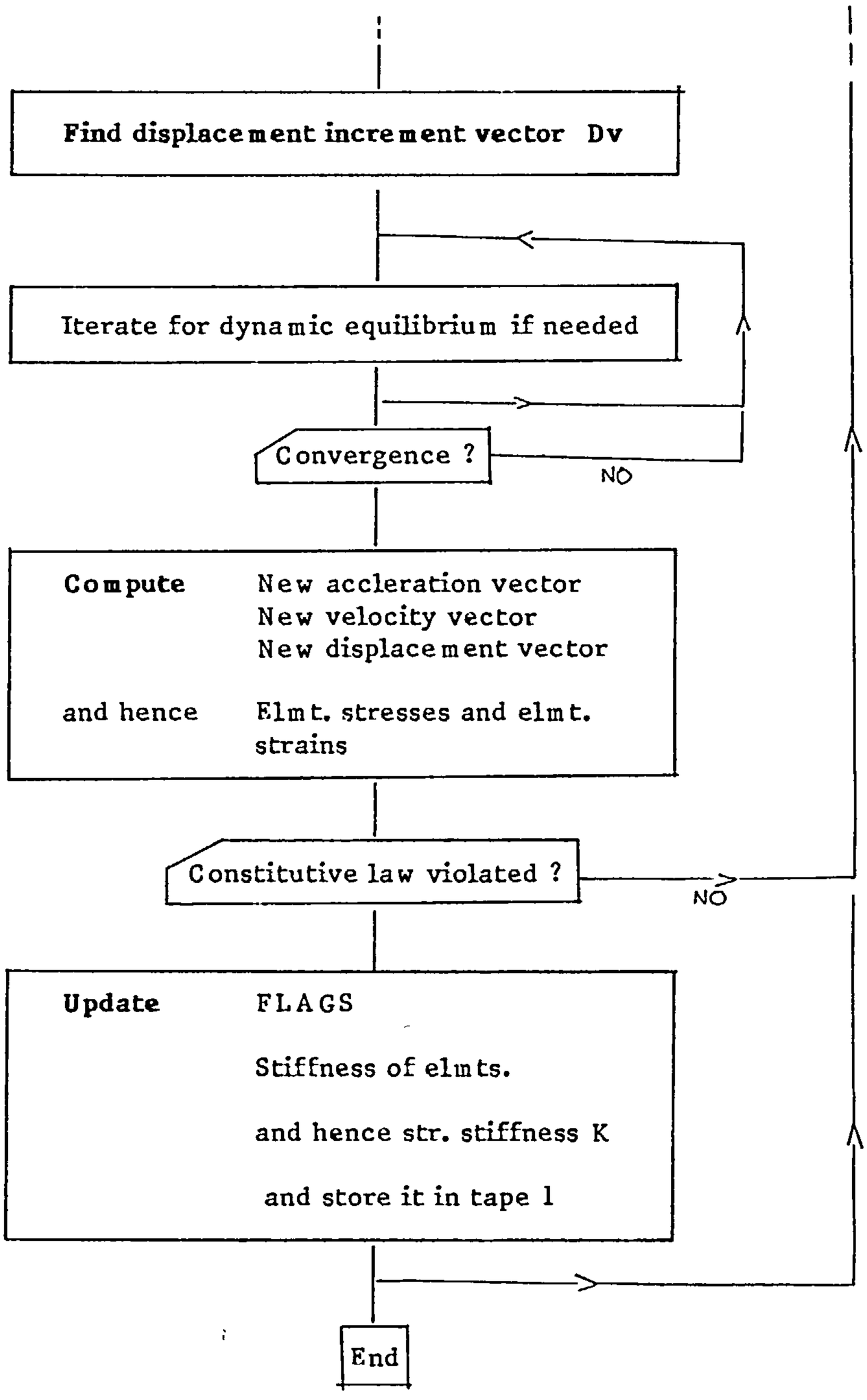
Find displacement increment vector Dv
Iterate for dynamic equilibrium if needed
Convergence ?
NO
Compute
New accleration vector
New velocity vector
New displacement vector
and hence
Elmt. stresses and elmt. strains
Constitutive law violated ?
NO
Update
FLAGS
Stiffness of elmts.
and hence str. stiffness K
and store it in tape 1
End

CHAPTER SEVEN

NUMERICAL EXAMPLES

7.1 General

The object of this chapter is to demonstrate the usefulness and applicability of the nonlinear step-by-step dynamic analysis presented in the previous chapters and to validate the FE idealisations and the hysteretic laws discussed in chapter V. Four numerical examples were investigated. In the first three examples, analytical results using the proposed model are compared with experimental test results [42, 109]. In the last example, the model is compared with analytical results reached using existing models [30].

To widen the scope and the usefulness of the model, the tested samples were of different geometric characteristics. The model is first compared with a single wall (without openings) tested by Agrawal and Leslie [42] and then with a pair of coupled shear walls tested by Ariztizabal [109]. The need for good accuracy in predicting plastic deformations (or ductilities) of the coupling beams of the coupled shear walls is very important if they are to be used as a first line of paraseismic defence. Therefore a 20 storey coupled shear wall was analysed and the coupling beam ductilities compared with those computed using the model presented by Kannan and Powell [30].

For convenience the four structures under investigation in this chapter are disignated by SW1, SW2A, SW2B and SW3. Their material properties are presented as given by the investigators, however, estimations were made in cases where specific items of data were not available.

7.2 Single Wall (SW1)

One of the very few experimental models subjected to earthquake motion is the isolated wall model tested by Agrawal et al. [42]. The geometry and the cross sectional property are shown in fig. (7.1). A load of 2 kips is lumped at each floor level as shown in fig. (7.2). The material data of the model is given in table 7.1. The model was subjected to the simulated N-S component of El-Centro earthquake of May 1940. The time axis of the original record was compressed by a factor of five. The amplitudes of the earthquake were normalised for a maximum peak acceleration of 1.05g and the duration of the experiment was set to 1.5 second.

7.2.1 Experimental Results [42] : The information provided by the experimental data is given in table 7.2 and the cracking pattern of the model, after test, is given in fig. (7.3). The cracking pattern prediction according to Agrawal's analysis is shown in fig. (7.4). The wall was idealised as an assembly of FE but with three degrees of freedom at each node. A shear factor $\alpha = 0.1$ and a damping $z = 1.5\%$ of critical were assumed. The response acceleration and displacement at the three mass levels are shown in fig. (7.5a) and fig. (7.6) respectively and the base shear and base moment responses in fig. (7.7). Also shown in fig. (7.7) is the base acceleration. These responses were based on a computed natural frequency of 11.84 cps.

7.2.2 Predicted Responses : The FE discretisation of the model is shown in fig. (7.8a). The external masses were lumped at the floor levels. The material properties and the dynamic data used in the analysis were those given in table 7.1 and described in the previous section. In order to compare the responses of both analytical and experimental information given by Agrawal et al. [42], the same values of shear coefficient, damping, Poisson's ratio are used in this study. Two cases were considered as far as discretisation is concerned

a) the same number of elements as Agrawal's discretisation (i.e., 120 elements)

b) approximately the same number of degrees of freedom (DOF) as considered by Agrawal (i.e., 441 dof)

The damping matrix was assumed proportional to the stiffness matrix only. The predicted absolute maxima for the two cases are given in table 7.2. This shows that as the ndof increased, the maximum response results improved except for the first level acceleration which diverged yet more from the experimental maximum value.

The computed response history acceleration for case b) is shown in fig. (7.5b) and the response history displacement, base shear and base moment in figs. (7.6) and (7.7) along with those given by Agrawal [42] for comparison. Figure (7.8) shows the instantaneous "photography" of the structure at different time steps obtained analytically. From these figures and as far as cracking and yielding patterns are concerned the following observations can be made:

i) First cracks started at the base level in the outer elements and spread to the higher levels and the inner elements of the first level.

ii) The cracking started almost horizontally at the outer elements and while propagating towards the inner elements the direction of the cracks changed substantially.

iii) the yielding of steel occured mostly in the first floor and was confined to longitudinal wires.

7.2.3 <u>Discussion:</u> Generally, analytical results are in agreement with those presented by Agrawal et al. [42] for the same number of degrees of freedom. There are still some discrepancies with respect to the experimental results.

However, a preliminary study revealed that as time step decreases the maximum displacement response slightly increases and the maximum base moment and base shear decrease. This study was made just for the first 0.5 second duration. In view of this preliminary study good agreement with experimental results can be expected as time increment decreases.

As can be seen from fig. (7.8f), the predicted crack pattern agreed quite well with the experimental one although not quite with Agrawal's model at the top of the specimen. The predicted yielding of steel was also more widespread than Agrawal's model. This may explain the generally lower values of displacements found by Agrawal as compared with those obtained in this study. Also, the predicted patterns indicated that local crushing due to excessive compression occured at the two bottom outermost elements as clearly shown by fig. (7.8f). Whether or not this yielding of steel and crushing of concrete was present after the experimental tests could not be ascertained from the available reference [42].

7.3 Coupled Shear Wall (SW2A ; SW2B)

7.3.1 Description of the Experimental Models: The procedure described in this investigation was applied to two 10 storey coupled wall models tested at the University of Illinois earthquake simulator by Ariztizabal [109]. The two coupled walls are designated as SW2A and SW2B. The dimensions of the models are shown in fig. (7.9). The models are made up of two shear walls having a cross sectional area of 1" by 7" each and a height of 90". The walls are connected at each floor level by a connecting beam of 4 in. length and 1 by 1.5 in. cross section. A weight of 0.5 kip is placed at each floor level (fig. 7.9). Material properties for the models are listed in table 7.3.1 and the assumed stiffness and strength of the different members are given in table 7.3.2. The models were subjected to the base motion representing the signals

of the El Centro N-S component earthquake. The original time axis was compressed by a factor of 2.5 and the amplitudes of acceleration records were normalised to give a maximum peak value of 0.92g.

The two coupled wall models (SW2A, SW2b) have essentially the same geometric properties. In order to demonstrate the importance of the coupling beam strength in the yield sequence , the coupling beam reinforcement areas in SW2B were twice as much as those in SW2A. The reinforcement cross sections for SW2A and SW2B are shown in fig. (7.10). The duration of the record used after time compression was 15 seconds. However it was recognised by Ariztizabal [109] that most of the structural failures occured within the first 3 seconds. Therefore in this study only the first 3 seconds (or 3 x 2.5 sec. of the original record) is considered for convenience and economy.

7.3.2 Experimental Responses [109]: The maximum responses provided by the tests are listed in table 7.3.3 for both SW2A and SW2B. The failure patterns after testing are shown in fig. (7.11). The experimental response history of acceleration and displacement are shown in fig. (7.12) and fig. (7.13). For convenience only the acceleration and the displacement history at level 10, level 7, and level 4 are given. The base shear and base moment histories were also monitored by Ariztizabal. However these were difficult to trace from the report and therefore are not shown here.

7.3.3 Predicted Responses: In order to compare the experimental data given in the previous section and the predicted response using the computer program developed for this investigation, the information not readily available such as coupling beam strengths and stiffness properties needed as input were derived and are shown in table 7.3.2. The damping factor was assumed equal to 2% of critical and the damping matrix was assumed to be a linear combination of mass and stiffness matrix. The time interval used in the response calculation was chosen to be 0.00025s. The Poisson's ratio and the shear reduction factor α

were assumed to be 0.2 and 0.5 respectively. For comparison, the computed history response acceleration and displacement are shown along with the corresponding experimental responses in figs. (7.12) and (7.13). The base shear and base moment histories are shown in fig. (7.14). The absolute maximum analytical responses were predicted as shown in table 7.3.3. The sequences of cracking and yielding of all constituent elements were recorded during the computer run and are shown in fig. (7.15) for various time steps over the duration of the excitation.

7.3.4 Discussion: Again, the analytical maximum response displacement and acceleration (fig. 7.12 - 7.13) are in good consistency with the experimental ones. In general, the predicted displacements were the lower bound to the experimental displacements and the predicted accelerations were the upper bound. However, as previously stated, if a smaller time interval and a finer discretisation are chosen and accurate material properties assessed then better compliance could be expected.

The displacement wave forms indicate clearly that the structure oscillated primarely in the first mode and that the peak acceleration at each level accured at the same time. The overall features of the response history are similar to those of the test. The times when the absolute maximum displacement at top floor and the maximum base moment occured are comparable to the corresponding times recorded in the test. The maximum positive and negative responses indicate that the structure was subjected to loads of the same order of magnitude in both directions. The base moment and base shear responses were dominated by the first mode as well, as can be seen from fig. (7.14).

The failure mechanisms at the end of the runs were also in good agreement with the test results. The analytical crack pattern however was found more widespread particularly at the lower levels than the tested model

seems to show. Furthermore, yielding of the coupling beams at levels 4, 5 and 6 was predicted by the analysis but were not reported by test results. This might be due to shrinkage cracks before test, which can slightly change the stress distribution and hence failure mechanism. Ariztizabal [109] did not record the sequence of failures at intermediate time intervals and therefore no comparison could be made in this respect.

Although similar response histories and maxima were reached for both SW2A and SW2B, the crack pattern and the extent of yielding and the damage in the two structures were quite different as anticipated. The following failure sequences were predicted by the present analysis (fig. 7.15):

t= 0.00s:

Both structures SW2A and SW2B were assumed elastic and isotropic. No cracks due to shrinkage or otherwise were taken into consideration.

t= 0.75s:

Cracks began to form at the connecting beams of the 4^{th}, 5^{th}, and 6^{th} floor (t=0.32s) and spread rapidly towards top and bottom floors.

t= 1.50s:

SW2A: The cracking is total at the coupling beams ends and yielding has already started at floors 4, 5 and 9. Some scattered cracks were also predicted in the outer elements at the bottom of the wall.

SW2B: No yielding was shown in the coupling beams at this stage, however all the coupling beams were cracked at their ends and more frequent cracks were present at the bottom of the wall.

t= 2.25s:

SW2A: yielding at the coupling beam ends is almost complete except

in the first two floors. the cracks now spread towards inner elements of the wall particularly within the first two levels where 2 sets of cracks were frequent. In the outer elements and at levels 6, and 7 one set of cracks took place.

- SW2B: Again no substantial yielding occur in the coupling beams except at floor 4. However in the two outer most elements at the base level, crushing was detected.

t= 3.00s:

SW2A: the second floor coupling beam yielded but the first floor coupling beam did not. Cracking spread towards the inner elements at the top levels and reached the 8^{th} and 9^{th} storey. Crushing also accured (t=2.47s) at the outer elements of the walls.

SW2B: Crushing of three more elements at the base level and yielding of the coupling beams at level 4, 5, and 6 were monitored.

As can be deducted from the previous discussions, the critical damage in structure SW2B started in the walls at the base level before any substantial formation of hinges at the coupling beam ends occured, whilst in structure SW2A, failure in the wall started after almost all coupling beams yielded. Moreover, the crushing of the walls at the outer elements in SW2B before yielding of the steel showed that the coupled shear wall acted as a single cantilever wall as the coupling was so strong. This demonstrates once again the importance of the relative stiffness and strength of the coupling beams with respect to those of the walls to control the mode and sequence of the failure pattern of aseismic structures.

7.4 Plastic Deformation Prediction (SW3)

The use of coupled shear walls in seismic resistant design has a great potential because of their tremendous capabilities for dissipating the energy input from an earthquake. Also it is well recognised that dissipation of energy should mainly be assured through inelastic deformation of the coupling beams without substantial loss of strength. A good prediction of these deformations by any model is therefore most important. Therefore the purpose of this section is twofold:

i) Test the validity of the model and its ability to predict plastic deformations accurately.

ii) Examine the results and use them as preliminary analysis to chapter VIII and deduct a strategy to be adopted for the chapter VIII.

A 20 storey coupled wall was considered for this purpose. Keeping the walls elastic, the plastic deformations enforced upon the coupling beams were recorded and the rotational ductilities computed as

$$\mu_r = \frac{\Theta_{max}}{\Theta_y} \simeq \frac{\Theta_p + \Theta_y}{\Theta_y} \qquad 7.2$$

$$\mu_r = 1 + \frac{\Theta_p}{\Theta_y} \qquad 7.3$$

in which μ_r= rotational ductility

Θ_{max}= maximum rotation of hinge

Θ_p, Θ_y= rotation at yield and plastic rotation respectively

The analysis was performed using the computer program developed in this study and results were compared with those given using DRAIN-2D. DRAIN-2D is a dynamic computer program developed in The University of California, Berkeley, in which columns and walls can only be treated as line elements.

7.4.1 Description of the Structure and Modeling: As previously stated, a 20 storey coupled shear wall was considered in this investigation. The structure was assumed to be fixed at its base. Its geometric, dynamic and strength properties are given in table 7.4.1. Its discretisation is shown in fig. (7.16). Three runs using different discretisations and analytical models were made, these were:

i) SW3a: Both walls and beams were idealised as line elements. This run was performed using the computer program DRAIN-2D. Takeda's model was used to simulate the nonlinear hysteresis of coupling beams.

ii) SW3b: This run was made using the computer program developed in this investigation. Again both walls and beams were idealised as line elements, however, in addition to Takeda's model assumption for the simulation of the nonlinear deformations, bond slip effect was taken into consideration as described in chapter V.

iii) SW3c: The finite element (FE) approach developed in this investigation was used. Bond slip model was also considered in this run.

The yield moment of all coupling beams was assumed constant (100 kip-ft). The damping factor, Shear reduction factor and Poisson's ratio were chosen as 2% of critical, 0.5, and 0.2 respectively. The damping matrix was assumed as a linear combination of mass and stiffness matrix.

7.4.2 Nonlinear Dynamic Procedure and Results: Assuming a mass representing a floor weight of 4 kips lumped at each floor level, the structure described above, was excited by the first 6 seconds of 1940 El Centro earthquake accelerogram with a peak acceleration amplitude of 0.33g (fig. 7.17). The equations of motion were solved using the step-by-step numerical integration method with a time increment of 0.00025 sec. when using FE approach and 0.005 sec. when using line elements. The maximum plastic

deformations enforced upon the coupling beams were recorded and the corresponding maximum ductility demands on each coupling beam were computed using eqn. 7.2 and are shown in fig. (7.18).

7.4.3 Ductility Demand Variation: As can be seen from fig. (7.18), the ductility demands are slightly higher in SW3b than in SW3a. This increase reflects the direct influence of bond slip which normally increases the maximum rotations and hence the ductility demands. As far as this example is concerned bond slip effect seems to be minor, however this must not be taken as a generalisation. In a study made by the author, it was found that the effect of bond slip increased substantially for higher earthquake intensity and varied also with the frequency content of the design accelerogram. Comparison between the results of SW3a, SW3b and SW3c as illustrated by fig. (7.18) yields the following observations:

i) The maximum ductility distribution over the height of the structure were comparable for all the coupled walls.

ii) Ductility demands obtained in SW3c were lower in the first eight floors than those in SW3a and SW3b. The maximum variation was about 13%.

iii) Ductility demands in SW3c were higher from level 9 upwards than those of SW3a and SW3b. The maximum variation was about 14.5%.

iv) Ductility demands in SW3b were generally higher than those in SW3a.

Many factors can be at the source of these discrepancies but the most obvious one seems to be the inherent behaviour of the models assumed at the first place. Generally however, the maximum ductilities obtained by any model were comparable.

7.4.4 Effect of Coupling Beam Yieding Moment Variation: To examine the influence of the yield moment variation, the 20 storey coupled shear walls SW3a, SW3b and SW3c described above were subdivided in 4 zones of 5 storeys each from the base and only the absolute maximum ductility in each of these zones were considered for convenience. For a yield moment M_{min}=100 kip-ft, the following ductilities were recorded (see above section)

zone	μ_0		
	SW3a	SW3b	SW3c
1	13.51	13.98	11.20
2	17.43	18.20	14.24
3	22.24	23.09	24.48
4	22.78	23.93	26.50

The yield moment was then increased progressively by a value corresponding to a variation (dM/M_{min}) equal to 0.50, 1.00 and 1.50 respectively and the corresponding ductility variation ($d\mu/\mu_o$) at each zone was computed. The results were as follows:

dM/Mmin	zone	$d\mu/\mu_0$		
		SW3a	SW3b	SW3c
0.50	1	0.370	0.375	0.390
	2	0.370	0.390	0.400
	3	0.390	0.380	0.400
	4	0.420	0.410	0.420

1.00	1	0.560	0.560	0.570
	2	0.560	0.550	0.580
	3	0.580	0.570	0.600
	4	0.610	0.590	0.620
1.50	1	0.660	0.665	0.680
	2	0.670	0.666	0.690
	3	0.690	0.680	0.695
	4	0.710	0.690	0.720

The results show clearly that although the ductility demands might be different using different models and for a given yielding moment as demonstrated in the previous section by comparing SW3a, SW3b and SW3c, the ductility variations ($d\mu/\mu_o$) in terms of the yield moment variation (dM/M_{min}) were very close. This shows that the ductility variations are almost invariant with respect to any model as the yield moment varied.

TABLE 7.1 Material Properties of SW1

Properties	
CONCRETE	
Young's modulus of elasticity	$E_c = 3.8\ 10^6$ psi
Uniaxial compressive strength	$f_c = 4720$ psi
Tensile strength	$f_{ct} = 409$ psi
Poisson's ratio	$\mu = 0.1$
Maximum compressive strain	$\epsilon_{max} = .003$
STEEL REINFORCEMENT	
Young's modulus of elasticity	$E_s = 2.9\ 10^7$ psi
Young's modulus at strain hardening	$E_{sh} = 7.03\ 10^4$ psi
Yield stress	$f_y = 53500$ psi
Yield strain	$\epsilon_y = 1.845\ 10^{-3}$
Ultimate strain	$\epsilon_u = 0.08$

TABLE 7.2 Experimental and Analytical Maxima

DESIGNATION	TEST	Proposed analysis	
		SW1(294 dof)	SW1(450 dof)
natural freq. (cps)	8.5	13.02	11.05
response acc.			
1st floor	1.00g	0.69g	0.61g
2nd floor	1.73g	1.31g	1.48g
3rd floor	2.03g	2.50g	2.29g
response disp. (dble amplitude)			
1st floor	0.30in	0.17in	0.21in
2nd floor	0.70in	0.48in	0.62in
3rd floor	1.15in	0.87in	0.99in
response base shear (kips)	4.00	6.21	5.88
response base moment (kip-in)	163	197	189

TABLE 7.3.1 Material Properties of SW2a and SW2b

Properties		
CONCRETE		
Young's modulus of elasticity	$E_c = 3.1\ 10^6$	psi
Uniaxial compressive strength	$f_c = 4500$	psi
Tensile strength	$f_{ct} = 403$	psi
Poisson's ratio	$\mu = 0.2$	
Maximum compressive strain	$C_{max} = .003$	
STEEL REINFORCEMENT		
Young's modulus of elasticity	$E_s = 2.9\ 10^7$	psi
Young's modulus at strain hardening	$E_{sh} = 7.03\ 10^4$	psi
Yield stress	$f_y = 72000$	psi
Yield strain	$C_y = .00248$	
Ultimate strain	$C_u = 0.08$	

TABLE 7.3.2 Stiffness and Strength Properties of Coupling Beams

Properties	SW2a	SW2b
moment-rotation relationship		
i) elastic slope, kip-in	622	810
ii) slope at yield, kip-in	20	25
iii) cracking momt,kip-in	0.15	0.15
iv) yielding momt,kip-in	1.56	2.90

TABLE 7.3.3 Experimental and Analytical Maxima

DESIGNATION	TEST				PROPOSED ANALYSIS			
	SW2a		SW2b		SW2a		SW2b	
	pos	neg	pos	neg	pos	neg	pos	neg
response acc. (g)								
4th floor	1.11	-0.95	1.11	-1.19	1.15	-1.25	1.16	-1.23
7th floor	1.07	-0.98	1.10	-1.00	1.21	-1.27	1.26	-1.13
10th floor	2.00	-1.58	1.58	-1.84	2.11	-1.77	1.72	-1.98
response disp. (inch)								
4th floor	0.70	-0.60	0.71	-0.55	0.57	-0.63	0.69	-0.53
7th floor	1.41	-1.18	1.43	-1.02	1.19	-0.93	1.23	-0.87
10th floor	2.13	-1.74	2.05	-1.47	1.93	-1.63	1.78	-1.26
response base shear (kips)	3.33	-3.38	3.90	-3.92	2.63	-2.77	2.73	-2.91
response base moment (kip.in)	200	-197	185	-199	182	-177	190	-187
natural freq. (cps)								
i) before run	4.80		4.80		5.00		5.00	
ii) after run	2.06		2.00		2.43		2.54	

TABLE 7.4.1 Material Properties of SW3

Properties	
CONCRETE	
Young's modulus of elasticity	Ec= 3.2 10^6 psi
Poisson's ratio	μ = 0.2
ELEMT STIFFNESSES (EI)	
Wall	9.6 10^9 kip.in^2
coupling beams	4.45 10^7 kip.in^2
ELEMENT STRENGTHS	
Wall	Elastic
coupling beams	Variable
FLOOR MASS	4.00 kips . s^2 / in
NATURAL FREQUENCY	10.90 cps
DAMPING FACTOR	z= 2% of critical

Reinforcement

Vertically: No.8 wires 1" c/c

Horizontally: No.8 wires 2" c/c

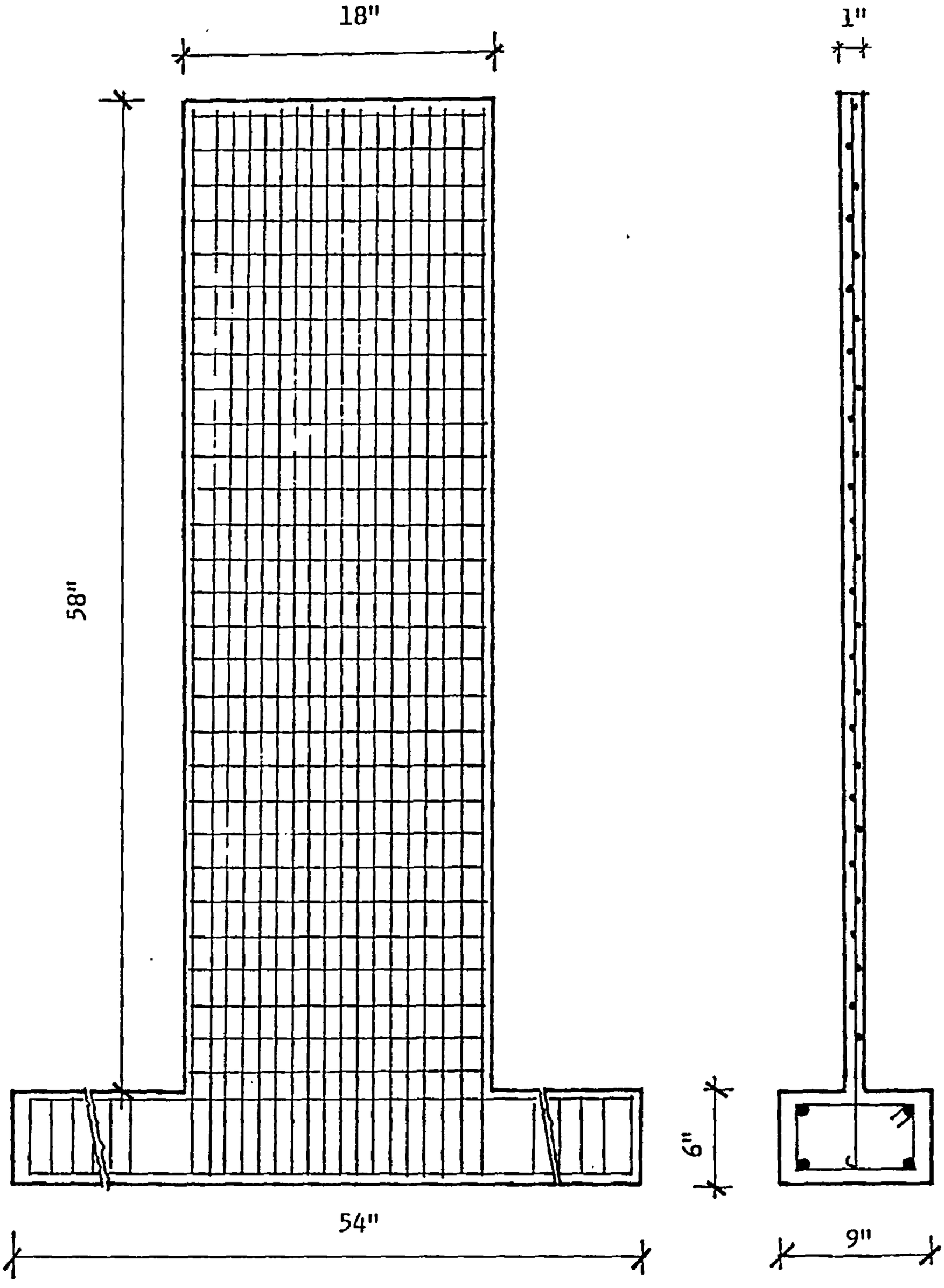

Elevation

Cross section

FIG. 7.1 GEOMETRY AND REINFORCEMENT OF SW1

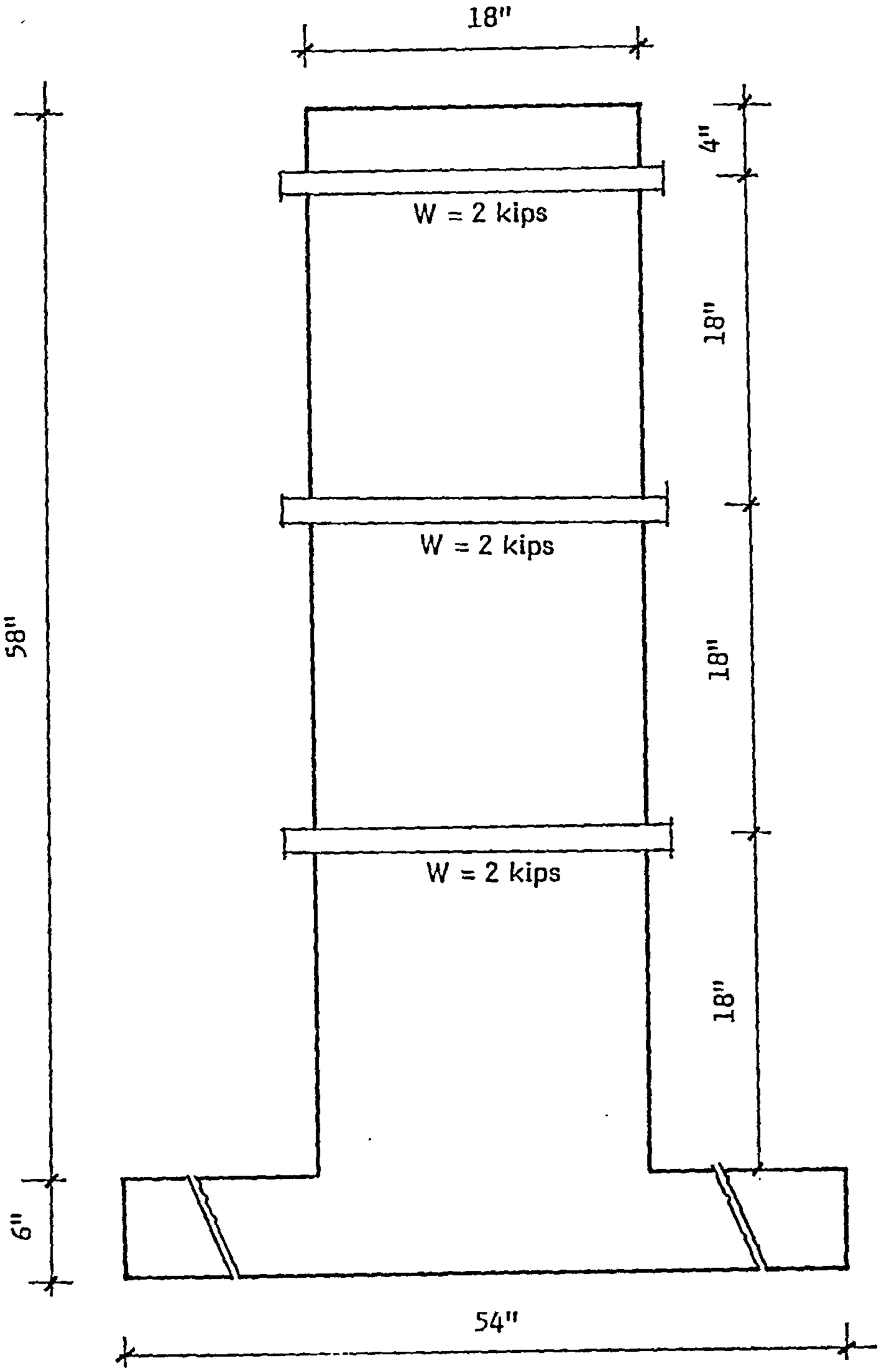

FIG. 7.2 POSITION OF THE FLOOR WEIGHTS

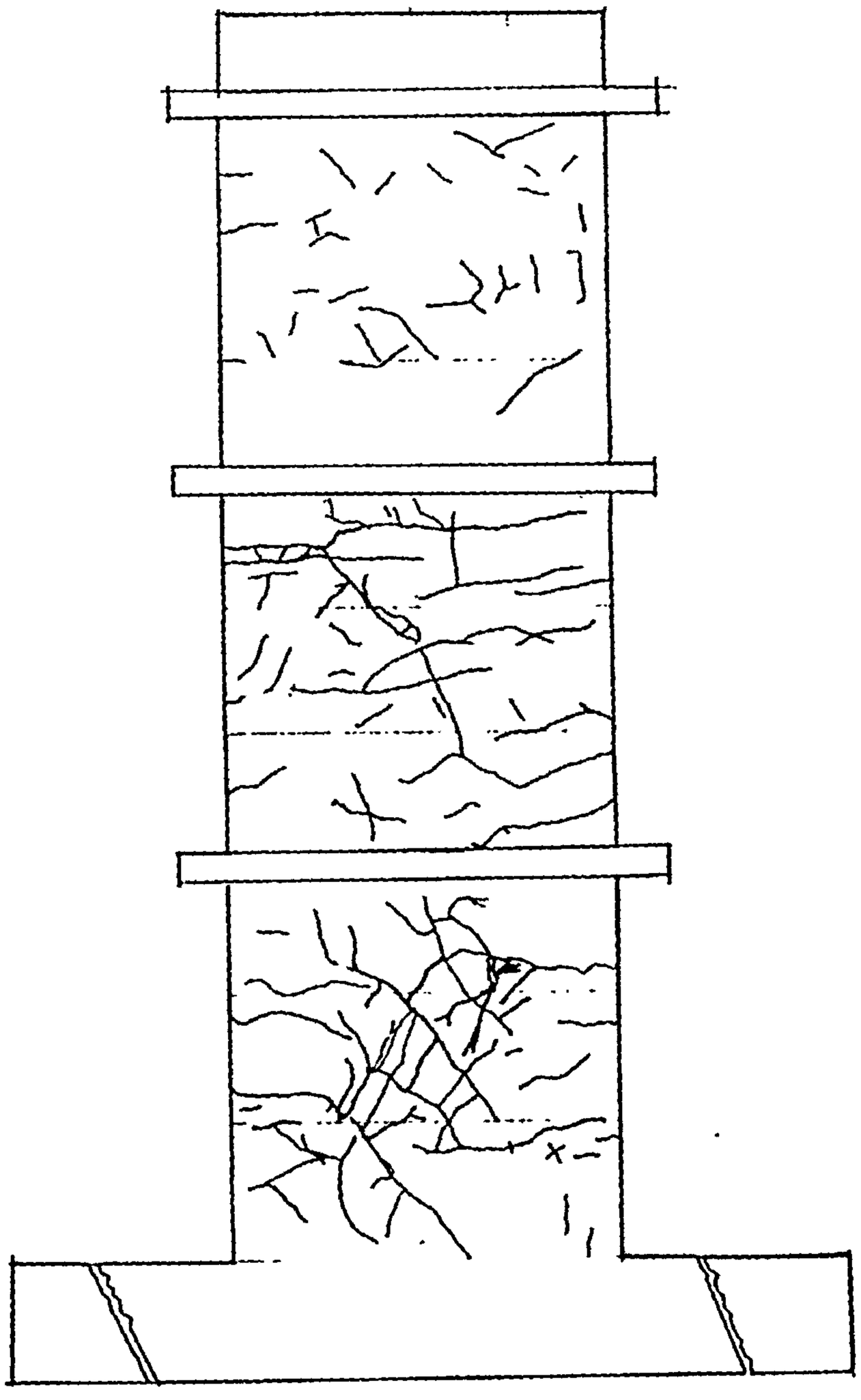

FIG. 7.3 EXPERIMENTAL CRACK PATTERN FOR SW1 [42]

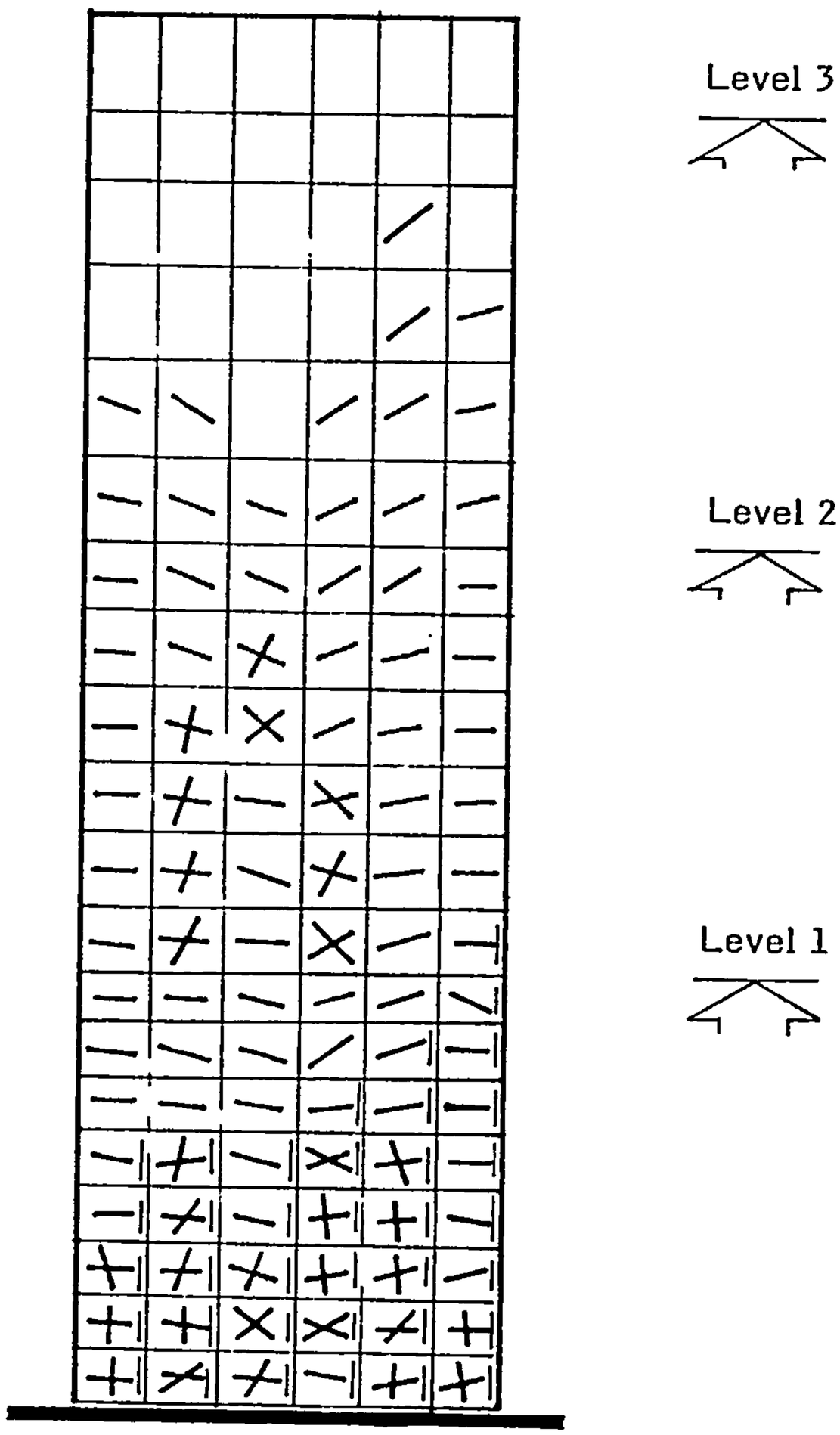

FIG. 7.4 CRACK PATTERN ACCORDING TO AGRAWAL'S ANALYTICAL MODEL [42]

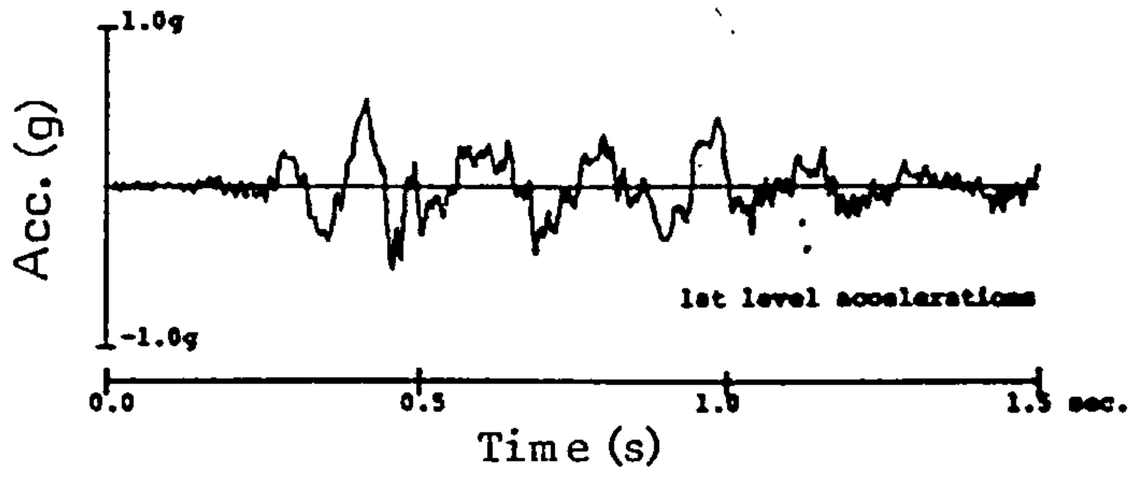

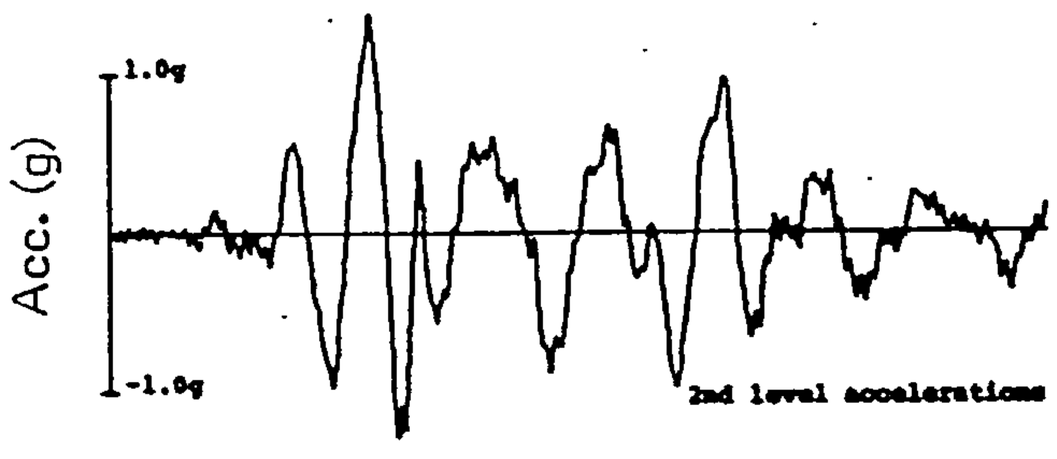

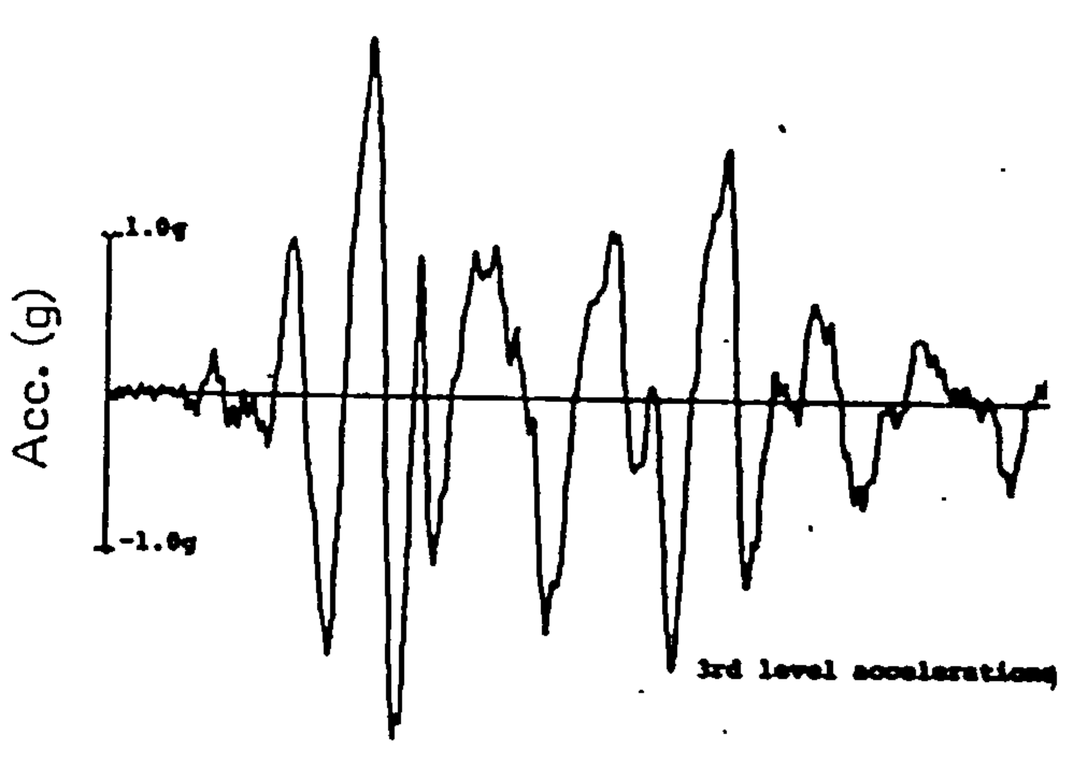

FIG. 7.5a ACCELERATION RESPONSE OF SW1 ACCORDING TO AGRAWAL

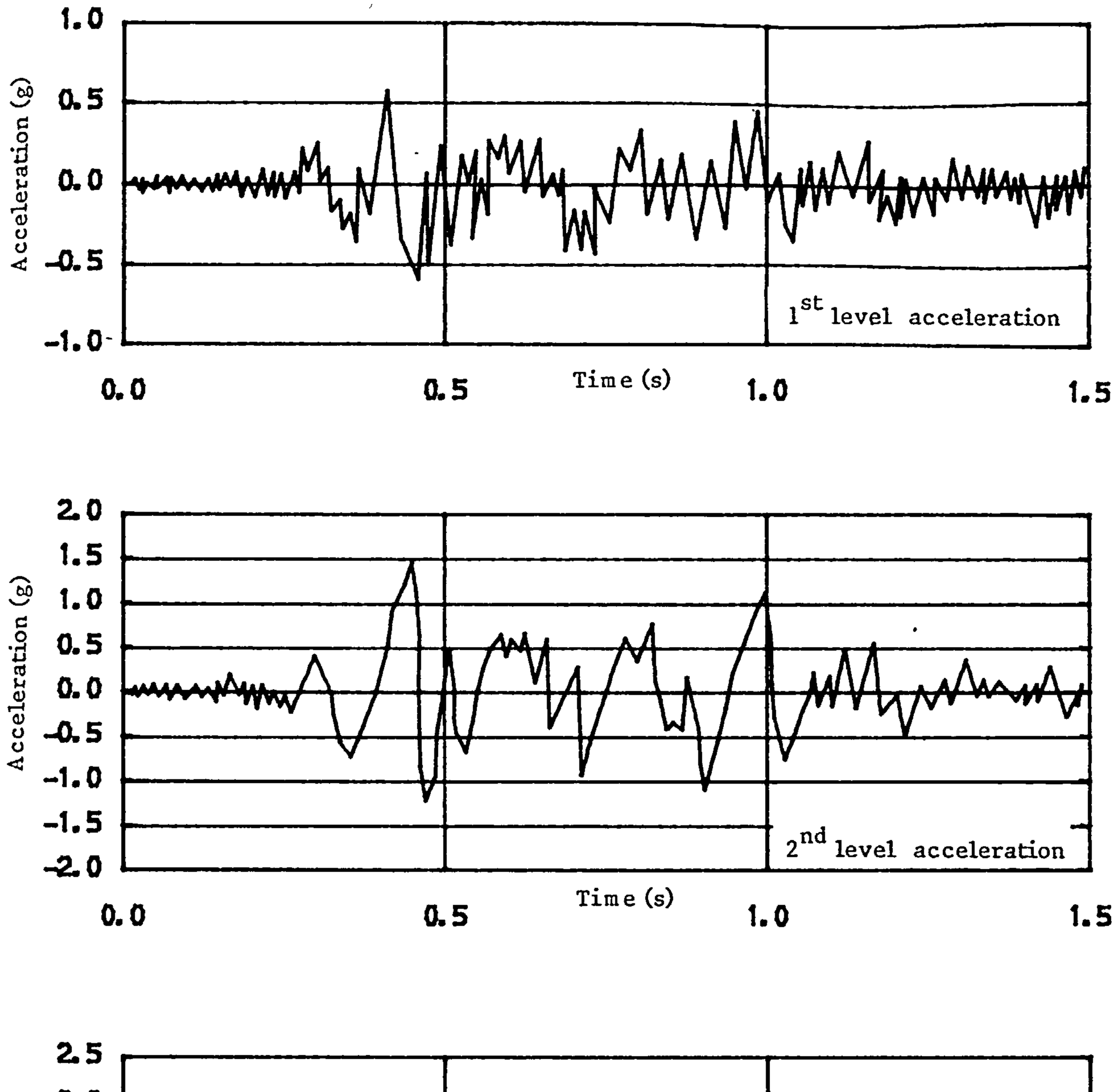

FIG. 7.5b PREDICTED ACCELERATION RESPONSE OF SW1

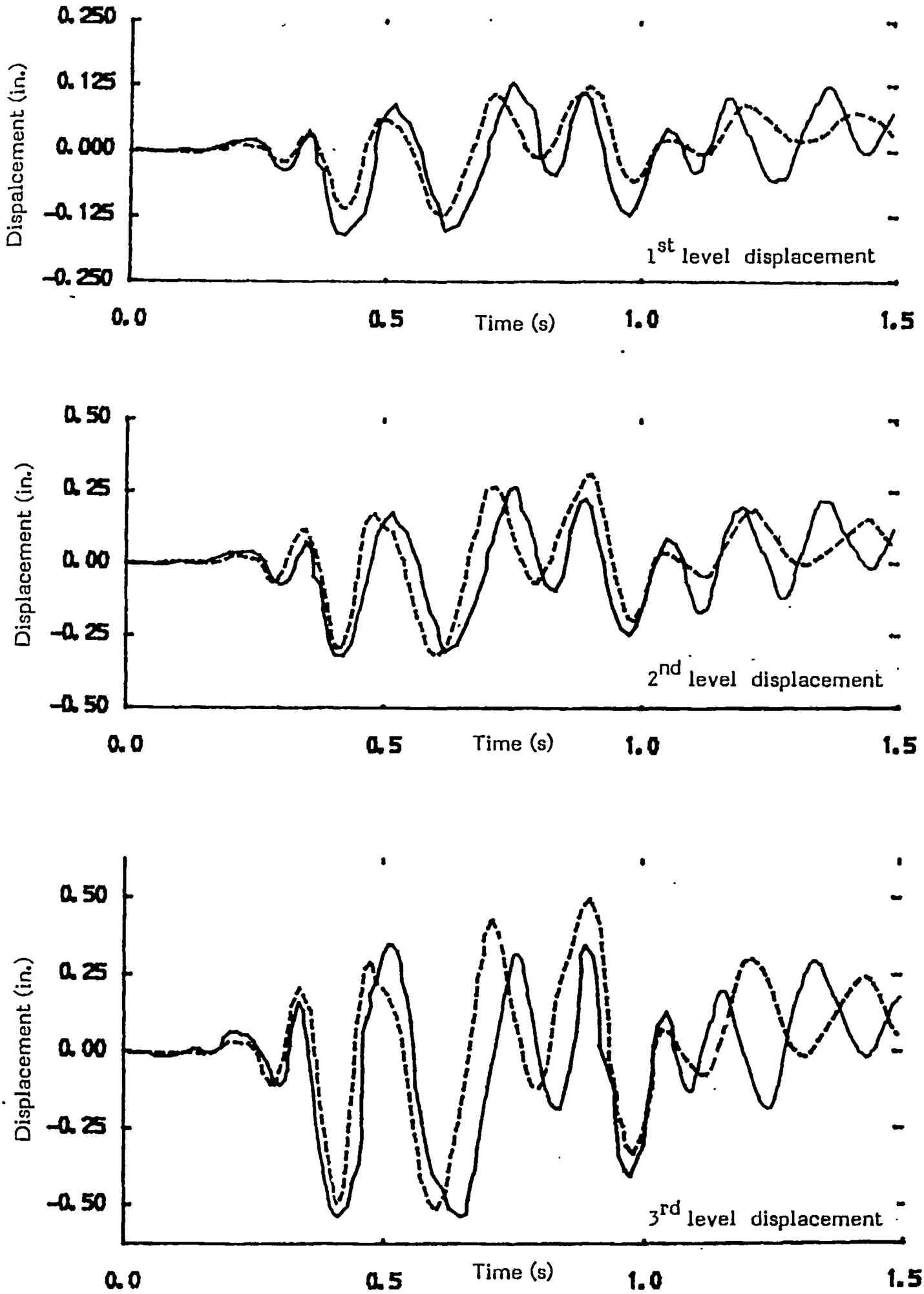

FIG. 7.6 DISPLACEMENT RESPONSE IN SW1

---- AGRAWAL [42]
———— PRESENT MODEL

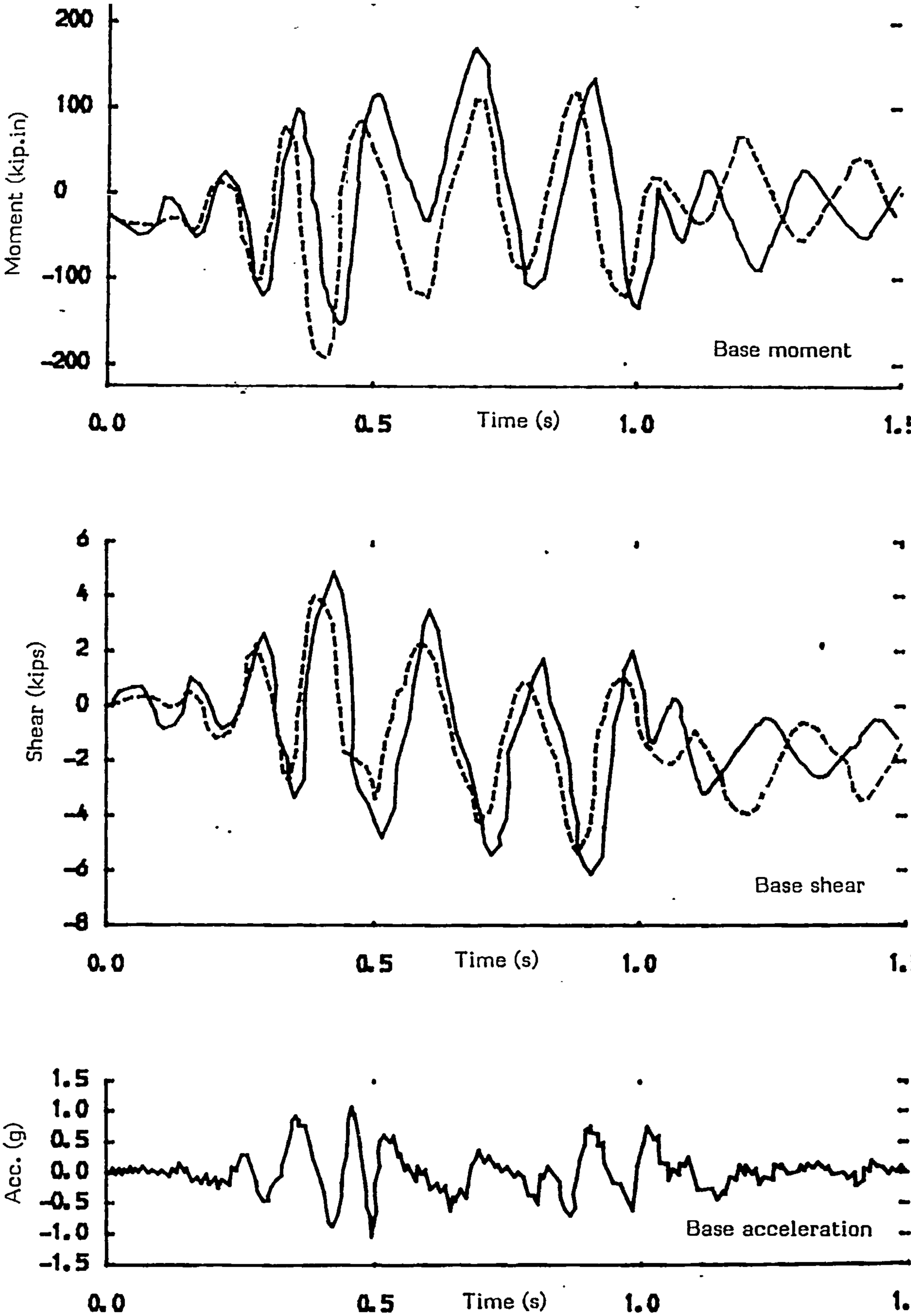

FIG. 7.7 BASE MOMENT & BASE SHEAR RESPONSE IN SW1

--- AGRAWAL [42]
——— PRESENT MODEL

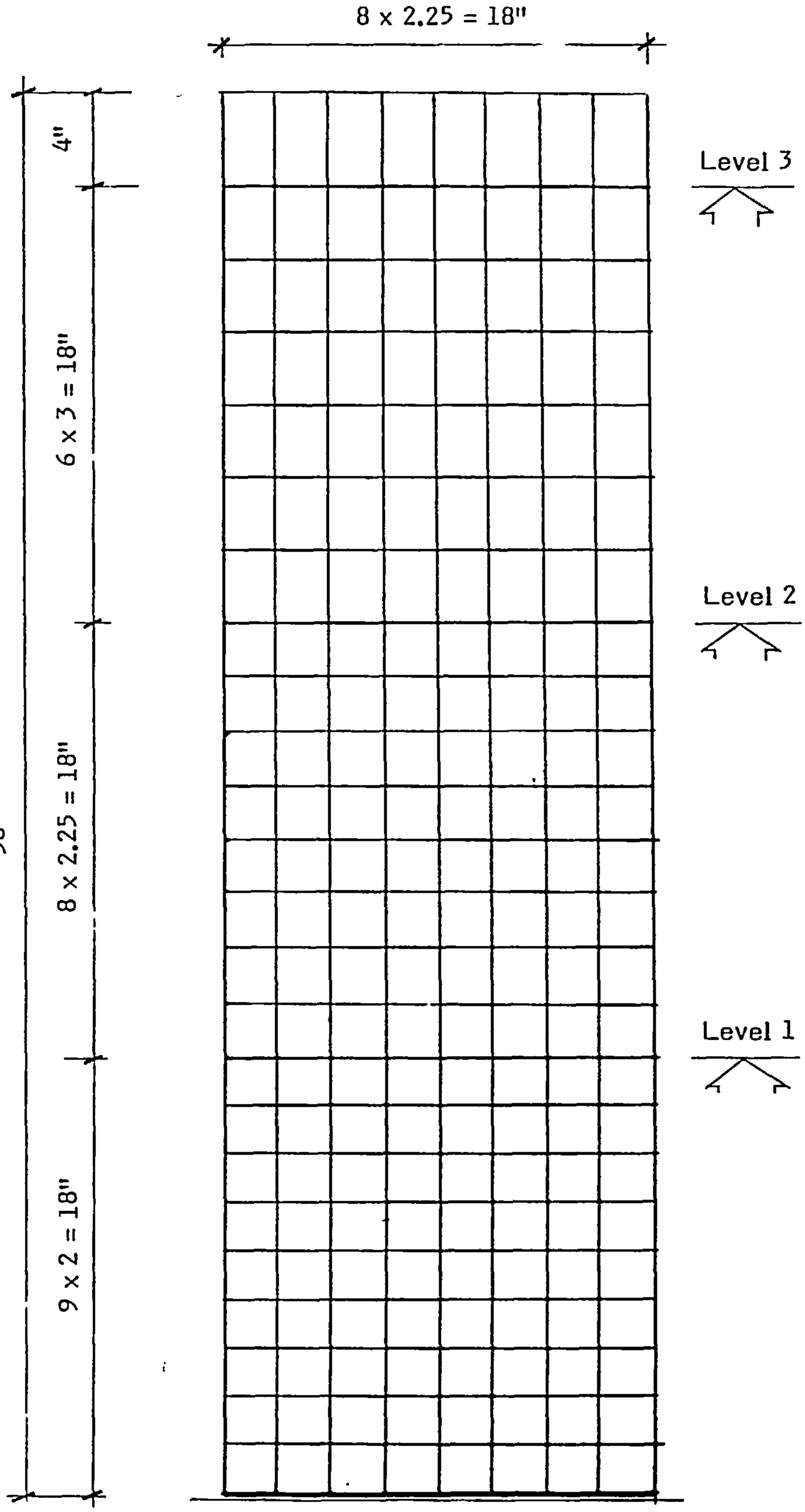

FIG. 7.8a ANALYTICAL FAILURE PREDICTION OF SW1
Time = 0.00 sec.

Open crack
Closed crack
Yielding of steel
Crushed element

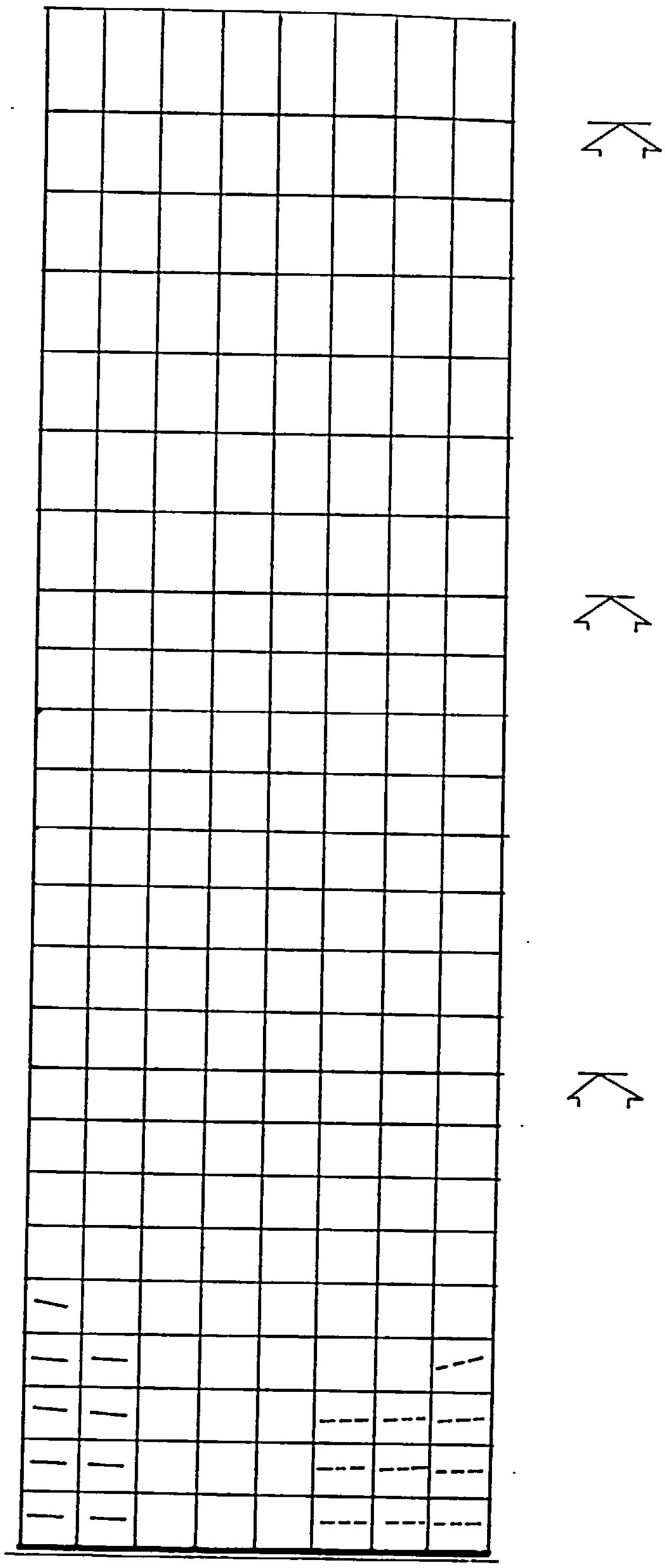

FIG. 7.8b ANALYTICAL FAILURE PREDICTION OF SW1
Time = 0.30 sec.

— Open crack
--- Closed crack
| Yielding of steel
◣ Crushed element

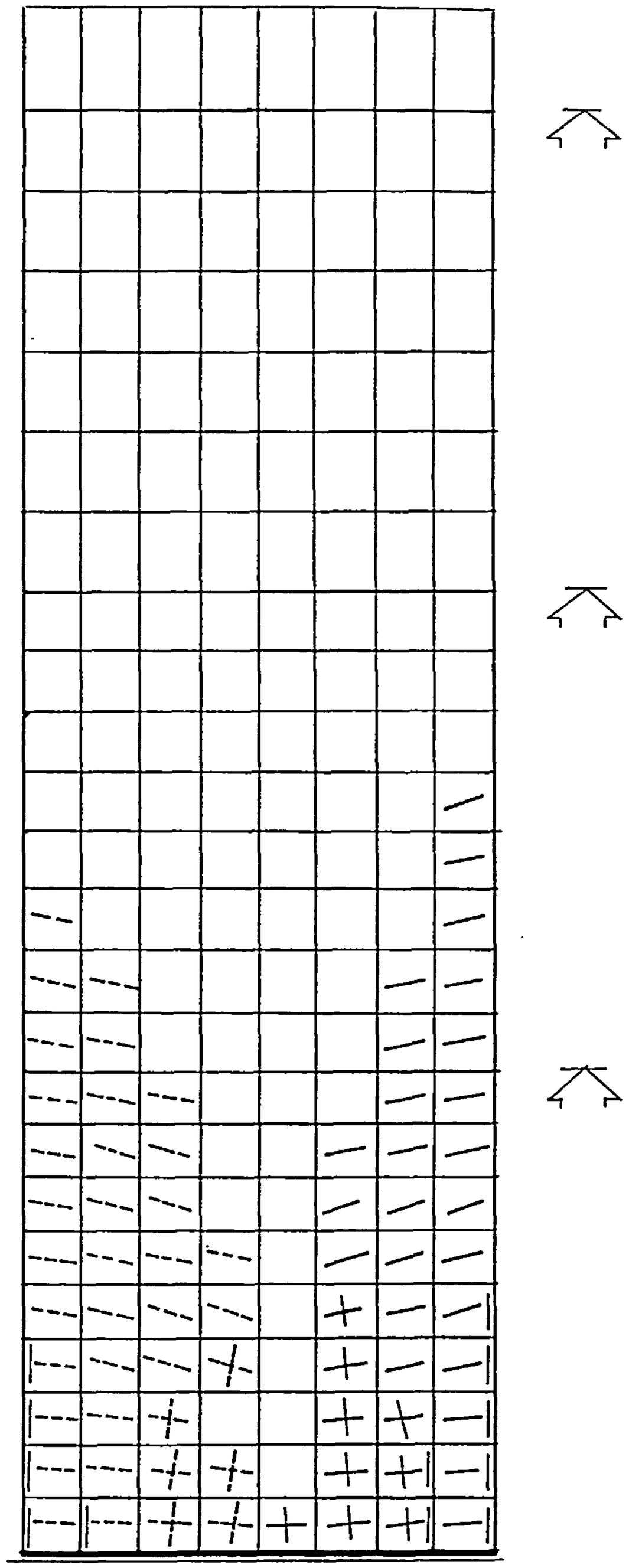

Open crack
Closed crack
Yielding of steel
Crushed element

FIG. 7.8c ANALYTICAL FAILURE PREDICTION OF SW1
Time = 0.60 sec.

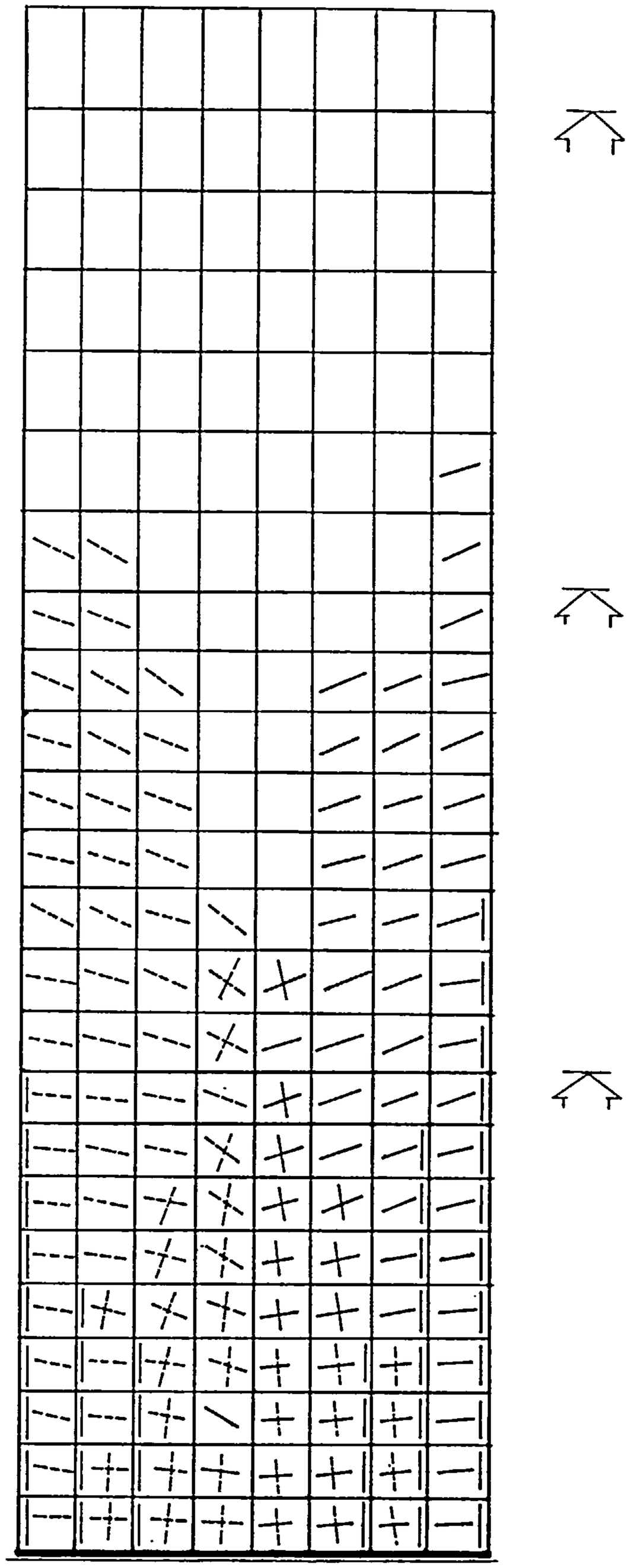

Open crack
Closed crack
Yielding of steel
Crushed element

FIG. 7.8d ANALYTICAL FAILURE PREDICTION OF SW1
Time = 0.90 sec.

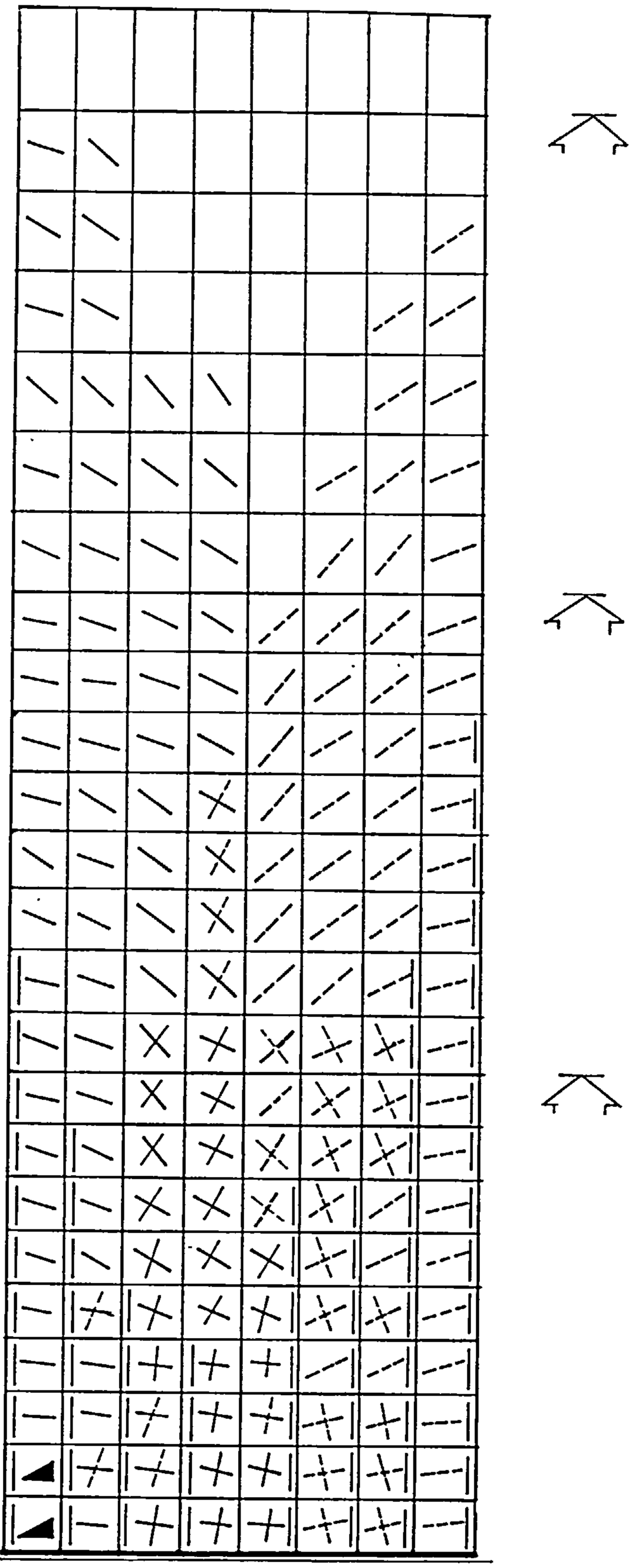

FIG. 7.8e ANALYTICAL FAILURE PREDICTION OF SW1
Time = 1.20 sec.

Open crack
Closed crack
Yielding of steel
Crushed element

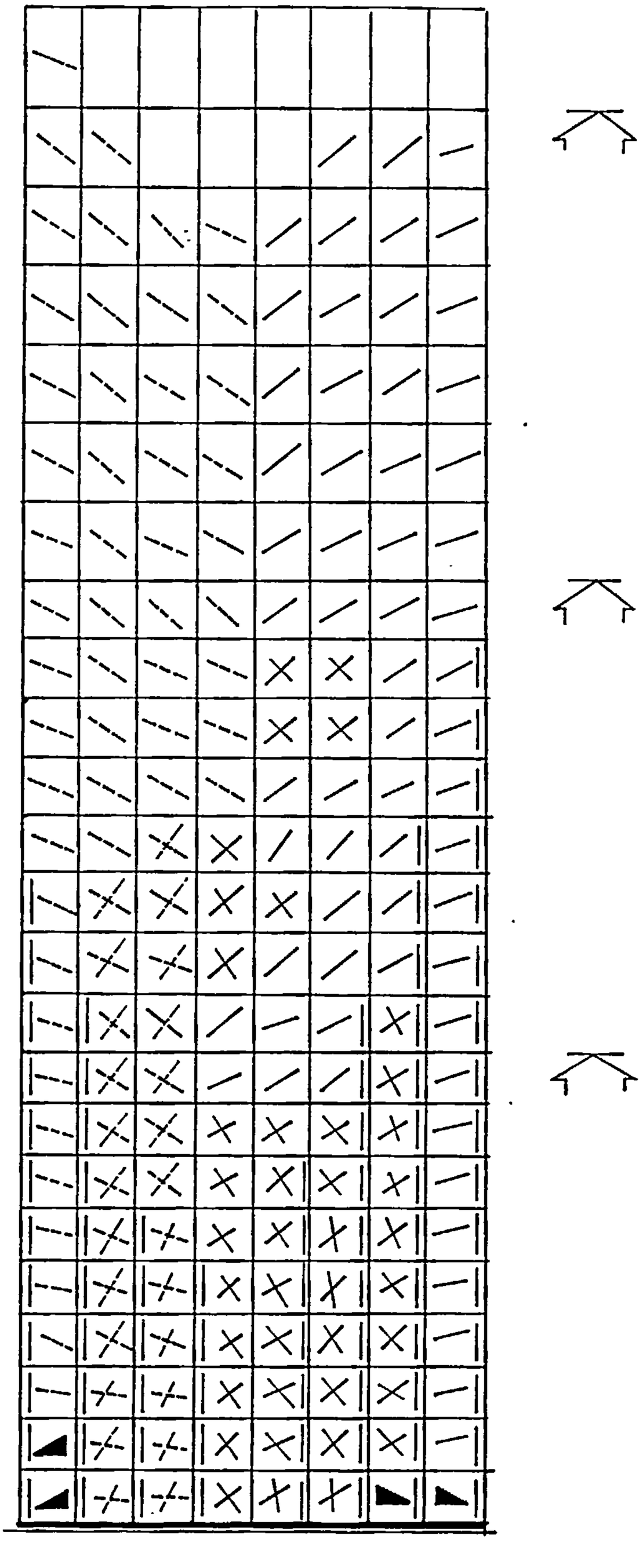

FIG. 7.8f ANALYTICAL FAILURE PREDICTION OF SW1
Time = 1.50 sec.

Open crack
Closed crack
Yielding of steel
Crushed element

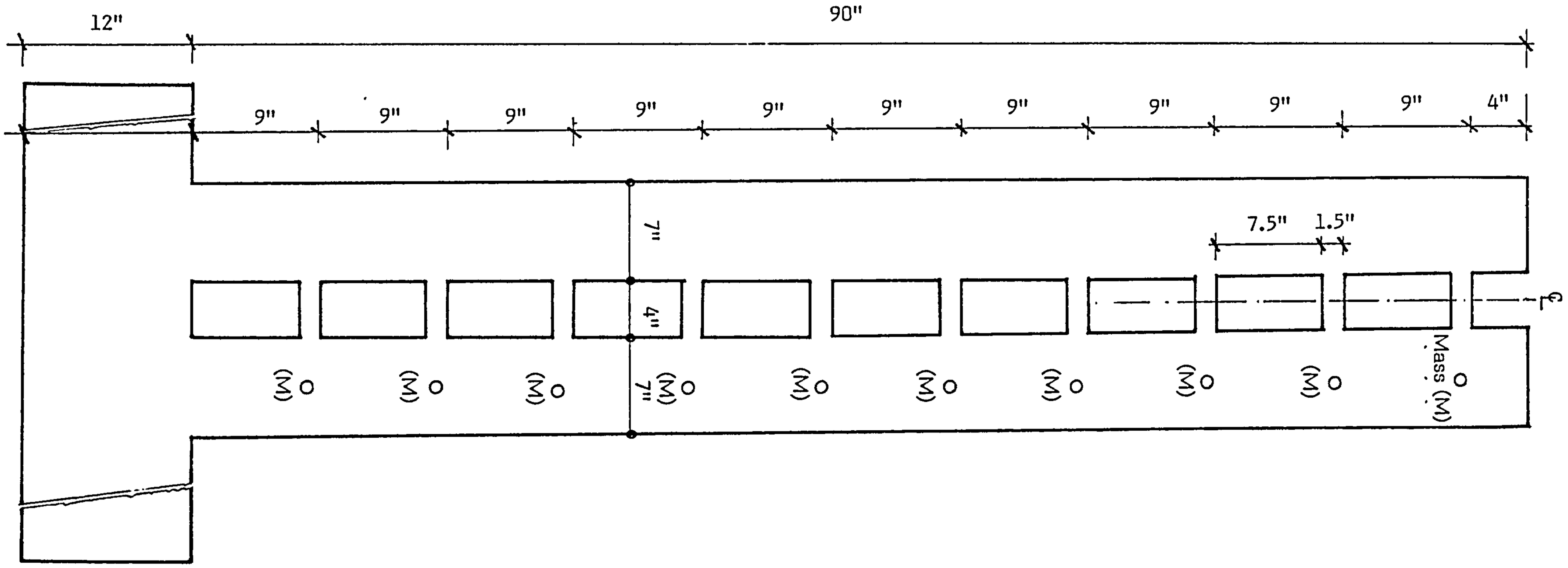

FIG. 7.9 GEOMETRICAL PROPERTIES OF SW2A AND SW2B

a) SW2A

Walls from base to level 6

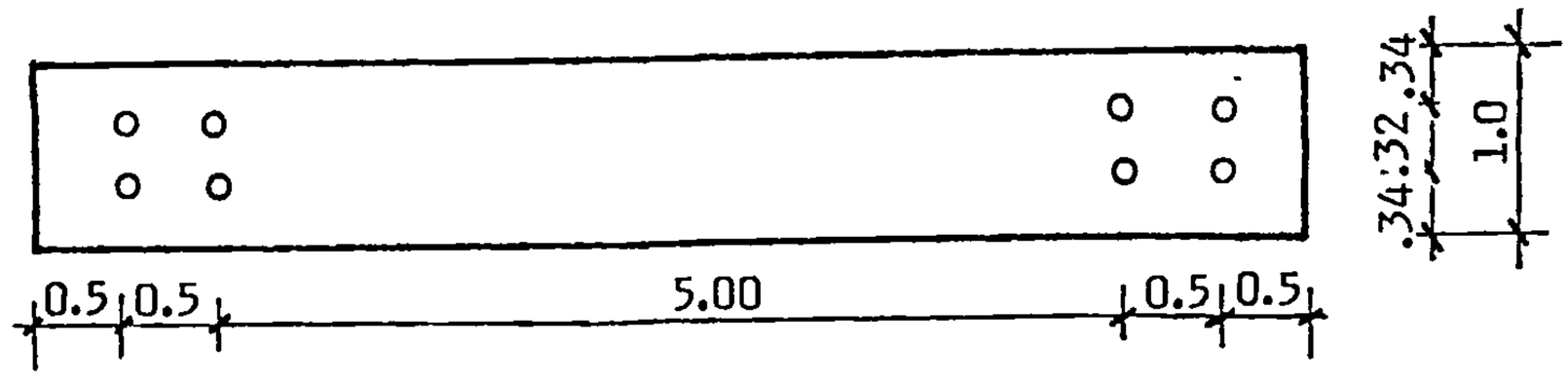

Walls from level 6 to level 10

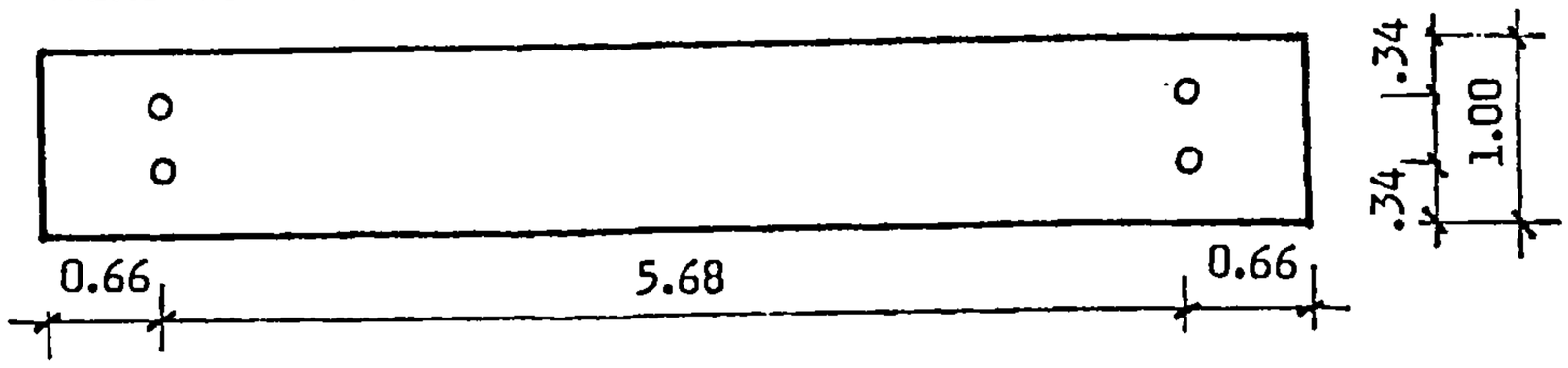

Coupling beams

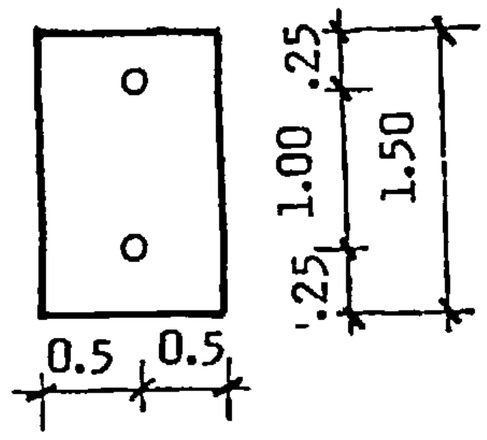

ALL REIFORCING BARS
No. 8 Wires

b) SW2B

Walls from base to level 10

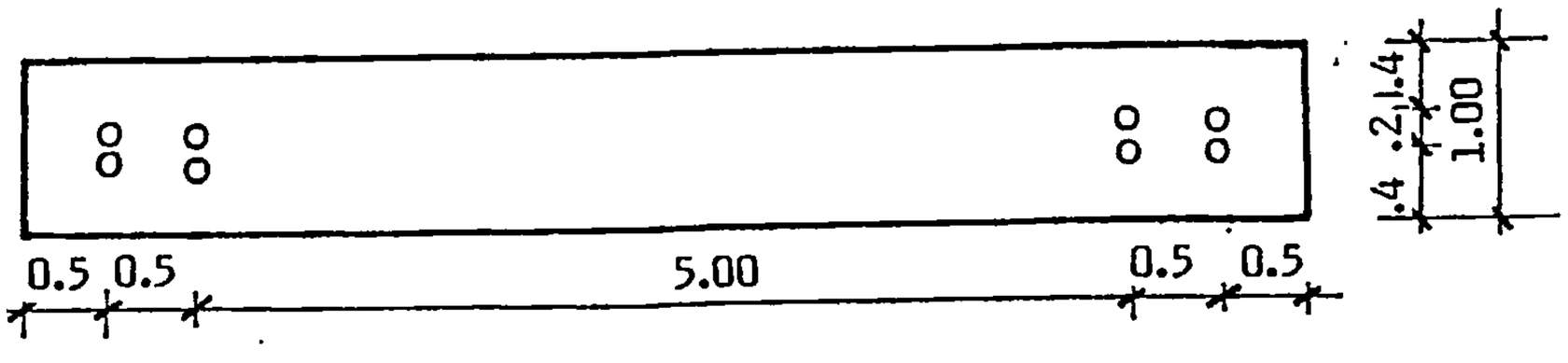

Coupling beams

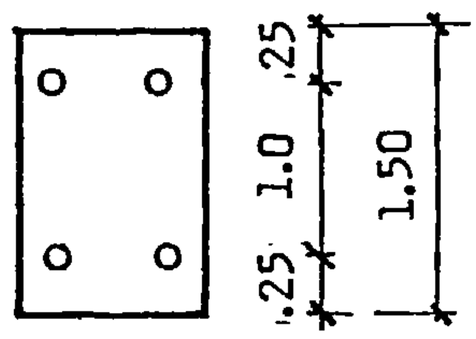

FIG. 7.10 CROSS SECTIONAL PROPERTIES OF SW2A and SW2B

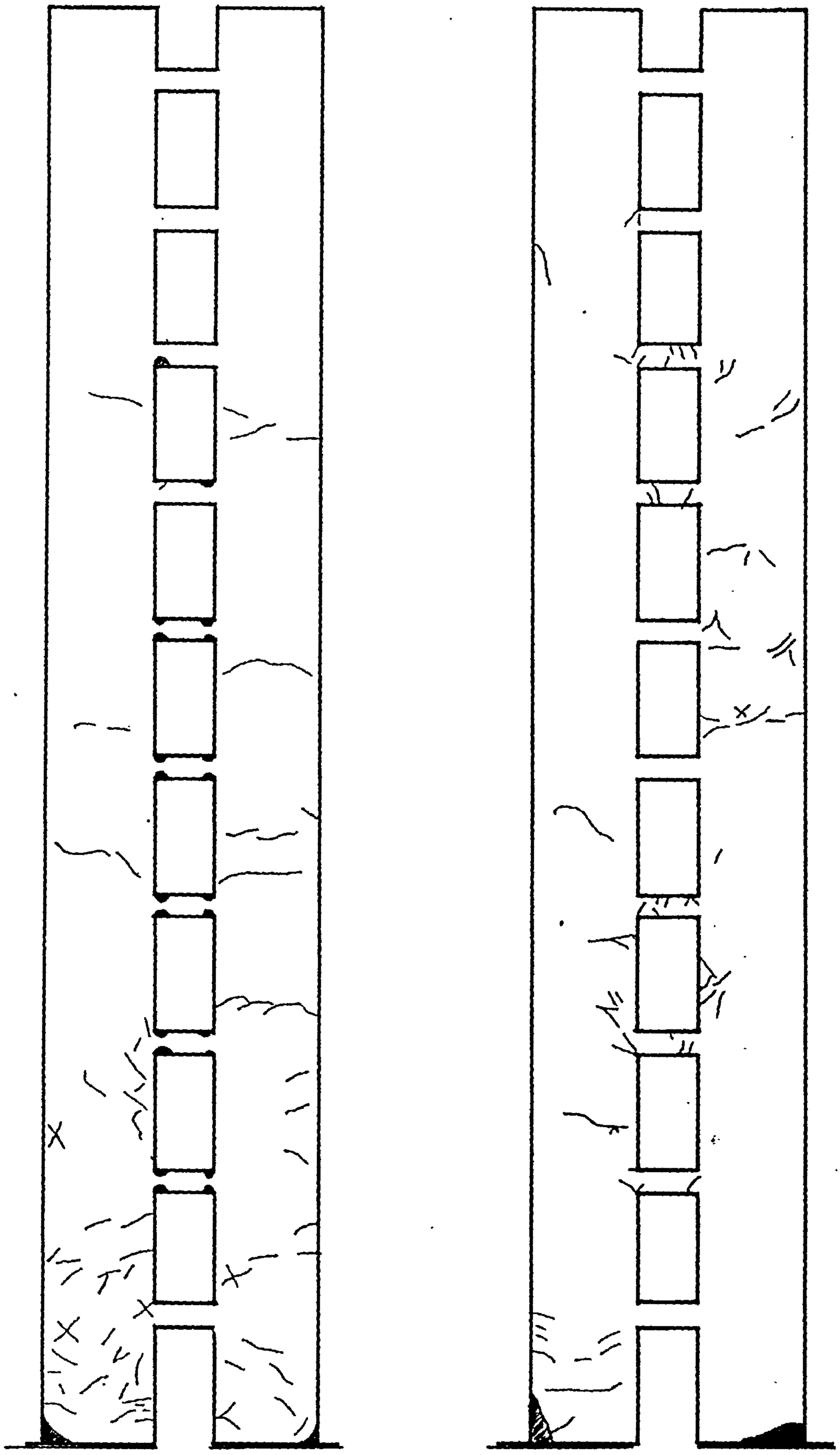

FIG. 7.11 EXPERIMENTAL FAILURE PATTERN OF SW2A and SW2B

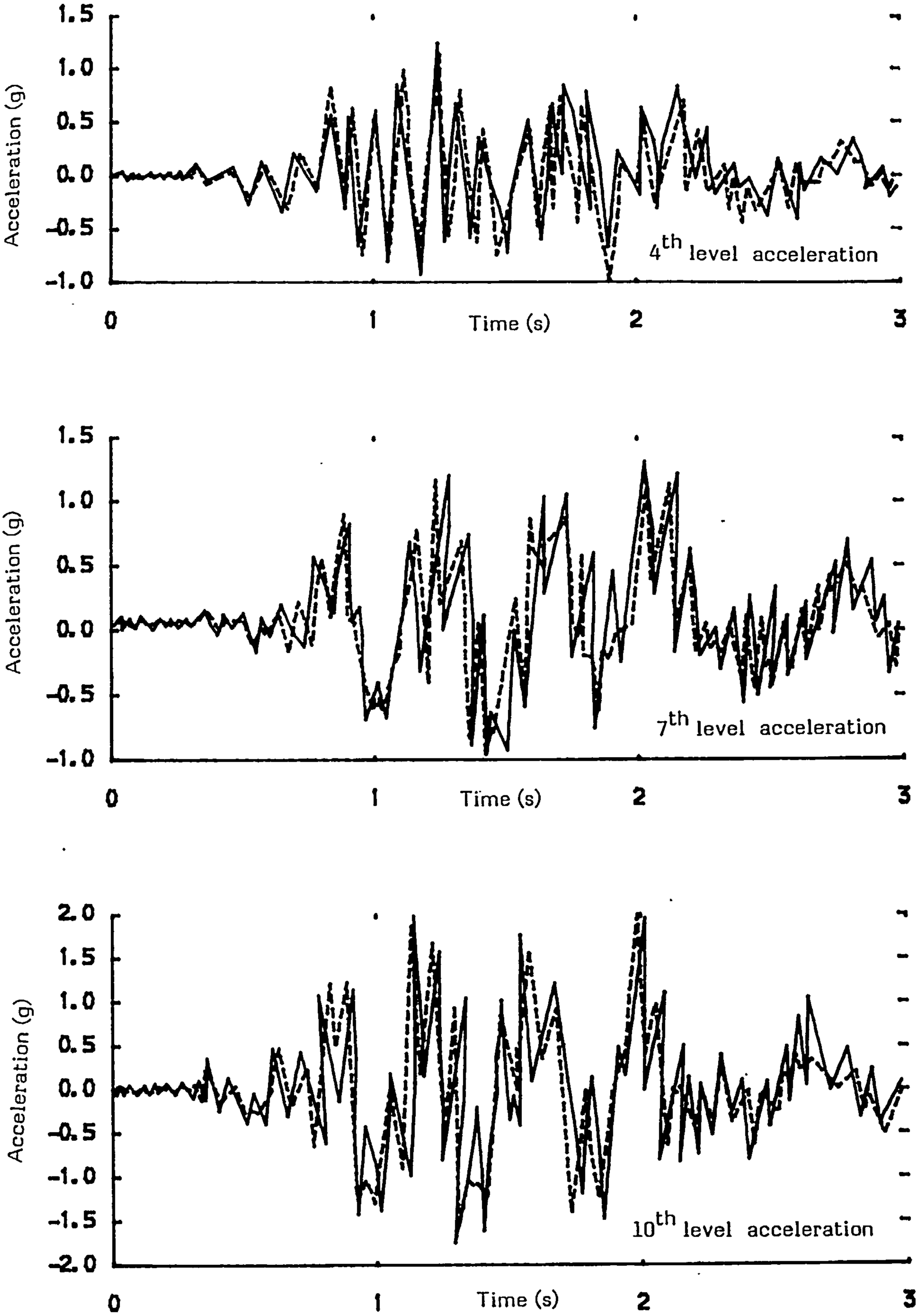

FIG. 7.12a ACCELERATION RESPONSE IN SW2A

_ _ _ EXPERIMENTAL [109]
____ PREDICTED

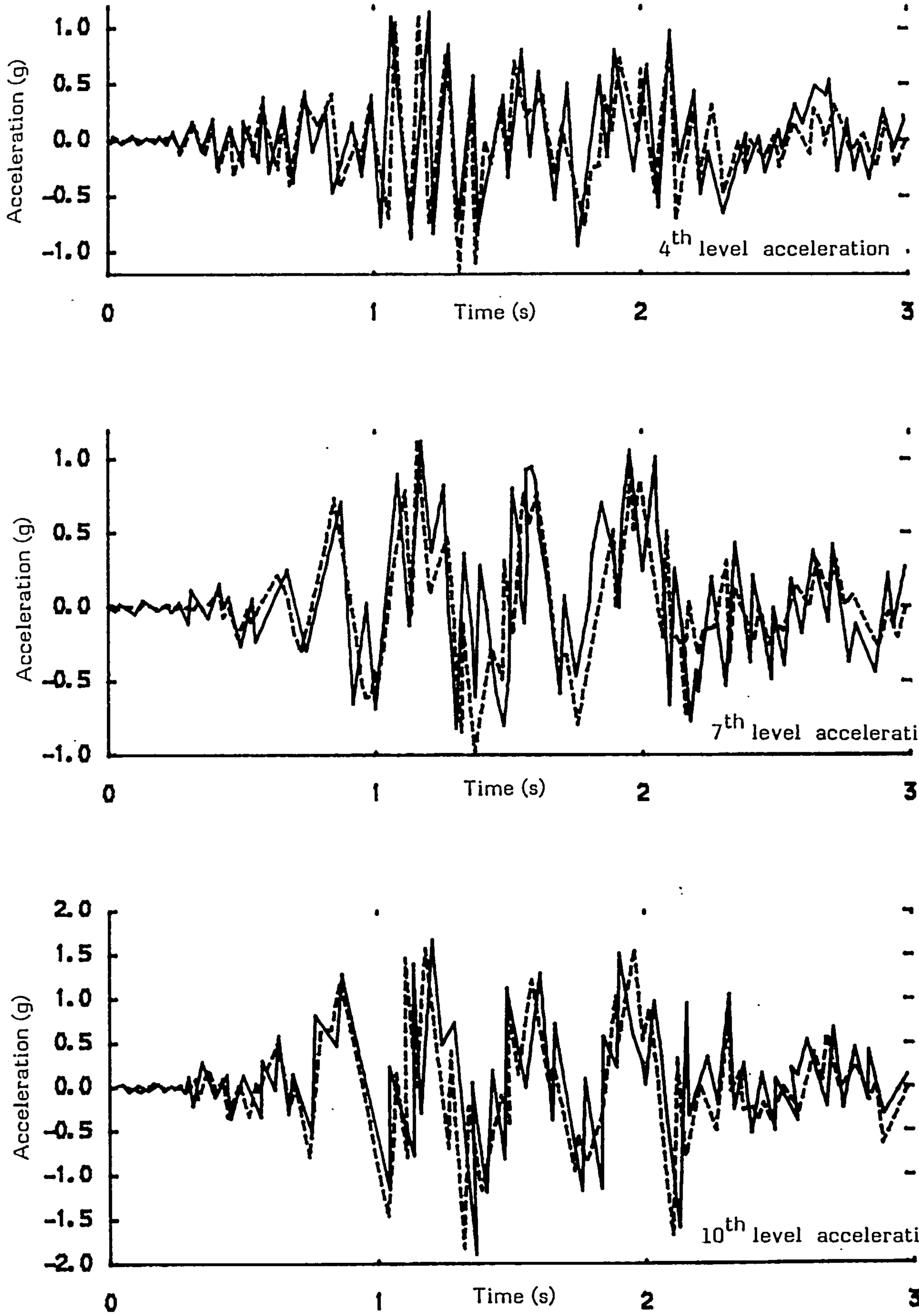

FIG. 7.12b ACCELERATION RESPONSE IN SW2B

_ _ _ EXPERIMENTAL [109]
_____ PREDICTED

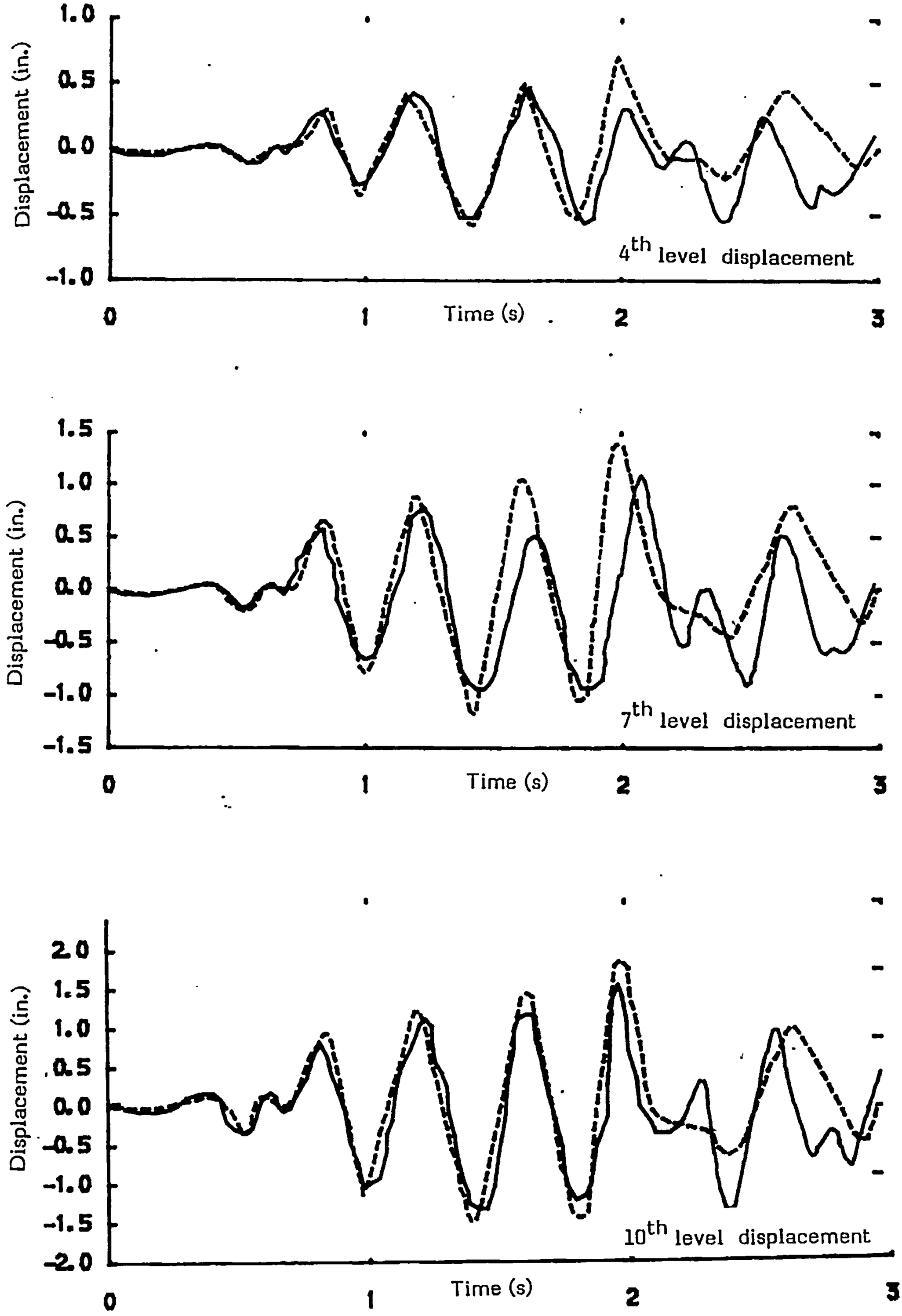

FIG. 7.13a DISPLACEMENT RESPONSE IN SW2A

---- EXPERIMENTAL [109]
———— PREDICTED

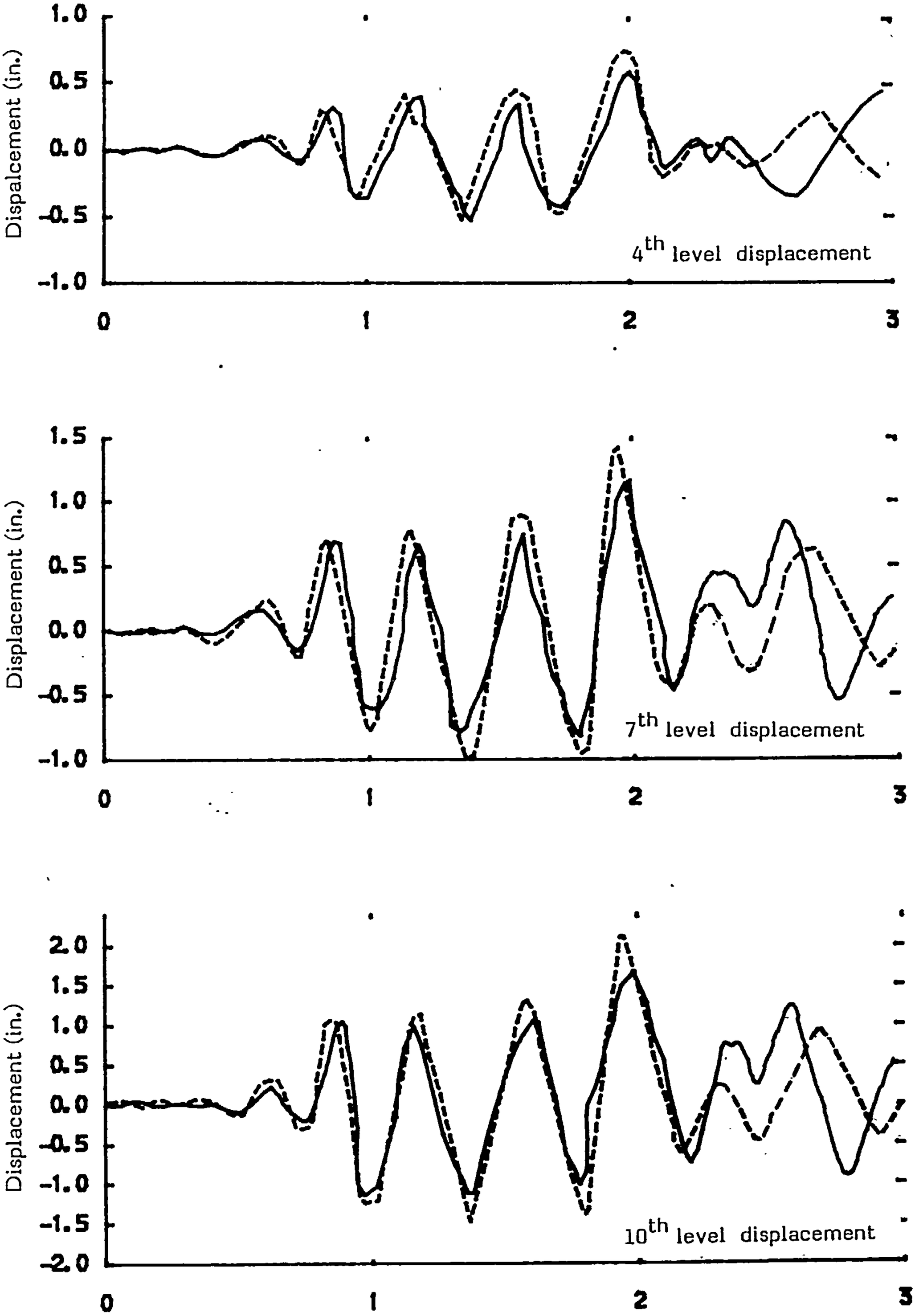

FIG. 7.13b DISPLACEMENT RESPONSE IN SW2B

---- EXPERIMENTAL [109]
———— PREDICTED

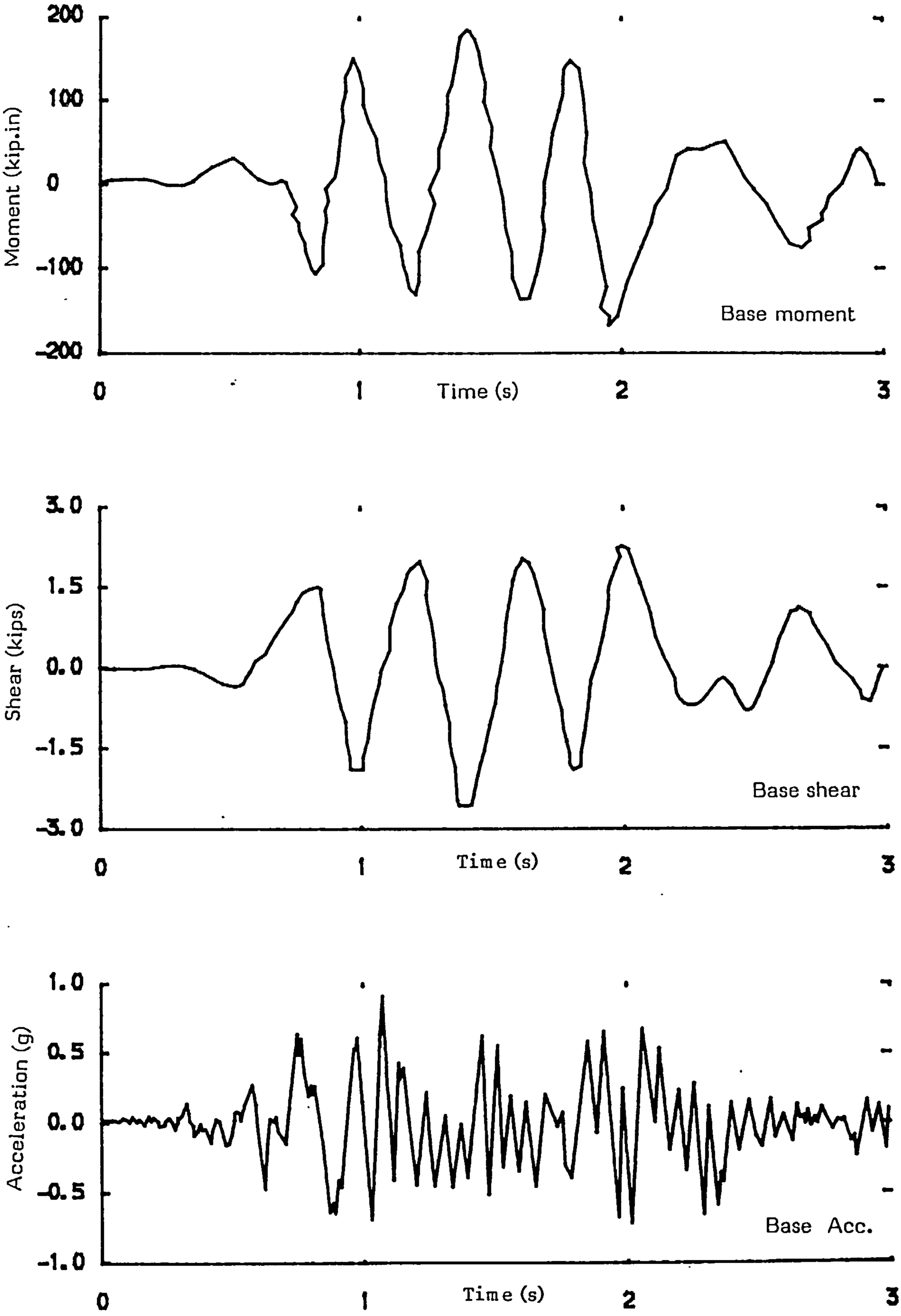

FIG. 7.14a BASE SHEAR & BASE MOMENT RESPONSE IN SW2A

---- EXPERIMENTAL [109]
____ PREDICTED

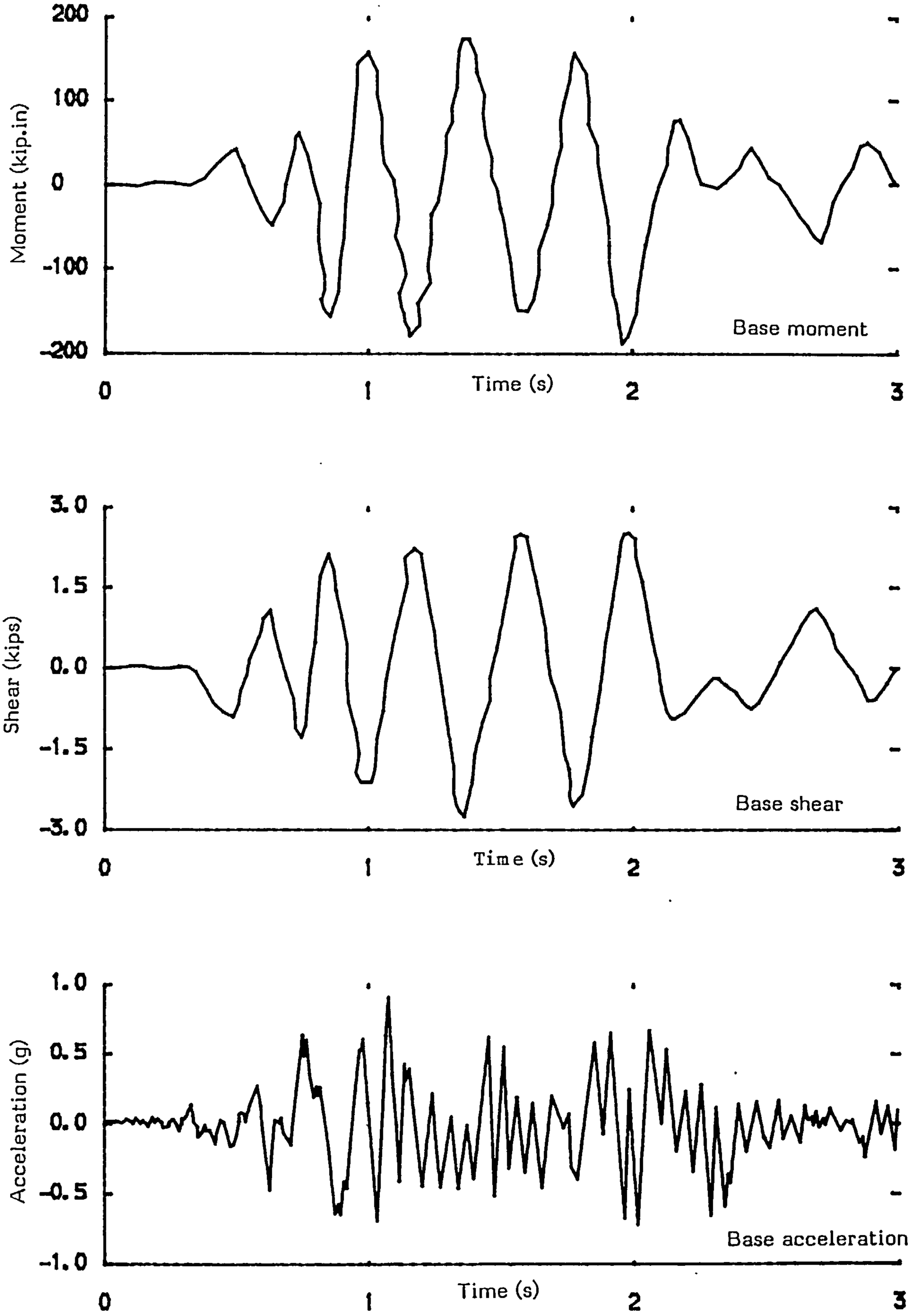

FIG. 7.14b BASE SHEAR & BASE MOMENT RESPONSE IN SW2B

---- EXPERIMENTAL [109]
———— PREDICTED

a) SW2A

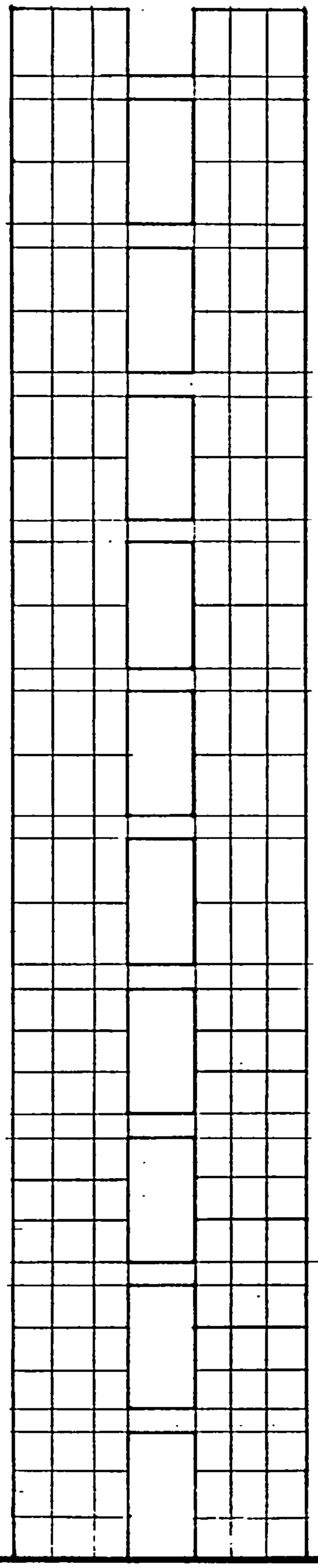

b) SW2B

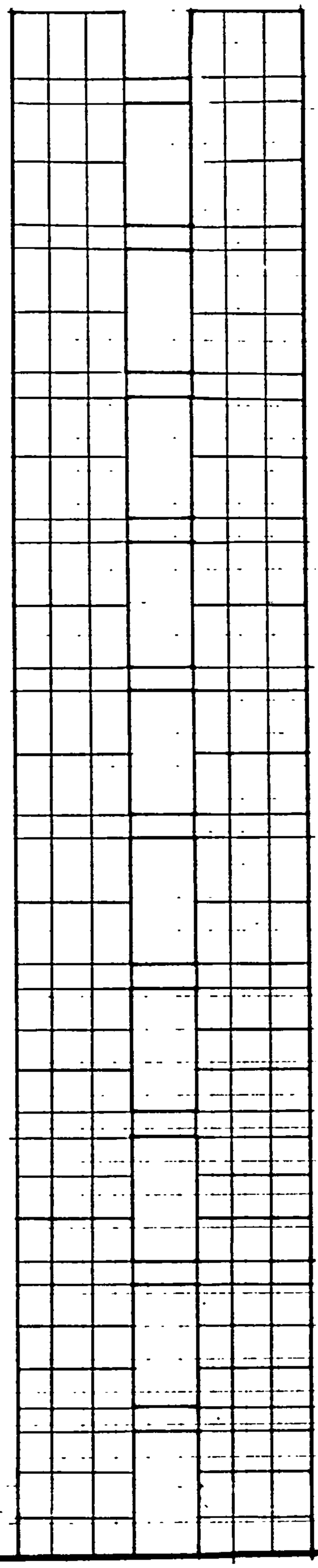

FIG. 7.15a ANALYTICAL FAILURE PREDICTION OF SW2A & SW2B
Time = 0.00 sec.

Open crack
Closed crack
Yielding of steel
Crushed element

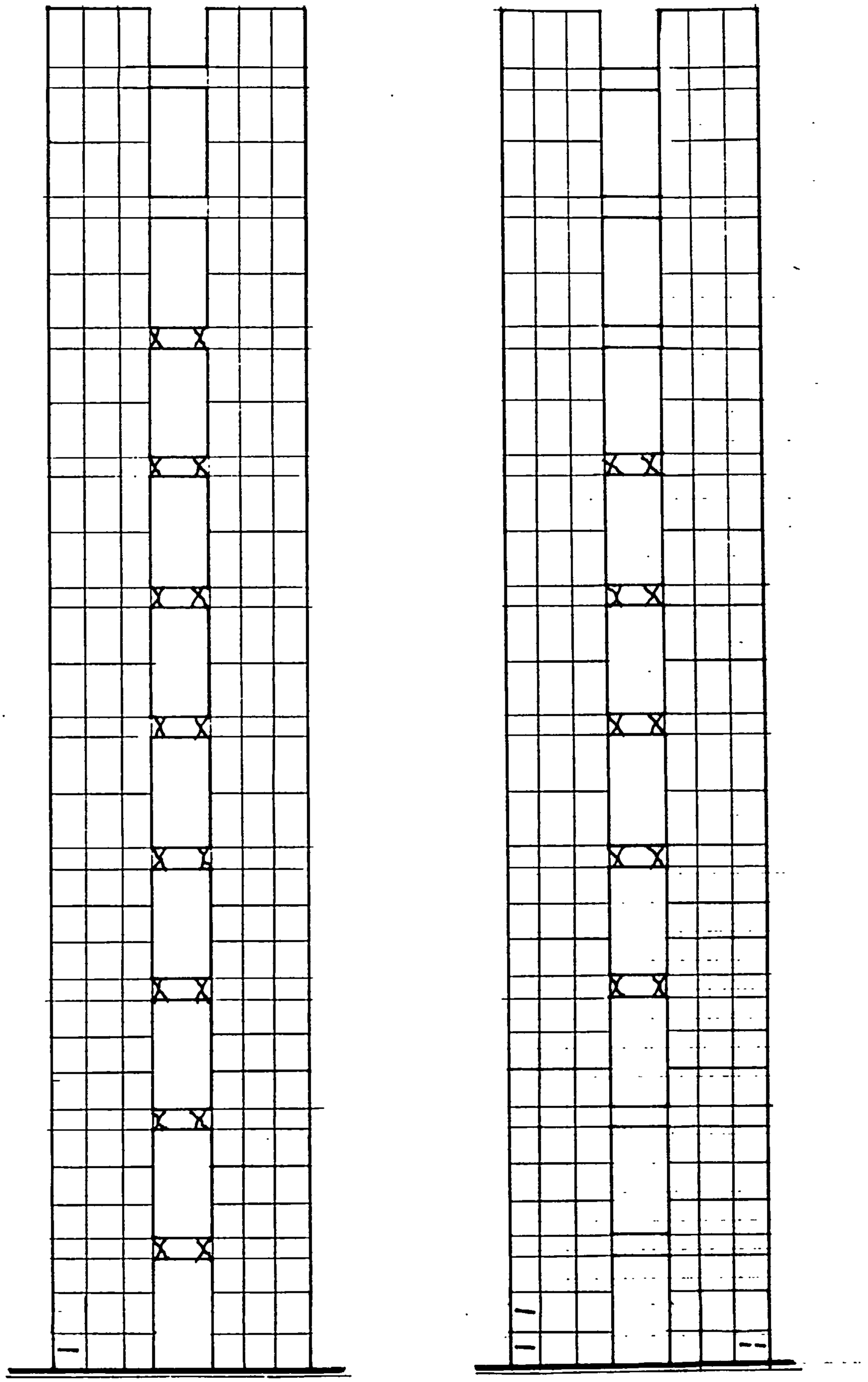

FIG. 7.15b ANALYTICAL FAILURE PREDICTION OF SW2A & SW2B
Time = 0.75 sec.

Open crack
Closed crack
Yielding of steel
Crushed element

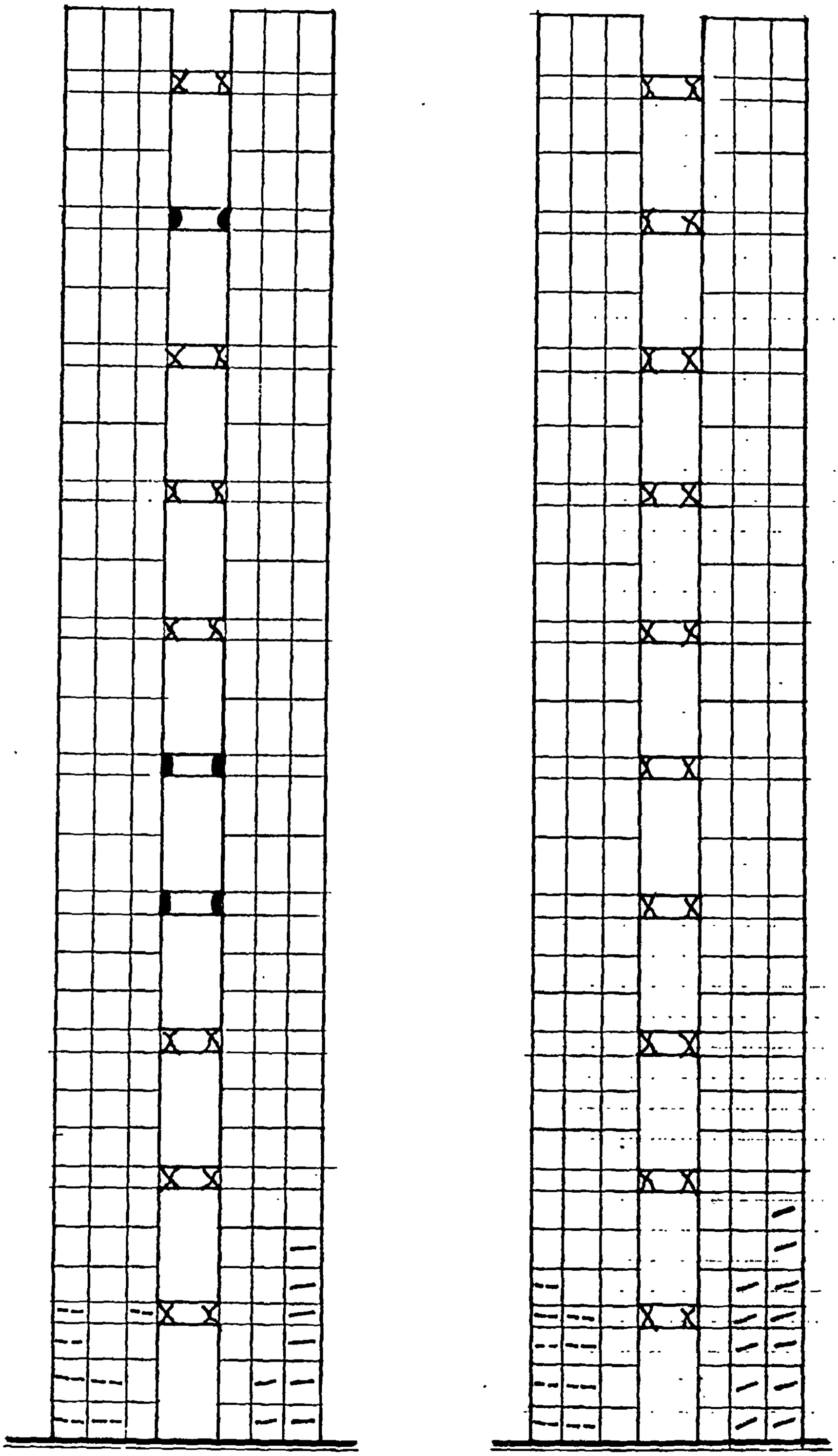

FIG. 7.15c ANALYTICAL FAILURE PREDICTION OF SW2A & SW2B
Time = 1.50 sec.

Open crack
Closed crack
Yielding of steel
Crushed element

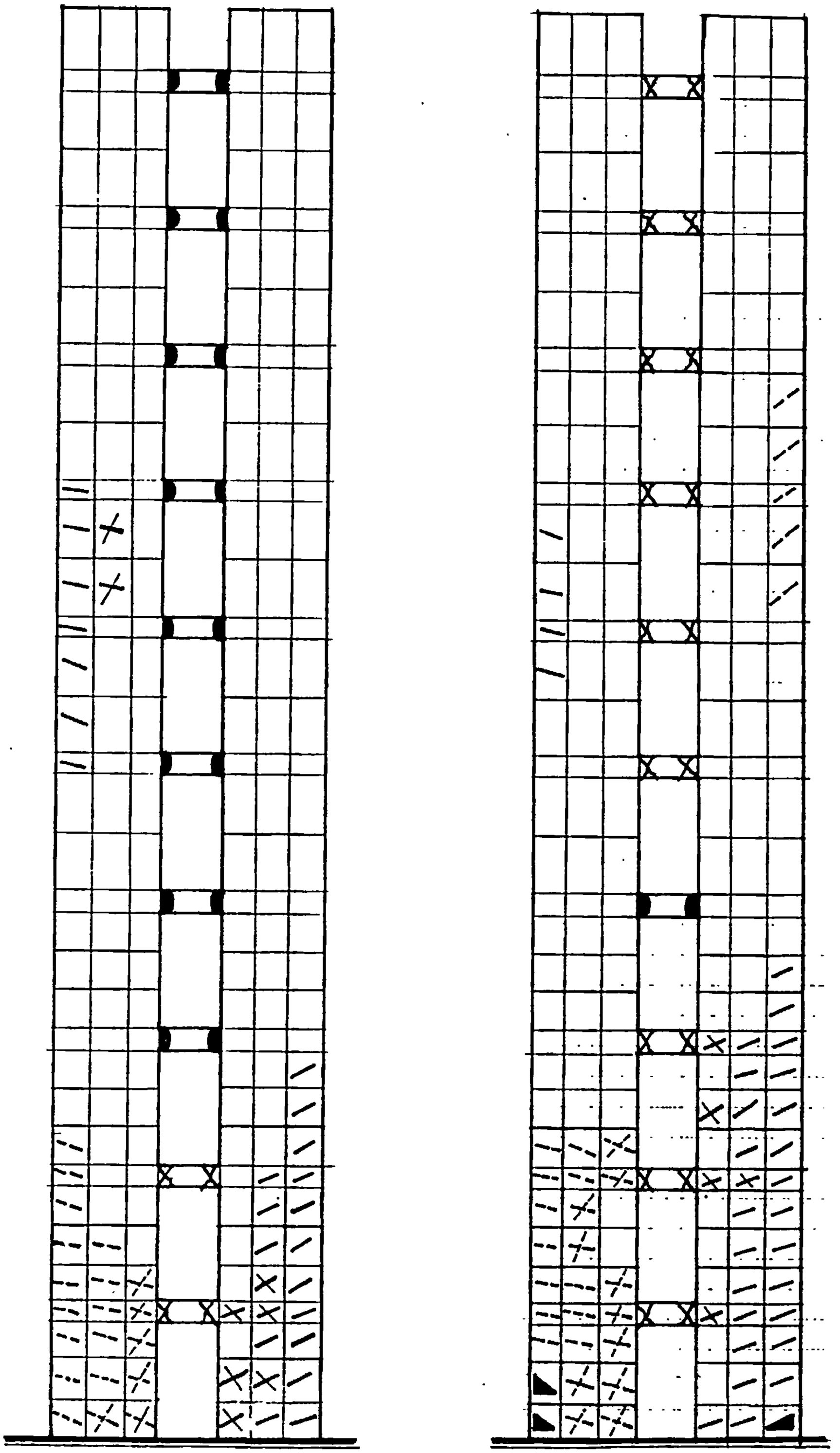

FIG. 7.15d ANALYTICAL FAILURE PREDICTION OF SW2A & SW2B
Time = 2.25 sec.

Open crack
Closed crack
Yielding of steel
Crushed element

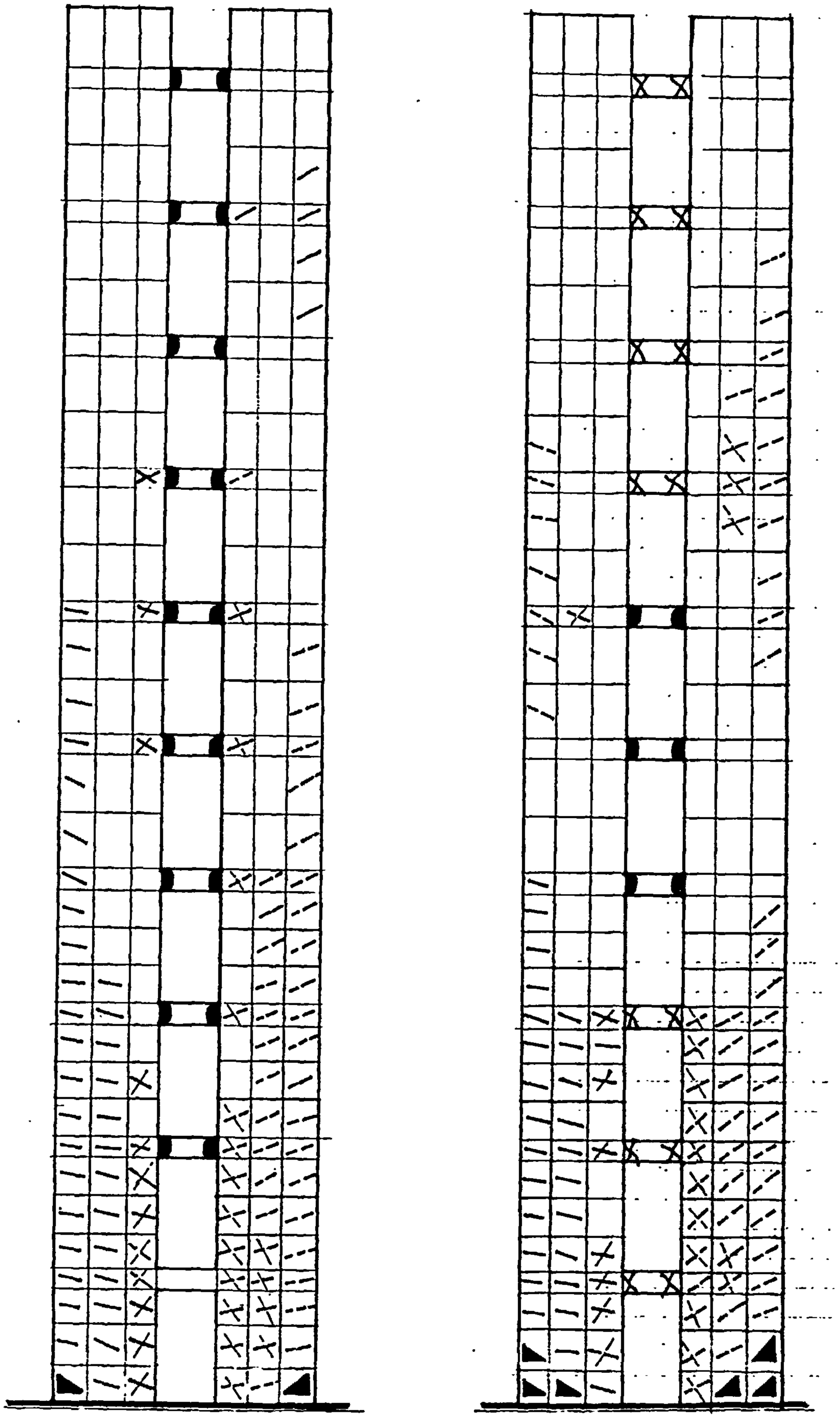

FIG. 7.15e ANALYTICAL FAILURE PREDICTION OF SW2A & SW2B
Time = 3.00 sec.

Open crack
Closed crack
Yielding of steel
Crushed element

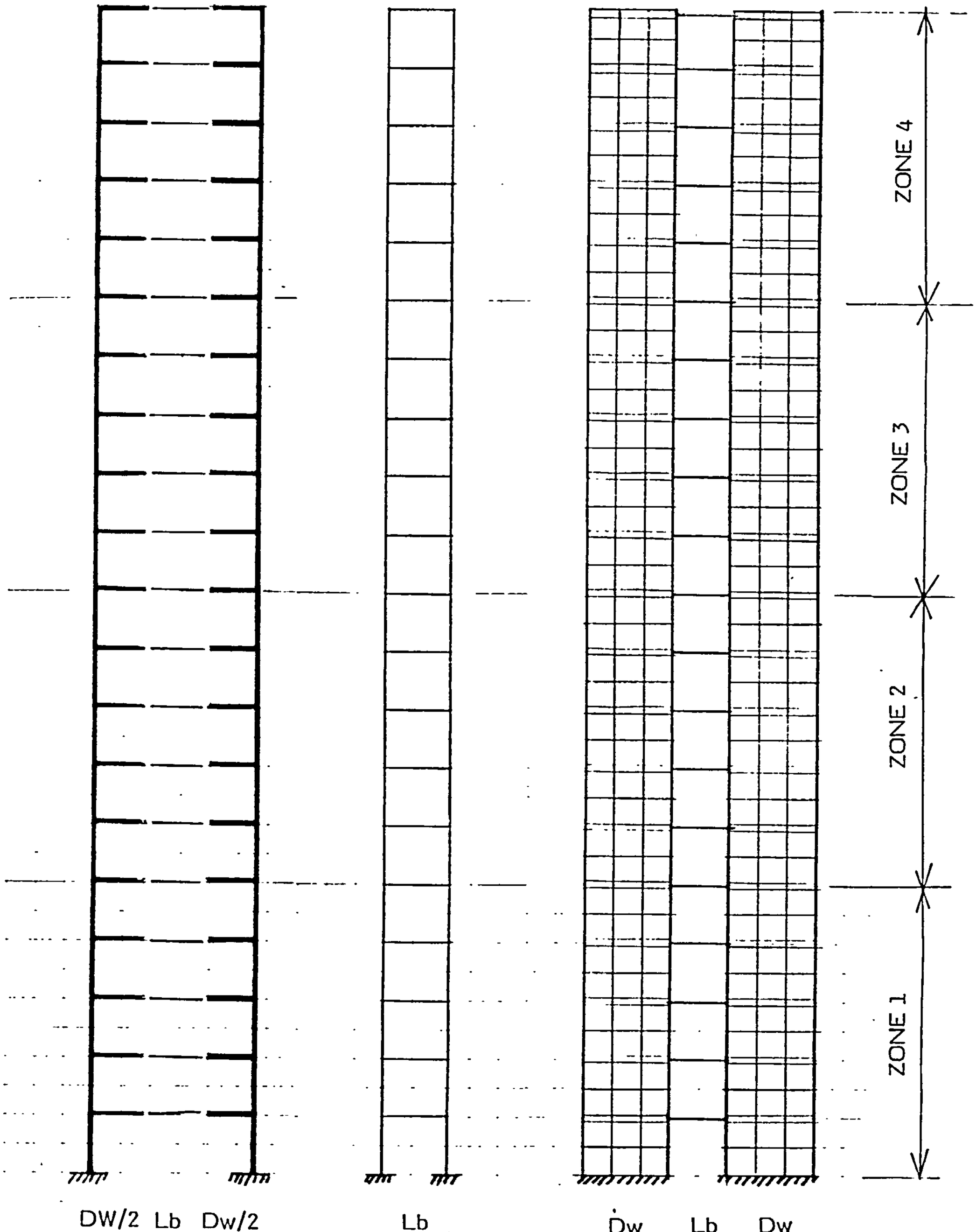

FIG. 7.16 DISCRETISATION OF THE 20 STOREY COUPLED SHEAR WALL SW3

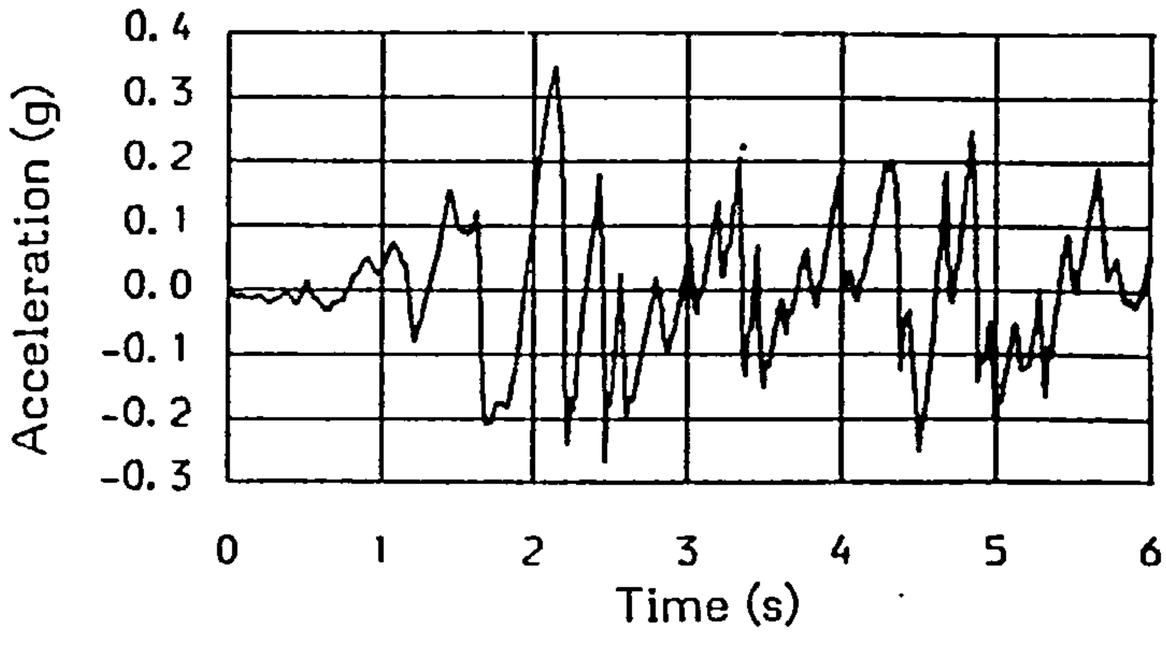

FIG. 7.17 FIRST 6 SECONDS OF EL CENTRO ACCELEROGRAM (N-S)

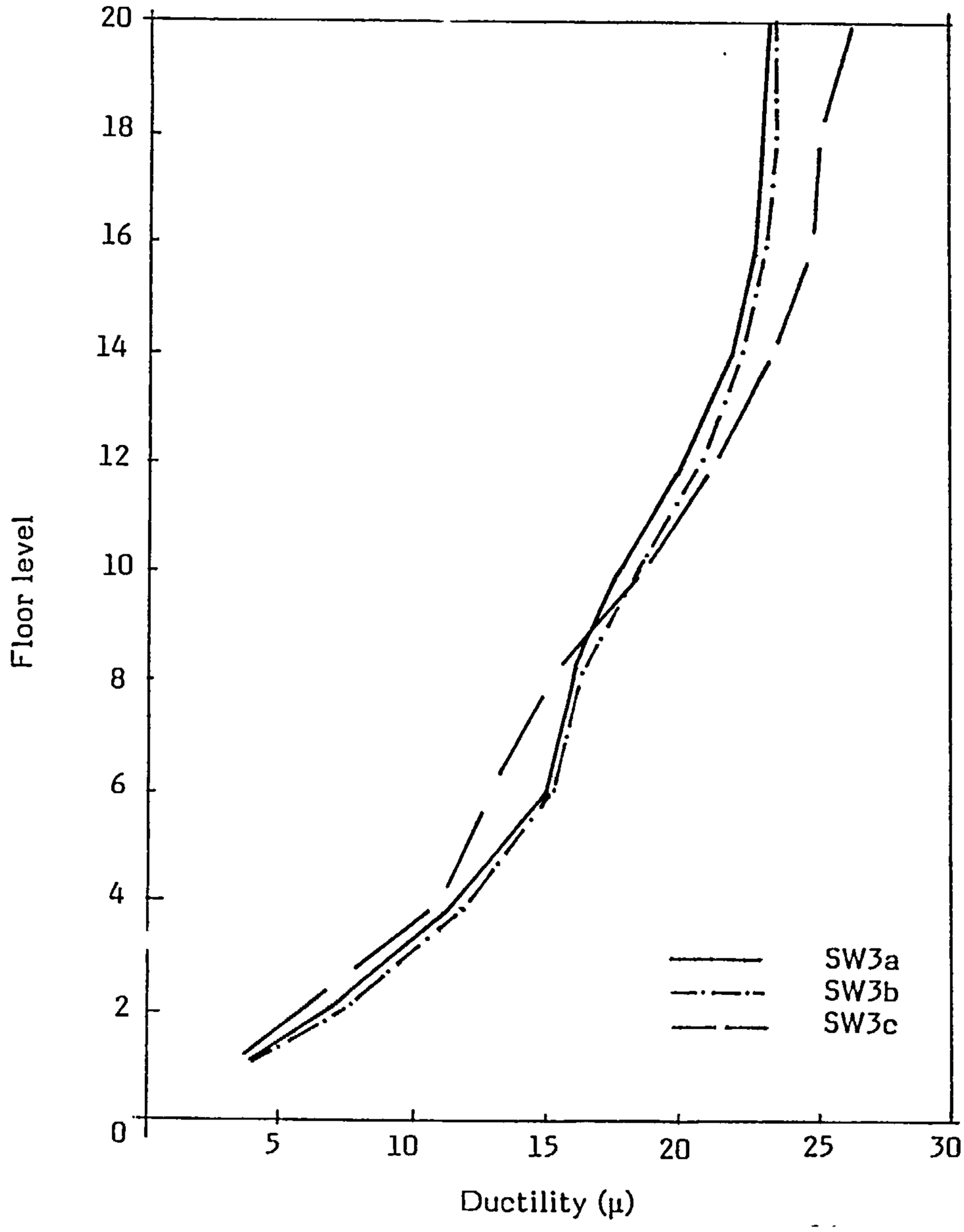

FIG. 7.18 DUCTILITY DEMANDS FOR VARIOUS DISCRETISATIONS

CHAPTER EIGHT

OPTIMUM NONLINEAR ANALYSIS OF COUPLED SHEAR WALLS

8.1 Introduction

In locations of possible seismic activities coupled shear walls are a form of construction often used. This is due to their ability to dissipate the energy input whilst retaining a great deal of their structural stability. One way of dissipating this energy is to allow the connecting beams to deform plastically whilst confining the rest to remain elastic. This is the preferred form of deformation because

i) Failure in the walls may lead to the collapse of the entire structure

ii) Axial forces which might be high in the walls tend to reduce their capability to deform

iii) It is easier and more economical to repair horizontal members than vertical ones

To achieve such a philosophy, the practice to purposely moderate the strength of the coupling beams allowing them to yield ahead of the walls, has been the desired behaviour among many seismic experts for the last few years. By doing so however, there is a risk that the coupling beams will undergo plastic deformations beyond their real capacity and hence may lead to an undesired behaviour and sometimes to the collapse of the entire structure.

These plastic deformations of the connecting beams are defined and limited by the mathematical model assumed for the inelastic material behaviour. The model most used in connection with the dynamic response of reinforced concrete members is the experimentally based hysteretic Takeda's

moment - rotation relationship [29] (fig. 8.1). This limit is often expressed by the ductility demand, μ, which is expressed in terms of the maximum and the yield rotations (Θmax, Θy) as

$$\mu = \frac{\Theta_{max}}{\Theta_y} \qquad 8.1$$

Paulay [86] and others [75-77] have shown that doubly reinforced concrete beams have a ductility demand capability of between 4 and 10. The actual value depends among other factors upon the amount of tension and shear reinforcement present in the beam.

In the past trial-and-error methods have been used to evaluate the moment capabilities of the connecting beams for specified ductility demands. Initial values were chosen and the coupled shear walls subjected to a nonlinear analysis for a given accelerogram. These initial values were then modified according to the calculated ductility demands and the procedure repeated until the ductility demands were within the required acceptable values.

The efficency of the above method is obviously limited and in this dissertation a method is proposed that will optimise the procedure. This is made possible by using a ductility decay curve. This curve has been obtained for a number of coupled shear walls with a range of geometrical dimensions.

The minimum moment capacities of the connecting beams, or groups of connecting beams, can be avaluated using the relevant code of practice. Using these minimum values the coupled shear wall is subjected to a nonlinear dynamic analysis for a specified accelerogram. The required ductility demand can then be expressed as a percentage of the initial ductility demand. Using the ductility decay curve, the increase in the moment capacity can be obtained. A further analysis can then be carried out to check the validity of the modified values.

8.2 Nonlinear Dynamic Procedure

Each coupled shear wall model was analysed using DRAIN-2D program [30] developed at the University of California, Berkeley. This program was preferred because it is less time consuming for comparable results (see section 7.4.4). The dynamic response of a coupled shear wall to an earthquake acceleration record is determined using a step-by-step numerical integration. The acceleration record used was the first six seconds of the N-S component of El Centro earthquake scaled to give a peak value of 0.33g as shown in fig. (8.2). For convenience, the structures were subdivided over their height into zones of 5 storeys each from the base and only the absolute maximum values in each zone was considered. As the computer program assumes a constant acceleration scheme during a time step, it is important to optimise this time step to balance accuracy and economy. A time step of 0.01 second was found to be appropriate as no substantial improvement was noticed for smaller values.

The stiffness matrix of the coupled shear walls was formulated by the direct stiffness method. The matrix is then modified locally whenever a member goes plastic. This is done according to the nonlinear cyclic behaviour for reinforced concrete members defined by Takeda's model. The fundamental periods of the structures were computed using the F.E dynamic program developed in this research. DRAIN-2D does not have the capability to carry out a free vibration analysis. Finally the damping is assumed to be proportional to both the stiffness and the mass matrix.

8.3 Influence of Various Factors on Ductility Demand

The prediction of ductilities and hence plastic deformations is of paramount importance. The accuracy of these predictions depends on many assumptions related to the mathematical model chosen, the initial stiffness and the strain hardening parameter assumed etc... to name but a few. Therefore before developing the ductility decay curve in detail, the different factors which might influence the ductility demands are examined and their effects evaluated. A 20 and a 30 storey coupled walls (SW1 and SW2) were chosen for this investigation. Their geometric and dynamic characteristics are given in fig. (8.3).

8.3.1 Effect of Stiffness Degradation on SW2: As previously stated Takeda's model with stiffness degradation capability was used. The stiffness degradation is simulated by reducing the unloading and reloading stiffnesses. The unloading stiffness, Ku, depends on the maximum hinge rotation and is controlled by the input parameter α as shown in fig. (8.1). α must be non negative and chosen such that the unloading slope is steeper than the reloading one in order to avoid a negative hysteresis loop, similarly the reloading stiffness is controlled by a parameter β.

i) Unloading Slope Variation: The influence of the unloading stiffness Ku is investigated. Setting My = 100 kip.ft for all the coupling beams and the walls elastic, the ductility demands in the coupling beams were computed for various values of α and a constant $\beta = 0$. The results are shown in table 8.1. The relevant ductility demand variations $d\mu(\%)$ with respect to the ductility demand μ_0, corresponding to $\alpha = 0$ and $\beta = 0$, are also shown in table 8.1 between brackets and are plotted against the variable α for zone 1 in fig. (8.4). Table 8.1 and fig. (8.4) show clearly that ductility demand increases with increasing α.

To examine the effects of the strength of the coupling beams on this variation, two more values of yield moments were considered My = 150 and My = 200 kip.ft and similar procedure was followed. The results are also shown in table 8.1 and the variation $d\mu_{(\%)}$ for the first zone is also plotted in fig. (8.4) for comparison. As can be seen, as α varies from 0 to 0.40, $d\mu_{(\%)}$ varies from 0 to a maximum value of

2.77 % for My = 100 kip.ft

7.67 % for My = 150 kip.ft

9.92 % for My = 200 kip.ft

This shows that the variation of ductility demand is higher for stronger coupling beams.

ii) Reloading Slope Variation: Similarly, the ductility demand on the coupling beams were computed for a varying parameter β and a constant α of 0.40. The results are shown in table 8.2 for values of yield moment of 100, 150, and 200 kip.ft respectively. The ductility variation of $d\mu_{(\%)}$ defined with respect to μ_o, corresponding to $\alpha = 0.40$ and $\beta = 0$, is now plotted against β for zone 1 in fig. (8.5). The results show that

a) The ductility variation was not substantial as β varied.

b) The ductility variation increases with increasing β.

c) The ductility variation is lesser for stronger coupling beams.

8.3.2 Effect of Strain Hardening on SW2: When subjected to a reversal of loading, the behaviour of a beam can be basically described by its moment-rotation relationship. The latter can either be idealised as elastic perfectly plastic, i.e., no strain hardening is accounted for (p = 0 in fig. (8.1)) or as elasto-plastic with strain hardening ($p \neq 0$). As far as reinforced concrete is concerned, a more realistic model would be the one which takes into account strain hardening effect.

Depending on the designer's judgement, various values of p can be chosen as an input to simulate strain hardening. Therefore, in the following section an attempt is made to examine the effect of the variation of the parameter p on the ductility demands of the coupling beams of the coupled shear wall SW2. The walls were kept elastic throughout the entire earthquake history and no stiffness degradation effect was considered. The value of the strain hardening parameter p was varied from 0.01 to 0.16 and the consequent changes in plastic deformations were recorded. Further more, to examine the possible influence of beam strength on the magnitude of these changes, three values of yield moment have been considered (My = 100, My = 150 and My = 200 kip.ft), the results are shown in table 8.3 and plotted against p in fig. (8.6) for zone 6.

The results show clearly that ductiliy demand decreases as the strain hardening parameter p increases. The variation of ductility demand depends also on the level of yielding of the coupling beams as it is greater for smaller yield moments My.

8.3.3 Effect of Beam Depth:

i) General Considerations: As a preliminary study an 8 storey coupled wall subjected to typical equivalent static loads was investigated. The depth of the coupling beams were varied keeping all the remaining geometry the same. The displacement pattern of this coupled wall depended very much on the size of the coupling beams as shown in fig. (8.7a). the depth of the coupling beams has therefore a considerable effect on the stress and deformation characteristics of the entire structure. When the depth was only one foot, both left and right walls deflected equally and the point of contraflexure was almost in the midspan of the coupling beam. This agreed remarquably well with the assumption made in the approximate methods of analysis. As the depth of the coupling beams was increased however, the behaviour of the coupled shear wall was noted to vary towards that of a single solid wall.

The interaction between the walls and the coupling beams was also investigated. Fig. (8.7b) shows the variation of the bending moments in the coupling beams with their depth. The interstorey variation of the bending moment is seen to increase substantially with the depth of the beam. This was found to be a very important phenomenon concerning the strength and the energy absorbing capability of the structure. The similarity of the inter storey bending moments of the coupling beams when they are slender yields the following consequences:

a) Yielding in the beams occur approximately at the same time thus improving their energy dissipation capability.

b) A straight forward design and construction of the coupling beams.

c) The approximate nonlinear method of analysis which assumes that all beams are hinged, and that the points of contraflexure are at midspan, becomes more acceptable.

ii) Effect of the Depth of Coupling Beams on their Ductility: Increasing the beam depth increases the initial stiffness (i.e. the first slope of the moment-rotation curve) and hence, for the same yield moment, reduces the yield rotation. To examine the effect of the beam depth Hb on the ductility demand, the 30 storey coupled shear wall (SW2) was considered. Varying the beam depth and keeping all the remaining data and zoning the same and setting the yield moment My = 100 kip.ft, the following ductility demands were recorded:

ZONE	DUCTILITY DEMAND (μ)		
	Hb = 1'	Hb = 2'	Hb = 3'
1	1.00	6.48	22.08
2	1.13	8.32	27.60
3	1.50	12.79	35.26
4	1.81	14.67	39.33
5	1.81	14.06	35.97
6	2.18	16.47	41.23

The infuence of the beam depth is considerable as is confirmed by the above table. The results show yet again that the parameters which define the yield point, namely the initial stiffness and the yield strength, have a particular effect on the ductility demand.

8.3.4 Effect of Coupling Beam Length on Ductility Demand: It can be anticipated that an increase in the length of the coupling beams leads to a greater flexibility and hence to an increase in ductility demands. It is however desirable to evaluate the extent of this increase and the nature of its variation as affected by the coupling beam length. In order to examine the effect of this variable, three twenty storey coupled walls were considered in addition to SW1 previously described. All four structures were the same except that the coupling beam length and hence the dynamic characteristics were varied. The maximum ductility demands were computed for each of the structures as follows:

Zone \ Beam Length	μ_{max} 4'	7'	10'	14'
1	9.71	13.51	15.11	15.40
2	10.33	17.43	20.37	21.60
3	8.81	22.24	26.17	28.08
4	9.57	22.77	27.32	29.63

The maximum ductility demands in the 4 zones are plotted against the beam length Lb, and also 1/Lb in fig. (8.8). The figure shows, as expected, the increase of ductility demand with increasing length. Furthermore, the maximum ductility demand seems to be almost inversely proportional to the coupling beam length. Note however, that the rate of increase in ductility demand decreases after the beam length has reached approximately 10 ft.

8.3.5 <u>Effect of Damping:</u> To assess the effect of the energy absorbing mechanism, which is present in structures even before the onset of yielding due to damping effect, a viscous damping form was assumed. Three damping factors namely 5%, 10% and 15% of critical were considered. To appreciate the influence of structure flexibility, i.e., its frequency of vibration, on the extent of the effect of damping, a coupled shear wall of 10 storeys (SW3) in addition to the 20 storey coupled wall (SW1) was considered. SW3 has the same properties, except the number of storeys and hence the total height, as SW1. The coupling beams yield moments were set to 100 kip.ft for SW1 and 80 kip.ft for SW3. The ductility demands in the coupling beams were then computed and the results are shown in table 8.4 and fig. (8.9). From these the following observations can be seen :

i) The effect of damping is substantial and therefore a great care should be exercised in its choice.

ii) The maximum reductions in ductility demands $D\mu_{(10\%)}$ and $D\mu_{(15\%)}$ with respect to $\mu_{(5\%)}$, i.e.,

$$D\mu_{(i\%} = \frac{\mu(5\%) - \mu(i\%)}{\mu_{(i\%)}} . 100 \qquad 8.2$$

were as follows:

	$D\mu_{(5\%)}$	$D\mu_{(10\%)}$	$D\mu_{(15\%)}$
SW3 (10 storeys)	0.0	25%	35%
SW1 (20 storeys)	0.0	32%	50%

8.3.6 Effect of Actual Stiffness of Coupling Beams: The importance of the choice of the original stiffness to be used along with the assumed nonlinear moment-rotation relationship must be emphasised. Depending on the designer, different initial rigidities ($EI_{initial}$) for the same cross section can be assumed ranging from the rigidity of the gross section to the rigidity below that of the cracked section (fig. 8.10). The influence of such an assumption on the ductility demand on the coupling beams of the coupled shear walls is most important and in this section attempts are made to assess the extent af this influence.

The 20 storey coupled shear wall (SW1) was chosen to illustrate this point. Its material, geometric and dynamic characteristics are given in fig. (8.3). Four typical values of $EI_{initial}$ were assumed as follows

	Run S1	Run S2	Run S3	Run S4
$EI_{initial}$	EI_{gross}	$0.8EI_{gross}$	$0.6EI_{gross}$	$0.4EI_{gross}$

The ductility demands upon the coupling beams are shown in table 8.5 and plotted in fig. (8.11) for the four rigidity values considered. The figure shows clearly that the influence is very substantial and the maximum variation of the ductility demand reached 120% in this study. It is interesting to note that ductility demand varied almost in proportion with the initial rigidity $EI_{initial}$.

8.3.7 Summary: The following conclusions can be drawn.

a) The ductility demand increases with increasing unloading parameter α and its variation is greater for stronger coupling beams. A maximum variation of 10% was obtained in this investigation.

b) The ductility demand increases with increasing reloading parameter β. Its variation however, is smaller for stronger coupling beams. The maximum variation obtained was 6.3%.

c) Generally the ductility demand decreases with increasing strain hardening parameter p. Its variation becomes smaller as the coupling beams become stronger.

d) The factors affecting the yield point in the moment - rotation relationship such as the depth of the coupling beams, the yield moments and the initial stiffness have a particular influence on ductility demand and should therefore be assessed with great care.

e) Damping effect on ductility demand is very substantial (up to 50% in this study) and is slightly higher for more flexible structures. Therefore its choice should taken with caution.

8.5 Optimal Nonlinear Analysis

8.5.1 Effect of Coupling Beam Strength on Ductility Demand: In coupled shear wall systems the strength of the coupling beams not only affects the degree of coupling between the walls but also controls the sequence of yielding and the magnitude of ductility demand of the different members of the structure. The direct influence of coupling beam strength variation is shown in fig. (8.12). the figure represents the response of a 20 storey coupled shear wall (SW1) for three levels of moment capacity namely 100, 200 and 300 kip.ft respectively. These curves show that ductility demands are in direct relation to the coupling beam moment capacity. They also show that as the moment capacity increases the ductility demand variation and the maximum ductility demand decreases.

8.5.2 Ductility Decay Curve: Obviously when a coupled shear wall is subjected to a dynamic loading, its coupling beams are stressed differently throughout the height of the structure and produce therefore different ductility demands according to their stiffness and yielding moments. Varying all the coupling beam yield moments equally produced the variation of ductility demands shown in fig. (8.12). However it is of interest to investigate the influence of the yield moment variation of one set of coupling beams on the others. To carry out such a study it was decided for practicality and economy to subdivide the structures into zones of five storeys each over their height. Instead of considering each individual beam separately, the absolute maximum response in each zone was considered. The degree of accuracy is therefore in direct relation with the number of zones.

The coupled shear walls SW1 and SW2 which are defined in fig. (8.13) were first considered. Initially all the zones are assumed to have the minimum moment capacity. This value will be dependent upon the minimum amount of reinforcement present in the beams. This is stipulated by most codes of

practice. A typical value is that recommended by the ACI code [48]. This is given by

$$p_{min} = p'_{min} = 200/f_y \qquad 8.3$$

in which p_{min} = minimum tensile reinforcement percentage

p'_{min} = minimum compressive reinforcement percentage

fy = yielding steel stress in psi

To allow the steel to yield before the concrete is crushed, an upper limit is also recommended for flexural steel ratio. The maximum value must not exceed half of that producing balanced failure [86]. Hence

$$\underset{(p')}{p} < 0.5 \cdot \frac{(.85f'c\beta_1)}{f_y} \cdot \frac{(.003Es)}{.003Es+f_y} \cdot \frac{p'f'_s\ \beta_1}{f_y} \qquad 8.4$$

where f'c = Compressive strength of concrete

β_1 = Constant (generally equal to 0.85)

f_y = Steel yield stress

f's = Compressive steel stress

Es = Steel modulus of eleasticity

For the walls SW1 and SW2 the minimum yield moment capacity was assumed to be equal to 100 kip.ft. Applying the nonlinear dynamic analysis to these walls, the ductility demand (μ_{min}) was determined for each zone . These values are tabulated in table 8.6a. The yield moment of zone 1 was then increased keeping all the others equal to the minimum recommended (My_{min}). The resulting ductility demands on all zones in terms of the yielding moment at zone 1 are shown in fig. (8.14a) and fig. (8.15a) for SW1 and SW2 respectively. Similarly, the infuence of the increase of yield moment in zone 2 keeping all the others equal to My_{min} are shown in fig. (8.14b) and fig. (8.15b). the same procedure for all zones follows and the results are shown in

fig. (8.14) for SW1 and fig. (8.15) for SW2. These two sets of figures show quite clearly

i) the necessity to vary the moment capacity of the connecting beams along the height of the coupled shear walls.

ii) that the variation of the ductility demand of a particular zone is dependent, in the main, upon the variation of moment capacity within that zone. Therefore a good approximation can be expected by assuming the effects of the other zones negligible.

The variation in ductility demand of a particular zone can be represented as a percentage of the ductility demand at minimum moment capacity. These values are tabulated, for all zones, in table 8.7 for the walls SW1 and SW2. The average values of the coupled walls considered are shown in table 8.6b. These variations are shown in graphical form in fig. (8.16) as the ductility decay curves.

8.4.3 <u>Applications:</u> Three examples of the use of the ductility decay curve are shown in table 8.8. Table 8.8a shows the process for the wall SW1 which is subdivided into four zones and a required ductility demand of 6 is assumed. Again it was assumed that the minimum moment My_{min} was 100 kip.ft. The initial ductility demands for all zones at this capacity (μ_{min}) are shown in the first column. For each zone the ductility demand required (μ_r) can be represented as a fraction of the initial ductility demand (μ_{min}). This is shown in column 2 as (μ_r/μ_{min}). Using the ductility decay curve the ratio (dM/My_{min}) can be read off and the moment capacity required can be calculated as

$$My = My_{min} + dM \qquad 8.5$$

This is shown in column 6. A nonlinear dynamic analysis was again carried out

and the ductility demand values are shown in column 7. Similarly tables 8.8b and 8.8c show the process for walls SW2 and SW3.

It can be seen from these tables that the required and computed ductility demands are within 10% of one another for walls SW1 and SW3. This is not the case for SW2 where the maximum difference in zone 5 is 29%. This show quite clearly that the ductility decay curve for SW2 does not describe its behaviour accurately enough and therefore the ductilities in SW2 need to be improved.

This improvement may be carried out using two different approaches:

i) By modifying the ductility decay curve

ii) By using the slope of the ductility decay curve.

The first procedure which can be seen from table 8.9 and fig. (8.17), uses the computed ductility demands (μ_g) that are shown in table 8.8b. Using the ratios obtained in table 8.9a the modified SW2 decay curve is obtained in fig. (8.17). Using this curve with the original ductility ratios (μ_r/μ_{min}) the modified values of (dM/My_{min}) and hence the required moment (My) are obtained. These values are again used in the nonlinear dynamic analysis and the computed values of ductility demands are shown in table 8.9b.

This modification of the ductility decay curve for one particular coupled shear wall supports the possibility of using one curve for all the coupled shear walls. To test the validity of modifying a standard curve for any wall, the curve representing wall SW3 was utilized. This curve was used to determine the yield moments required for wall SW2. Using this curve the moments shown in table 8.10a were used producing the ductility demands (μ_g) shown. The ratios (dM/My_{min}) and (μ_g/μ_{min}) were then used to modify the original curve. This shown in fig. (8.18).

This modified curve was then used along with the original ductility ratios to evaluate the required moment capacity My. The resulting ductility

demands are shown in table 8.10b. A second modification to the original curve can be made by considering the latest moment and ductility ratios. This second modification is shown in fig. (8.18). This curve was then used to obtain the values shown in table 8.10c and the nonlinear dynamic analysis produced the final ductility demands shown.

The second procedure uses a simplified trilinear curve derived from the ductility decay curve and whose three branches have a slope of 2.5, 5.0 and 10.0 respectively. The procedure can be seen from table 8.11 and fig. (8.19). Using the computed ductility (μ_g) and the original ductility (μ_o), the rate by which the computed ductility has been underestimated with respect to the required ductility (μ_r) can be computed. This is given by the ratio

$$\frac{\mu_r - \mu_o}{\mu_o} \qquad 8.6$$

and is shown in column (7) of table 8.11.

Depending upon this ratio and the derived yield moment My shown in column (5), the slope which is to be used is set from fig. (8.19). This is given in column (8). If the ratio given in equation 8.6 ranges over two or three slopes as it is the case for zones 3 to 6, then it must devided proportionally as shown in column (9). Multiplying the slope by the corresponding ratio, the ratio dM_g/M_{min} and hence the required reduction dM_g of the yield moment is obtained (columns 10 & 11). The final yield moments are then deducted. These are shown in column (12) and the resulting ductilities in column (13).

As can be seen from column (13), the improved ductilities obtained are very close to the required ductility μ_r. This clearly shows that the procedure is simple, optimal and leads to a greater accuracy for a minimum effort.

8.5 Conclusion and summary: The method described is a major improvement on the existing trial - and -error process. For any particular wall it has been shown that the use of a ductility decay curve produces accurate values of the moment capacities to produce the required ductility demands. When the original curve for a wall does not produce an accurate set of results then the curve can be modified.

In generalising the method, one ductility decay curve only was used. In the particular case shown the most conservative curve was used. again by modifying the curve form accurate values of yield moments are achieved for a predetermined ductility demand.

Table 8.1 Effect of Unloading Stiffness Degradation

		μ_1	μ_2	μ_3	μ_4	μ_5	μ_6
M_y = 100	α = 0	6.49 (0%)	8.32	12.80	14.69	14.08	16.49
	α = 0.1	6.56 (1.08)	8.45	12.81	14.61	13.96	16.38
	α = 0.2	6.62 (2.06)	8.50	12.86	14.61	13.96	16.34
	α = 0.3	6.66 (2.62%)	8.51	12.86	14.56	13.98	16.34
	α = 0.4	6.67 (2.77%)	8.49 (2.04%)	12.85 (-39%)	14.52 (-1.16%)	14.04 (-0.28%)	16.39 (-0.69%)
M_y = 150	0.	3.79 (0.0)	4.68	7.09	7.97	7.33	8.48
	0.1	3.90 (2.90)	4.76	7.10	7.94	7.39	8.52
	0.2	3.97 (4.75)	4.82	7.13	7.95	7.45	8.59
	0.3	4.04 (6.60)	4.85	7.16	7.96	7.49	8.64
	0.4	4.08 (7.67)	4.87 (4.06)	7.16 (.99)	7.96 (-.13)	7.53 (+2.73)	8.70 (2.59)
M_y = 200	0.	2.62 (0)	3.03	4.48	4.95	4.32	4.95
	0.1	2.70 (3.05)	3.09	4.50	4.95	4.35	4.99
	0.2	2.76 (5.34)	3.14	4.50	4.95	4.39	5.05
	0.3	2.82 (7.63)	3.19	4.52	4.96	4.43	5.09
	0.4	2.88 (9.92%)	3.22 (6.27%)	4.53 (1.12%)	4.97 (0.40%)	4.46 (3.24)	5.13 (3.64)

Table 8.2 Effect of Reloading Stiffness Degradation

	β	μ_1	μ_2	μ_3	μ_4	μ_5	μ_6
M_y = 100	0.	6.64 (0)	8.45	12.80	14.41	14.09	16.44
	0.1	6.68 (0.60)	8.58	12.78	14.41	14.07	16.42
	0.2	6.73 (1.36)	8.71	12.77	14.41	14.06	16.40
	0.3	6.77 (1.96)	8.83	12.78	14.42	14.04	16.38
	0.4	6.80 (2.41%)	8.93	12.78	14.42	14.04	16.38
	0.5	6.80 (2.41%)	8.98 (6.27%)	12.78 (-0.16)	14.42 (0.0&)	14.04 (0.35)	16.38 (0.36)
M_y = 150	0.	4.12 (0)	4.86	7.15	7.94	7.57	8.75
	0.1	4.15 (0.73)	4.94	7.13	7.93	7.57	8.74
	0.2	4.16 (0.97)	5.00	7.14	7.94	7.56	8.73
	0.3	4.16 (0.97)	5.01	7.14	7.94	7.56	8.73
	0.4	4.17 1.21%)	5.03	7.14	7.94	7.56	8.73
	0.5	4.17 (1.21%)	5.03 (3.50)	7.14 (-0.14)	7.94 (0.0)	7.56 (-0.13)	8.73 (-0.23)
M_y = 200	0.	2.92 (0)	3.24	4.54	4.97	4.49	5.17
	0.1	2.93 (0.34)	3.25	4.55	4.98	4.48	5.17
	0.2	2.93 (0.34)	3.26	4.55	4.98	4.48	5.17
	0.3	2.93 (0.34)	3.26	4.54	4.97	4.48	5.17
	0.4	(0.34)	3.27	4.54	4.97	4.48	5.17
	0.5	(0.34)	3.27 (.93%)	4.54 (0.0)	4.97 (0.0)	4.48 (-0.22)	5.17 (0.0)

Table 8.3 Effect of Strain Hardening

	Str. Hard. parameter (P)	$\mu_{(1)}$	$\mu_{(2)}$	$\mu_{(3)}$	$\mu_{(4)}$	$\mu_{(5)}$	$\mu_{(6)}$
M_y = 100	.01	6.44	8.18	14.40	16.7	16.17	18.95 (0.0)
	.02	6.42	8.19	13.92	16.11	15.59	18.26 (-3.64)
	.04	6.47	8.30	13.16	15.14	14.55	17.05 (-10.03)
	.06	6.49	8.34	12.47	13.27	13.62	15.95 (-15.83)
	.08	6.30	8.32	11.81	13.47	12.80	14.98 (-20.95)
	.10	6.48	8.27	11.26	12.78	12.06	14.09 (-25.65)
	.12	6.44	8.19	10.75	12.13	11.39	13.28 (-29.92)
	.14	6.40	8.08	10.26	11.52	10.79	12.56 (-33.72)
	.16	6.34 (1.55)	7.96 (+1.95)	9.83 (-31.74)	10.97 (-34.31)	10.22 (-36.80)	11.87 (-37.36)
M_y = 150	.01	3.76	4.59	7.73	8.80	8.19	9.49 (0.0)
	.02	3.78	4.62	7.57	8.58	7.96	9.17 (-3.4)
	.04	3.79	4.67	7.25	8.17	7.53	8.72 (-8.1)
	.06	3.79	4.68	6.96	7.79	7.13	8.26 (-13.0)
	.08	3.79	4.68	6.69	7.46	6.78	7.85 (-17.3)
	.10	3.76	4.66	6.43	7.16	6.45	7.46 (-21.5)
	.12	3.77	4.63	6.20	6.88	6.14	6.88 (-27.5)
	.14	3.75	4.58	6.00	6.63	5.85	6.78 (-28.6)
	.16	3.73 (-.80)	4.53 (-.13)	5.80 (-24.97)	6.38 (-27.50)	5.59 (-31.75)	6.46 (-31.93)
M_y = 200	.01	2.63	3.03	4.75	5.29	4.69	5.42 (0.0)
	.02	2.63	3.03	4.68	5.20	4.60	5.30 (-2.21)
	.04	2.63	3.03	4.55	5.03	4.41	5.06 (-6.64)
	.06	2.62	3.02	4.41	4.86	4.23	4.84 (-10.70)
	.08	2.61	3.01	4.30	4.72	4.06	4.63 (-14.58)
	.10	2.59	2.98	4.17	4.56	3.90	4.44 (-18.08)
	.12	2.58	2.96	4.07	4.44	3.76	4.27 (-21.22)
	.14	2.56	2.93	3.96	4.31	3.62	4.11 (-24.17)
	.16	2.54 (-3.42)	2.90 (-4.29)	3.86 (-18.74)	4.19 (-20.79)	3.50 (-25.37)	3.95 (-27.12)

Table 8.4 Influence of Damping on Ductility Demand

Floor Level	20 STOREYS		
	Ductility 5% Damp	Ductility 10%	Ductility 15%
20	22.68	15.33	11.35
19	22.74	15.40	11.40
18	22.77	15.46	11.37
17	22.68	15.44	11.19
16	22.52	15.36	10.94
15	22.24	15.19	10.79
14	21.71	14.88	10.58
13	20.92	14.39	10.33
12	19.85	13.74	7.99
11	18.56	13.12	9.59
10	17.43	12.56	9.74
9	16.53	12.26	10.07
8	15.74	12.29	10.58
7	15.44	12.27	10.72
6	14.70	11.87	10.42
5	13.51	10.96	9.67
4	11.82	9.53	8.46
3	9.64	7.66	6.85
2	6.99	5.48	4.85
1	3.76	2.91	2.51
Max. reduction with respect (to 5%)	0.0	32%	50%

10 STOREYS		
5%	10%	15%
17.30	12.95	11.25
17.23	12.94	11.25
16.80	12.74	11.06
15.82	12.24	10.57
14.29	11.57	9.88
12.96	11.16	9.47
12.39	10.43	8.75
11.01	9.09	7.54
8.57	6.97	5.72
4.89	3.92	3.19
0.0	25%	35%

Table 8.5 Effect of Initial Stiffness

Floor Level	RUN S1 EI = 309.3 10^3 kip.ft^2	RUN S2 (0.8 EI)	RUN S3 (0.6 EI)	RUN S4 (0.4 EI)
20	22.68	18.85	14.74	10.28
19	22.74	18.90	14.77	10.30
18	22.77	18.91	14.88	10.29
17	22.68	18.83	14.69	10.23
16	22.52	18.67	14.54	10.12
15	22.24	18.40	14.31	9.93
14	21.71	17.93	13.91	9.63
13	20.92	17.24	13.35	9.21
12	19.85	16.33	12.67	8.66
11	18.56	15.23	11.72	8.02
10	17.43	14.28	10.97	7.50
9	16.53	13.48	10.30	6.99
8	15.74	12.78	9.75	6.63
7	15.44	12.53	9.55	6.49
6	14.70	11.93	9.08	6.17
5	13.51	10.95	8.33	5.65
4	11.82	9.57	7.28	4.93
3	9.64	7.81	5.98	4.00
2	6.99	5.65	4.27	2.87
1	3.76	3.02	2.26	1.50

Table 8.6

a) DUCTILITY DEMAND AT My_{min}

b) DUCTILITY DECAY

a)

ZONE	DUCTILITY DEMAND AT My_{min} (μ_{min})				
	SW1	SW2	SW3	SW4	SW5
1	13.51	6.48	9.95	9.36	8.02
2	17.43	8.32	12.51	12.14	10.54
3	22.24	12.79	13.64	11.93	13.46
4	22.77	14.67		14.73	13.38
5		14.06		17.69	16.94
6		16.07		18.03	18.16

b)

dM / My_{min}	DUCTILITY DECAY (μ_r / μ_{min})				
	SW1	SW2	SW3	SW4	SW5
0.5	0.61	0.61	0.64	0.62	0.61
1.0	0.42	0.40	0.46	0.43	0.42
1.5	0.32	0.28		0.32	0.31
2.0	0.25		0.29	0.25	0.24
3.0	0.18	0.12	0.23	0.17	0.18

Table 8.7

a) Average Variation of Ductility Demand in SW1
b) Average Variation of Ductility Demand in SW1

a)

$\frac{\mu}{\mu_{min}}$ \ $\frac{dM}{My_{min}}$	0.5	1.0	1.5	2.0	3.0
$\frac{\mu 1}{\mu 1_{min}}$	0.63	0.44	0.34	0.28	0.19
$\frac{\mu 2}{\mu 2_{min}}$	0.63	0.44	0.32	0.26	0.20
$\frac{\mu 3}{\mu 3_{min}}$	0.61	0.42	0.31	0.23	0.17
$\frac{\mu 4}{\mu 4_{min}}$	0.58	0.41	0.28	0.22	0.17
AVERAGE $\frac{\mu}{\mu_{min}}$	**0.61**	**0.42**	**0.32**	**0.25**	**0.18**

b)

$\frac{\mu}{\mu_{min}}$ \ $\frac{dM}{My_{min}}$	0.5	1.0	1.5	3.0
$\frac{\mu 1}{\mu 1_{min}}$	0.63	0.44	0.29	0.12
$\frac{\mu 2}{\mu 2_{min}}$	0.61	0.41	0.30	0.12
$\frac{\mu 3}{\mu 3_{min}}$	0.62	0.42	0.31	0.13
$\frac{\mu 4}{\mu 4_{min}}$	0.61	0.41	0.29	0.12
$\frac{\mu 5}{\mu 5_{min}}$	0.59	0.39	0.27	0.11
$\frac{\mu 6}{\mu 6_{min}}$	0.57	0.36	0.23	0.11
AVERAGE $\frac{\mu}{\mu_{min}}$	**0.61**	**0.40**	**0.28**	**0.12**

Table 8.8 DECAY CURVE BASED & COMPUTED DUCTILITIES

a) SW1
b) SW2
c) SW3

a) **SW1** $\mu_r = 6$ $My_{min} = 100$ kip.ft 4 zones

ZONE	μ_{min}	$\frac{\mu_r}{\mu_{min}}$	$\frac{dM}{M_{min}}$	dM	My	μ_g computed
1	13.51	.444	0.98	98	198	5.88
2	17.43	.344	1.35	135	235	5.48
3	22.24	.270	1.72	172	272	5.65
4	22.77	.263	1.74	174	274	5.72

b) **SW2** $\mu_r = 4$ $My_{min} = 100$ kip.ft 6 zones

ZONE	μ_{min}	$\frac{\mu_r}{\mu_{min}}$	$\frac{dM}{M_{min}}$	dM	My	μ_g computed
1	6.48	.617	0.50	50	150	3.95
2	8.32	.481	0.79	79	179	3.83
3	12.79	.313	1.34	134	234	3.17
4	14.67	.273	1.53	153	253	3.10
5	14.06	.284	1.48	148	248	2.86
6	16.47	.243	1.66	166	266	2.92

c) **SW3** $\mu_r = 6$ $My_{min} = 100$ kip.ft 3 zones

ZONE	μ_{min}	$\frac{\mu_r}{\mu_{min}}$	$\frac{dM}{M_{min}}$	dM	My	μ_g computed
1	9.95	.600	0.60	60	160	5.88
2	12.51	.480	0.93	93	193	5.66
3	13.64	.440	1.08	108	208	5.55

Table 8.9 IMPROVEMENT IN ACCURACY OF DUCTILITY DEMAND IN SW2

ZONE	μ_{min}	μ_g	$\frac{\mu_g}{\mu_{min}}$	$\frac{dM}{M_{min}}$	$\frac{\mu_r}{\mu_{min}}$	$\frac{dM}{M_{min}}$	My	μ_g
1	6.48	3.95	.610	0.50	.617	0.50	150	3.92
2	8.32	3.83	.460	0.79	.481	0.72	172	3.99
3	12.79	3.17	.248	1.34	.313	1.12	212	3.85
4	14.67	3.10	.211	1.53	.273	1.25	225	3.91
5	14.06	2.86	.203	1.48	.284	1.22	222	3.38
6	16.47	2.92	.177	1.66	.243	1.34	234	3.45

(a) (b)

Table 8.10

STANDARD AND MODIFIED DUCTILITY DECAY AS APPLIED TO SW2

	ZONE	$\frac{\mu_r}{\mu_o}$	$\frac{dM}{My_{min}}$	My	μ_g	$\frac{\mu_g}{\mu_o}$	
STANDARD CURVE	1	.617	.578	157.8	3.88	.59	(a)
	2	.481	.921	192.1	3.52	.423	
	3	.313	1.772	277.2	2.33	.174	
	4	.273	2.210	321.0	1.99	.136	
	5	.284	2.074	307.4	1.14	.081	
	6	.243	2.652	365.2	1.02	.062	
MODIFIED CURVE 1	1	.617	.524	152.4	3.80	.59	(b)
	2	.481	.790	179.0	3.78	.454	
	3	.313	1.260	226.0	3.49	.272	
	4	.273	1.40	240.0	3.48	.237	
	5	.284	1.36	236.0	2.68	.191	
	6	.243	1.520	252.0	2.85	.173	
MODIFIED CURVE 2	1	.617	.492	149.0	3.92		(c)
	2	.481	.730	173.0	3.94		
	3	.313	1.158	215.0	3.73		
	4	.273	1.270	227.0	3.84		
	5	.284	1.24	224.0	3.23		
	6	.243	1.340	234.0	3.54		

TABLE 8.11 SLOPE APPROACH TO IMPROVE DUCTILITY ACCURACY

ZONE	μ_o	$\frac{\mu_r}{\mu_o}$	$\frac{dM}{M_{min}}$	My	μ_g	$\frac{\mu_r-\mu_g}{\mu_o}$	Slope	$\frac{\mu}{\mu_o}-\frac{\mu_r}{\mu_o}$	$\frac{dM_g}{M_{min}}$	dM_g	My = My-dM_g	μfinal
(1)	(2)	(3)	(4)	(5)	(6)	(7)	(8)	(9)	(10)	(11)	(12)	(13)
1	6.48	.617	0.578	158.	3.88	0.02	2.5	0.02	0.05	5	153.	3.69
2	8.32	.481	0.921	192.	3.52	0.06	2.5	0.06	0.15	15	177.	3.75
3	12.79	.313	1.772	277.	2.23	0.13	$\frac{10.}{5.0}$	$\frac{.037}{.093}$	$\frac{0.37}{0.46}$	83	194.	4.01
4	14.67	.273	2.210	321.	1.99	0.13	$\frac{10.}{5.0}$	$\frac{.077}{.053}$	$\frac{0.77}{0.26}$	103.	218.	4.28
5	14.06	.284	2.074	307.	1.14	0.20	$\frac{\frac{10.}{5.0}}{2.5}$	$\frac{\frac{.066}{.100}}{.034}$	$\frac{\frac{0.66}{0.50}}{0.08}$	123.	184.	3.80
6	16.47	.243	2.652	365.	1.02	0.17	$\frac{10.}{5.0}$	$\frac{.107}{.063}$	$\frac{1.07}{0.31}$	138.	227.	3.89

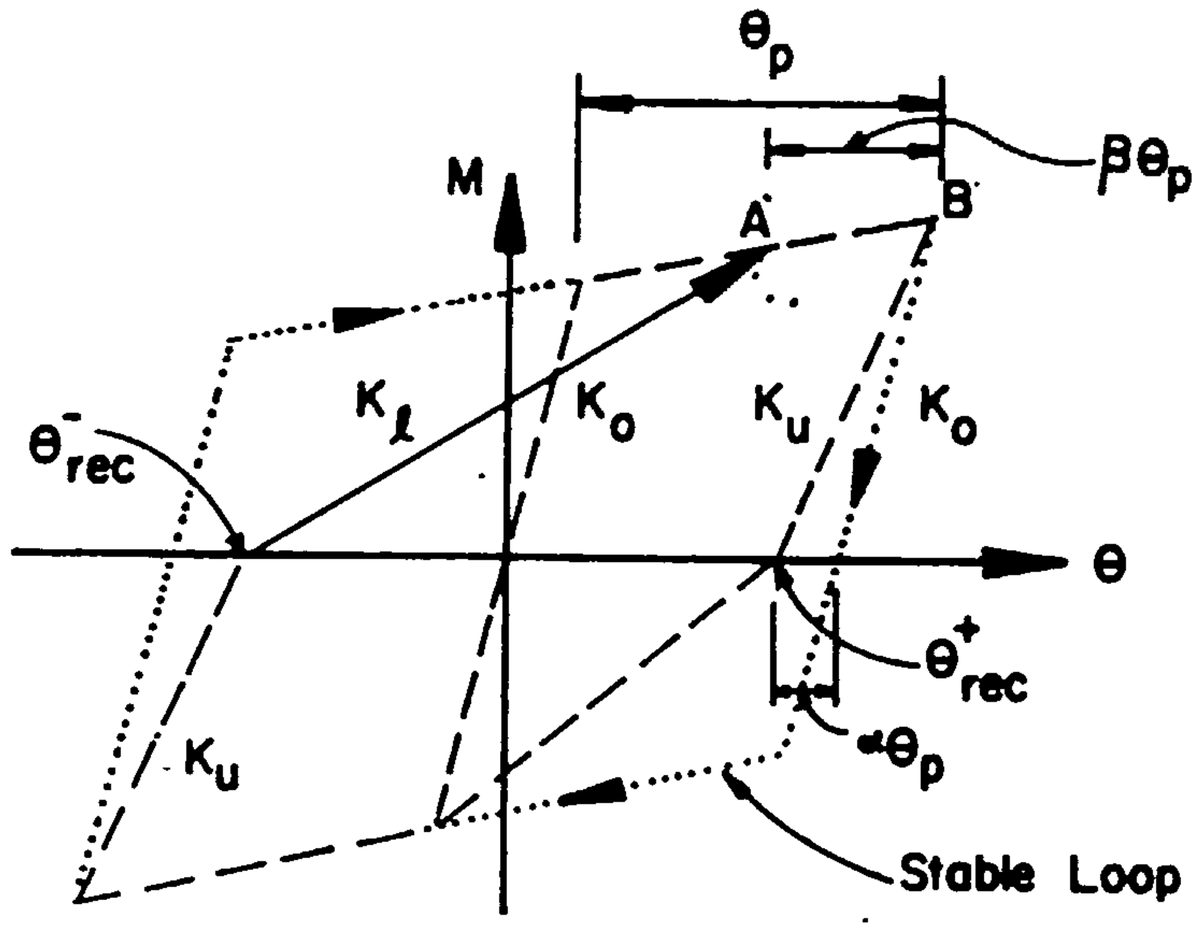

FIG. 8.1 TAKEDA MODEL OF THE MOMENT-ROTATION RELATIONSHIP OF R/C BEAMS

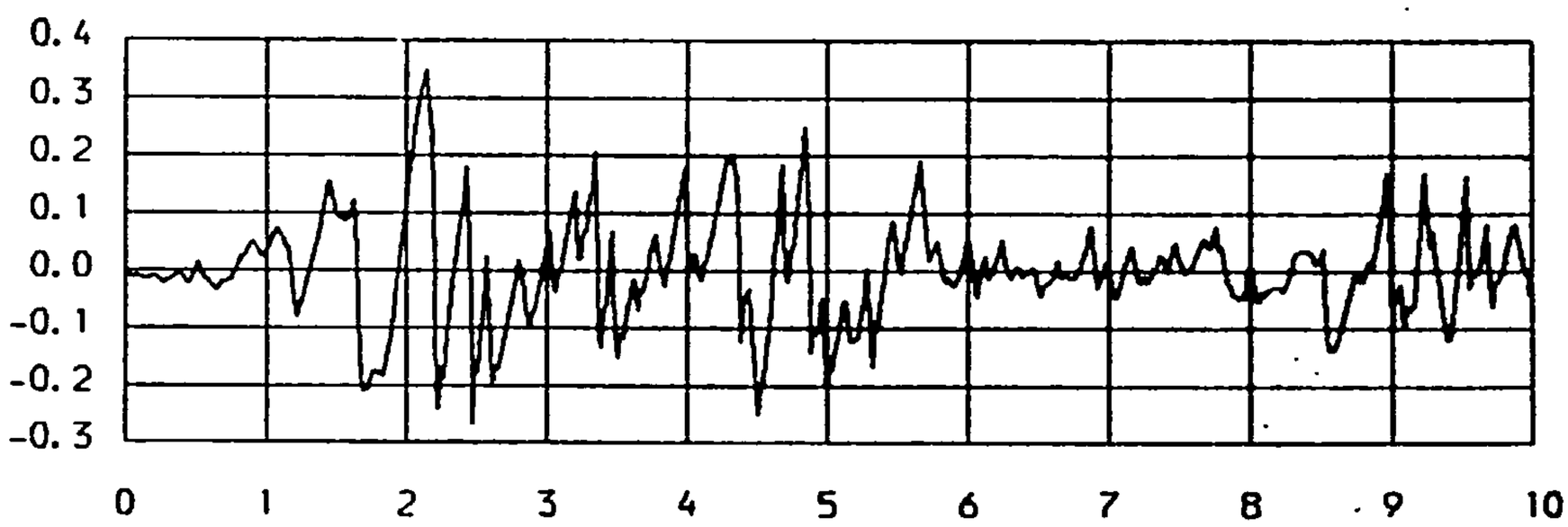

FIG. 8.2 FIRST 10 SEC. OF EL CENTRO ACCELEROGRAM N/S COMPONENT, MAY 1940

FIG. 8.3 Geometric and Dynamic Characteristics of SW1 and SW2

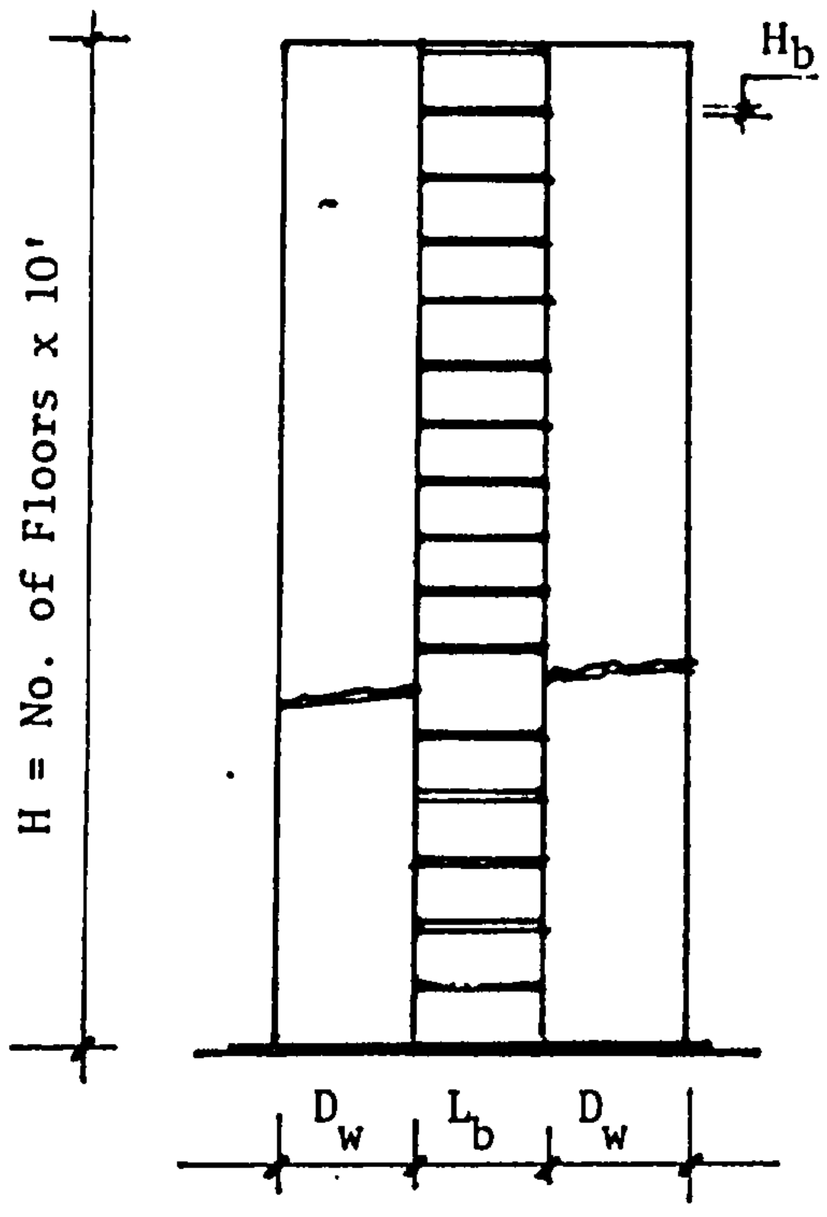

	PROPERTIES	
20 STOREYS (SW1)	Beam Stiffness (EI_b)	30.93 10^4 kip ft^2
	Wall Stiffness (EI_w)	66.80 10^6 kip ft^2
	Wall Width (D_w)	12 ft
	Beam Length (L_b)	7 ft unless stated
	Beam depth (H_b)	2 ft " "
	Total Height (H)	200 ft " "
	Thickness	1 ft
	Beam Strength	Variable
	Wall Strength	Elastic
	Fundamental Period	1.8475 seconds
	Lumped Floor Mass	6.22 kips
30 STOREYS (SW2)	Beam Stiffness	30.93 10^4 kip ft^2
	Wall Stiffness	66.80 10^6 Kip ft^2
	Beam Length	7 ft unless stated
	Beam Depth	2 ft " "
	Total Height	300 ft " "
	Thickness	1 ft
	Beam Strength	Variable
	Wall Strength	Elastic
	Fundamental Period	3.7846 seconds
	Lumped Mass/Floor	6.22 kips

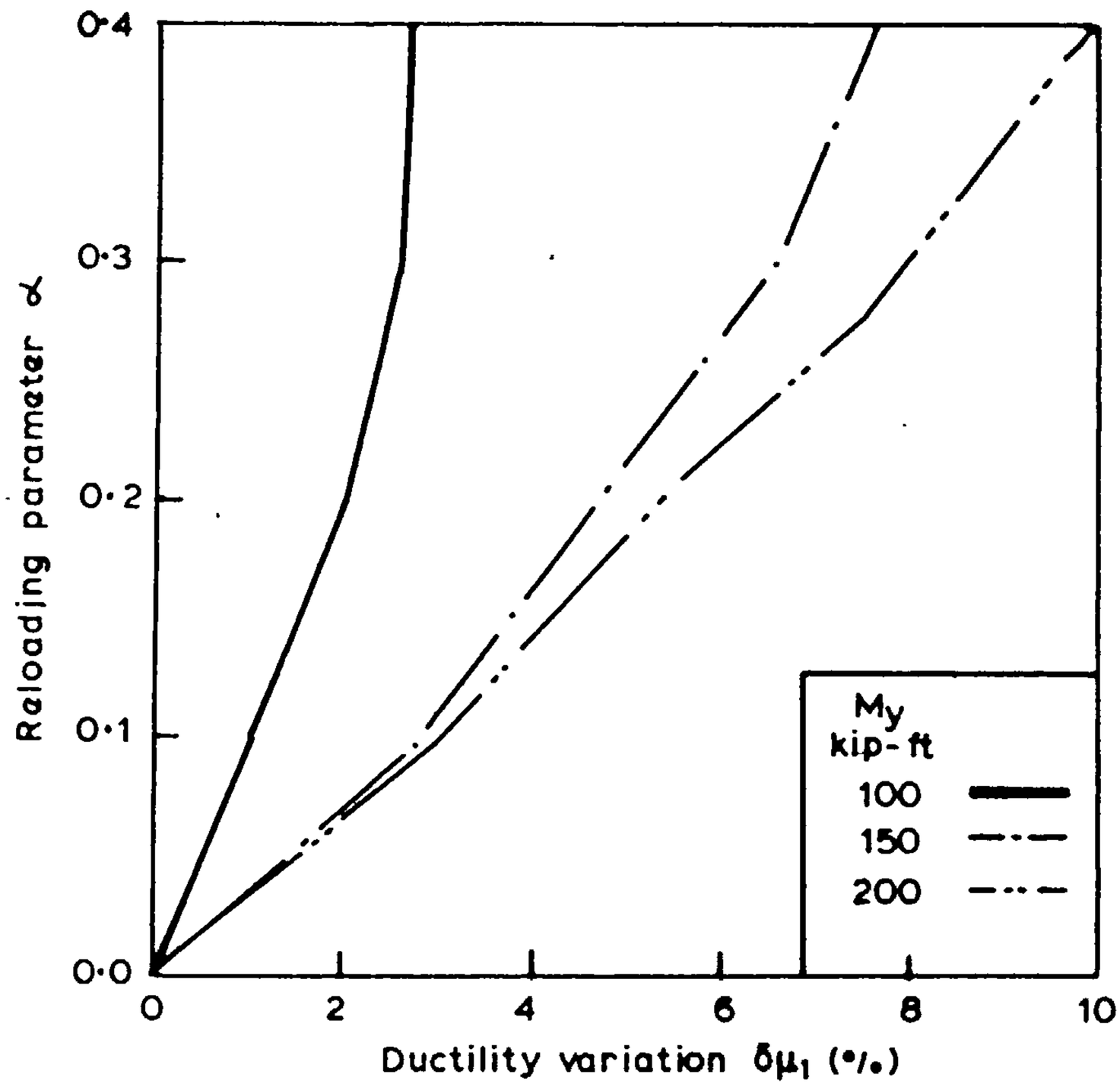

FIG. 8.4 EFFECT OF UNLOADING PARAMETER.

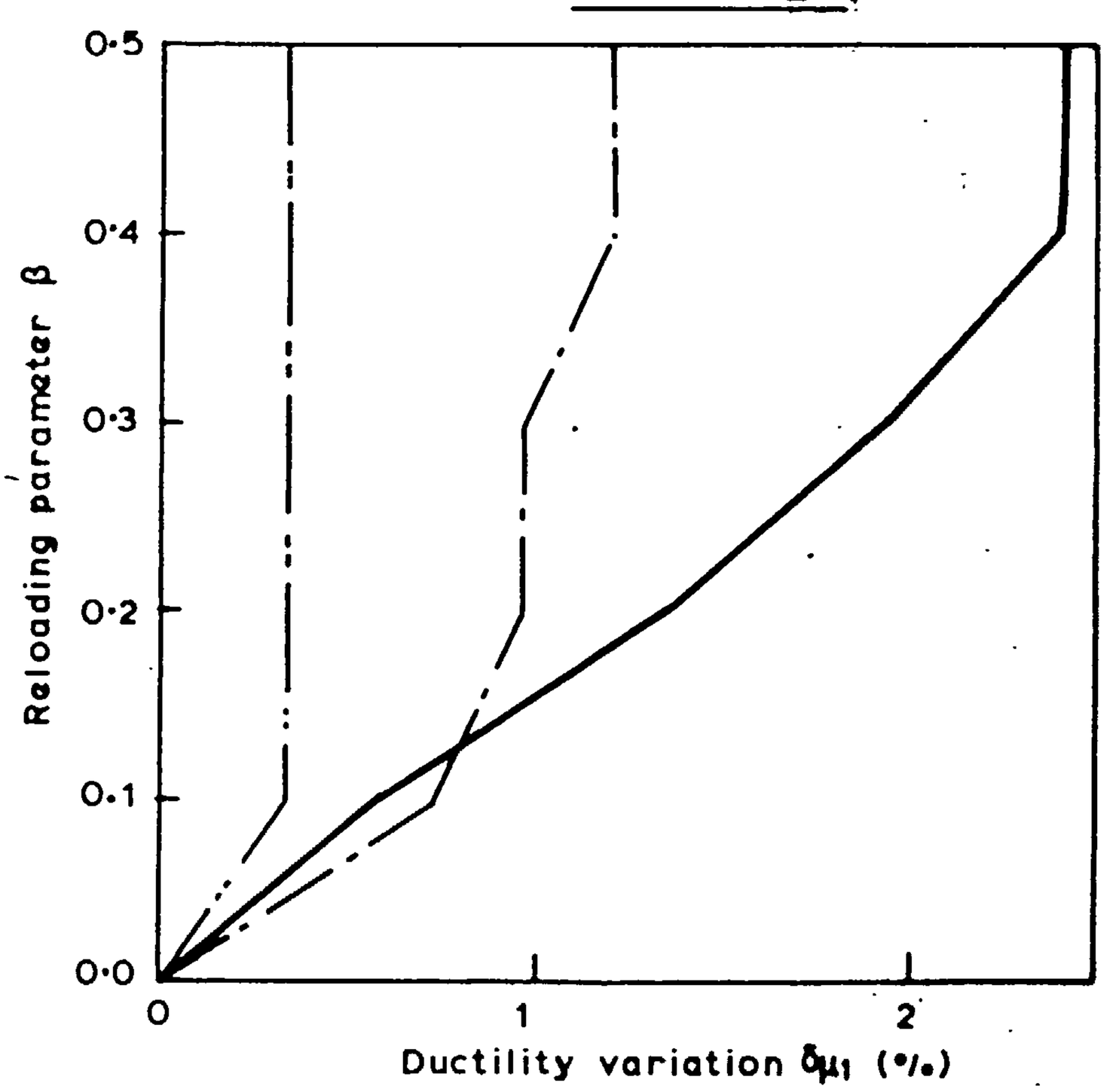

FIG. 8.5 EFFECT OF RELOADING PARAMETER β.

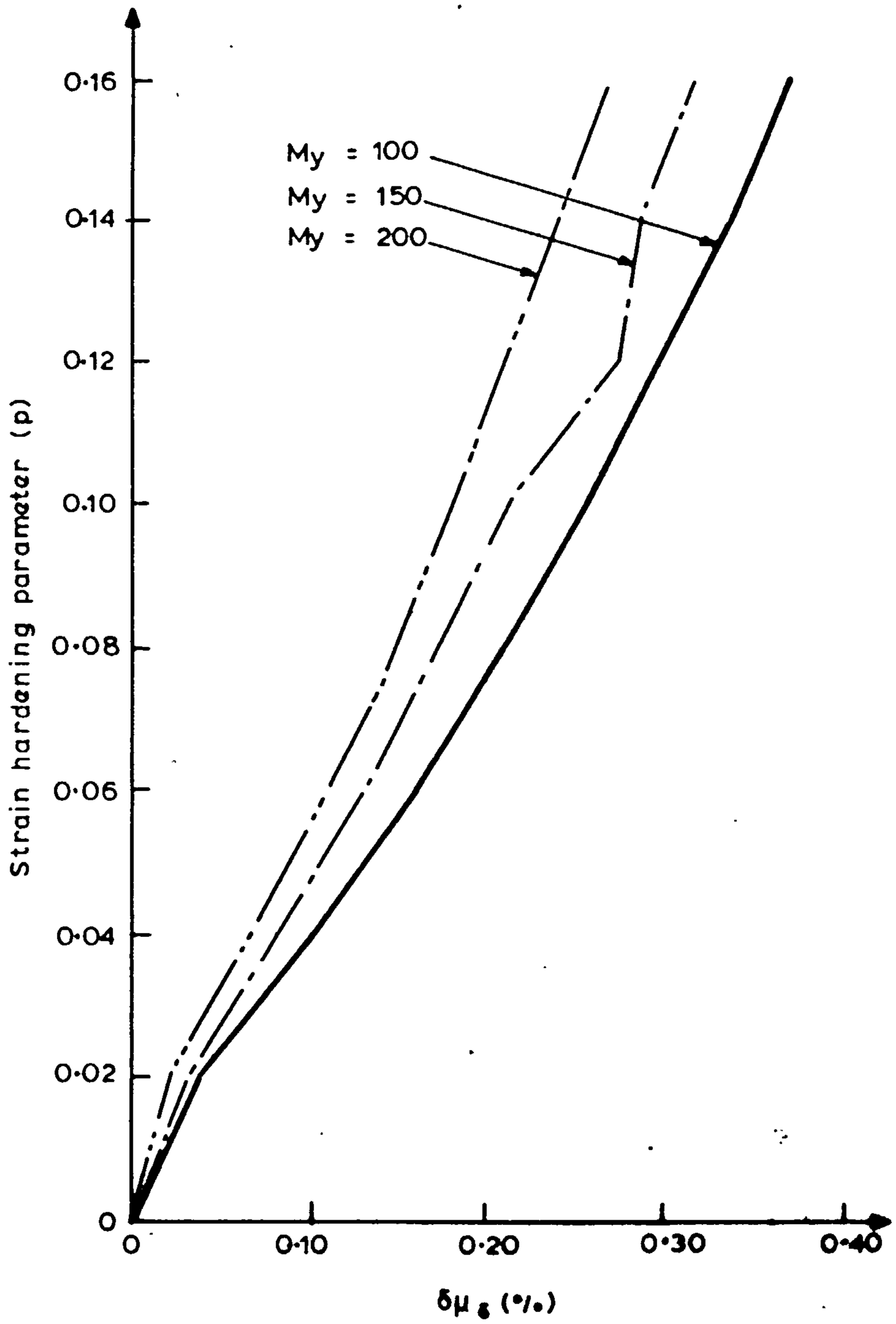

FIG. 8.6 EFFECT OF STRAIN HARDENING ON DUCTILITY DEMAND:

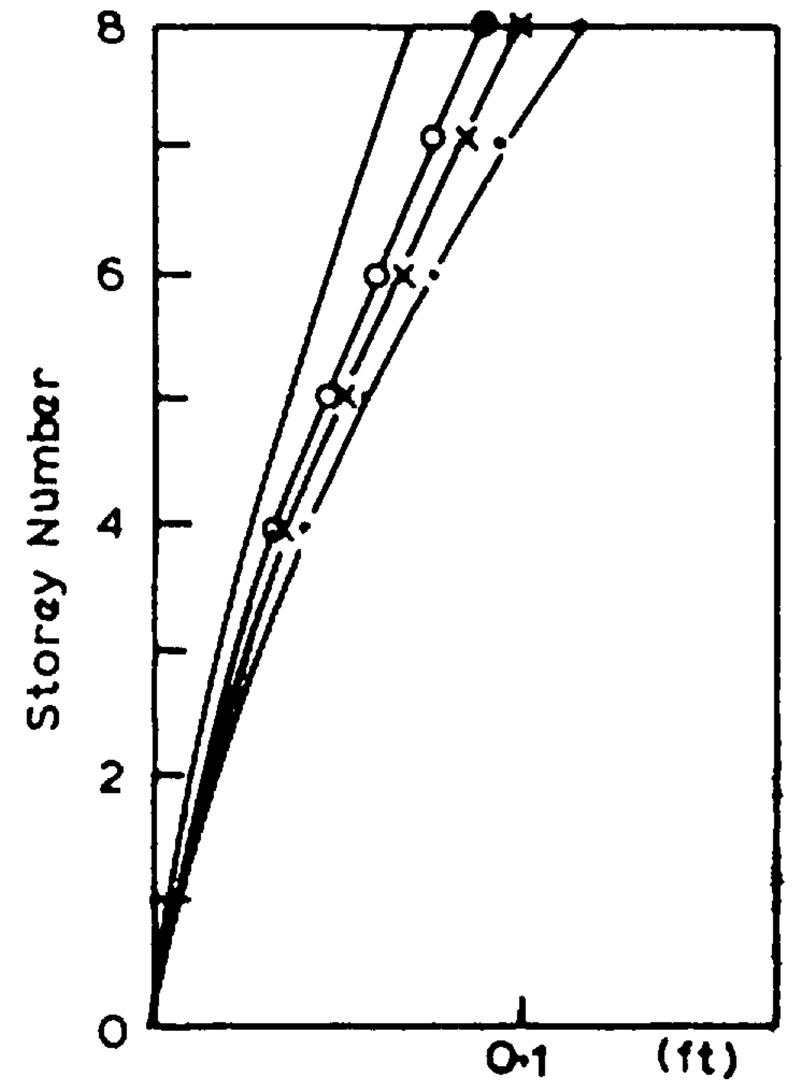

a) Lateral displacement

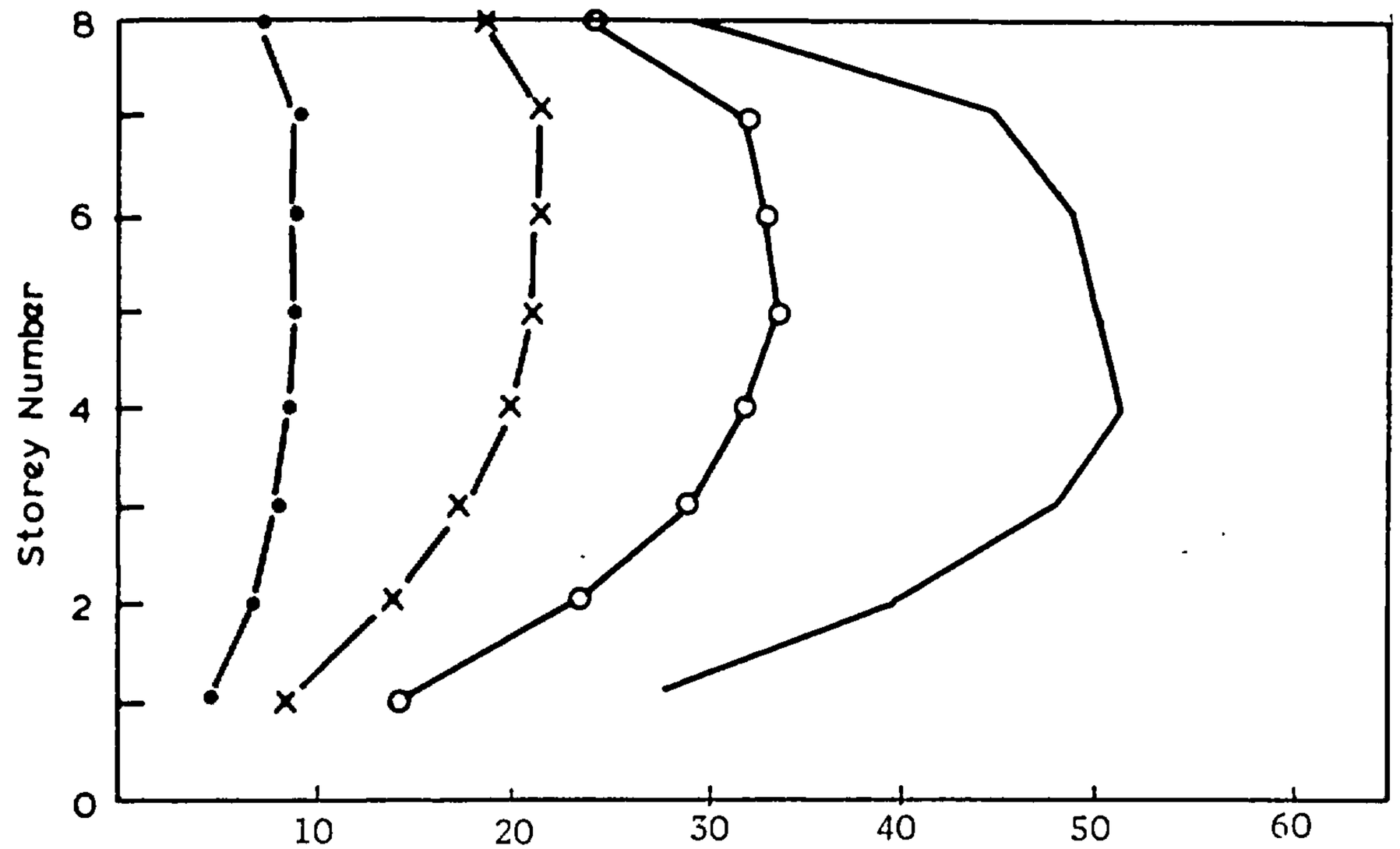

b) Bending moment in coupling beams (kip-ft)

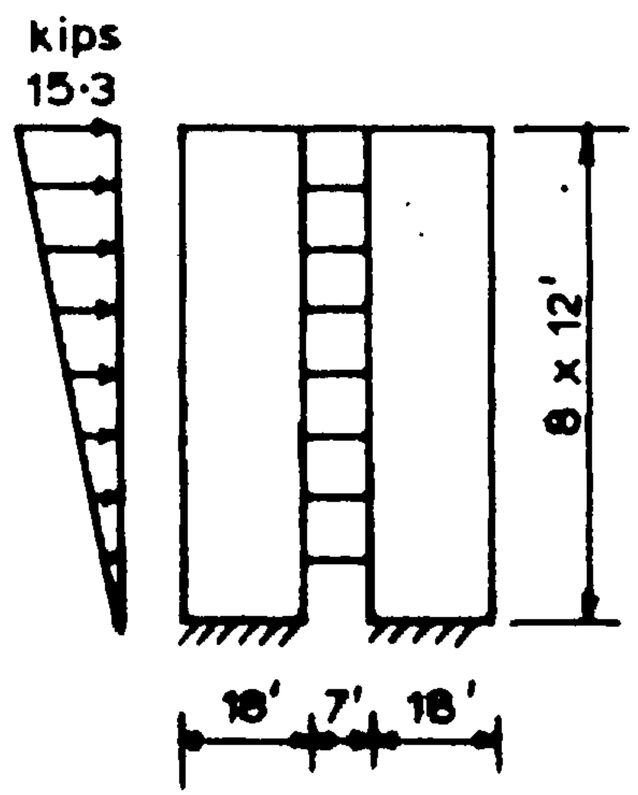

Beam depth (ft)	Designation
1·0	—•—
1·5	—x—
2·0	—o—
3·0	———

FIG. 8.7 EFFECT OF BEAM DEPTH ON

a) Overall behaviour of the structure

b) Bending Moments in coupling beams

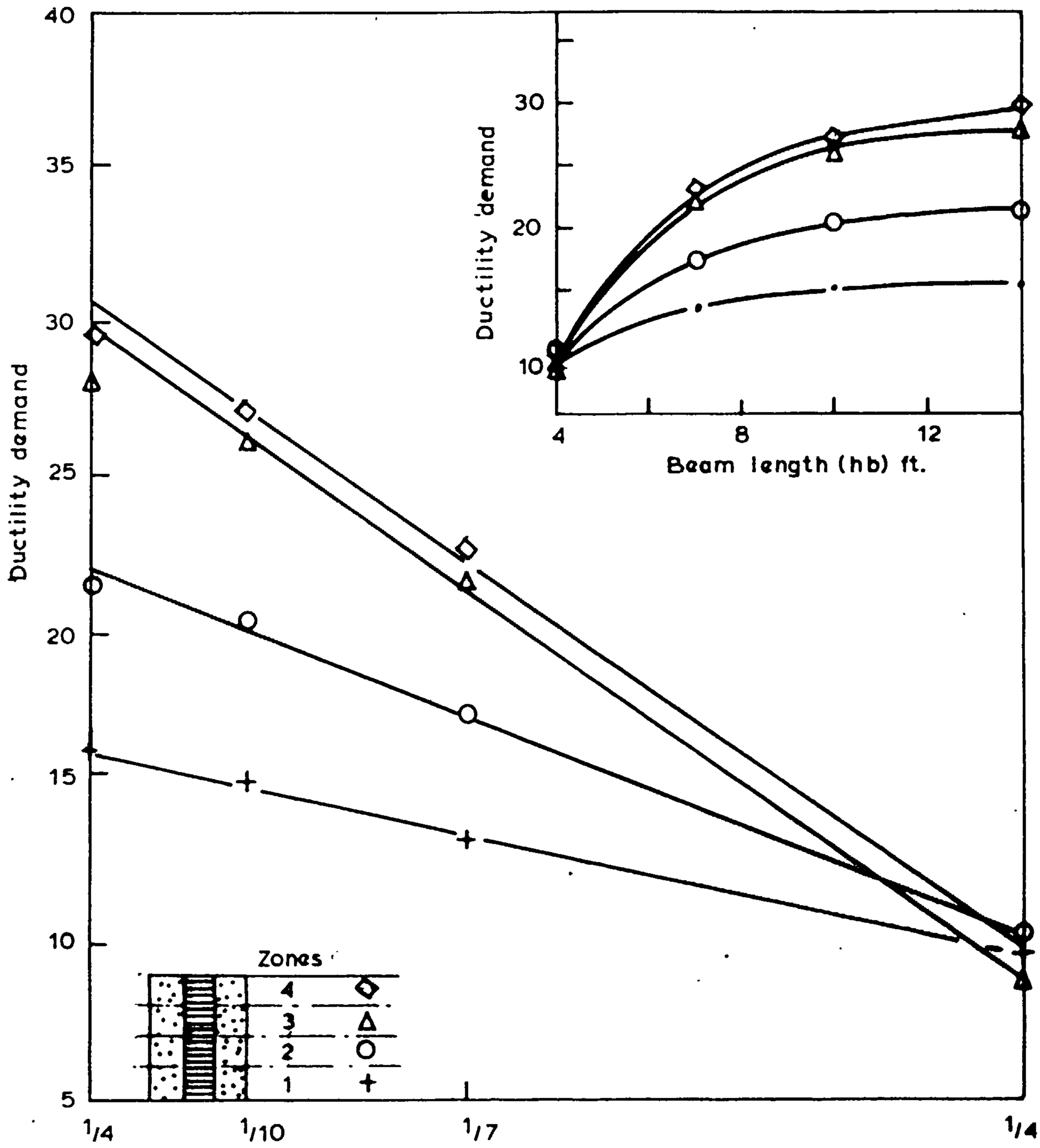

FIG. 8.8 DUCTILITY DEMAND - BEAM LENGTH RELATIONSHIP.

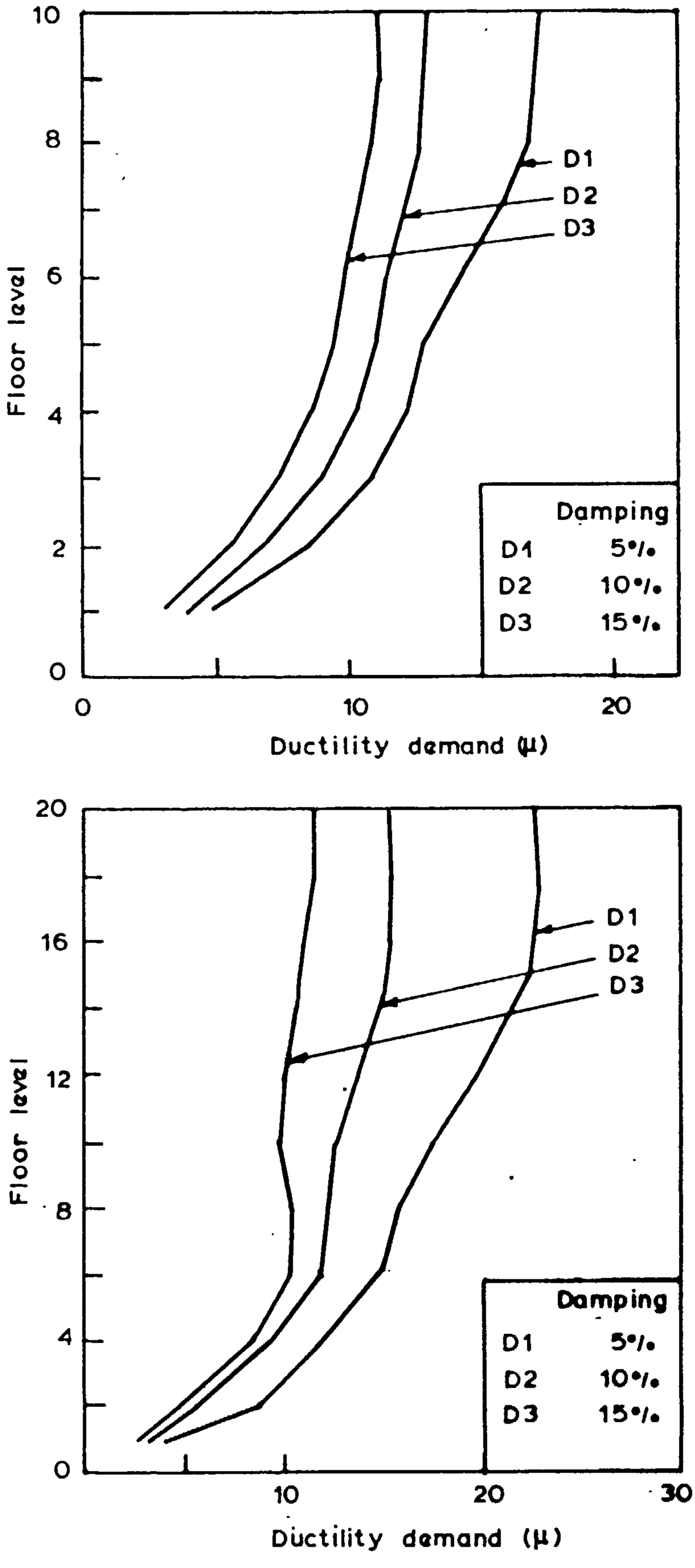

FIG. 8.9 EFFECT OF DAMPING ON DUCTILITY DEMAND OF 10 & 20 STOREY COUPLED WALLS.

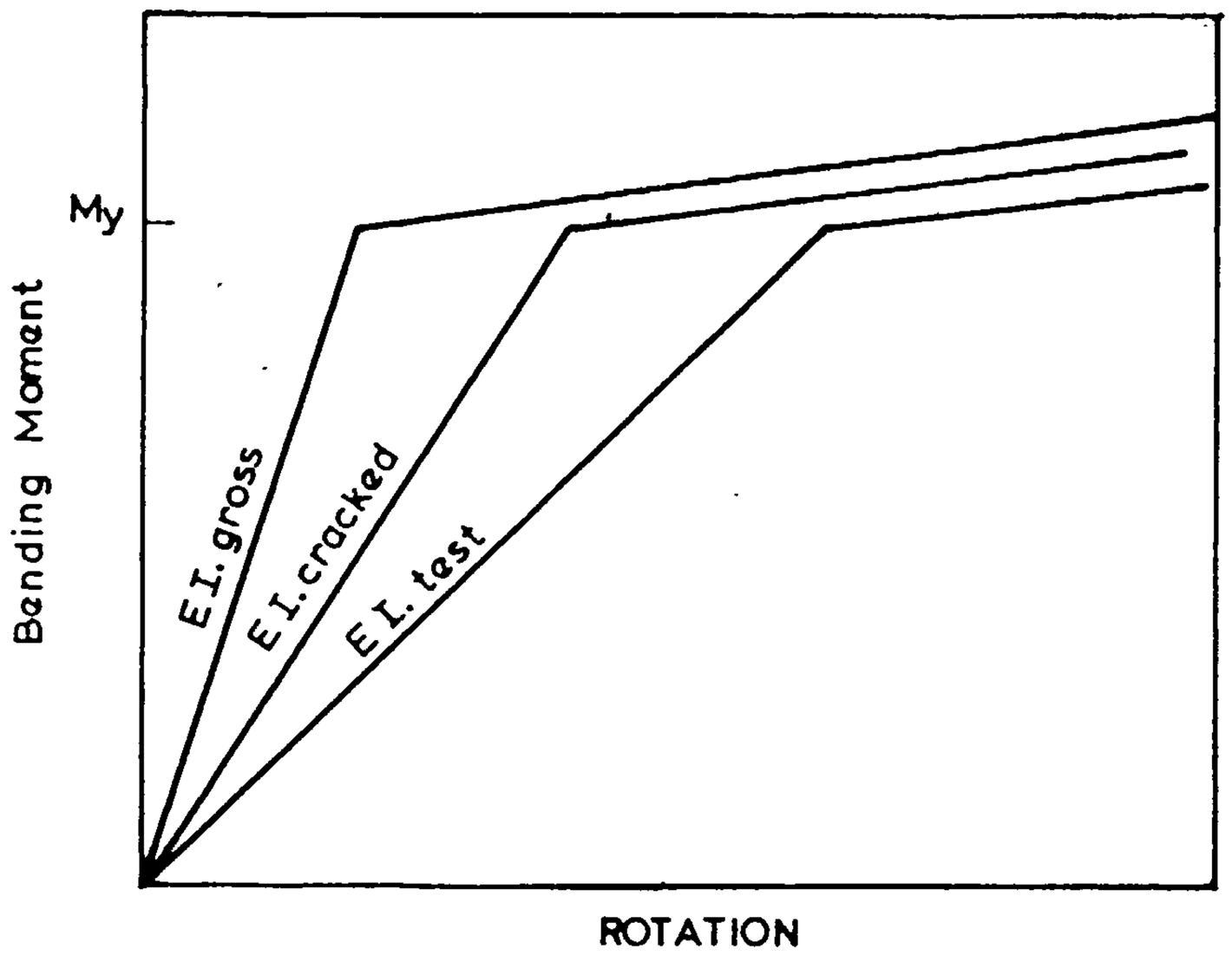

FIG. 8.10 THE DIFFERENT ALTERNATIVE FOR THE INITIAL ACTUAL STIFFNESS EIa.

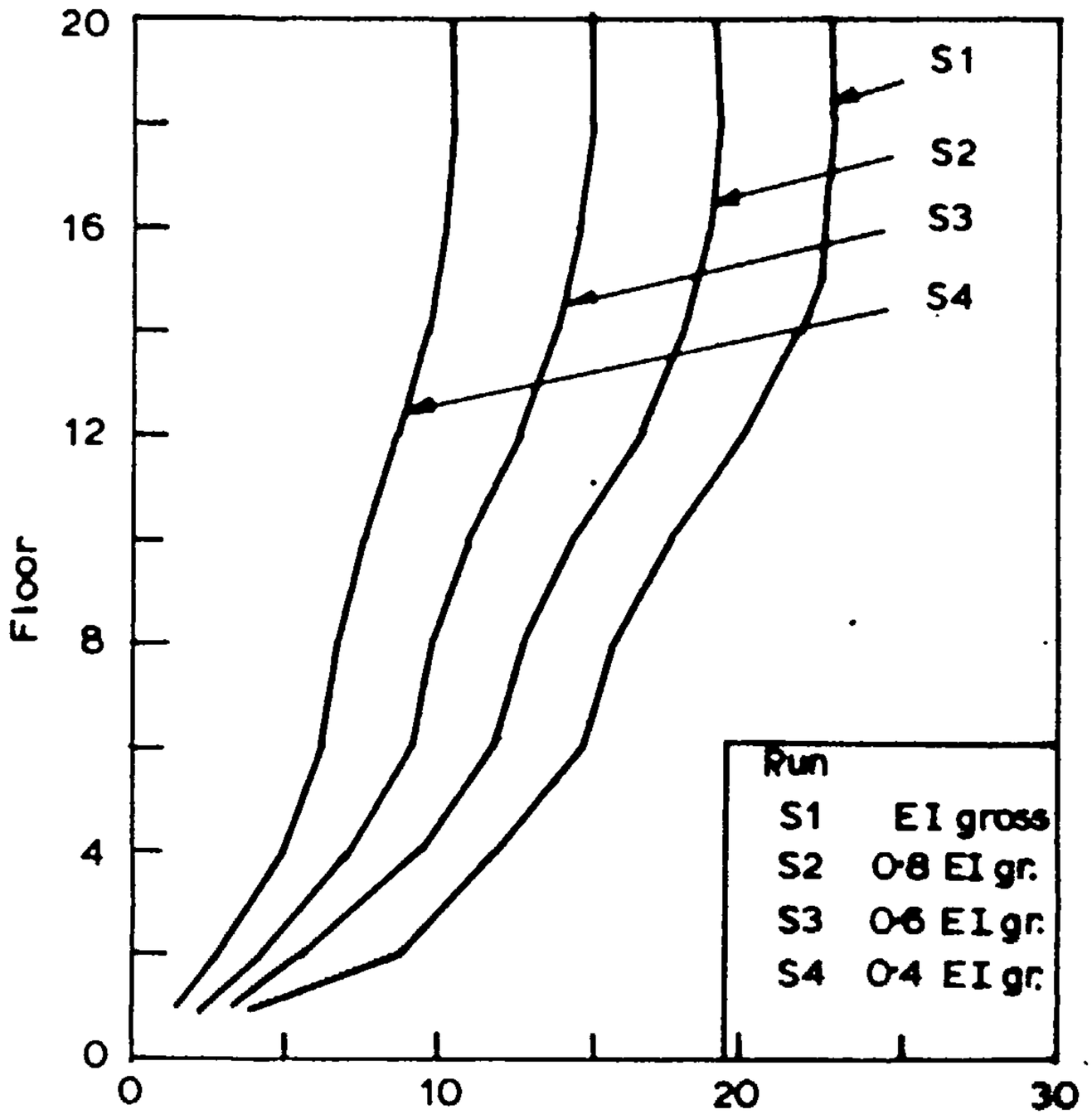

FIG. 8.11 INFLUENCE OF INITIAL HINGE RIGIDITY ON DUCTILITY DEMAND OF A 20 STOREY R/SHEAR WALL.

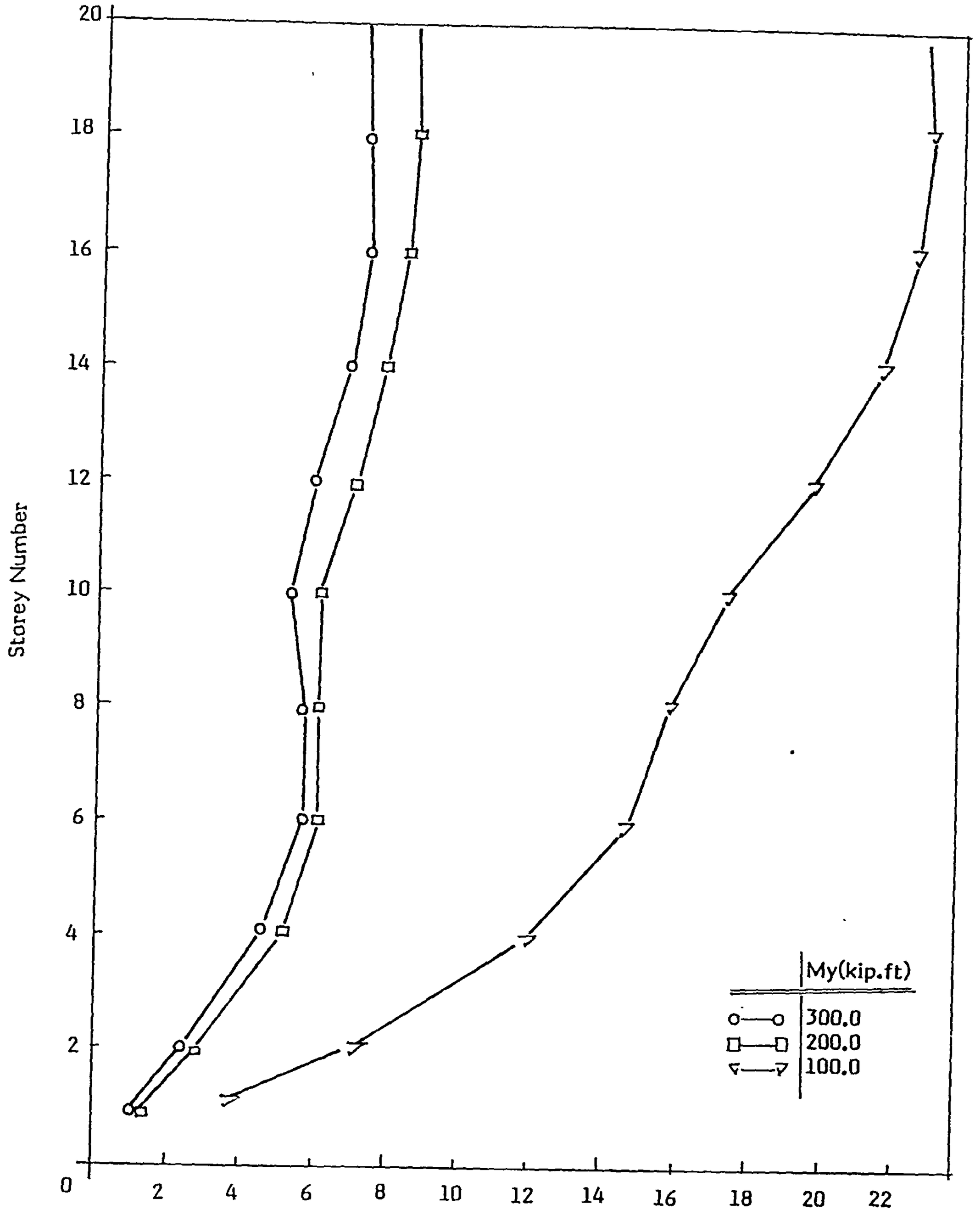

FIG. 8.12 INFLUENCE OF COUPLING BEAM YIELD MOMENT ON DUCTILITY DEMAND

FIG. 8.13 GEOMETRIC AND DYNAMIC PROPERTIES OF THE COUPLED SHEAR WALLS

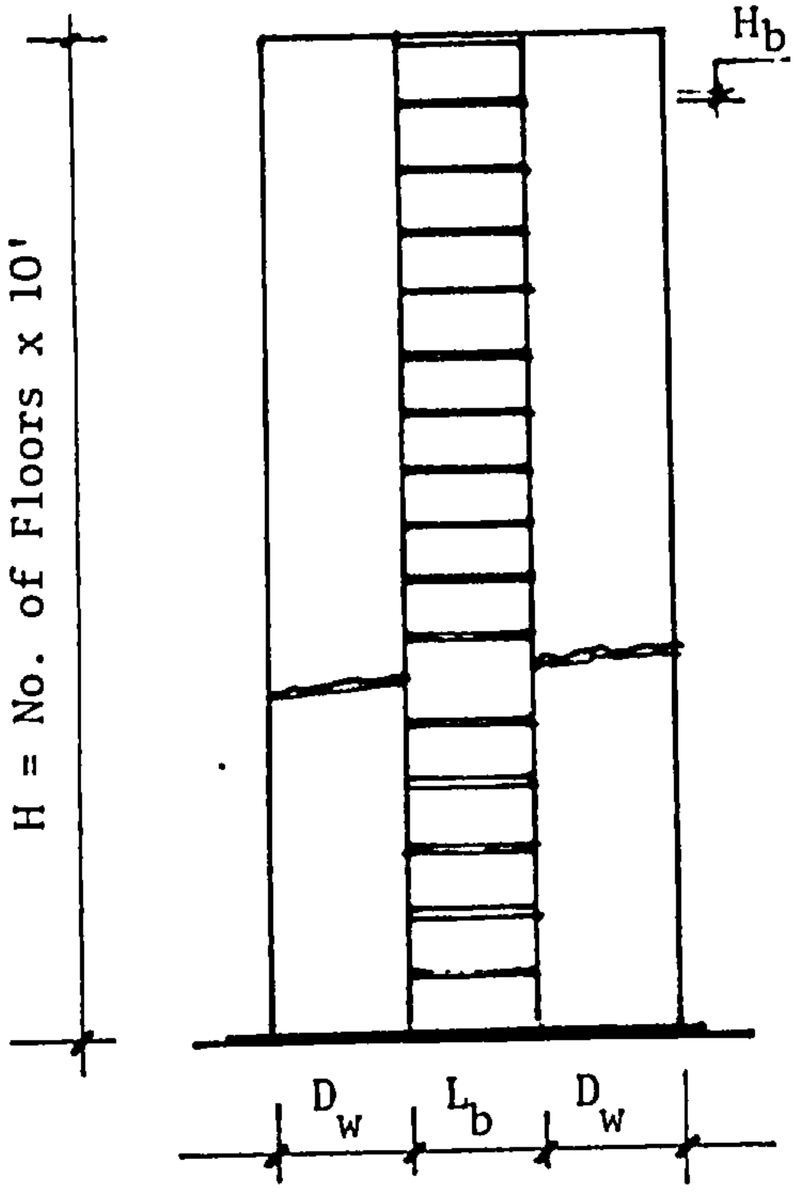

	SW1	SW2	SW3	SW4	SW5
Dw (ft)	12	12	12	18	15
H (ft)	200	300	100	300	300
Lb (ft)	7	7	7	7	10
Hb (ft)	2	2	2	2	2
H_f (ft)	10	10	10	10	10
Fundamental Period (sec.)	1.85	3.78	0.55	2.50	2.88
Wall Rigidity (EI_w/H_f) (kip.ft)	$6.68\ 10^6$	$6.68\ 10^6$	$6.68\ 10^6$	$2.25\ 10^6$	$2.88\ 10^6$
Beam Rigidity (EI_b/Lb) (kip.ft)	$4.42\ 10^4$	$4.42\ 10^4$	$4.42\ 10^4$	$4.42\ 10^4$	$3.09\ 10^4$
Lumped Mass (kips)	6.22	6.22	6.22	6.22	6.22

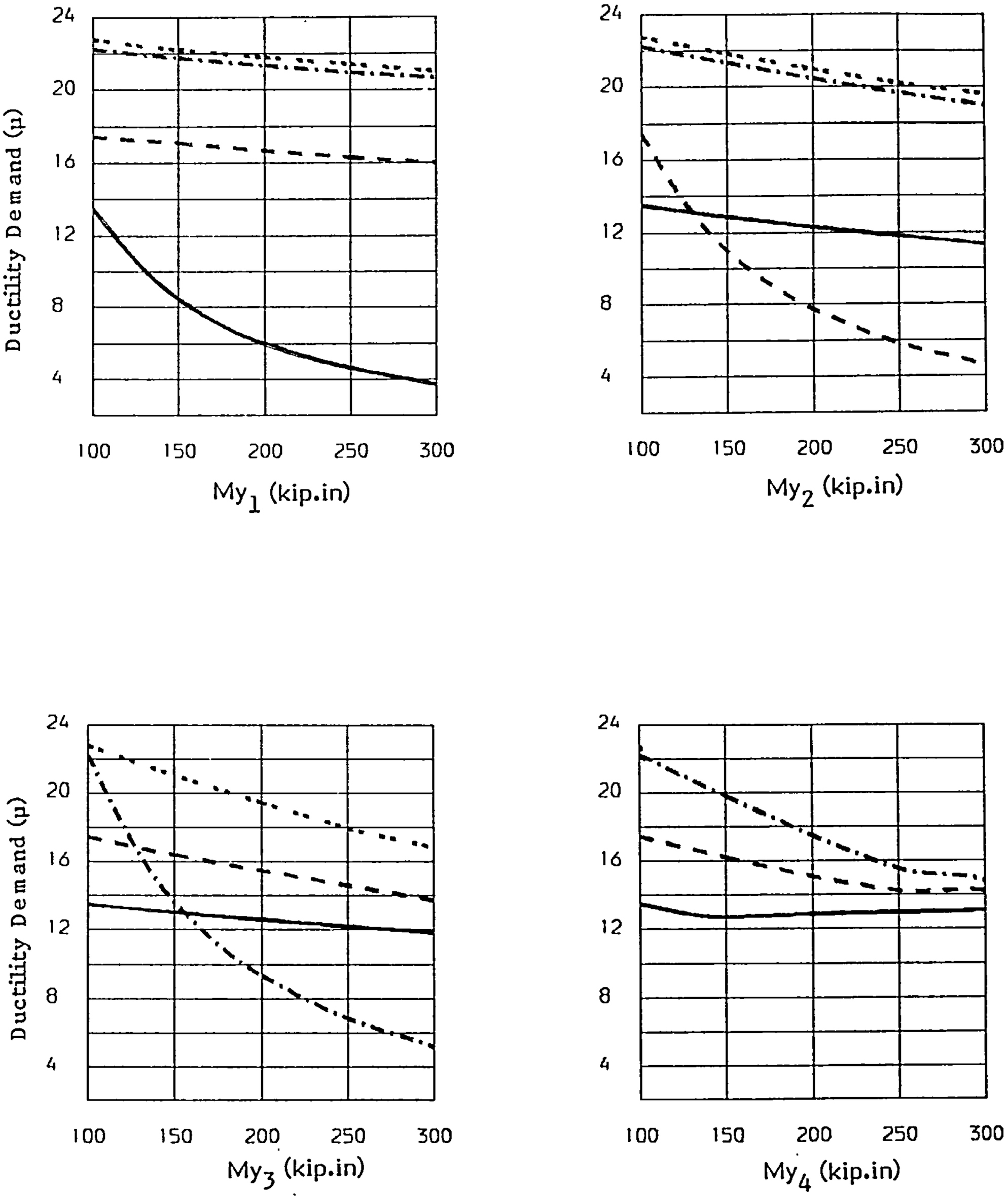

FIG. 8.14 **VARIATION OF DUCTILITY DEMAND IN THE VARIOUS ZONES DUE TO**

(a) My_1 (b) My_2 (c) My_3 (d) My_4

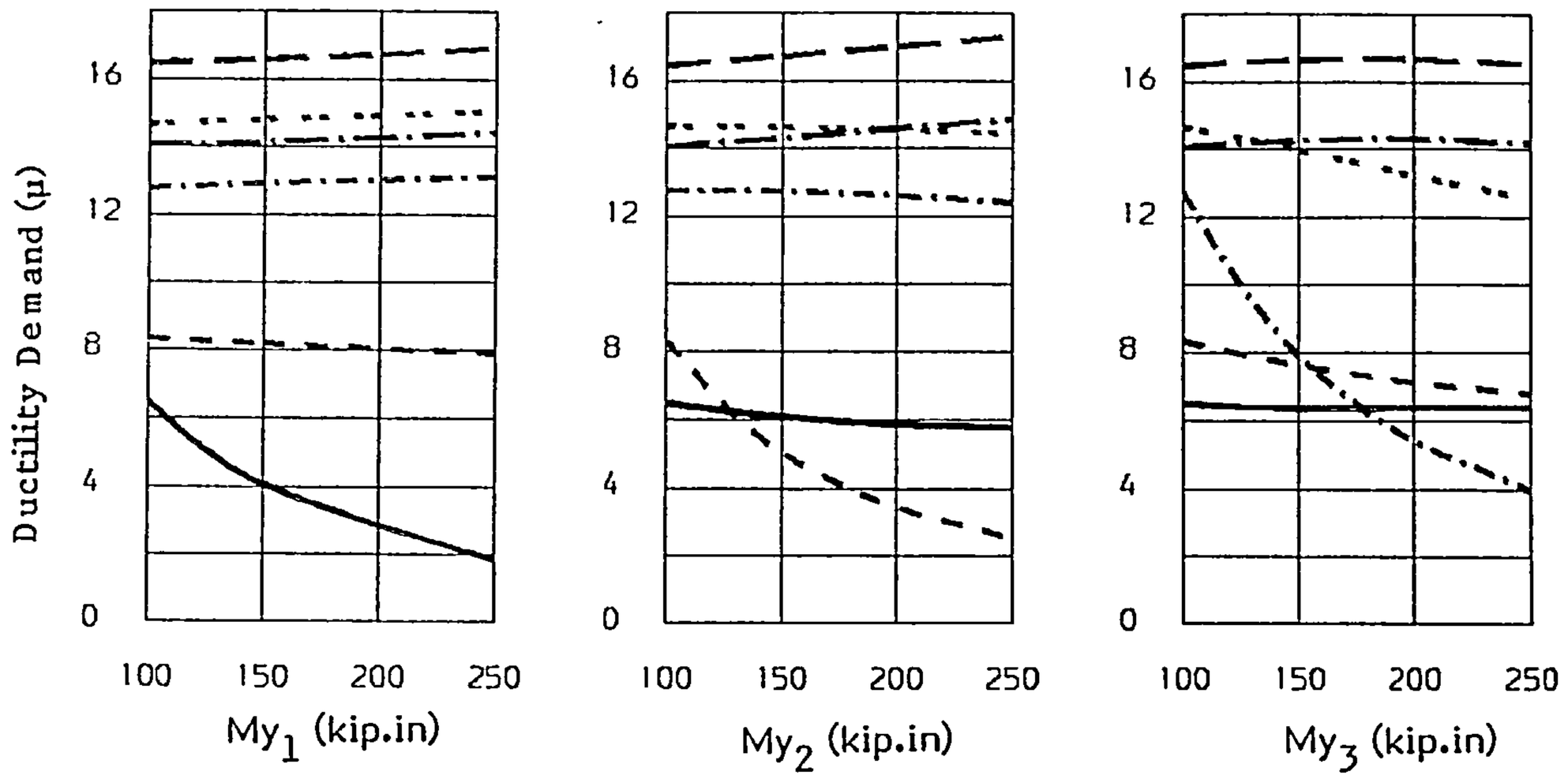

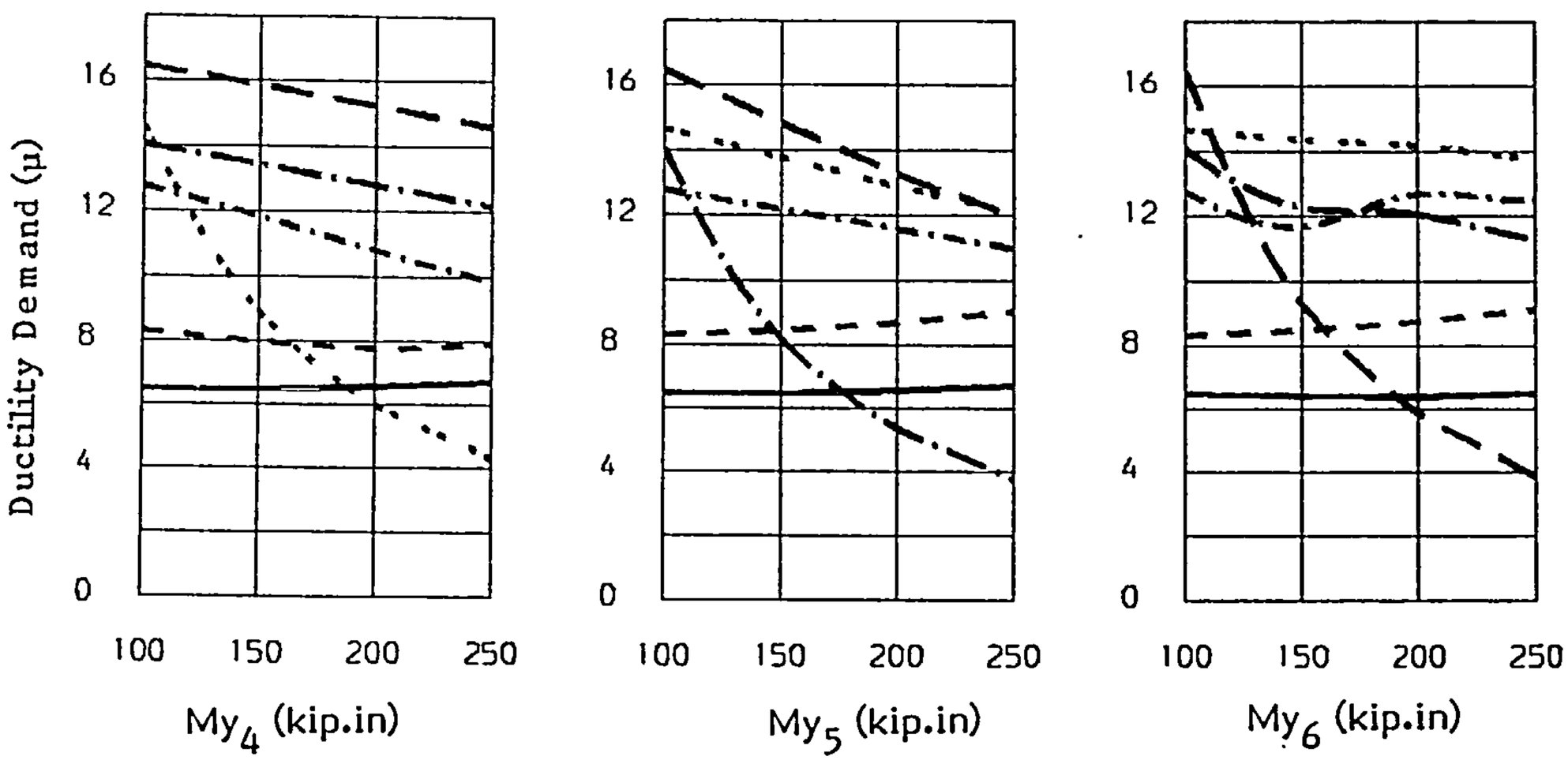

Zone	
1	———
2	— — —
3	—·—·—
4	-- -- --
5	——·——
6	—— ——

FIG. 8.15 VARIATION OF DUCTILITY DEMAND IN THE VARIOUS ZONES DUE TO

(a) My_1 (b) My_2 (c) My_3
(d) My_4 (e) My_5 (f) My_6

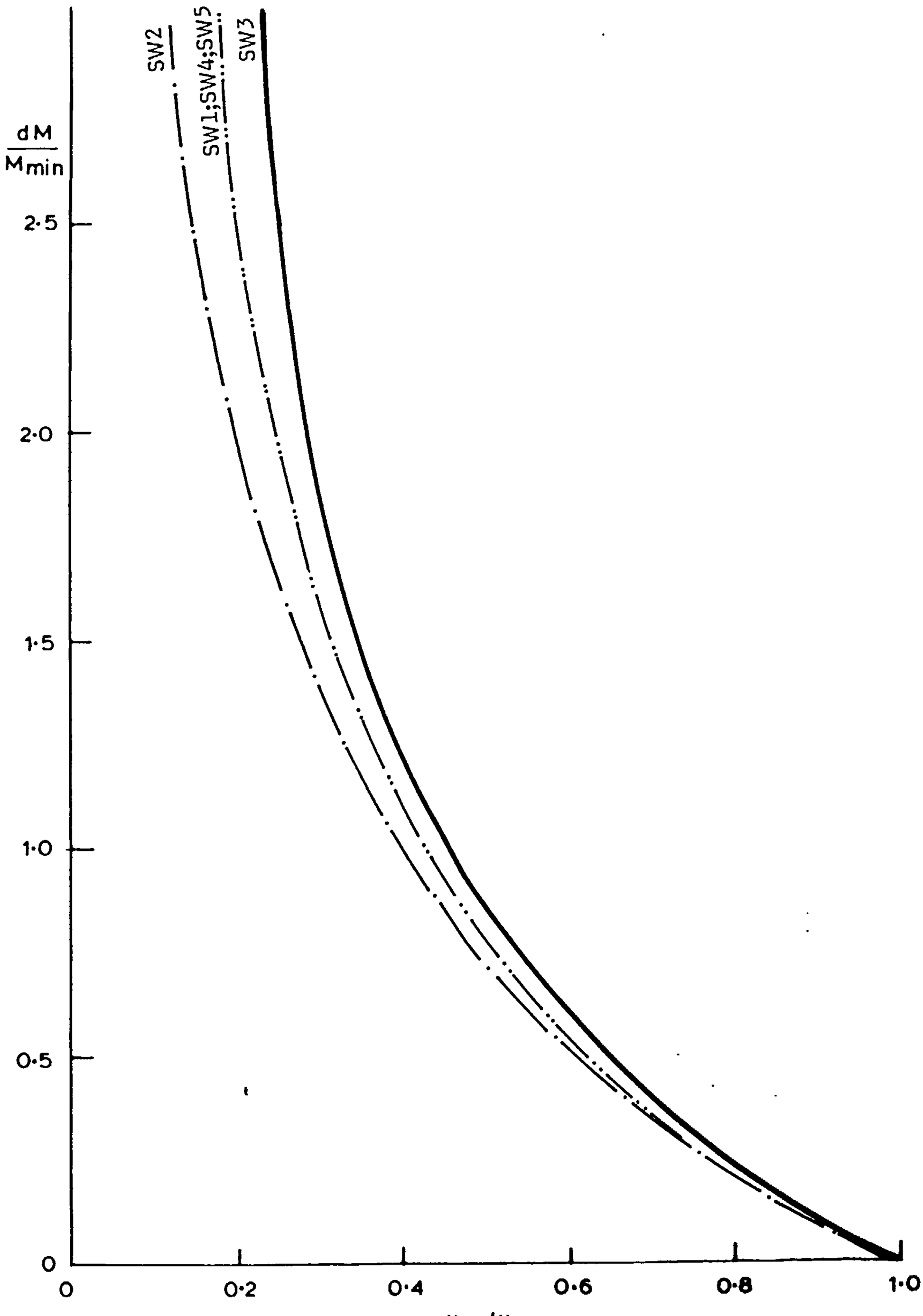

FIG. 8.16 DECAY CURVES FOR DUCTILITY DEMANDS

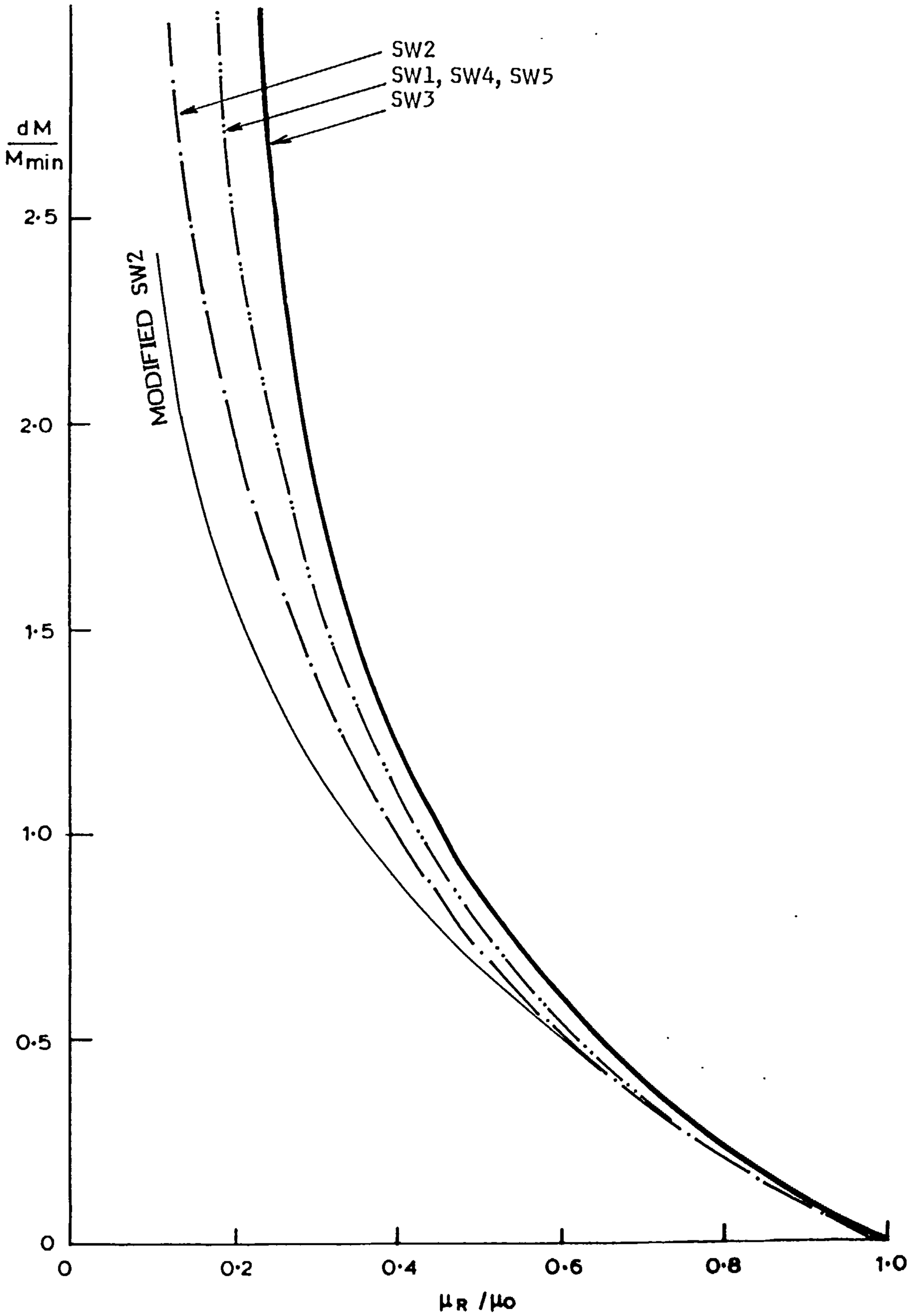

FIG. 8.17 MODIFICATION OF DECAY CURVE SW2

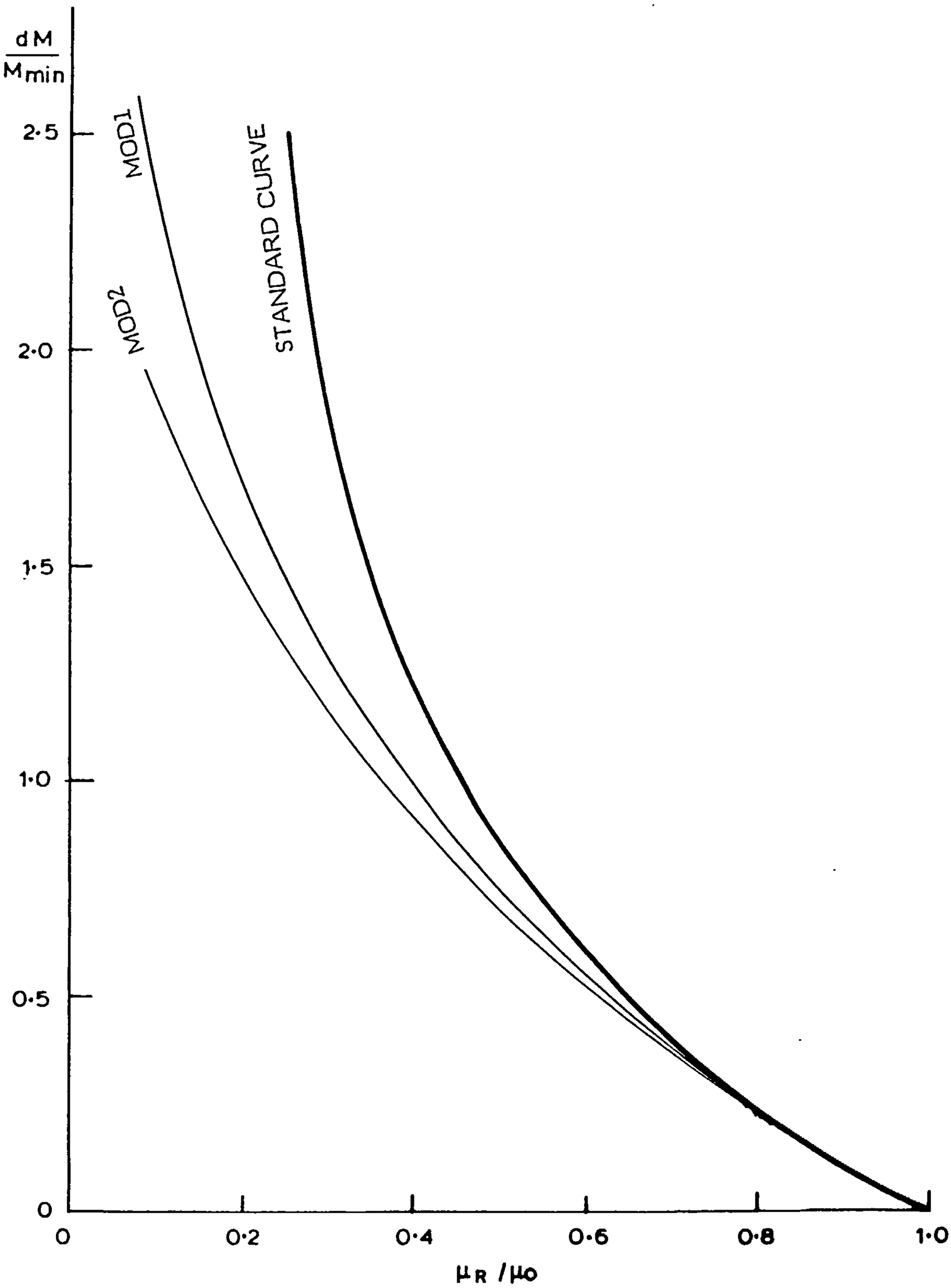

FIG. 8.18 SUCCESSIVE MODIFICATION OF THE STANDARD DECAY CURVE

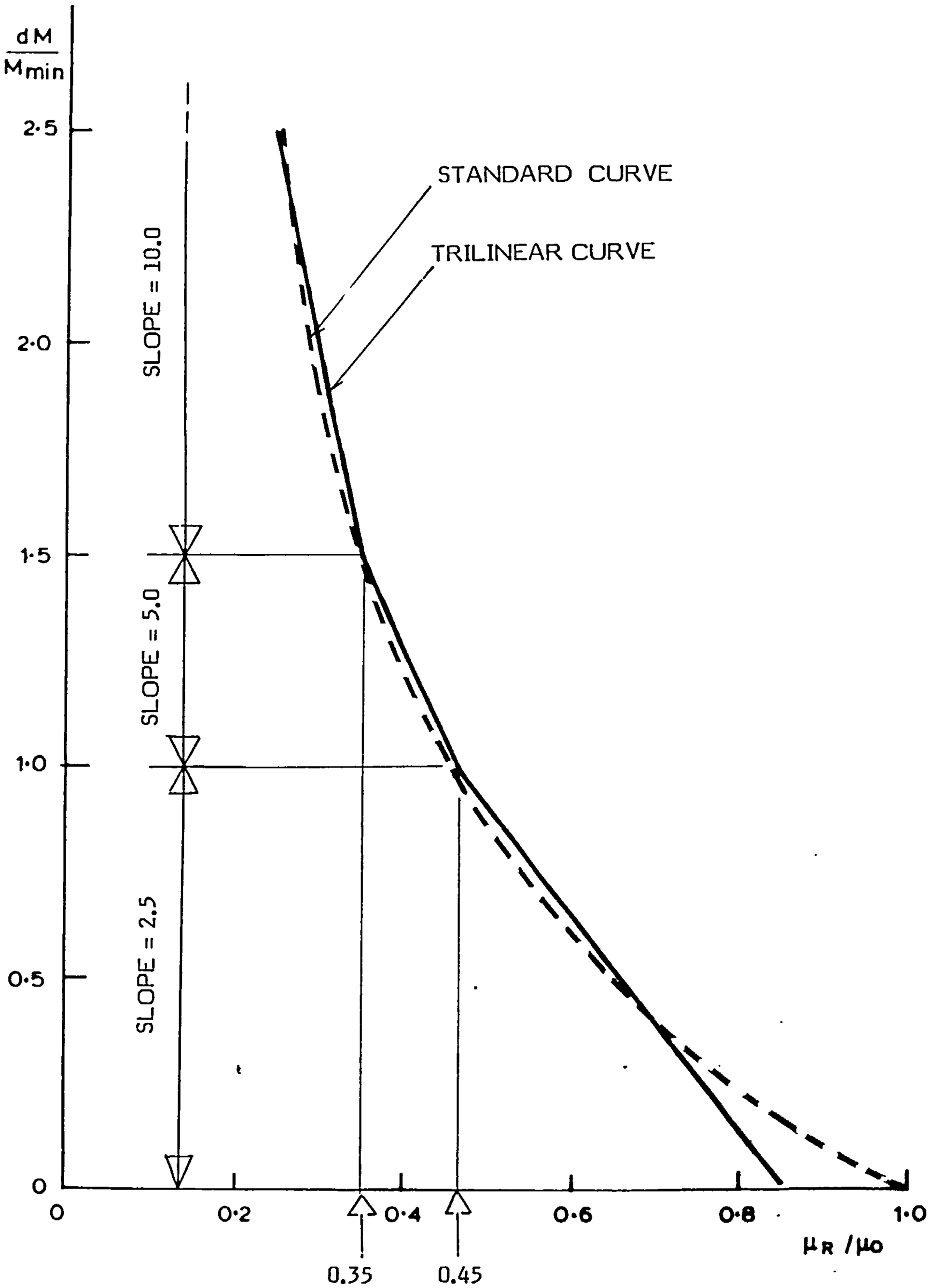

FIG. 8.19 APPROXIMATE TRILINEAR CURVE AND ASSUMED SLOPES

REFERENCES

1. ROSMAN, R.,
Approximate Analysis of Shear Walls Subject to Lateral Loads,
ACI Journal, American Concrete Institute, Proceedings, June 1964,
Vol. 61, pp. 717-733

2. COULL, A., CHOUDHURY, J.R.,
Stresses and Deflections in Coupled Shear Walls,
ACI Journal, American Concrete Institute, Proceedings, Feb. 1967,
Vol. 64, pp. 65-72

3. COULL, A., CHOUDHURY, J.R.,
Analysis of Coupled Shear Walls,
ACI Journal, American Concrete Institute, Proceedings, Sept. 1967,
Vol. 64, pp. 587-593

4. COULL, A., IRWIN, A.W.,
Design of Connecting Beams in Coupled Shear Walls,
ACI Journal, American Concrete Institute, Proceedings, Mar. 1969,
Vol. 66, pp. 205-209

5. TSO, W.K., CHAN, H.B.,
Dynamic Analysis of Plane Coupled Shear Walls,
Journal of the Engineering Mechanics Division, ASCE, Vol. 97,
No. EM1, Feb. 1971, pp. 33-48

6. COULL, A., MUKHERJEE, P.R.,
Free Vibrations of Coupled Shear Walls,
Journal of Earthquake Engineering And Structural Dynamics, Vol. 2,
1973, pp. 171-183

7. COULL, A., MUKHERJEE, P.R.,
Approximate Analysis of Free Vibration of Planar Coupled Shear Walls,
Journal of Earthquake Engineering And Structural Dynamics, Vol. 1,
1973, pp. 387-405

8. ZIENKIEWICZ, O.C.,
The Finite Element Method in Engineering Science,
McGraw-Hill Book Co., London, 1971.

9. CLOUGH, W.R.,
Analysis of Structural Vibrations and Dynamic Response,
Japan-U.S Seminar on Matrix Methods of Structural Analysis and Design,
August 1969,Tokyo, Japan.

10. PAULAY, T.,
An Elasto-Plastic Analysis of Coupled Shear Walls,
ACI Journal, American Concrete Institute, Proceedings, Nov. 1970,
Vol. 67, pp. 915-922

11. WALPOLE,W.R., SHEPHERD, R.,
Elasto-Plastic Seismic Response of Reinforced Concrete Frame,
Journal of the Structural Division, ASCE, Vol. 106, No ST6,
June 1980, pp. 1295-1310.

12. CLOUGH, R.W., PENZIEN, J.,
Structural Dynamics
McGraw-Hill, New York, 1975.

13. GUERRA, O.R., ESTEVA, L.E.,
Equivalent Properties and Ductility Requirements in Seismic Analysis of Nonlinear Systems,
Proceedings of the Sixth World Conference on Earthquake Engineering,
Vol. 5, Jan. 1977, pp. 263-268.

14. NEWMARK, N.M., HALL, W.J.,
Procedures and Criteria for Earthquake Resistant Design,
Building Practices for Disaster Mitigation, Building Science Series,
No.46, national Bureau of Standards, Feb. 1973, pp. 209-236.

15. ANAGNOSTOPOULOS, S.A., HAVILAND,R.W., BIGGS, J.M.,
Use of Inelastic Response Spectra in Aseismic Design,
Journal of the Structural Division, ASCE, Vol. 104, No ST1,
Jan. 1978, pp. 95-109.

16. LAI, S.P., BIGGS, J.M.,
Inelastic Response Spectra for Aseismic Building Design,
Journal of the Structural Division, ASCE, Vol. 106, No ST6,
June 1980, pp. 1295-1310.

17. SHIBATA, A., SOZEN, M.A.,
The Substitute Structure Method for Seismic Design in R/C
Journal of the Structural Division, ASCE, Vol. 102, No ST1,
Jan. 1976, pp. 1-18.

18. HUDSON, D.E.,
Equivalent Viscous Friction for Hysteretic Systems With Earthquake-Like Excitations,
Proceedings of the Third World Conference on Earthquake Engineering,
Vol. 2, 1965 , pp. 601-609.

19. IWAN, W.D.,
Response of Multi-Degree-of-Freedom Yielding Systems,
Journal of the Engineering Mechanics Division, ASCE, Vol. 94,
No. EM2, Apr. 1968, pp. 421-437.

20. JENNINGS, P.C.,
Equivalent Viscous Damping for Yielding Structures,
Journal of the Engineering Mechanics Division, ASCE, Vol. 94,
No. EM1, Feb. 1968, pp. 103-116.

21. GIBERSON, M.F.,
The Response of Nonlinear Multi-Storey structures Subjected to earthquake Excitations,
Earthquake Research Laboratory, California Institute of Technology,
Pasadena, 1967.

22. CLOUGH, R.W., BENUSKA, K.L., WILSON, E.L.,
Inelastic Earthquake Response of Tall Buildings,
Proceedings of the Third World Conference on Earthquake Engineering,
Vol. 2, New Zealand 1965 , pp. 68-84.

23. AOYAMA, H.,
Moment-Curvature Characteristics of Reinforced Concrete Members Subjected to Axial Load and Reversal of bending,
Proceedings of International Symposium on the Flexural Mechanics of R/C, ASCE-ACI, Miami, Nov. 1964, pp. 183-212.

24. OTANI, S.,
Inelastic Analysis of R/C Frame Structures,
Journal of the Structural Division, ASCE, Vol. 100,
No. ST7, July 1974, pp. 1433-1449.

25. AKTAN, E., PECKNOLD, D.A.W., SOZEN, M.A.,
R/C Column Earthquake Response in Two Dimensions
Journal of the Structural Division, ASCE, Vol. 100,
No. ST10, Oct. 1974, pp. 1999-2015.

26. TAKAYANAGI, T., SCHNOBRICH, W.C.,
Computed Behaviour of R/C Coupled Shear Walls.
Research No SRS 434, University of Illinois, Urbana-Champaign,
Dec 1976.

27. EMORI, K., SCHNOBRICH, W.C.,
Inelastic Behaviour of Concrete Frame-Wall Structures,
Journal of the Structural Division, ASCE, Vol. 107,
No. ST1, Jan. 1981, pp. 145-164.

28. KENT, D.C., PARK, R.,
Flexural Members With Confined Concrete
Journal of the Structural Division, ASCE, Vol. 97, No ST7,
July 1971, pp. 1969-1990.

29. TAKEDA, T., SOZEN, M.A., NIELSEN, N.,
R/C Response To Simulated Earthquakes
Journal of the Structural Division, ASCE, Vol. 96, No ST12,
Dec. 1970, pp. 2557-2573.

30. KANNAN, A.E., POWELL, G.H.,
A General Purpose Computer Program For Dynamic Analysis of Inelastic
Plane Structures (DRAIN2-D),
Reports No EERC 73-6 and EERC 73-22, University of California,
Berkeley, Apr. 1973 (Revised Aug. 1975).

31. NGO, D., SCORDELIS, A.C.,
Finite Element Analysis of R/C Beams
ACI Journal, American Concrete Institute, Proceedings, Vol. 64, No. 3,
March 1967, pp. 152-163.

32. NILSON, A.H.,
Nonliner Analysis of R/C by Finite Element Method
ACI Journal, American Concrete Institute, Proceedings, Vol. 65, No. 9,
sept. 1968, pp. 757-766.

33. SUIDAN, M., SCHNOBRICH, W.C.,
Finite Element Analysis of Reinforced Concrete
Journal of the Structural Division, ASCE, Vol. 99, No ST10,
Oct. 1973, pp. 2109-2122.

34. AGRAWAL, A.B.,JAEGER, L.G., MUFTI, A.A.,
Crack Propagation and Plasticity of R/C Shear Wall Under Monotonic
and Cyclic Loading,
Conference on FEM in Engineering, Adelaide, Australia, Dec. 1976.

35. SCHNOBRICH, W.C.,
Behaviour of R/C Structures Predicted by Finite Element Method,
An International Journal, Computers and Structures, Vol. 7, No. 3,
June 1977, pp. 365-376.

36. DARWIN, D., PECKNOLD, D.A.W.,
Analysis of R/C Shear Panels Under Cyclic Loading,
Journal of the Structural Division, ASCE, Vol. 102, No ST2,
Feb. 1976, pp. 355-369.

37. RASHID, U.R.,
Analysis of Prestressed Concrete Pressure Vessels,
Nuclear Eng. and Design, Vol. 7, No. 4, Apr. 1968, pp. 334-344.

38. CERVENKA, V., GERSTLE, K.H.,
Inelastic Analysis of R/C Panels,
Part I: Theory, IABSE Publications, Vol. 31-II, 1971, pp. 31-45.

39. CERVENKA, V., GERSTLE, K.H.,
Inelastic Analysis of R/C Panels,
Part II: Experimental Verification and Application, IABSE Publications,
Vol. 32-II, 1972, pp. 25-39.

40. VALLIAPPAN, S., DOOLAN, T.F.,
Nonlinear Stress Analysis of Reinforced Concrete,
Journal of the Structural Division, ASCE, Vol. 98, No ST4,
Apr. 1972, pp. 885-898.

41. YUZUGULU, O., SHNOBRICH, W.C.,
A Numerical Procedure for the Determination of the Behaviour of a Shear Wall Frame System,
ACI Journal, American Concrete Institute, Proceedings, Vol. 70, July 1973, pp. 474-479.

42. AGRAWAL, A.B., JAEGER, L.G., MUFTI, A.A.,
Response of R/C Shear Wall Under Ground Motions,
Journal of the Structural Division, ASCE, Vol. 107, No ST2,
Feb. 1981, pp. 395-411.

43. HOUSNER, G.W.,
Behaviour of Structures During Earthquakes,
Journal of the Engineering Mechanics Division, ASCE, Vol. 85,
No. EM4, Oct. 1959, pp. 109-129.

44. PAULAY, T.,
Coupling Beams of R/C Shear Walls,
Journal of the Structural Division, ASCE, Vol. 97, No ST3,
Mar. 1971, pp. 843-862.

45. PAULAY, T.,
Simulated Seismic Loading of Spandrel Beams,
Journal of the Structural Division, ASCE, Vol. 97, No ST9,
Sept. 1971, pp. 2407-2419.

46. PAULAY, T., PRIESTLEY, M.J.N., SYNGE, A.J.,
Ductility in Earthquake Squat Shear Walls
ACI Journal, American Concrete Institute, Proceedings, Vol. 79-26, July-Aug. 1982, pp. 257-269.

47. ALLEN, C.M., JAEGER, L.G., FENTON, V.C.,
Ductility of Reinforced Concrete Shear Walls,
Publication SP36-6, Committee 442, Response of Multistorey Concrete Structures to Lateral Forces, Detroit, 1973.

48. A C I COMMITTEE 318,
Building Code Requirements for Reinforced Concrete,
ACI 318-17, American Concrete Institute, Detroit, 1977.

49. S E A O C SEISMOLOGY COMMITTEE
Structural Engineers Association of California,
Recommended Lateral Forces Requirements and Commentary,
171 Second Street, San Fransisco, California, 94105.

50. U B C Uniform Building Code,
International Conference of Building Officials,
5260 South Workman Mill Road, Whittier, California, 90601.

51. N B C National Building Code,
Associate Committee NBC, National Building Code of Canada, 1970,
National Research Council, Ottawa, Canada.

52. BERTERO, V.V.,
Seismic Behaviour of R/C Wall Structure Systems,
Proceedings of the 7th. World Conference on Earthquake Eng., Vol. 6,
Turkey, 1980.

53. COULL, A., CHOO, B.S.,
Simplified Elasto-Plastic Analysis of Coupled Shear Walls,
The Institution of Civil Eng., Part II, Vol. 73, June 1982, pp. 365-381.

54. FINTEL, M., GHOSH, S.K.,
Inelastic Response History Analysis of the Aseismic Design of a 31 Storey Frame Wall Building,
Journal of Earthquake Engineering And Structural Dynamics, Vol. 9,
1981, pp. 543-556.

55. FINTEL, M., GHOSH, S.K.,
Case Study of Aseismic Design of a 16 Storey Coupled Shear Wall Using Inelastic Dynamic Analysis,
ACI Journal, American Concrete Institute, Proceedings, Vol. 79, May-June 1982, pp. 171-179.

56. DERETCHO, A.T.,
Dynamic Inelastic Response of Coupled Shear Walls as Affected by Axial Forces,
Study No. 14, Nonlinear design of Concrete Structures, Solid Mechanics Div., University of Waterloo, Ontario, Canada, Aug. 7-9, 1979.

57. WEE, H.J.,
Free Vibration Analysis and Transient Response of Shear Wall Structures by Finite Element Method,
M. Eng. Thesis, Civ. Eng. Dept, Univ. of Liverpool, 1976.

58. OWEN, D.R.J., HINTON, E.,
Finite Elements Method in Plasticity, Theory & Practice,
Pineridge Press Limited, Swansea, U.K., 1980.

59. DESAI, C.S., ABEL, J.F.,
Introduction to the FEM: A Numerical Method for Engineering Analysis,
Van Norstrand Reisnhold Company, New York, 1972.

60. CHEUNG, Y.K., YEO, M.F.,
A Practical Introduction To Finite Element Analysis,
Pitman Int. Company, London, 1979.

61. COOK, R.D.,
Concepts and Applications of Finite Element Analysis,
John Wiley & Sons, New York, 1974.

62. TIMOSHENKO, S., GOODIER, J.N.,
Theory of Elasticity,
McGraw-Hill, New York, 1951.

63. WILSON, E.L., TAYLOR, R.L., DOHERTY, W.P., GHABOUSSI, J.,
Incompatible Displacement Models,
International Symposium on Numerical Computer Methods in Structural Mechanics, Univ. of Illinois, Urbana, Sept. 1971.

64. JIMINEZ, R., WHITE, R.N., GERGELY, P.,
Cyclic Shear and Dowel Action Models in R/C,
Journal of the Structural Division, ASCE, Vol. 108, No ST5,
May 1982, pp. 1106-1123.

65. AGRAWAL, A.B., MUFTI, A.A., JAEGER, L.G.,
Discussion on Analysis of R/C Shear Panels Under Cyclic Loading,
Journal of the Structural Division, ASCE, Vol. 103, No ST1,
Jan. 1977, pp. 302-304.

66. SAIIDI, M.,
Hysteresis Model for Reinforced Concrete,
Journal of the Structural Division, ASCE, Vol. 108, No ST5,
May 1982, pp. 1077-1087.

67. SINHA, B.P., GERTLE, K., TULIN, L.G.,
Stress-Strain Relationships for Concrete Under Cyclic Loading,
ACI Journal, American Concrete Institute, Proceedings, Vol. 61, Jan. 1964, pp. 195-211.

68. SOLEIMANI, D., POPOV, E.P., BERTERO, V.V.,
hysteretic Behaviour of R/C Beam-Column Subassemblages,
ACI Journal, American Concrete Institute, Proceedings, Vol. 76, Nov. 1979, pp. 1179-1195.

69. IWAN, W.D.,
Estimating Inelastic Response Spectra from Elastic Spectra,
Earthquake Eng. and Str. Dynamics, Vol. 8, No.4, July-Aug. 1980, pp. 375-388.

70. TANSIRIKONGKOL, V., PECKNOLD, D.A.,
Approximate Model Analysis of Bilinear Mdof Systems,
Journal of the Eng. Mech. Division, ASCE, Vol. 106, No EM2, Apr. 1980, pp. 361-376.

71. WIEGEL, R.L., Editor,
Earthquake Engineering,
Prentice-Hall, 1970.

72. BERTERO, V.V., SAGAJESKI, S.W.,
Optimal Inelastic Design of Seismic Resistant R/C Framed Structures,
Nonlinear Design of Concrete Structures,
CSCE-ASCE-ACI-CEB International Symposium, University of Waterloo, Ontario, Canada, Aug. 7-9, 1979.

73. SEED, H.B., IDRISS, I.M.,
Influence of Soil Conditions on Ground Motions During Earthquake,
Journal of Soil Mech. and Foundation Div., ASCE, Vol. 95, SM1, Jan. 1969, pp.99-137.

74. DERETCHO, A.T., FUGELSO, L.E., FINTEL, M.
Structural Walls in Earthquake Resistant Buildings - Analytical Investigation, Dynamic Analysis of Isolated Walls, Input Motions, Final Report to the National Science Foundation, RANN, Under Grant No ENV74-14766, Portland Cement Association, Dec. 1977.

75. DERETCHO, A.T., GHOSH, S.K., IQBAL, M., FINTEL, M.,
Strength, Stiffness and Ductility required in R/C Structural Walls For Earthquake Resistance,
ACI Journal, American Concrete Institute, Proceedings, Vol. 76, Aug. 1976, pp. 875-896.

76. A T C
Tentative Provisions For the Developement of Seismic Regulations For Buildings, Applied Technology Council ATC-3, San Fransisco, 1978.

77. FINTEL, M., Editor,
Handbook Concrete Engineering,
Van Nostran Reinhold Company, 1974.

78. FINTEL, M., GHOSH, S.K.,
Explicit Inelastic Dynamic Procedure For Aseismic Structures,
ACI Journal, American Concrete Institute, Proceedings, Vol. 79, March-Apr. 1982, pp. 110-118.

79. FINTEL, M., GHOSH, S.K.,
Design of Walled Structures of Earthquake Loading,
Nonlinear Design of Concrete Structures,
CSCE, ASCE, ACI, CEB, International Symposium, University of Waterloo, Ontario, Canada, Aug. 7-9, 1979.

80. CORLEY, W.G., SCANLON, A.,
Dynamic Modeling of Structural Walls,
Design for Dynamic Loading, The Use of Model Analysis,
Edited by G.S.T Armer & F.K Garas, Construction Press, 1982.

81. GHOSHY, B.,
Modelling of Supporting Cores Subjected to Dynamic Loading,
Design for Dynamic Loading, The Use of Model Analysis,
Edited by G.S.T Armer & F.K Garas, Construction Press, 1982.

82. MAHIN. S.A., BERTERO, V.V.,
An Evaluation of Inelastic Seismic Design Spectra,
Journal of the Structural Division, ASCE, Vol. 107, No ST9,
Sept. 1981, pp. 1777-1795.

83. RAJU, I.S., RAO, G.V., MURTHY, T.V.G.K.,
Eingenvalues and Eigenvectors of Large Order Banded Matrices,
Journal of Computer and Structures, Vol. 4, 1974, pp. 549-558.

84. STOODLEY, K.D.C., LEWIS, T., STAINTON, G.L.S.,
Applied stastical Techniques,
University of Bradford, Ellis Horwood Limited, 1980.

85. ANDERSON, C.J., BERTERO, V.V.,
Effects of Gravity Load on Vertical Ground Acceleration on the Seismic Response of Multistorey Frames, 4th World Conference on Earthquake Eng., Rome, 1974.

86. PAULAY, T., PARK, R.,
Reinforced Concrete Structures,
John Wiley & Sons, New York, 1975, 769 pp.

87. POPOVICS, S.,
A Numerical Approach to the Complete Stress-Strain Curve of Concrete,
Cement & Concrete Research, 3, 1973, pp. 583-599.

88. KARSAN, I.D., JIRSA, J.O.,
Behaviour of Concrete Under Biaxial Stresses,
Journal of the Structural Division, ASCE, Vol. 95, No ST12,
Dec. 1969, pp. 2543-2563.

89. KUPFER, H., HILSDORF, H.K., RUSH, H.,
Behaviour of Concrete Under Biaxial Stresses,
ACI Journal, American Concrete Institute, Proceedings, Vol. 66,
Aug. 1969, pp. 656-666.

90. DULASKA, H.,
Dowel Action of Reinforcement Crossing Cracks in Concrete,
ACI Journal, American Concrete Institute, Proceedings, Vol. 69-70, Dec.
1972, pp. 754-757.

91. PAULAY, T., FENWICK, R.C.,
Mechanism of Shear Resistance of Concrete beams,
Journal of the Structural Division, ASCE, Vol. 94, No ST10,
Oct. 1968, pp. 2325-2350.

92. PRZEMIENIECKI, J.S.,
Theory of Matrix Structural Analysis,
McGraw-Hill Book Co., New York, 1968.

93. PAULAY, T., LOEBER, P.J.,
Shear Transfer by Aggregate Interlock,
ACI, Special Publication, SP42, Vol. 1, 1973.

94. CEDOLIN, L., DEIPOLI, S.,
Finite Element Studies of Shear Critical R/C Beams,
Journal of the Eng. Mech. Division, ASCE, Vol. 103, No EM3,
June 1977, PP. 395-410.

95. AL-MAHAIDI, R.H., NILSON, A.H.,
Nonlinear Finite Element Analysis of R/C Deep Members,
Research Report No 79-1, Dept. of Str. Eng., Cornell University, Itheca,
New york, Jan. 1979.

96. ZIENKIEWICZ. O.C., VALLIAPPAN, S., KING, I.P.,
Elasto-Plastic Solution of Engineering Problems, Initial Stress FE Approach, International Journal of Numerical Methods in Eng., Vol. 1, Jan. 1969, pp. 75-100.

97. BANON, H., BIGGS, J.M., IRVINE, H.M.,
Seismic Damage of Reinforced Concrete Frames,
Journal of the Structural Division, ASCE, Vol. 107, No ST9, Sept. 1981, pp. 1713-1729.

98. FERGUSSON, P.M.,
Reinforced Concrete Fundamentals,
Third Edidion, John Wiley & Sons, 1981.

99. NILSON, A.H.,
Internal Measurement of Bond Slip,
ACI Journal, American Concrete Institute, Proceedings, Vol. 69, July 1972, pp. 439-441.

100. OTANI, S., SOZEN, M.A.,
Behaviour of Multistorey R/C Frames During Earthquakes,
Civ. Eng. Studies, Str. Research Series, No 392, Univ. of Illinois, Urbana, July 1974.

101. ABRAMS, D.P., SOZEN, M.A.,
Measured Hysteresis Relationships For Small Scale Beams,
Civ. Eng. Studies, Str. Research Series, No 432, Univ. of Illinois, Urbana, Nov. 1976.

102. NEWMARK, N.M.,
A Method of Computation For Structural Dynamics,
Journal of the Eng. Mech. Division, ASCE, Vol. 85, No EM3, March 1959, pp. 67-94.

103. WILSON, E.L.,
A Computer Program For the Dynamic Stress Analysis of Underground Structures, SESM, Report 68-1, Dept. of Civ. Eng., Univ. of California, Betkeley, 1968.

104. WILSON, E.L., PENZIEN, J.,
Evaluation of Orthogonal Damping Matrices,
International Journal of Numerical Methods in Eng., Vol. 4, 1972, pp. 11-30.

105. HART, G.C., RAMASWAMI, V.,
Earthquake Design of Buildings and Damping,
Journal of the Structural Division, ASCE, Vol. 101, No ST1, Jan.1975, pp. 11-30.

106. BERGAN, P.G., CLOUGH, R.W.,
Technical Notes, Convergence Criteria For Iterative Processes,
AIAA Journal, Vol. 10, No. 8, Aug. 1972, pp. 1107-1108.

107. PORTER, F.L., POWELL, G.H.,
Static and Dynamic Analysis of Inelastic Frame Structures,
Report No EERC 71-3, Eatrhquake Eng. Meeting, baltimore, April 1971.

108. BELYTSCHKO, T.,
A Survey of Numerical Methods and Computer Programs For Dynamic,
Structural Analysis, Nuclear Eng. & Design, Vol. 1, Apr. 1976, pp. 23-34.

109. ARISTIZABAL-OCHOA, J.D.,
Dynamic Response of Coupled Shear Wall Systems,
Journal of the Structural Division, ASCE, Vol. 108, No ST8,
Aug. 1982, pp. 1846-1857.

110. PAULAY, T., SANTHKUMAR, A.R.,
Ductile Behaviour of Coupled Shear Walls,
Journal of the Structural Division, ASCE, Vol. 102, No ST1,
Jan. 1976, pp. 93-108.

111. HOUSNER, G.W.,
Spectrum Intensities of Strong Motion Earthquakes,
Proceedings of 1952 Symposium on Earthquakes and Blast Effect on
Structures, Earthquake Eng. Research Inst., 1952.

APPENDIX A

DESIGN EXAMPLE

The following example is intented to illustrate the use of the Inelastric Spectrum Analysis to coupled shear walls as presented in chapter four (4).

Consider the following data:

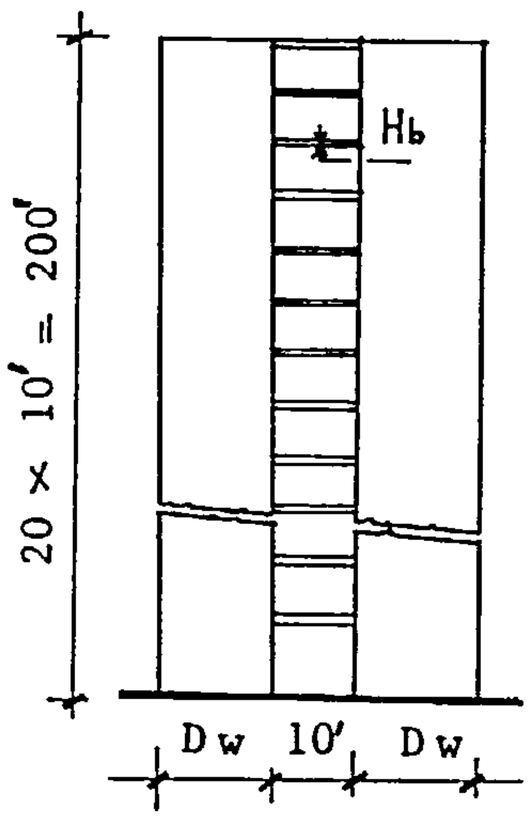

The wall depth Dw or the beam depth Hb are to be determined by the designer. The building is in a zone of strong motion earthquakes. The extra storey mass M = 4 kips.

$Ec = 464.10^3$ ksf = 3222 ksi

Es = 23810 ksi

$\epsilon y = 0.0021$

fy = 50 ksi

i) Selection of the design ductility:

The design ductility should reflect the importance of the building. If it is a hospital for instance, which should be preserved even after the event of a strong earthquake, the μ_d would be small, say $\mu_d = 1$, while for less 'important' structures the design ductility may be greater. Let us assume a ductility factor $\mu_d = 2$ for our case.

ii) Selection of Maximum Acceptable Drift:

According to the material of the components of the building and the extent of damage judged acceptable, the maximum admissible drift is set, say dmax = .01h. This yields the maximum yield drift as:

$$d_{y,max} = \frac{d_{max}}{\mu_d} = .005h$$

iii) Frequency of the Structure:

For $d_{y,max}$ = .005h, figure (4.14) yields the maximum period ,i.e.,

$$T_{1,max} = 1.0 \text{ sec.}$$

and hence the minimum frequency

$$f_{1,min} = \frac{1}{T_{1,max}} = 1.0 \text{ cps}$$

iv) Dimensioning:

It is very important to note that the minimum frequency $f_{1,min}$ is that of the structure without extra mass m. For $f_{1,min}$ = 1.0 (cps), figure (4.9) yields the following possibilities for Dw_{min} and Hb_{min}:

Dw_{min}	Hb_{min}	
21	0.30'	
18'	0.50'	
15'	1.00'	
12'	1.40'	chosen Dw = 12' & Hb = 2'

v) Beam Strength:

Assuming d = 21 in

z = 5.12 = 60 in

and applying equation (4.21), the hinge spread length lp can be approximated as:

$$lp = 0.5x21 + .05x60 = 13.5 \text{ in}$$

From fig. (4.15), the maximum rotation can be approximated as:

$$\theta_{max} = \frac{d_{max}}{h} = 0.01 \text{ rd}$$

Assuming a rotational ductility factor μ_b = 5, the yield rotation can be computed using equation 4.19, i.e.,

$$\theta_y = \frac{\theta_{max}}{\mu_b} = \qquad 0.002 \text{ rd}$$

and hence the yield curve (eqn. 2.20)

$$\varphi_y = \frac{\theta_y}{lp} = \ 1.48\ 10^{-4}\ in^{-1}$$

From fig. (4.16) the neutral axis depth at yield can be set:

$$k_{ud} = d \ - \frac{\epsilon_y}{\varphi_y} \ = \ 6.83 \text{ in}$$

and so can the strains ϵc and $\epsilon's$

$$\epsilon c = \frac{k_{ud}\, \epsilon_y}{d\text{-}k_{ud}} = 1.01\ 10^{-3}$$

$$\epsilon's = \frac{(k_{ud}\text{-}d')\, \epsilon_y}{d\text{-}k_{ud}} = 1.01\ 10^{-3}$$

and hence the max stresses

$$fc = Ec\ \epsilon c = 3.25 \text{ ksi}$$

$$fs' = Es\ \epsilon's = 13.50 \text{ ksi}$$

Assuming a rectangular stress shape and As = A's, the equilibrium equation 2.22 yields:

$$As\ fy = 0.4fc\ k_{ud}\ b + f's\ A's$$

and hence

$$As = A's = 2.29 \text{ in}^2$$

and

$$\underline{My = 2430 \text{ k-in}}$$

APPENDIX B

DIAGRAMS FOR 2nd AND 3rd NATURAL FREQUENCIES

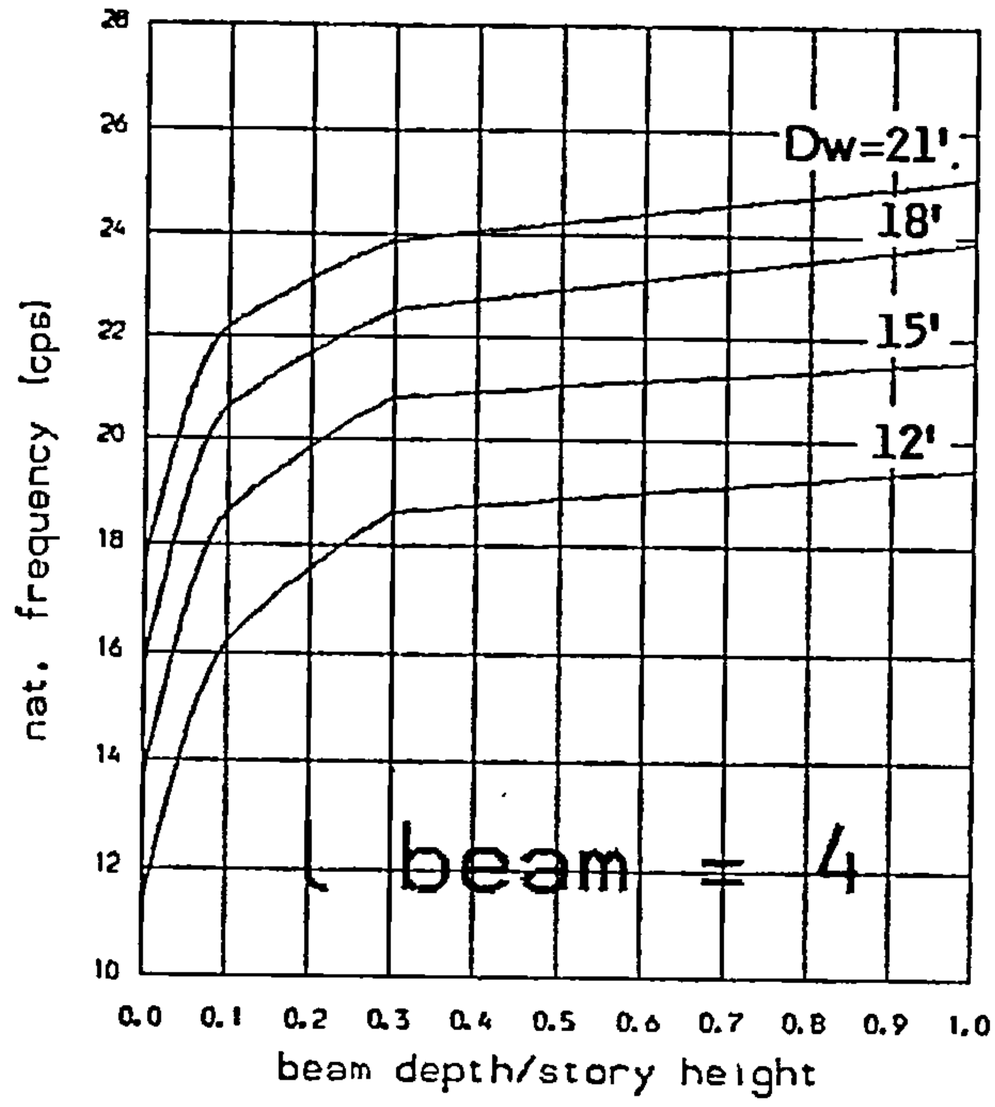

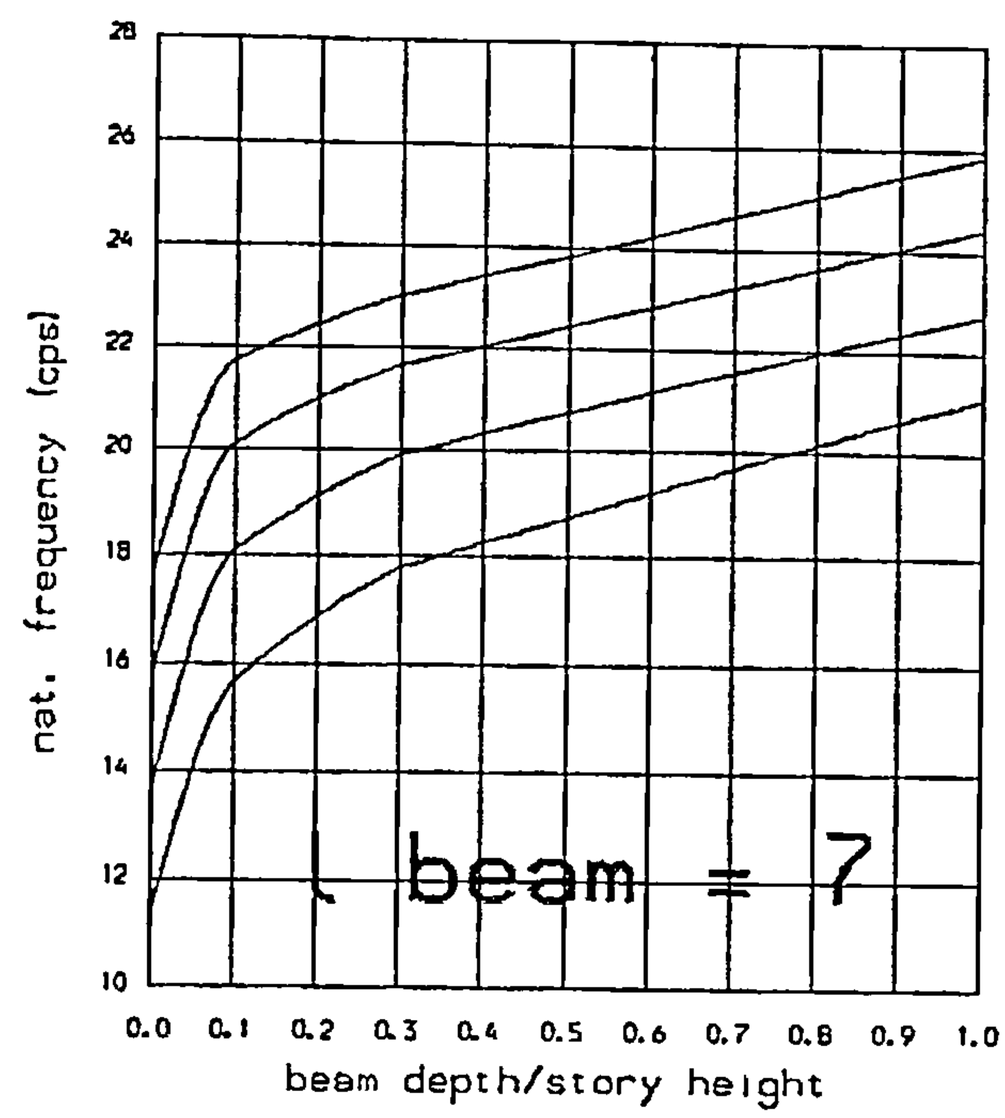

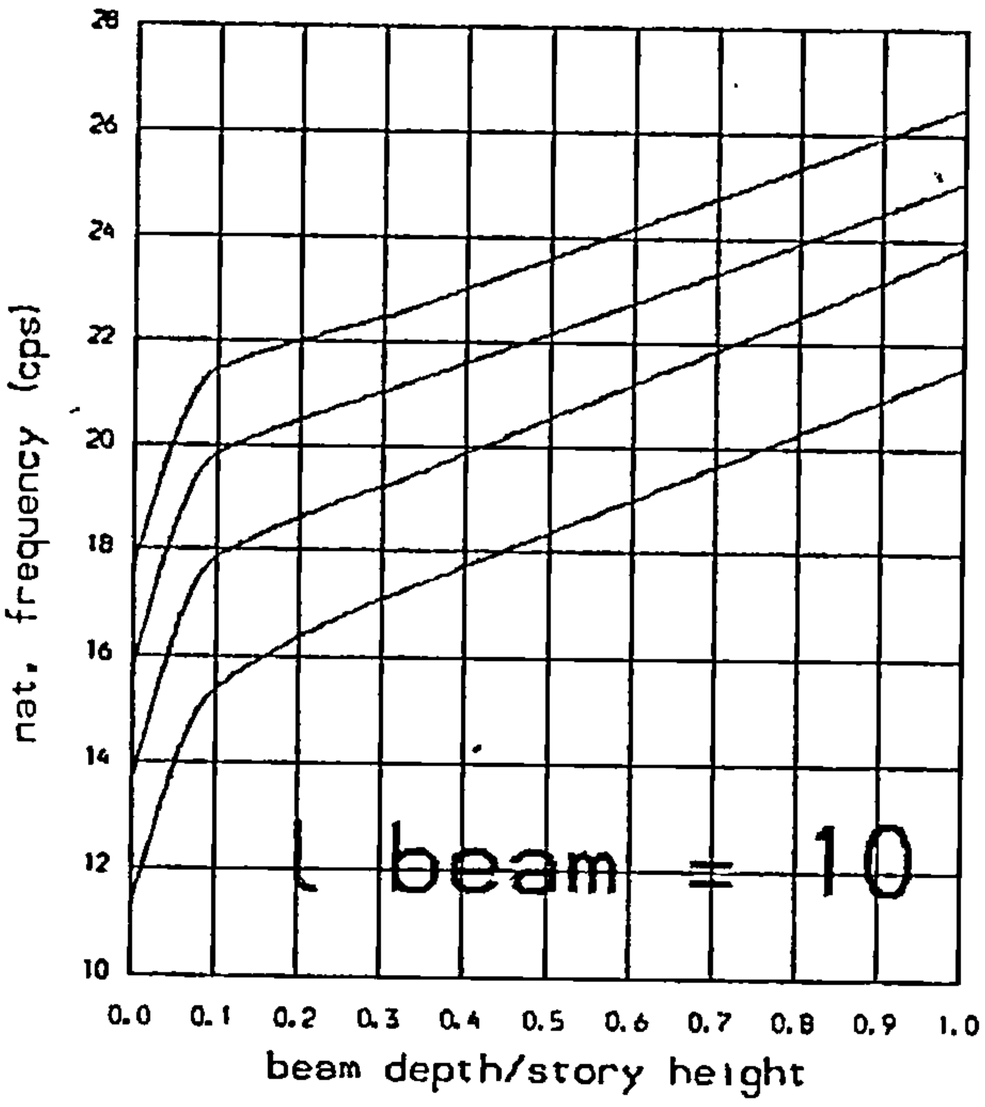

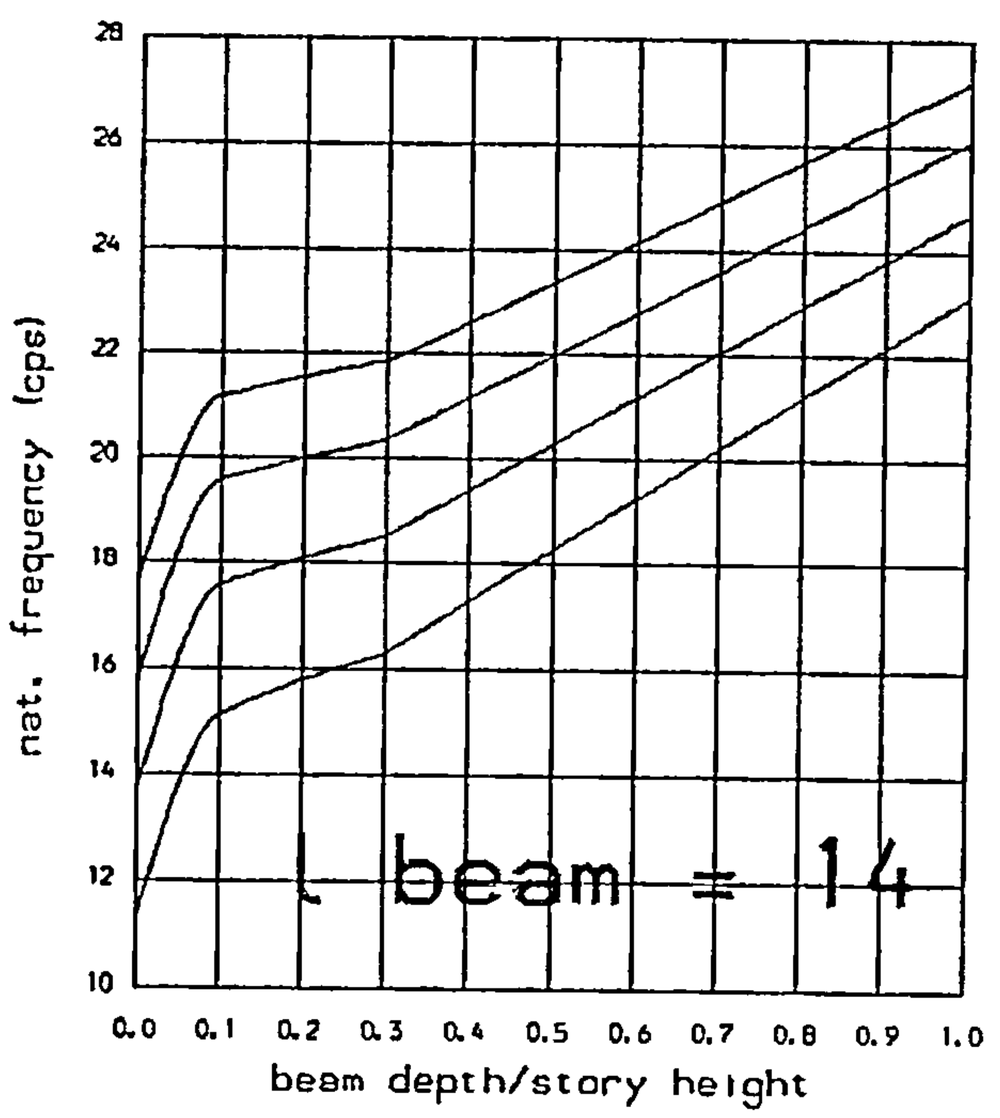

FIG. B.1

Variation of 2 nd. natural freqency with beam depth and wall width (DV) .

Total height : 100 ft
Nb of storeys : 10
Selfweight : yes
Extra story mass : none

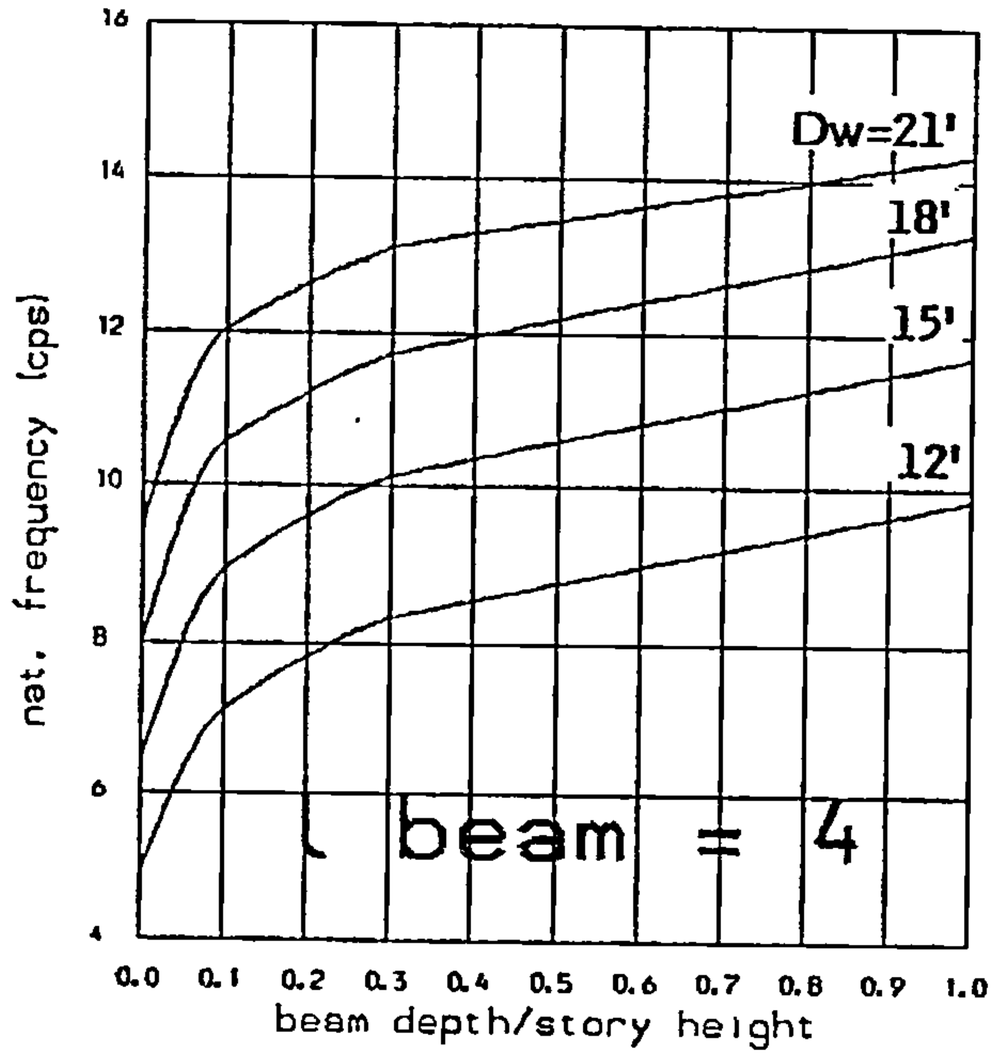

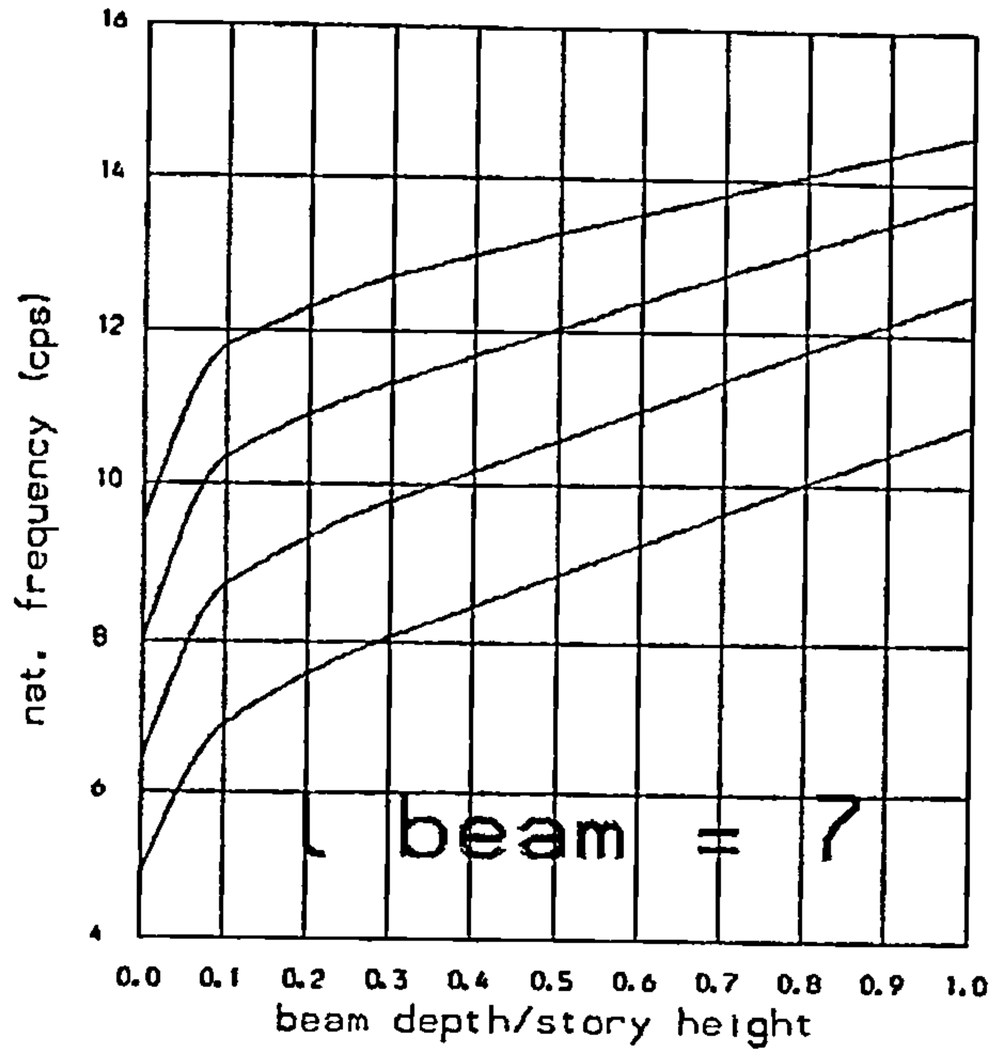

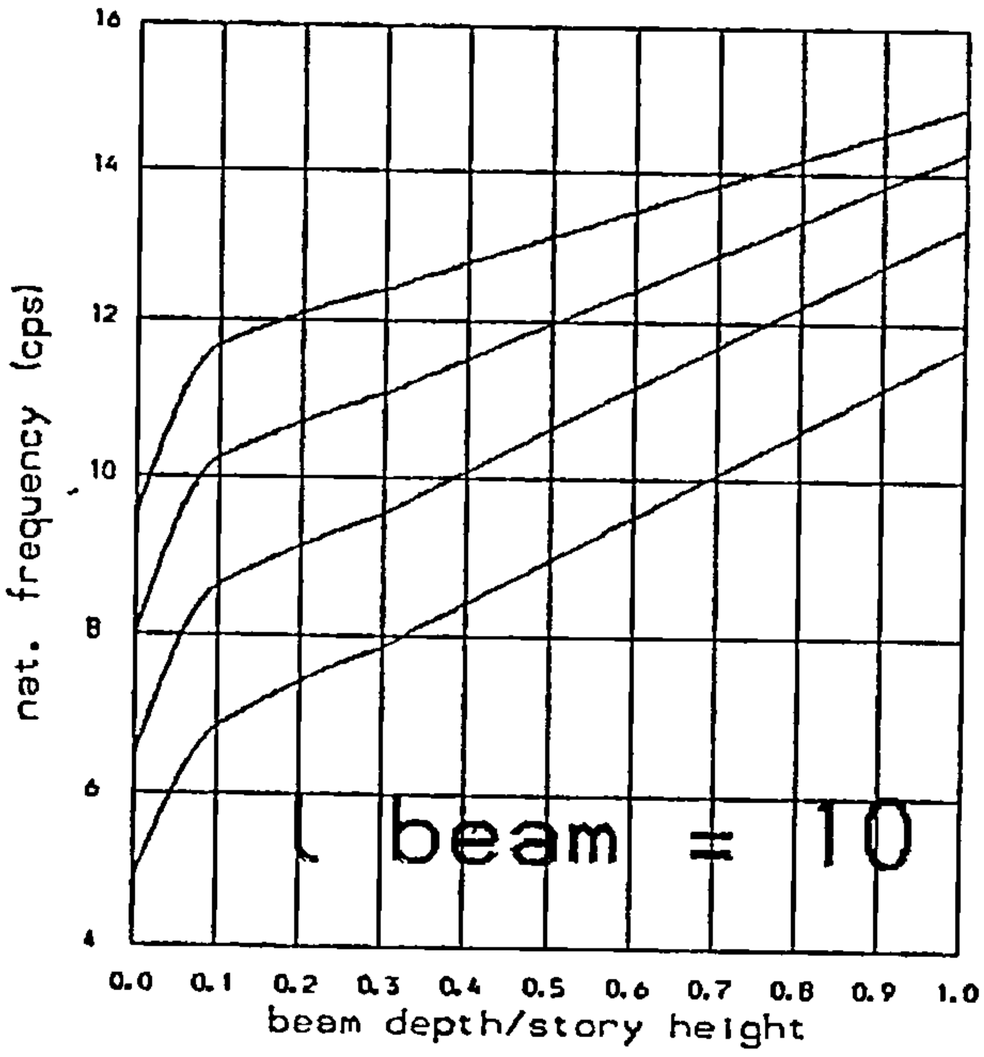

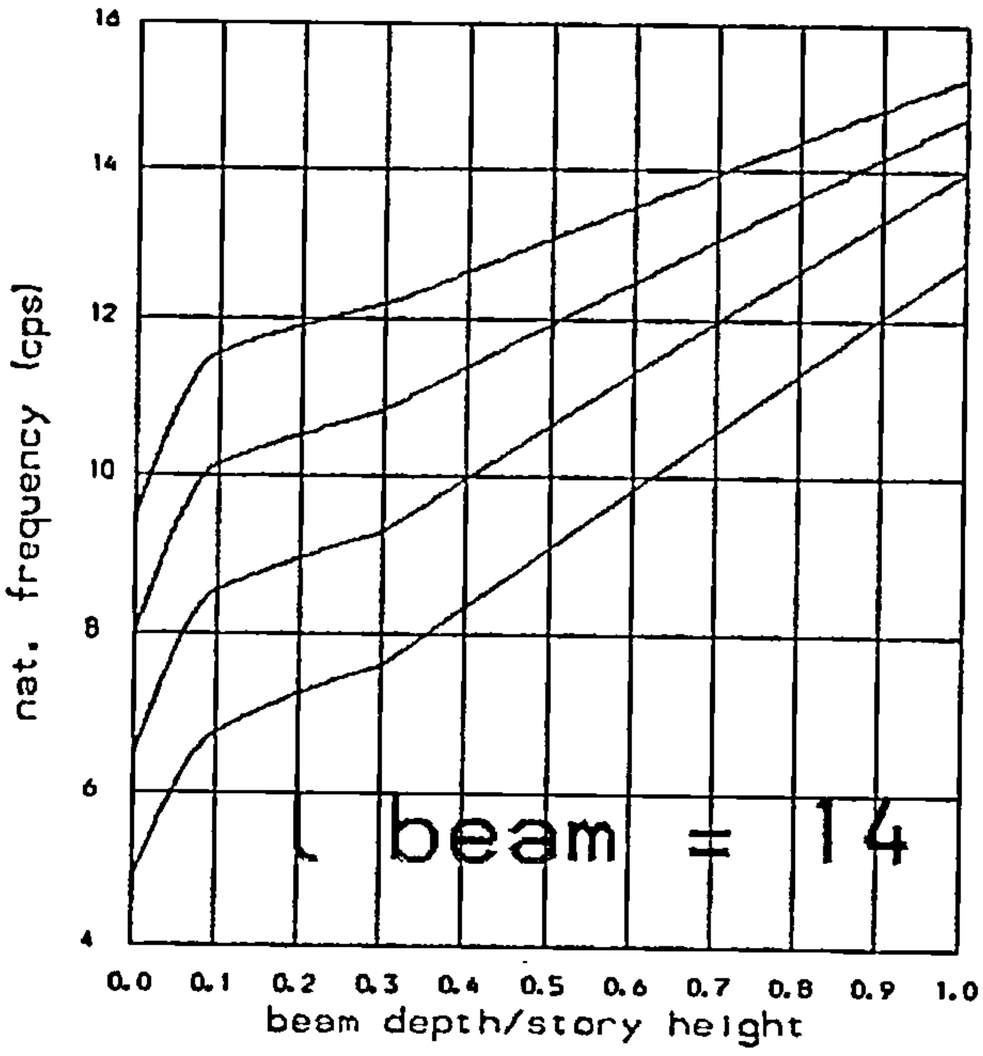

FIG. B.2

Variation of 2 nd. natural freqency with beam depth and wall width (DW) .

Total height : 100 ft
Nb of storeys : 10
Selfweight : yes
Extra story mass : 4.kips

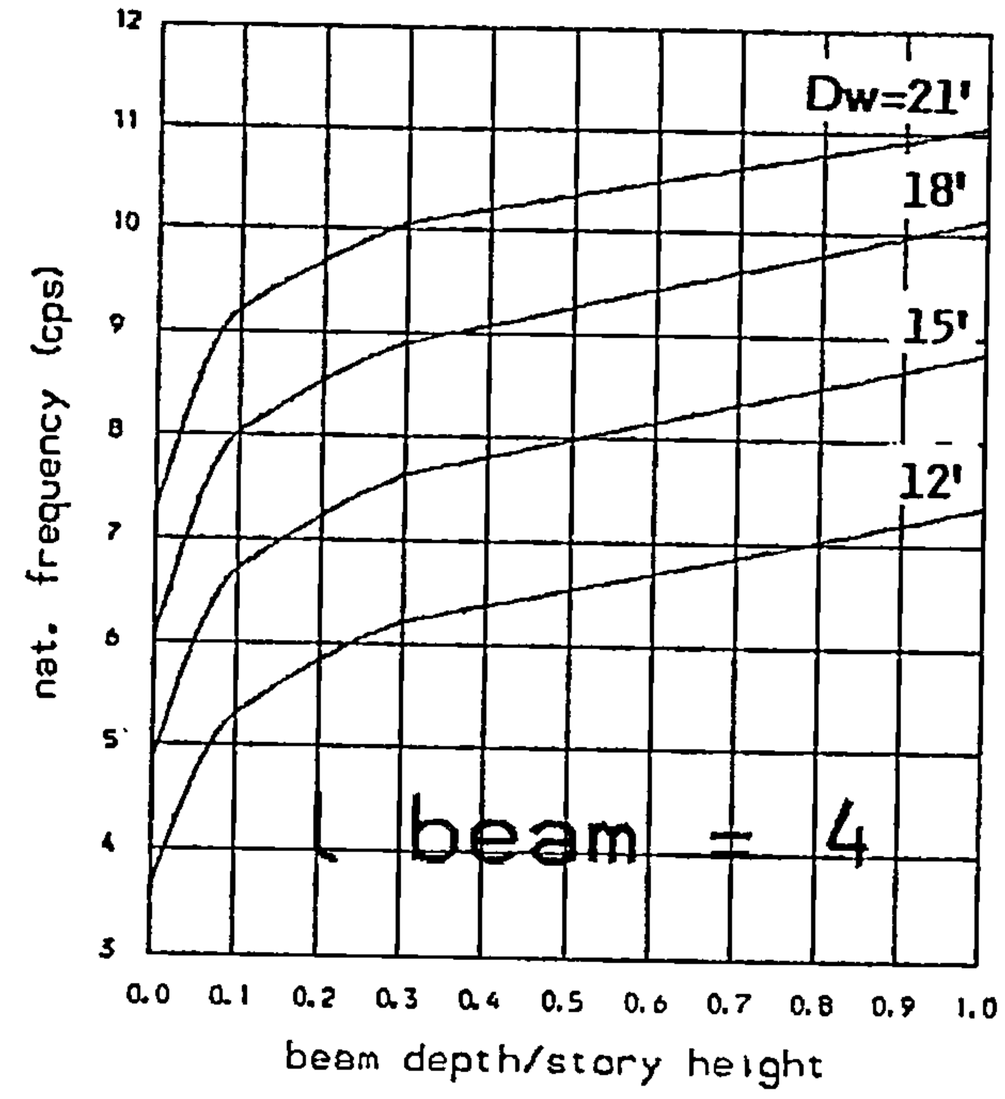

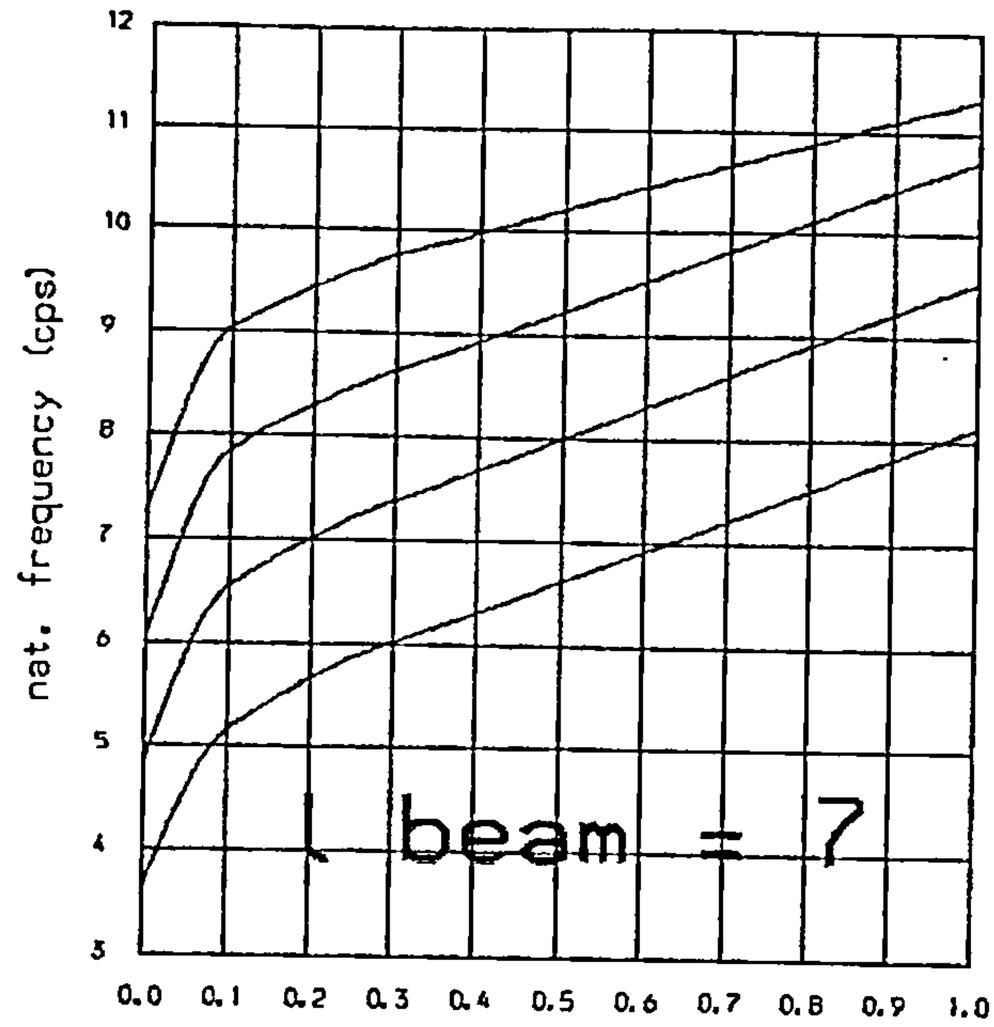

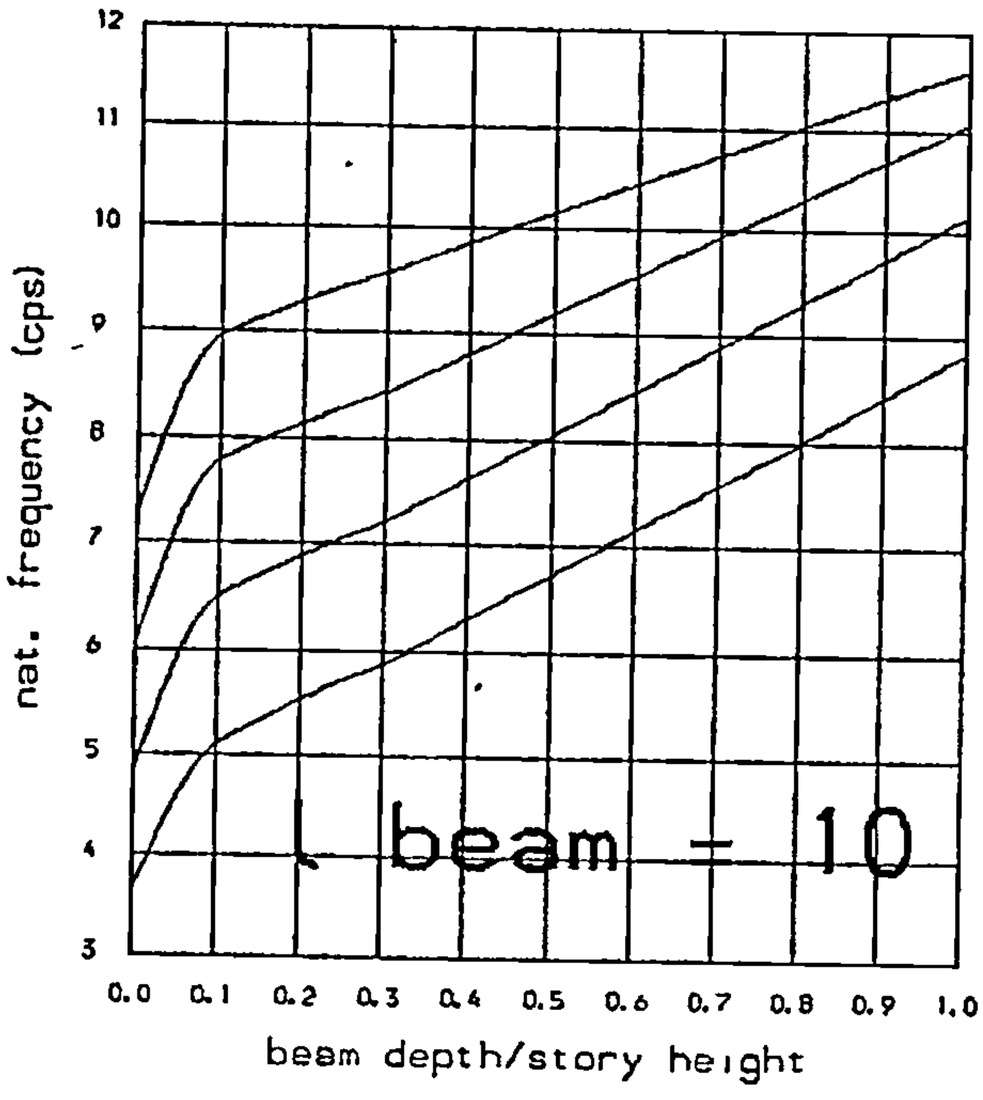

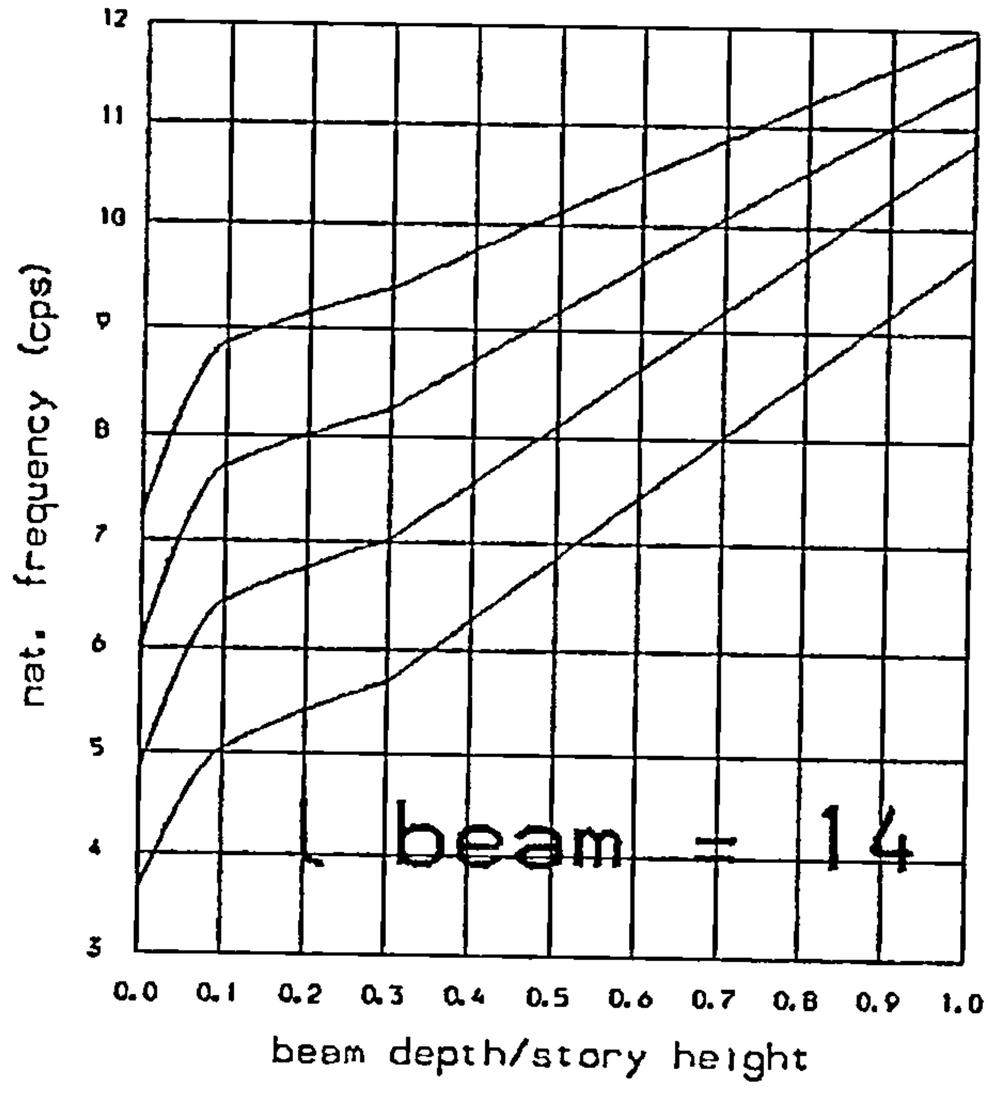

FIG. B.3
Variation of 2 nd. natural freqency with beam depth and wall width (DV).

Total height : 100 ft
Nb of storeys : 10
Selfweight : yes
Extra story mass : 8.kips

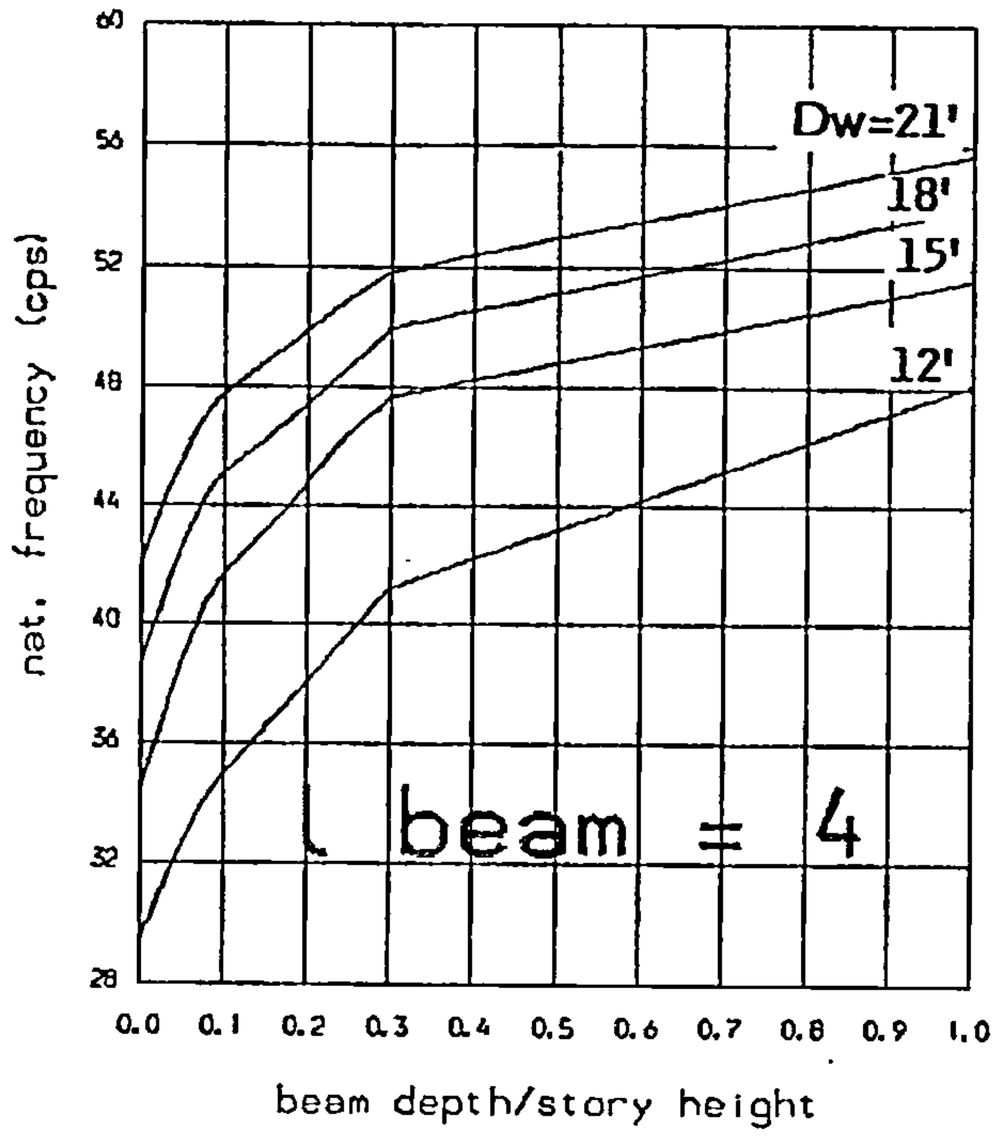

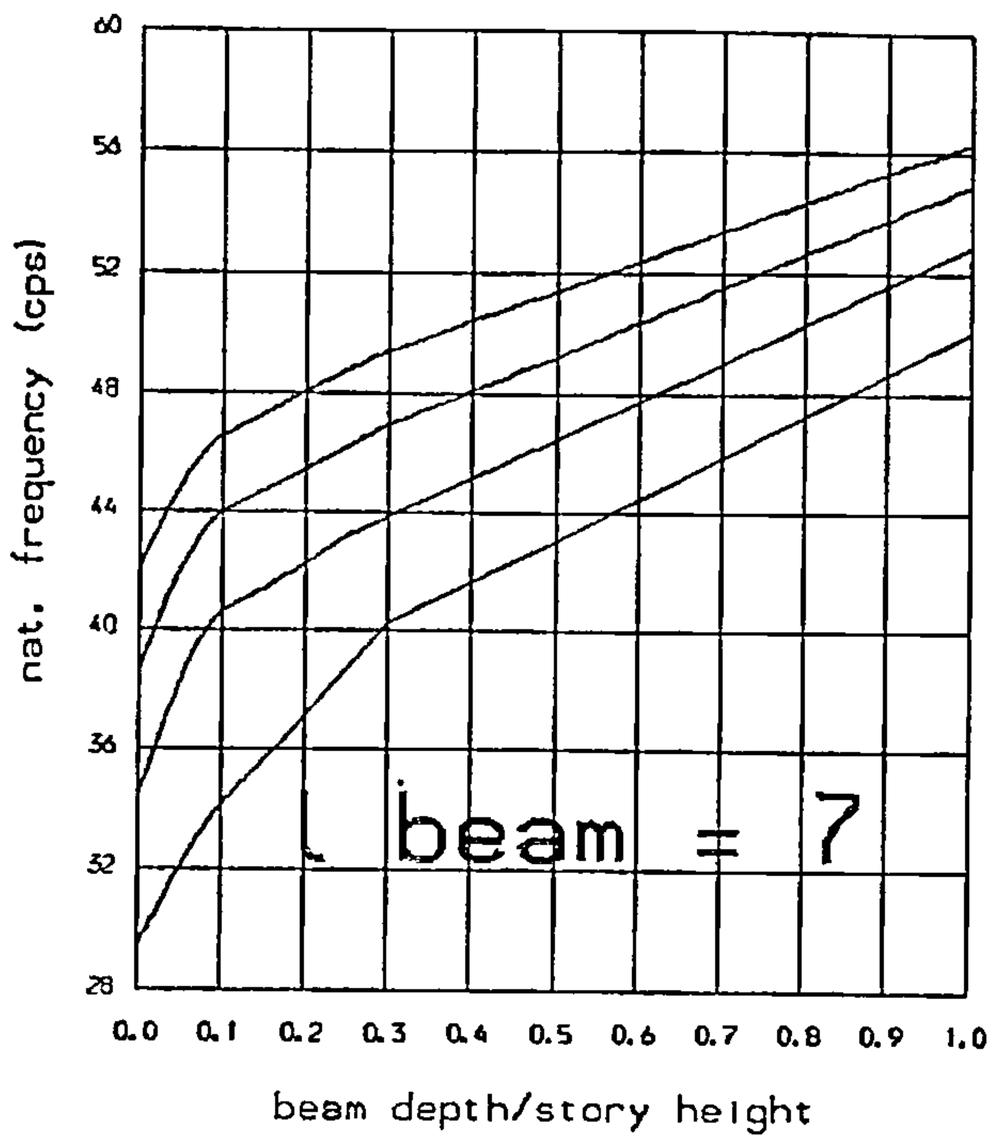

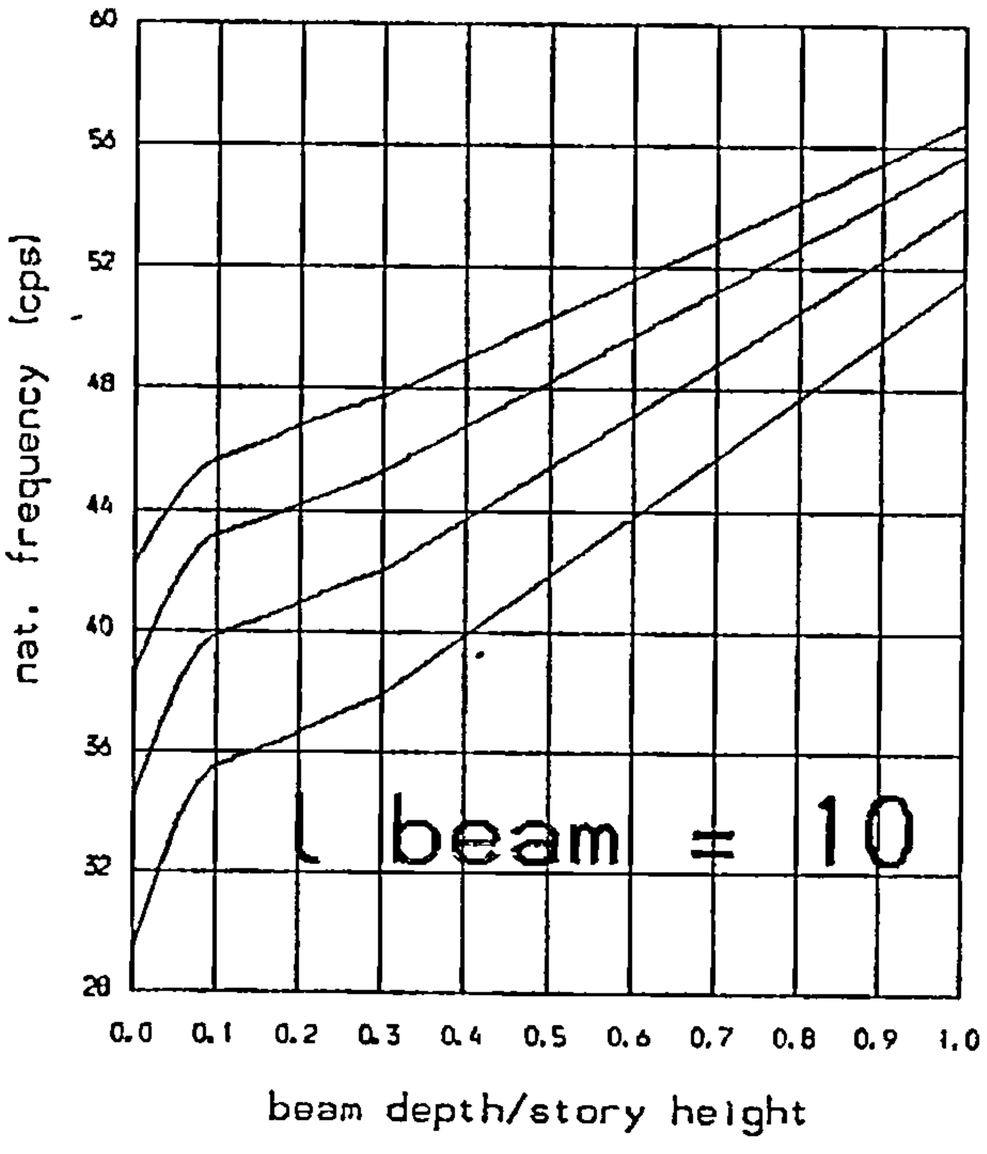

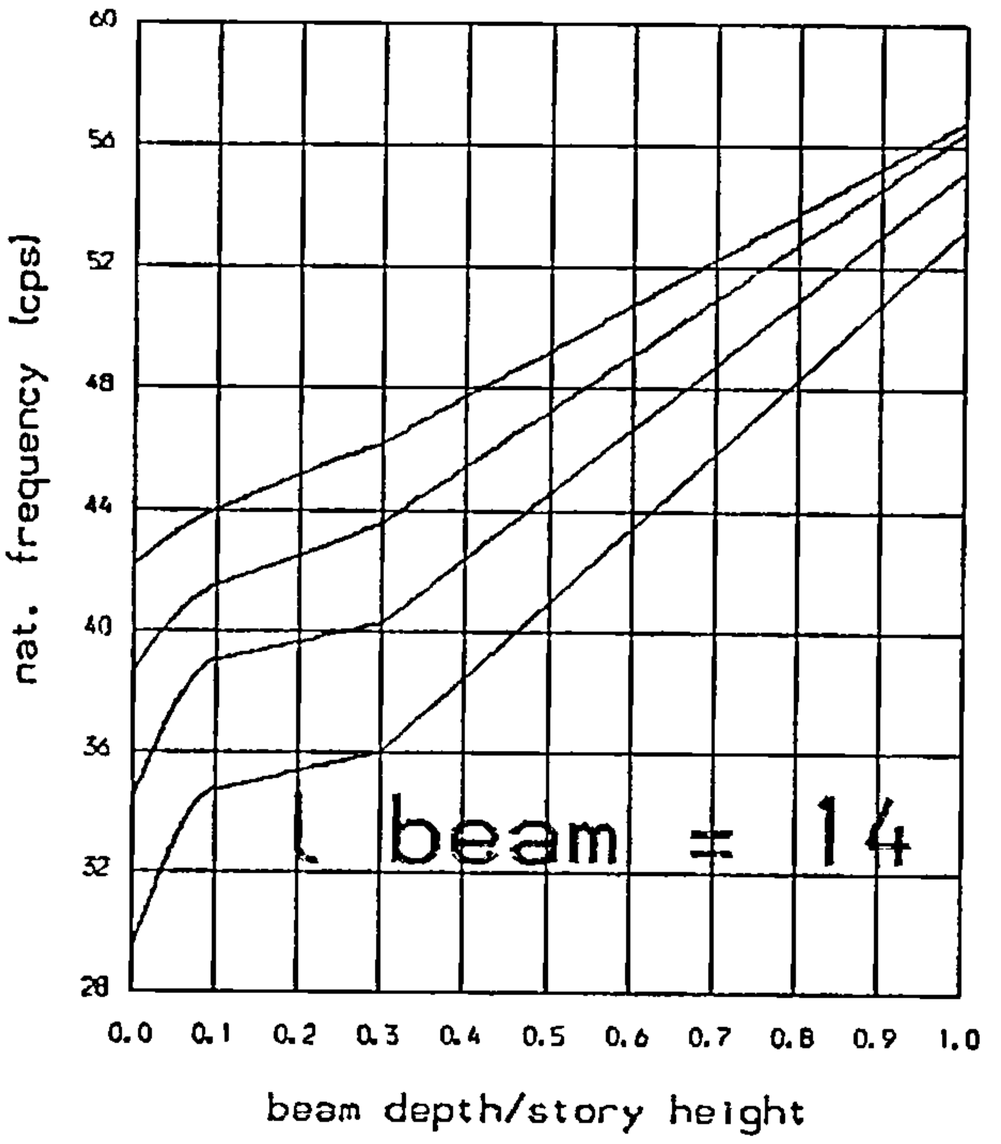

FIG. B.4
Variation of 3 rd. natural freqency with beam depth and wall width (DW) .

Total height	:	100 ft
Nb of storeys	:	10
Selfweight	:	yes
Extra story mass	:	none

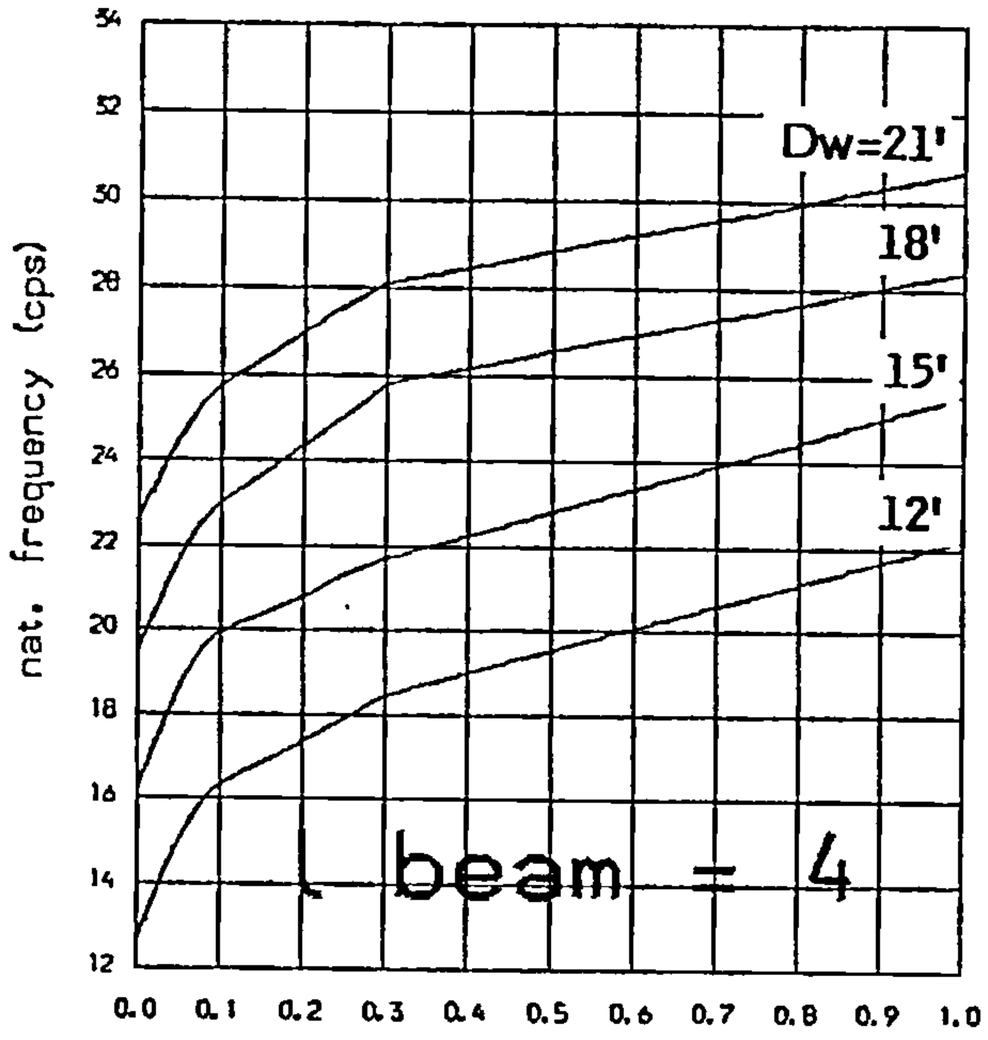

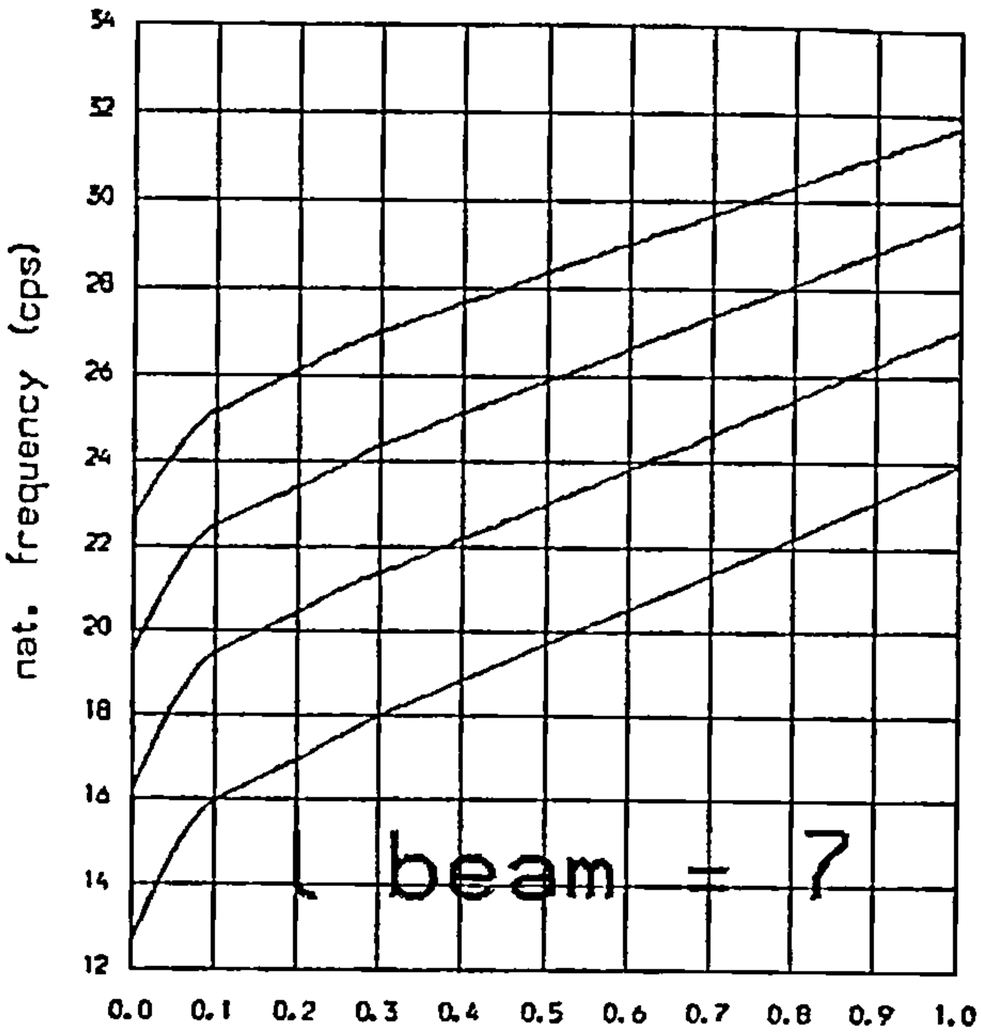

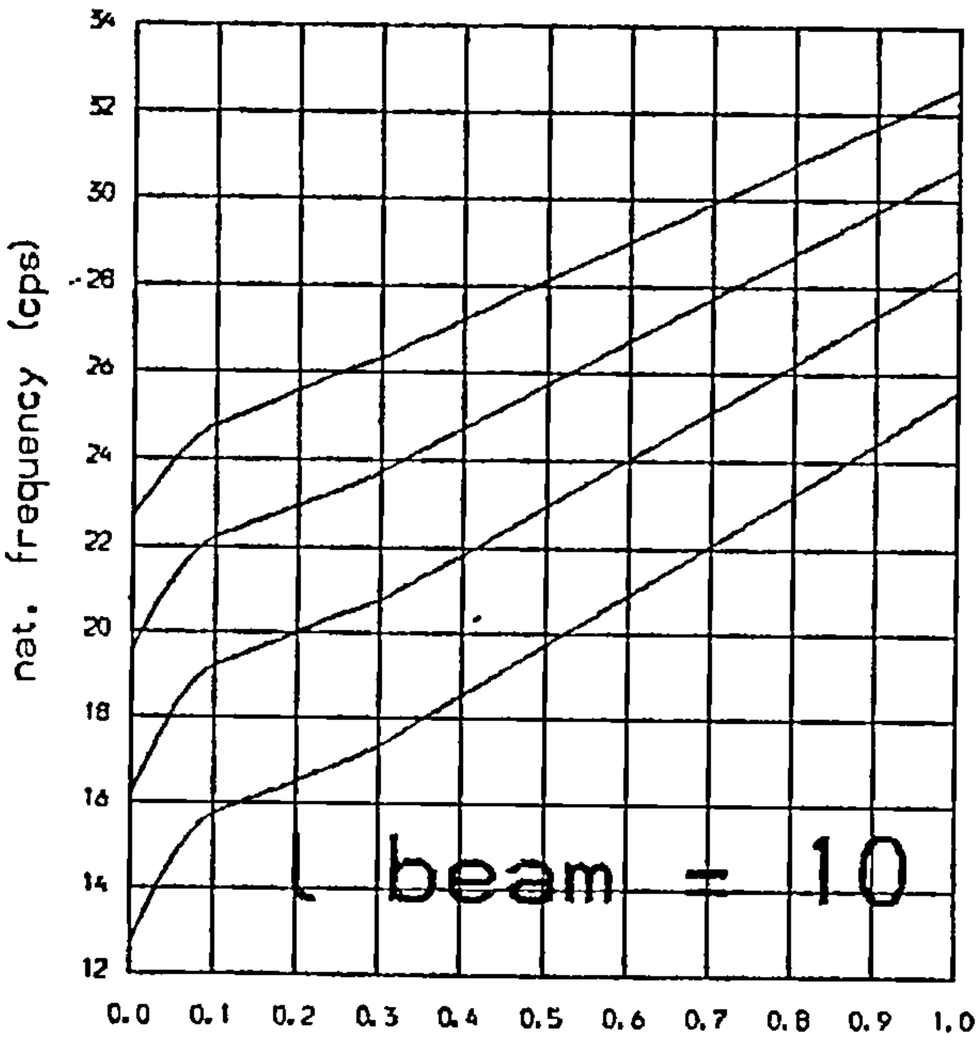

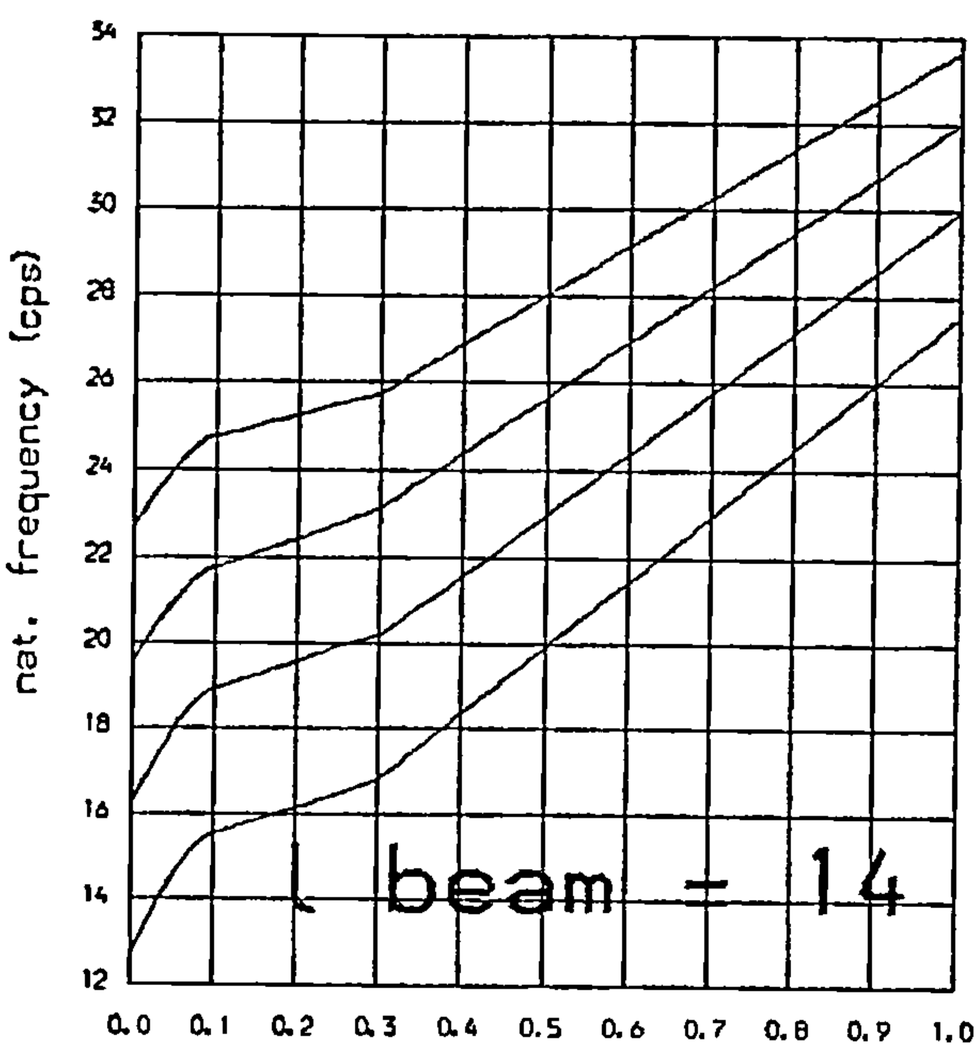

FIG. B.5

Variation of 3 rd. natural freqency with beam depth and wall width (DW).

Total height	:	100 ft
Nb of storeys	:	10
Selfweight	:	yes
Extra story mass	:	4.kips

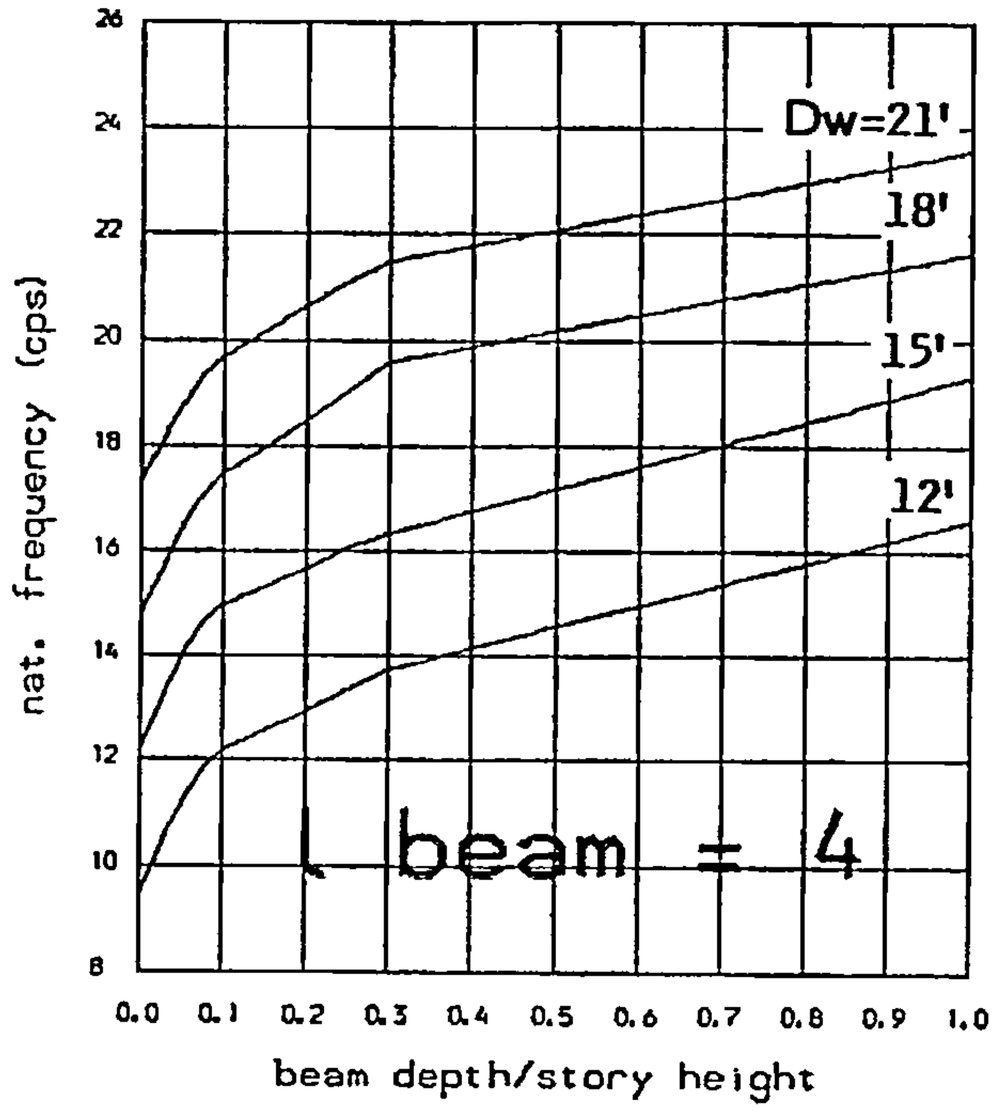

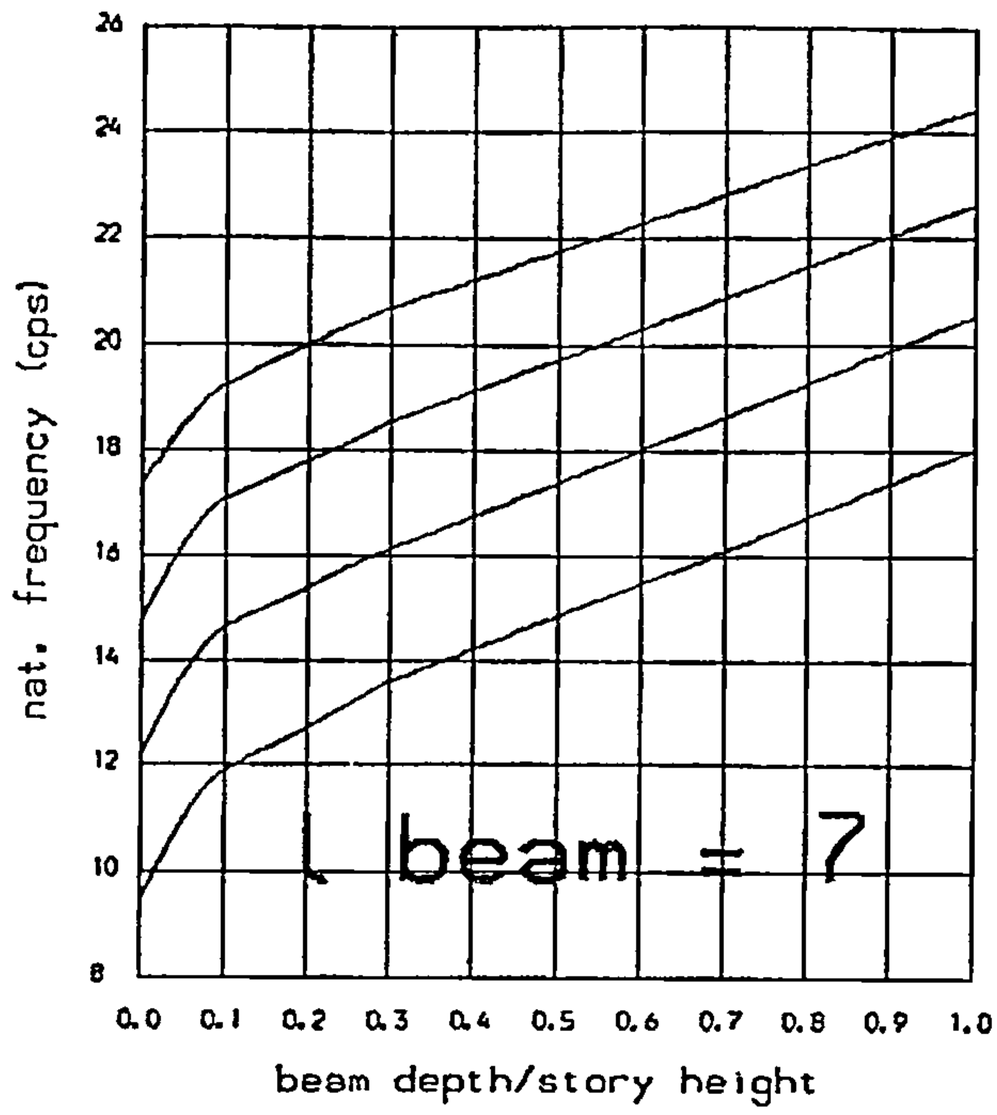

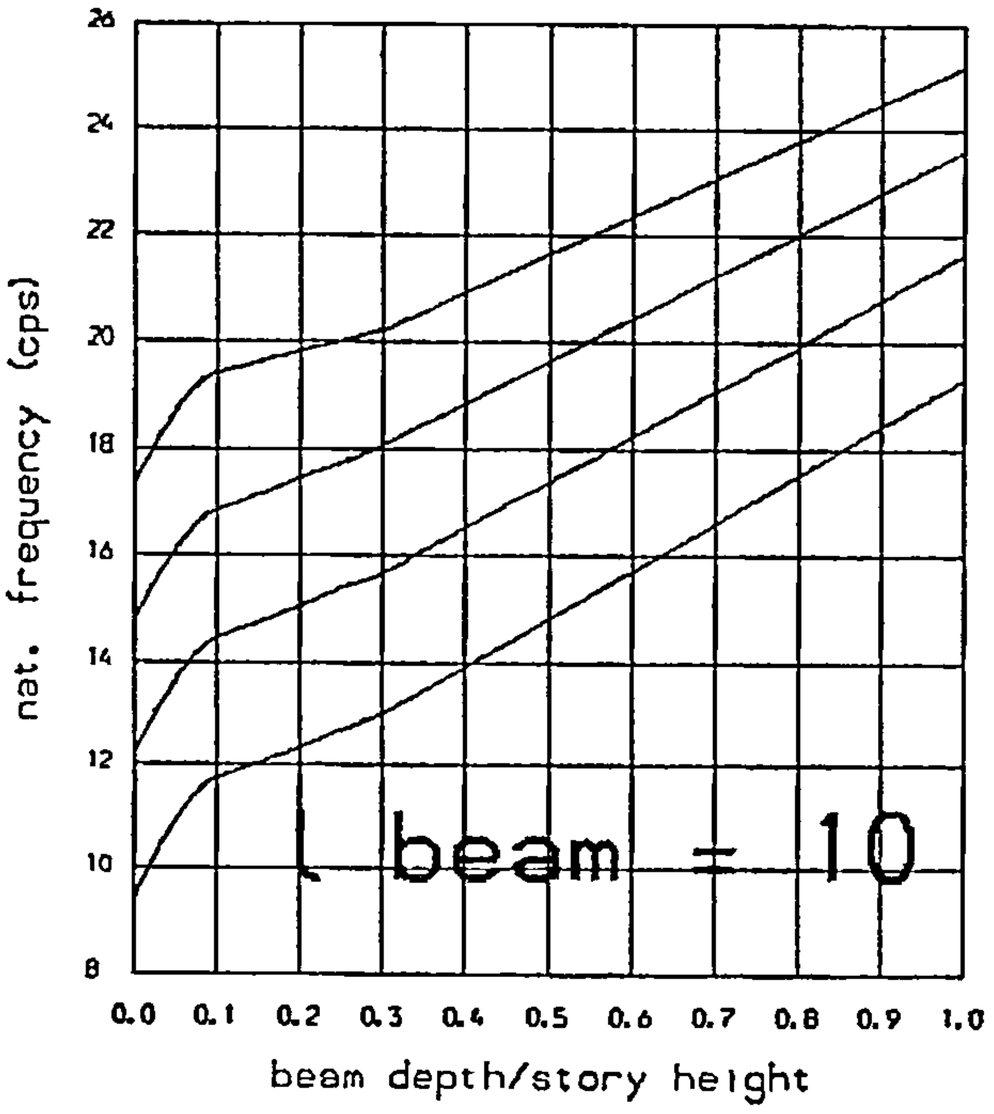

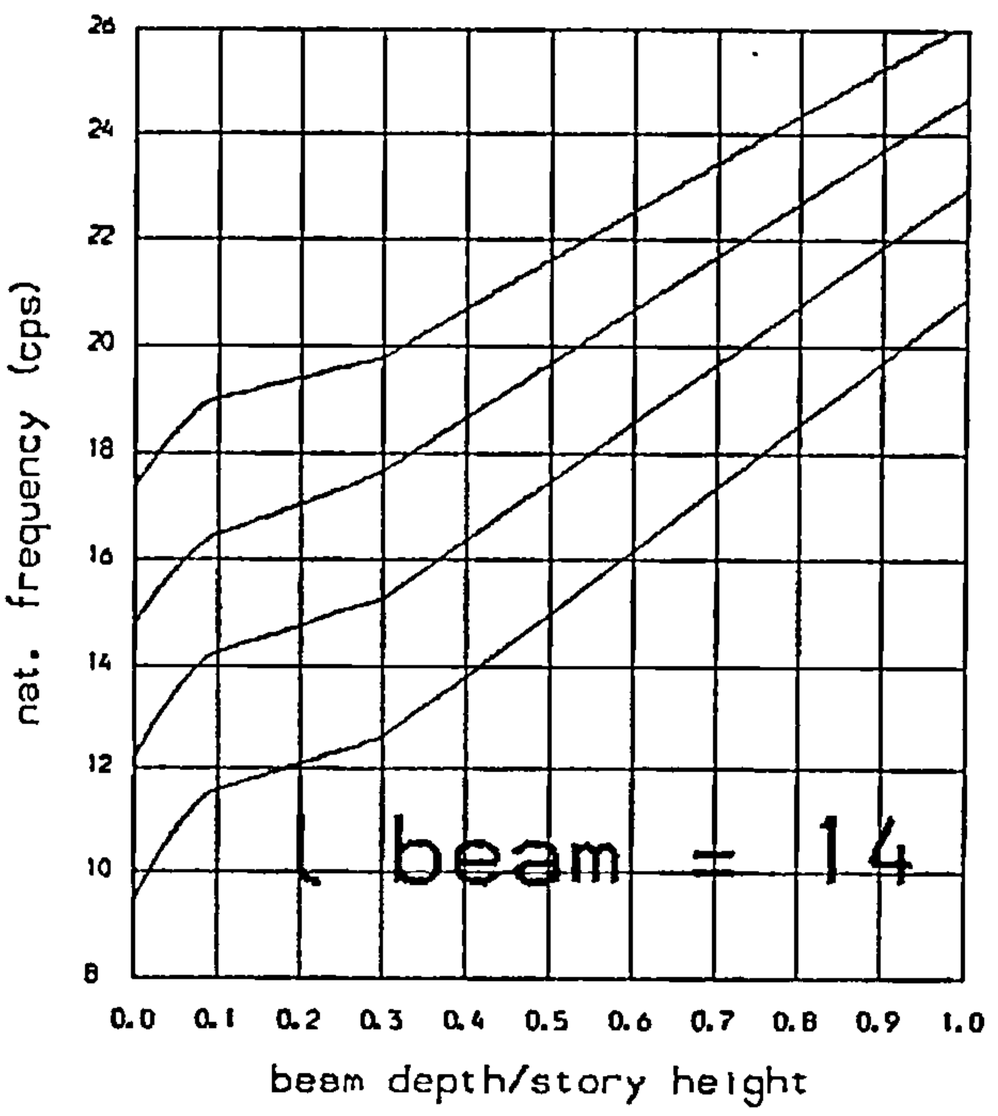

FIG. B.6

Variation of 3 rd. natural freqency with beam depth and wall width (DW) .

Total height	:	100 ft
Nb of storeys	:	10
Selfweight	:	yes
Extra story mass	:	8.kips

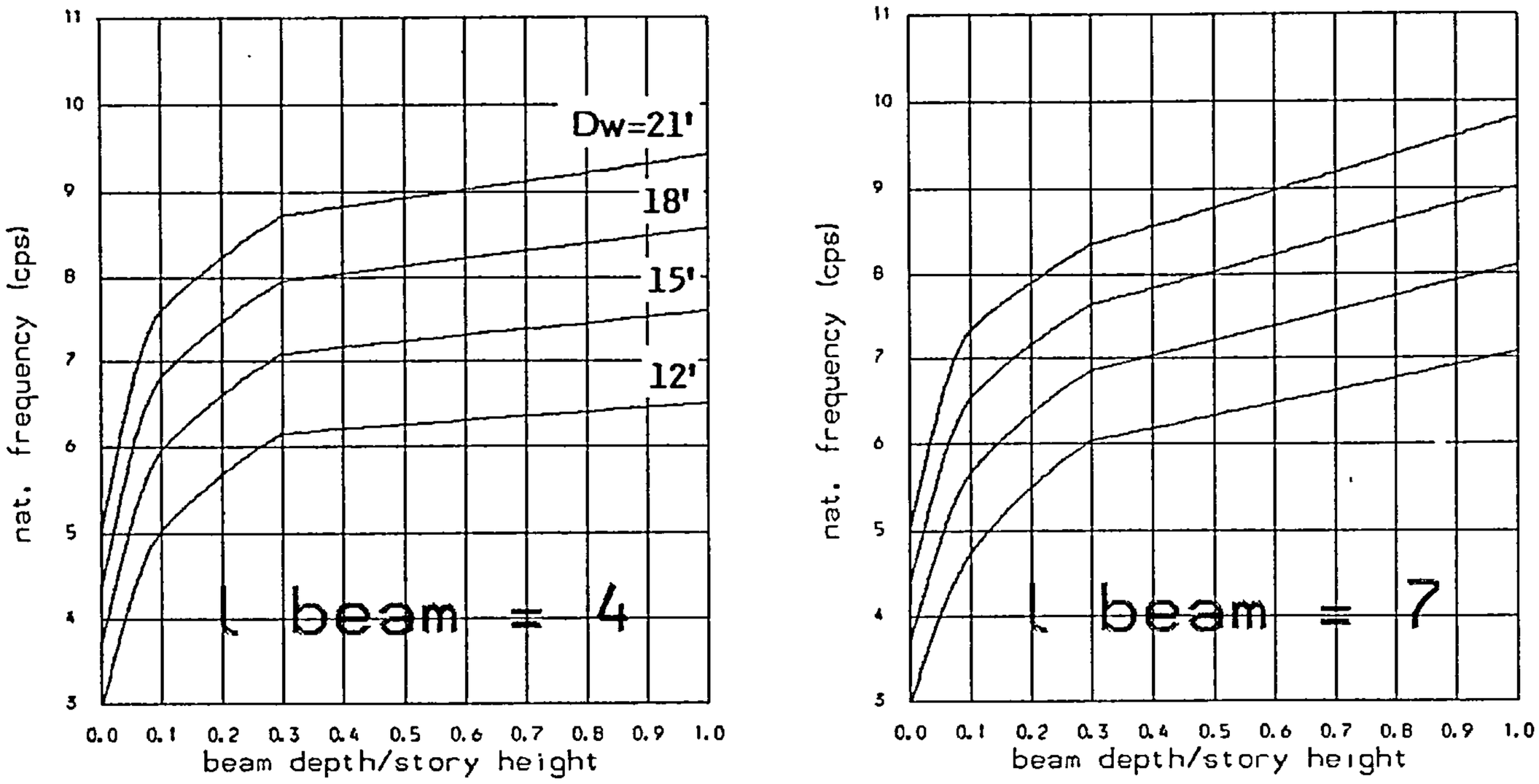

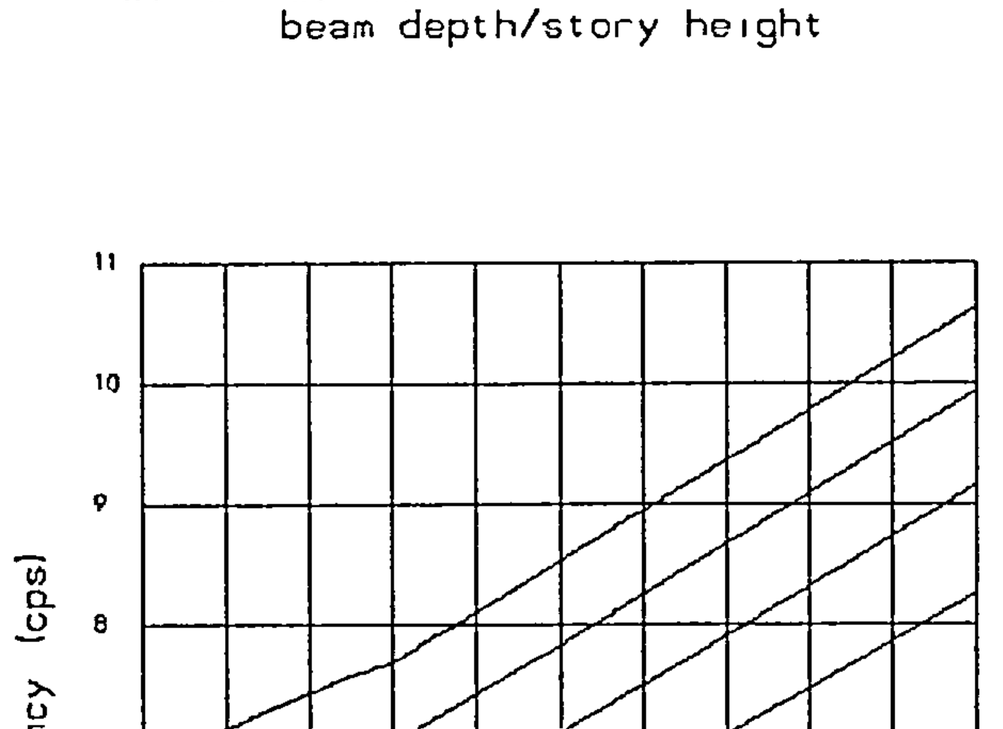

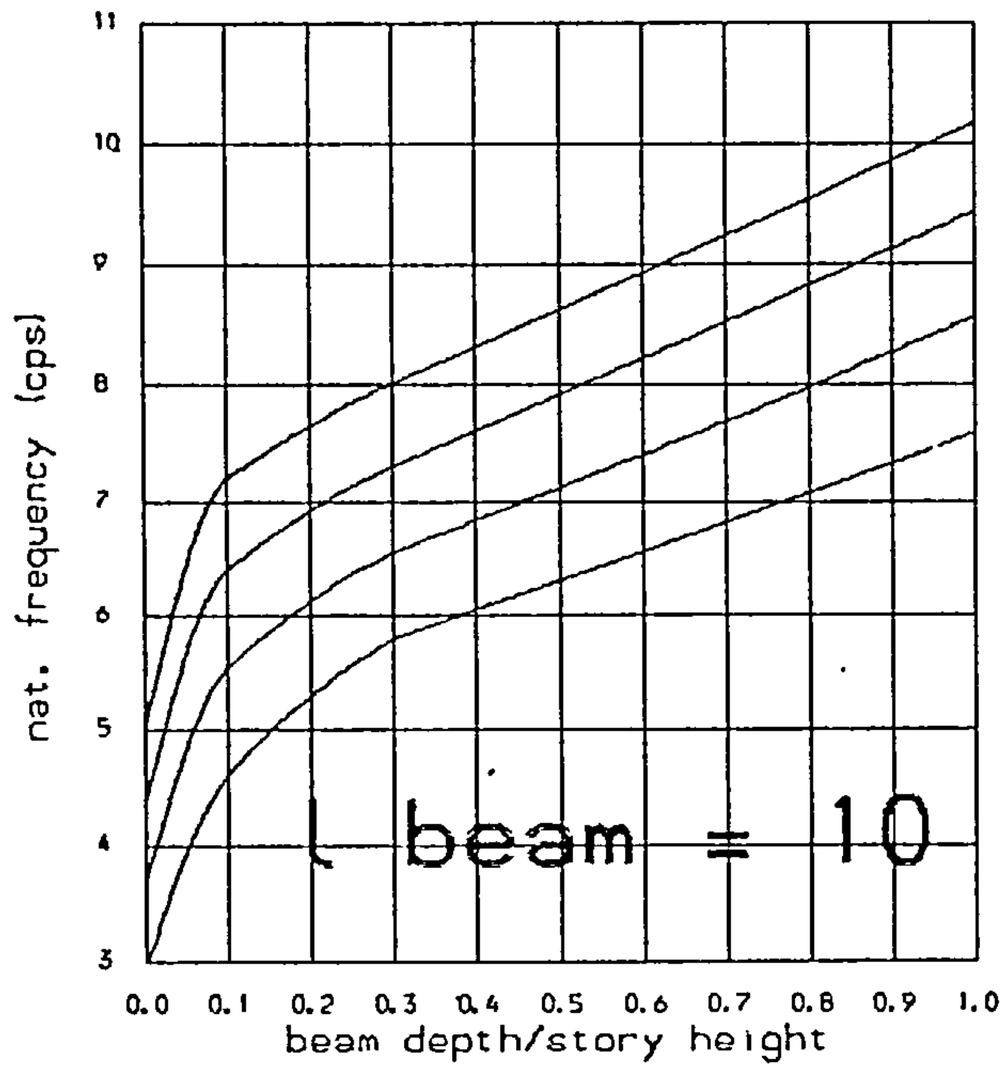

FIG. B.7

Variation of 2 nd. natural freqency with beam depth and wall width (DV).

Total height	:	200 ft
Nb of storeys	:	20
Selfweight	:	yes
Extra story mass	:	none

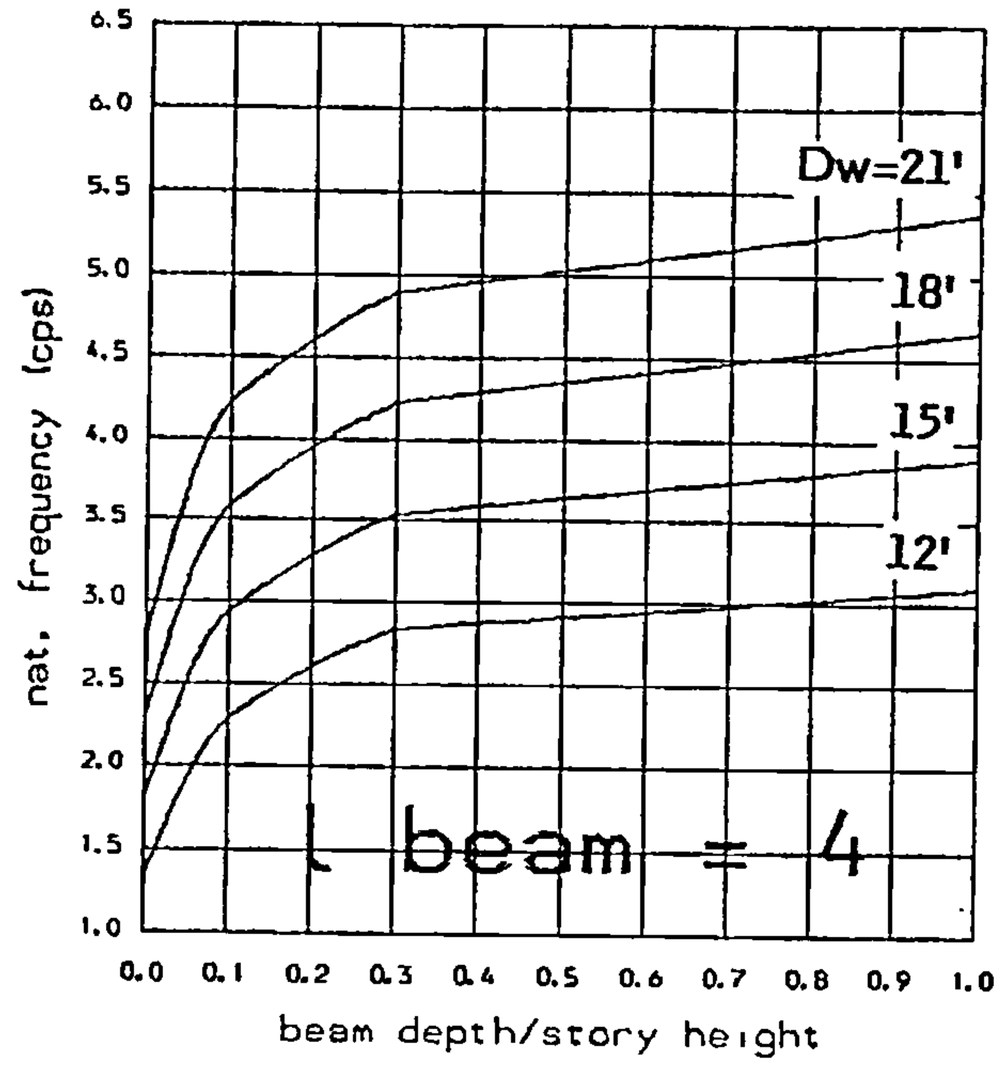

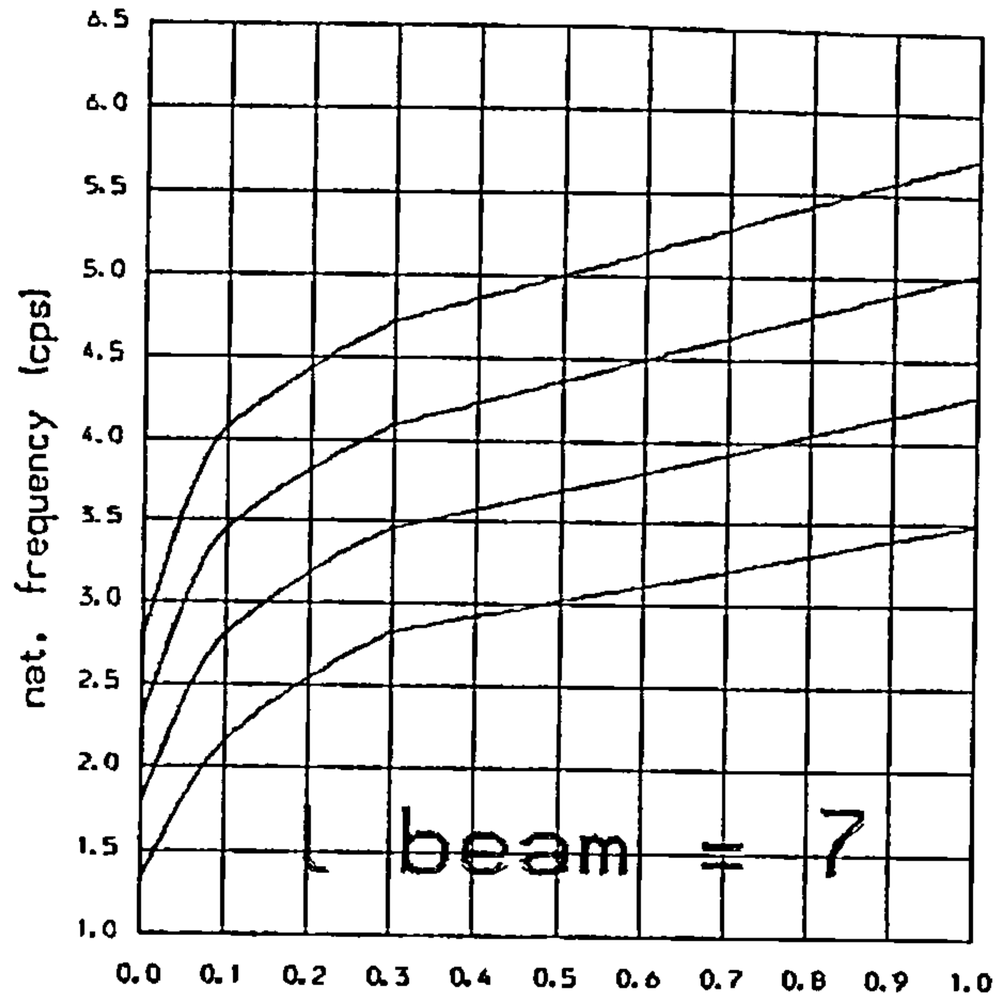

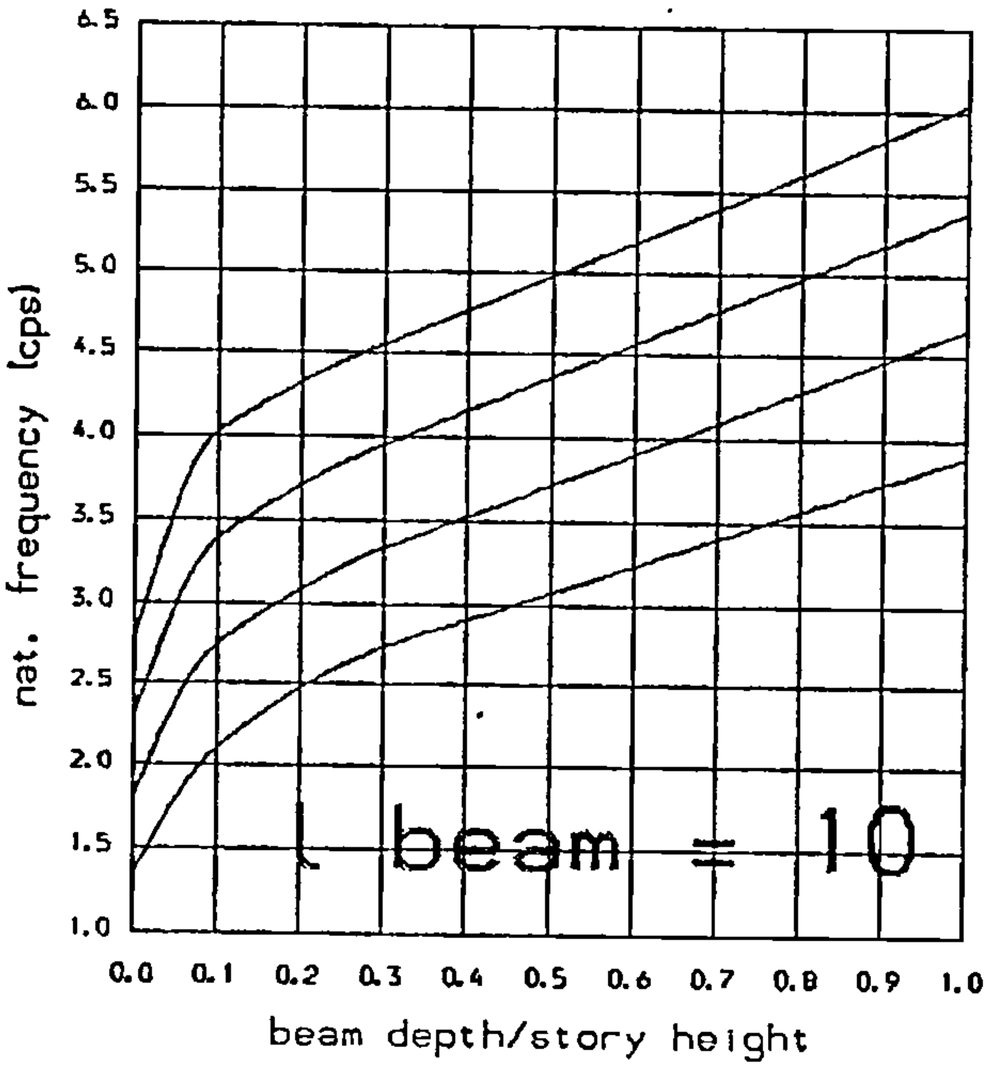

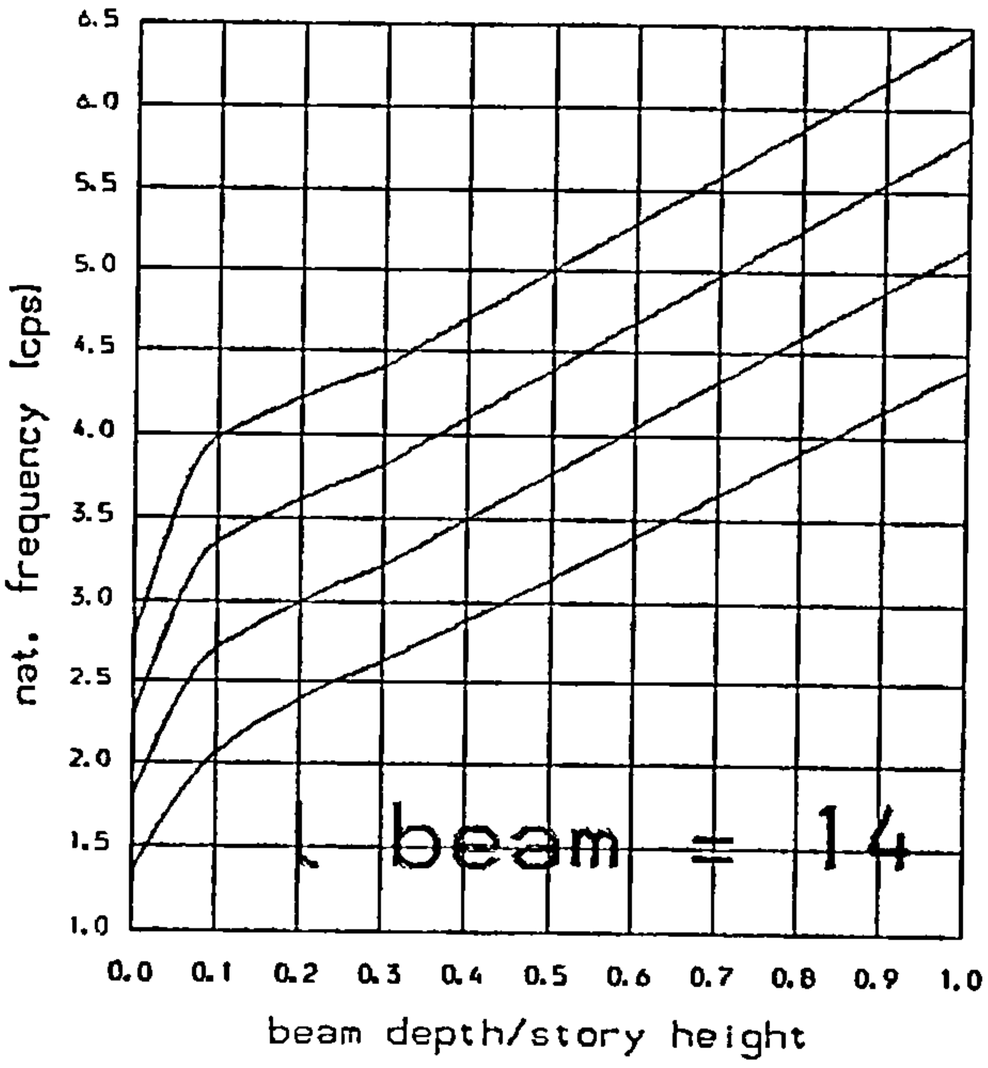

FIG. B.8

Variation of 2 nd. natural freqency with beam depth and wall width (DV) .

Total height	:	200 ft
Nb of storeys	:	20
Selfweight	:	yes
Extra story mass	:	4.kips

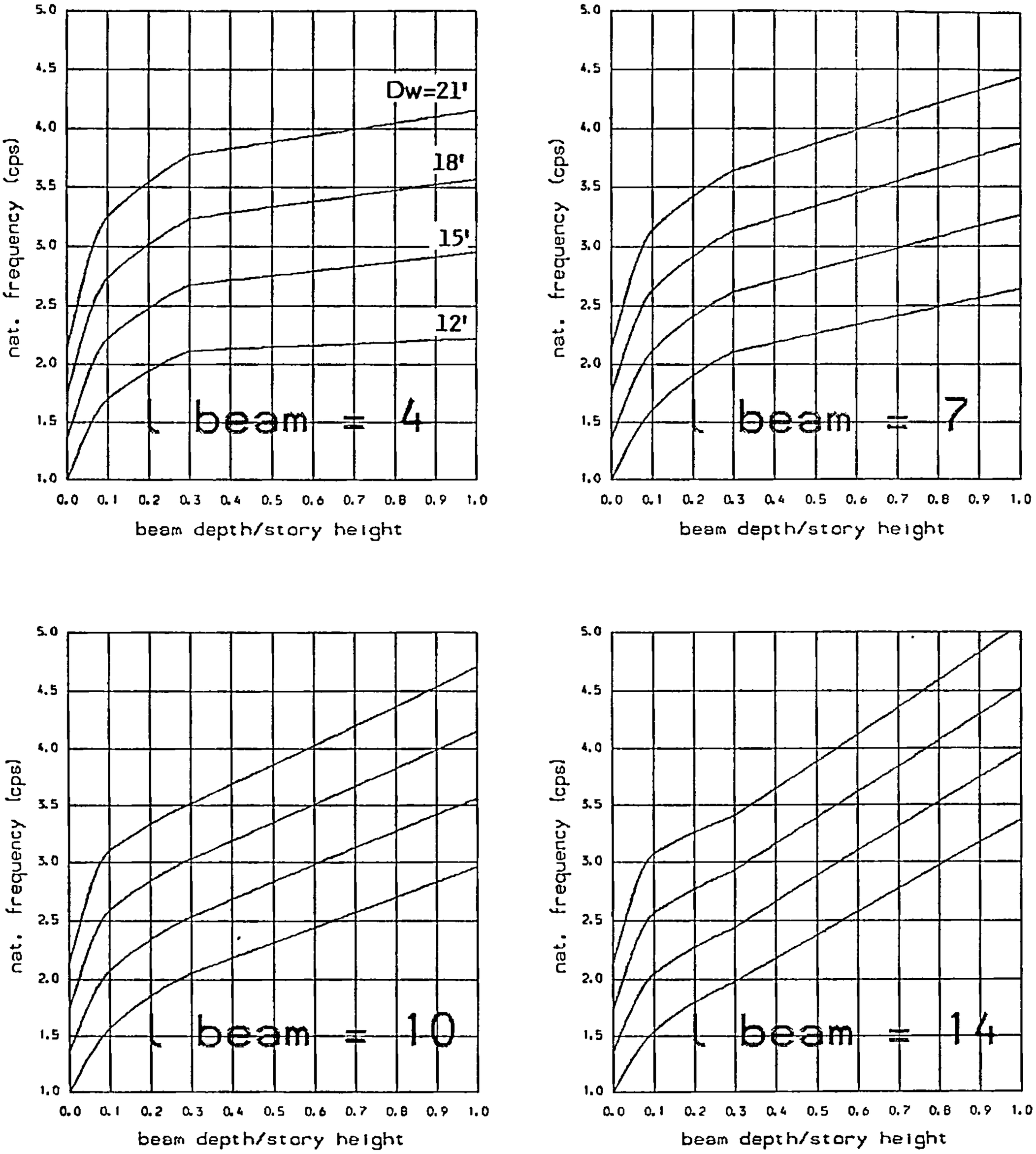

FIG. B.9

Variation of 2 nd. natural freqency with beam depth and wall width (DV) .

Total height	:	200 ft
Nb of storeys	:	20
Selfweight	:	yes
Extra story mass	:	8.kips

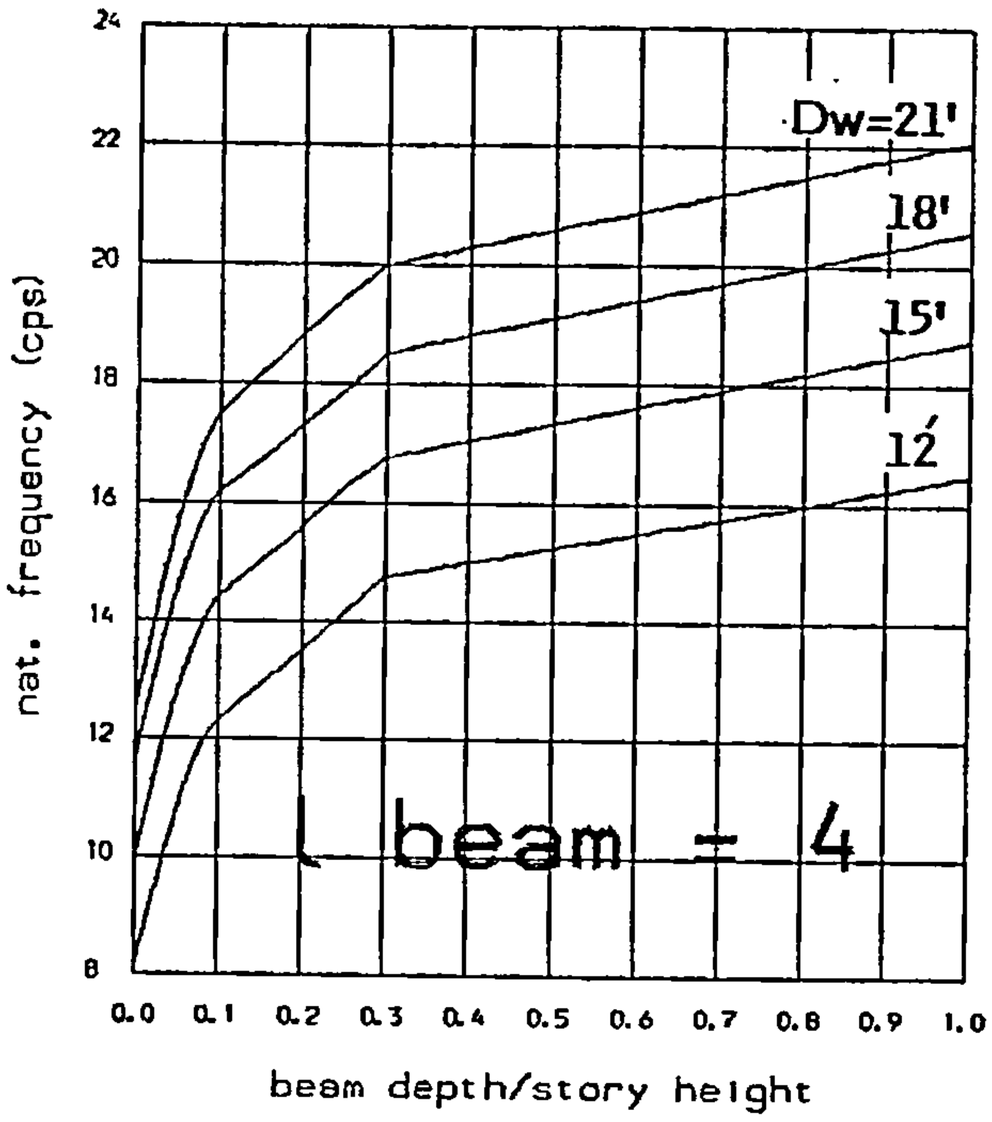

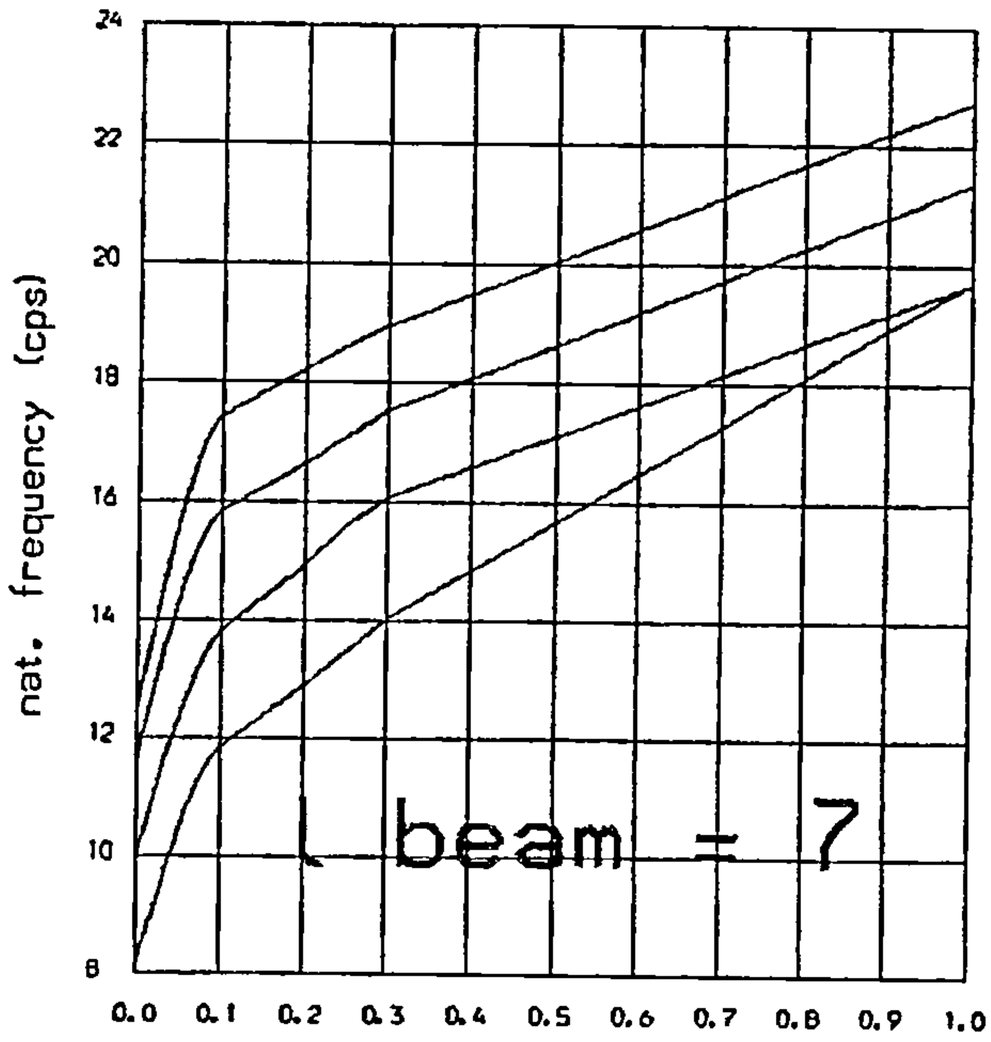

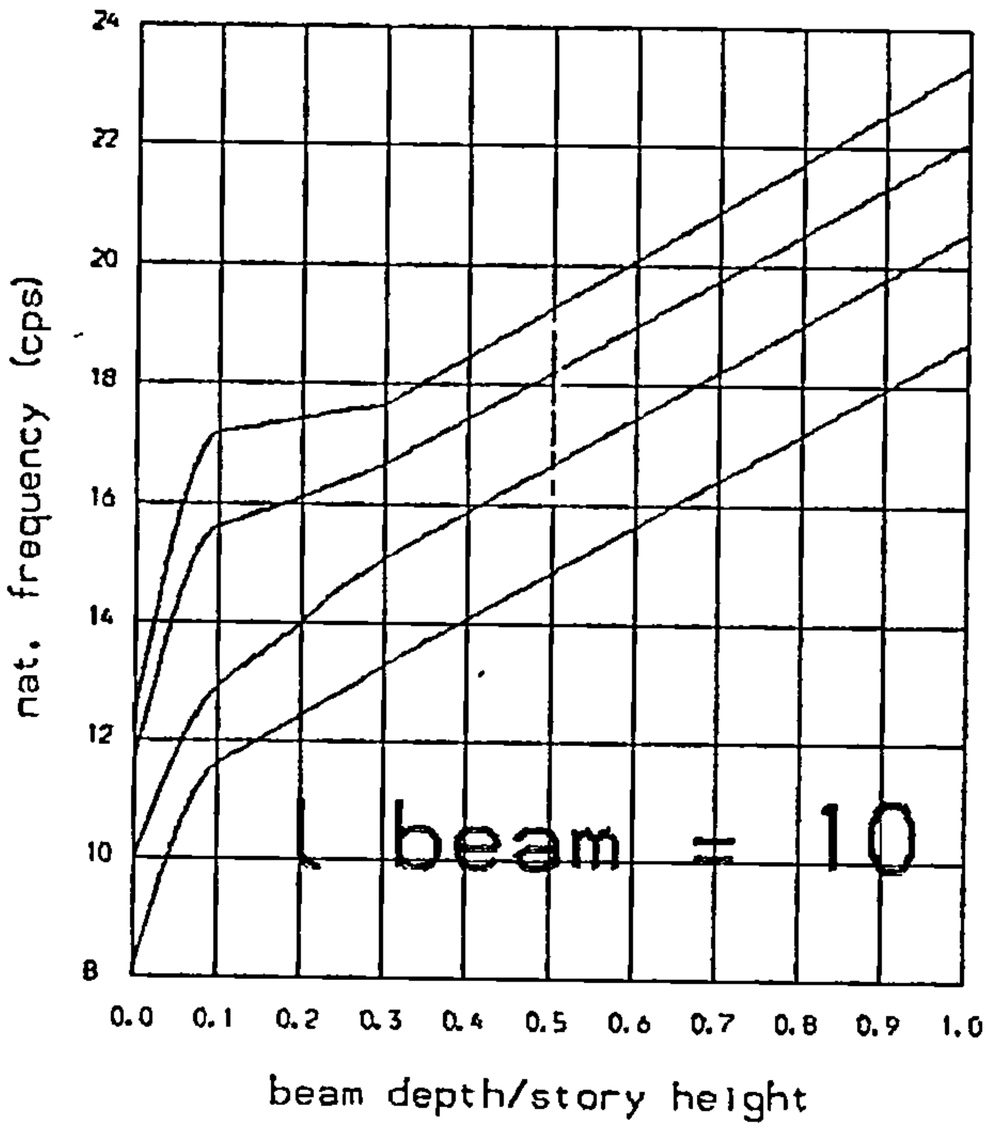

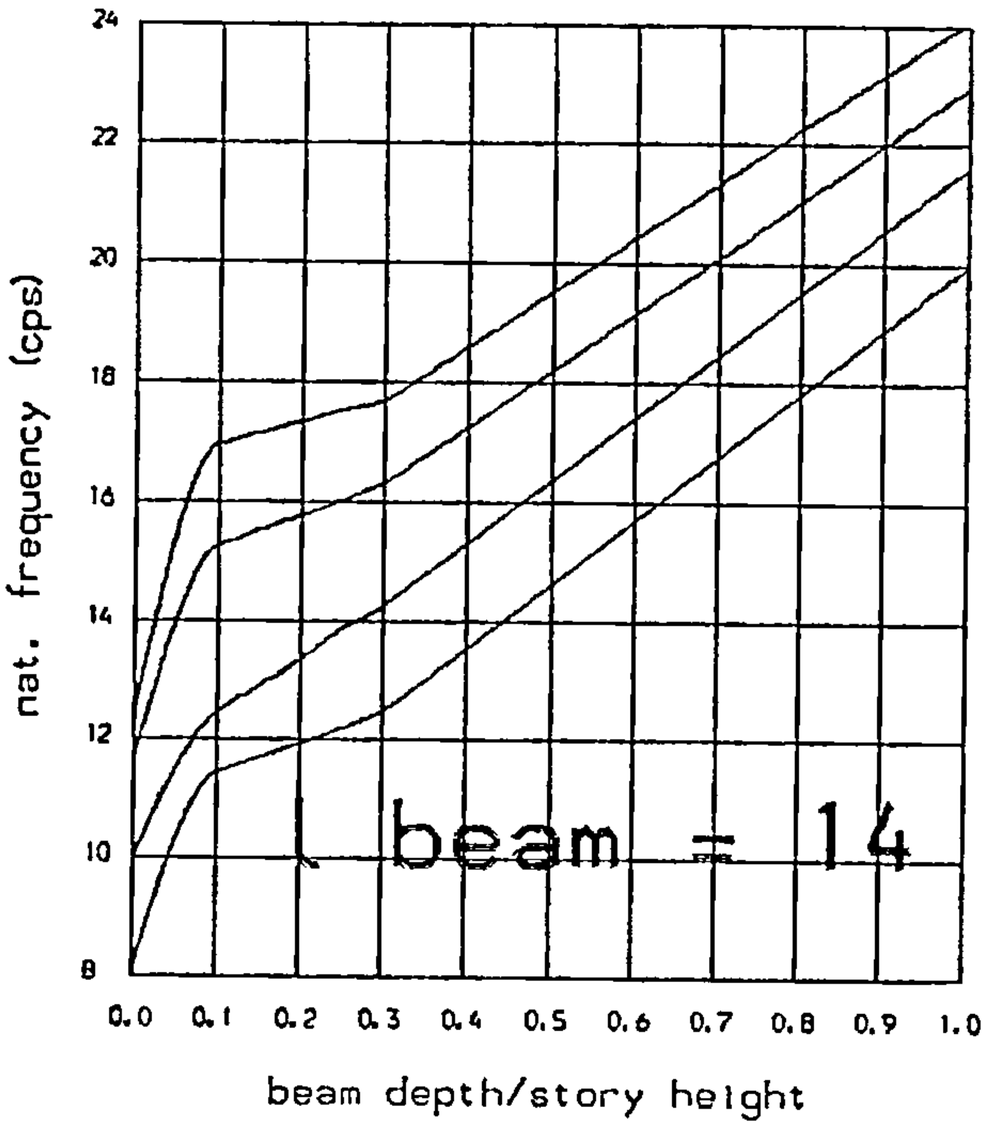

FIG. B.10

Variation of 3 rd. natural freqency with beam depth and wall width (DW) .

Total height : 200 ft
Nb of storeys : 20
Selfweight : yes
Extra story mass : none

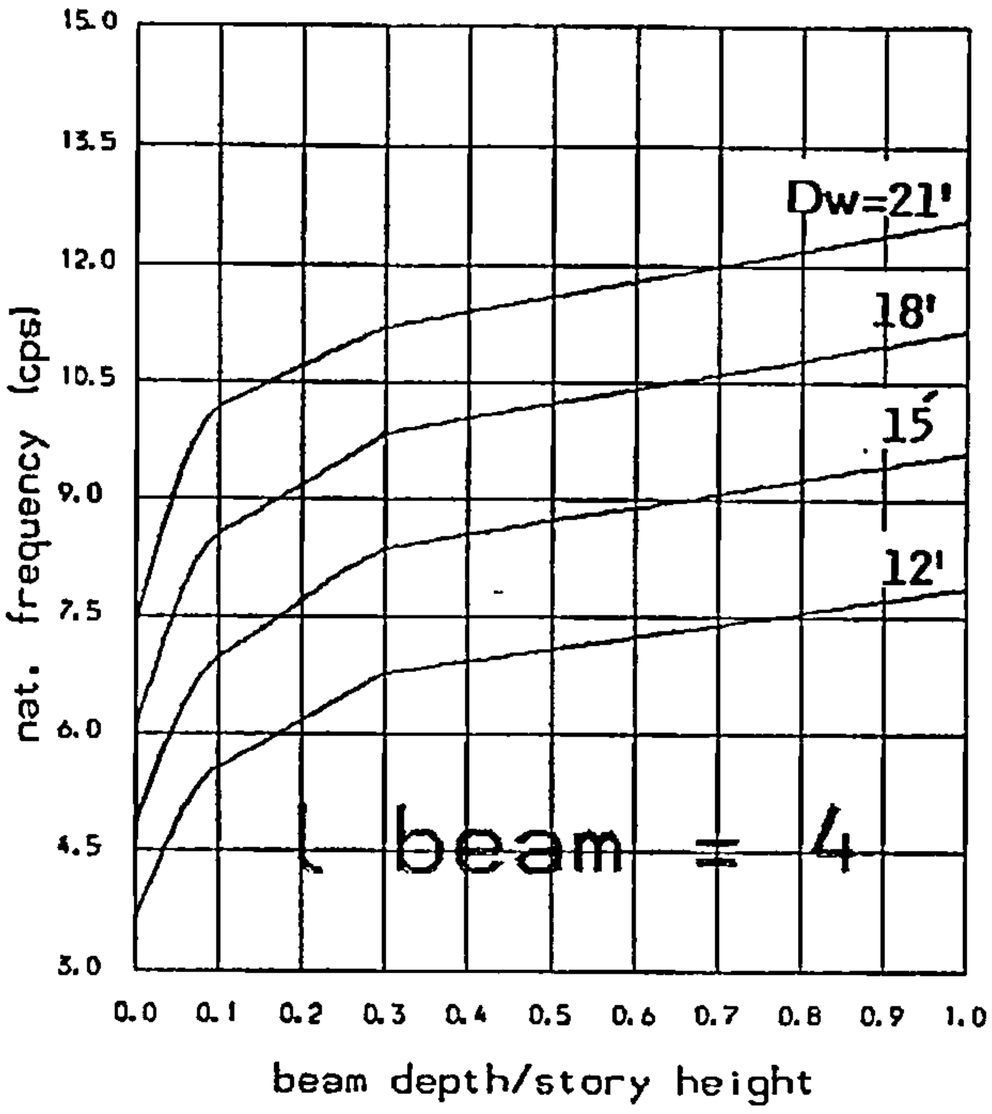

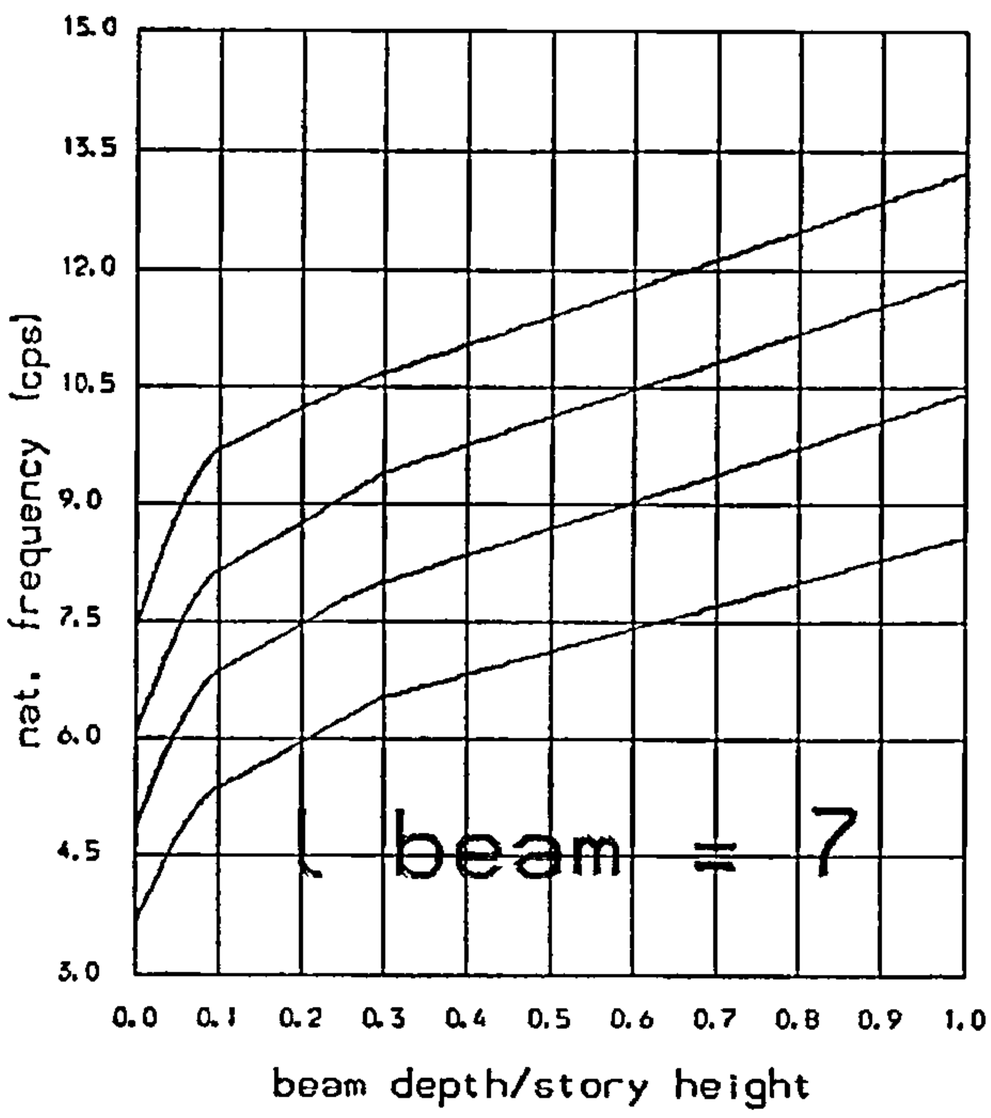

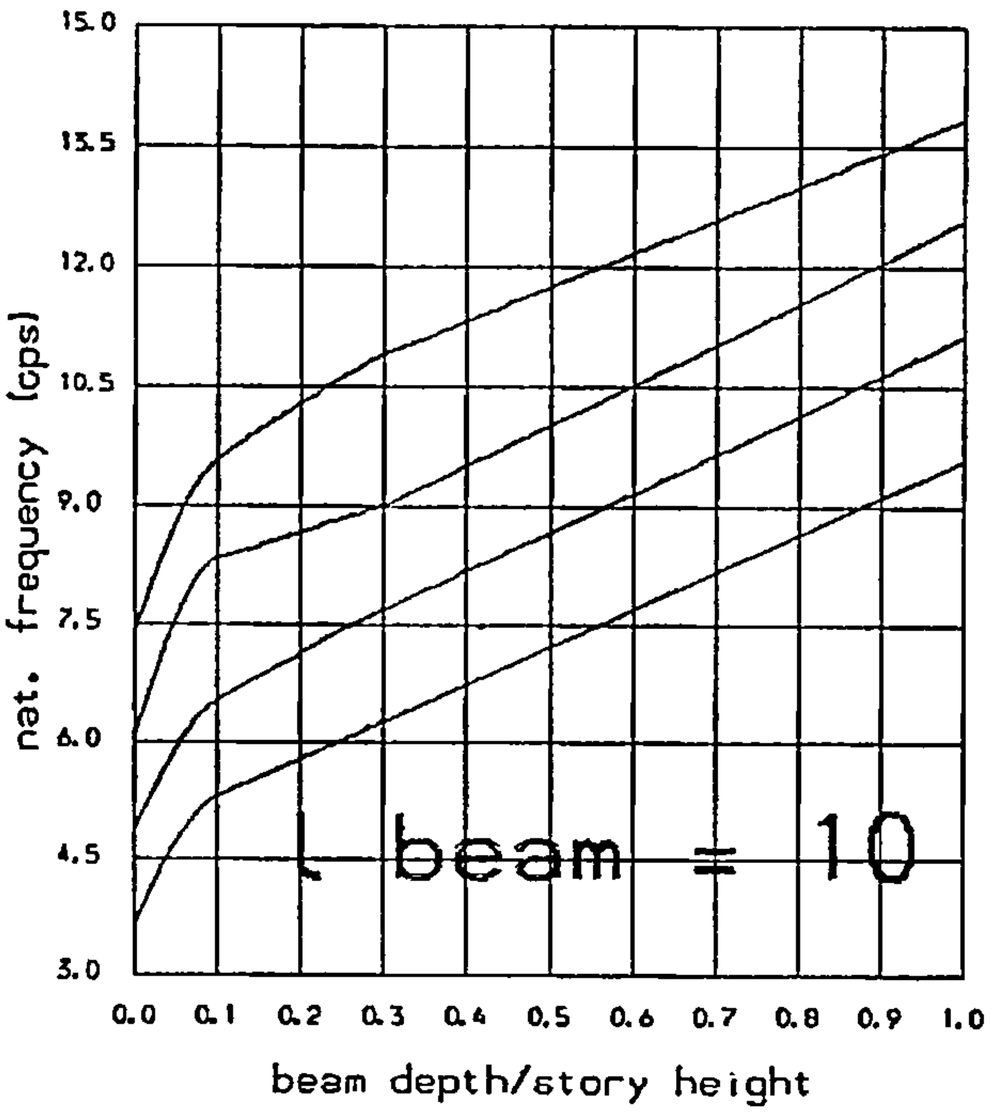

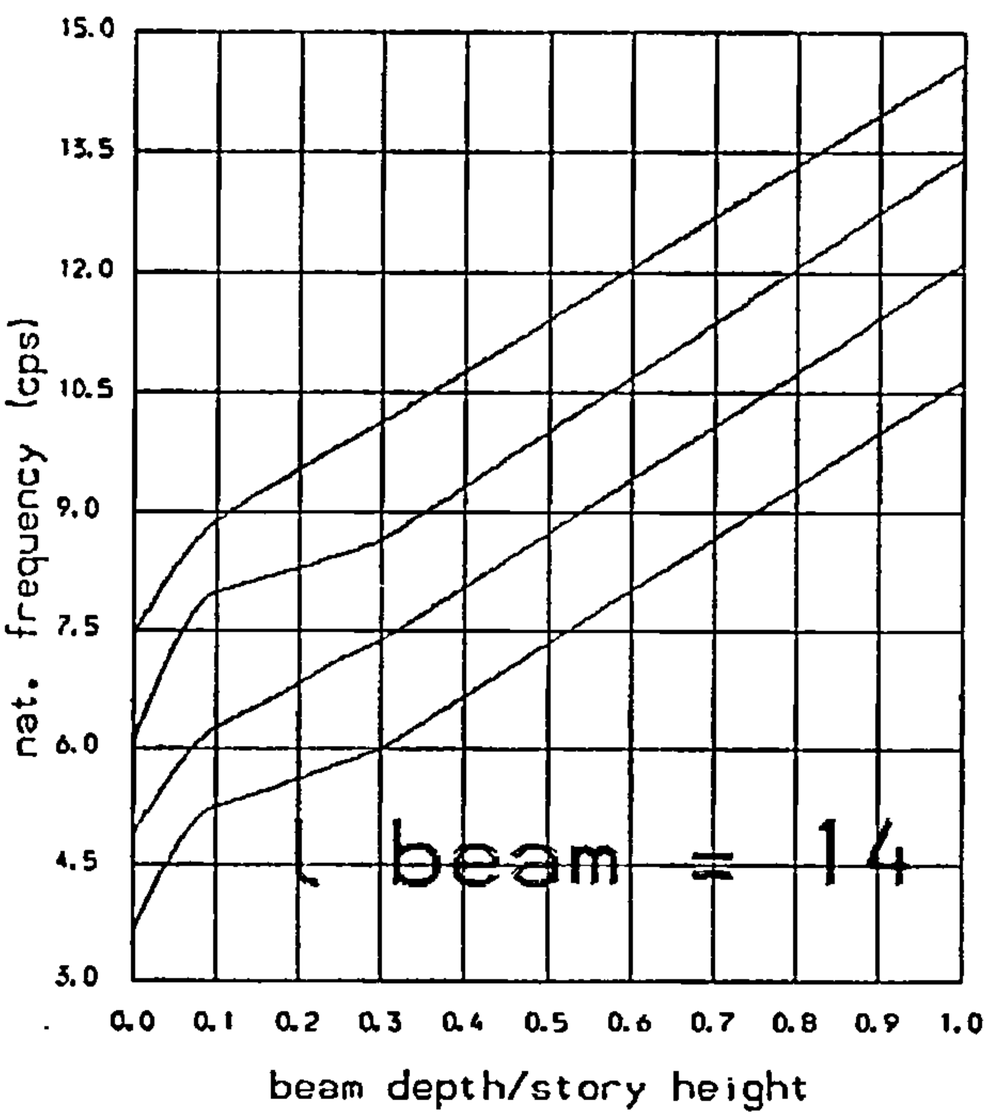

FIG. B.11

Variation of 3 rd. natural freqency with beam depth and wall width (DV) .

Total height	: 200 ft
Nb of storeys	: 20
Selfweight	: yes
Extra story mass	: 4.kips

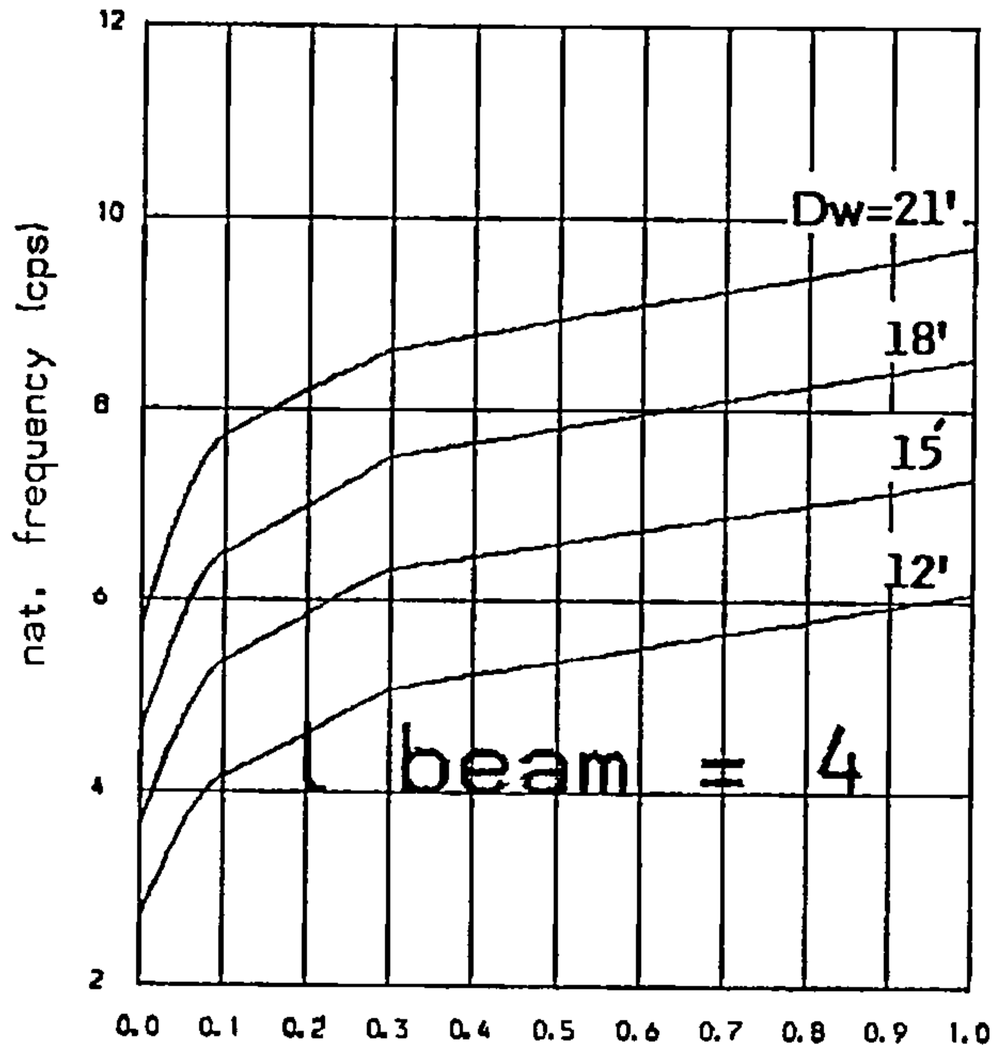

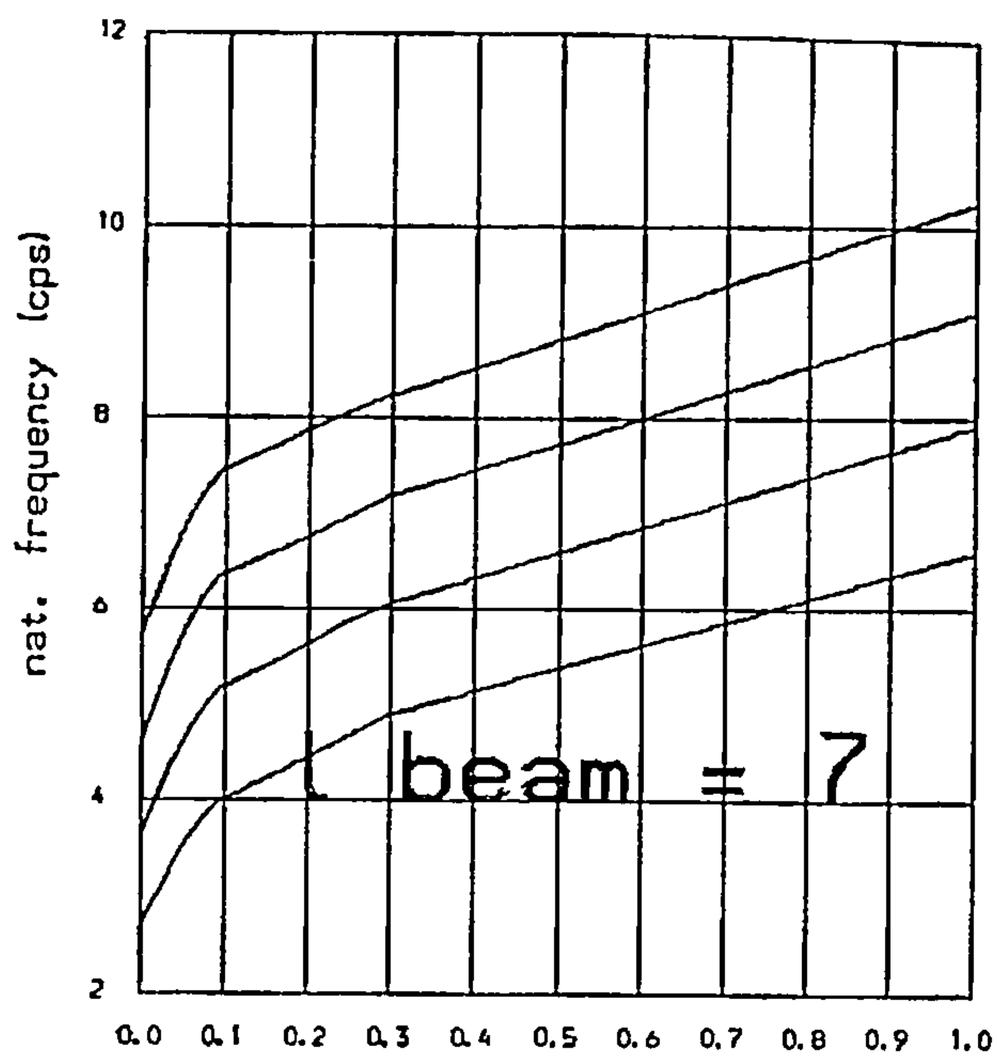

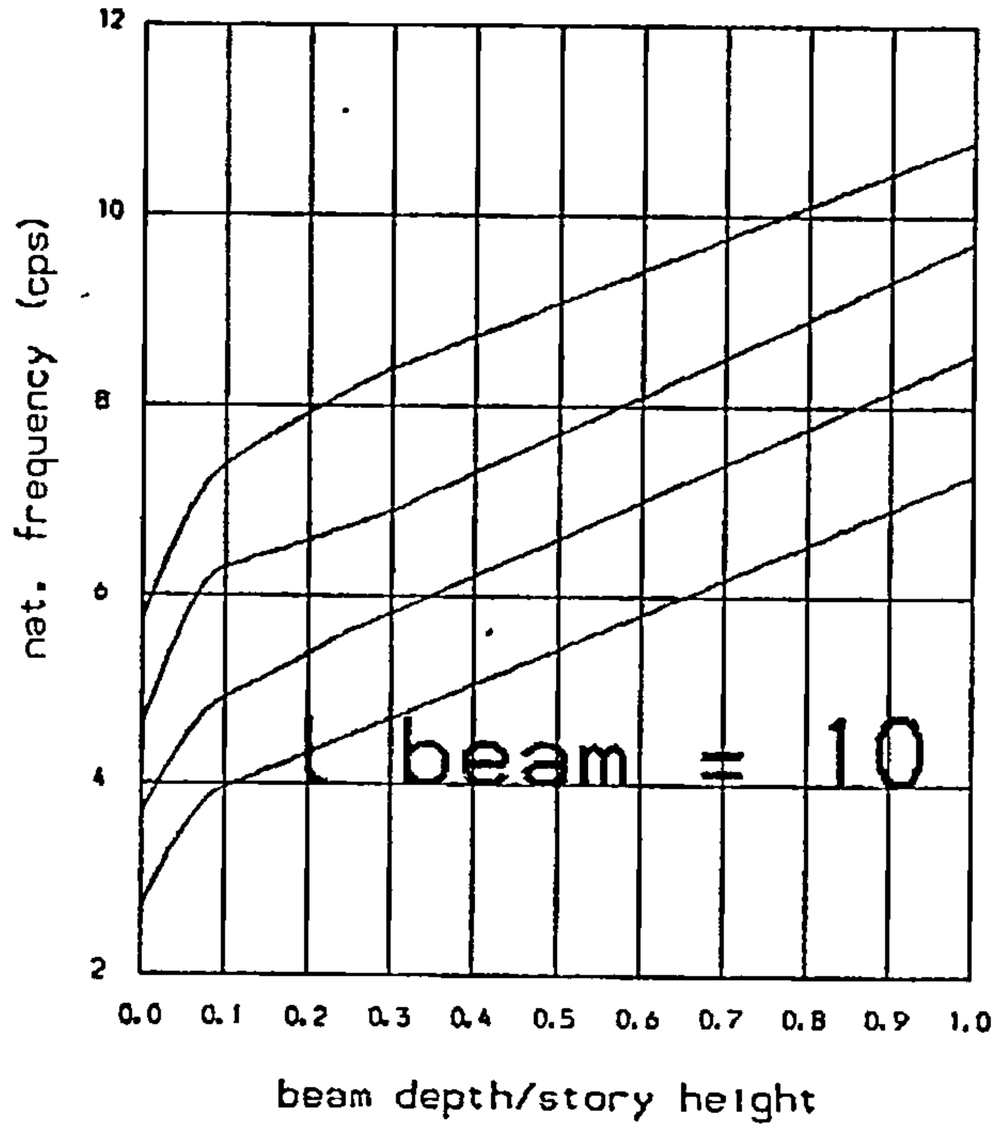

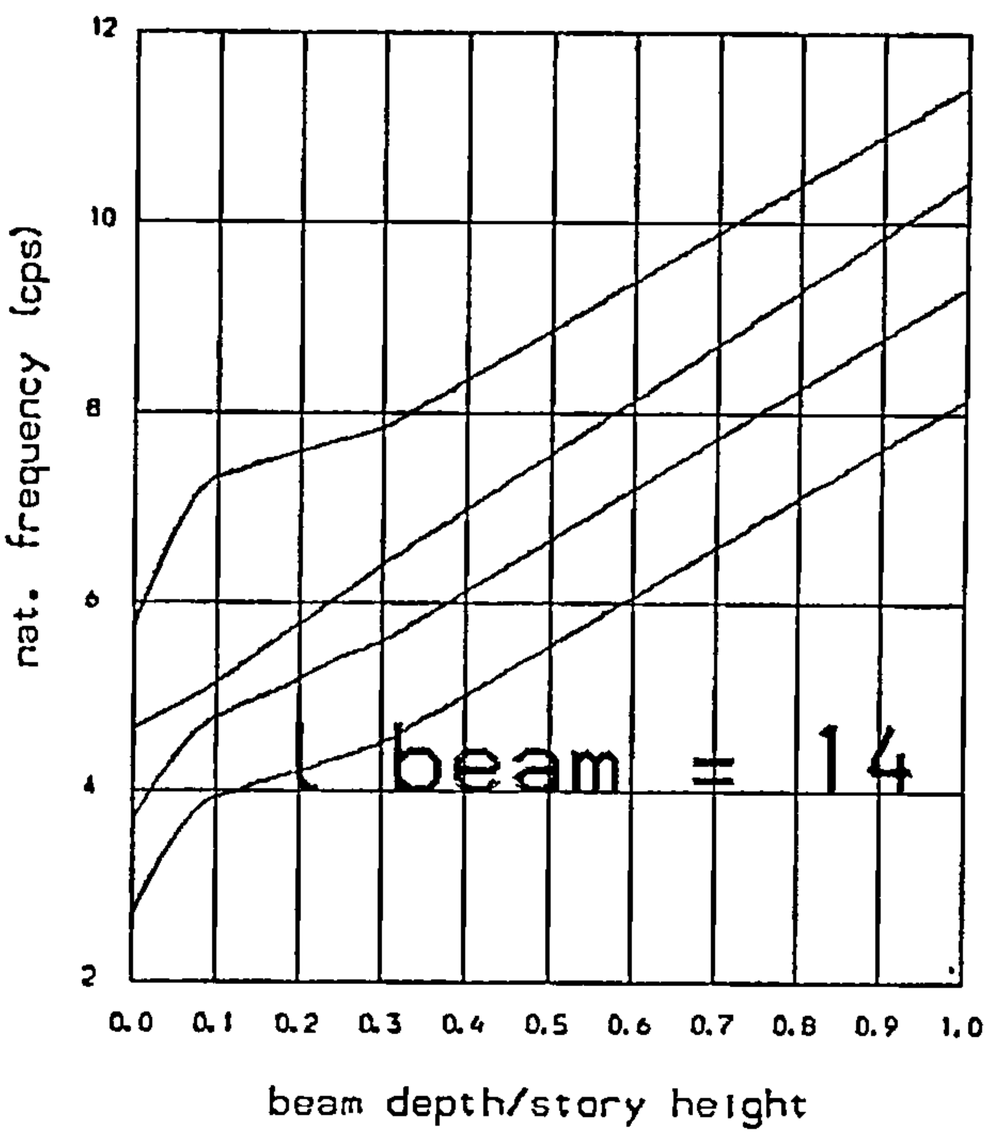

FIG. B.12

Variation of 3 rd. natural freqency with beam depth and wall width (DW) .

Total height	:	200 ft
Nb of storeys	:	20
Selfweight	:	yes
Extra story mass	:	8.kips

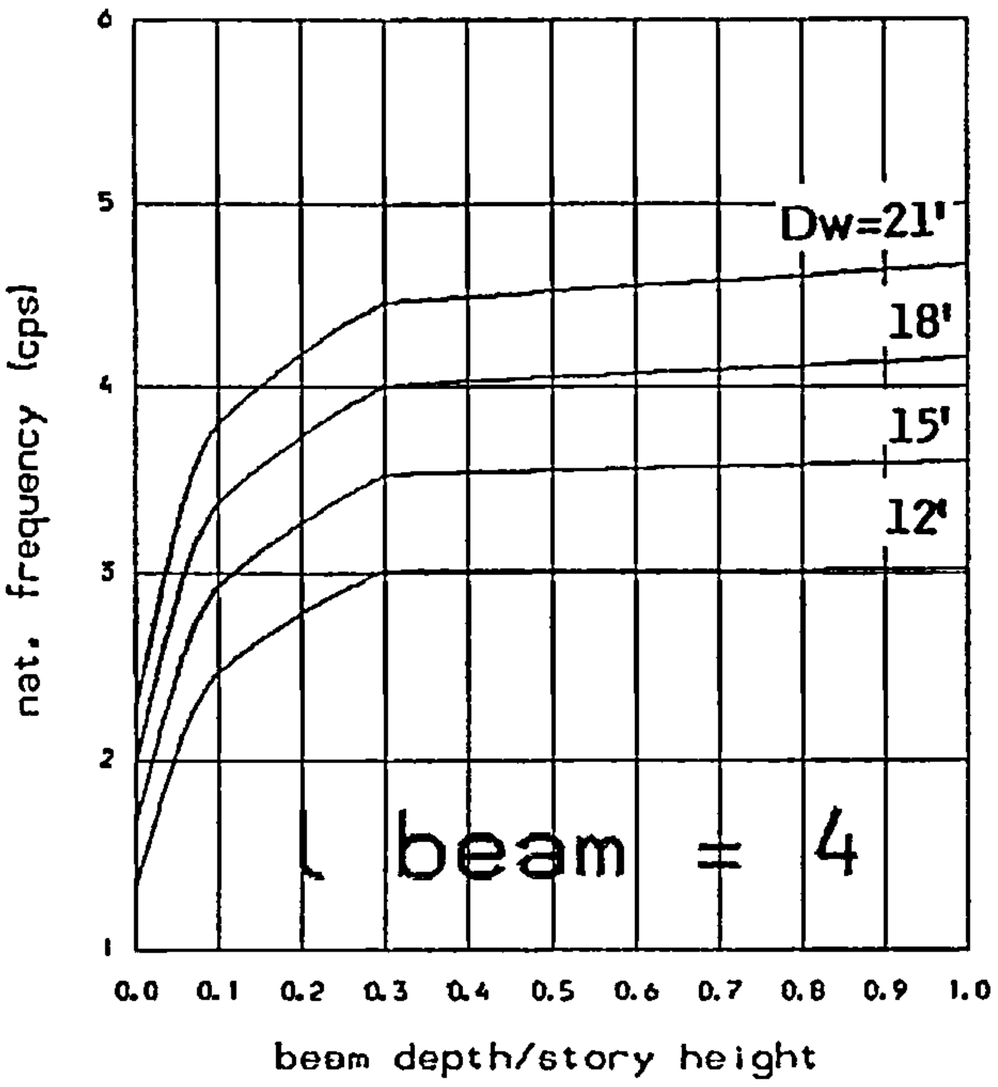

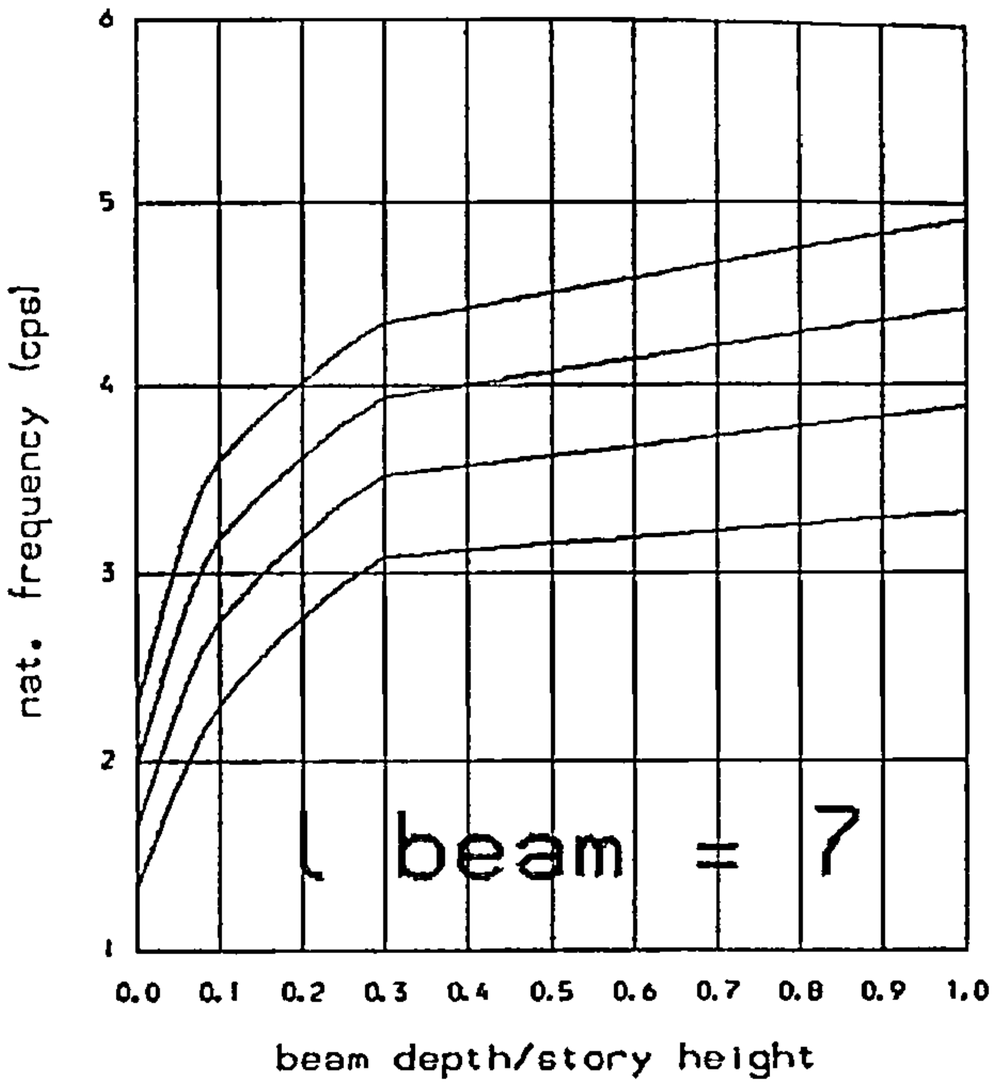

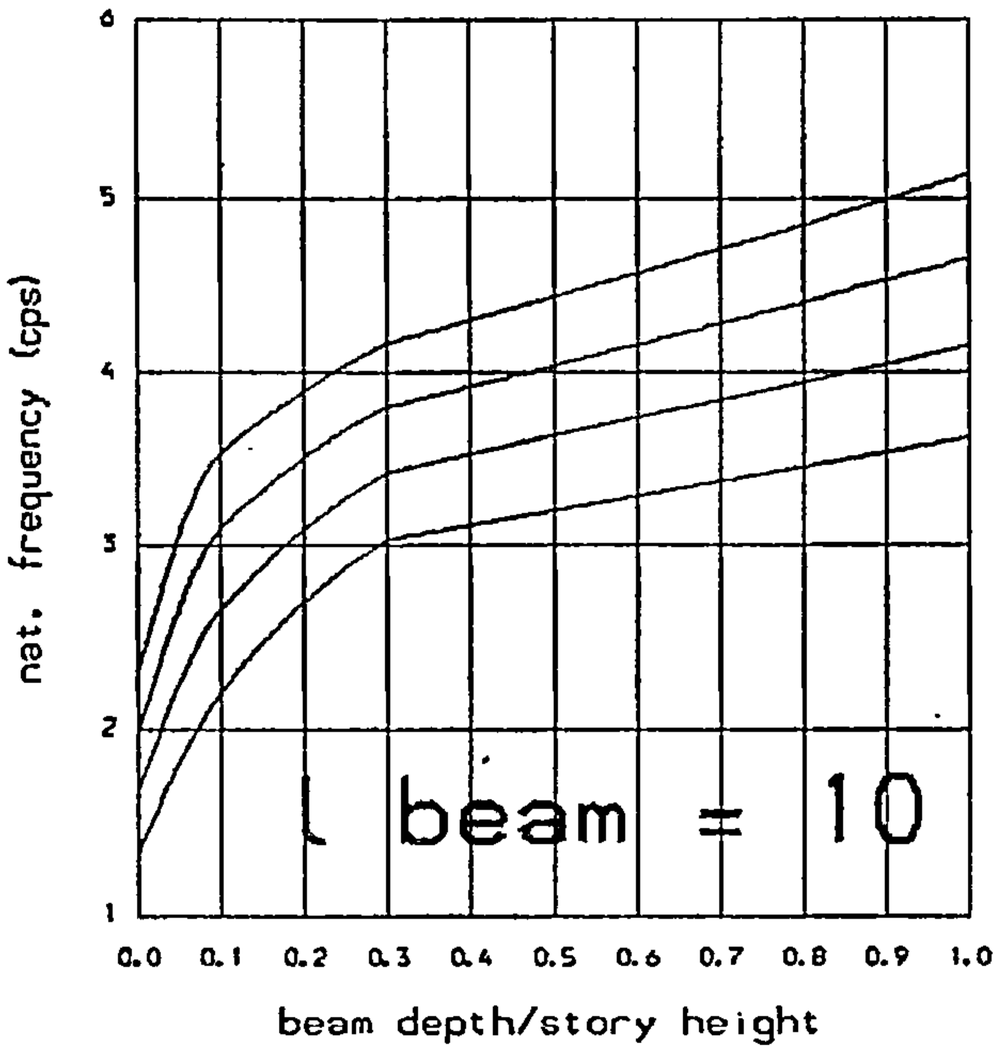

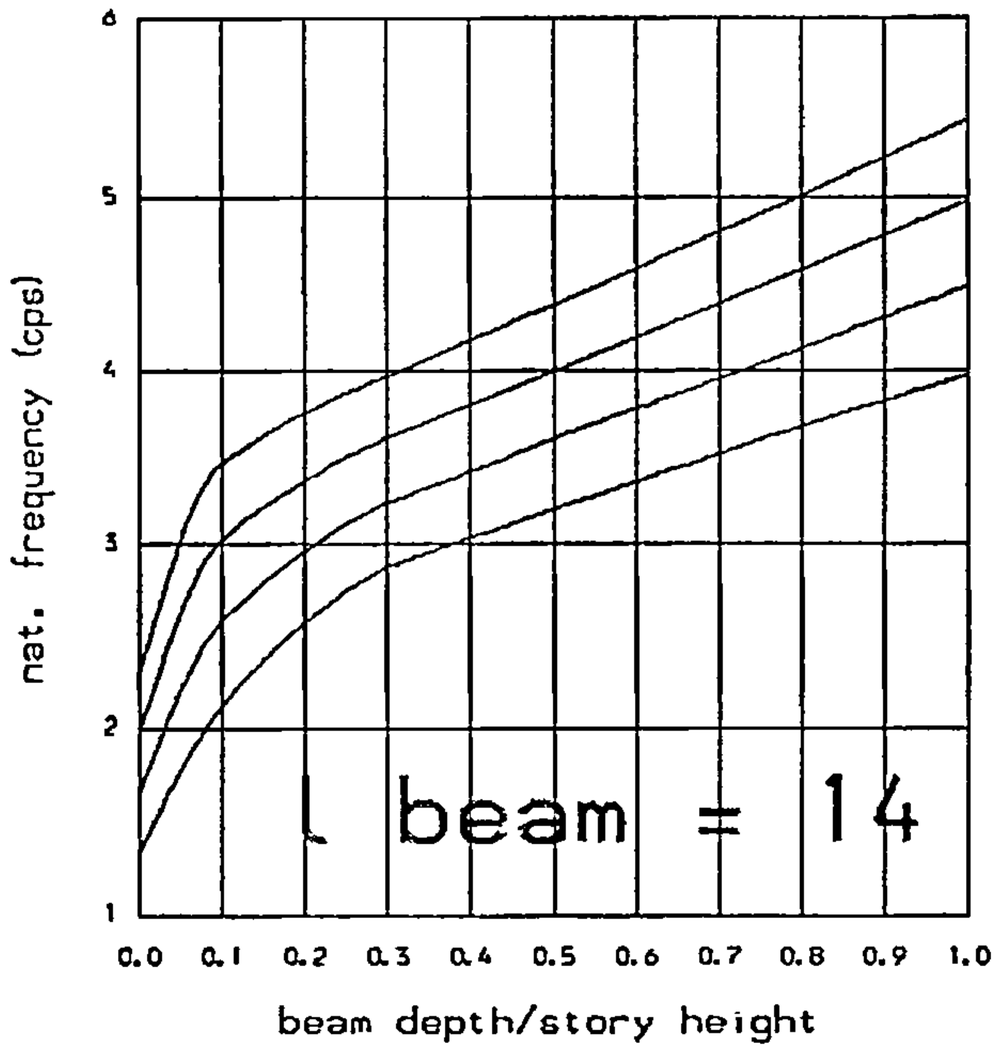

FIG. B.13

Variation of 2 nd. natural freqency with beam depth and wall width (DW).

Total height : 300 ft
Nb of storeys : 30
Selfweight : yes
Extra story mass : none

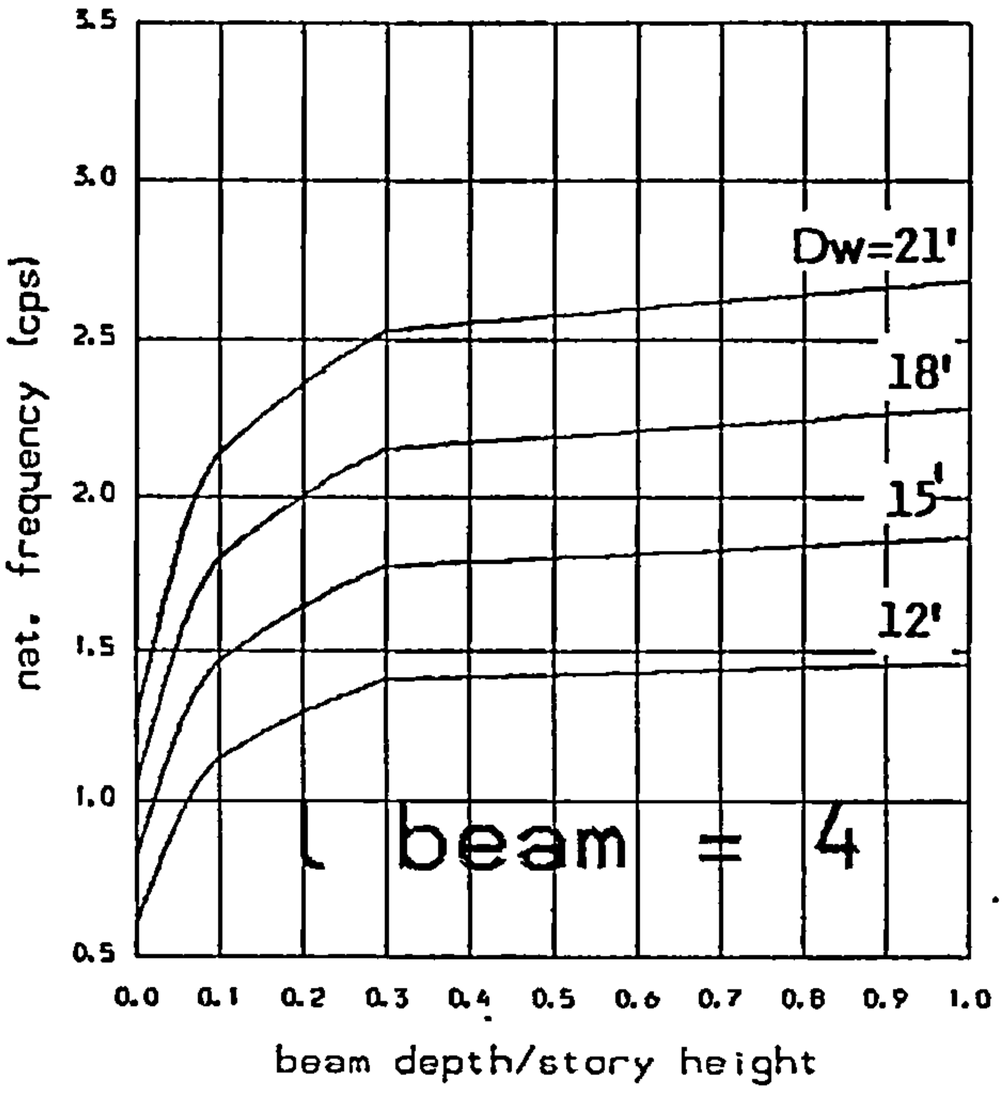

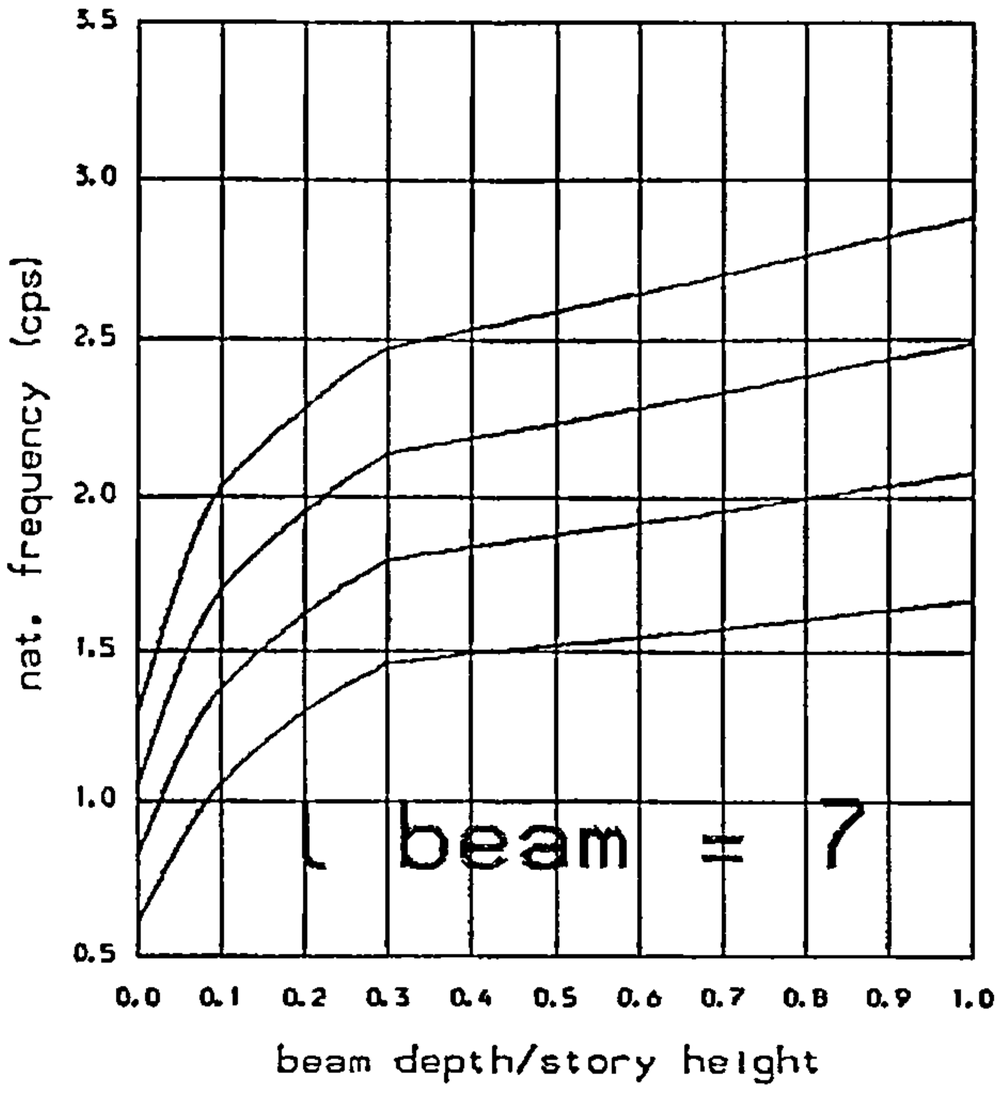

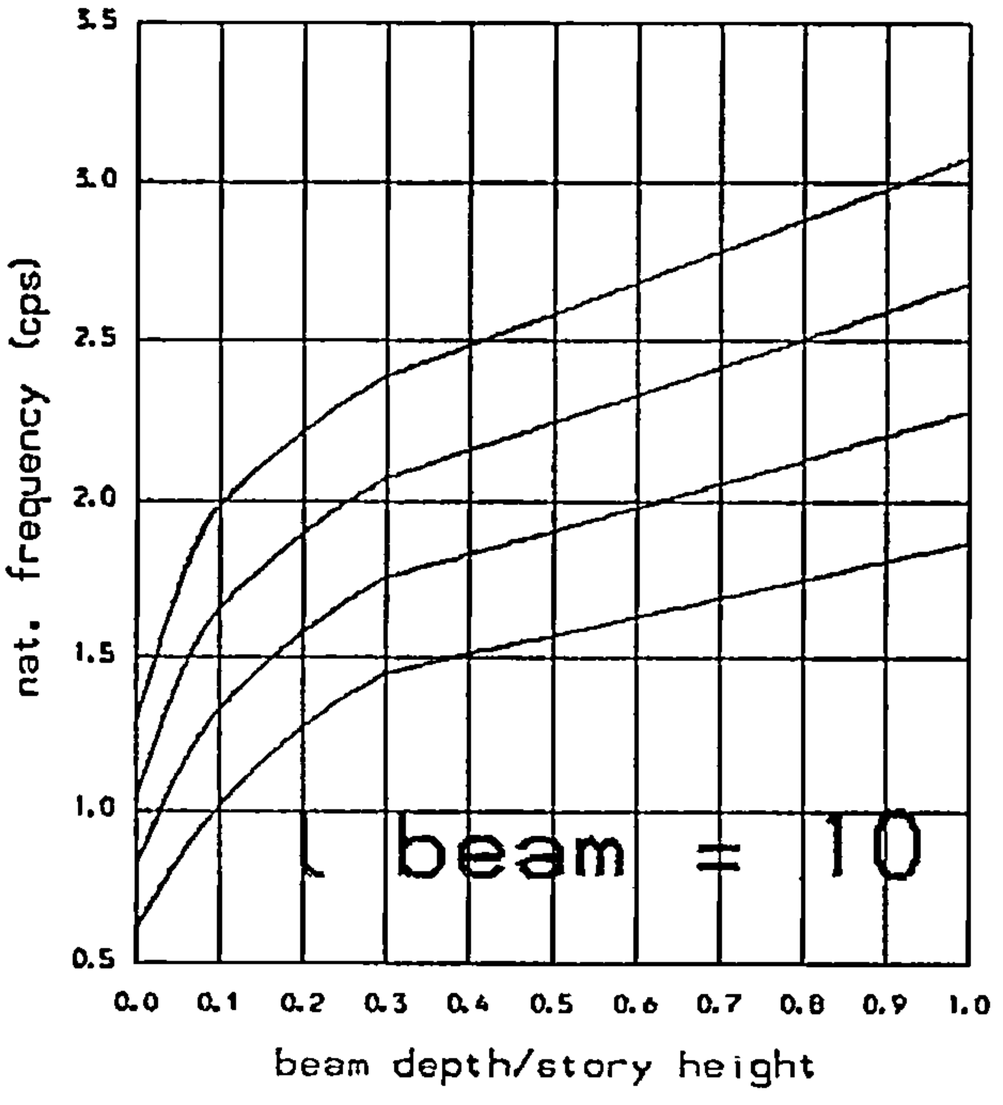

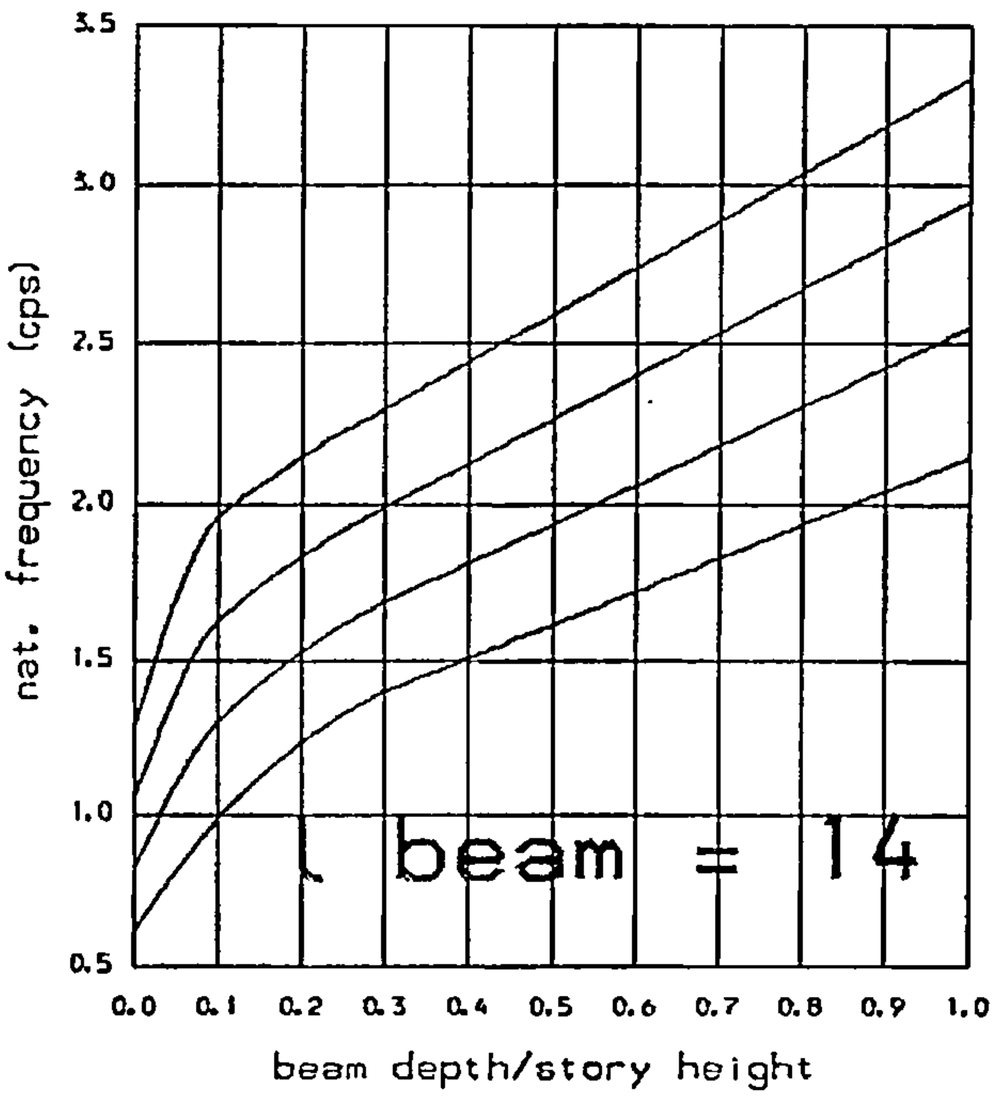

FIG. B.14

Variation of 2 nd. natural freqency with beam depth and wall width (DW) .

Total height	: 300 ft
Nb of storeys	: 30
Selfweight	: yes
Extra story mass	: 4.kips

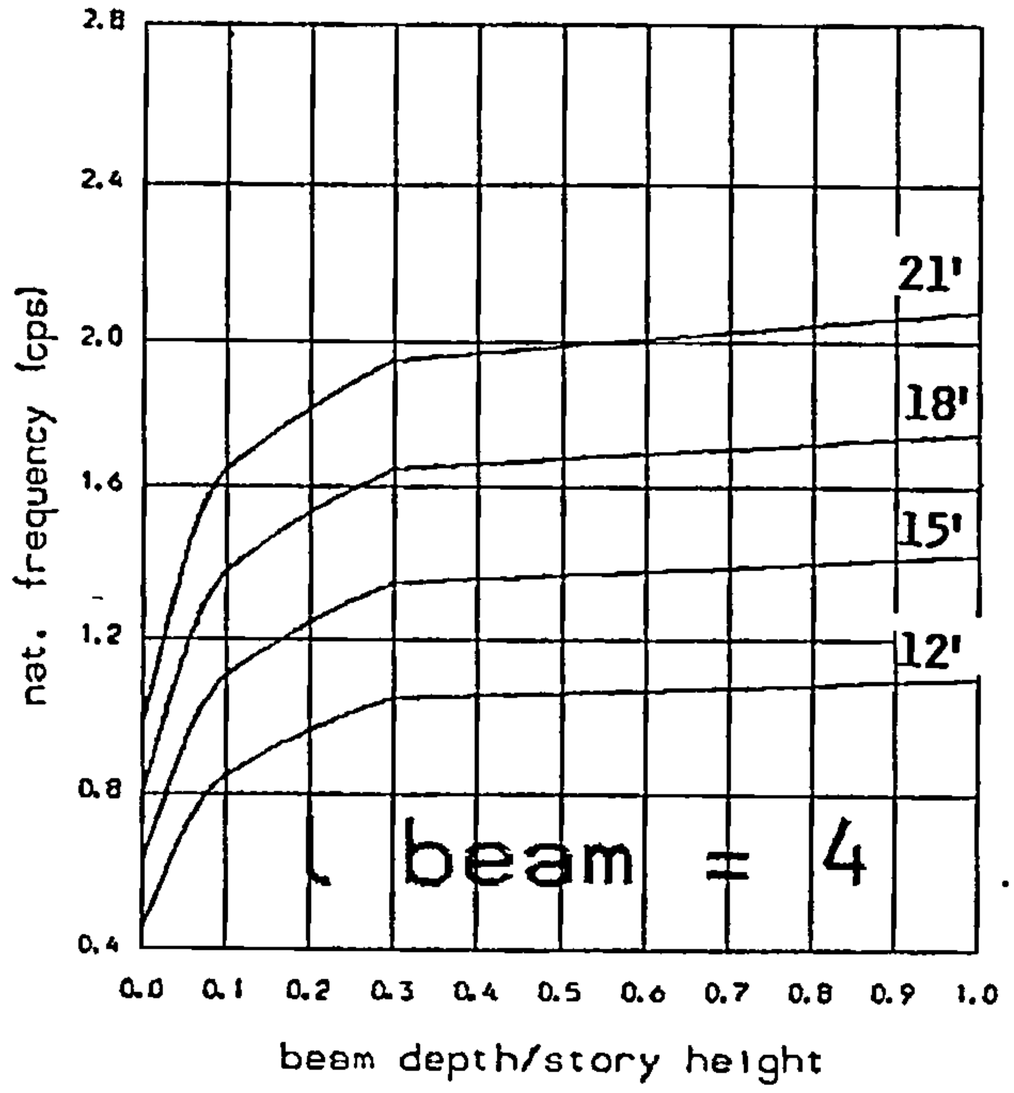

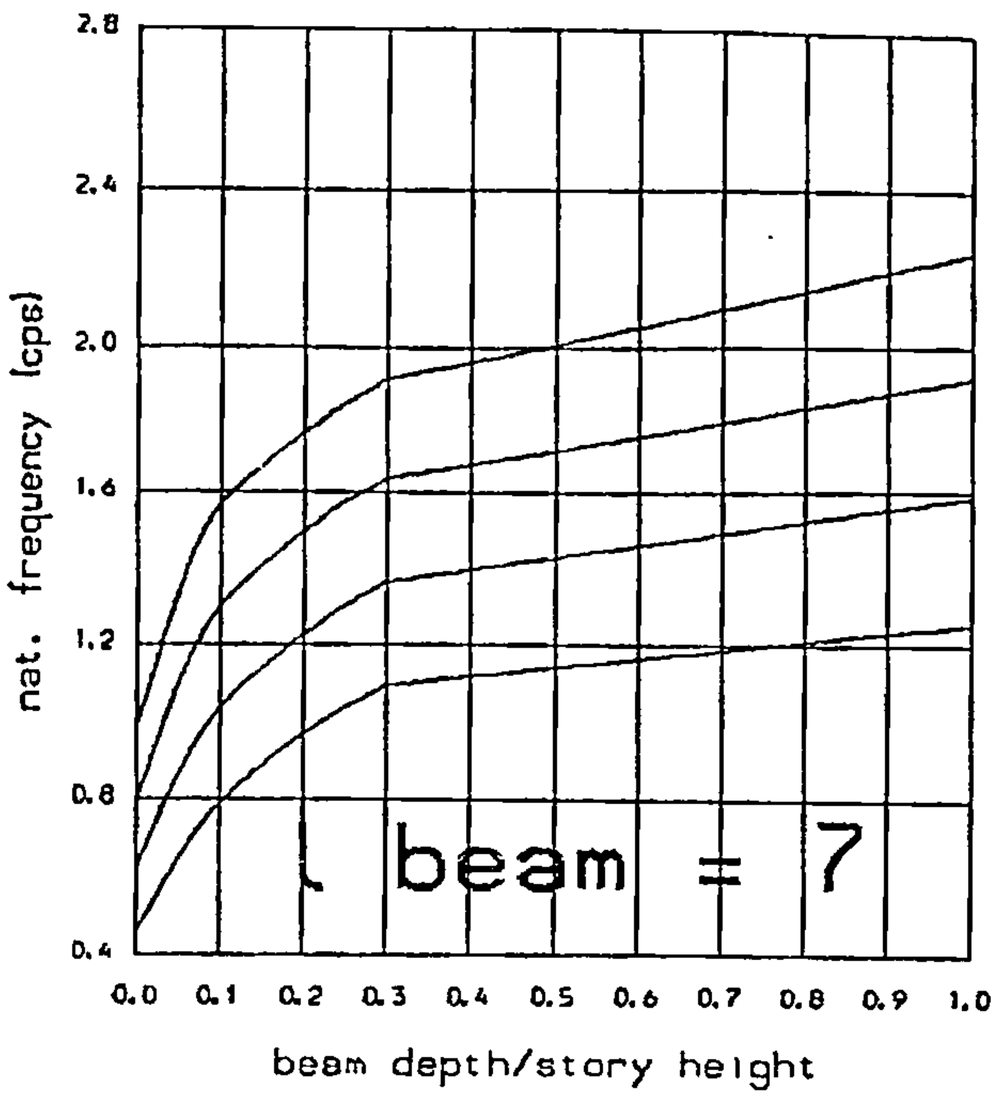

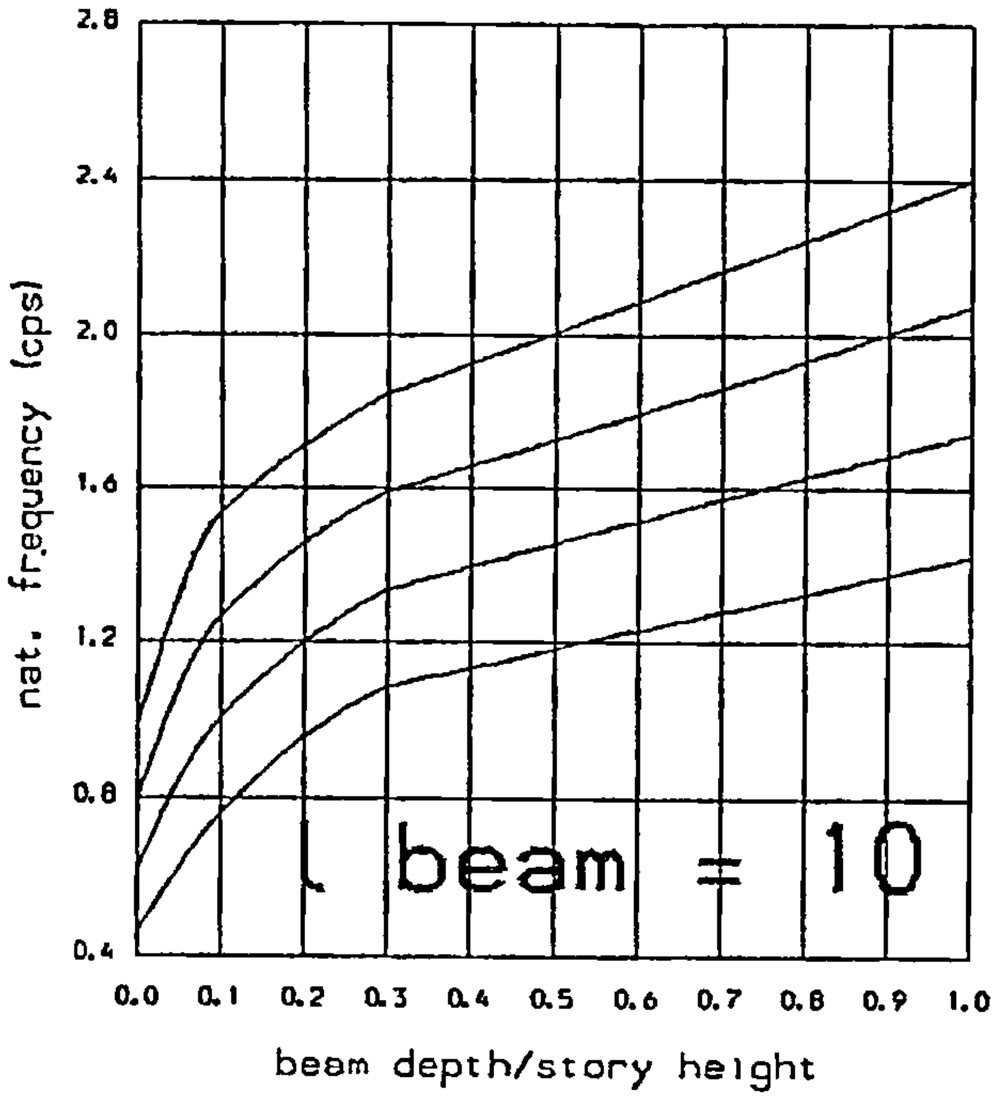

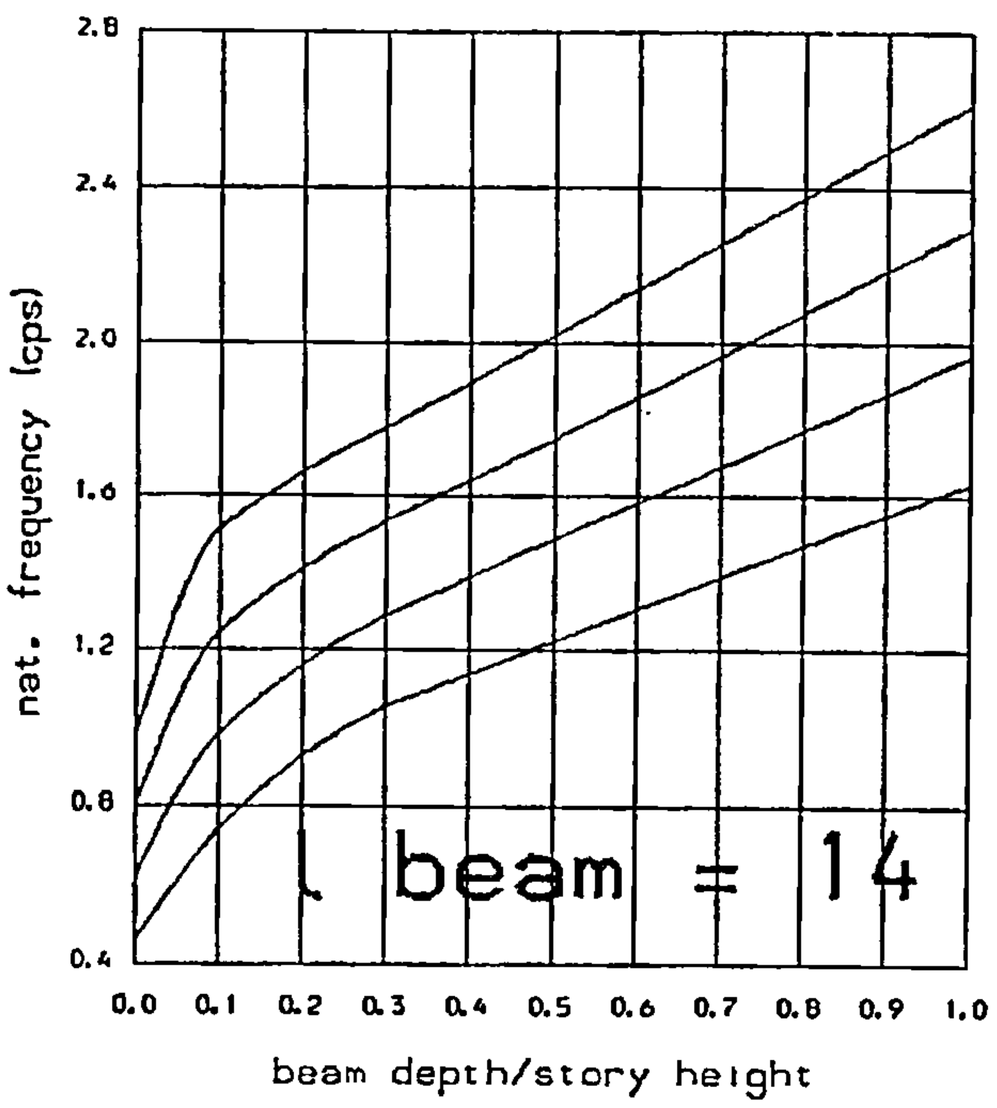

FIG. B.15
Variation of 2 nd. natural freqency with beam depth and wall width (DW).

Total height	:	300 ft
Nb of storeys	:	30
Selfweight	:	yes
Extra story mass	:	8.kips

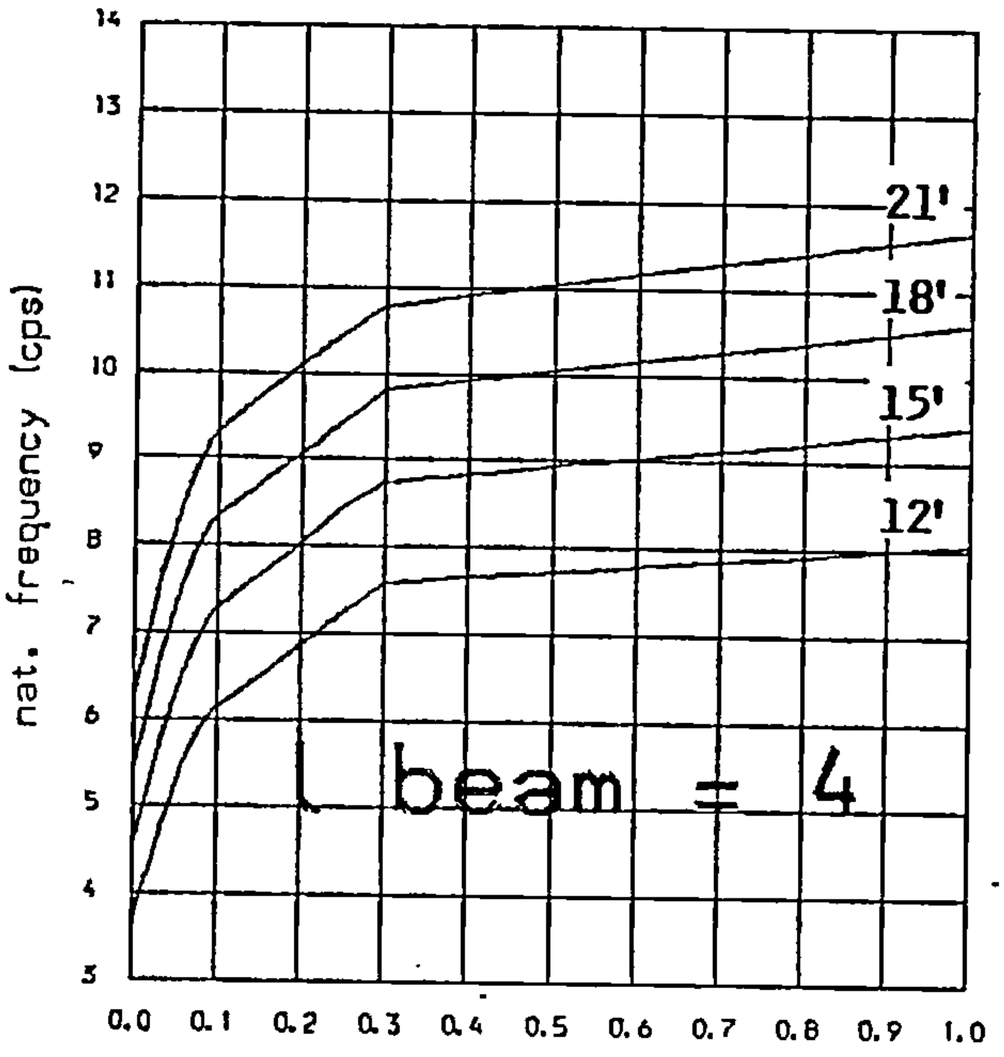

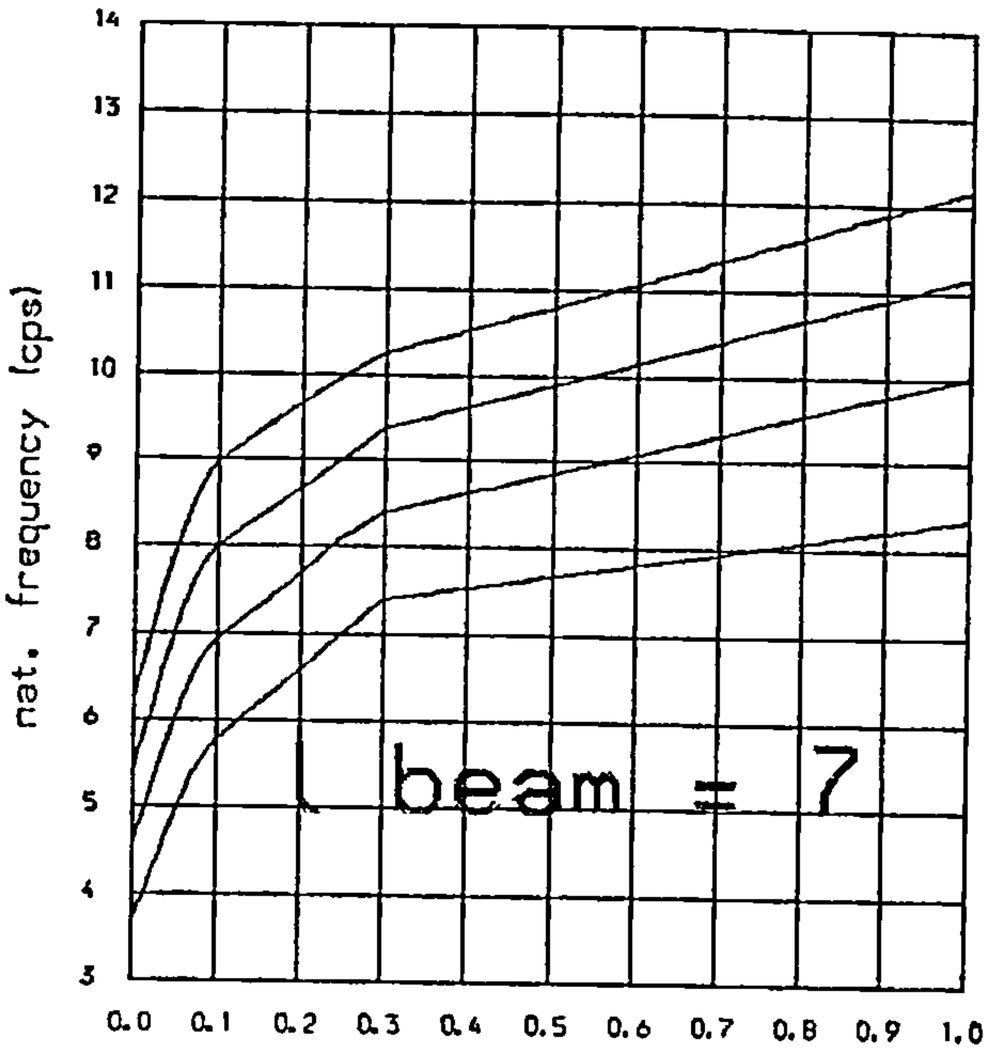

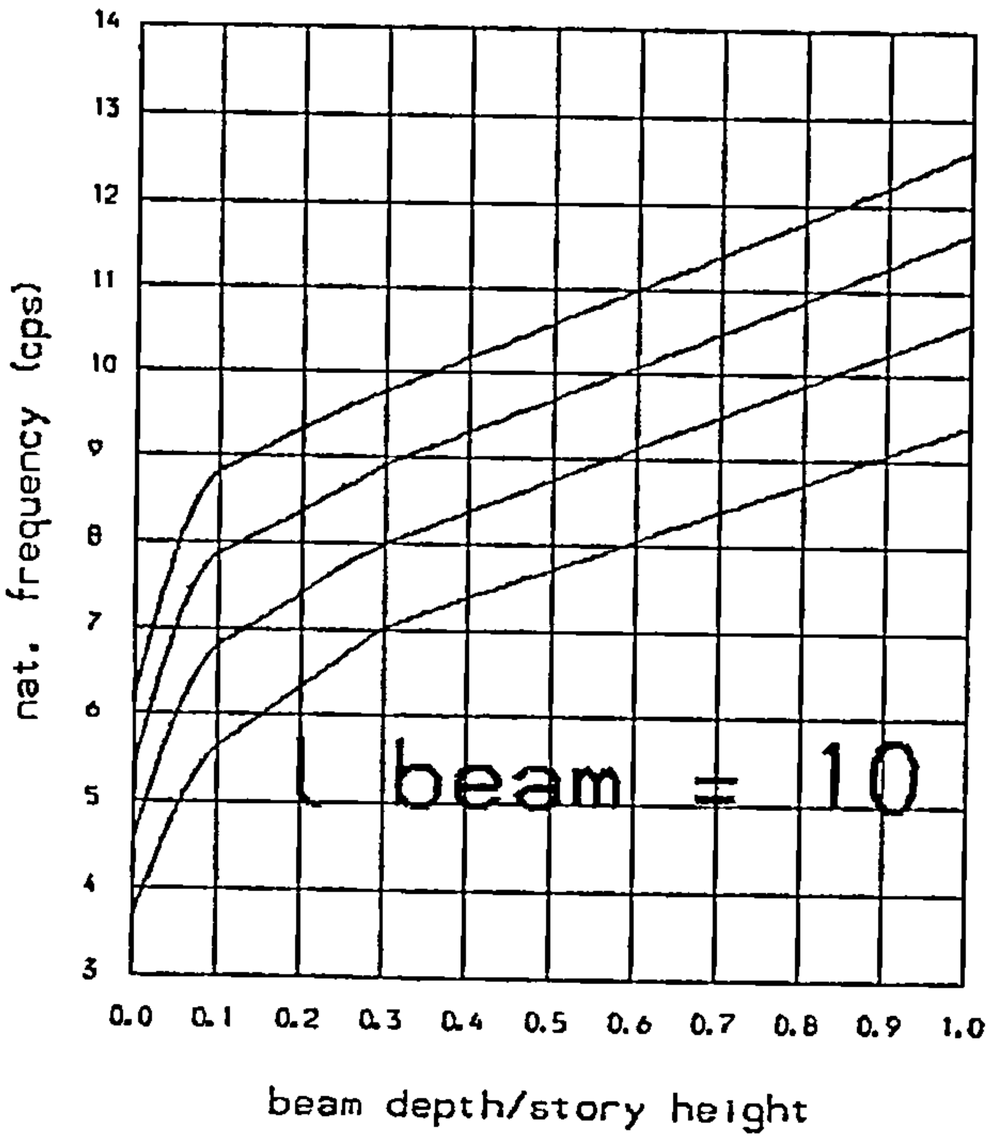

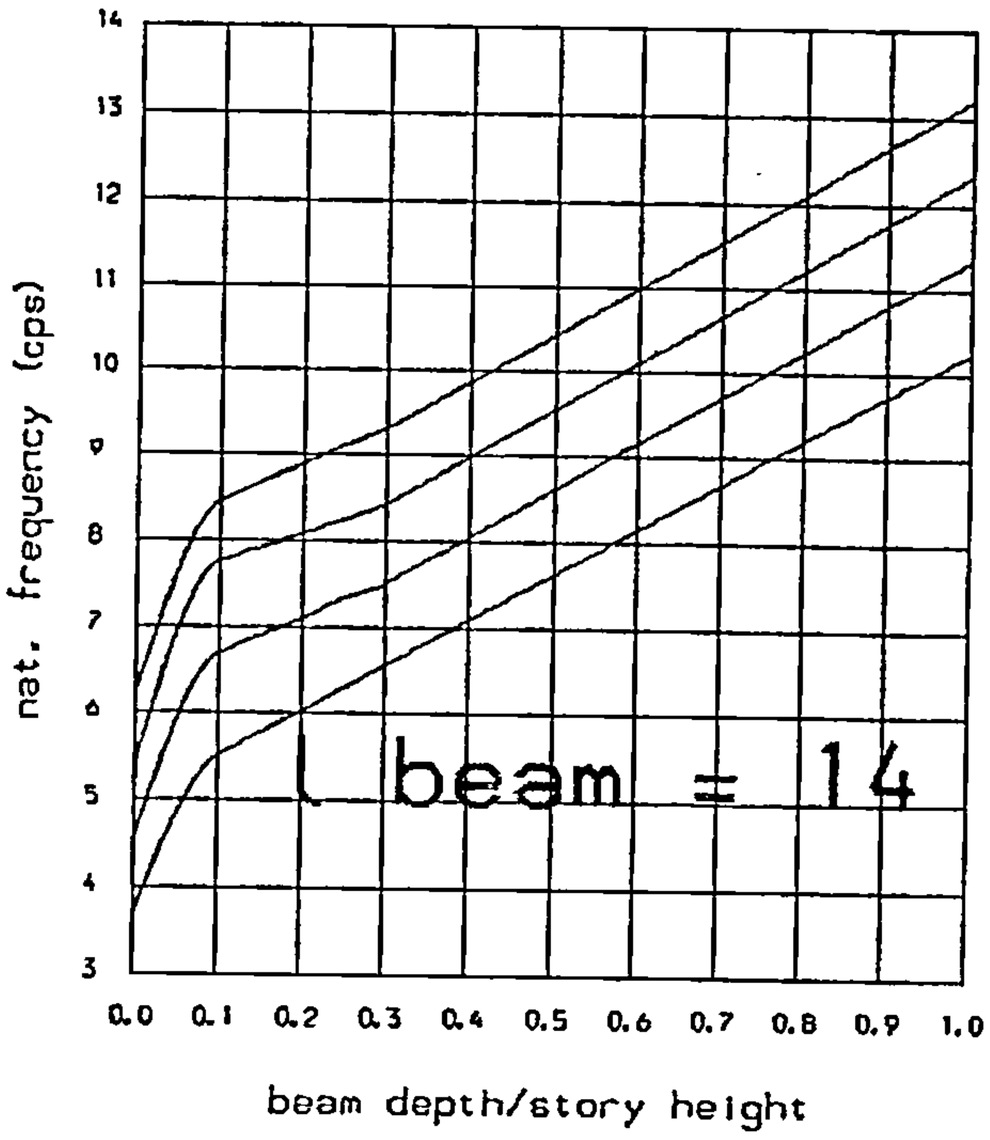

FIG. B.16

Variation of 3 rd. natural freqency with beam depth and wall width (DV) .

Total height	:	300 ft
Nb of storeys	:	30
Selfweight	:	yes
Extra story mass	:	none

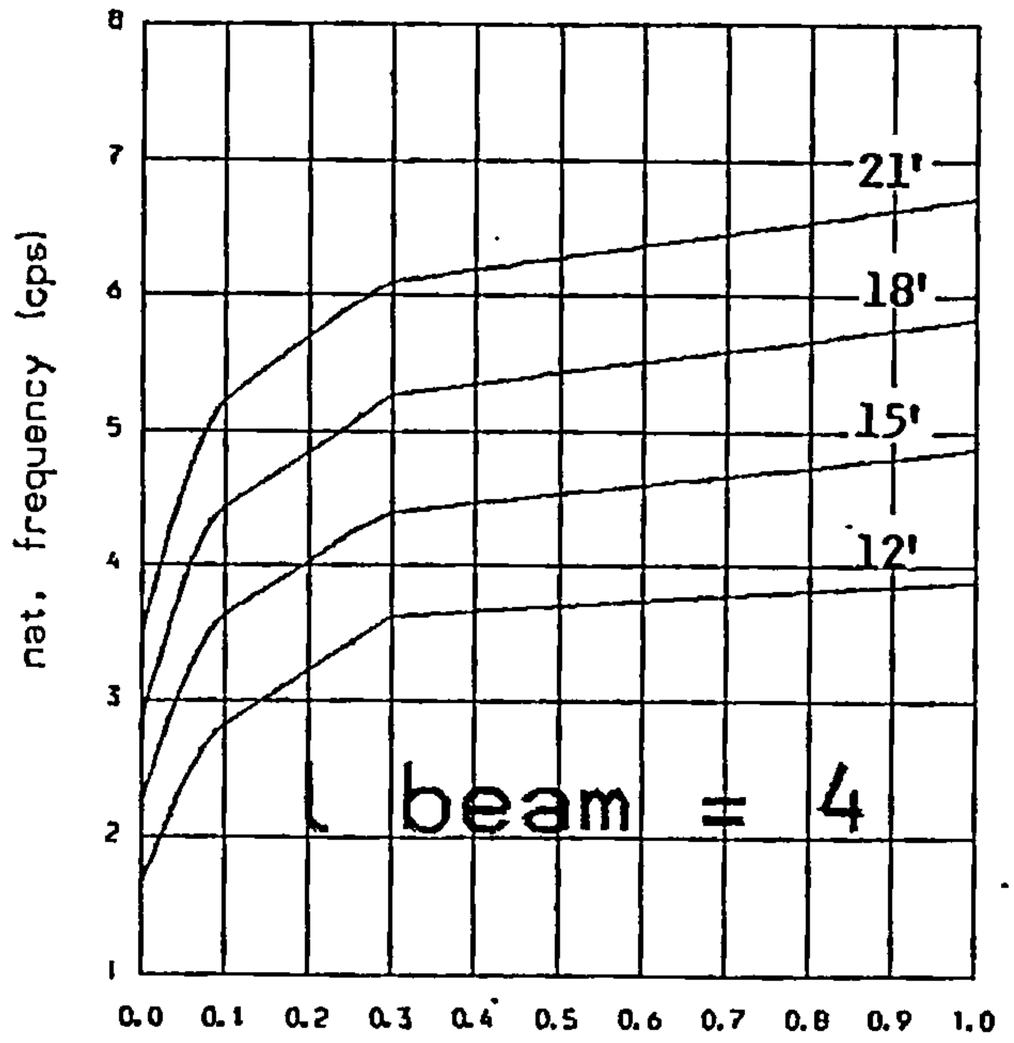

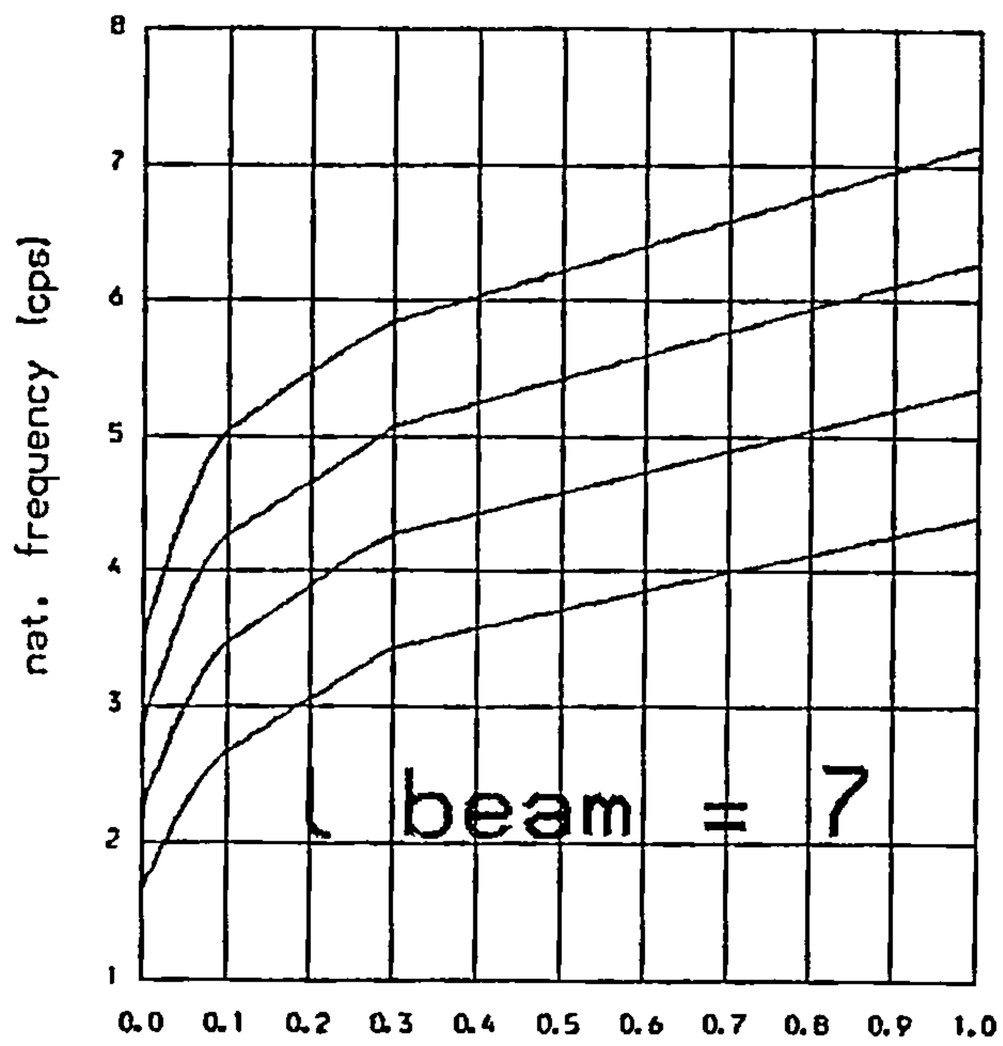

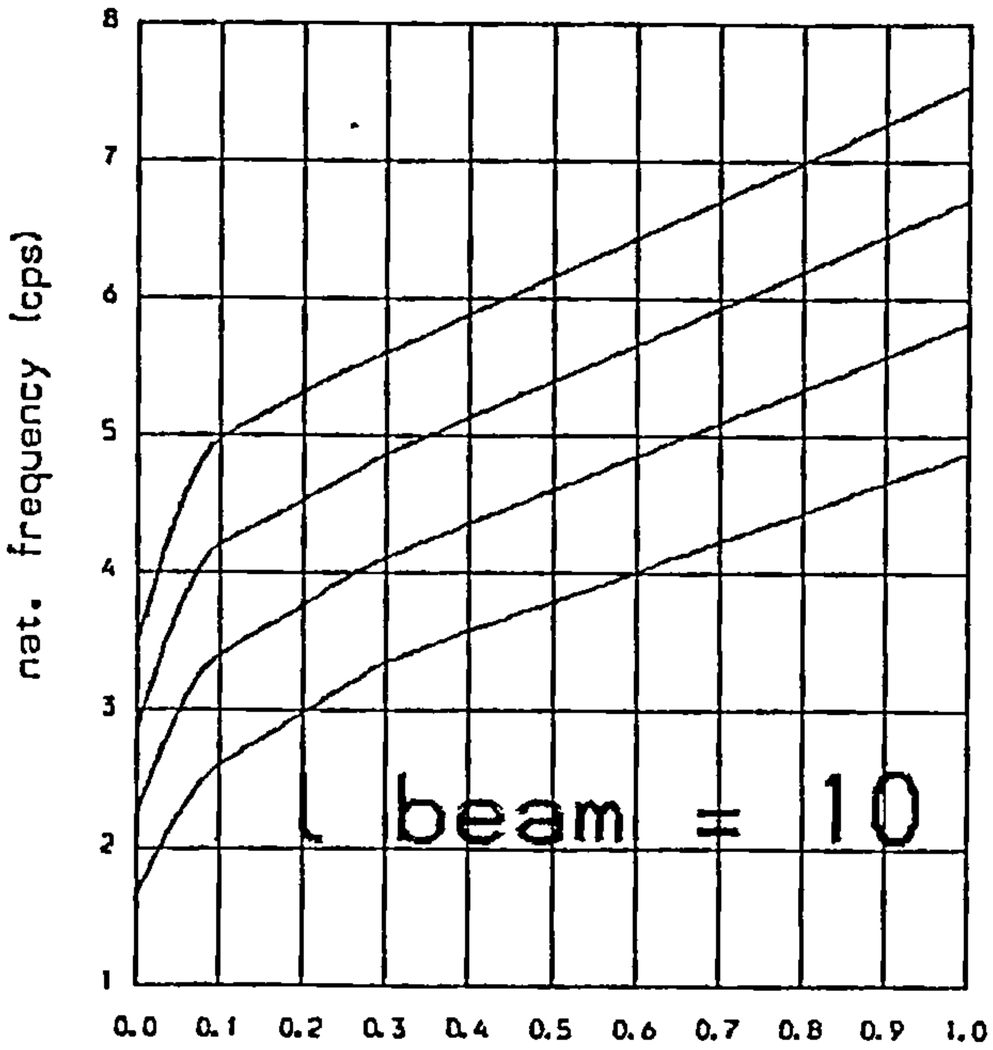

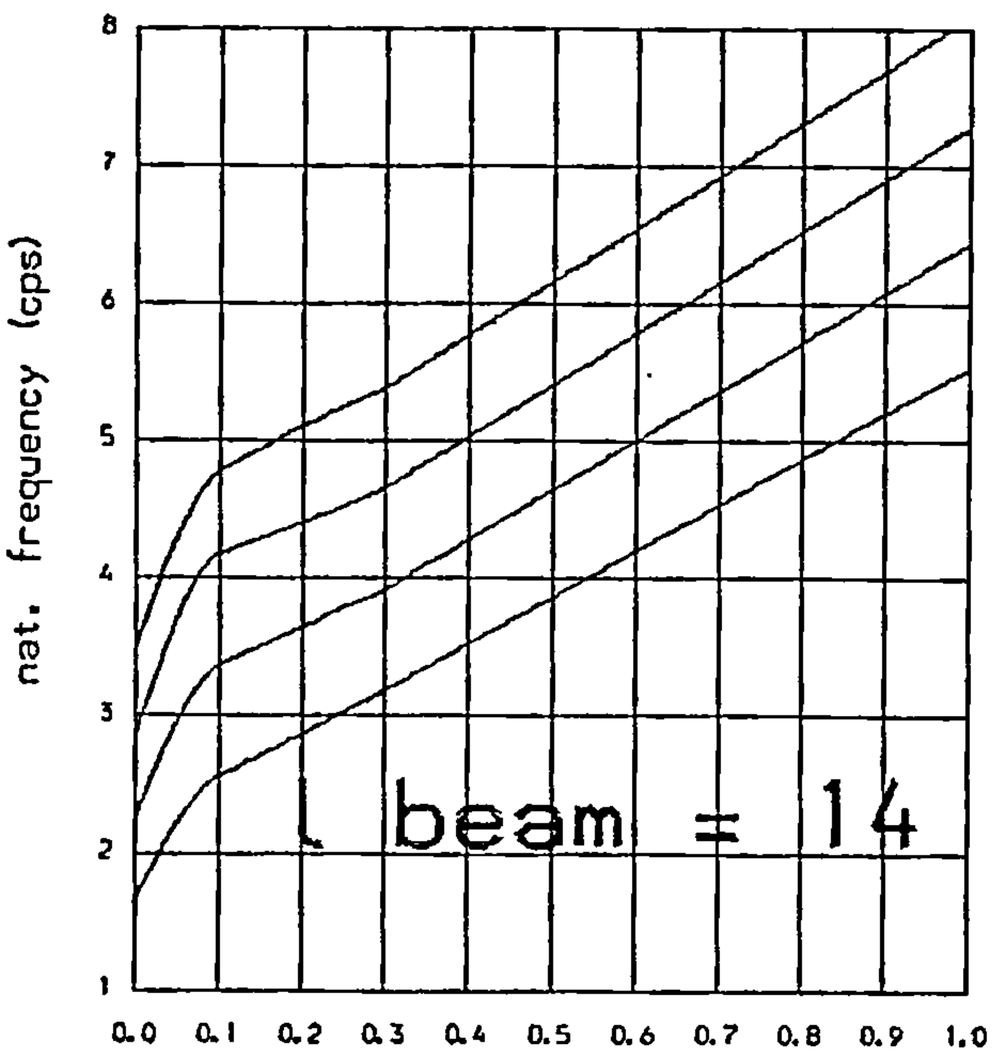

FIG. B.17

Variation of 3 rd. natural freqency with beam depth and wall width (DV) .

Total height	:	300 ft
Nb of storeys	:	30
Selfweight	:	yes
Extra story mass	:	4.kips

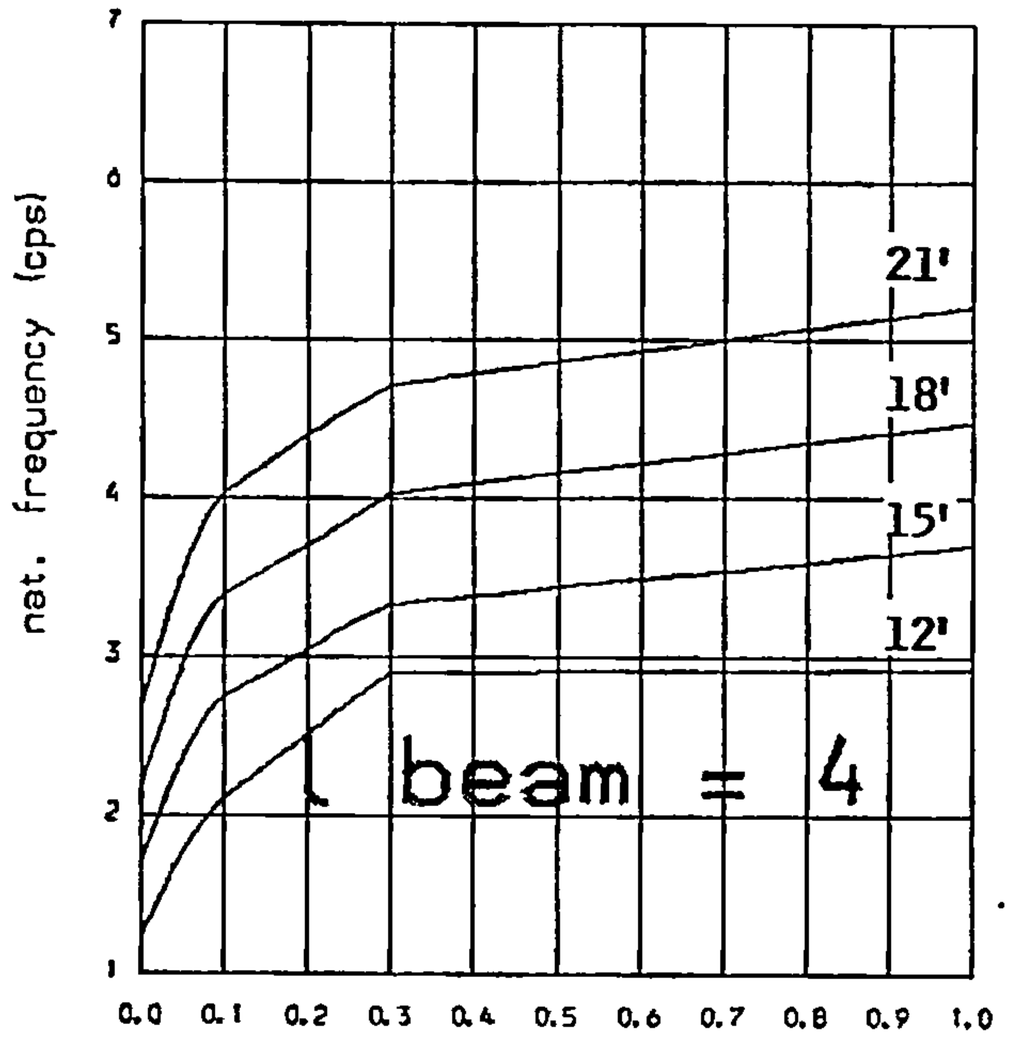

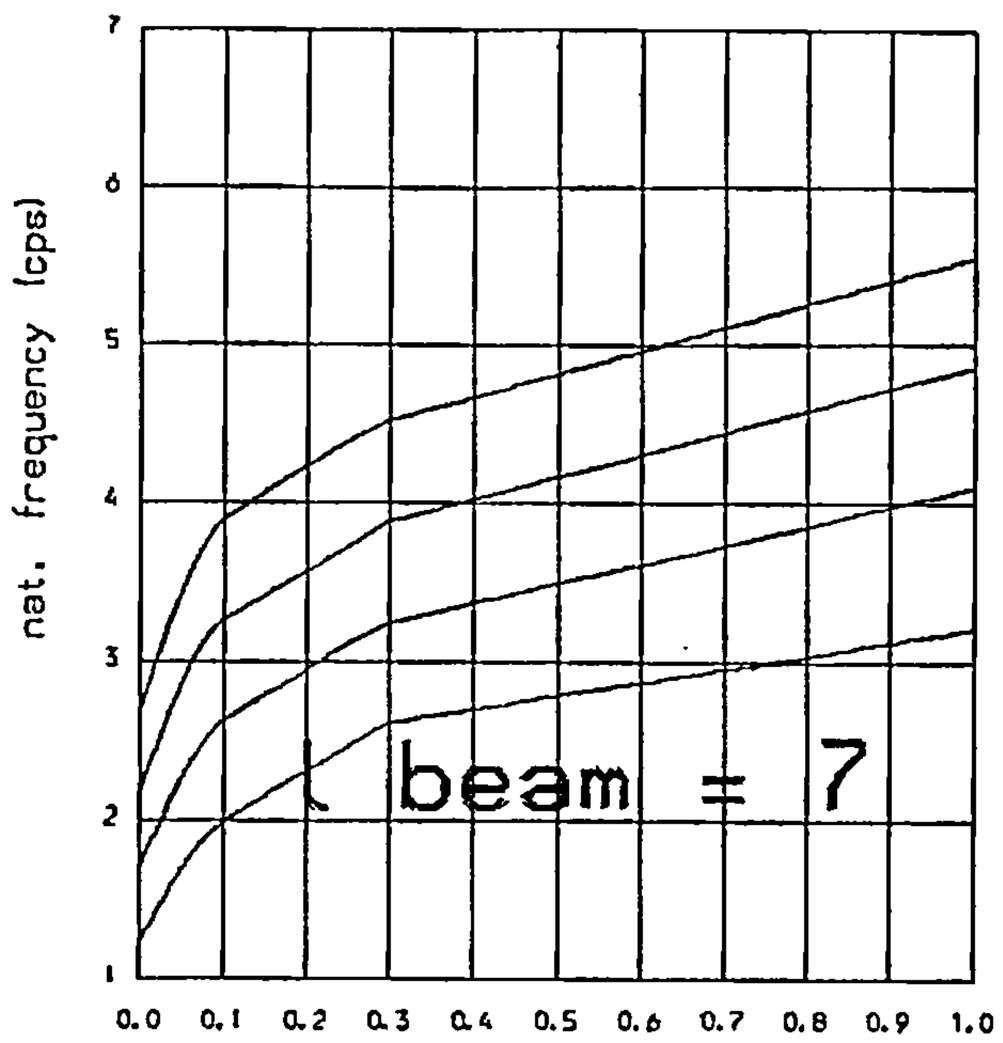

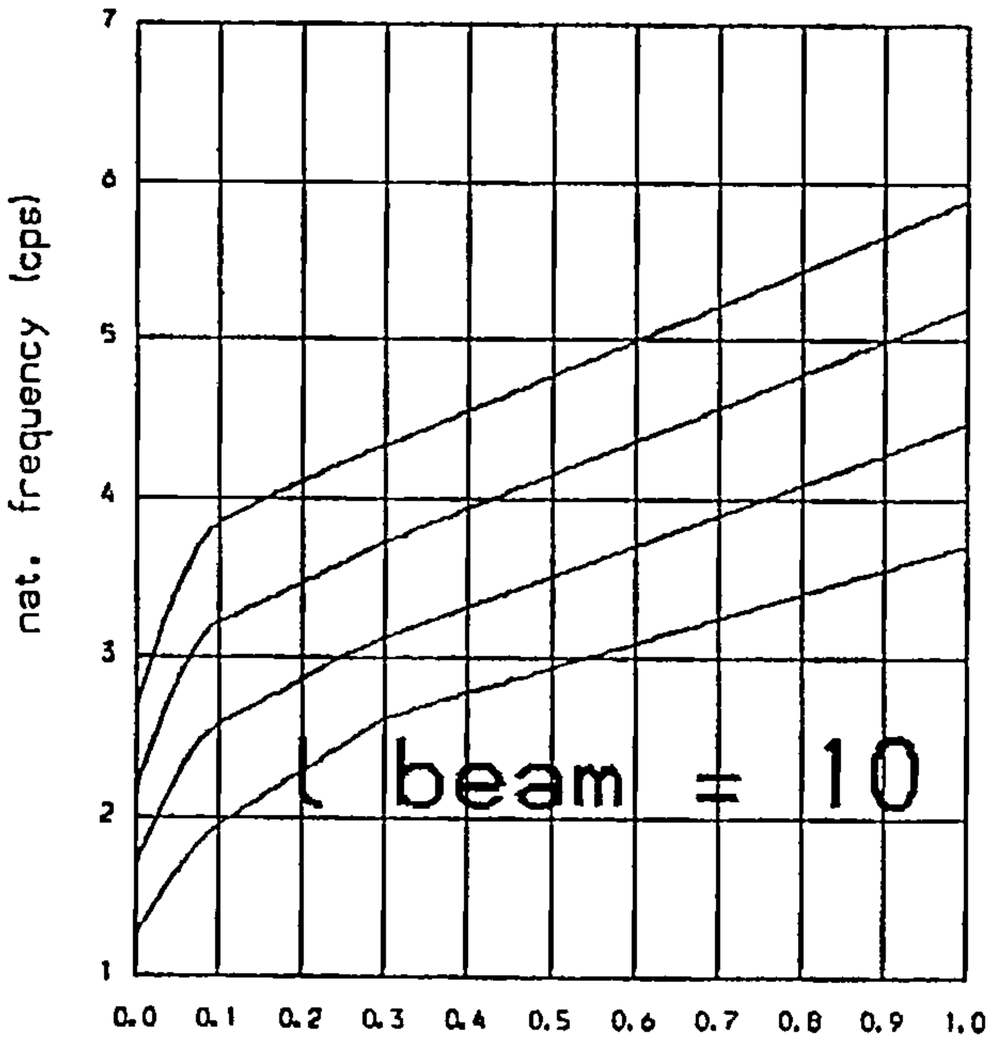

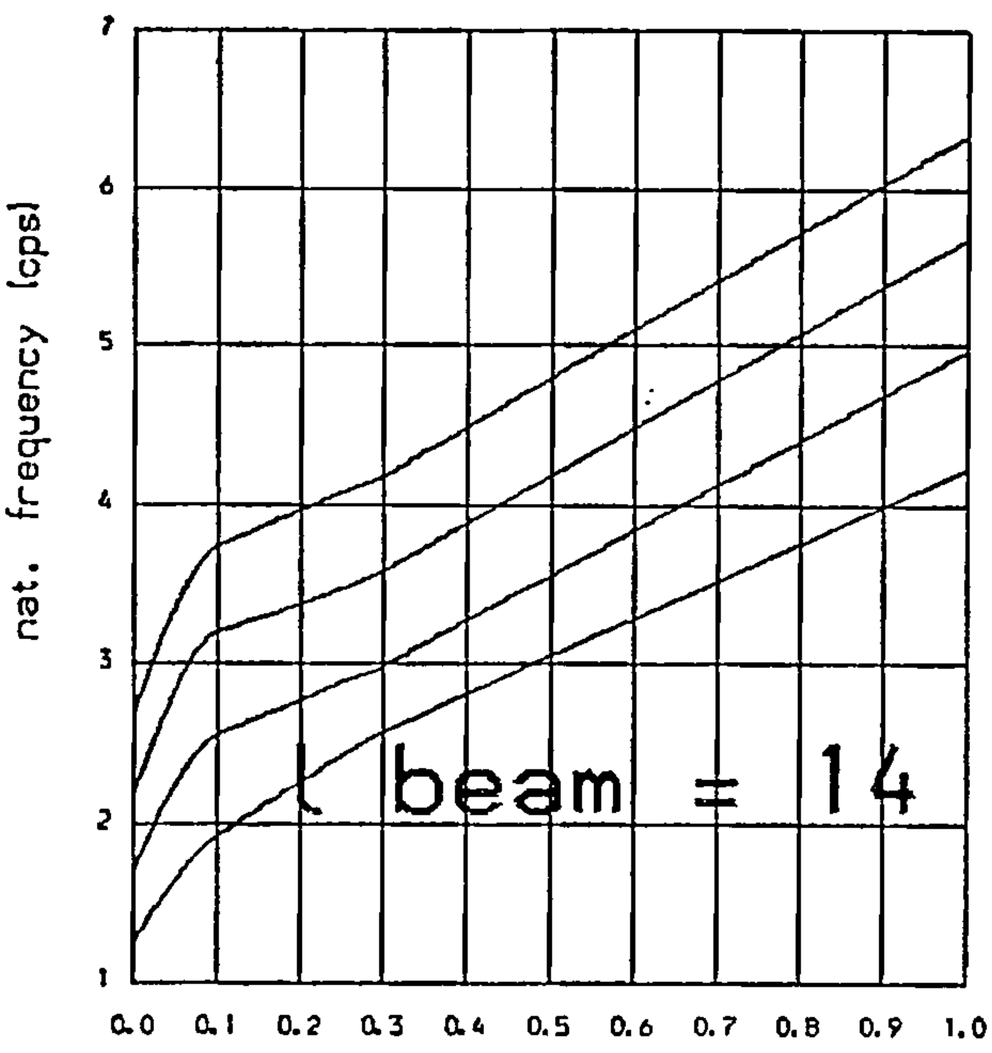

FIG. B.18

Variation of 3 rd. natural freqency with beam depth and wall width (DV) .

Total height	:	300 ft
Nb of storeys	:	30
Selfweight	:	yes
Extra story mass	:	8.kips

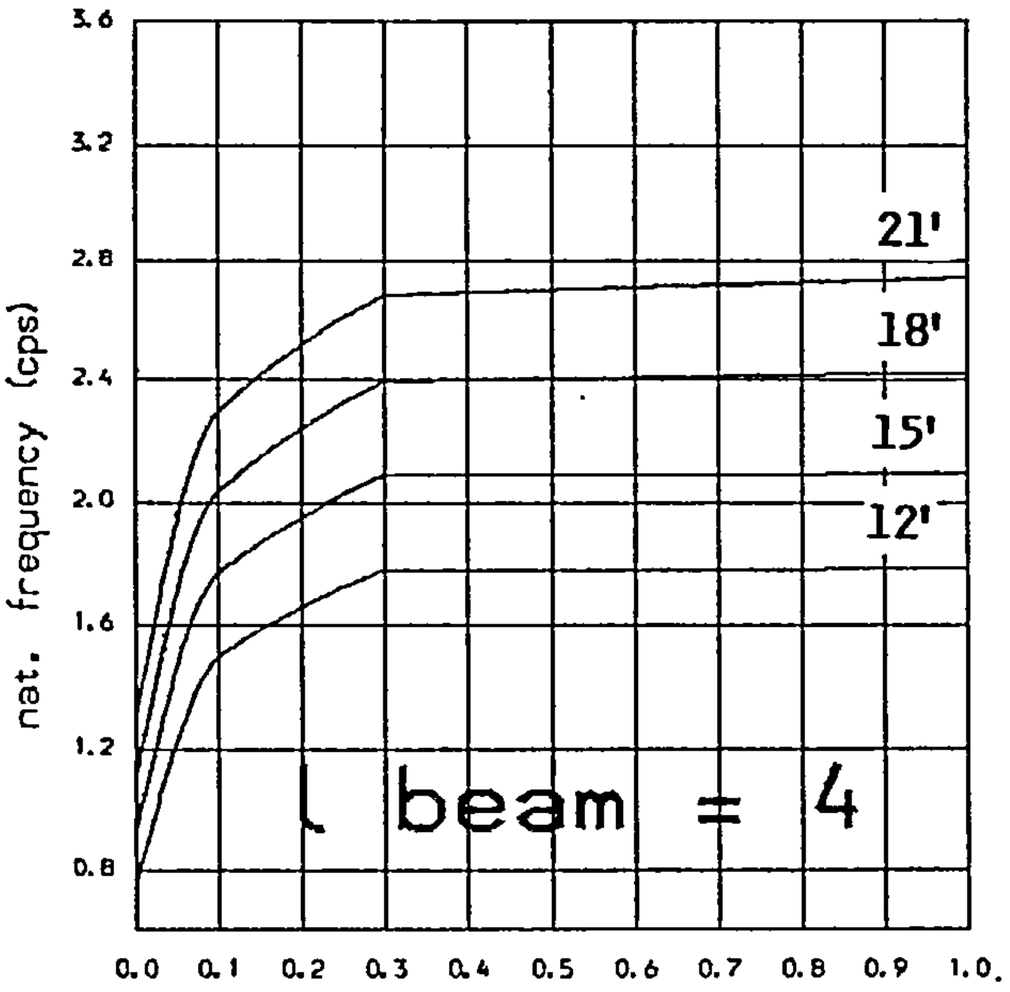

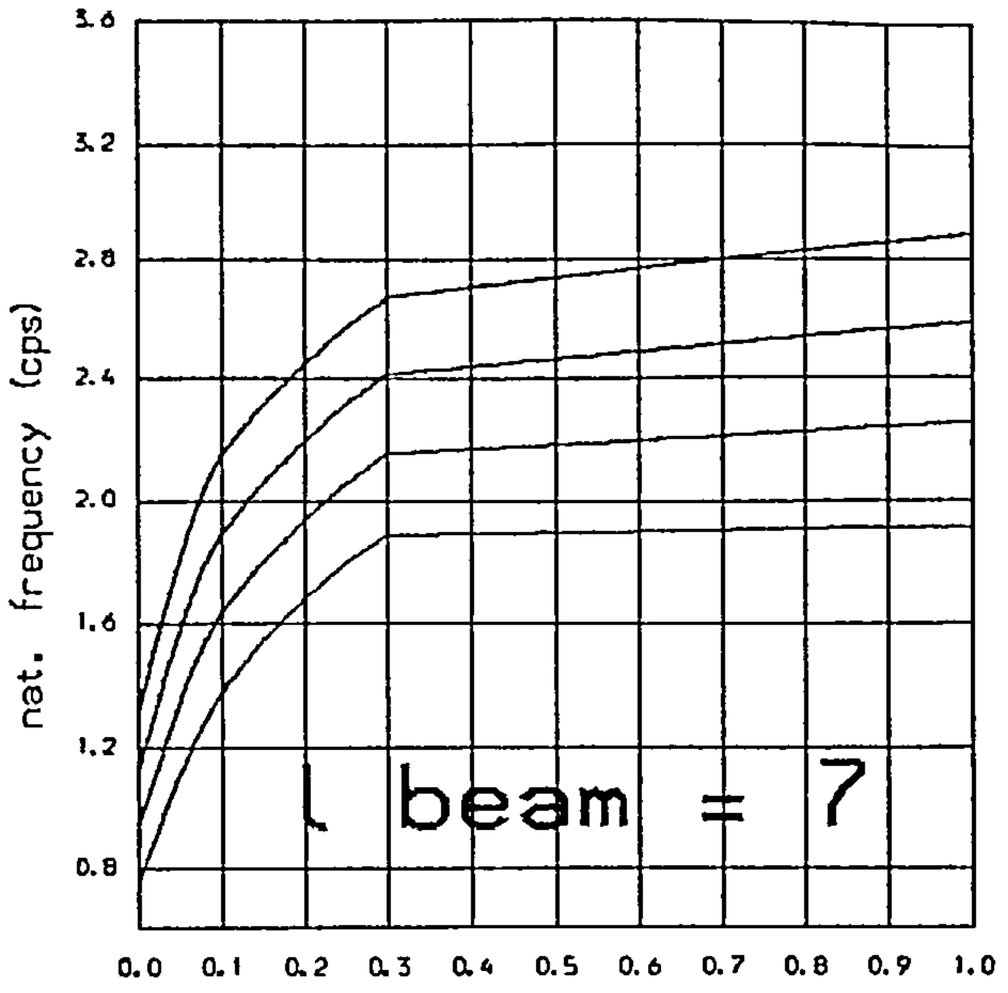

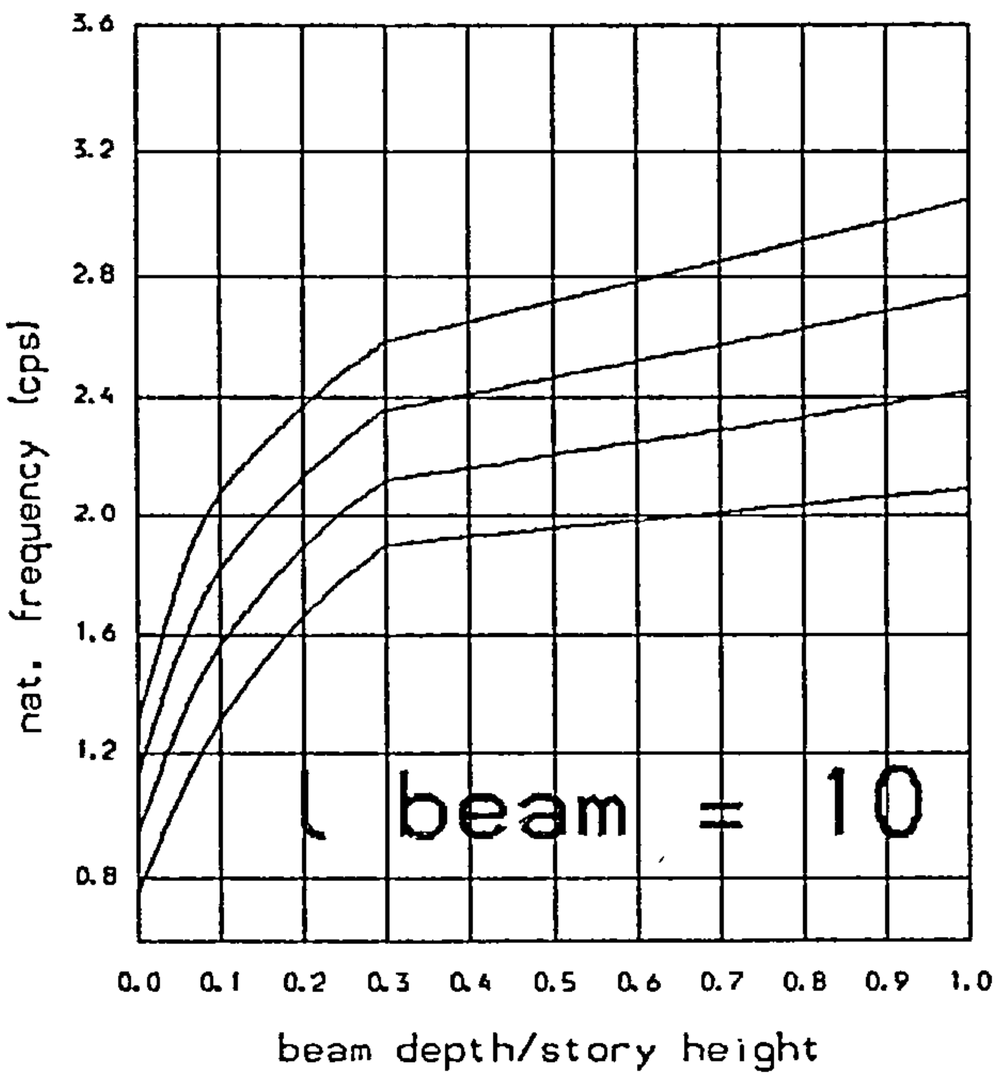

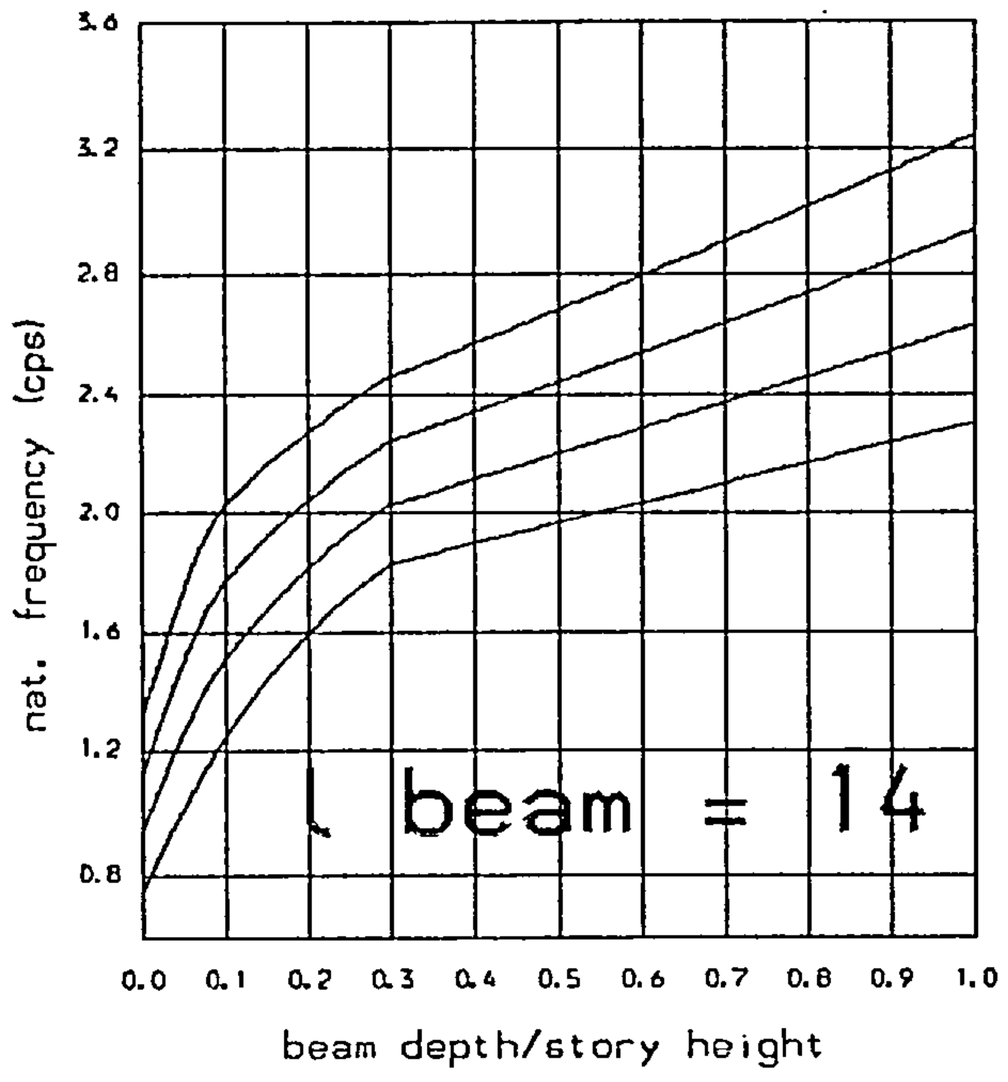

FIG. B.19

Variation of 2 nd. natural freqency with beam depth and wall width (DW) .

Total height : 400 ft
Nb of storeys : 40
Selfweight : yes
Extra story mass : none

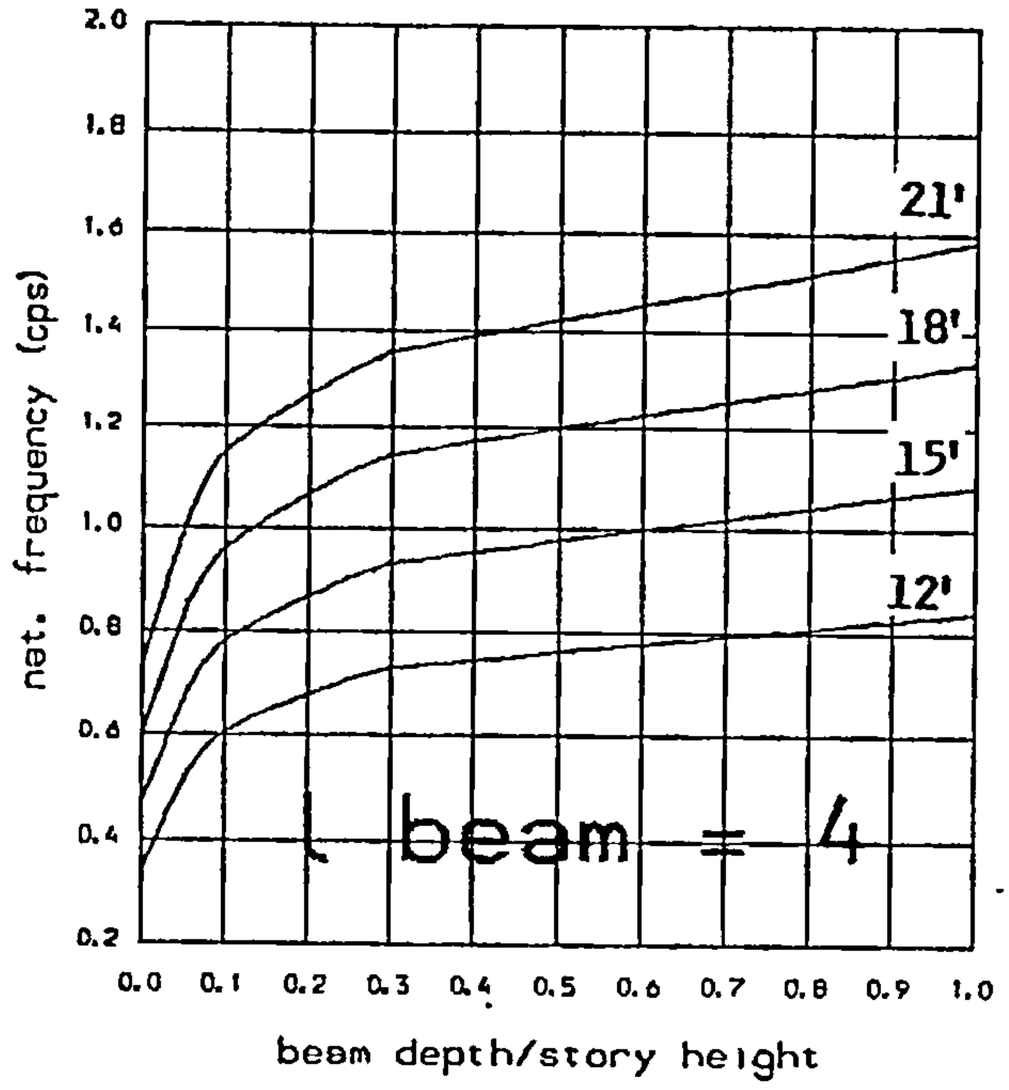

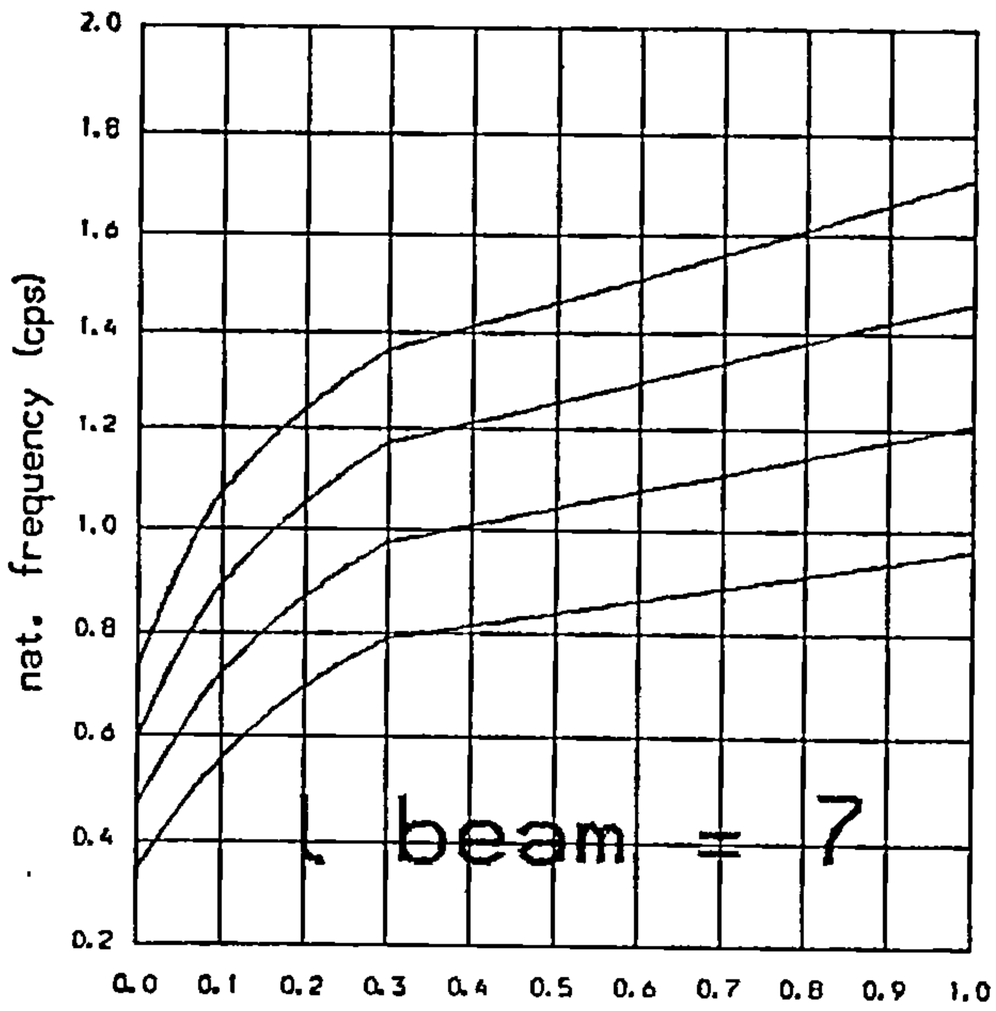

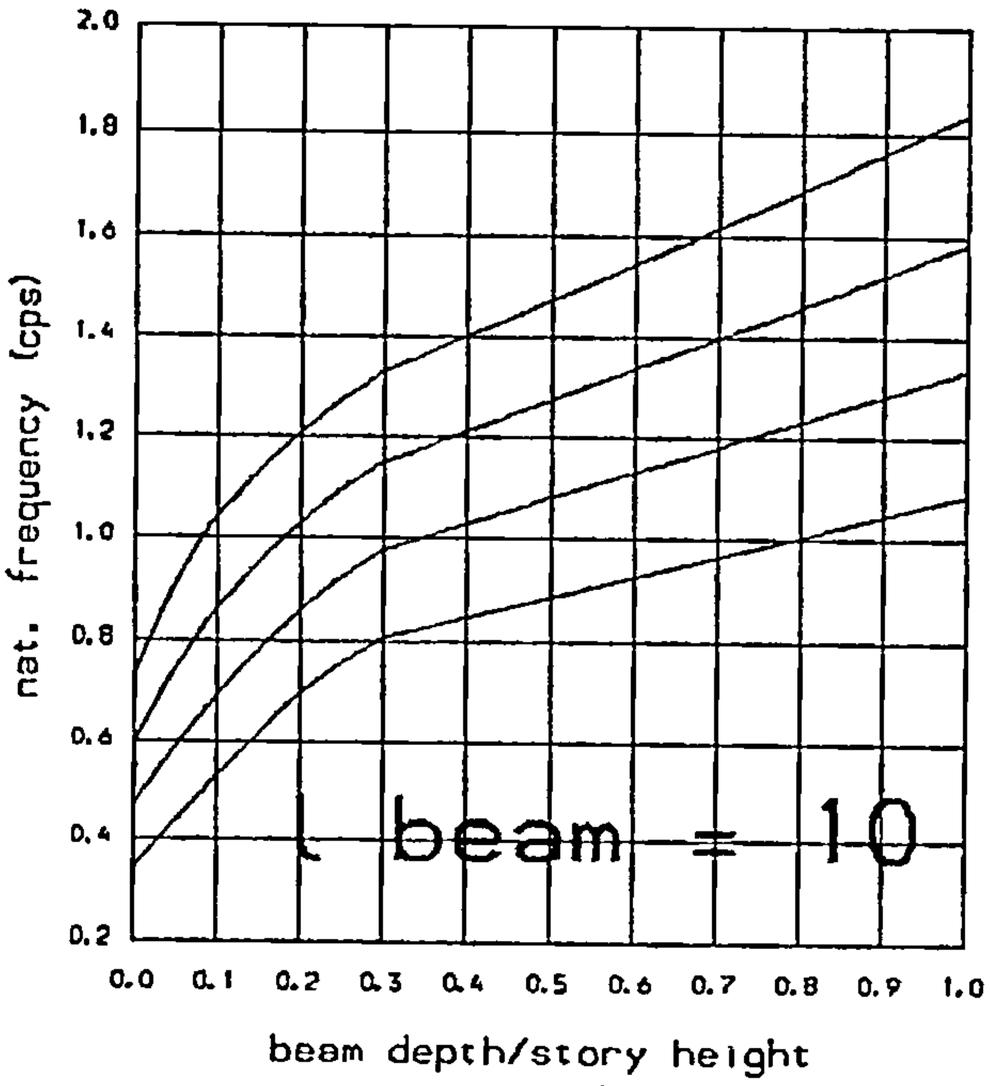

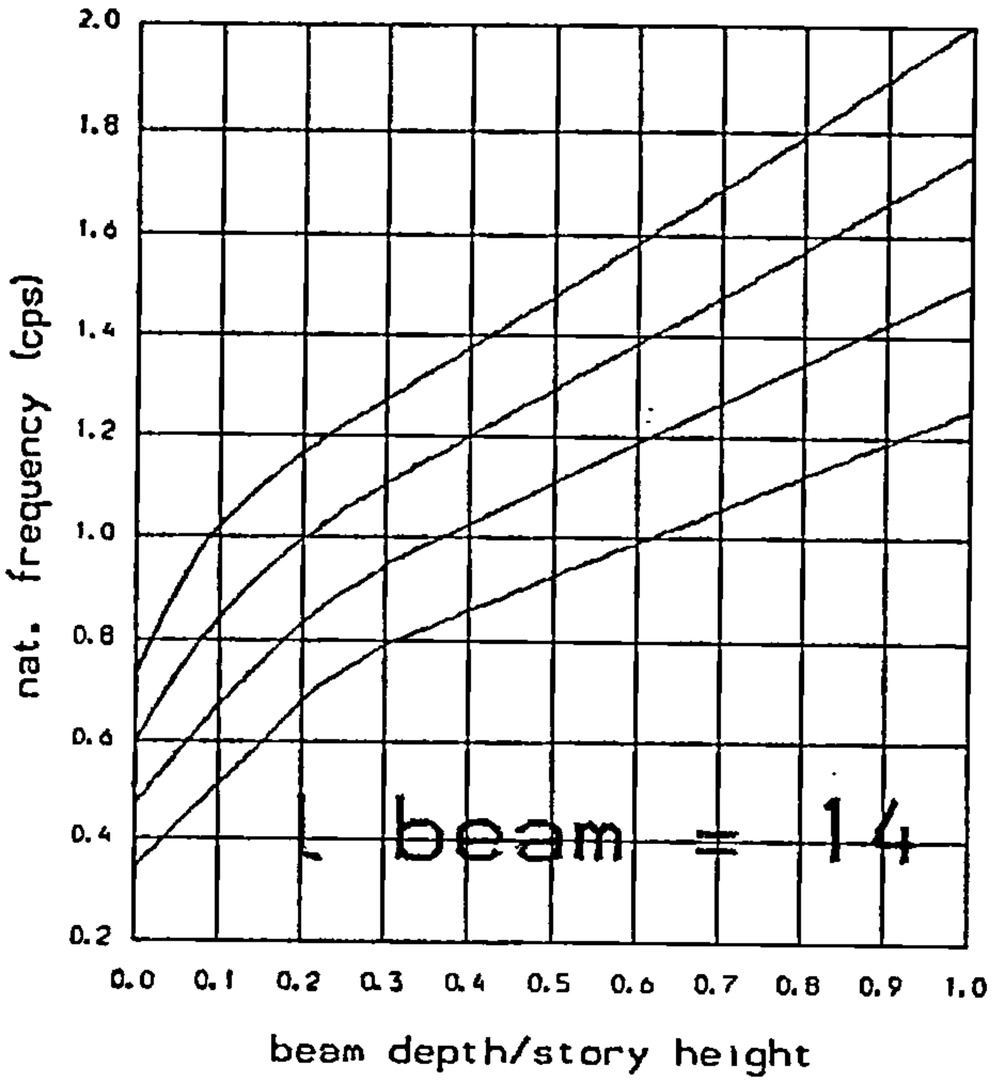

FIG. B.20

Variation of 2 nd. natural freqency with beam depth and wall width (DV) .

Total height	: 400 ft
Nb of storeys	: 40
Selfweight	: yes
Extra story mass	: 4.kips

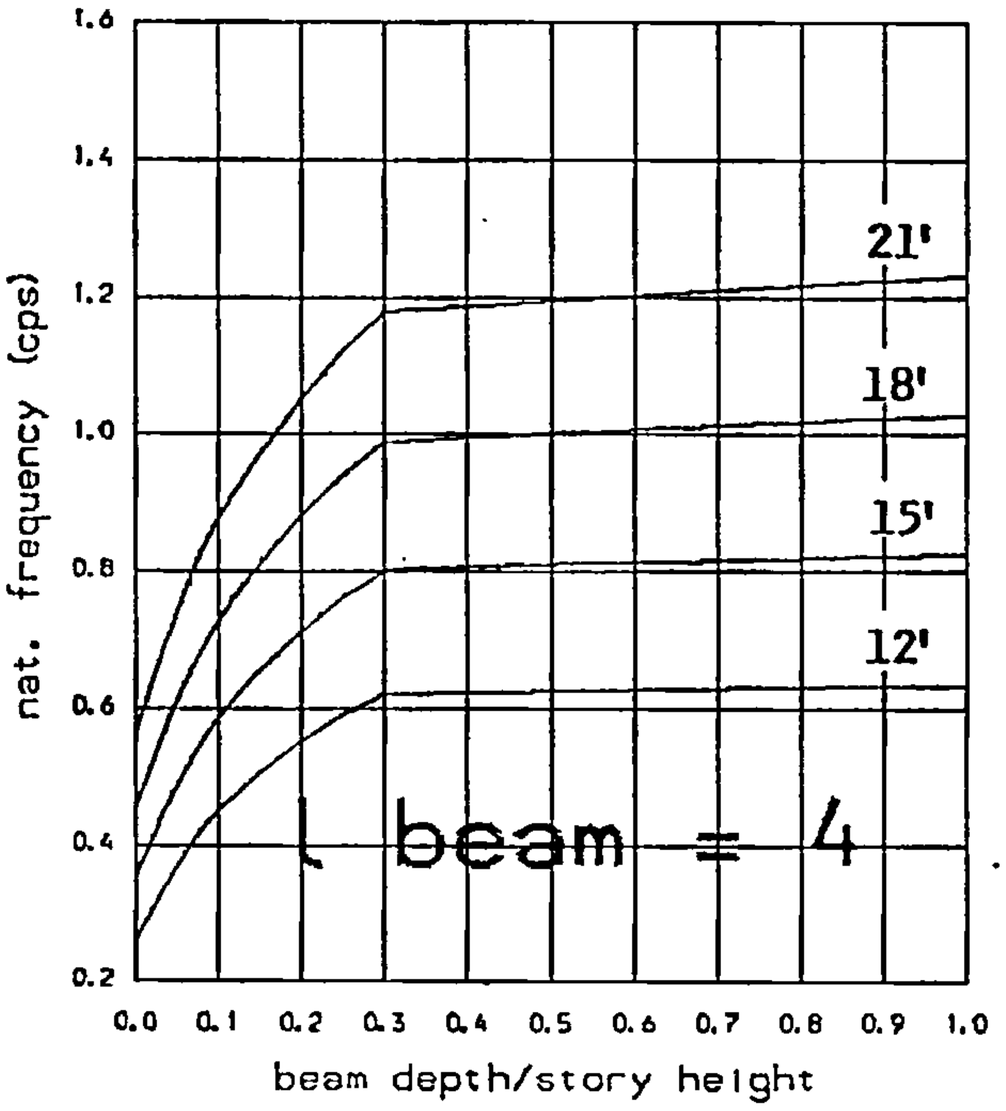

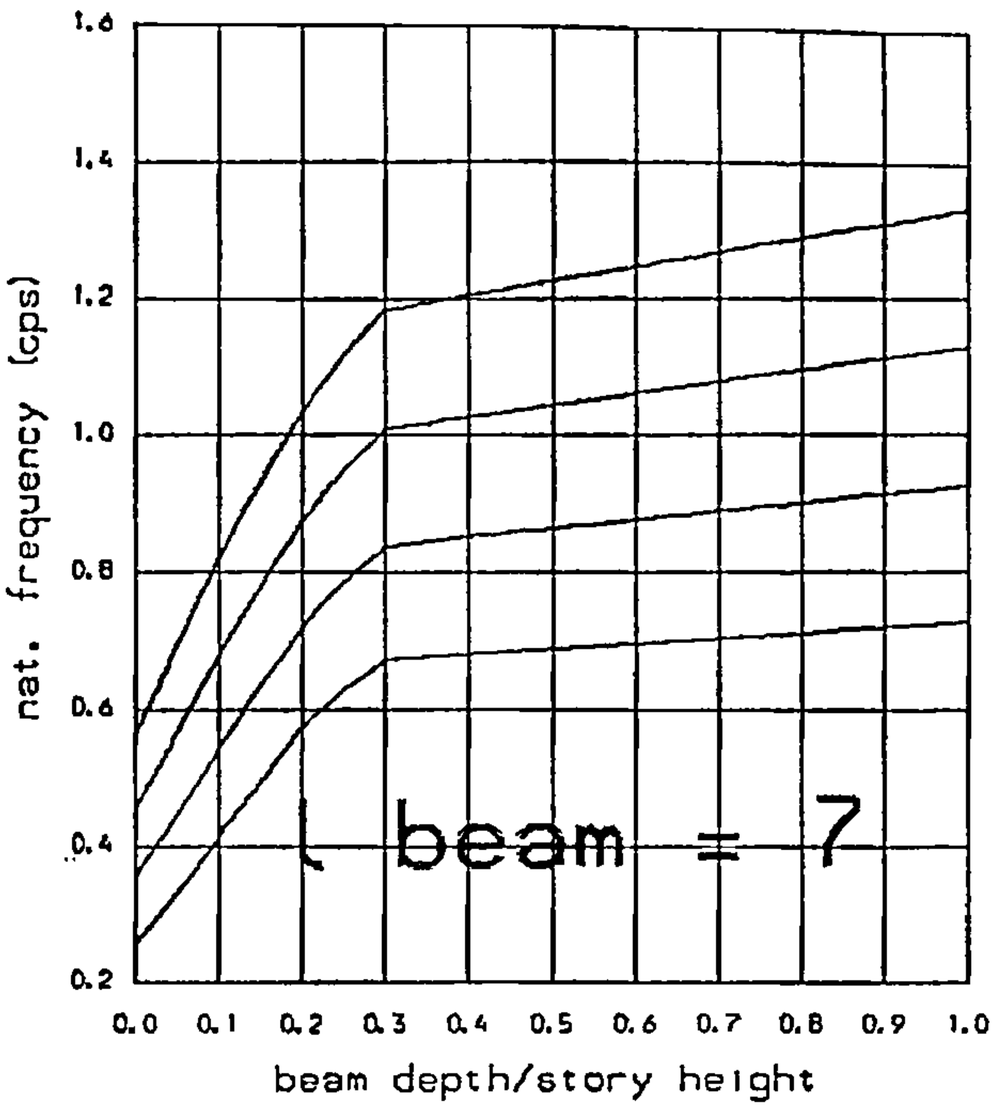

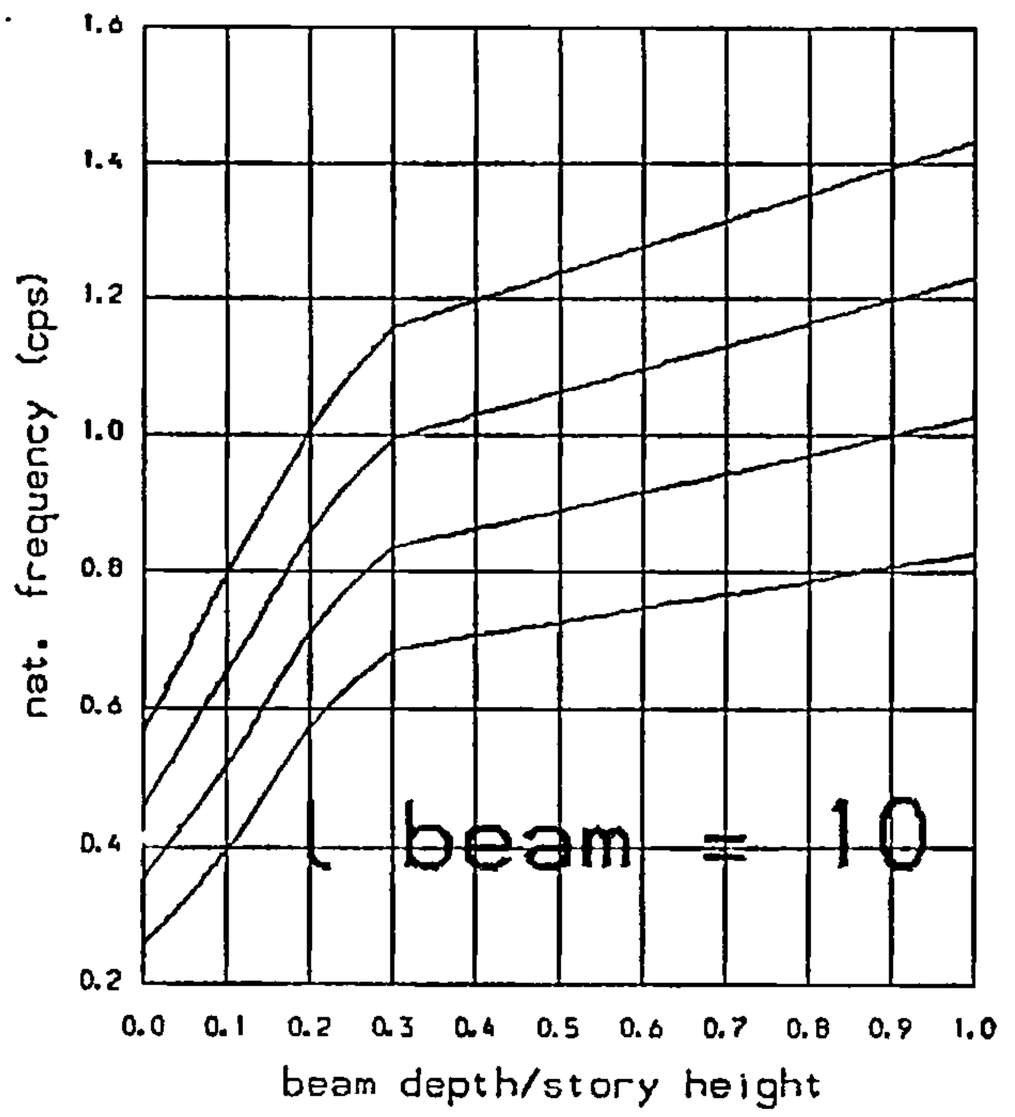

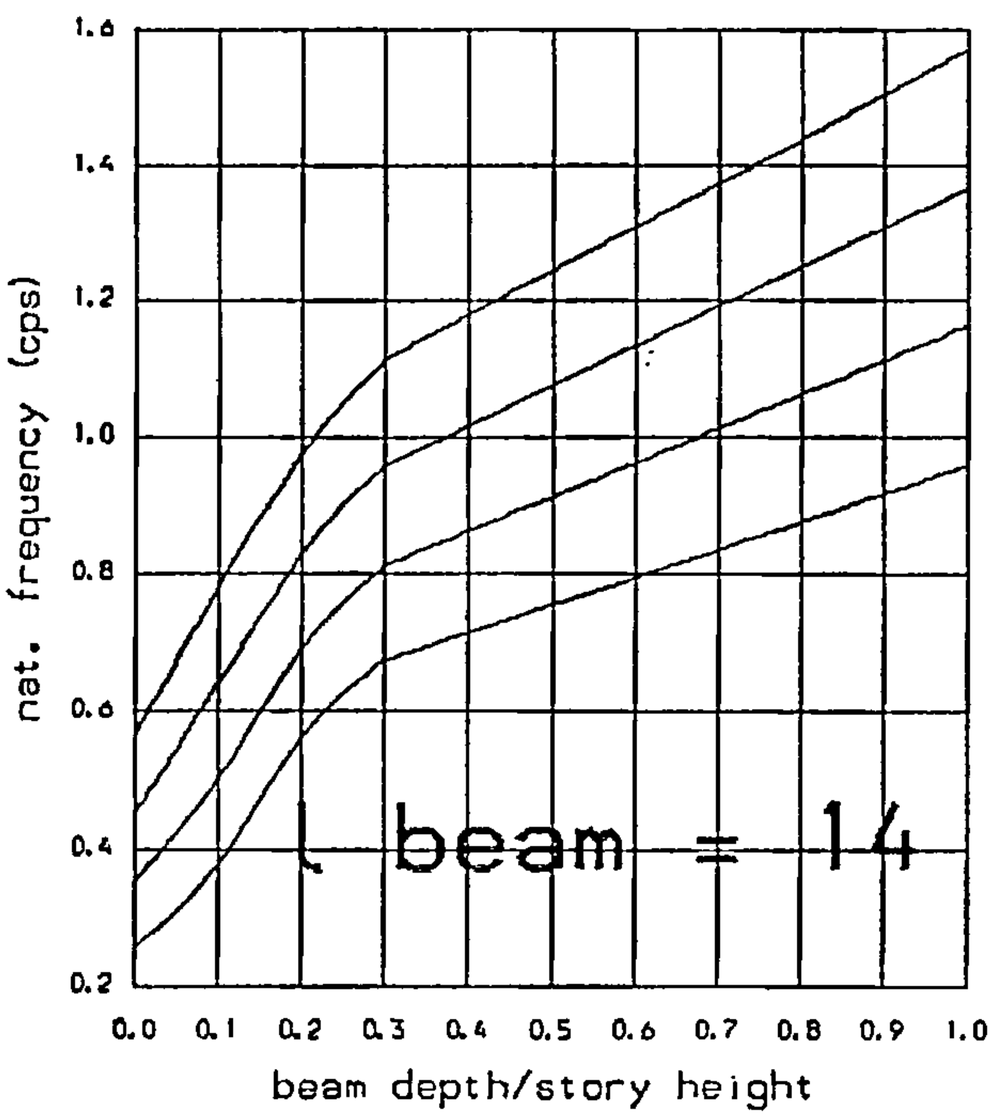

FIG. B.21

Variation of 2 nd. natural freqency with beam depth and wall width (DV) .

Total height	: 400 ft
Nb of storeys	: 40
Selfweight	: yes
Extra story mass	: 8.kips

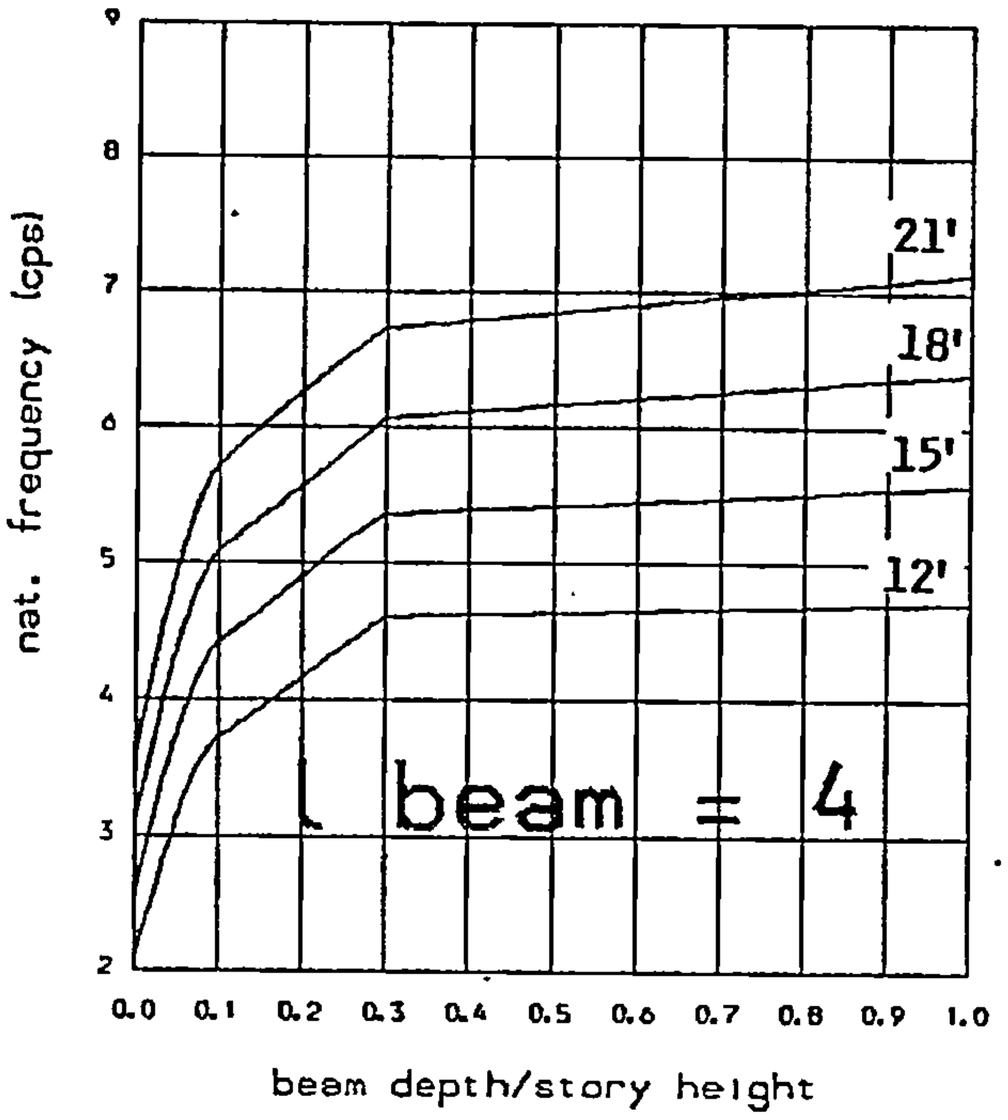

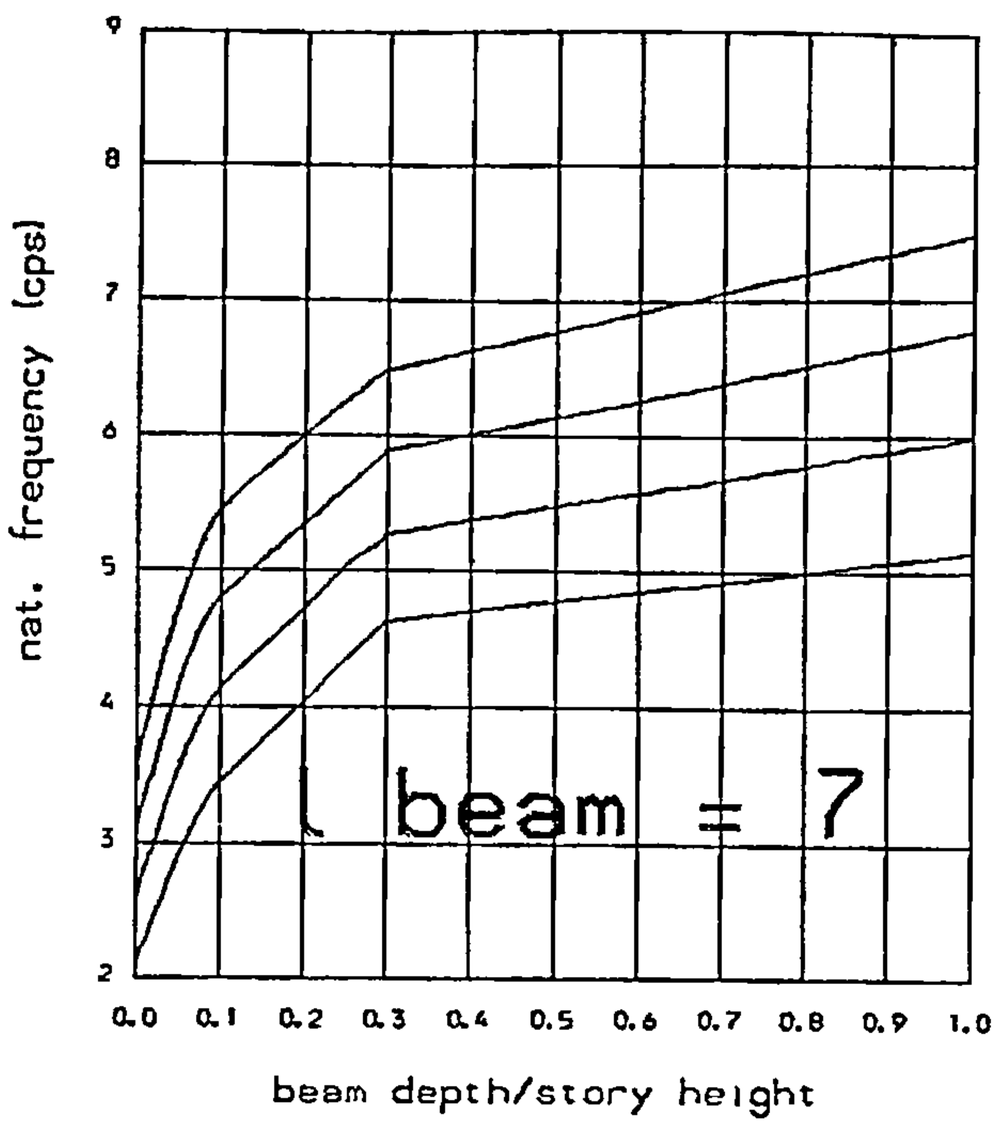

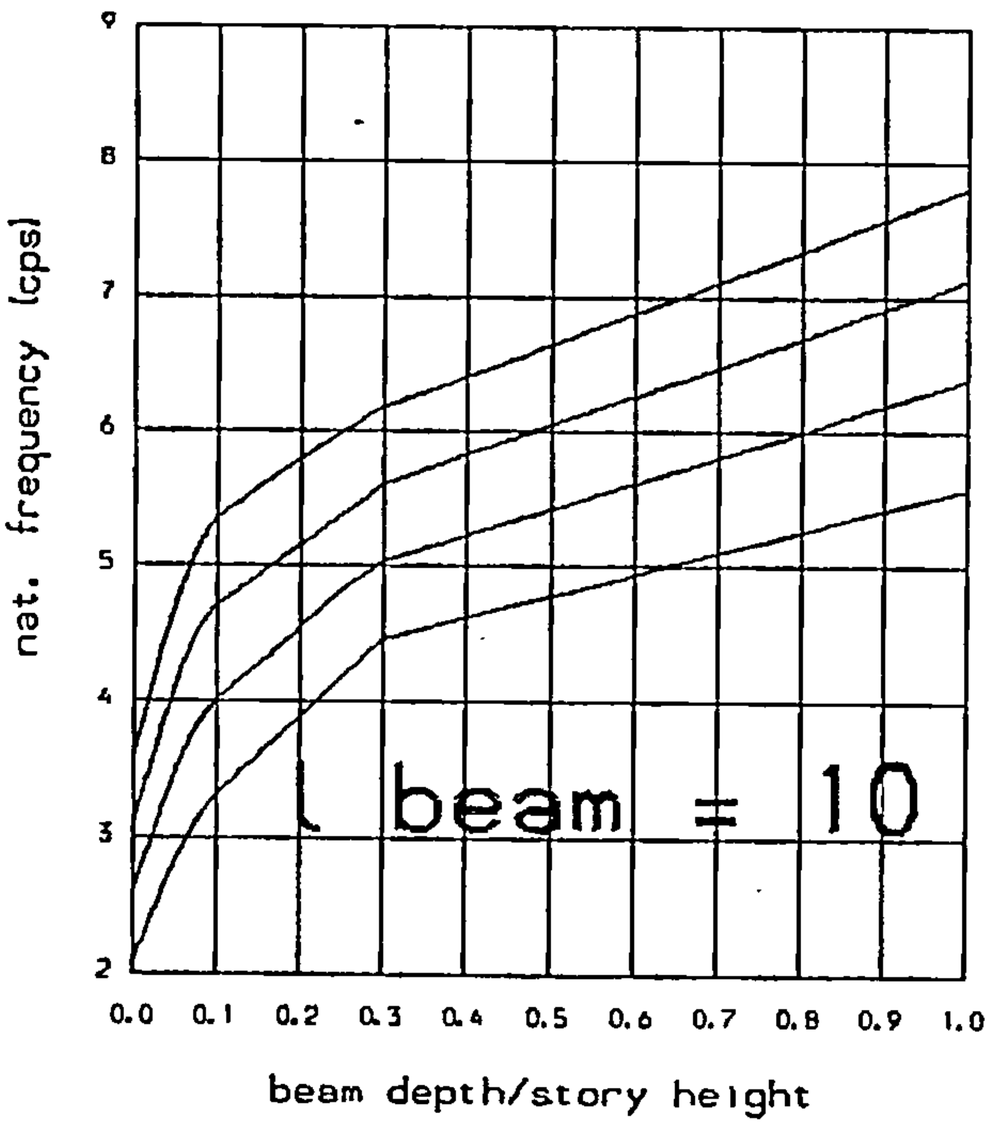

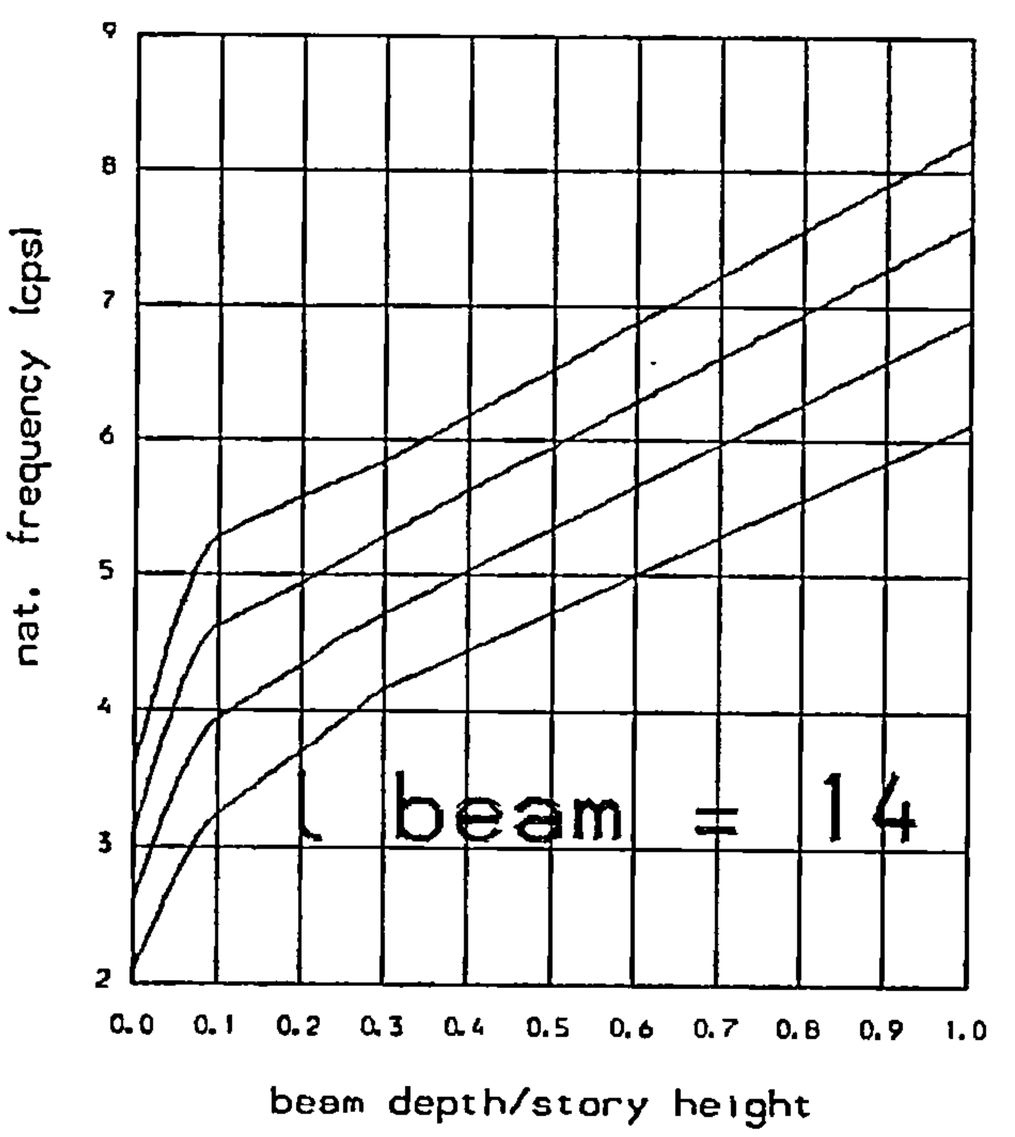

FIG. B.22

Variation of 3 rd. natural freqency with beam depth and wall width (DW) .

Total height	:	400 ft
Nb of storeys	:	40
Selfweight	:	yes
Extra story mass	:	none

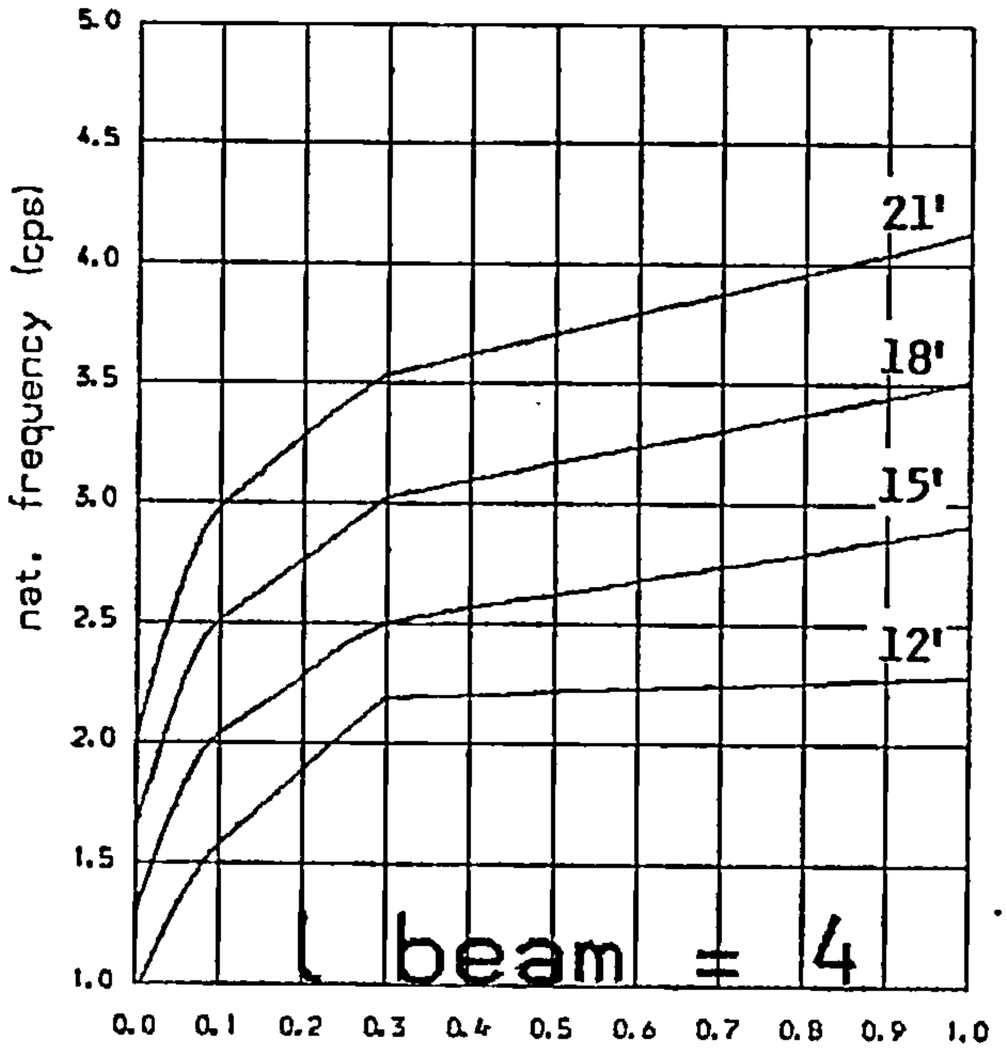

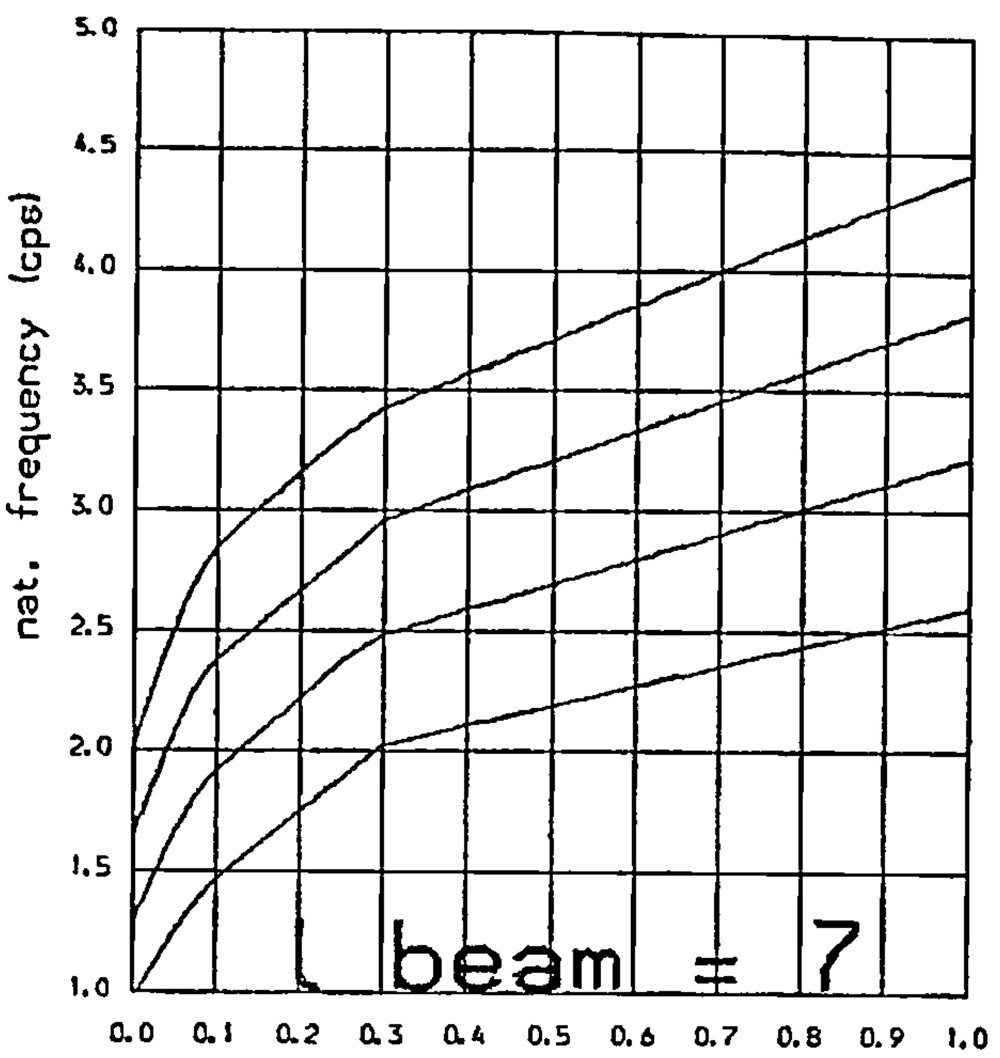

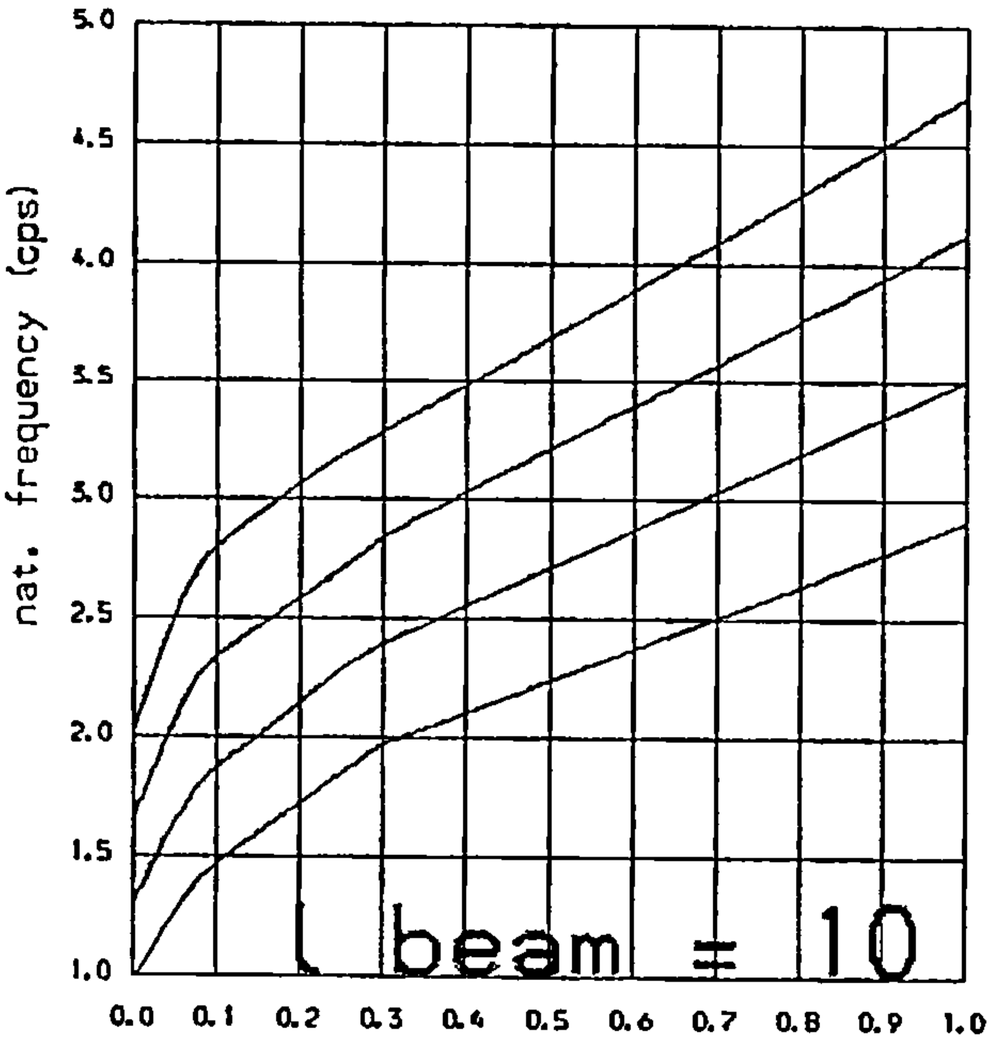

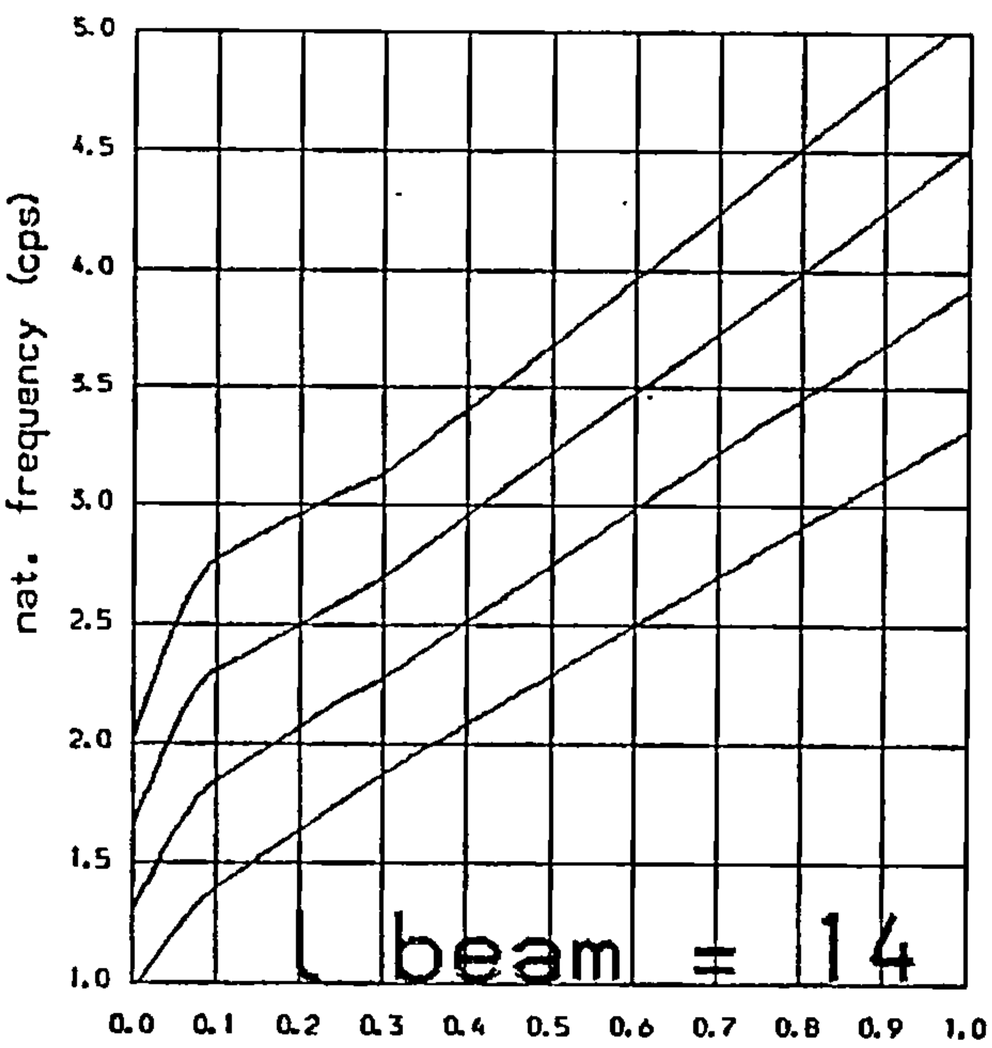

FIG. B.23

Variation of 3 rd. natural freqency with beam depth and wall width (DV) .

Total height	: 400 ft
Nb of storeys	: 40
Selfweight	: yes
Extra story mass	: 4.kips

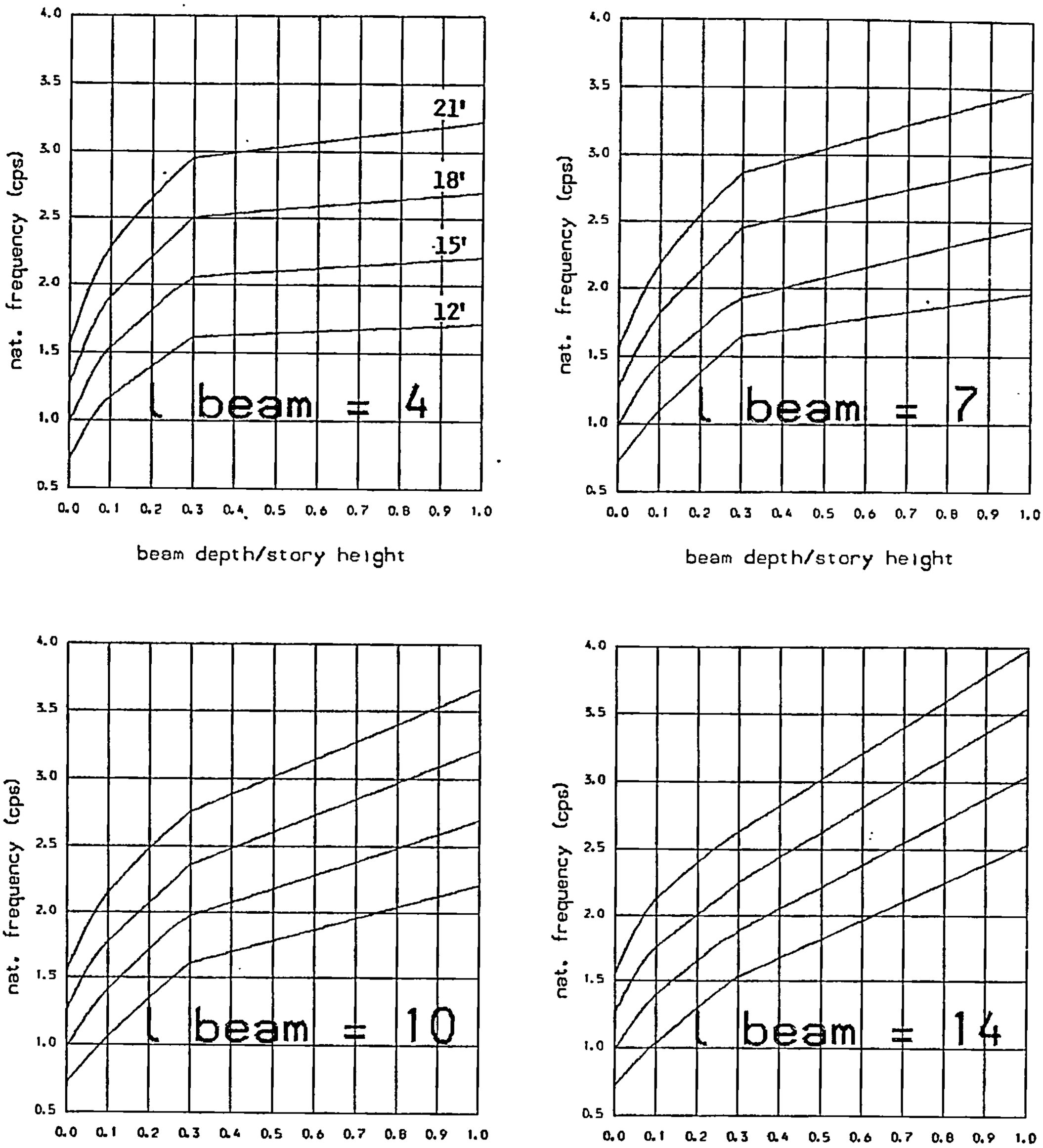

FIG. B.24	Total height	: 400 ft
Variation of 3 rd. natural	Nb of storeys	: 40
freqency with beam depth	Selfweight	: yes
and wall width (DV) .	Extra story mass	: 8.kips

C-1 COMPUTER PROGRAM FLOW CHART

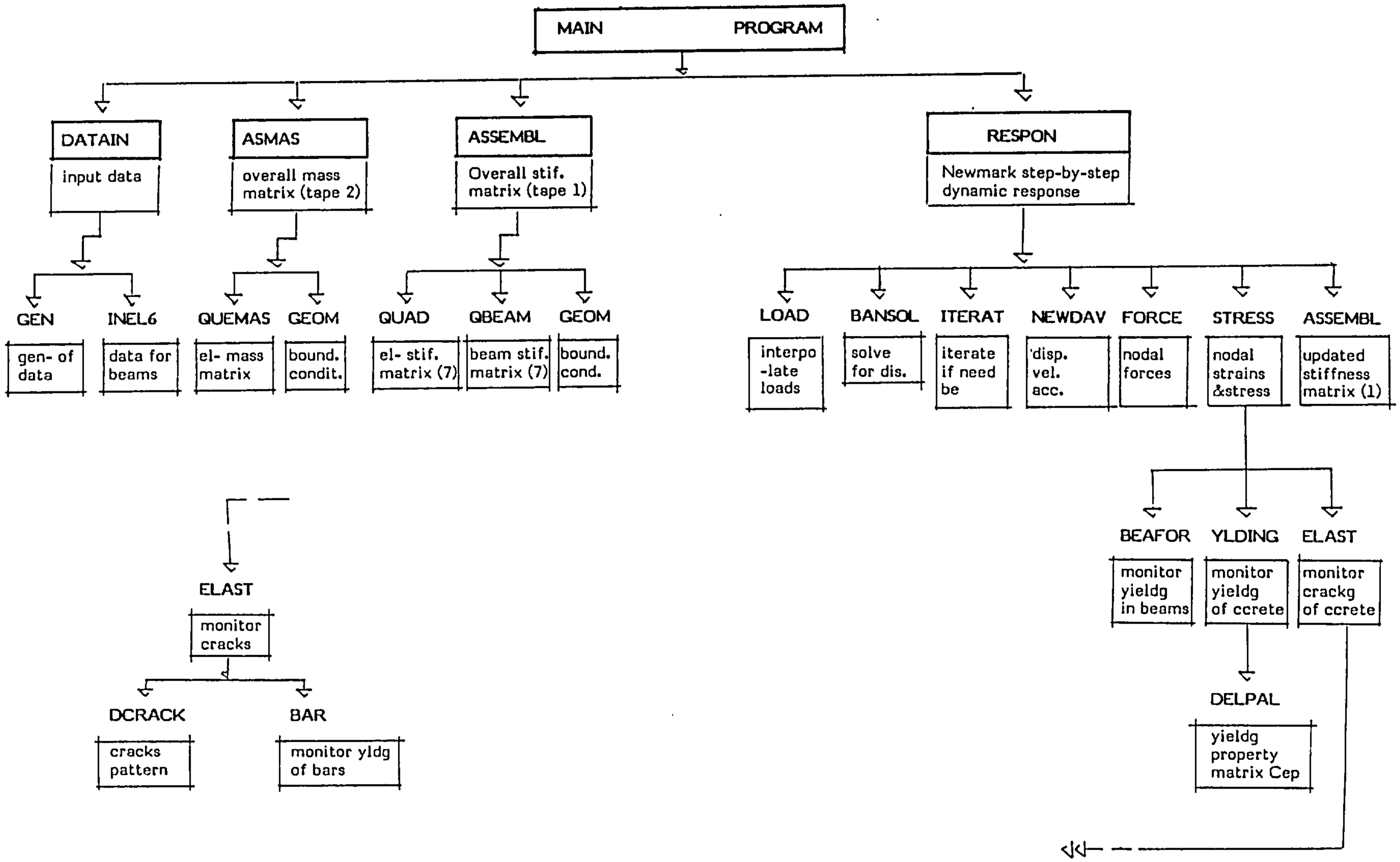

C-2 DESCRIPTION OF THE INPUT DATA

Card 1	(I5, 3X, 9A8)	Nb. and Title of the problem
Card 2	(4I5)	Control information card
	IPRINT	0 = none, 1 = print stiffness & mass matrices
	MODIF	0 = none, 1 = non conforming mode used
	NDYNAN	0 = static, 1 = dynamic
	NDFORS	0 = none, 1 = print forces & stresses
Card 3	(7I5)	Basic data
	NNP	Number of nodal points
	NEL	Total number of elements
	NEL2	number of beam elements
	NBOUN	Number of restrained elements
	NBODY	0 = None, 1 = Self weight included in y dir.
	NOPT	1 = plane strain, 2 = plane stress
	NMAT	Number of different materials
Card 4	(I10, 4F10.5)	Coordinates
	KODE(I)	1 = restrained in x-direction 2 = restrained in y-direction 3 = restrained in both directions
	X(I)	Node abscissa
	Y(I)	Node ordinate
	ULX(I)	Static load in x-direction
	VLY(I)	Static load in y-direction

Card 5	(6I5)	Element nodes, type and material
	IE(I,1)	First node of the element
	IE(I,2)	Second node of the element
	IE(I,3)	Third node of the element
	IE(I,4)	Fourth node of the element
	IE(I,5)	Material type
	IE(I,6)	1 = quadrilateral elment, 2 = Beam element
Card 6	(2F10.4)	Reinforcement
	PXX	Reinforcement ratio in x-direction
	PYY	Reinforcement ratio in y-direction
Card 7	(4F12.2)	Material properties (As many as NMAT)
	E	Young's modulus of concrete
	PR	Poisson's ratio of concrete
	RO	Mass density of concrete
	TH	Thickness of the elements
Card 8	(3F12.5, F15.2, F12.5)	Steel properties
	EPSY	Yield strain of steel
	EPSUL	Ultimate strain of steel
	SIGY	Yield stress of steel
	ES	Young's modulus of steel
	ESH	Modulus of steel at strain hardening

Card 9	(I5,3F10.0,3F5.0,2F10.0)	Omit if NEL2=0, Beam elemt property
	I	Stiffness pattern number beginning with 1
	FTYP(I,1)	EI, Flexural stiffness of the member
	FTYP(I,2)	EA, Axial stiffness of the member
	FTYP(I,3)	GA, Shear stiffness of the member
	FTYP(I,4)	Flexural stiffness factor k_{ii}
	FTYP(I,5)	Flexural stiffness factor k_{jj}
	FTYP(I,6)	Flexural stiffness factor k_{ij}
	FTYP(I,7)	Strain hardening ratio at node i
	FTYP(I,8)	Strain hardening ratio at node j
Card 10	(I5, 7F10.0)	Omit if NEL2=0, Hinge properties
	ITP	Stiffness pattern number beginning with 1
	FTYP(I,9)	Hinge stiffness at node i
	FTYP(I,10)	Hinge stiffness at node j
	FTYP(I,11)	α_i, unloading parameter for end i
	FTYP(I,12)	α_j, unloading parameter for end j
	FTYP(I,13)	β_i, loading parameter for end i
	FTYP(I,14)	β_j, loading parameter for end j
Card 11	(I5, 5X, 2F10.0)	Omit if NEL2=0, Yielding Moments
	K	Yielding surface number
	BMMY(1)	Yield moment at first end
	BMMY(2)	Yield moment at second end
Card 12	(2I5)	Mass codes
	KMAS	0 lumped, 1 consistent mass assumed
	NSEC	Number of external mass patterns

Card 13	(4(2I5, F8.3)	Omit if NSEC = 0, (as many as NSEC)
	LUM(1)	Starting node where the mass is to be applied
	LUM(2)	Ending node where the mass is to be applied
	EXMAS	Value of the external mass
Card 14	(6I5)	Basic dynamic data
	INT	0 = initial disp. and derivatives all zero 1 = initial disp. and velocity are given. 2 = initial disp. and derivatives all given
	NPRINT	Nb. of steps after which results to be printed
	NSTEP	Total number of steps
	MAXSTEP	Maximun number of steps
	NTYP	0 = Force function, 1 = Earthquake accelerogram
	NP	Number of loading pairs
Card 15	(5F8.5, F10.5)	
	C1	Damping constant for mass matrix
	C2	Damping constant for stiffness matrix
	DELT	Operator factor, usually 0
	DT	Time increment
	TIME	Initial time
	GACC	Acceleration of gravity
Card 16	(3F10.4)	Concrete strength
	EPSLIM	Minimum strain after which concrete crushes
	YIELD	Compressive strength of concrete
	SIGMI1	Tensile strength of concrete

Card 17	(3I5)		
		NFIX	Number of fixed points
		NVEC	10 = x-component only 01 = y-component only 11 = x-component and y-component
		MSPAC	Nb. of steps after which results are printed
Card 18	(2F10.4)		Acc. record (as many as NP)
		P(1,K)	Time
		P(2,K)	Acceleration in g units

COMPUTER PROGRAM LISTING

```
C*****************************************************************
C                                                                *
C  NONLINEAR ANALYSIS OF COUPLED SHEAR VALLS SUBJECTED           *
C  TO EARTHQUAKE FORCES BY THE FINITE ELEMENT METHOD.            *
C                                                                *
C*****************************************************************
      COMMON/DATA/ NNP,NEL,NMAT,NOPT,NBODY,KMAS,MODIF,NEL2
      COMMON/THREE/R(200),AK(200,40)
      COMMON/DISP/X(100),Y(100),ULX(100),VLY(100),
     *KODE(100)
      COMMON/NODE/IE(60,6)
      COMMON/STEEL/PX(80),PY(80)
      COMMON/PROTY/E(4),PR(4),RO(4),TH(4)
      COMMON/TWO/IBAND,NEQ
      DIMENSION TITLE(9)
      DEFINE FILE 3(200,64,L,I5),7(200,512,L,K6)
      DEFINE FILE 8(200,1152,L,III)
C     DATA STAR /1H*/
      DATA MAXEL,MAXNP,MAXMAT,MAXBV / 80,100,4,40 /
   10 READ(5,11) NPROB,(TITLE(I),I=1,9)
   11 FORMAT(I5,3X,9A8)
      IF(NPROB.LE.0) GOTO49
      VRITE(6,12) NPROB,(TITLE(I),I=1,9)
   12 FORMAT(/8HIPROBLEM,I5,3H  .,9A8)
      READ(5,13) IPRINT,MODIF,NDYNAN,NDFORS
   13 FORMAT(4I5)
      IF(MODIF.NE.0) VRITE(6,14)
   14 FORMAT(/10X,'***NON-CONFORMING**'/)
C
C  INPUT ALL THE STRUCTURE INFORMATION
C
      CALL DATAIN (MAXEL,MAXNP,MAXMAT,ISTOP)
      MAXDOF=2*MAXNP
      MAXDIF=0
      DO 20 I=1,NEL
      DO 20 J=1,4
      DO 20 K=1,4
      LL=IABS(IE(I,J)-IE(I,K))
      IF(LL.GT.MAXDIF) MAXDIF=LL
   20 CONTINUE
      IBAND=2*(MAXDIF+1)
      NEQ=2*NNP
      IF(IBAND.GT.MAXBV) GOTO 39
      IF(ISTOP.GT.0) GOTO 49
      N1=0
C
C    FORM STIFFNESS MATRIX
C
      CALL ASEMBL(ISTOP,MAXEL,MAXNP,MAXDOF,MAXBV,N1)

      IF(ISTOP.GT.0) GOTO 49
      IF(IPRINT.EQ.0) GOTO 76
      VRITE(6,82)
      DO75I=1,NEQ
      VRITE(6,78) I
      VRITE(6,79) (AK(I,J),J=1,IBAND)
   75 CONTINUE
   76 CONTINUE
C
C  FORM MASS MATRIX
C
  103 FORMAT(////15X,'*****ERROR******')
      CALL ASEMAS(ISTOP,R,AK,MAXDOF,MAXBV,X,Y,KODE,MAXNP,MAXEL)
      IF(ISTOP.GT.0) VRITE(6,103)
      IF(ISTOP.GT.0) GO TO 49
      IF(IPRINT.EQ.0) GOTO 90
      VRITE(6,83)
      DO80I=1,NEQ
      VRITE(6,78) I
      VRITE(6,79) (AK(I,J),J=1,IBAND)
   80 CONTINUE
   78 FORMAT( I5,'XXXX NEW LINE ******************************
     ************************************************')
   79 FORMAT( 5X,10E10.3)
   82 FORMAT( //10X,'***** STIFFNESS MATRIX *****' // )
   83 FORMAT( //10X,'XXXXX MASS MATRIX *****'//)
   90 CONTINUE
C
C  COMPUTE NODAL RESPONSES
C
      CALL RESPON(AK,R,KMAS,MAXDOF,MAXEL,MAXNP,NEQ,IBAND,NEL,MAXBV)
   39 VRITE(6,40)IBAND,MAXBV
   40 FORMAT(///'BANDWIDTH=',I5,'EXCEEDS MAX=',I5/)
   49 STOP
      END
C
C  ASSEMBLE OVERALL STIFFNESS MATRIX AND STORE IN TAPE 7
C
      SUBROUTINE ASEMBL(ISTOP,MAXEL,MAXNP,MAXNEQ,MAXBV,N1)
      COMMON/DATA/ NNP,NEL,NMAT,NOPT,NBODY,KMAS,MODIF,NEL2
      COMMON/THREE/ R(200),AK(200,40)
      COMMON/DISP/X(100),Y(100),ULX(100),VLY(100),KODE(100)
      COMMON/NODE/IE(80,6)
      COMMON/STEEL/PX(80),PY(80)
      COMMON/PROTY/E(4),PR(4),RO(4),TH(4)
      COMMON/TWO/IBAND,NEQ
      DIMENSION LP(8),OK(12,12),O(8),OKV(64)
      ISTOP=0
      DO 2 I=1,NEQ
      R(I)=0.0
      DO 2 J=1,IBAND
    2 AK(I,J)=0.0
      TAREA=0.0
      NEL1=NEL2
      DO 10 M=1,NEL
      IF(IE(M,5).GT.0) GOTO 11
      ISTOP=ISTOP+1
      VRITE(6,1111)M
 1111 FORMAT(1X,19HERROR ISTOP ELEMT= ,I5)
      GOTO 10
   11 CONTINUE
      MTYP2=IE(M,6)
      IF(N1.NE.0)GO TO 90
      IF(MTYP2.NE.2)GO TO 1620
      NEL1=NEL1-1
      MM=NEL2-NEL1
C
C  BEAM ELEMENT STIFFNESS
C
      CALL OBEAM(MM,AREA,OK,O,MAXEL,MAXNP,N1,M)
      GO TO 104
C
C  QUADRILATERAL ELEMENT STIFFNESS
C
 1620 CALL QUAD(M,AREA,OK,O,MAXEL,MAXNP,X,Y,N1)
  104 TAREA=TAREA+AREA
      IF(M.EQ.NEL) VRITE(6,101) TAREA
  101 FORMAT(///1H ,21HTOTAL AREA OF VALL = ,F12.3)
      GO TO 105
   90 READ(7'M)(OKV(K),K=1,64)
      IV=0
      DO 1110 I1=1,8
      DO 1110 J1=1,8
      IV=IV+1
 1110 OK(I1,J1)=OKV(IV)
  105 LIM=8
      DO 60 I=2,LIM,2
      IJ=I/2
      LP(I-1)=2*IE(M,IJ)-1
   60 LP(I)=2*IE(M,IJ)
      DO 50 LL=1,LIM
      I=LP(LL)
      IF(N1.NE.0)X(LL)=0.0
      R(I)=R(I)+O(LL)
      DO 50 MM=1,LIM
      J=LP(MM)-I+1
      IF(J.LE.0) GOTO 50
      AK(I,J)=AK(I,J)+OK(LL,MM)
   50 CONTINUE
C
C  BOUNDARY CONDITIONS CONSIDERATION
C
   10 CONTINUE
      DO55N=1,NNP
      IF(KODE(N).EQ.3) GOTO 55
      K=2*N
      IF(KODE(N).EQ.1) GOTO 57
      R(K-1)=R(K-1)+ULX(N)
      IF(KODE(N).NE.0) GOTO 55
   57 R(K)=R(K)+VLY(N)
   55 CONTINUE
      DO70M=1,NNP
      IF(KODE(M).GE.0.AND.KODE(M).LE.3) GO TO 72
      ISTOP=ISTOP+1
      GOTO 70
   72 IF(KODE(M).EQ.0) GOTO70
      IF(KODE(M).EQ.2) GOTO 71
      M11=2*M-1
      CALL GEOME(ULX(M),M11,R,AK,MAXNEQ,MAXBV,1)
      IF(KODE(M).EQ.1) GOTO 70
   71 M11=2*M
      CALL GEOME(VLY(M),M11,R,AK,MAXNEQ,MAXBV,1)
   70 CONTINUE
      REVIND 1
      VRITE(1) ((AK(I,J),J=1,IBAND),I=1,NEQ)
      IF(ISTOP.EQ.0) GOTO 81
      VRITE(6,100) ISTOP
  100 FORMAT(////42H SOLUTION VILL NOT BE PERFORMED BECAUSE OF,I5,15H
     1DATA ERRORS  /)
   81 RETURN
      END
C
C  FORM BEAM ELEMENT STIFFNESS MATRIX & STORE IN TAPE 7
C
      SUBROUTINE OBEAM(M,AREA,OK,O,MAXEL,MAXNP,N1,NM)
      COMMON/INFEL/EKHIP(20),EKHJP(20),EKH(20,2),KODYX(20,2),
     1            ND(4),KODY(20,2),BMY(20,2,6),RY(20,2,6),
     2              IND(20,2),EKEP(20,2,6),REVPT(20,2),BMTOT(20,2),
     3              SFTOT(20,2),FTOT(20,2),RTOT(20,2),ROTPP(20,2),
     4              ROTPN(20,2),ROTSP(20,2),ROTSN(20,2),EK1(20,2),
     5              RY1(20,2,2),RA(20,2,2),RB(20,2,2),BMA(20,2,2),
     6              BMB(20,2,2),RREC(20,2,2),ALPHA(20,2),BETA(20,2),
     7              EEXP(20),AXIAL(20,2)
      COMMON/DATA/NNP,NEL,NMAT,NOPT,NBODY,KMAS,MODIF,NEL2
      COMMON/PROTY/E(4),PR(4),RO(4),TH(4)
      COMMON/NODE/IE(80,6)
      COMMON/BEAM/S0,S1,S2,S3,S4,A(12,12)
      COMMON/DISP/X(100),Y(100),ULX(100),VLY(100),KODE(100)
      DIMENSION OK(12,12),O(8),OK1(12,12),OKV(64),AT(12,12)
      I=IE(NM,1)
      J=IE(NM,2)
      K=IE(NM,3)
      L=IE(NM,4)
      MTYP=IE(NM,5)
      BL=ABS(X(J)-X(I))
      AL=ABS(Y(L)-Y(I))
      AREA=AL*BL
      CROS=AL*TH(MTYP)
      S=CROS*AL*AL/12.
      S0=E(MTYP)*CROS/BL
      ALFA=0.5
      SF=0.5
      G=0.4*E(MTYP)
   12 DO 10 K=1,12
      DO 10 L=1,12
      OK1(K,L)=.0
```

```
10  OK(K,L)=0 00
    A1=BL/(3 *E(MTYP)*S)
    B=-A1/2
    C=1 /(ALFA*SF*CROS*G*BL)
    D=1 /EKH(M,1)
    E1=1 /EKH(M,2)
    F1=A1+C+D
    F2=B+C
    F3=F2
    F4=A1+C+E1
    DETT=F1*F4-F2*F3
    OK(1,1)=S0
    OK(1,4)=-S0
    OK(4,1)=-S0
    OK(4,4)=S0
    OK(3,3)=F1/DETT
    OK(3,6)=-F2/DETT
    OK(6,3)=-F3/DETT
    OK(6,6)=F4/DETT
    S1=OK(3,3)
    S2=OK(3,6)
    S3=OK(6,3)
    S4=OK(6,6)
    DO 11 I=1,12
    DO 11 J=1,12
    AT(I,J)= 0
11  A(I,J)=0 0
    A(1,1)=.5
    A(1,7)=.5
    A(2,2)= 5
    A(2,8)= 5
    A(3,1)=1./AL
    A(3,7)=-1 /AL
    A(4,3)=.5
    A(4,5)= 5
    A(5,4)=.5
    A(5,6)=.5
    A(6,3)=1 /AL
    A(6,5)=-1 /AL
    CALL TRANS(12,12,12,12,12,12,A,AT)
    CALL MATMUL(12,12,12,12,12,12,12,12,12,AT,OK,OK1)
    CALL MATMUL(12,12,12,12,12,12,12,12,12,OK1,A,OK)
    IF(KODY(M,1) NE 0) GO TO 2110
    OK(2,2)=OK(2,2)+10 **12.
    OK(8,8)=OK(8,8)+10.**12.
    OK(2,8)=OK(2,8)+10 **12
    OK(8,2)=OK(8,2)+10 **12.
2110 IF(KODY(M,2).NE 0) GO TO 2111
    OK(4,4)=OK(4,4)+10 **12
    OK(6,6)=OK(6,6)+10.**12.
    OK(4,6)=OK(4,6)+10 **12.
    OK(6,4)=OK(6,4)+10.**12.
2111 IV=0
    DO 1110 I1=1,8
    DO 1110 J1=1,8
    IV=IV+1
    OKV(IV)=OK(I1,J1)
1110 CONTINUE
    WRITE(7'NM X OKV(K),K=1,64)
    IF(N1.GT 2)GO TO 99
    WRITE(6,103)N1
    WRITE(6,101)((OK(I1,J1),J1=1,8),I1=1,8)
101  FORMAT(1X,8E14.5)
103  FORMAT(3X,30HBEAM  STIF. INITIAL AT  STEP= ,I3//)
102  DO 20 I=1,8
 20  Q(I)=0 00
    IF (NBODY.EQ.0)GO TO 99
    TBODYF=RO(MTYP)*TH(MTYP)*AREA
    BODYF=TBODYF/4.
    DO 60 I=2,8,2
    Q(I)=-BODYF
    IF(NBODY.EQ 2)Q(I-1)=BODYF
 60  CONTINUE
 99  RETURN
    END
C
C  FORM QUADRILATERAL ELEMENT STIFFNESS MATRIX & STORE IN TAPE 7
C
    SUBROUTINE QUAD(M,AREA,CK,Q,MAXEL,MAXNP,X,Y,N1)
    COMMON/DATA/ NNP,NEL,NMAT,NOPT,NBODY,KMAS,MODIF,NEL2
    COMMON/PROTY/E(4),PR(4),RO(4),TH(4)
    COMMON/TWO/IBAND,NEQ
    COMMON/NODE/IE(60,6)
    COMMON/GAUSS/CORD(5,5),WEIGHT(5,5)
    DIMENSION X(MAXNP),Y(MAXNP)
    DIMENSION XE(4,2),Q(8),CK(12,12),TOK(12,12),CB(12,12),TCB(3,12)
    DIMENSION OKV(64),CBV(144),C(3,3)
    I=IE(M,1)
    J=IE(M,2)
    K=IE(M,3)
    L=IE(M,4)
    MTYP=IE(M,5)
    AREA=0 0
    A=X(J)-X(I)
    F=X(K)-X(I)
    G=Y(J)-Y(I)
    H=Y(K)-Y(I)
    AREA1=(A*H-F*G)/2.0
    A=X(K)-X(I)
    F=X(L)-X(I)
    G=Y(K)-Y(I)
    H=Y(L)-Y(I)
    AREA2=(A*H-F*G)/2 0
    AREA=AREA1+AREA2
    DO10N=1,4
    NN=IE(M,N)
    XE(N,1)=X(NN)
    XE(N,2)=Y(NN)
10  CONTINUE
    DO 12 II=1,8
12  Q(II)=0 0
    DO13 II=1,12
    DO13JJ=1,12
    CB(JJ,II)=0 0
13  OK(II,JJ)=0.0
    NC=2
    DO20I2=1,NC
    ETA=CORD(I2,NC)
    WEIG1=WEIGHT(I2,NC)
    DO20J2=1,NC
    XI=CORD(J2,NC)
    WEIG2=WEIGHT(J2,NC)
    CALL FUNK(XE,XI,ETA,TOK,TCB,MTYP,M,NMAT,NOPT,N1,X,Y,C)
    FACT=WEIG1*WEIG2
    DO 15 I1=1,12
    DO15J1=1,12
15  OK(I1,J1)=OK(I1,J1)+TOK(I1,J1)*FACT
20  CONTINUE
    DO25II=1,12
    DO25JJ=1,12
25  OK(II,JJ)=OK(II,JJ)*TH(MTYP)
    DO 30L1=1,4
    IF(L1.EQ.1.OR L1 EQ.2) ETA=-1.0
    IF(L1.EQ.3 OR.L1 EQ.4) ETA=1.0
    IF(L1 EQ 1 OR.L1 EQ.4) XI=-1.0
    IF(L1.EQ 2.OR.L1.EQ.3) XI=1.0
    CALL FUNK(XE,XI,ETA,TOK,TCB,MTYP,M,NMAT,NOPT,N1,X,Y,C)
    DO30I1=1,3
    II=I1+3*(L1-1)
    DO30J1=1,12
 30 CB(II,J1)=TCB(I1,J1)
    IF(MODIF.EQ.0)GO TO 55
C
C  ELIMINATE  INCOMPATIBLE  MODES
C
    DO 50 I1=1,4
    L1=12-I1
    K1=L1+1
    DO 50 J1=1,L1
    PIV=OK(J1,K1)/OK(K1,K1)
    DO 40J2=1,12
 40 CB(J2,J1)=CB(J2,J1)-PIV*CB(J2,K1)
    DO 50 J2=1,L1
 50 OK(J1,J2)=OK(J1,J2)-PIV*OK(K1,J2)
 55 IV=0
    DO 1110 I1=1,8
    DO 1110 J1=1,8
    IV=IV+1
    OKV(IV)=OK(I1,J1)
1110 CONTINUE
    IF(M NE.1)GO TO 259
    WRITE(6,229)
    WRITE(6,228)(OKV(J),J=1,64)
229 FORMAT(10X,'STIF. 1ST ELEMT COMPUTED IN QUAD V. C MATRIX'//)
228 FORMAT(1X,4F18.7)
259 WRITE(7'M X OKV(K),K=1,64)
    IV=0
    DO 1111 I1=1,12
    DO 1111 J1=1,12
    IV=IV+1
    CBV(IV)=CB(I1,J1)
1111 CONTINUE
    WRITE(8'M X CBV(K),K=1,144)
    IF(M.EQ.1)WRITE(6,118)N1
    IF(M.EQ.1)
   1WRITE(6,119)((CB(I,J),J=1,12),I=1,12)
118 FORMAT(/3X,28HCB MATRIX INITIAL  AT STEP= ,I3//)
119 FORMAT(6E15.6)
    IF(NBODY.EQ.0) GOTO99
    TBODYF=AREA*RO(MTYP)*TH(MTYP)
    BODYF=TBODYF/4.0
    DO60I=2,8,2
    Q(I)=-BODYF
    IF(NBODY.EQ.2) Q(I-1)=BODYF
 60 CONTINUE
 99 IF(M.NE.1)GO TO 199
    WRITE(6,705)
    WRITE(6,706)((C(I,J),J=1,3),I=1,3)
705 FORMAT(//5X,18HC MATRIX FROM QUAD//)
706 FORMAT(5X,3F15.5)
199 RETURN
    END
C
C  GAUSIAN  CONSTANTS
C
    BLOCK DATA
    COMMON/GAUSS/ CORD(5,5),WEIGHT(5,5)
    DATA CORD/0.0,0 0.0,0.0,0.0,0.0,
   A-0.5773502691,0.5773502691,0.0,0 0,0.0,
   B-0.7745966692,0.0,0.7745966692,0.0,0.0,
   C-0.8611363115,-0 3399810435,0.3399810435,0.8611363115,0.0,
   D-0 9061798459,-0.5384693101,0.0,0.5384693101,0.9061798459/
    DATA WEIGHT/0 0,0.0,0.0,0.0,0 0,0 0,
   E1.0,1 0,0 0,0 0,0.0,
   F0.5555555555,0.8888888888,0.5555555555,0 0,0.0,
   G0 3478548451,0.6521451548,0.6521451548,0.3478548451,0.0,
   H0 236926885,0 4786286704,0.5688888888,0.4786286704,0.236926885/
    END
C
C  FORM  MATRIX  BT . C   B
C
    SUBROUTINE FUNK(XE,XI,ETA,TOK,TCB,MTYP,M,NMAT,NOPT,N1,X,Y,C)
    COMMON/PROTY/ E(4),PR(4),RO(4),TH(4)
    COMMON/STEEL/PX(80),PY(80)
    COMMON/BARR/EPSY,EPSUL,SIGY,ES,ESH
    DIMENSION B(3,12),C(3,3),DXY(2,6),BT(12,3)
```

```
      DIMENSION XE(4,2),TOK(12,12),TCB(3,12)
      DIMENSION X(100),Y(100)
      C1=ES*PX(M)
      C2=ES*PY(M)
      DO 20 I=1,3
      DO 20 J=1,12
      BT(J,I)=0.0
      TCB(I,J)=0.0
   20 B(I,J)=0.0
      DO 25 I=1,12
      DO 25 J=1,12
   25 TOK(I,J)=0.0
      IF(NI.NE.0)GO TO 10
      C(1,3)=0.0
      C(2,3)=0.0
      C(3,1)=0.0
      C(3,2)=0.0
      IF(NMAT.EQ.1.AND.M.GT.1) GOTO 10
      IF(NOPT.EQ.2) GOTO2
      CF=E(MTYP)/((1.0+PR(MTYP))*(1.0-2.0*PR(MTYP)))
      C(1,1)=CF*(1.0-PR(MTYP))
      C(1,2)=CF*PR(MTYP)
      C(2,1)=C(1,2)
      C(2,2)=C(1,1)
      C(3,3)=CF*(1.0-2.0*PR(MTYP))/2.0
      GOTO5
    2 CF=E(MTYP)/(1.0-PR(MTYP)**2)
      C(1,1)=CF
      C(1,2)=PR(MTYP)*CF
      C(2,1)=C(1,2)
      C(2,2)=CF
      C(3,3)=CF*(1.0-PR(MTYP))/2.0
    5 C(1,1)=C(1,1)+C1
      C(2,2)=C(2,2)+C2
   10 CONTINUE
      CALL BMAT(XE,XI,ETA,B,BT,DET)
      CALL MATMUL(3,3,3,12,3,12,3,3,12,C,B,TCB)
      CALL MATMUL(12,3,3,12,12,12,12,3,12,BT,TCB,TOK)
      DO 30 I=1,12
      DO 30 J=1,12
   30 TOK(I,J)=TOK(I,J)*DET
      RETURN
      END
C
C  FORM  B  MATRIX
C
      SUBROUTINE BMAT(XE,XI,ETA,B,BT,DET)
      DIMENSION B(3,12),BT(12,3),XE(4,2),DXY(2,6)
      CALL JACOBI(XE,XI,ETA,DET,DXY)
      DO 25 I=1,6
      II=2*I-1
      B(1,II)=DXY(1,I)
      B(2,II+1)=DXY(2,I)
      B(3,II)=DXY(2,I)
      B(3,II+1)=DXY(1,I)
   25 CONTINUE
      CALL TRANS(3,12,12,3,3,12,B,BT)
      RETURN
      END
C
C  FORM  JACOBIAN  MATRIX  AND  ITS  DETERMINANT
C
      SUBROUTINE JACOBI(XE,XI,ETA,DET,DXY)
      DIMENSION XE(4,2),DXY(2,6),AJ(2,2),DXE(2,4),TXE(2,6)
      DXE(1,1)=-(1.0-ETA)/4.0
      DXE(1,2)=(1.0-ETA)/4.0
      DXE(2,2)=(-1.0-XI)/4.0
      DXE(2,1)=-(1.0-XI)/4.0
      DXE(1,3)=(1.0+ETA)/4.0
      DXE(2,3)=(1.0+XI)/4.0
      DXE(1,4)=-(1.0+ETA)/4.0
      DXE(2,4)=(1.0-XI)/4.0
      CALL MATMUL(2,4,4,2,2,2,2,4,2,DXE,XE,AJ)
      DET=AJ(1,1)*AJ(2,2)-AJ(1,2)*AJ(2,1)
      TEM=AJ(1,1)
      AJ(1,1)=AJ(2,2)
      AJ(2,2)=TEM
      AJ(1,2)=-AJ(1,2)
      AJ(2,1)=-AJ(2,1)
      DO10I=1,2
      DO10J=1,2
   10 AJ(I,J)=AJ(  ,J)/DET
      DO20I=1,2
      DO20J=1,4
   20 TXE(I,J)=DXE  I,J)
      TXE(1,5)=-2.  1XI
      TXE(1,6)=0.0
      TXE(2,5)=0.0
      TXE(2,6)=-2.0*ETA
      CALL MATMUL(2,2,2,6,2,6,2,2,6,AJ,TXE,DXY)
      RETURN
      END
C
C  FORM  TRANSPOSE OF A  MATRIX A, I.E., B = AT
C
      SUBROUTINE TRANS(II,JJ,KK,LL,K,L,AA,BB)
      DIMENSION AA(II,JJ),BB(KK,LL)
      DO10I=1,K
      DO10J=1,L
   10 BB(J,I)=AA(I,J)
      RETURN
      END
C
C  FORM PRODUCT OF TVO MATRICES A AND B AS  C = A . B
C
      SUBROUTINE MATMUL(II,JJ,KK,LL,MM,NN,K,L,M,AA,BB,CC)
      DIMENSION AA(II,JJ),BB(KK,LL),CC(MM,NN)
      DO10I=1,K
      DO10J=1,M
      CC(I,J)=0.0
      DO10J1=1,L
   10 CC(I,J)=CC(I,J)+AA(I,J1)*BB(J1,J)
      RETURN
      END
C
C  FORM  OVERALL  MASS  MATRIX
C
      SUBROUTINE ASEMAS(ISTOP,R,AMS,MAXNEQ,MAXBV,X,Y,KODE,MAXNP,MAXEL)
      COMMON/DATA/ NNP,NEL,NMAT,NOPT,NBODY,KMAS,MODIF,NEL2
      COMMON/PROTY/E(4),PR(4),RO(4),TH(4)
      COMMON/TVO/IBAND,NEQ
      COMMON/NODE/IE(80,6)
      DIMENSION X(MAXNP),Y(MAXNP),KODE(MAXNP)
      DIMENSION AMS(MAXNEQ,MAXBV),R(MAXNEQ)
      DIMENSION OK(8,8),LP(8),LUM(150,2),EXMAS(150)
      READ(5,100) KMAS,NSEC
      IF(NSEC.LE.0) GOTO 5
      READ(5,110) ((LUM(I,J),J=1,2),EXMAS(I),I=1,NSEC)
      VRITE(6,120) KMAS,NSEC
      VRITE(6,130) ((LUM(I,J),J=1,2),EXMAS(I),I=1,NSEC)
    5 CONTINUE
      DO10I=1,NEQ
      DO10J=1,IBAND
   10 AMS(I,J)=0.0
      IF(KMAS.EQ.2) GO TO 235
      DO 35 M=1,NEL
      MTYP=IE(M,5)
      IF(MTYP.GT.0) GOTO 15
      ISTOP=ISTOP+1
      VRITE(6,220)
  220 FORMAT(5X,'******ERROR 1******')
      GOTO 35
   15 MTYP2=IE(M,6)
      NODE1=IE(M,1)
      NODE2=IE(M,2)
      NODE3=IE(M,3)
      NODE4=IE(M,4)
      A=X(NODE2)-X(NODE1)
      F=X(NODE3)-X(NODE1)
      G=Y(NODE2)-Y(NODE1)
      H=Y(NODE3)-Y(NODE1)
      AREA1=ABS((A*H-F*G)/2.0)
      A=X(NODE3)-X(NODE1)
      F=X(NODE4)-X(NODE1)
      G=Y(NODE3)-Y(NODE1)
      H=Y(NODE4)-Y(NODE1)
      AREA2=ABS((A*H-F*G)/2.0)
      AREA=AREA1+AREA2
      CALL QUAMAS(OK,AREA,MTYP,KMAS)
  300 LIM=8
      DO20 I=2,LIM,2
      IJ=I/2
      LP(I-1)=2*IE(M,IJ)-1
   20 LP(I)=2*IE(M,IJ)
  125 DO30LL=1,LIM
      IP=LP(LL)
      DO 30 MM=1,LIM
      JP=LP(MM)-IP+1
      IF(JP.LE.0) GOTO 30
      AMS(IP,JP)=AMS(IP,JP)+OK(LL,MM)
   30 CONTINUE
   36 CONTINUE
  235 IF(NSEC.LE.0) GOTO 39
      DO 38 II=1,NSEC
      N1=LUM(II,2)
      DO 36 J1=1,N1
      NP1=2*(LUM(II,1)+J1-1)
      NP2=NP1-1
      AMS(NP1,1)=AMS(NP1,1)+EXMAS(II)
   36 AMS(NP2,1)=AMS(NP2,1)+EXMAS(II)
   38 CONTINUE
   39 CONTINUE
      DO60MP=1,NNP
      IF(KODE(MP).GE.0.AND.KODE(MP).LE.3) GOTO 40
      ISTOP=ISTOP+1
      VRITE(6,230)
  230 FORMAT(5X,'******ERROR 2 ******')
      GOTO 60
   40 IF(KODE(MP).EQ.0) GOTO 60
      IF(KODE(MP).EQ.2) GOTO 50
      MII=2*MP-1
      CALL GEOME(0.0,MII,R,AMS,MAXNEQ,MAXBV,2)
   50 IF(KODE(MP).EQ.1) GOTO 60
      MII=2*MP
      CALL GEOME(0.0,MII,R,AMS,MAXNEQ,MAXBV,2)
   60 CONTINUE
      REVIND 2
      DO70I=1,NEQ
   70 VRITE(2) (AMS(I,J),J=1,IBAND)
  100 FORMAT(2I5)
  110 FORMAT(4(2I5,F8.3))
  120 FORMAT(//,15X,'**** KMASS ',I5,10X,'**** NSEC =',I5,//)
  130 FORMAT(//15X,'**** EXTRA LUMPED MASS ****',//,(4(6X,2I5,F10.3)))
   80 RETURN
      END
C
C  FORM  ELEMENT  MASS  MATRIX
C
      SUBROUTINE QUAMAS(OK,AREA,MTYP,KMAS)
      COMMON/PROTY/E(4),PR(4),RO(4),TH(4)
      DIMENSION OK(8,8)
      DO10 I=1,8
      DO10 J=1,8
   10 OK(I,J)=0.0
      CONST=0.25*AREA*TH(MTYP)*RO(MTYP)
      IF(KMAS.EQ.0) GOTO 20
```

```
      IF(KMAS EQ 0) GOTO 20
      OK(1,1)=0 44444444*CONST
      OK(1,3)=0 22222222*CONST
      OK(1,5)=0 11111111*CONST
      OK(1,7)=0 22222222*CONST
      OK(2,2)=0 44444444*CONST
      OK(2,4)=0 22222222*CONST
      OK(2,6)=0 11111111*CONST
      OK(2,8)=0.22222222*CONST
      OK(3,1)=0 22222222*CONST
      OK(3,3)=0 44444444*CONST
      OK(3,5)=0 22222222*CONST
      OK(3,7)=0 11111111*CONST
      OK(4,2)=0 22222222*CONST
      OK(4,4)=0 44444444*CONST
      OK(4,6)=0 22222222*CONST
      OK(4,8)=0 11111111*CONST
      OK(5,1)=0 11111111*CONST
      OK(5,3)=0 22222222*CONST
      OK(5,5)=0 44444444*CONST
      OK(5,7)=0 22222222*CONST
      OK(6,2)=0.11111111*CONST
      OK(6,4)=0 22222222*CONST
      OK(6,6)=0 44444444*CONST
      OK(6,8)=0 22222222*CONST
      OK(7,1)=0 22222222*CONST
      OK(7,3)=0.11111111*CONST
      OK(7,5)=0 22222222*CONST
      OK(7,7)=0 44444444*CONST
      OK(8,2)=0 22222222*CONST
      OK(8,4)=0 11111111*CONST
      OK(8,6)=0 22222222*CONST
      OK(8,8)=0.44444444*CONST
      GO TO 40
   20 DO 30 L=1,8
   30 OK(L,L)=CONST
   40 RETURN
      END
C
C  ROTATE BANDED MATRIX TO HALF BAND
C
      SUBROUTINE GEOME(U,N,RD,AKM,NDIM,MDIM,IC)
      COMMON/TVO/IBAND,NEQ
      DIMENSION RD(NDIM),AKM(NDIM,MDIM)
      IF(IC EQ.2) GOTO 200
      DO100 M=2,IBAND
      K=N-M+1
      IF(K.LE.0) GOTO 50
      RD(K)=RD(K)-AKM(K,M)*U
      AKM(K,M)=0.0
   50 K=N+M-1
      IF(K.GT.NEQ) GOTO100
      RD(K)=RD(K)-AKM(N,M)*U
      AKM(N,M)=0 0
  100 CONTINUE
      AKM(N,1)=1.0
      RD(N)=U
      GOTO 400
  200 CONTINUE
      DO300MM=2,IBAND
      J=N-MM+1
      IF(J.LE 0) GOTO 250
      AKM(J,MM)=0.0
  250 J=N+MM-1
      IF(J.GT.NEQ) GOTO 300
      AKM(N,MM)=0.0
  300 CONTINUE
      AKM(N,1)=1.0
  400 RETURN
      END
C
C  I) SOLVE AK.U=R FOR U  IF  KKK = 2
C II) TRIANGULARISE  MATRIX  AK  IF  KKK>< 2
C
      SUBROUTINE BANSOL(KKK,AK,R,NEQ,IBAND,NDIM,MDIM)
      DIMENSION AK(NDIM,MDIM),R(NDIM)
      NRS=NEQ-1
      NR=NEQ
      IF(KKK.EQ 2) GOTO 200
      DO120N=1,NRS
      M=N-1
      NRM=NR-M
      MR=MIN0(IBAND,NRM)
      PIVOT=AK(N,1)
      DO120L=2,MR
      CP=0.0
      IF(PIVOT EQ.0.0) GOTO 100
      CP=AK(N,L)/PIVOT
  100 CONTINUE
      I=M+L
      J=0
      DO110K=L,MR
      J=J+1
  110 AK(I,J)=AK(I,J)-CP*AK(N,K)
  120 AK(N,L)=CP
      IF(KKK.EQ.1) GOTO 400
  200 DO220N=1,NRS
      M=N-1
      NRM=NR-M
      MR=MIN0(IBAND,NRM)
      CP=R(N)
      R(N)=0 0
      IF(AK(N,1).EQ 0 0) GOTO 210
      R(N)=CP/AK(N,1)
  210 CONTINUE
      DO 220 L=2,MR
      I=M+L
  220 R(I)=R(I)-AK(N,L)*CP
      IF(AK(NR,1) EQ 0 0) GOTO 230
      R(NR)=R(NR)/AK(NR,1)
      GOTO 240
  230 R(NR)=0 0
  240 CONTINUE
      DO 320 I=1,NRS
      N=NR-I
      M=N-1
      NRM=NR-M
      MR=MIN0(IBAND,NRM)
      DO 320 K=2,MR
      L=M+K
  320 R(N)=R(N)-AK(N,K)*R(L)
  400 RETURN
      END
C
C  COMPUTE  BEAM  ELEMENT  FORCES
C  MONITOR  BEAM  ELEMENT  STATE  FOLLOWING  TAKEDA  RULES
C
      SUBROUTINE BEAFOR(CK,IAA,NM,DISPI,X,Y,NI,MAXNP,DISP,
     1                  MAXEL,KBAL,M,ITV)
      COMMON/INFEL/EKHIP(20),EKHJP(20),EKH(20,2),KODYX(20,2),
     1             NDX(4),KODY(20,2),BMY(20,2,6),RY(20,2,6),
     2             IND(20,2),EKEP(20,2,6),REVPT(20,2),BMTOT(20,2),
     3             SFTOT(20,2),FTOT(20,2),RTOT(20,2),ROTPP(20,2),
     4             ROTPN(20,2),ROTSP(20,2),ROTSN(20,2),EKI(20,2),
     5             RYI(20,2,2),RA(20,2,2),RB(20,2,2),BMA(20,2,2),
     6             BMB(20,2,2),RREC(20,2,2),ALPHA(20,2),BETA(20,2),
     7             EEXP(20),AXIAL(20,2)
      COMMON/RESP/DVRI,DVRJ,BML(20,2),DBM(20,2),MINDX(20,2)
      COMMON/DATA/NNP,NEL,NMAT,NOPT,NBODY,KMAS,MODIF,NEL2
      COMMON/NODE/IE(80,6)
      COMMON/BEAM/S0,S1,S2,S3,S4,A(12,12)
      DIMENSION EDIS(8,1),OK(8,8),Q(8),EDIS1(8),A1(8,8),DISP(8,1)
      DIMENSION DISPI(200),X(100),Y(100),OKV(64),FT(8),OK0(8,8),
     1          OK2(12,12)
      IF(NM.EQ NEL2) VRITE(6,1113)XJ,KODY(J,1),KODY(J,2),J=1,NEL2)
 1113 FORMAT(1X,'EL=',I5,'KODY(1)=',I6,'KODY(2)=',I6/)
      KODYX(NM,1)=KODY(NM,1)
      KODYX(NM,2)=KODY(NM,2)
      K1=IE(M,1)
      K2=IE(M,2)
      K3=IE(M,3)
      K4=IE(M,4)
      BL=ABS(X(K2)-X(K1))
      AL=ABS(Y(K4)-Y(K1))
      DO 10 I=1,4
      NN=IE(M,I)
      EDIS(2*I-1,1)=DISPI(2*NN-1)
   10 EDIS(2*I,1)=DISPI(2*NN)
      DO 21 I=1,8
      DO 21 J=1,8
   21 A1(I,J)=A(I,J)
      CALL MATMUL(8,8,8,1,8,1,8,8,1,A1,EDIS,EDIS1)
      VRITE(6,987)(EDIS1(I),I=1,8)
  987 FORMAT(1X,'*EDIS1 ARRAY FROM BEAFOR* ',8F8.5//)
      DO 1110 I1=1,8
      DO 1110 J1=1,8
      OK0(I1,J1)=OK(I1,J1)
 1110 CONTINUE
      VRITE(6,202) M
      VRITE(6,201)((OK(I,J),J=1,8),I=1,8)
  201 FORMAT(1X,8E12.5)
  202 FORMAT(4X,' BEAM  STIF  FROM BEAFOR  OF  ELMT = ',I3//)
      DBM(NM,1)=S1*EDIS1(3)+S2*EDIS1(6)
      DBM(NM,2)=S3*EDIS1(3)+S4*EDIS1(6)
      IF(NI.NE.1)GO TO 20
      DO 12 I=1,2
      RTOT(NM,I)=0.0
      SFTOT(NM,I)=0.0
      ROTPP(NM,I)=.0
      ROTPN(NM,I)=.0
      ROTSP(NM,I)=.0
      ROTSN(NM,I)=0.
      KODY(NM,I)=0
      AXIAL(NM,I)=0.0
   12 BMTOT(NM,I)=0 0
   20 BMTOT1=BMTOT(NM,1)
      BMTOT2=BMTOT(NM,2)
      BML(NM,1)=BMTOT(NM,1)+DBM(NM,1)
      BML(NM,2)=BMTOT(NM,2)+DBM(NM,2)
      AXIAL(NM,1)=AXIAL(NM,1)+S0*(EDIS1(1)-EDIS1(4))
      AXIAL(NM,2)=AXIAL(NM,2)-S0*(EDIS1(1)-EDIS1(4))
      FACAC=0.0
   30 FACTOR=1.-FACAC
      KFAC=0
      DO 341 IEND=1,2
      KOD1=KODY(NM,IEND)
      IF(DBM(NM,IEND).EQ.0.)GO TO 340
      REMIND=1.
      IF(IND(NM,IEND).EQ 2)REMIND=-1.
C
C     RULE  1
C
      IF(KODY(NM,IEND).NE.0)GO TO 50
      IF(DBM(NM,IEND).GT.0.)GO TO 40
      FAC=(BMY(NM,IEND,2)-BMTOT(NM,IEND))/DBM(NM,IEND)
      IF(FAC GE.FACTOR)GO TO 340
      FACTOR=FAC
      BM=BMY(NM,IEND,2)
      ROT=RY(NM,IEND,2)
      KFAC=IEND
      KODE=2
      EK=EKEP(NM,IEND,2)
      IDK=2
      GO TO 340
   40 FAC=(BMY(NM,IEND,1)-BMTOT(NM,IEND))/DBM(NM,IEND)
      IF(FAC GE.FACTOR)GO TO 340
      FACTOR=FAC
```

```
      FACTOR=FAC
      BM=BMY(NM,IEND,1)
      ROT=RY(NM,IEND,1)
      KFAC=IEND
      KODE=1
      EK=EKEP(NM,IEND,2)
      IDK=1
      GO TO 340
   50 KOD=KODY(NM,IEND)
      GO TO(60,60,100,150,170,220,240,260,280,300,320),KOD
C
C     RULE    2.
C
   60 IF(REMIND*DBM(NM,IEND) LT 0.0)GO TO 70
      MIND(NM,IEND)=IND(NM,IEND)
      GO TO 340
   70 KODY(NM,IEND)=3
      IDD=IND(NM,IEND)
      BMT=BMTOT(NM,IEND)
      BMTEST=(BMB(NM,IEND,IDD)-BMT)*REMIND
      IF(BMTEST GE.0 )GO TO 90
      EKU=BMT/(ALPHA(NM,IEND)*RTOT(NM,IEND)+(1 -ALPHA(NM,IEND))*
     1BMT/EK1(NM,IEND))
      IDM=3-IDD
      EKUMIN=(BMT-BMA(NM,IEND,IDM))/(RTOT(NM,IEND)-RA(NM,IEND,IDM))
      IF(EKU LT.EKUMIN)EKU=EKUMIN
      IF(EKEP(NM,IEND,1) LE EKU)EKU=EKEP(NM,IEND,1)
      IF(ALPHA(NM,IEND) LE 0 )EKU=EK1(NM,IEND)
      EKEP(NM,IEND,1)=EKU
      BMB(NM,IEND,IDD)=BMT
      RB(NM,IEND,IDD)=RTOT(NM,IEND)
      RA(NM,IEND,IDD)=(1.-BETA(NM,IEND))*RTOT(NM,IEND)+BETA(NM,IEND)*
     1RY1(NM,IEND,IDD)
      BMA(NM,IEND,IDD)=BMT-((RTOT(NM,IEND))-(RA(NM,IEND,IDD)))*
     1EKEP(NM,IEND,2)
      IF(BETA(NM,IEND) GT.0.0)GO TO 80
      RA(NM,IEND,IDD)=RTOT(NM,IEND)
      BMA(NM,IEND,IDD)=BMT
   80 RREC(NM,IEND,IDD)=RTOT(NM,IEND)-BMB(NM,IEND,IDD)/EKEP(NM,IEND,1)
      IDB=3-IDD
      RREC(NM,IEND,IDB)=RB(NM,IEND,IDB)-BMB(NM,IEND,IDB)/
     1                  EKEP(NM,IEND,1)
      RCTEST=RREC(NM,IEND,IDB)*REMIND
      IF(RCTEST GT.0.) RREC(NM,IEND,IDB)=0 0
   90 EKH(NM,IEND)=EKEP(NM,IEND,1)
      REVPT(NM,IEND)=RTOT(NM,IEND)-BMT/EKH(NM,IEND)
      FACTOR=0.
      KFAC=0
      GO TO 340
C
C     RULE .......3. .
C
  100 IF(REMIND*DBM(NM,IEND) LT.0 0)GO TO 110
      IDD=IND(NM,IEND)
      FAC=(BMY(NM,IEND,IDD)-BMTOT(NM,IEND))/DBM(NM,IEND)
      IF(FAC.GE FACTOR)GO TO 340
      FACTOR=FAC
      BM=BMY(NM,IEND,IDD)
      ROT=RY(NM,IEND,IDD)
      KFAC=IEND
      KODE=IEND
      KODE=IDD
      IDK=IDD
      EK=EKEP(NM,IEND,2)
      GO TO 340
  110 FAC=-BMTOT(NM,IEND)/DBM(NM,IEND)
      IF(FAC.GE.FACTOR)GO TO 340
      FACTOR=FAC
      BM=0.
      ROT=REVPT(NM,IEND)
      KFAC=IEND
      KODE=4
      IDK=3-IND(NM,IEND)
      IDD=3-IDK
CNEV LOADING SLOPE
      RTEST=(RREC(NM,IEND,IDD)-ROT)*REMIND
      IF(RTEST.GT.0 0)GO TO 120
      BMY(NM,IEND,IDK)=BMA(NM,IEND,IDK)
      RY(NM,IEND,IDK)=RA(NM,IEND,IDK)
      GO TO 13
  120 RBA=RB(NM,IEND,IDK)-RA(NM,IEND,IDK)
      RPR=ROT-RREC(NM,IEND,IDD)
      RRR=RREC(NM,IEND,IDK)-RREC(NM,IEND,IDD)
      RXA=RBA*(RPR/RRR)**EEXP(NM)
      RY(NM,IEND,IDK)=RA(NM,IEND,IDK)+RXA
      BMY(NM,IEND,IDK)=BMA(NM,IEND,IDK)+RXA*EKEP(NM,IEN,2)
  130 EKL=BMY(NM,IEND,IDK)/(RY(NM,IEND,IDK)-ROT)
C CHECK  MAX  SLOPE
      IF(EKL LT EKEP(NM,IEND,1))GO TO 140
      EKL=0 999*EKEP(NM,IEND,1)
      RY(NM,IEND,IDK)=(ROT*EKL+BMA(NM,IEND,IDK)-RA(NM,IEND,IDK)*
     *EKEP(NM,IEND,2))/
     1(EKL-EKEP(NM,IEND,2))
      BMY(NM,IEND,IDK)=EKL*(RY(NM,IEND,IDK)-ROT)
  140 EKEP(NM,IEND,3)=EKL
      EK=EKEP(NM,IEND,3)
      GO TO 340
C
C .RULE ..    .. 4 .
C
  150 IF(REMIND*DBM(NM,IEND) LT 0 0)GO TO 160
      IDD=IND(NM,IEND)
      MIND(NM,IEND)=3
      FAC=(BMY(NM,IEND,IDD)-BMTOT(NM,IEND))/DBM(NM,IEND)
      IF(FAC GE FACTOR)GO TO 340
      FACTOR=FAC
      BM=BMY(NM,IEND,IDD)
      ROT=RY(NM,IEND,IDD)
      KFAC=IEND
      KODE=IEND
      KODE=IDD
      IDK=IDD
      EK=EKEP(NM,IEND,2)
      GO TO 340
  160 KODY(NM,IEND)=5
      EKH(NM,IEND)=EKEP(NM,IEND,1)
      REVPT(NM,IEND)=RY(NM,IEND,3)-BMY(NM,IEND,3)/EKH(NM,IEND)
      FACTOR=0.
      KFAC=0
      GO TO 340
C
C  RULE..... 5...
C
  170 IF(REMIND*DBM(NM,IEND).LT.0. )GO TO 180
      FAC=(BMY(NM,IEND,3)-BMTOT(NM,IEND))/DBM(NM,IEND)
      IF(FAC.GE.FACTOR)GO TO 340
      FACTOR=FAC
      BM=BMY(NM,IEND,3)
      ROT=RY(NM,IEND,3)
      KFAC=IEND
      KODE=4
      IDK=IND(NM,IEND)
      EK=EKEP(NM,IEND,3)
      GO TO 340
  180 FAC=-BMTOT(NM,IEND)/DBM(NM,IEND)
      IF(FAC GE.FACTOR)GO TO 340
      FACTOR=FAC
      BM=0.
      ROT=REVPT(NM,IEND)
      KFAC=IEND
      KODE=6
      IDK=3-IND(NM,IEND)
      IDD=3-IDK
C NEV LOAD  SLOPE
      RTEST=(RREC(NM,IEND,IDD)-ROT)*REMIND
      IF(RTEST.GT.0. )GO TO 190
      BMY(NM,IEND,IDK)=BMA(NM,IEND,IDK)
      RY(NM,IEND,IDK)=RA(NM,IEND,IDK)
      GO TO 200
  190 RBA=RB(NM,IEND,IDK)-RA(NM,IEND,IDK)
      RPR=ROT-RREC(NM,IEND,IDD)
      RRR=RREC(NM,IEND,IDK)-RREC(NM,IEND,IDD)
      RXA=RBA*(RPR/RRR)**EEXP(NM)
      RY(NM,IEND,IDK)=RA(NM,IEND,IDK)+RXA
      BMY(NM,IEND,IDK)=BMA(NM,IEND,IDK)+RXA*EKEP(NM,IEND,2)
  200 EKL=BMY(NM,IEND,IDK)/(RY(NM,IEND,IDK)-ROT)
      IF(EKL.LT EKEP(NM,IEND,1))GO TO 210
      EKL=0.999*EKEP(NM,IEND,1)
      RY(NM,IEND,IDK)=(ROT*EKL+BMA(NM,IEND,IDK)-RA(NM,IEND,IDK)*
     1EKEP(NM,IEND,2))
     2/(EKL-EKEP(NM,IEND,2))
      BMY(NM,IEND,IDK)=EKL*(RY(NM,IEND,IDK)-ROT)
  210 EKEP(NM,IEND,4)=EKL
      EK=EKEP(NM,IEND,4)
      GO TO 340
C
C. . RULE...6..
C
  220 IF(REMIND*DBM(NM,IEND).LT.0. )GO TO 230
      IDD=IND(NM,IEND)
      MIND(NM,IEND)=4
      FAC=(BMY(NM,IEND,IDD)-BMTOT(NM,IEND))/DBM(NM,IEND)
      IF(FAC GE.FACTOR) GO TO 340
      FACTOR=FAC
      BM=BMY(NM,IEND,IDD)
      ROT=RY(NM,IEND,IDD)
      KFAC=IEND
      KODE=IDD
      IDK=IDD
      EK=EKEP(NM,IEND,2)
      GO TO 340
  230 KODY(NM,IEND)=7
      EKH(NM,IEND)=EKEP(NM,IEND,1)
      REVPT(NM,IEND)=RY(NM,IEND,4)-BMY(NM,IEND,4)/EKH(NM,IEND)
      FACTOR=0.
      KFAC=0
      GO TO 340
C
C ...RULE...7...
C
  240 IF(REMIND*DBM(NM,IEND).LT.0.0)GO TO 250
      FAC=(BMY(NM,IEND,4)-BMTOT(NM,IEND))/DBM(NM,IEND)
      IF(FAC GE.FACTOR)GO TO 340
      FACTOR=FAC
      BM=BMY(NM,IEND,4)
      ROT=RY(NM,IEND,4)
      KFAC=IEND
      KODE=6
      IDK=IND(NM,IEND)
      EK=EKEP(NM,IEND,4)
      GO TO 340
  250 FAC=-BMTOT(NM,IEND)/DBM(NM,IEND)
      IF(FAC.GE FACTOR)GO TO 340
      FACTOR=FAC
      BM=0
      ROT=REVPT(NM,IEND)
      KFAC=IEND
      KODE=8
      IDK=3-IND(NM,IEND)
      EKEP(NM,IEND,5)=BMY(NM,IEND,3)/(RY(NM,IEND,3)-REVPT(NM,IEND))
      EK=EKEP(NM,IEND,5)
      GO TO 340
C
C     RULE.. 8
C
  260 IF(REMIND*DBM(NM,IEND).LT.0 0)GO TO 270
      MIND(NM,IEND)=5
      FAC=(BMY(NM,IEND,3)-BMTOT(NM,IEND))/DBM(NM,IEND)
```

```
      FAC=(BMY(NM,IEND,3)-BMTOT(NM,IEND))/DBM(NM,IEND)
      IF(FAC GE FACTOR)GO TO 340
      FACTOR=FAC
      BM=BMY(NM,IEND,3)
      ROT=RY(NM,IEND,3)
      KFAC=IEND
      KODE=4
      IDK=IND(NM,IEND)
      EK=EKEP(NM,IEND,3)
      GO TO 340
  270 KODY(NM,IEND)=9
      EKH(NM,IEND)=EKEP(NM,IEND,1)
      REVPT(NM,IEND)=RY(NM,IEND,5)-BMY(NM,IEND,5)/EKH(NM,IEND)
      FACTOR=0
      KFAC=0
      GO TO 340
C
C ..  RULE   9 ...
C
  280 IF(REMIND*DBM(NM,IEND) LT 0 0)GO TO 290
      FAC=(BMY(NM,IEND,5)-BMTOT(NM,IEND))/DBM(NM,IEND)
      IF(FAC GE FACTOR)GO TO 340
      FACTOR=FAC
      BM=BMY(NM,IEND,5)
      ROT=RY(NM,IEND,5)
      KFAC=IEND
      KODE=8
      IDK=IND(NM,IEND)
      EK=EKEP(NM,IEND,5)
      GO TO 340
  290 FAC=-BMTOT(NM,IEND)/DBM(NM,IEND)
      IF(FAC GE FACTOR)GO TO 340
      FACTOR=FAC
      BM=0 0
      KFAC=IEND
      ROT=REVPT(NM,IEND)
      KODE=10
      IDK=3-IND(NM,IEND)
      EKEP(NM,IEND,6)=(BMY(NM,IEND,4))/(RY(NM,IEND,4)-REVPT(NM,IEND))
      EK=EKEP(NM,IEND,6)
      GO TO 340
C
C.   RULE. .10  .
C
  300 IF(REMIND*DBM(NM,IEND).LT 0 0)GO TO 310
      MIND(NM,IEND)=6
      FAC=(BMY(NM,IEND,4)-BMTOT(NM,IEND))/DBM(NM,IEND)
      IF(FAC GE FACTOR)GO TO 340
      FACTOR=FAC
      BM=BMY(NM,IEND,4)
      ROT=RY(NM,IEND,4)
      KFAC=IEND
      KODE=6
      IDK=IND(NM,IEND)
      EK=EKEP(NM,IEND,4)
      GO TO 340
  310 KODY(NM,IEND)=11
      EKH(NM,IEND)=EKEP(NM,IEND,1)
      REVPT(NM,IEND)=RY(NM,IEND,6)-BMY(NM,IEND,6)/EKH(NM,IEND)
      FACTOR=0.0
      KFAC=0
      GO TO 340
C
C   RULE   11
C
  320 IF(REMIND*DBM(NM,IEND) LT 0 0)GO TO 330
      FAC=(BMY(NM,IEND,6)-BMTOT(NM,IEND))/DBM(NM,IEND)
      IF(FAC GE FACTOR)GO TO 340
      FACTOR=FAC
      BM=BMY(NM,IEND,6)
      ROT=RY(NM,IEND,6)
      KFAC=IEND
      KODE=10
      IDK=IND(NM,IEND)
      EK=EKEP(NM,IEND,6)
      GO TO 340
  330 FAC=-BMTOT(NM,IEND)/DBM(NM,IEND)
      IF(FAC.GE FACTOR)GO TO 340
      FACTOR=FAC
      BM=0
      ROT=REVPT(NM,IEND)
      KFAC=IEND
      KODE=8
      IDK=3-IND(NM,IEND)
      EKEP(NM,IEND,5)=BMY(NM,IEND,3)/(RY(NM,IEND,3)-REVPT(NM,IEND))
      EK=EKEP(NM,IEND,5)
  340 CONTINUE
  341 CONTINUE
C
C  *** UPDATE  MOMENTS **********
C
      DO 400 IEND=1,2
      IF(IEND EQ KFAC)GO TO 390
      BMTOT(NM,IEND)=BMTOT(NM,IEND)+FACTOR*DBM(NM,IEND)
      RTOT(NM,IEND)=RTOT(NM,IEND)+FACTOR*DBM(NM,IEND)/EKH(NM,IEND)
      IF(KODY(NM,IEND) EQ 0)GO TO 400
      KOD=KODY(NM,IEND)
      GO TO (350,350,400,350,400,350,400,350,400,350,400), KOD
  350 IDD=MIND(NM,IEND)
      BMY(NM,IEND,IDD)=BMTOT(NM,IEND)
      RY(NM,IEND,IDD)=RTOT(NM,IEND)
      DROT=DBM(NM,IEND)*FACTOR/EKH(NM,IEND)
      IF(KOD GT 2)GO TO 370
      IF(DROT.LT 0 )GO TO 360
      ROTPP(NM,IEND)=ROTPP(NM,IEND)+DROT
      GO TO 400
  360 ROTPN(NM,IEND)=ROTPN(NM,IEND)+DROT
      GO TO 400
  370 IF(DROT LT 0 )GO TO 380
      ROTSP(NM,IEND)=ROTSP(NM,IEND)+DROT
      GO TO 400
  380 ROTSN(NM,IEND)=ROTSN(NM,IEND)+DROT
      GO TO 400
  390 BMTOT(NM,IEND)=BM
      RTOT(NM,IEND)=ROT
      KODY(NM,IEND)=KODE
      EKH(NM,IEND)=EK
      IND(NM,IEND)=IDK
  400 CONTINUE
C  .CHECK  COMPLETION  OF  CYCLE
      FACAC=FACAC+FACTOR
      IF(FACAC.GT.0.999)GO TO 410
      CALL QBEAM(NM,AREA,QK2,Q,MAXEL,MAXNP,N1,M)
      DBM(NM,1)=S1*EDIS1(3)+S2*EDIS1(6)
      DBM(NM,2)=S3*EDIS1(3)+S4*EDIS1(6)
      GO TO 30
C .. SHEAR  FORCES  ..
  410 DSF=(-BMTOT(NM,1)+BMTOT1+BMTOT(NM,2)-BMTOT2)/BL
      SFTOT(NM,1)=SFTOT(NM,1)+DSF
      SFTOT(NM,2)=SFTOT(NM,2)-DSF
      KST=0
      IF(KODYX(NM,1).NE.KODY(NM,1).OR.KODYX(NM,2) NE.KODY(NM,2))
     !KST=1
      VRITE(6,147)N1,KST
  147 FORMAT(/5X,6HSTEP= ,I2,2X,5HKST= ,I2,/)
      DO 53 I1=1,8
   53 FT(I1)=0 0
      IF(KST.NE 1)GO TO 56
      KBAL=KBAL+1
      CALL QBEAM(NM,AREA,QK2,Q,MAXEL,MAXNP,N1,M)
      DO 58 I1=1,8
      DO 58 J1=1,8
   58 QK0(I1,J1)=QK0(I1,J1)-QK2(I1,J1)
      CALL MATMUL(8,8,8,1,8,1,8,8,1,QK0,EDIS,FT)
   56 VRITE(3'M X FT(I1),I1=1,8)
C NB !! TOTAL DISP = EDIS1 (6,1)
      CALL MATMUL(8,8,8,1,8,1,8,8,1,A1,DISP,EDIS1)
      IF(NM.EQ NEL2 AND.ITV.EQ 0) VRITE(6,11)
      IF(NM EQ.NEL2.AND.ITV.EQ 0) VRITE(6,101)
      IF(NM.EQ NEL2.AND.ITV.EQ.0) VRITE(6,111)
     1  (J,(AXIAL(J,I),SFTOT(J,I),BMTOT(J,I),ROTPP(J,I),ROTPN(J,I
     2   I=1,2),J=1,NEL2)
   11 FORMAT(1H1,'***OUTPUT TABLE 2.1 END BEAM FORCES****'//)
  101 FORMAT(//8H    NODE,11X,5HAXIAL,13X,5HSHEAR,12X,6HMOMENT,
     !12X,'X-DISP.',12X,'Y-DISP.',12X,'Y-ROTAT.'/)
  111 FORMAT(1H ,I6,6E18.6/7X,6E18.6)
      RETURN
      END
C
C  FORM  NODAL  FORCES
C
      SUBROUTINE FORCE(R,MAXEL,MAXNEQ,MAXNP,XFORCE,YFORCE,
     *X,Y,NEQ,DISPI,N1,KBAL,IT,TIME)
      COMMON/DATA/ NNP,NEL,NMAT,NOPT,NBODY,KMAS,MODIF,NEL2
      COMMON/NODE/IE(80,6)
      DIMENSION R(NEQ)
      DIMENSION X(MAXNP),Y(MAXNP)
      DIMENSION XFORCE(MAXNP),YFORCE(MAXNP)
      DIMENSION EDIS(8,1),QK(8,8),Q(8),QKV(64),DISPI(200)
      IF(IT.EQ.0) VRITE(6,11) TIME
      INDEX=0
      DO 5 K=1,MAXNP
      XFORCE(K)=0.0
      YFORCE(K)=0.0
    5 CONTINUE
      NEL1=NEL2
      DO 80 M=1,NEL
      MTYP2=IE(M,6)
      DO 20 I=1,4
      NN=IE(M,I)
      EDIS(2*I-1,1)=R(2*NN-1)
   20 EDIS(2*I,1)=R(2*NN)
      READ(7'M X QKV(K),K=1,64)
      IV=0
      DO 1110 I1=1,8
      DO 1110 J1=1,8
      IV=IV+1
      QK(I1,J1)=QKV(IV)
 1110 CONTINUE
      IF(MTYP2.NE.2)GO TO 63
      VRITE(6,61)
      VRITE(6,62 X((QK(I1,J1),J1=1,8),I1=1,8)
   61 FORMAT(8X,'  BEAM  STIF.  FROM 7 CALLED IN RTINE FORCE '/)
   62 FORMAT(1X,8E14.6)
   63 CALL MATMUL(8,8,8,1,8,1,8,8,1,QK,EDIS,Q)
      IF(INDEX.EQ.1) VRITE(6,100) M
      IF(MTYP2.NE.2)GO TO 1620
      NEL1=NEL1-1
      MM=NEL2-NEL1
C
C  IF  BEAM  ELEMENT  CALL  BEAFOR
C
      CALL BEAFOR(QK,IAA,MM,DISPI,X,Y,N1,MAXNP,EDIS,MAXEL,KBAL,M
 1620 DO 60 II=1,4
      NN=IE(M,II)
      XFORCE(NN)=XFORCE(NN)+Q(2*II-1)
      YFORCE(NN)=YFORCE(NN)+Q(2*II)
      IF(INDEX EQ.1) VRITE(6,110) NN,Q(2*II-1),Q(2*II)
   60 CONTINUE
   80 CONTINUE
  100 FORMAT(/25X,'ELEMENT NUMBER=',I5/,5X,'NODE',12X,'X-STRESS'
     1,12X,'Y-STRESS')
  110 FORMAT(I10,2E20 8)
      IF(IT NE 0) GO TO 141
C     VRITE(6,120)
      DIS=0 0
      FOR=0 0
```

```
      FOR=0 0
      AMOMT=0
      DO90JJ=1,NNP
      J=NNP+1-JJ
      DIS=DIS+R(2*J-1)
      FOR=FOR+XFORCE(J)
C     WRITE(6,130) J,X(J),Y(J),R(2*J-1),R(2*J),XFORCE(J),
C    *YFORCE(J)
      IF(X(J) NE 0 0)GO TO 90
C     WRITE(6,22) DIS,FOR
      AMOMT=AMOMT+FOR*Y(J)
C     WRITE(6,33)
      IF(Y(J) EQ 0 )WRITE(6,122)AMOMT
  122 FORMAT(5X,'BASE MOMT = ',F12 3/)
      IF(JJ EQ NNP) GO TO 90
      FOR=0 0
      DIS=0 0
   90 CONTINUE
  141 FOR=XFORCE(33)+XFORCE(53)+XFORCE(73)
      AMOMT=XFORCE(33)*Y(33)+XFORCE(53)*Y(53)+XFORCE(73)*Y(73)
      WRITE(13,123) TIME,FOR,AMOMT
      WRITE(6,123) TIME,FOR,AMOMT
  123 FORMAT(3F15 4)
   11 FORMAT(1H1,'**** OUTPUT TABLE 2 2 FORCE ON EACH NODE AT TIME = ',
     1       F6 4//)
   22 FORMAT(5X,'**** TOTAL VALUE AT THIS SECTION ****',F15.5,F40.5)
   33 FORMAT(5X,'**************************************************')
  120 FORMAT(3X,'NODE',5X,'X',5X,'Y',10X,'U-DISP',8X,'V-DISP',
     18X,'X-FORCE',8X,'Y-FORCE'/)
  130 FORMAT(I8,2F6 3,4F15 6)
  140 FORMAT(//15X,'**** ELEMENT STIFFNESS ON TAPE NO 7 WAS WRONG',5X,
     15X,'XXX M=',I5,5X,'XXX MM=',I5//)
      RETURN
      END
C
C  COMPUTE  STRESSES   AND  STRAINS
C  CHECK  YIELDING  OR  CRUSHING  OF  CONCRETE  BY  CALL  YIELDG
C  CHECK CRACKING OF CONCRETE AND YIELDING OF STEEL BY CALL ELAST
C  UPDATE  STIFFNESS  MATRIX  CONSEQUENTLY
C  FORM  ELEMENT  PSEUDO-LOADS  AND  STORE IN TAPE  3
C
      SUBROUTINE STRESS(R,X,Y,SIG1A,SIG2A,EPSA,SIGA,MAXNEQ,
     *MAXEL,MAXNP,N1,NEQ,KBAL,IFLAG,TIME,IT,DISPI)
      COMMON/DATA/ NNP,NEL,NMAT,NOPT,NBODY,KMAS,MODIF,NEL2
      COMMON/GAUSS/CORD(5,5),WEIGHT(5,5)
      COMMON/NODE/IE(80,6)
      COMMON/PROTY/E(4),PR(4),RO(4),TH(4)
      COMMON/STEEL/PX(80),PY(80)
      COMMON/YLDI/EPSLIM,YIELD,SIGMII
      COMMON/STATE/ NSIN(100),KOD(100),IPEL(100),KBAR(100),TITA(100),
     1              EPSMAX(100),EPSMIN(100)
      COMMON/BOUND/ NBOUN
      DIMENSION R(NEQ)
      DIMENSION X(MAXNP),Y(MAXNP),ND(100),ALFA1(100),
     1          SIG1(100),SIG2(100)
      DIMENSION SIG1A(MAXNP),SIG2A(MAXNP),EPSA(MAXNEQ),SIGA(MAXNEQ)
      DIMENSION CB(3,12),TCB(12,12),DISP(12,1),SIGB(3)
      DIMENSION B(3,12),EPSB(3),BT(12,3),EPSAA(3)
      DIMENSION XE(4,2),CB2(12,12),TCB2(3,12),TCB3(3,12),FT1(12),
     *OK(12,12),TOK(12,12),OK3(12,12),SIGAA(3),C(3,3),CC(3,3),FT(12),
     *TOK3(12,12),OKV(64),CBV(144)
      DIMENSION XFORCE(100),YFORCE(100),SHEAR(100)
      DIMENSION XDEF(100),YDEF(100),SDEF(100)
      DIMENSION V(300),RR(300),SS1(100),SS2(100),OK1(8,8),DISP1(8,1),
     1          SS3(100),LP(8),DELTA(3),DISP1(200),OK0(8,8)
      DO 6 I2=1,NNP
      SS1(I2)=0 0
      SS2(I2)=0 0
      SS3(I2)=0 0
      XFORCE(I2)=.0
      YFORCE(I2)=.0
      SHEAR(I2)=.0
      ALFA1(I2)=0
      ND(I2)=0
      XDEF(I2)= 0
      YDEF(I2)=0 0
      SDEF(I2)= 0
      SIG1(I2)= 0
    6 SIG2(I2)= 0
      DO 2 I=1,12
      DO 2 J=1,12
      CB2(I,J)=0 0
    2 OK3(I,J)=0 0
      DO 5 I=1,3
      SIGB(I)= 0
      EPSB(I)=0 0
      DO 5 J=1,3
      CC(I,J)=0 0
      C(I,J)=0 0
      DO 5 N2=1,12
      B(I,N2)=0 0
      CB(I,N2)=0 0
      BT(N2,I)=0 0
      TCB2(I,N2)=0 0
      TCB3(I,N2)=0 0
    5 DISP(N2,1)=0.0
      DO 79 I=1,MAXNEQ
      V(I)=0 0
   79 RR(I)=0 0
      IAA=0
   10 DO 60 NM=1,NEL
      MTYP2=IE(NM,5)
      IF(MTYP2 NE 1)GO TO 60
      DO 65 N=1,4
      MM=IE(NM,N)
      XE(N,1)=X(MM)
      XE(N,2)=Y(MM)
   65 CONTINUE
      DO 20 J=1,4
      NN=IE(NM,J)
      DISP(2*J-1,1)=R(2*NN-1)
   20 DISP(2*J,1)=R(2*NN)
      IF(INDX.EQ 2) WRITE(6,200)NM
      READ(8'NM)(CBV(K),K=1,144)
      IV=0
      DO 1110 I1=1,12
      DO 1110 J1=1,12
      IV=IV+1
      TCB(I1,J1)=CBV(IV)
 1110 CONTINUE
      IF(NM EQ.1.AND.IFLAG.EQ.0)WRITE(6,17)
      IF(NM EQ 1.AND.IFLAG.EQ 0) WRITE(6,19)((TCB(I,J),J=1,12),I=
   17 FORMAT(3X,17HCB MATRIX FROM 8./)
   19 FORMAT(6E15.5)
      IBB=0
      DO 30 L1=1,4
      NN=IE(NM,L1)
 C100 FORMAT(10X,I5,3E20 8)
  200 FORMAT(/15X,'STRESSES IN THE ELEMENT NO.= ',I5,//11X,'NODE'
     112X,'X-STRESS',12X,'Y-STRESS',8X,'SHEAR-STRESS')
      IF(L1.EQ 1.OR L1.EQ.2)ETA=-1.
      IF(L1.EQ.3 OR L1 EQ 4)ETA=1
      IF(L1.EQ.1.OR.L1.EQ 4)XI=-1.
      IF(L1.EQ 2 OR.L1 EQ.3)XI=1.0
      CALL BMAT(XE,XI,ETA,B,BT,DET)
      CALL MATMUL(3,12,12,1,3,1,3,12,1,B,DISP,EPSB)
      XDEF(NN)=XDEF(NN)+EPSB(1)
      YDEF(NN)=YDEF(NN)+EPSB(2)
      SDEF(NN)=SDEF(NN)+EPSB(3)
      DO 25 KK=1,3
      II=KK+3*(L1-1)
      DO 25 LL=1,12
   25 CB(KK,LL)=TCB(II,LL)
      CALL MATMUL(3,12,12,1,3,1,3,12,1,CB,DISP,SIGB)
      XFORCE(NN)=XFORCE(NN)+SIGB(1)
      YFORCE(NN)=YFORCE(NN)+SIGB(2)
      SHEAR(NN)=SHEAR(NN)+SIGB(3)
      ND(NN)=ND(NN)+1
   30 CONTINUE
   60 CONTINUE
      DO 82 K=1,NNP
      XFORCE(K)=XFORCE(K)/ND(K)
      YFORCE(K)=YFORCE(K)/ND(K)
      SHEAR(K)=SHEAR(K)/ND(K)
      XDEF(K)=XDEF(K)/ND(K)
      YDEF(K)=YDEF(K)/ND(K)
      SDEF(K)=SDEF(K)/ND(K)
      SP=(XFORCE(K)+YFORCE(K))/2.
      SM=(XFORCE(K)-YFORCE(K))/2.
      SQ=SM**2+SHEAR(K)**2
      DS=SQRT(SQ)
      SIG1(K)=SP+DS
      SIG2(K)=SP-DS
      IF(SM.EQ 0.0)ALFA1(K)=3.141592/2.
      IF(SM.EQ.0. )GO TO 92
      ALFA1(K)= 5*ATAN(SHEAR(K)/SM)
   92 ALFA1(K)=ALFA1(K)*180./3 1415926
   82 CONTINUE
      IF(IT.NE.0) GO TO 749
      WRITE(6,300)N1
      WRITE(6,1010)(K,X(K),Y(K),XFORCE(K),YFORCE(K),SHEAR(K),
     1              SIG1(K),SIG2(K),ALFA1(K),K=1,NNP)
      WRITE(6,400)
      WRITE(6,301)N1
      WRITE(6,1011)(K,X(K),Y(K),XDEF(K),YDEF(K),SDEF(K),K=1,NNP)
  300 FORMAT(1H1,//'*****STRESSES  ON  EACH  NODE AT  STEP=',I5,
     1       2X,'****'/2X,7H  NODE ,8X,1HX,9X,1HY,6X,8HSIGMA(X),
     2       8HSIGMA(Y),6X,8HTAU(X,Y),6X,8HSIGMA(1),6X,8HSIGMA(2
     3       5HANGLE)
  301 FORMAT(1H1,//'*****STRAINS ON  EACH NODE  AT  STEP= ',I5,
     1       2X,'****'/2X,7H  NODE ,8X,1HX,9X,1HY,8X,8HEPSIL(X),
     2       9X,8HEPSIL(Y),9X,8HEPS(X,Y))
  400 FORMAT(4X,'**************************************************
 1010 FORMAT(I8,2F10.2,6E14.6)
 1011 FORMAT(I8,2F10.2,E14.5,2X,E14.5,2X,E14.5)
  749 ICC=0
      IFLAG=IFLAG+1
      IF(IFLAG.GT.0) GO TO 3431
      DO 431 NN=1,NNP
      MTYP=1
      EPSAA(1)=EPSA(3*NN-2)
      EPSAA(2)=EPSA(3*NN-1)
      EPSAA(3)=EPSA(3*NN)
      SIGAA(1)=SIGA(3*NN-2)
      SIGAA(2)=SIGA(3*NN-1)
      SIGAA(3)=SIGA(3*NN)
      SIG1AA=SIG1A(NN)
      SIG2AA=SIG2A(NN)
      EPSB(1)=XDEF(NN)
      EPSB(2)=YDEF(NN)
      EPSB(3)=SDEF(NN)
      SIGB(1)=XFORCE(NN)
      SIGB(2)=YFORCE(NN)
      SIGB(3)=SHEAR(NN)
      SIG1B=SIG1(NN)
      SIG2B=SIG2(NN)
      P1B=EPSB(1)
      P2B=EPSB(2)
      PPB=EPSB(3)
      DO 292 I3=1,3
  292 DELTA(I3)=0.0
      RR(3*NN-2)=SIGB(1)
      RR(3*NN-1)=SIGB(2)
      RR(3*NN)=SIGB(3)
      IF(NN LE.NBOUN) GO TO 1292
      IF(IPEL(NN).EQ.3) GO TO 1292
      IF(SIGB(1) GE 0 0 OR SIGB(2).GE 0 0) GO TO 1432
```

```
      IF(SIGB(1) GE 0 0.OR SICB(2) GE 0 0) GO TO 1432
      EPS=SQRT(P1B*P1B+P2B*P2B-P1B*P2B+1 5*PPB*PPB)
      KR=KBAR(NN)
C
      CALL YIELDG(EPSAA,EPSB,SIGAA,SIGB,SIG1AA,SIG1B,SIG2AA,SIG2B,
     *            NN,N1,MAXNEQ,MAXNP,IPEL,C,EPS,MTYP,KR,DELTA)
C
      GO TO 1292
 1432 DELSI1=0 0
      DELSI2=0.0
      IF(SIG1B LT..0.AND SIG1B GT.YIELD OR
     1SIG2B LT. 0 AND SIG2B.GT YIELD) GO TO 1292
      IF(SIG1B LT YIELD) DELSI1=SIG1B-YIELD
      IF(SIG2B LT.YIELD) DELSI2=SIG2B-YIELD
      ALFA= ALFA1(NN)*3 1415926/180
      C1=COS(ALFA)
      S1=SIN(ALFA)
      SN2=SIN(2*ALFA)
      DELTA(1)=DELSI1*C1**2+DELSI2*S1**2
      DELTA(2)=DELSI1*S1**2+DELSI2*C1**2
      DELTA(3)=DELSI1*SN2* 5-DELSI2*SN2* 5
 1292 SS1(NN)=DELTA(1)
      SS2(NN)=DELTA(2)
      SS3(NN)=DELTA(3)
  431 CONTINUE
C     WRITE(6,3330)
C3330 FORMAT(/10X,'***  ERROR PAST YIELDG  ***'//)
 3431 DO 39 J=1,NNP
   39 ND(J)=0
      DO 31 NM=1,NEL
      DO 906 I1=1,3
      DO 906 J1=1,3
  906 CC(I1,J1)=0 0
      DO 907 I1=1,12
      DO 907 J1=1,12
  907 QK3(I1,J1)=0 0
      MTYP2=IE(NM,6)
      MTYP=IE(NM,5)
      IF(MTYP2.EQ 2)GO TO 31
      DO 66 N=1,4
      MM=IE(NM,N)
      DISPI(2*N-1,1)=DISPI(2*MM-1)
      DISPI(2*N,1)=DISPI(2*MM)
      XE(N,1)=X(MM)
      XE(N,2)=Y(MM)
   66 CONTINUE
      DO 32 I=1,4
      NN=IE(NM,I)
      EPSAA(1)=EPSA(3*NN-2)
      EPSAA(2)=EPSA(3*NN-1)
      EPSAA(3)=EPSA(3*NN)
      SIGAA(1)=SIGA(3*NN-2)
      SIGAA(2)=SIGA(3*NN-1)
      SIGAA(3)=SIGA(3*NN)
      SIG1AA=SIG1A(NN)
      SIG2AA=SIG2A(NN)
      EPSB(1)=XDEF(NN)
      EPSB(2)=YDEF(NN)
      EPSB(3)=SDEF(NN)
      SIGB(1)=XFORCE(NN)
      SIGB(2)=YFORCE(NN)
      SIGB(3)=SHEAR(NN)
      SIG1B=SIG1(NN)
      SIG2B=SIG2(NN)
      ALFA=ALFA1(NN)
C
      CALL ELAST(EPSAA,EPSB,SIGAA,SIGB,SIG1AA,SIG2AA,SIG1B,
     *           SIG2B,ALFA,N1,NN,NM,MAXNEQ,MAXNP,C,KBAL,IFLAG,MTYP)
C
      DO 34 I1=1,3
      DO 34 J1=1,3
   34 CC(I1,J1)=CC(I1,J1)+C(I1,J1)
   32 CONTINUE
      DO 36 I1=1,3
      DO 36 J1=1,3
   36 CC(I1,J1)=.25*CC(I1,J1)
C     IF(NM NE.1)GO TO 707
C     WRITE(6,705)
C     WRITE(6,706)((CC(I,J),J=1,3),I=1,3)
  705 FORMAT(/5X,' CC MATRIX FROM ELAST'//)
  706 FORMAT(5X,3F15.5)
  707 NC=2
      DO 57 I2=1,NC
      ETA=CORD(I2,NC)
      VEIG1=VEIGHT(I2,NC)
      DO 57 J2=1,NC
      XI=CORD(J2,NC)
      VEIG2=VEIGHT(J2,NC)
      FACT=VEIG1*VEIG2
      CALL BMAT(XE,XI,ETA,B,BT,DET)
      CALL MATMUL(3,3,3,12,3,12,3,3,12,CC,B,TCB3)
      CALL MATMUL(12,3,3,12,12,12,12,3,12,BT,TCB3,TQK3)
      DO 15 I1=1,12
      DO 15 J1=1,12
   15 QK3(I1,J1)=QK3(I1,J1)+TQK3(I1,J1)*FACT*TH(MTYP)*DET
   57 CONTINUE
      DO 33 I=1,4
      DO 746 J=1,12
      FT(J)=0 0
  746 FT1(J)=0 0
      NN=IE(NM,I)
      DELTA(1)=SS1(NN)
      DELTA(2)=SS2(NN)
      DELTA(3)=SS3(NN)
      IF(I EQ.1 OR I.EQ 2)ETA=-1
      IF(I EQ 3 OR.I.EQ 4)ETA=1.
      IF(I EQ.1.OR I.EQ 4)XI=-1.
      IF(I EQ.2 OR I EQ 3)XI=1
      CALL BMAT(XE,XI,ETA,B,BT,DET)
      CALL BMAT(XE,XI,ETA,B,GT,DET)
      CALL MATMUL(3,3,3,12,3,12,3,3,12,CC,B,TCB2)
      DO 95 I1=1,3
      I1=I1+3*(I-1)
      DO 95 J1=1,12
   95 CB2(I1,J1)=TCB2(I1,J1)
      CALL MATMUL(12,3,3,1,12,1,12,3,1,BT,DELTA,FT1)
      DO 747 J1=1,8
  747 FT(J1)=FT(J1)+FT1(J1)
   33 CONTINUE
      IF(MODIF.EQ 0) GO TO 877
C INCOMP.   MODES   ...  ..
      DO 50 I1=1,4
      L1=12-I1
      K1=L1+1
      DO 50 J1=1,L1
      PIV=QK3(J1,K1)/QK3(K1,K1)
      DO 40J2=1,12
   40 CB2(J2,J1)=CB2(J2,J1)-PIV*CB2(J2,K1)
      DO 50 J2=1,L1
   50 QK3(J1,J2)=QK3(J1,J2)-PIV*QK3(K1,J2)
  877 IV=0
      DO 1111 I1=1,12
      DO 1111 J1=1,12
      IV=IV+1
      CBV(IV)=CB2(I1,J1)
 1111 CONTINUE
C     IF(NM.NE.1)GO TO 602
C     WRITE(6,1113)
 1113 FORMAT(10X,'  CB FROM STRESS V. CC MATRIX'//)
C     WRITE(6,1114)((CB2(I2,J2),J2=1,12),I2=1,12)
 1114 FORMAT(6E15.6)
  602 WRITE(8'NM)(CBV(K),K=1,144)
  600 IV=0
      READ(7'NM)(QKV(K),K=1,64)
      DO 1112 I1=1,8
      DO 1112 J1=1,8
      IV=IV+1
      QK0(I1,J1)=QKV(IV)
      QK0(I1,J1)=QK0(I1,J1)-QK3(I1,J1)
      QKV(IV)=QK3(I1,J1)
 1112 CONTINUE
      CALL MATMUL(8,8,8,1,8,1,8,8,1,QK0,DISP1,FT1)
      DO 1723 KL=1,8
 1723 FT(KL)=FT(KL)+FT1(KL)
C
C   PSEUDO LOADS
C
      WRITE(3'NM)(FT(K),K=1,8)
  229 FORMAT (10X,'STIF. 1ST ELEMT COMPUTED IN QUAD V. C MATRIX'/
  228 FORMAT(1X,4F18.7)
  259 WRITE(7'NM)(QKV(K),K=1,64)
   31 CONTINUE
      IF(IT.EQ.0)
     1WRITE (6,990)N1,TIME
      DO 2482 K=1,NNP
      GAMA=TITA(K)*180 /3.1415926
      IF(IT.EQ.0)WRITE(6,991) K,NSIN(K),KOD(K),IPEL(K),KBAR(K),GAM
      EPSA(3*K-2)=XDEF(K)
      EPSA(3*K-1)=YDEF(K)
      EPSA(3*K)=SDEF(K)
      SIGA(3*K-2)=RR(3*K-2)
      SIGA(3*K-1)=RR(3*K-1)
      SIGA(3*K)=RR(3*K)
      SP=(SIGA(3*K-2)+SIGA(3*K-1))/2.
      SM=(SIGA(3*K-2)-SIGA(3*K-1))/2.
      SQ=SM**2+SIGA(3*K)**2
      DS=SQRT(SQ)
      SIG1A(K)=SP+DS
 2482 SIG2A(K)=SP-DS
  990 FORMAT (8X,28H** STATE OF ELEMTS AT STEP= ,I3,2X,6HTIME= ,F6
     16X,5HPOINT,10X,4HNSIN,5X,4HKODE,5X,4HIPEL,5X,4HKBAR,10X,'TITA
  991 FORMAT (7X,I3,10X,I3,5X,I3,5X,I3,5X,I3,8X,F10.4)
      RETURN
      END
C
C  READ  INPUT  DATA  FOR  BEAM  ELEMNTS
C
      SUBROUTINE INEL6(X,Y,N,NM)
      COMMON/DATA/NNP,NEL,NMAT,NOPT,NBODY,KMAS,MODIF,NEL2
      COMMON/INFEL/EKHIP(20),EKHJP(20),EKH(20,2),KODYX(20,2),
     1            ND(4),KODY(20,2),BMY(20,2,6),RY(20,2,6),
     2             IND(20,2),EKEP(20,2,6),REVPT(20,2),BMTOT(20,2),
     3             SFTOT(20,2),FTOT(20,2),RTOT(20,2),ROTPP(20,2),
     4             ROTPN(20,2),ROTSP(20,2),ROTSN(20,2),EK1(20,2),
     5             RY1(20,2,2),RA(20,2,2),RB(20,2,2),BMA(20,2,2),
     6             BMB(20,2,2),RREC(20,2,2),ALPHA(20,2),BETA(20,2),
     7             EEXP(20),AXIAL(20,2)
      COMMON/ELEM/KSF(2),FTYP(60,14),BMMY(20,70,2),EEXPN(60),ASTN(60
      COMMON/NODE/IE(80,6)
      DIMENSION IMT(60),AST(2)
      DIMENSION X(100),Y(100)
      DATA AST(1),AST(2)/2H   ,2H */
      WRITE(6,20)
   20 FORMAT(////16H STIFFNESS TYPES//
     1        18H   BEAM PROPERTIES//
     2     2X,5H TYPE,7X,28HREFERENCE SECTION PROPERTIES,5X,
     3        26HFLEXURAL STIFFNESS FACTORS,4X,15HHARDENING RATIO/
     4     2X,5H  NO.,8X,2HEI,10X,2HEA,10X,2HGA,8X,2HII,8X,2HJJ,8X,
     5        2HIJ,9X,1HI,7X,1HJ/)
 1010 FORMAT(//6110)
      IMT(N)=0
      ASTN(N)=AST(1)
      READ(5,30)I,(FTYP(N,J),J=1,8)
      READ(5,32)ITP,(FTYP(N,J),J=9,14),EEXPN(N)
   30 FORMAT(I5,3F10 0,3F5.0,2F10 0)
   32 FORMAT(I5,7F10 0)
      IF(FTYP(N,9) NE.0. )GOTO 40
      IMT(N)=1
```

```
      IMT(N)=1
      IMBT=N
      FTYP(IMBT,9)=FTYP(IMBT,1)*1 E8
      FTYP(IMBT,10)=FTYP(IMBT,1)*1 E8
      ASTN(N)=AST(2)
   40 WRITE(6,50)I,(FTYP(N,J),J=1,8)
   50 FORMAT(2X,I4,2X,3E12 4,F9 3,2F10 3,2X,2F8.5)
   60 CONTINUE
      WRITE(6,70)
   70 FORMAT(/19H   HINGE PROPERTIES//
     1       7H   TYPE,7X,15HHINGE STIFFNESS,5X,20HUNLOADING PARAMETERS,
     2       7X,18HLOADING PARAMETERS/4X,3HNO.,8X,1HI,11X,1HJ,10X,2HAI,
     3       8X,2HAJ,10X,2HBI,8X,2HBJ,7X,1HN/)
      WRITE(6,90)ASTN(N),N,(FTYP(N,J),J=9,14),EEXPN(N)
   80 CONTINUE
   90 FORMAT(1X,A2,I3,E14.4,E12 4,F10 3,F10 3,F12.3,F10 3,F9 2)
C
C    YIELDING  MOMENTS
C
  140 WRITE(6,150)
  150 FORMAT(////19H YIELD MOMENT TYPES//
     1       5H TYPE,5X,8HPOSITIVE,5X,8HNEGATIVE/
     2       5H NO ,5X,8H MOMENT ,5X,8H MOMENT /)
      DO 187 I=1,2
      READ(5,160)K,BMMY(N,I,1),BMMY(N,I,2)
      WRITE(6,170)N,BMMY(N,I,1),BMMY(N,I,2)
  160 FORMAT(I5,5X,2F10 0)
  170 FORMAT(I4,2F13 2)
      BMMY(N,I,2)=-ABS(BMMY(N,I,2))
  187 CONTINUE
  180 CONTINUE
      KODYX(N,1)=0
      KODYX(N,2)=0
      KODY(N,1)=0
      KODY(N,2)=0
      EKH(N,1)=0.
      EKH(N,2)=0.
      DO 189 I1=1,2
      DO 189 J1=1,2
      EKEP(N,I1,J1)=0 0
  189 CONTINUE
  181 CONTINUE
      KST=0

C   .HINGESTRAIN HARDENING RATIO

  410 IMBT=N
      FT7=FTYP(IMBT,7)
      FT8=FTYP(IMBT,8)
      I1=IE(NM,1)
      J1=IE(NM,2)
      FL=ABS(X(J1)-X(I1))
      EIL=FTYP(IMBT,1)/FL
      IF(IMT(IMBT).EQ 0)GO TO 420
      PSH=FTYP(IMBT,7)
      SKH=FTYP(IMBT,9)
      FT7=PSH/(SKH*(1.-PSH)/(3 *EIL)+1.)
      PSH=FTYP(IMBT,8)
      SKH=FTYP(IMBT,10)
      FT8=PSH/(SKH*(1.-PSH)/(3 *EIL)+1.)
  920 FORMAT(///4X,':. NODES. .',5X,I5,5X,I5/)
  420 EKH(IMBT,1)=FTYP(IMBT,9)
      EKEP(IMBT,1,1)=EKH(IMBT,1)
      EKEP(IMBT,1,2)=EKH(IMBT,1)*FT7
      EKH(IMBT,2)=FTYP(IMBT,10)
      EKEP(IMBT,2,1)=EKH(IMBT,2)
      EKEP(IMBT,2,2)=EKH(IMBT,2)*FT8
      EKHIP(IMBT)=EKH(IMBT,1)
      EKHJP(IMBT)=EKH(IMBT,2)
      IND(IMBT,1)=1
      IND(IMBT,2)=1
      ALPHA(IMBT,1)=FTYP(IMBT,11)
      ALPHA(IMBT,2)=FTYP(IMBT,12)
      BETA(IMBT,1)=FTYP(IMBT,13)
      BETA(IMBT,2)=FTYP(IMBT,14)
      EEXP(IMBT)=EEXPN(IMBT)
C
C... YIELD  MOMENT  AND  ROTATIONS
C
      KSFI=1
      KSFJ=2
      BMY(IMBT,1,1)=BMMY(IMBT,KSFI,1)
      RY(IMBT,1,1)=BMY(IMBT,1,1)/EKH(IMBT,1)
      BMY(IMBT,1,2)=BMMY(IMBT,KSFI,2)
      RY(IMBT,1,2)=BMY(IMBT,1,2)/EKH(IMBT,1)
      BMY(IMBT,2,1)=BMMY(IMBT,KSFJ,1)
      RY(IMBT,2,1)=BMY(IMBT,2,1)/EKH(IMBT,2)
      BMY(IMBT,2,2)=BMMY(IMBT,KSFJ,2)
      RY(IMBT,2,2)=BMY(IMBT,2,2)/EKH(IMBT,2)
      BMA(IMBT,1,1)=BMY(IMBT,1,1)
      BMB(IMBT,1,1)=BMY(IMBT,1,1)
      RA(IMBT,1,1)=RY(IMBT,1,1)
      RB(IMBT,1,1)=RY(IMBT,1,1)
      BMA(IMBT,1,2)=BMY(IMBT,1,2)
      BMB(IMBT,1,2)=BMY(IMBT,1,2)
      RA(IMBT,1,2)=RY(IMBT,1,2)
      RB(IMBT,1,2)=RY(IMBT,1,2)
      BMA(IMBT,2,1)=BMY(IMBT,2,1)
      BMB(IMBT,2,1)=BMY(IMBT,2,1)
      RA(IMBT,2,1)=RY(IMBT,2,1)
      RB(IMBT,2,1)=RY(IMBT,2,1)
      BMA(IMBT,2,2)=BMY(IMBT,2,2)
      BMB(IMBT,2,2)=BMY(IMBT,2,2)
      RA(IMBT,2,2)=RY(IMBT,2,2)
      RB(IMBT,2,2)=RY(IMBT,2,2)
      RREC(IMBT,1,1)=0
      RREC(IMBT,1,2)=0
      RREC(IMBT,2,1)=0
      RREC(IMBT,2,2)=0
      EK1(IMBT,1)=EKEP(IMBT,1,1)
      EK1(IMBT,2)=EKEP(IMBT,2,1)
      RY1(IMBT,1,1)=RY(IMBT,1,1)
      RY1(IMBT,1,2)=RY(IMBT,1,2)
      RY1(IMBT,2,1)=RY(IMBT,2,1)
      RY1(IMBT,2,2)=RY(IMBT,2,2)
  182 CONTINUE
      RETURN
      END
C
C  READ  INPUT  GENERAL  DATA
C
      SUBROUTINE DATAIN(MAXEL,MAXNP,MAXMAT,ISTOP)
      COMMON/DATA/NNP,NEL,NMAT,NOPT,NBODY,KMAS,MODIF,NEL2
      COMMON/DISP/X(100),Y(100),ULX(100),VLY(100),
     *KODE(100)
      COMMON/NODE/IE(80,6)
      COMMON/STEEL/PX(80),PY(80)
      COMMON/BARR/EPSY,EPSUL,SIGY,ES,ESH
      COMMON/PROTY/E(4),PR(4),RO(4),TH(4)
      COMMON/BOUND/ NBOUN
      ISTOP=0
      READ(5,100) NNP,NEL,NEL2,NBOUN,NBODY,NOPT,NMAT
      IF(NNP.LE MAXNP) GOTO 200
      ISTOP=ISTOP+1
  200 WRITE(6,201) NNP
      IF(NEL.LE.MAXEL) GOTO 202
      ISTOP=ISTOP+1
  202 WRITE(6,203) NEL
      IF(NMAT.LE.MAXMAT) GOTO 204
      ISTOP=ISTOP+1
  204 WRITE(6,205) NMAT
      WRITE(6,206) NBODY
      WRITE(6,207) NOPT
C
C    READ IN NODAL POINT GEOMETRY AND FORCES
C
      WRITE(6,208)
      WRITE(6,209)
      IF(NEL2.NE.0) GO TO 2006
      READ (5,101)(KODE(J),X(J),Y(J),ULX(J),VLY(J),J=1,NNP)
      READ (5,103)(IE(J,1),IE(J,2),IE(J,3),IE(J,4),IE(J,5),
     *IE(J,6),J=1,NEL)
      GO TO 2007
 2006 CALL GEN (NEL,NNP)
 2007 WRITE(6,102)(J,X(J),Y(J),ULX(J),VLY(J),J=1,NNP)
C
C   READ IN ELEMENT CONFIGURATION AND TYPE
C
      WRITE(6,229)
      WRITE(6,210)
      WRITE(6,211)
      WRITE(6,104)(J,IE(J,1),IE(J,2),IE(J,3),IE(J,4),IE(J,5),
     *IE(J,6),J=1,NEL)
      READ(5,1109) PXX,PYY
 1109 FORMAT (2F10.4)
  115 DO 105 N=1,NNP
      PY(N)=PYY
  105 PX(N)=PXX
  106 CONTINUE
C
C    READ IN MATERIAL PROPERTIES
C
      WRITE(6,214)
      WRITE(6,215)
      READ(5,109)(E(I),PR(I),RO(I),TH(I),I=1,NMAT)
      WRITE(6,110)(I,E(I),PR(I),RO(I),TH(I),I=1,NMAT)
      READ(5,50) EPSY,EPSUL,SIGY,ES,ESH
   50 FORMAT(3F12.5,F15.2,F12.5)
      IF(NEL2.EQ.0) GO TO 1620
      NEL1=NEL2
      DO1620 NM=1,NEL
      MTYP2=IE(NM,6)
      IF(MTYP2.NE.2)GO TO 1620
      NEL1=NEL1-1
      MM=NEL2-NEL1
      CALL INEL6(X,Y,MM,NM)
 1620 CONTINUE
 1000 FORMAT(I5,3X,I5)
  100 FORMAT(7I5)
  101 FORMAT(I10,4F10.5)
  103 FORMAT(6I5)
  113 FORMAT(4I5)
  107 FORMAT(I5,3F10.5)
  201 FORMAT(1H ,8X,25HNUMBER OF NODAL POINTS = ,I6/)
  203 FORMAT(1H ,12X,23HNUMBER OF ELEMENTS   = ,I6/)
  205 FORMAT(1H ,7X,26HNUMBER OF ELEMENT TYPES = ,I6/)
  206 FORMAT(1H ,2X,31HBODY FORCES(1=Y-DIR X 0=NONE) = ,I6/)
  207 FORMAT(1H ,1X,32H(1PLANE STRAIN X 2PLANE STRESS) = ,I6/)
  208 FORMAT(//1H ,9X,5HNODAL,8X,1HX,10X,1HY,12X,1HX,12X,1HY)
  209 FORMAT(1H ,9X,5HPOINT,6X,5HCOORD,6X,5HCOORD,8X,5HFORCE,8X,5HFORC(
     *//)
  102 FORMAT(1H ,10X,I3,6X,F6.2,5X,F6.2,4X,F8.2,5X,F8.2)
  229 FORMAT(1H ,20HRECTANGULAR ELEMENTS/)
  210 FORMAT(////1H ,8X,7HELEMENT,11X,5HNODES)
  211 FORMAT(1H ,10X,3HNO.,5X,1H1,6X,1H2,6X,1H3,6X,1H4,5X,4HTYPE,
     *4X,4HTYP2///)
  104 FORMAT((1H ,10X,5(I3,4X),I3,3X,I3))
  114 FORMAT((1H ,10X,4(I3,4X),I3))
  212 FORMAT(////1H ,9X,5HNODAL,7X,1HX,7X,1HY,7X,1HY)
  213 FORMAT(1H ,9X,5HPOINT,5X,4HDISP,4X,4HDISP,4X,4HROTA/)
  108 FORMAT(1H ,10X,I3,7X,F3 1,5X,F3 1,5X,F3.1)
  214 FORMAT(////1H ,8X,8HMATERIAL,2X,7HELASTIC,4X,9HPOISSON'S)
  215 FORMAT(1H ,10X,3HNO.,5X,7HMODULUS,6X,5HRATIO,4X,7HDENSITY,3X,
     * 9HTHICKNESS//)
  109 FORMAT(4F12.2)
  110 FORMAT(10X,I2,5X,F12.2,4X,F6 2,6X,F6.2,7X,F6.2)
      RETURN
```

```
      RETURN
      END
C
C  NONLINEAR  DYNAMIC  RESPONSE  FOLLOWING  NEWMARK-0 METHOD
C
      SUBROUTINE RESPON( AK,R,KMAS,MAXDOF,MAXEL,MAXNP,NEQ,IBAND,NEL,
     1                   MAXBV )
      COMMON/DAMP/C1,C2,DT,NP
      COMMON/NODE/IE(80,6)
      COMMON/STEEL/PX(80),PY(80)
      COMMON/DISP/X(100),Y(100),ULX(100),VLY(100),KODE(100)
      COMMON/DYCOF/AMS(200),AA(200),BB(200),U1(200),V1(200),A1(200)
      COMMON/BARR/EPSY,EPSUL,SIGY,ES,ESH
      COMMON/YLDI/EPSLIM,YIELD,SIGM11
      COMMON/STATE/ NSIN(100),KOD(100),IPEL(100),KBAR(100),TITA(100),
     1              EPSMAX(100),EPSMIN(100)
      DIMENSION R(NEQ),AK(NEQ,IBAND)
      DIMENSION CH(100),CV(100),T(100)
      DIMENSION BN(30),P(3,150),TNED(5,2)
      DIMENSION SIG1A(100),SIG2A(100),SIGA(200),EPSA(200)
      DIMENSION DISPI(200),CK(200,30)
      N1=0
      NNP=NEQ/2
      IFLAG=0
      REWIND 1
      READ(1) ((AK(I,J),J=1,IBAND),I=1,NEQ)
      REWIND 2
      DO 5 I=1,NEQ
      READ (2) (BN(J),J=1,IBAND)
      AMS(I)=BN(1)
      DISPI(I)=0.0
    5 CONTINUE
      DO 35 I=1,MAXNP
      TITA(I)=0.0
      SIG1A(I)=0.0
   35 SIG2A(I)=0.0
      DO 37 J=1,MAXDOF
      SIGA(J)=0.0
   37 EPSA(J)=0.0
      READ(5,10) INT,NPRINT,NSTEP,MAXSTP,NTYP,NP
      READ(5,50) C1,C2,DELT,DT,TIME,GACC
      READ(5,52) EPSLIM,YIELD,SIGM11
      READ(5,10) NFIX,NVEC,MSPAC,MSTRS,NEED,IT
      IF(MSTRS.EQ.0) GOTO 15
      READ(5,60) (TNED(I,1),TNED(I,2),I=1,NEED)
   15 DO 116 N=1,NNP
      EPSMIN(N)=-EPSY
      EPSMAX(N)=EPSY
      NSIN(N)=1
      IPEL(N)=1
      KOD(N)=0
  116 KBAR(N)=1
      DO 20 I=1,NNP
      CH(I)=0.0
      CV(I)=0.0
      T(I)=0.0
      IF(I.LE.NFIX) GOTO 20
      IF(NVEC.EQ.11.OR.NVEC.EQ.10) CH(I)=1.0
      IF(NVEC.EQ.11.OR.NVEC.EQ.01) CV(I)=1.0
   20 CONTINUE
      IF(NTYP) 22,24,22
   22 DO 23 I=2,NEQ,2
      N=I/2
      CH(N)=-CH(N)*GACC*AMS(I-1)
   23 CV(N)=-CV(N)*GACC*AMS(I)
   24 CONTINUE
      IF(NFIX.LT.NNP) GO TO 26
      READ(5,10) NVC
      DO25I=1,NVC
   25 READ(5,90) II,CH(II),CV(II)
   90 FORMAT(I5,2F10.5)
   26 CONTINUE
      READ(5,61) ((P(I,J),I=1,2),J=1,NP)
   61 FORMAT(2F10.4)
      DO 62 I=1,NP
      P(1,I)=P(1,I)/5.
      P(2,I)=P(2,I)*1.05/.3194
   62 P(3,I)=0.0
      IF(INT.EQ.0) GO TO 100
      READ(5,30) (U1(I),I=1,NEQ)
      READ(5,30) (V1(I),I=1,NEQ)
      IF(INT.EQ.1) GOTO 120
      READ(5,30) (A1(I),I=1,NEQ)
      GOTO 215
  100 DO 110 I=1,NEQ
      U1(I)=0.0
  110 V1(I)=0.0
  120 CONTINUE
      DO 130 I=1,NEQ
      A1(I)=0.0
  130 R(I)=U1(I)+C2*V1(I)
      DO 200 I=1,NEQ
      K=NEQ-I+1
      IF(K-IBAND)150,150,140
  140 K=IBAND
  150 DO 160 J=1,K
      IJ=I+J-1
  160 A1(I)=A1(I)+AK(I,J)*R(IJ)
      IF(I-IBAND)180,170,170
  170 L=IBAND-1
      GO TO 190
  180 L=I-1
      IF(L)200,200,190
  190 II=I
      DO 195 J=1,L
      II=II-1
  195 A1(I)=A1(I)+AK(II,J+1)*R(II)
  200 CONTINUE
C
C  CALL LOAD  FOR  INCREMENTAL  FORCES
C
      CALL LOAD( AK,AMS,R,P,AA,BB,T,CH,CV,NEQ,IBAND,TIME,N1,NFIX,IFLA(
     1           U1)
      DO 210 M=1,NEQ
      IF(AMS(M).EQ.0.0) GO TO 210
      A1(M)=(R(M)-A1(M))/AMS(M)-C1*V1(M)
  210 CONTINUE
      WRITE(6,300)
  215 CONTINUE
      BITA= 25*((1.+DELT)**2)
      ALPHA= 5+DELT
      DEAL=ALPHA/BITA
      A0=1 /(BITA*DT*DT)
      A11=DEAL/DT
      A2=1./(BITA*DT)
      A3=(.5/BITA)-1
      A4=DEAL-1
      A5=DT*( 5*DEAL-1.)
      A6=A0
      A7=-A2
      A8=-A3
      A9=(1.-ALPHA)*DT
      A10=ALPHA*DT
      CON1=1.+C2*A11
      CON2=C1*A11+A0
      B2=6./DT**2.+C1*3./DT
      B1=3*C2/DT+1.
      IF(KMAS.EQ.0) WRITE(6,305)
      IF(KMAS.GT.0) WRITE(6,310)
      IF(NTYP.EQ.0) WRITE(6,317)
      IF(NTYP.GT.0) WRITE(6,318)
      WRITE(6,315) INT,NPRINT,NSTEP,NTYP,NP
      WRITE(6,320) DT,ALPHA,BITA,DELT,C1,C2,GACC
      WRITE(6,335) (I,TNED(I,1),TNED(I,2),I=1,NEED)
      WRITE(6,325) ( I,T(I),CH(I),CV(I),I=1,NNP)
      WRITE(6,330) (J,P(1,J),P(2,J),P(3,J),J=1,NP)
      WRITE(6,400) TIME
      WRITE(6,345) (I,U1(2*I-1),U1(2*I),V1(2*I-1),V1(2*I),A1(2*I-1),
     *A1(2*I),I=1,NNP)
  300 FORMAT(1H1,15X,'**** THE FORCED RESPONSE PROBLEM *****',//15X,
     1           '*******NEWMARK BETA METHOD ****** *',//)
  305 FORMAT(//,15X,'****LUMPED MASS MATRIX WAS USED ****',//)
  310 FORMAT(//,15X,'**** CONSISTENT MASS MATRIX USED ****',//)
  315 FORMAT(//,10X,'** INT     ** NPRINT ** NSTEP  **NTYP     NP ****
     * // 6X,5I10)
  317 FORMAT(//15X,'**** FORCING FUNCTION RESPONSE ANALYSIS *****'//
  318 FORMAT(//15X,' **** EARTHQUAKE RESPONSE HISTORY ANALYSIS ****'
  320 FORMAT(//10X,'  TIME INTERVAL = ',F10.6,//15X,'ALPHA= ',F10.5,
     *' BITA = ',F10.5,5X,' DELT = ',F10.5,//15X, ' CONST1 =',F10.5,
     *' CONST2 = ',F10.5,5X,' GACC = ',F10.5)
  325 FORMAT(//10X,' **** FORCE VECTOR ****',//(I10,F10.4,2F15.6))
  330 FORMAT(//10X,'**** FORCE FUNCTION ****',//(I10,F10.4,2F15.6))
  335 FORMAT(//10X,'**** FORCES AND STRESSES CALCULATED AT FOLLOVING
     *E INTERVAL'//5X,'STEP',16X,'FROM',18X,'TO',//I8,4X,2F20.5)
  400 FORMAT(///15X,' INITIAL CONDITION AT TIME = ',F8.5//)
  345 FORMAT(//(5X,I5,6F15.5))
      KK=1
      IDO=0
      IEQUIL=20
      KEQUIL=0
      REWIND 1
      READ(1X(AK(I,J),J=1,IBAND),I=1,NEQ)
      DO 101 M=1,NEQ
      DO 102 L=1,IBAND
  102 CK(M,L)=AK(M,L)*C2
  101 CK(M,1)=CK(M,1)+AMS(M)*C1
      REWIND 10
      WRITE(10) ((CK(I,J),J=1,IBAND),I=1,NEQ)
      DO 280 N1=1,NSTEP
      KBAL=0
      TIME=TIME+DT
      IF(N1.NE.1.AND.IDO.EQ.0)GO TO 266
      REWIND 1
      READ(1X(AK(I,J),J=1,IBAND),I=1,NEQ)
      DO 250 M=1,NEQ
      DO 245 L=1,IBAND
  245 AK(M,L)=AK(M,L)+A11*CK(M,L)
  250 AK(M,1)=AK(M,1)+AMS(M)*A0
      CALL BANSOL(1,AK,R,NEQ,IBAND,NEQ,IBAND)
      REWIND 4
      WRITE(4X(AK(I,J),J=1,IBAND),I=1,NEQ)
  266 DO 265 I=1,NEQ
      AA(I)=-V1(I)*A2-A1(I)*A3
  265 BB(I)=-A4*V1(I)-A5*A1(I)
      CALL LOAD( AK,AMS,R,P,AA,BB,T,CH,CV,NEQ,IBAND,TIME,N1,NFIX,IFLA
     1           U1)
      REWIND 4
      READ(4X((AK(I,J),J=1,IBAND),I=1,NEQ)
C
C  SOLVE  FOR  DISPLACEMENT  INCREMENT
C
      CALL BANSOL(2,AK,R,NEQ,IBAND,NEQ,IBAND)
      DO 270 I=1,NEQ
  270 DISPI(I)=R(I)
      KEQUIL=KEQUIL+1
      IT=IEQUIL-KEQUIL
      IF(IT.EQ.0) KEQUIL=0
C
C  ITERATE  FOR  CONVERGENCE  IF  NEEDED
C
      IF(TIME.LT.0.10) GO TO 27
      CALL ITERAT(A0,A11,A2,A3,A4,A5,A6,A7,A8,A9,A10,C1,C2,DISPI,
     1       IBAND,NEQ,AK,R,AMS,A1,V1,U1,N1,AA)
   27 DO 271 I=1,NEQ
      R(I)=A7*V1(I)+A8*A1(I)+A6*DISPI(I)
      V1(I)=V1(I)+A9*A1(I)+A10*R(I)
      A1(I)=R(I)
```

```
      A1(I)=R(I)
      U1(I)=DISPI(I)+U1(I)
  271 R(I)=U1(I)
      CALL NEWDAV(U1,V1,A1,N1,TIME)
  278 CALL FORCE(R,MAXEL,MAXDOF,MAXNP,ULX,VLY,X,Y,NEQ,DISPI,N1,KBAL,IT,
     1            TIME)
      CALL STRESS(R,X,Y,SIG1A,SIG2A,EPSA,SIGA,MAXDOF,MAXEL,
     1     MAXNP,N1,NEQ,KBAL,IFLAG,TIME,IT,DISPI)
  279 CONTINUE
      WRITE(6,1002) N1,KBAL
 1002 FORMAT(/10X,'** AT  STEP = ',I5,5X,'***  KBAL = ',I5/)
      IF(KBAL.EQ.0)GO TO 260
      DO 299 J=1,NNP
      ULX(J)=0.0
  299 VLY(J)=0.0
      IDO=IDO+1
      CALL ASEMBL(ISTOP,MAXEL,MAXNP,MAXDOF,MAXBW,N1)
  280 CONTINUE
   10 FORMAT(6I5)
   30 FORMAT(5F15.5)
   50 FORMAT(5F8.5,F10.5)
   52 FORMAT(3F10.4)
   60 FORMAT(6F10.4)
      RETURN
      END
      SUBROUTINE ITERAT(A0,A11,A2,A3,A4,A5,A6,A7,A8,A9,A10,C1,C2,DISPI,
     *      IBAND,NEQ,AK,R,AMS,A1,V1,U1,N1,R1)
      DIMENSION AK(NEQ,IBAND),R(NEQ)
      DIMENSION DISPI(200),AMS(200),A1(200),V1(200),U1(200)
      DIMENSION R1(200)
      ITE=0
      RTOL=0.0010
      ITEMAX=20
  500 DO 10 I=1,NEQ
      R1(I)=0.0
   10 R(I)=U1(I)+DISPI(I)
      ITE=ITE+1
      DO 20 I=1,NEQ
   20 R(I)=C2*(A11*DISPI(I)-A4*V1(I)-A5*A1(I))+R(I)
      REWIND 1
      READ (1) ((AK(I,J),J=1,IBAND),I=1,NEQ)
      DO 700 I=1,NEQ
      K=NEQ-I+1
      IF(K-IBAND)650,650,640
  640 K=IBAND
  650 DO 660 J=1,K
      IJ=I+J-1
  660 R1(I)=AK(I,J)*R(IJ)+R1(I)
      IF(I-IBAND)680,670,670
  670 L=IBAND-1
      GO TO 690
  680 L=I-1
      IF(L)700,700,690
  690 II=I
      DO 695 J=1,L
      II=II-1
  695 R1(I)=R1(I)+AK(II,J+1)*R(II)
  700 CONTINUE
      FAC1=A0+A11*C1
      FAC2=-A2-A4*C1
      FAC3=-A3-A5*C1
      DO 40 I=1,NEQ
      R(I)=FAC1*DISPI(I)+FAC2*V1(I)+FAC3*A1(I)
      R(I)=-AMS(I)*R(I)
   40 R(I)=R(I)-R1(I)
C     WRITE(6,900)(R(I),I=1,NEQ)
C 900 FORMAT(3F24.8)
      REWIND 9
      READ (9) (R1(I),I=1,NEQ)
      DO 60 I=1,NEQ
   60 R(I)=R(I)+R1(I)
   61 REWIND 4
      READ (4) ((AK(I,J),J=1,IBAND),I=1,NEQ)
      CALL BANSOL (2,AK,R,NEQ,IBAND,NEQ,IBAND)
      DNORM=0
      DINORM=0.0
      DO 300 I=1,NEQ
      R1(I)=U1(I)+DISPI(I)+R(I)
      DNORM=DNORM+R1(I)*R1(I)
  300 DINORM=DINORM+R(I)*R(I)
      TOL=DNORM*RTOL
      IF(DINORM.LT.TOL) GO TO 400
      DO 120 I=1,NEQ
      DISPI(I)=DISPI(I)+R(I)
  120 R(I)=R1(I)
      IF(ITE.LT.ITEMAX) GO TO 500
      WRITE(6,2010)N1,ITE
      WRITE(6,2020)
  400 ICOUNT=2
      WRITE(6,2222) N1,ITE
 2222 FORMAT(/10X,'** AT  STEP = ',I3,3X,'NBR OF ITERATIONS = ',I2/)
      RETURN
 2010 FORMAT(///32HEQUILIBRIUM  ITERATION IN STEP= ,I5,/
     1          32HNUMBER OF ITERATIONS          = ,I5//)
 2020 FORMAT(///28HITERATION LIMIT REACHED STOP)
      END
C
C  COMPUTE  UPDATED  DISPL ,  VEL.  AND  ACC.  VECTORS
C
      SUBROUTINE NEWDAV(DISP,VEL,ACC,N1,TIME)
      COMMON/DATA/NNP,NEL,NMAT,NOPT,NBODY,KMAS,MODIF,NEL2
      DIMENSION  VEL(200),ACC(200),DISP(200)
      WRITE(6,70)N1,TIME
      DO 103 II=1,NNP
      WRITE(6,345)I, DISP(2*I-1),DISP(2*I)
  103 CONTINUE
      WRITE(12,347) TIME,DISP(65),DISP(105),DISP(155)
      WRITE(6,347) TIME,DISP(65),DISP(105),DISP(155)
   70 FORMAT(//10X,'****STEP NO= ',I5,5X,'***TIME= ',F12.8,//
     *2H ,'NODE',7X,'XDISP',9X,'Y-DISP')
  345 FORMAT(2X,I5,2F15.6)
  347 FORMAT(F15.5,10X,3F15.5)
      RETURN
      END
C
C  FORM  UPDATED  ELASTICITY  MATRIX  C
C
      SUBROUTINE ELAST(EPSAA,EPSB,SIGA,SIGB,SIG1AA,SIG2AA,SIG1B,
     *          SIG2B,ALFA,N1,NN,NM,MAXNEQ,MAXNP,C,KBAL,IFLAG,MTYP)
      COMMON/PROTY/E(4),PR(4),RO(4),TH(4)
      COMMON/YLDI/EPSLIM,YIELD,SIGMI1
      COMMON/STEEL/PX(80),PY(80)
      COMMON/STATE/ NSIN(100),KOD(100),IPEL(100),KBAR(100),TITA(100),
     1              EPSMAX(100),EPSMIN(100)
      DIMENSION EPSAA(3),EPSB(3),SIGB(3),SIGA(3),C(3,3),CS(3,3),DELTA(
      P1A=EPSAA(1)
      P2A=EPSAA(2)
      PPA=EPSAA(3)
      P1B=EPSB(1)
      P2B=EPSB(2)
      PPB=EPSB(3)
      ALFA=ALFA*3.1415926/180.
      BITA0=TITA(NN)
      DO 5 I=1,3
      DO 5 J=1,3
    5 C(I,J)=0.0
      IF(IPEL(NN).EQ.3)GO TO 10
   92 SB1=SIGB(1)
      SB2=SIGB(2)
      SB3=SIGB(3)
      S1A=SIG1AA
      S1B=SIG1B
      S2A=SIG2AA
      S2B=SIG2B
      ST=SIGMI1
      IF(BITA0.EQ.0.0) GO TO 141
      PI=3.1415926
      C1=COS(BITA0)
      S1=SIN(BITA0)
      SS2=SIN(2*BITA0)
      C2=COS(BITA0-PI/2.)
      S2=SIN(BITA0-PI/2.)
      EPER1=P1B*C1*C1+P2B*S1*S1-PPB*C1*S1
      EPER2=P2B*C2*C2+P1B*S2*S2-PPB*C2*S2
      SPER11=SB1*S1*S1+SB2*C1*C1-2.*SB3*C1*S1
      SPER12=SB1*C2*C2+SB2*S2*S2-2.*SB3*S2*C2
      SPER1=-PR(MTYP)*SPER11/E(MTYP)
      SPER2=-PR(MTYP)*SPER22/E(MTYP)
  141 KD=KOD(NN)
      CALL DCRACK(C,KD,NN,NM,N1,S1B,S2B,ALFA,EPER1,EPER2,SPER1,SPER2,
     1            S1A,S2A,ST,MTYP,KBAL,SPER11,SPER22,BITA0)
      TITA(NN)=BITA0
      KOD(NN)=KD
   10 CALL BAR(NSIN,KBAR,CS,P2B,P2A,NN,NM,N1,EPSMAX,EPSMIN,IFLAG,MTYP,
     1         KBAL)
      DO 35 I=1,3
      DO 35 J=1,3
   35 C(I,J)=C(I,J)+CS(I,J)
   20 RETURN
      END
C
C  MONITOR  OPENING  OR  CLOSING  OF  CRACKS
C
      SUBROUTINE DCRACK(C,KD,NN,NM,N1,S1B,S2B,ALFA,EPER1,EPER2,SPER1,
     1           SPER2,S1A,S2A,ST,MTYP,KBAL,SPER11,SPER22,BITA0)
      DIMENSION C(3,3)
      KD1=KD
      IF(KD.NE.0)GO TO 5
      IF(S1B.GT.ST)KD=1
      IF(S2B.GT.ST.AND.KD.EQ.1)KD=3
      IF(S2B.GT.ST.AND.KD.EQ.0)KD=2
      GO TO 340
    5 GO TO (110,120,130,140,150,160,170,180),KD
  110 IF(EPER1.LT.SPER1)KD=4
      IF(S2B.GT.ST.AND.KD.EQ.4) KD=5
      IF(S2B.GT.ST.AND.KD.EQ.1) KD=3
      GO TO 340
  120 IF(EPER2.LT.SPER2)KD=6
      IF(S1B.GT.ST.AND.KD.EQ.6) KD=7
      IF(S1B.GT.ST.AND.KD.EQ.2) KD=3
      GO TO 340
  130 IF(EPER1.LT.SPER1) GO TO 131
      IF(EPER2.LT.SPER2) KD=7
      GO TO 340
  131 KD=5
      IF(EPER2.LT.SPER2) KD=8
      GO TO 340
  140 IF(SPER11.GT..0.AND.SPER12.GT.ST)KD=3
      IF(SPER11.GT.0.AND.SPER12.LT.ST)KD=1
      IF(SPER11.GT.0.0)GO TO 340
      IF(SPER12.GT.ST)KD=5
      GO TO 340
  150 IF(SPER11.LT.0.0)GO TO 151
      KD=3
      IF(EPER2.LT.SPER2) KD=7
      GO TO 340
  151 IF(EPER2.LT.SPER2) KD=8
      GO TO 340
  160 IF(SPER12.LT.0.0)GO TO 161
      KD=2
      IF(SPER11.GT.ST)KD=3
      GO TO 340
  161 IF(SPER11.GT.ST)KD=7
      GO TO 340
  170 IF(SPER12.LT.0.0)GO TO 171
      KD=3
      IF(EPER1.LT.SPER1) KD=5
```

```
      IF(EPER1 LT SPER1 ) KD=5
      GO TO 340
  171 IF(EPER1 LT.SPER1 ) KD=8
      GO TO 340
  180 IF(SPER11 LT 0 0)GO TO 181
      KD=7
      IF(SPER12 GT. 0 ) KD=3
      GO TO 340
  181 IF(SPER12 GT  0 )KD=5
  340 IF(KD.EQ 0 ) BITA0=0 0
      IF(KD.EQ 0 ) GO TO 988
      IF(KD1 NE 0 ) GO TO 988
      BITA0=ALFA
  988 CALL CRAC(C,BITA0,KD,NN,NM,N1,MTYP,KBAL )
      IF(KD1 NE KD ) KBAL=KBAL+1
      RETURN
      END
C
C  FORM  C  MATRIX  OF  CRACKED  ELEMENTS
C
      SUBROUTINE CRAC(C,BITA0,KD,NN,M,N1,MTYP,KBAL )
      COMMON/STEEL/PX(80),PY(80)
      COMMON/PROTY/E(4),PR(4),RO(4),TH(4)
      COMMON/BOUND/ NBOUN
      DIMENSION C(3,3),T(3,3),D(3,3),CT(3,3)
C SHEAR FACTOR = NU
      IAA=0
      NU= 5
      DO 10 I=1,3
      DO 10 J=1,3
      CT(I,J)=0 0
   10 C(I,J)=0 0
      PI=3 1415926
      A1=E(MTYP)/(1 -PR(MTYP)*PR(MTYP))
      B1=A1*PR(MTYP)
      IF(KD.EQ 0 OR NN LE.NBOUN)GO TO 110
      GO TO (120,130,140,110,130,110,120,110),KD
  110 C(1,1)=A1
      C(1,2)=B1
      C(2,1)=B1
      C(2,2)=A1
      C(3,3)=A1*(1.-PR(MTYP))/2.
      GO TO 100
  120 ANGLE=BITA0+PI/2
      C(1,1)=E(MTYP)
      C(3,3)=A1*(1 -PR(MTYP))*NU/2.
      GO TO 50
  130 ANGLE=BITA0
      C(2,2)=E(MTYP)
      C(3,3)=A1*(1 -PR(MTYP))*NU/2.
      GO TO 50
  140 C(3,3)=A1*(1 -PR(MTYP))*NU/2.
      ANGLE=BITA0
      IF(IAA GT 0)ANGLE=BITA0+PI/2.
   50 S1=SIN(ANGLE)
      C1=COS(ANGLE)
      T(1,1)=C1*C1
      T(1,2)=S1*S1
      T(1,3)=C1*S1
      T(2,1)=S1*S1
      T(2,2)=C1*C1
      T(2,3)=-C1*S1
      T(3,1)=-2 *C1*S1
      T(3,2)=2.*C1*S1
      T(3,3)=C1*C1-S1*S1
      DO 60 IR=1,3
      DO 60 IC=1,3
      D(IR,IC)=0.0
      DO 70 IN=1,3
   70 D(IR,IC)=D(IR,IC)+T(IN,IR)*C(IN,IC)
   60 CONTINUE
      DO 90 IR=1,3
      DO 90 IC=1,3
      C(IR,IC)=0 0
      DO 80 IN=1,3
   80 C(IR,IC)=C(IR,IC)+D(IR,IN)*T(IN,IC)
   90 C(IC,IR)=C(IR,IC)
      IF(KD.NE.3) GO TO 100
      IF(IAA.NE 0) GO TO 96
      DO 95 I=1,3
      DO 95 J=1,3
   95 CT(I,J)=C(I,J)
      IAA=IAA+1
      GO TO 140
   96 DO 97 I=1,3
      DO 97 J=1,3
   97 C(I,J)=C(I,J)+CT(I,J)
  100 RETURN
      END
C
C  CHECK  YIELDING  OF  CONCRETE  (VON MISES FLOW)  OR CRUSHING
C
      SUBROUTINE YIELDG(EPSAA,EPSB,SIGAA,SIGB,SIG1A,SIG1B,SIG2A,
     *SIG2B,NN,N1,MAXNEQ,MAXNP,IPEL,C,EPS,MTYP,KR,DELTS)
      COMMON/YLDI/EPSLIM,YIELD,SIGMI1
      COMMON/STEEL/ PX(80),PY(80)
      COMMON/BARR/EPSY,EPSUL,SIGY,ES,ESH
      COMMON/PROTY/ E(4),PR(4),RO(4),TH(4)
      DIMENSION EPSAA(3),EPSB(3),SIGB(3),SIGAA(3),C(3,3),DELTA(3)
      DIMENSION DELSIG(3),DELEPS(3),TAU(3),DEPS(3),DELTM(3),DELTS(3)
      DIMENSION IPEL(MAXNP)
      IPEL1=IPEL(NN)
      C1=ES*PX(NN)
      GO TO (  540,550,540,550,540,560 ),KR
  540 EY=ES
      GO TO 570
  550 EY=ESH
      GO TO 570
  560 EY=0 0
  570 C2=EY*PY(NN)
      IF(EPS.LT EPSLIM) IPEL(NN)=3
      IF(IPEL(NN).EQ.3) GO TO 106
      YLD=YIELD
      A11=E(MTYP)/(1.-PR(MTYP)**2.)+C1
      A12=E(MTYP)/(1.-PR(MTYP)**2.)+C2
      B1=A1*PR(MTYP)
      B2=E(MTYP)/(2.*(1 +PR(MTYP)))
      DO 10 I=1,3
      TAU(I)=0.0
      DELSIG(I)=SIGB(I)-SIGAA(I)
   10 DELEPS(I)=EPSB(I)-EPSAA(I)
C     DELSIG(1)=A11*DELEPS(1)+B1*DELEPS(2)
C     DELSIG(2)=B1*DELEPS(2)+A12*DELEPS(2)
C     DELSIG(3)=B2*DELEPS(3)
      DO 20 I=1,3
   20 TAU(I)=SIGAA(I)+DELSIG(I)
      SX=TAU(1)
      SY=TAU(2)
      SXY=TAU(3)
      F=SQRT(SX*SX-SX*SY+SY*SY+3*SXY*SXY)+YLD
      IF(F)30,30,40
   30 IPEL(NN)=1
C     DO 50 I=1,3
C  50 SIGB(I)=TAU(I)
      GO TO 500
   40 IF(IPEL(NN).EQ.1)GO TO 45
      IPEL(NN)=2
      RATIO=0 0
      DO 42 I=1,3
   42 TAU(I)=SIGAA(I)
      GO TO 150
   45 IPEL(NN)=2
      DO 300 I1=1,3
  300 TAU(I1)=SIGAA(I1)
      SX=TAU(1)
      SY=TAU(2)
      SXY=TAU(3)
      DX=DELSIG(1)
      DY=DELSIG(2)
      DXY=DELSIG(3)
      F1=SX*SX+SY*SY-SX*SY+3 *SXY*SXY-YLD*YLD
      F2=DX*DX+DY*DY-DX*DY+3.*DXY*DXY
      F3=DX*SX+DY*SY+3 *SXY*DXY
      F4=F3*F3-F2*F1
      IF (F4.LT.0.0) F4=0.0
      RATIO=(-F3+SQRT(F4))/F2
      VRITE(6,99)F1,F2,F3,RATIO
   99 FORMAT(10X,'F1=',F8.5,'F2=',F8.5,'F3=',F8.5,'RATIO=',F8.5/)
  910 FORMAT(/4X,'NODE= ',I3,3X,'YIELDG FUNCTION F1 = ',F12.8//)
      DO 55 I1=1,3
   55 TAU(I1)=SIGAA(I1)+RATIO*DELSIG(I1)
  150 MM=20.*SQRT(F)/(-YLD)+1
      IF(MM.GT.20) MM=20
      XM=(1.-RATIO)/FLOAT(MM)
      DO 60 I1=1,3
   60 DEPS(I1)=XM*DELEPS(I1)
      DO 83 I1=1,3
      DELTA(I1)=0.0
   83 DELTM(I1)=0.0
      DO 80 IM=1,MM
      CALL DELPAL(TAU,DEPS,C,YLD,MTYP)
C     C(1,1)=C(1,1)+C1
C     C(2,2)=C(2,2)+C2
      DO 70 I1=1,3
      DO 70 J1=1,3
      DELTM(I1)=C(I1,J1)*DEPS(I1)
   70 TAU(I1)=TAU(I1)+DELTM(I1)
      SX=TAU(1)
      SY=TAU(2)
      SXY=TAU(3)
      FA=SX*SX-SX*SY+SY*SY+3.*SXY*SXY
      FB=YLD*YLD
      F=FA-FB
      IF(F LE 1.E-04)GO TO 80
      COEF=SQRT(FB/FA)
      DO 82 I1=1,3
      DELTA(I1)=DELTA(I1)+DELTM(I1)
   82 TAU(I1)=TAU(I1)*COEF
   80 CONTINUE
      DO 475 I1=1,3
  475 DELTS(I1)=DELTA(I1)
C     DO 75 I1=1,3
C  75 SIGB(I1)=TAU(I1)
  106 IF(IPEL(NN).NE.3)GO TO 500
      IF(IPEL1.EQ.3)GO TO 500
      DO 575 I1=1,3
  575 DELTS(I1)=SIGB(I1)
      VRITE(6,699) NN,N1
  699 FORMAT(/5X,6HNODE= ,I3,5X,17HCRUSHED AT STEP= ,I3/)
  500 RETURN
      END
C
C  FORM  C  MATRIX  OF  YIELDED  CONCRETE  ELEMENT
C
      SUBROUTINE DELPAL(TAU,DEPS,C,YLD,MTYP)
      COMMON/PROTY/E(4),PR(4),RO(4),TH(4)
      DIMENSION TAU(3),C(3,3),DEPS(3)
      D1=PR(MTYP)/(PR(MTYP)-1.)
      SM=(TAU(1)+TAU(2))/3
      SX=TAU(1)-SM
      SY=TAU(2)-SM
      SS=TAU(3)
      H=2.*D1/3
      P=SS/(1.+PR(MTYP))
      R=SX*SX+SY*SY+2 *PR(MTYP)*SY*SX
      Q=R+2 *(1 -PR(MTYP))*P
      C(1,1)=SY*SY+2.*P
```

```
      C(1,1)=SY*SY+2 *P
      C(1,2)=-SX*SY+2 *PR(MTYP)*P
      C(1,3)=-(SX+PR(MTYP)*SY)*SS/(1 +PR(MTYP))
      C(2,1)=C(1,2)
      C(2,2)=SX*SX+2.*P
      C(2,3)=-(SY+PR(MTYP)*SX)*SS/(1 +PR(MTYP))
      C(3,1)=C(1,3)
      C(3,2)=C(2,3)
      C(3,3)=R/(2 *(1.+PR(MTYP)))
      DO 10 I1=1,3
      DO 10 J1=1,3
   10 C(I1,J1)=(E(MTYP)/Q)*C(I1,J1)
      RETURN
      END
C
C  CHECK  YIELDING  OF  STEEL  REINFORCEMENT
C
      SUBROUTINE BAR(NSIN,KBAR,CS,P2B,P2A,NN,NM,NI,EPSMAX,EPSMIN,IFLAG,
     1                MTYP,KBAL)
      COMMON/PROTY/E(4),PR(4),RO(4),TH(4)
      COMMON/NODE/ IE(80,6)
      COMMON/STEEL/ PX(80),PY(80)
      COMMON/BARR/EPSY,EPSUL,SIGY,ES,ESH
      DIMENSION EPSMAX(100),EPSMIN(100),KBAR(100),NSIN(100),CS(3,3)
      E1=ES/E(MTYP)
      C1=E(MTYP)*E1*PX(NN)
      DO 2 I=1,3
      DO 2  J=1,3
    2 CS(I,J)=0.0
      CS(1,1)=C1
      KR=KBAR(NN)
      KR1=KR
      IF(IFLAG.GT.1)GO TO 5
      IF(P2B.LT.0.0) NSIN(NN)=2
    5 KK1=NSIN(NN)
      GO TO (110,120),KK1
  110 IF(P2B.GE.EPSUL) KR=6
      GO TO (10,20,30,40,50,340) , KR
   10 IF(P2B.LT.EPSY) GO TO 340
      KR=2
      EPSMIN(NN)=P2B-2 *EPSY
      GO TO 340
   20 IF(P2B.LT.P2A) GO TO 21
      EPSMIN(NN)=P2B-2.*EPSY
      GO TO 340
   21 KR=3
      EPSMAX(NN)=P2B
      GO TO 340
   30 IF(P2B.LT.P2A) GO TO 31
      IF(P2B.LT.EPSMAX(NN))GO TO 340
      KR=2
      EPSMAX(NN)=P2B
      GO TO 340
   31 IF(P2B.GT.EPSMIN(NN)) GO TO 340
      KR=4
      EPSMAX(NN)=P2B+2*EPSY
   40 IF(P2B.GT.P2A) GO TO 41
      EPSMAX(NN)=P2B+2.*EPSY
      GO TO 340
   41 KR=5
      EPSMIN(NN)=P2B
      GO TO 340
   50 IF(P2B.LT.P2A) GO TO 51
      IF(P2B.LT.EPSMAX(NN))GO TO 340
      KR=2
      EPSMIN(NN)=P2B-2 *EPSY
      GO TO 340
   51 IF(P2B.GT.EPSMIN(NN)) GO TO 340
      KR=4
      EPSMAX(NN)=P2B+2*EPSY
      GO TO 340
  120 IF(P2B.LE.(-EPSUL))KR=6
      GO TO (210,220,230,240,250,340) ,KR
  210 IF(P2B.GT.(-EPSY))GO TO 340
      KR=2
      EPSMAX(NN)=P2B+2 *EPSY
      GO TO 340
  220 IF(P2B.GT.P2A) GO TO 221
      EPSMAX(NN)=P2B+2 *EPSY
      GO TO 340
  221 KR=3
      EPSMIN(NN)=P2B
      GO TO 340
  230 IF(P2B.LT.P2A) GO TO 231
      IF(P2B.LT.EPSMAX(NN))GO TO 340
      KR=4
      EPSMIN(NN)=P2B-2 *EPSY
      GO TO 340
  231 IF(P2B.GT.EPSMIN(NN)) GO TO 340
      KR=2
      EPSMAX(NN)=P2B+2*EPSY
  240 IF(P2B.LT.P2A) GO TO 241
      EPSMAX(NN)=P2B
      GO TO 340
  241 KR=5
      EPSMIN(NN)=EPSMAX(NN)-2 *EPSY
      GO TO 340
  250 IF(P2B.GT.P2A) GO TO 251
      IF(P2B.GT.EPSMIN(NN))GO TO 340
      KR=2
      EPSMAX(NN)=P2B+2 *EPSY
      GO TO 340
  251 IF(P2B.LE.EPSMAX(NN)) GO TO 340
      KR=4
      EPSMAX(NN)=P2B
  340 KBAR(NN)=KR
      GO TO (  540,550,540,550,540,560 ),KR
  540 EY=ES
      GO TO 570
  550 EY=ESH
      GO TO 570
  560 EY=0.0
  570 IF(KR.NE.KR1) KBAL=KBAL+1
      C2=EY*PY(NM)
      CS(2,2)=C2
      RETURN
      END
C
C  INCREMENTAL  LOAD VECTOR  (+ PSEUDO-LOADS IF NEED BE)
C
      SUBROUTINE LOAD(AK,AMS,R,P,AA,BB,T,CH,CV,NEQ,IBAND,TIME,NI,NFIX,
     1                IFLAG,U1)
      COMMON/DAMP/C1,C2,DT,NP
      COMMON/DATA/NNP,NEL,NMAT,NAPT,NBODY,KMAS,MODIF,NEL2
      COMMON/NODE/IE(80,6)
      DIMENSION AK(NEQ,IBAND),R(NEQ)
      DIMENSION AMS(200),FT(8),LP(8)
      DIMENSION AA(200),BB(200),CH(100),CV(100),T(100)
      DIMENSION P(3,150),U1(200)
      IF(NI.NE.0) GO TO 121
      REWIND 1
      READ(1) ((AK(I,J),J=1,IBAND),I=1,NEQ)
      GO TO 103
  121 REWIND 10
      READ(10)((AK(I,J),J=1,IBAND),I=1,NEQ)
  103 N=1
  100 TAU=TIME-T(N)
      IF(TAU) 50,150,150
  150 K=1
      IF(NP.LE.1) GOTO 155
   60 IF(TAU.GE.P(1,K).AND.TAU.LT.P(1,K+1)) GOTO 200
      K=K+1
      IF(K.GT.NP) GOTO 270
      GOTO 60
  200 D=P(1,K+1)-P(1,K)
      DH=P(2,K+1)-P(2,K)
      DV=P(3,K+1)-P(3,K)
      T1=TAU-P(1,K)
      FH=P(2,K)+T1*DH/D
      FV=P(3,K)+T1*DV/D
      GOTO 160
  155 CONTINUE
      FH=P(2,1)*COS(2.0*3.1416*P(1,1)*TAU)
      FV=P(3,1)*COS(2.0*3.1416*P(1,1)*TAU)
  160 IF(CH(N).EQ.0.0.AND.CV(N).EQ.0.0) GOTO 50
      IF(CH(N)) 300,250,300
  250 R(2*N-1)=0.0
  350 R(2*N)=CV(N)*FV
      GOTO 500
  300 R(2*N-1)=CH(N)*FH
      IF(CV(N)) 350,400,350
   50 R(2*N-1)=0.0
  400 R(2*N)=0.0
  500 N=N+1
      IF(NNP-N) 130,120,120
  120 IF(T(N)-T(N-1)) 100,140,100
  140 IF(TAU) 50,160,160
  130 IF(TIME) 230,270,230
  230 CONTINUE
  353 IF(NI.EQ.1.OR.IFLAG.EQ.0)GO TO 530
      IAA=0
      DO 340 N=1,NEL
      MTYP2=IE(N,6)
      DO 338 I=1,8
  338 FT(I)=.0
      LIM=8
      DO 339 I=2,LIM,2
      IJ=I/2
      LP(I-1)=2*IE(N,IJ)-1
  339 LP(I)=2*IE(N,IJ)
  341 READ(3'N)(FT(K),K=1,8)
C     IF(N.NE.1)GO TO 343
C     WRITE(6,1100)
C 343 WRITE(6,1101)N,(FT(I),I=1,8)
 1100 FORMAT(12X,20HFT ARRAY READ FROM 3//)
 1101 FORMAT(1X,I4,6X,8(F10.5,3X))
      DO 342 J=1,LIM
      I=LP(J)
      I1=2*NFIX
      IF(I.LE.I1) FT(J)=0.0
  342 R(I)=R(I)+FT(J)
  340 CONTINUE
  530 REWIND 9
      WRITE (9) (R(I),I=1,NEQ)
  531 DO 330 M=1,NEQ
  330 R(M)=R(M)-AMS(M)*AA(M)
      IBB=0
 1701 DO 700 I=1,NEQ
      K=NEQ-I+1
      IF(K-IBAND)650,650,640
  640 K=IBAND
  650 DO 660 J=1,K
      IJ=I+J-1
  660 R(I)=R(I)-AK(I,J)*BB(IJ)
      IF(I-IBAND)680,670,670
  670 L=IBAND-1
      GO TO 690
  680 L=I-1
      IF(L)700,700,690
  690 II=I
      DO 695 J=1,L
      II=II-1
  695 R(I)=R(I)-AK(II,J+1)*BB(II)
  700 CONTINUE
      IF (NI.EQ.0) GO TO 270
      IF (IBB.NE.0) GO TO 270
```

```
      REWIND 1
      READ( 1 ) (( AK( I,J ),J=1,IBAND ),I=1,NEQ )
      DO 1700 I=1,NEQ
 1700 BB( I )=U1( I )
      IBB=IBB+1
      GO TO 1701
  270 RETURN
      END
      SUBROUTINE GEN( NEL,NNP )
      COMMON/DISP/X( 100 ),Y( 100 ),ULX( 100 ),VLY( 100 ),KODE( 100 )
      COMMON/NODE/IE( 80,6 )
      READ( 5,100 ) NSP
      DO 5 ISP=1,NSP
    5 READ( 5,101 ) I,X( I ),Y( I )
      READ ( 5,102 ) ISCALE,JSCALE,NX,NY,DRX,DRY
      READ ( 5,103 ) DRBX,DRBY
      DO 10 K=1,ISCALE
      IAA=0
      LS=JSCALE-1
      DO 10 I=1,LS
      IAA=IAA+1
      DR=DRY
      IF( IAA.EQ.3 ) DR=DRBY
      Y( K+NY*I )=Y( K+NY*( I-1 ))+DR
      IF( IAA.EQ.3 )IAA=0
   10 CONTINUE
      DO 20 I=1,ISCALE
      KS=JSCALE-1
      DO 20 J=1,KS
      X( I+NY*J )=X( I+NY*( J-1 ))
   20 CONTINUE
      JMAX=16
      JAA=0
      IAA=0
      DO 30 M=1,NEL
      JAA=JAA+1
      IAA=IAA+1
      IMAX=4
      IF( M.GT.16 ) JMAX=19
      NNX=1
      IF( JMAX.EQ.19.AND.JAA.LE.4 ) IMAX=IMAX+1
      IF( IAA.EQ.IMAX.AND.JAA.NE.JMAX ) NNX=2
      IF( JMAX.EQ.19.AND.JAA.LE.4 ) IMAX=IMAX+1
      IF( M.NE.1 )GO TO 35
      IE( M,1 )=1
      IE( M,2 )=IE( M,1 )+NX
      IE( M,3 )=IE( M,2 )+NY
      IE( M,4 )=IE( M,1 )+NY
      GO TO 32
   35 DO 40 I=1,4
   40 IE( M,I )=IE( M-1,I )+NNX
   32 IE( M,5 )=1
      IE( M,6 )=1
      IF( JAA EQ.JMAX ) IE( M,6 )=2
      IF( IAA.EQ.IMAX )IAA=1
      IF( JAA.EQ JMAX )JAA=0
   30 CONTINUE
      DO 60 N=1,NNP
      ULX( N )=0.
      VLY( N )=0.
      KODE( N )=0
   60 IF( N.LE.ISCALE )KODE( N )=3
  100 FORMAT( I5 )
  101 FORMAT( I5,2F10.3 )
  102 FORMAT( 4I5,2F5.2 )
  103 FORMAT( 2F10.2 )
      RETURN
      END
```

APPENDIX D

PUBLICATIONS

ASSOCIATION FOR THE ADVANCEMENT
MODELLING AND SIMULATION TECHNIQUES
IN ENTERPRISES

ASSOCIATION POUR LA PROMOTION
DES TECHNIQUES DE MODELISATION
ET DE SIMULATION DANS L'ENTREPRISE

16 avenue de Grange-Blanche, 69160 TASSIN-LA-DEMI-LUNE, FRANCE

C. Thomas
Dept Civil Engineering
The University of Liverpool

31/3/1983

Dear Contributor,

Your proposal

Influence of stiffness degradation and strain hardening on the ductility demand of the coupling beams of coupled shear walls
by O. Chaallal & C. Thomas

for the International 83 AMSE Summer Conference "Modelling and Simulation" is accepted.

I invite you for the presentation (Nice: September 12-14, 1983).

The full texts are accepted up to the Conference, but I invite you to send them as soon as possible from now to allow the edition of the Proceedings in the shorter delay after the Conference. The participants will receive at the Conference the Volume of Summaries of accepted Communications.

The publication in the Proceedings implies the enrolment for the Conference. Papers accepted but not presented at the Conference will be published in AMSE Reviews.

Full texts must be typed (use good typewriter and ribbon) on standard sheets of paper of about 21 x 29,7 cm, with margins of 2 cm on the left and on the right. A short abstract precedes the text. We make a format reduction for the publication; so don't use too small characters.

All contributors will receive in due time the last Announcement of the Conference giving all informations. The Conference will be held at Nice University, Parc Valrose, Nice.

Sincerely yours,

G. MESNARD
President of the AMSE

INFLUENCE OF STIFFNESS DEGRADATION STRAIN HARDENING AND OTHER PARAMETERS ON DUCTILITY DEMAND OF COUPLED WALLS

by O. CHAALLAL and C. THOMAS*

1. INTRODUCTION

The use of coupled shear walls in seismic resistant design has a great potential because of their tremendous capabilities to dissipate the energy input from an earthquake. Also, it is recognised that this dissipation of energy is usually obtained by the inelastic deformations of the connecting beams. This is a preferred form of deformation because

i) Failure in the walls may lead to the collapse of the entire structure.

ii) Axial Forces, which might be high in the walls, tend to reduce their capability to deform.

iii) It is easier and more economical to repair horizontal members than vertical ones.

The prediction of the expected deformations in the coupling beams, and the different factors which might influence its extent, appear therefore to be of paramount importance. However, this evaluation can only be assessed after assuming a mathematical model of the inelastic material behaviour. The model most used in connection with the dynamic response of reinforced concrete members is the experimentally based hysteretic Takeda's moment-rotation relationship (ref. 1). This simulates two important reinforced concrete behavioural features namely stiffness degradation and strain hardening.

The objective of this study is to examine the variation of the ductility demands on the coupling beams of coupled walls as affected by

i) Stiffness degradation
ii) Strain hardening
iii) Depth of coupling beams
iv) Length of coupling beams
v) Damping
vi) Initial coupling beam stiffness.

2. PROCEDURE

A 20 and a 30 storey coupled shear wall (SW1 and SW2) were chosen for this investigation. Their geometric and dynamic characteristics are given in Fig. (1). The structures were subjected to the first 6 seconds of the N/S component of 1940 El-Centro earthquake with a scaled peak acceleration of 0.33g (Fig. 3). For convenience, the structures were subdivided over their height into zones of 5 storeys each from the base. Keeping the walls elastic, the maximum ductility demands (see section 5) enforced upon the coupling beams on each zone were computed.

3. ANALYTICAL MODEL

The walls of the structures are elastic allowing all nonlinearities to occur in the coupling beams. These are idealised as elastic line elements connected to nonlinear rotational springs in which inelastic deformations can take place. The masses were assumed lumped at each

* Civil Engineering Department, University of Liverpool, England.

floor level. The computer program DRAIN2-D (ref. 2) developed at the University of California, Berkeley, was used in this investigation. Dynamic response was determined using step-by-step numerical integration based on a constant acceleration during each time interval. A damping coefficient of 5% of critical was assumed and the damping matrix was computed as a linear combination of the stiffness and the mass matrix.

4. HYSTERESIS RULE

As previously stated, the hysteretic Takeda's model with stiffness degradation capability was used. The stiffness degradation is simulated by reducing the unloading and reloading stiffnesses. The unloading stiffness, K_u, depends on the maximum hinge rotation and is controlled by the input parameter α as shown in fig. (2). α must be non negative and chosen such that the unloading slope is steeper than the reloading one in order to avoid a negative hysteresis loop, similarly the reloading stiffness is controlled by a parameter β.

5. DUCTILITY DEMAND

When subjected to a severe earthquake, the structure must have the capability of undergoing inelastic deformation reversals without substantial loss of strength. These inelastic deformations are often defined as ductility demand. This can be measured in terms of strains, displacements, curvatures or rotations and is the ratio of the ultimate to yield value of the measure considered, i.e.,

$$\mu = \frac{\Delta_u}{\Delta_y} \qquad (1)$$

The ductility used in this study is the rotational one and is defined as:

$$\mu_r = \frac{\theta_{max}}{\theta_y} \qquad (2)$$

Where θ_{max} is the maximum absolute rotation and θ_y, the rotation corresponding to yield as shown in Fig. (2). The validity of such a ductility has been demonstrated by Fintel et al (ref. 4).

6. INFLUENCE OF YIELDING MOMENT ON DUCTILITY DEMAND

In a study submitted by the authors elsewhere (ref. 3), a decay curve representing the variation of ductility demand in terms of the variations in yielding moment has been presented (fig. 4). The curve was intended to optimize the existing trial and error procedure (refs. 4-5) and to provide the desired ductility with a very good approximation. Thus simplicity, economy and efficiency were achieved. The following steps describe the procedure:

a) Choose a minimum yield moment $M_{y\ min}$

b) Perform a nonlinear dynamic analysis and compute the corresponding ductilities μ_{min} in each members.

c) Compute the ratio (μ_r/μ_{min}) in which μ_r is the desired ductility.

d) From the curve of fig. (4) derive (dM/M_{min})

e) Now compute the needed moment variation as

$$dM = \frac{dM}{M_{min}} \quad M_{y\ min}$$

f) Compute the yield moment required

$$My = M_{y\,min} + dM$$

7. EFFECT OF STIFFNESS DEGRADATION ON SW2

7.1 Unloading Slope Variation. The influence of the variation of the unloading stiffness Ku is investigated. Setting My = 100 kip.ft for all the coupling beams and the walls elastic, the ductility demands were computed for various values of α and a constant $\beta = 0$. The results are shown in table 1. The relevant ductility demand variations $d\mu$ (%) with respect to the ductility demand μo, corresponding to $\alpha = 0$ and $\beta = 0$, are also shown in table 1 between brackets and are plotted against the variable α for zone 1 in fig. (5). Table 1 and fig. (5) show clearly that ductility demand increases with increasing α.

To examine the effects of the strength of the coupling beams on this variation, two more values of yield moments were considered My = 150 and My = 200 kip-ft and similar procedure was followed. The results are also shown in table 1 and the variation $d\mu_{(\%)}$ for the first zone is also plotted in fig. (5) for comparison. As can be seen, as α varies from 0 to 0.40, $d\mu_{(\%)}$ varies from 0 to a maximum value of

2.77 % for My = 100 kip ft

7.67 % for My = 150 kip ft

9.92 % for My = 200 kip ft

This shows that the variation of ductility demand is higher for stronger coupling beams.

7.2 Reloading Slope Variation. Similarly, the ductility demand on the coupling beams were computed for a varying parameter β and a constant α of 0.4. The results are shown in table 2 for values of yield moment (My) of 100, 150, and 200 kip.ft respectively. The ductility variation of $d\mu_{(\%)}$ defined with respect to μo, corresponding to $\alpha = 0.40$ and $\beta = 0$, is now plotted against β for zone (1) in fig. (6). The results show that

i) The ductility variation was not substantial as β varied.

ii) The ductility variation increases with increasing β.

iii) The ductility variation is lesser for stronger coupling beams.

8. EFFECT OF STRAIN HARDENING ON SW2

When subjected to reversal of loading, the behaviour of a beam can be basically described by its moment-rotation relationship. The latter can be idealised either as elastic perfectly plastic, i.e., no strain hardening is accounted for ($p = 0$ in fig. 2) or as elasto-plastic with strain hardening ($p \neq 0$). As far as reinforced concrete is concerned, a more realistic model would be the one which takes into account strain hardening effect.

Depending on the designer's judgement, various values of p can be chosen as an input to simulate strain hardening. Therefore, in the following section an attempt is made to examine the effect of the variation of p on the ductility demands of the coupling beams of the

coupled shear wall SW2. The walls were kept elastic throughout the entire earthquake history and no stiffness degradation effect was considered. The value of strain hardening parameter p was varied from 0.01 to 0.16 and the consequent changes in plastic deformation were recorded. Furthermore, to examine the possible influence of beam strength, on the magnitude of these changes, three values of yield moments have been considered (My = 100, My = 150 and My = 200 kip.ft), the results being shown in table 3. The variation of ductility demand $d\mu_{(\%)}$, defined with respect to μ_o which corresponds to p = 0.01, is also shown in table 3 and plotted against p in fig. (7) for zone 6.

The results show clearly that ductility demand decreases as the strain hardening parameter p increases. The variation of ductility demand depends also on the level of yielding of the coupling beams as it is greater for smaller yield moments My.

9. EFFECT OF BEAM DEPTH

9.1 General Considerations. In a preliminary study (ref. 6) an 8 storey coupled wall subjected to typical equivalent static loads was investigated. The depth of the coupling beams were varied keeping all the remaining geometry the same. The displacement pattern of this coupled wall depended very much on the size of the coupling beams as shown in fig. (8a). The depth of the coupling beams has therefore a considerable effect on the stress and deformation characteristics of the entire structure. When the depth was only 1ft, both left and right walls deflected equally and the point of contraflexure was almost in the midspan of the coupling beam. This agreed remarkably well with the assumption made in the approximate methods of analysis. As the depth of the coupling beams was increased however, the behaviour of the coupled wall was noted to vary towards the behaviour of a single solid wall.

The interaction between the walls and the coupling beams was also investigated. Figure 8(b) shows the variation of the bending moments in the coupling beams with their depth. The inter storey variation of the bending moments is seen to increase substantially with the depth of the beam. This was found to be a very important phenomenon concerning the strength of the energy absorbing capability of the structure. The similarity of the bending moments of the coupling beams when slender, yields the following consequences:

a) Yielding in the beams occur approximately at the same time thus improving the energy dissipation capability.

b) A straight forward design and construction of the coupling beams.

c) The approximate nonlinear method of analysis which assumes that all beams are hinged and that the point of contraflexure is at midspan, becomes more acceptable.

9.2 Effect of the Depth of Coupling Beams on their Ductility. Increasing the beam depth increases the initial stiffness (i.e. the first slope of the moment-rotation curve) and hence, for the same yield moment, reduces the yield rotation. To examine the effect of the beam depth Hb on the ductility demand, the 30 storey coupled shear wall (SW2) was considered. Varying the beam depth and keeping all the remaining data and zoning the same and setting the yield mo-

ment My = 100 kip.ft, the following ductility demands were recorded:

ZONE	DUCTILITY DEMAND (μ)		
	Hb = 1'	Hb = 2'	Hb = 3'
1	1.00	6.48	22.08
2	1.13	8.32	27.60
3	1.50	12.79	35.26
4	1.81	14.67	39.33
5	1.81	14.06	35.97
6	2.18	16.47	41.23

The influence of the beam depth is considerable as confirmed by the above table. The results show yet again that the parameters which define the yield point, namely the initial stiffness and the yield strength, have a particular effect on ductility demand.

10. EFFECT OF COUPLING BEAM LENGTH ON DUCTILITY DEMAND

It can be anticipated that an increase in the length of the coupling beams leads to a greater flexibility and hence to an increase in ductility demands. It is however desirable to evaluate the extent of this increase and the nature of its variation as affected by the coupling beam length. In order to examine the effect of this variable, three twenty storey walls were considered in addition to SW1 previously described. All four structures were the same except that the coupling beam length and hence the dynamic characteristics were varied. For convenience the structures were subdivided in 4 zones from base and the maximum ductility demands were computed for each of the structures as follows:

	μ max			
Zone \ Beam Length	4'	7'	10'	14'
1	9.71	13.51	15.11	15.40
2	10.33	17.43	20.37	21.60
3	8.81	22.24	26.17	28.08
4	9.57	22.77	27.32	29.63

The maximum ductility demand in the 4 zones are plotted against the beam length Lb, and also 1/Lb in Fig. (9). The figure shows, as expected, the increase of ductility demand with increasing length. Furthermore, the maximum ductility demand seems to be almost inversely proportional to the coupling beam length. Note however, that the rate of increase in ductility demand decreases after the beam length has reached approximately 10 ft.

11. EFFECT OF DAMPING

To assess the effect of energy absorbing mechanism, which is present in structures even before the onset of yielding due to damping effect, a viscous damping form was assumed. Three different damping factors namely 5%, 10% and 15% of critical were considered. To appreciate

the influence of structure flexibility, i.e. its frequency of vibration on the extent of the effect of damping, a coupled wall of 10 storeys (SW3) in addition to the 20 storey coupled wall (SW1) was considered. SW3 has the same properties, except the number of storeys and hence the total height, as SW1. The coupling beams yield moments were set to 100 kip.ft for SW1 and 80 kip.ft for SW3. The ductility demands in the coupling beams were then computed and the results are shown in table 4 and Fig. (10). From these the following observations can be seen.

i) The effect of damping is substantial and therefore great care should be exercised in its choice.

ii) The maximum reductions on ductility demands $\Delta\mu_{(10\%)}$ and $\Delta\mu_{(15\%)}$ with respect of $\mu_{(5\%)}$, i.e.,

$$\Delta\mu_{(i\%)} = \frac{|\mu_{(5\%)} - \mu_{(i\%)}|}{\mu_{(i\%)}} \cdot 100$$

were as follows:

	$\Delta\mu_{(5\%)}$	$\Delta\mu_{(10\%)}$	$\Delta\mu_{(15\%)}$
SW3 (10 storeys)	0.0	25%	35%
SW1 (20 storeys)	0.0	32%	50%

12. EFFECT OF ACTUAL STIFFNESS OF COUPLING BEAMS

The importance of the choice of the original stiffness to be used along with the assumed nonlinear moment-rotation relationship must be emphasised. Depending on the designer, different initial rigidities (EI initial) for the same cross section can be assumed ranging from the rigidity of the gross section to a rigidity below that of the cracked section (fig. 11). The influence of such an assumption on the ductility demand of the coupling beams of the coupled shear walls is most important and in this section attempts are made to assess the extent of this influence.

The 20 storey coupled wall (SW1) was chosen to illustrate this point. Its material, geometric and dynamic characteristics are given in table 1. For typical values of $EI_{initial}$ were assumed as follows

	Run S1	Run S2	Run S3	Run S4
$EI_{initial}$	EI_{gross}	$.8EI_{gross}$	$.6EI_{gross}$	$.4EI_{gross}$

The ductility demands upon the coupling beams are shown in table 5 and plotted in Fig. (12) for the four rigidity values considered. The figure shows clearly that the influence is very substantial and the maximum variation of the ductility demand reached 120% in this study. It is interesting to note that ductility demand varied almost in proportion with the initial rigidity $EI_{initial}$.

13. CONCLUSION & SUMMARY

The following conclusions can be drawn.

a) The ductility demand increases with increasing unloading parameters α and its variation is greater for stronger coupling beams. A maximum variation of approximately 10% was obtained in this investigation.

b) The ductility demand increases with increasing reloading parameter β. Its variation however, is smaller for stronger coupling beams. The maximum variation obtained was 6.3%.

c) Generally the ductility demand decreases with increasing strain hardening parameter p. Its variation becomes smaller as the coupling beams become stronger.

d) The factors affecting the yield point in the moment-rotation relationship such as the depth of the coupling beams, the yield moments and the initial stiffness have a particular influence on ductility demand and should therefore be assessed with great care.

e) Damping effect on ductility demand is very substantial (up to 50% in this study) and is slightly higher for more flexible structures. Therefore its choice should be taken with caution.

REFERENCES

1. TAKEDA, T., SOZEN, M.A., and NIELSEN, N.N.,
"Reinforced Concrete Response to Simulated Earthquake",
Jrnl. of Str. div., ASCE, 96, ST12, Dec.1970, pp.2557-2573.

2. KANAAN, A.E., and POWELL, G.H.
"A general purpose computer program for inelastic dynamic response of plane structures",
Report No. EERC 73-22, University of California, Berkeley, Aug.1975.

3. THOMAS, C. and CHAALLAL, O.
"A Ductility Decay Curve for Optimum Inelastic Analysis of R/C Coupled Walls",
paper submitted to ASCE for publication.

4. FINTEL, M., and GHOSH,
"Inelastic Response History Analysis of the Aseismic Design of a 31 Storey Frame Wall Building",
Earthquake Eng. and Str. dynamics, Vol. 9, pp.543-556, 1981.

5. DERETCHO, A.T.,
"Dynamic Inelastic Response of Coupled Shear Walls as affected by Axial Forces",
Study No. 14, Nonlinear Design of Concrete Structures, SolidMech. Div., University of Waterloo, Ontario, Canada, Aug.7-9, 1979.

6. CHAALLAL, O.,
Ph.D. Thesis to be submitted in the Department of Civil Engineering, University of Liverpool.

Table 1 Effect of Unloading Stiffness Degradation

		μ_1	μ_2	μ_3	μ_4	μ_5	μ_6
M_y = 100	α = 0	6.49 (0%)	8.32	12.80	14.69	14.08	16.49
	α = 0.1	6.56 (1.08)	8.45	12.81	14.61	13.96	16.38
	α = 0.2	6.62 (2.06)	8.50	12.86	14.61	13.96	16.34
	α = 0.3	6.66 (2.62%)	8.51	12.86	14.56	13.98	16.34
	α = 0.4	6.67 (2.77%)	8.49 (2.04%)	12.85 (-39%)	14.52 (-1.16%)	14.04 (-0.28%)	16.39 (-0.69%)
M_y = 150	0.	3.79 (0.0)	4.68	7.09	7.97	7.33	8.48
	0.1	3.90 (2.90)	4.76	7.10	7.94	7.39	8.52
	0.2	3.97 (4.75)	4.82	7.13	7.95	7.45	8.59
	0.3	4.04 (6.60)	4.85	7.16	7.96	7.49	8.64
	0.4	4.08 (7.67)	4.87 (4.06)	7.16 (.99)	7.96 (-.13)	7.53 (+2.73)	8.70 (2.59)
M_y = 200	0.	2.62 (0)	3.03	4.48	4.95	4.32	4.95
	0.1	2.70 (3.05)	3.09	4.50	4.95	4.35	4.99
	0.2	2.76 (5.34)	3.14	4.50	4.95	4.39	5.05
	0.3	2.82 (7.63)	3.19	4.52	4.96	4.43	5.09
	0.4	2.88 (9.92%)	3.22 (6.27%)	4.53 (1.12%)	4.97 (0.40%)	4.46 (3.24)	5.13 (3.64)

Table 2 Effect of Reloading Stiffness Degradation

	β	μ_1	μ_2	μ_3	μ_4	μ_5	μ_6
M_y = 100	0.	6.64 (0)	8.45	12.80	14.41	14.09	16.44
	0.1	6.68 (0.60)	8.58	12.78	14.41	14.07	16.42
	0.2	6.73 (1.36)	8.71	12.77	14.41	14.06	16.40
	0.3	6.77 (1.96)	8.83	12.78	14.42	14.04	16.38
	0.4	6.80 (2.41%)	8.93	12.78	14.42	14.04	16.38
	0.5	6.80 (2.41%)	8.98 (6.27%)	12.78 (-0.16)	14.42 (0.0%)	14.04 (0.35)	16.38 (0.36)
M_y = 150	0.	4.12 (0)	4.86	7.15	7.94	7.57	8.75
	0.1	4.15 (0.73)	4.94	7.13	7.93	7.57	8.74
	0.2	4.16 (0.97)	5.00	7.14	7.94	7.56	8.73
	0.3	4.16 (0.97)	5.01	7.14	7.94	7.56	8.73
	0.4	4.17 1.21%)	5.03	7.14	7.94	7.56	8.73
	0.5	4.17 (1.21%)	5.03 (3.50)	7.14 (-0.14)	7.94 (0.0)	7.56 (-0.13)	8.73 (-0.23)
M_y = 200	0.	2.92 (0)	3.24	4.54	4.97	4.49	5.17
	0.1	2.93 (0.34)	3.25	4.55	4.98	4.48	5.17
	0.2	2.93 (0.34)	3.26	4.55	4.98	4.48	5.17
	0.3	2.93 (0.34)	3.26	4.54	4.97	4.48	5.17
	0.4	(0.34)	3.27	4.54	4.97	4.48	5.17
	0.5	(0.34)	3.27 (.93%)	4.54 (0.0)	4.97 (0.0)	4.48 (-0.22)	5.17 (0.0)

Table 3 Effect of Strain Hardening

	Str. Hard. parameter (P)	$\mu_{(1)}$	$\mu_{(2)}$	$\mu_{(3)}$	$\mu_{(4)}$	$\mu_{(5)}$	$\mu_{(6)}$
M_y = 100	.01	6.44	8.18	14.40	16.7	16.17	18.95 (0.0)
	.02	6.42	8.19	13.92	16.11	15.59	18.26 (-3.64)
	.04	6.47	8.30	13.16	15.14	14.55	17.05 (-10.03)
	.06	6.49	8.34	12.47	13.27	13.62	15.95 (-15.83)
	.08	6.30	8.32	11.81	13.47	12.80	14.98 (-20.95)
	.10	6.48	8.27	11.26	12.78	12.06	14.09 (-25.65)
	.12	6.44	8.19	10.75	12.13	11.39	13.28 (-29.92)
	.14	6.40	8.08	10.26	11.52	10.79	12.56 (-33.72)
	.16	6.34 (1.55)	7.96 (+1.95)	9.83 (-31.74)	10.97 (-34.31)	10.22 (-36.80)	11.87 (-37.36)
M_y = 150	.01	3.76	4.59	7.73	8.80	8.19	9.49 (0.0)
	.02	3.78	4.62	7.57	8.58	7.96	9.17 (-3.4)
	.04	3.79	4.67	7.25	8.17	7.53	8.72 (-8.1)
	.06	3.79	4.68	6.96	7.79	7.13	8.26 (-13.0)
	.08	3.79	4.68	6.69	7.46	6.78	7.85 (-17.3)
	.10	3.76	4.66	6.43	7.16	6.45	7.46 (-21.5)
	.12	3.77	4.63	6.20	6.88	6.14	6.88 (-27.5)
	.14	3.75	4.58	6.00	6.63	5.85	6.78 (-28.6)
	.16	3.73 (-.80)	4.53 (-.13)	5.80 (-24.97)	6.38 (-27.50)	5.59 (-31.75)	6.46 (-31.93)
M_y = 200	.01	2.63	3.03	4.75	5.29	4.69	5.42 (0.0)
	.02	2.63	3.03	4.68	5.20	4.60	5.30 (-2.21)
	.04	2.63	3.03	4.55	5.03	4.41	5.06 (-6.64)
	.06	2.62	3.02	4.41	4.86	4.23	4.84 (-10.70)
	.08	2.61	3.01	4.30	4.72	4.06	4.63 (-14.58)
	.10	2.59	2.98	4.17	4.56	3.90	4.44 (-18.08)
	.12	2.58	2.96	4.07	4.44	3.76	4.27 (-21.22)
	.14	2.56	2.93	3.96	4.31	3.62	4.11 (-24.17)
	.16	2.54 (-3.42)	2.90 (-4.29)	3.86 (-18.74)	4.19 (-20.79)	3.50 (-25.37)	3.95 (-27.12)

Table 4 Influence of Damping on Ductility Demand

Floor Level	20 STOREYS		
	Ductility 5% Damp	Ductility 10%	Ductility 15%
20	22.68	15.33	11.35
19	22.74	15.40	11.40
18	22.77	15.46	11.37
17	22.68	15.44	11.19
16	22.52	15.36	10.94
15	22.24	15.19	10.79
14	21.71	14.88	10.58
13	20.92	14.39	10.33
12	19.85	13.74	7.99
11	18.56	13.12	9.59
10	17.43	12.56	9.74
9	16.53	12.26	10.07
8	15.74	12.29	10.58
7	15.44	12.27	10.72
6	14.70	11.87	10.42
5	13.51	10.96	9.67
4	11.82	9.53	8.46
3	9.64	7.66	6.85
2	6.99	5.48	4.85
1	3.76	2.91	2.51
Max. reduction with respect (to 5%)	0.0	32%	50%

10 STOREYS		
5%	10%	1
17.30	12.95	11
17.23	12.94	11
16.80	12.74	11
15.82	12.24	10
14.29	11.57	9
12.96	11.16	9
12.39	10.43	8
11.01	9.09	7
8.57	6.97	5
4.89	3.92	2
0.0	25%	3

Table 5 Effect of Initial Stiffness

Floor Level	RUN S1 EI = 309.3 10^3 kip.ft^2	RUN S2 (0.8 EI)	RUN S3 (0.6 EI)	RUN S4 (0.4 EI)
20	22.68	18.85	14.74	10.28
19	22.74	18.90	14.77	10.30
18	22.77	18.91	14.88	10.29
17	22.68	18.83	14.69	10.23
16	22.52	18.67	14.54	10.12
15	22.24	18.40	14.31	9.93
14	21.71	17.93	13.91	9.63
13	20.92	17.24	13.35	9.21
12	19.85	16.33	12.67	8.66
11	18.56	15.23	11.72	8.02
10	17.43	14.28	10.97	7.50
9	16.53	13.48	10.30	6.99
8	15.74	12.78	9.75	6.63
7	15.44	12.53	9.55	6.49
6	14.70	11.93	9.08	6.17
5	13.51	10.95	8.33	5.65
4	11.82	9.57	7.28	4.93
3	9.64	7.81	5.98	4.00
2	6.99	5.65	4.27	2.87
1	3.76	3.02	2.26	1.50

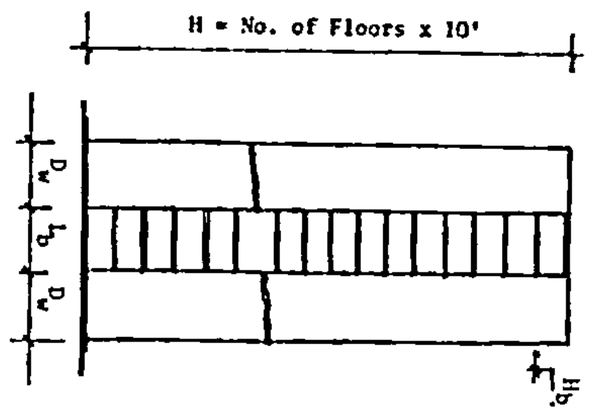

Fig. 1 Geometric and Dynamic Characteristics of SW1 and SW2

PROPERTIES	20 STOREYS (SW1)	30 STOREYS (SW2)
Beam Stiffness (EI_b)	30.93 10^3 kip ft^2	Wall Stiffness 30.93 10^3 kip ft^2
Wall Stiffness (EI_w)	66.80 10^3 kip ft^2	Beam Stiffness 66.80 10^3 kip ft^2
Wall Width (D_w)	12 ft	Beam Length 7 ft unless stated
Beam Length (L_b)	7 ft unless stated	Beam Depth 2 ft " "
Beam depth (H_b)	2 ft " "	Total Height 300 ft " "
Total Height (H)	200 ft " "	Thickness 1 ft
Thickness	1 ft	Beam Strength Variable
Beam Strength	Variable	Wall Strength Elastic
Wall Strength	Elastic	Fundamental Period 3.7846 seconds
Fundamental Period	1.8475 seconds	Lumped Mass/Floor 6.22 kips
Lumped Floor Mass	6.22 kips	

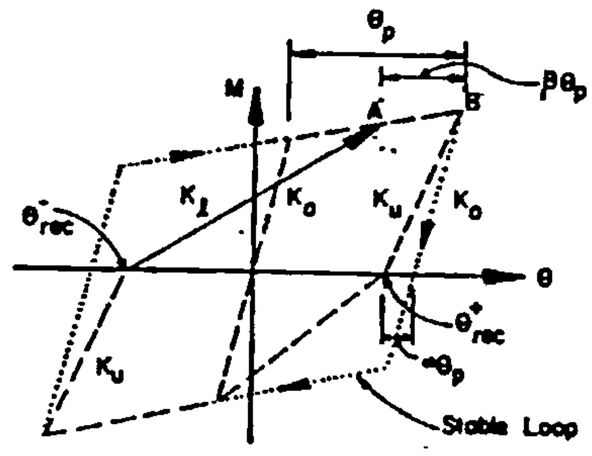

FIG. 2 TAKEDA MODEL OF THE MOMENT-ROTATION RELATIONSHIP OF R/C BEAMS

FIG. 3 FIRST 10 SEC. OF EL CENTRO ACCELEROGRAM N/S COMPONENT, MAY 1940

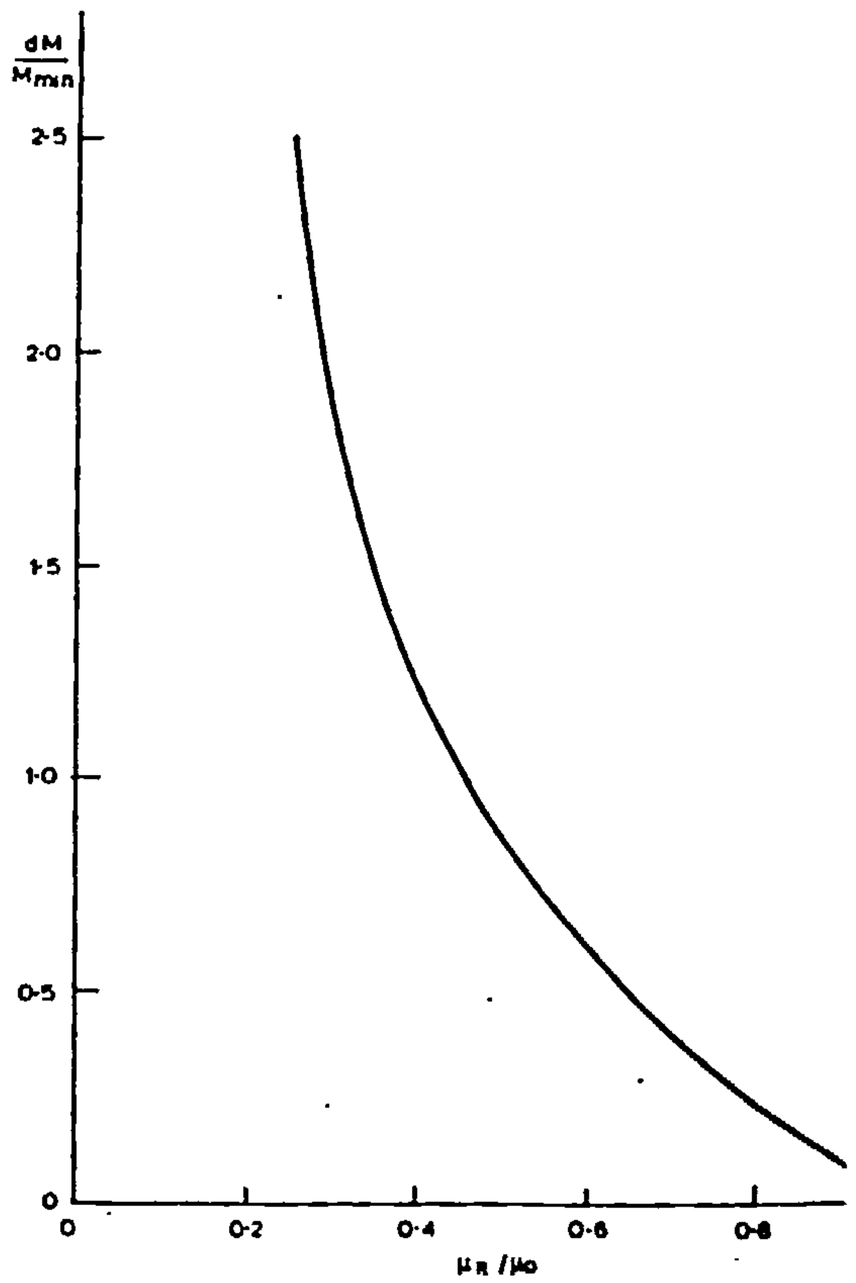

FIG. 4 DECAY CURVE FOR DUCTILITY DEMAI

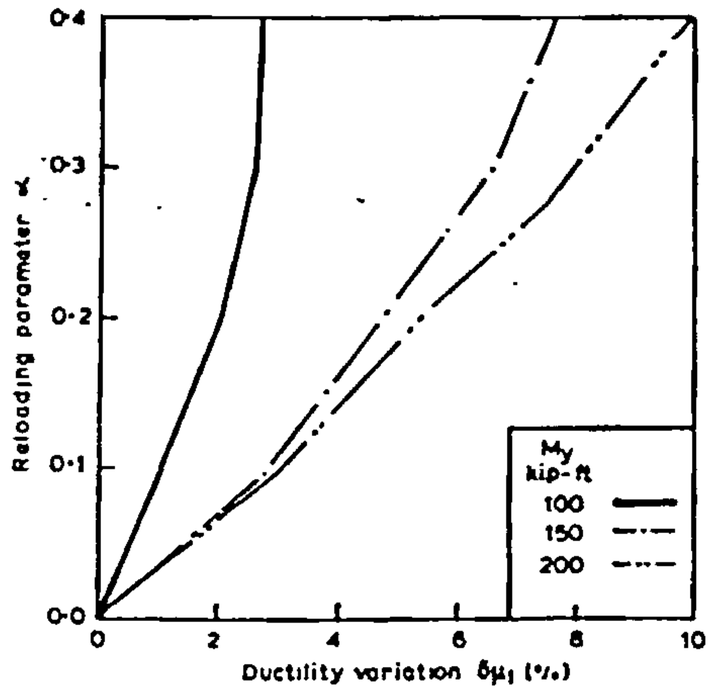

FIG. 5 EFFECT OF UNLOADING PARAMETER.

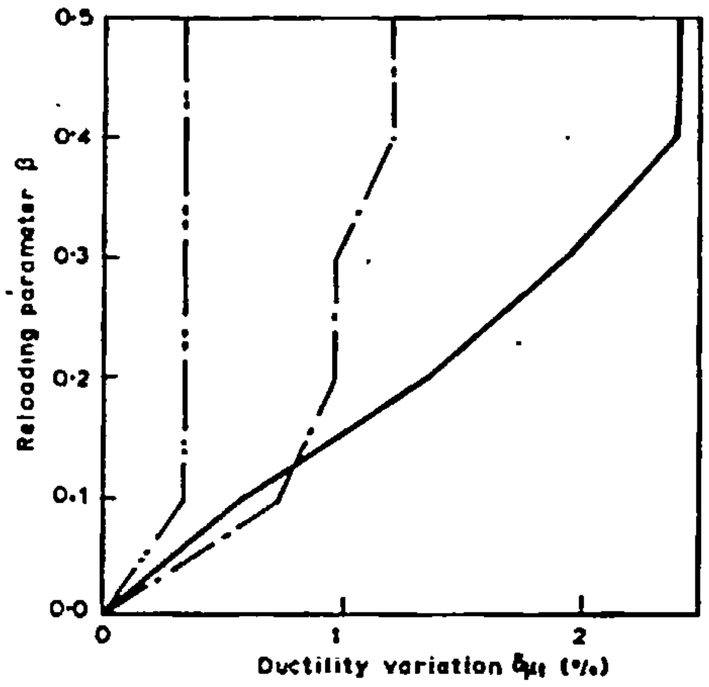

FIG. 6 EFFECT OF RELOADING PARAMETER β.

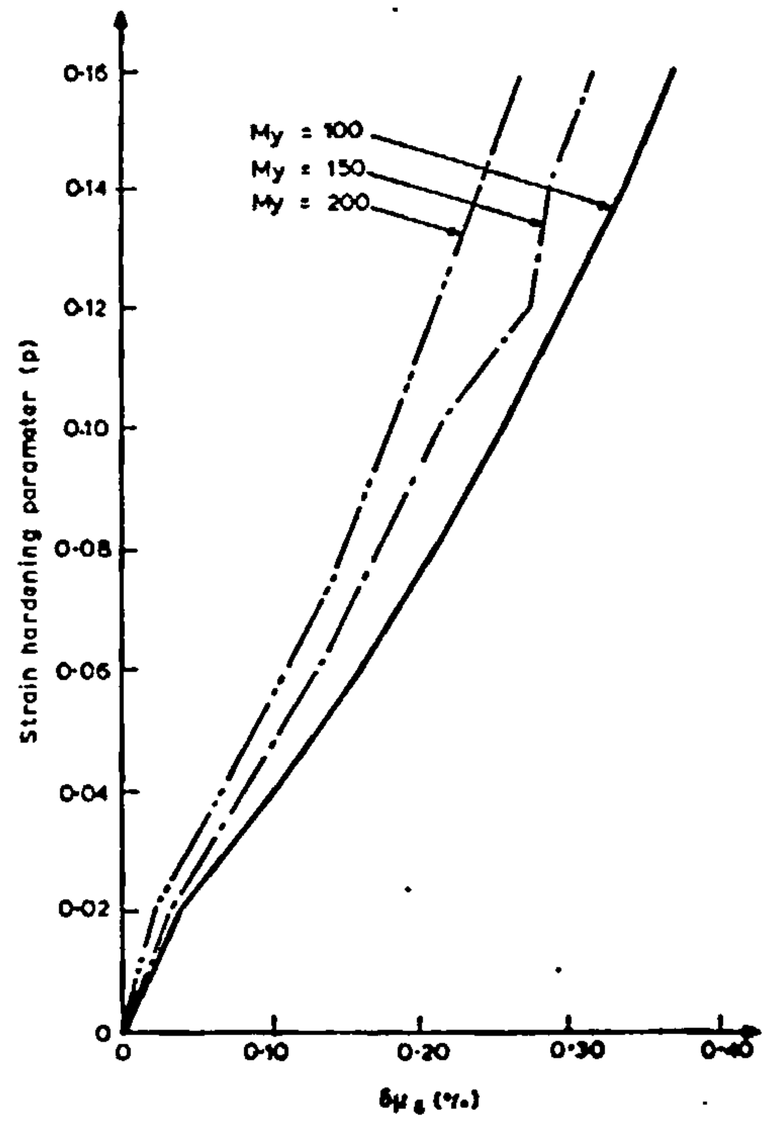

FIG. 7 EFFECT OF STRAIN HARDENING ON DUCTILITY DEMAND.

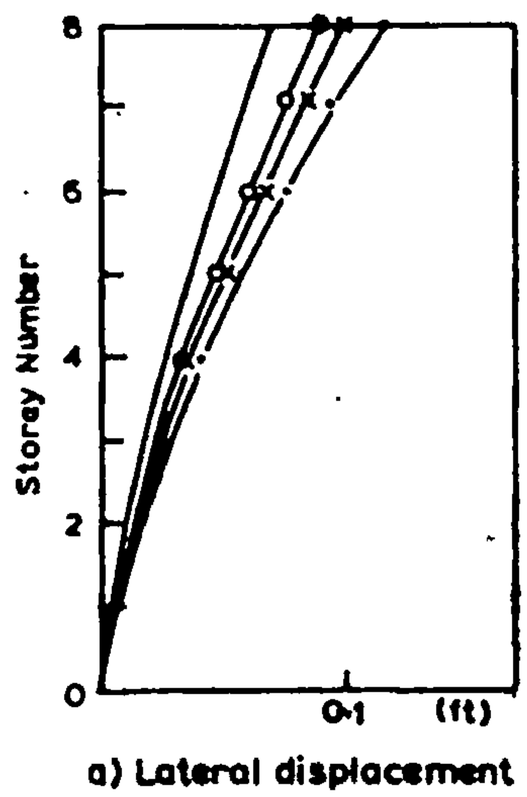

a) Lateral displacement

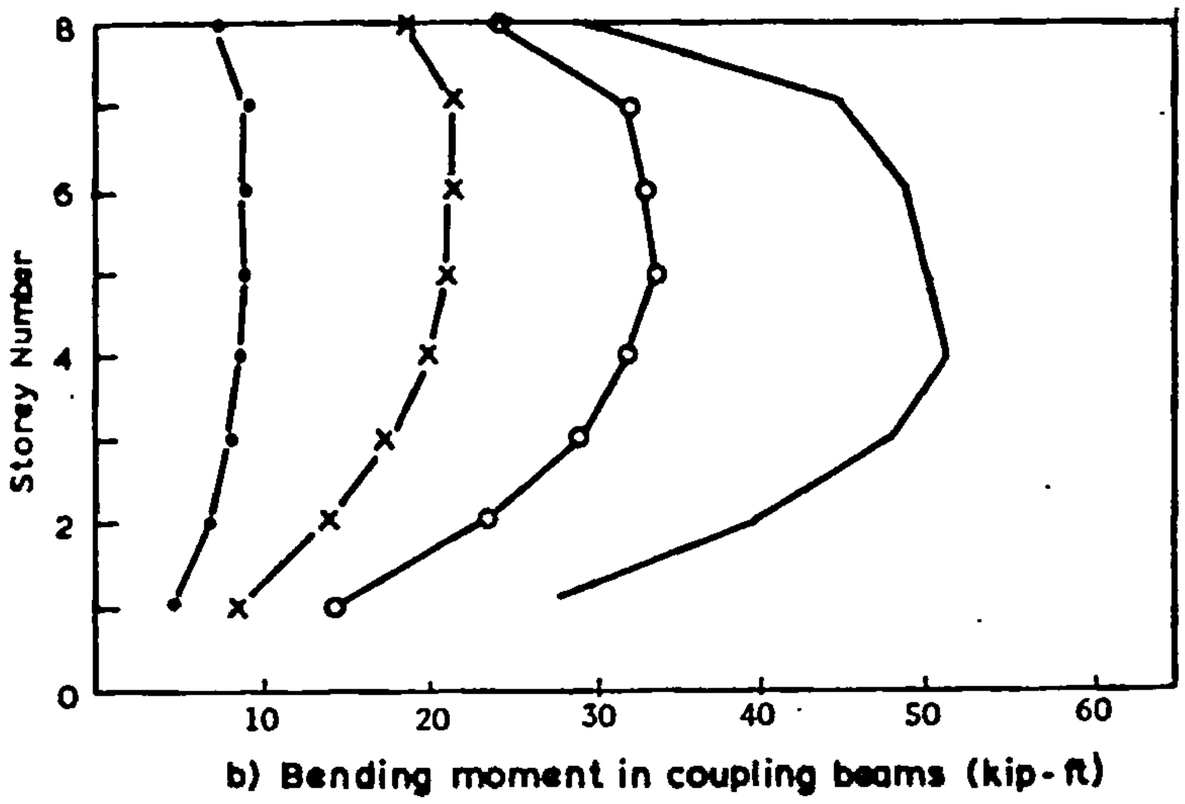

b) Bending moment in coupling beams (kip-ft)

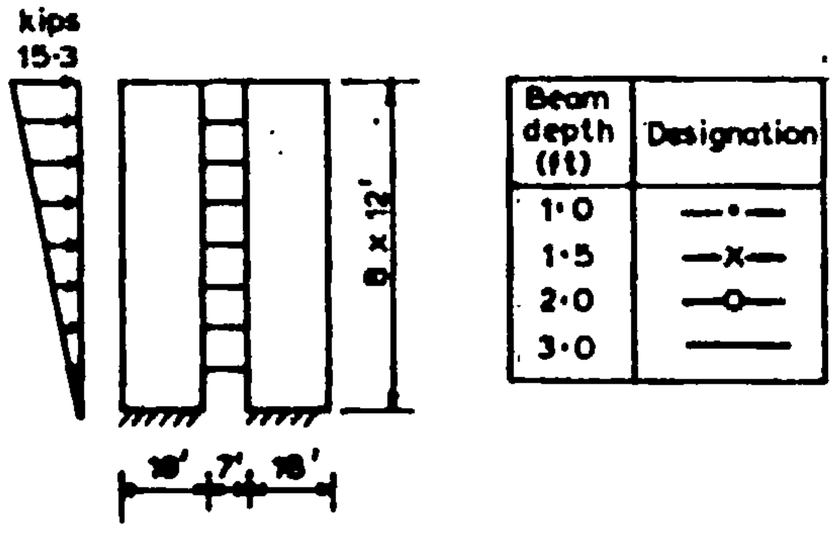

FIG. 8 EFFECT OF BEAM DEPTH ON

a) Overall behaviour of the structure

b) Bending Moments in coupling beams

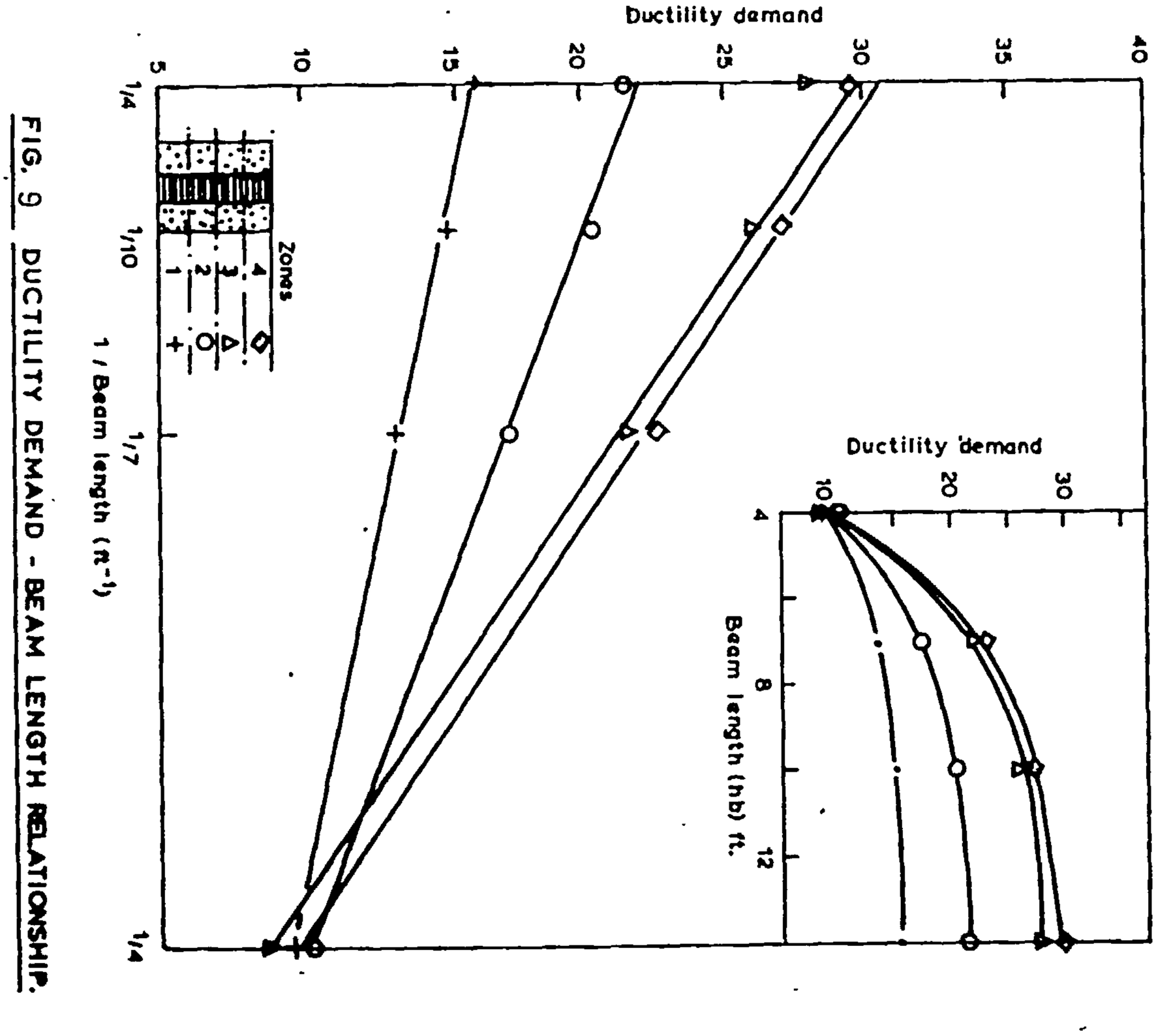

FIG. 9 DUCTILITY DEMAND - BEAM LENGTH RELATIONSHIP.

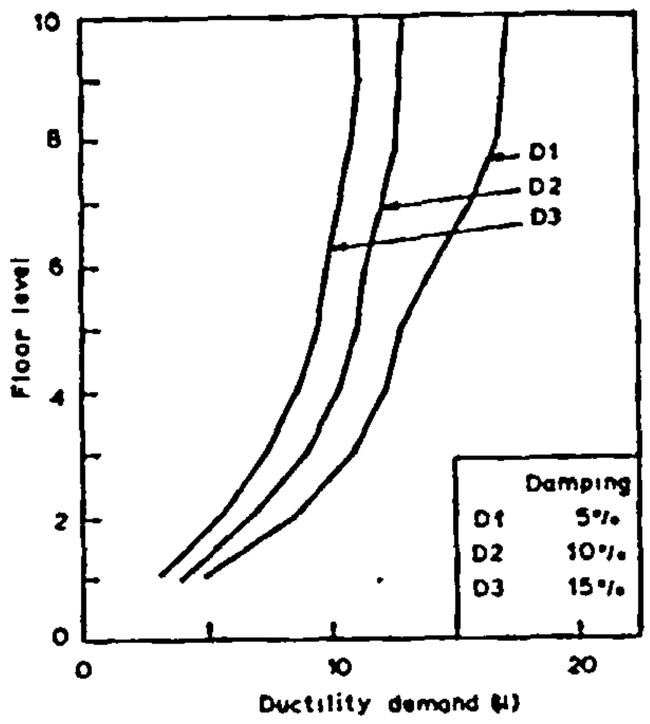

FIG. 10 EFFECT OF DAMPING ON DUCTILITY DEMAND OF 10 & 20 STOREY COUPLED WALLS.

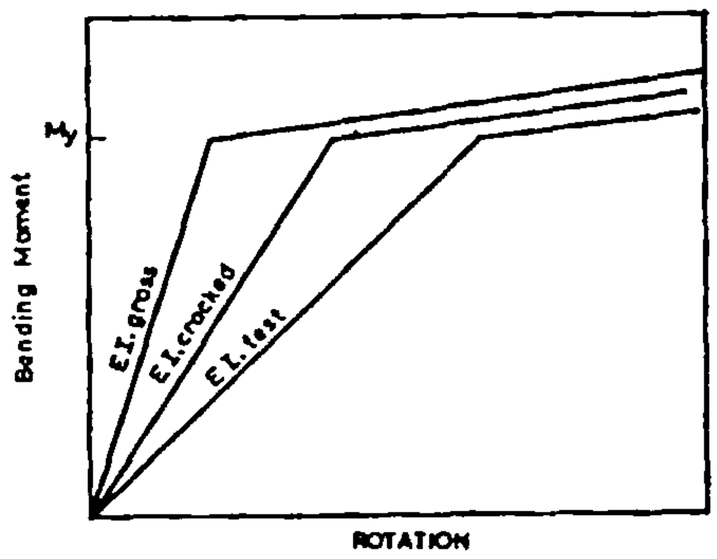

FIG. 11 THE DIFFERENT ALTERNATIVE FOR THE INITIAL ACTUAL STIFFNESS EIa.

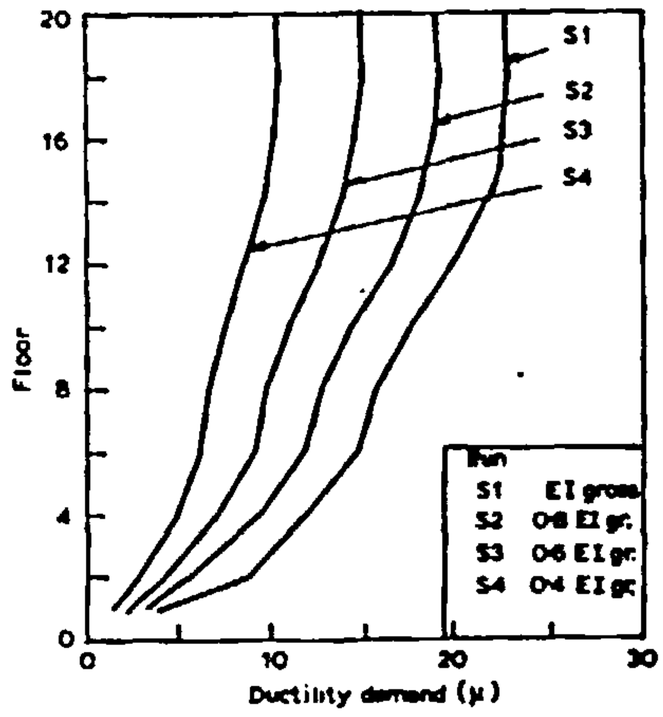

FIG. 12 INFLUENCE OF INITIAL HINGE RIGIDITY ON DUCTILITY DEMAND OF A 20 STOREY e/SHEAR WALL.

International Conference on

COMPUTER-AIDED ANALYSIS AND DESIGN OF CONCRETE STRUCTURES

SPLIT, YUGOSLAVIA

September 17th—21st 1984

DEPARTMENT OF CIVIL ENGINEERING
UNIVERSITY COLLEGE OF SWANSEA
SWANSEA SA2 8PP
UNITED KINGDOM
Telephone: 0792-205678

Dear Dr. Thomas,

Thank you for submitting your abstract for possible presentation at the International Conference on "Computer Aided Analysis and Design of Concrete Structures", to be held in Split, Yugoslavia, during September 1984.

This has been reviewed by the Programme Committee and I am pleased to inform you that it has been accepted for presentation. We shall be sending you instructions for suitable preparation of your manuscript in October of this year.

I look forward to meeting you in Split next year. Please write me if you have any queries regarding the Conference.

Yours sincerely,

Ernest Hinton

Dr. Ernest Hinton
for Organising Committee

THE NON LINEAR ANALYSIS OF

COUPLED SHEAR WALLS

USING DUCTILITY-DECAY CURVE

by

O. Chaallal & C. Thomas

(University of Liverpool, U.K.)

ABSTRACT

In recent years the philosophy behind the design of coupled shear walls in seismic zones has changed. Initially their inherent strength was used to resist lateral seismic loads. Over the last few years it is their ductility that has been used to absorb the energy input from an earthquake. This ductility has been introduced into the structure by allowing the connecting beams to deform plastically. The magnitude of these deformations is controlled by a concept, introduced by Paulay and others, called ductility demand (μ). With reference to Fig. 1 the definitions of ductility demand is

$$\mu = \frac{\text{rotation at failure}}{\text{rotation at yield}} = \frac{\theta max}{\theta y}$$

The limits of the ductility demand for doubly reinforced concrete connecting beams has been shown to be

$$4 \leq \mu \leq 10 \qquad \text{Equ. 1.}$$

The design procedure used has been to carry out a non linear analysis on a structure and to obtain ductility demand values at the connecting beams. Then by a process of trial, error and experience the yield moments at the connecting beams were modified and the process repeated. The values of the yield moments were modified until all the ductility demand values were within the limits specified by Equ. 1.

In this paper the authors show a different approach to the analysis. Depending upon the code of practice used the minimum yield amount (M_{min})

can be calculated for all connecting beams or zones of connecting beams. Using these values the ductility demands (μO) can be calculated by carrying out a non linear analysis as before. If the moment of one zone is increased by (dM), in several increments, and the ductility demands (μR) is obtained for all zones, the variations are as shown in Fig. 2 for a 4 zone structure. For all four zones this shows that the variation of the ductility demand in a particular zone is mainly dependent upon the increment of the moment applied to that zone only.

This variation can be shown graphically by producing a ductility decay curve. This is obtained by plotting the ratio $(\frac{dM}{M_{min}})$ against $(\frac{\mu R}{\mu O})$, and is shown in Fig. 3. Thus for any coupled shear wall a ductility decay curve can be obtained for a specified earthquake input.

This curve can now be used in a non linear analysis of a coupled shear wall. The procedure is as follows

(a) using the minimum yield moments of the connecting beams a non linear analysis can be carried out to obtain the initial ductility demands (μO).

(b) the required ductility demand is used as μR to calculate $(\frac{\mu R}{\mu O})$

(c) the ductility decay curve is then used to evaluate $(\frac{dM}{M_{min}})$ hence

$$M_y = (M_{min} + dM)$$

(d) Using these modified yield moments a non linear analysis is carried out again and the ductility demands obtained.

The models tested by the authors obtained values of ductility demands within 10% of the required values.

The method can be extended so that one ductility-decay curve can be used for most coupled shear walls.

Using one curve, steps a, b, c and d are carried out as above producing ductility demands (μg). If the values of (μg) are dissimilar to (μR) the following extra steps are carried out

(e) the ductility-decay is redrawn or recalculated by using the ratios $(\frac{\mu g}{\mu 0})$ and $(\frac{dM}{M_{min}})$

(f) with this new curve the ratio $(\frac{\mu R}{\mu 0})$ is used to calculate $(\frac{dM}{M_{min}})$.

Steps b, c and d are repeated to obtain new values of (μg). If the values of μg are dissimilar to μR then step e and f are repeated. The whole process is repeated until the values of μg are acceptably close to μR. Again examples are shown.

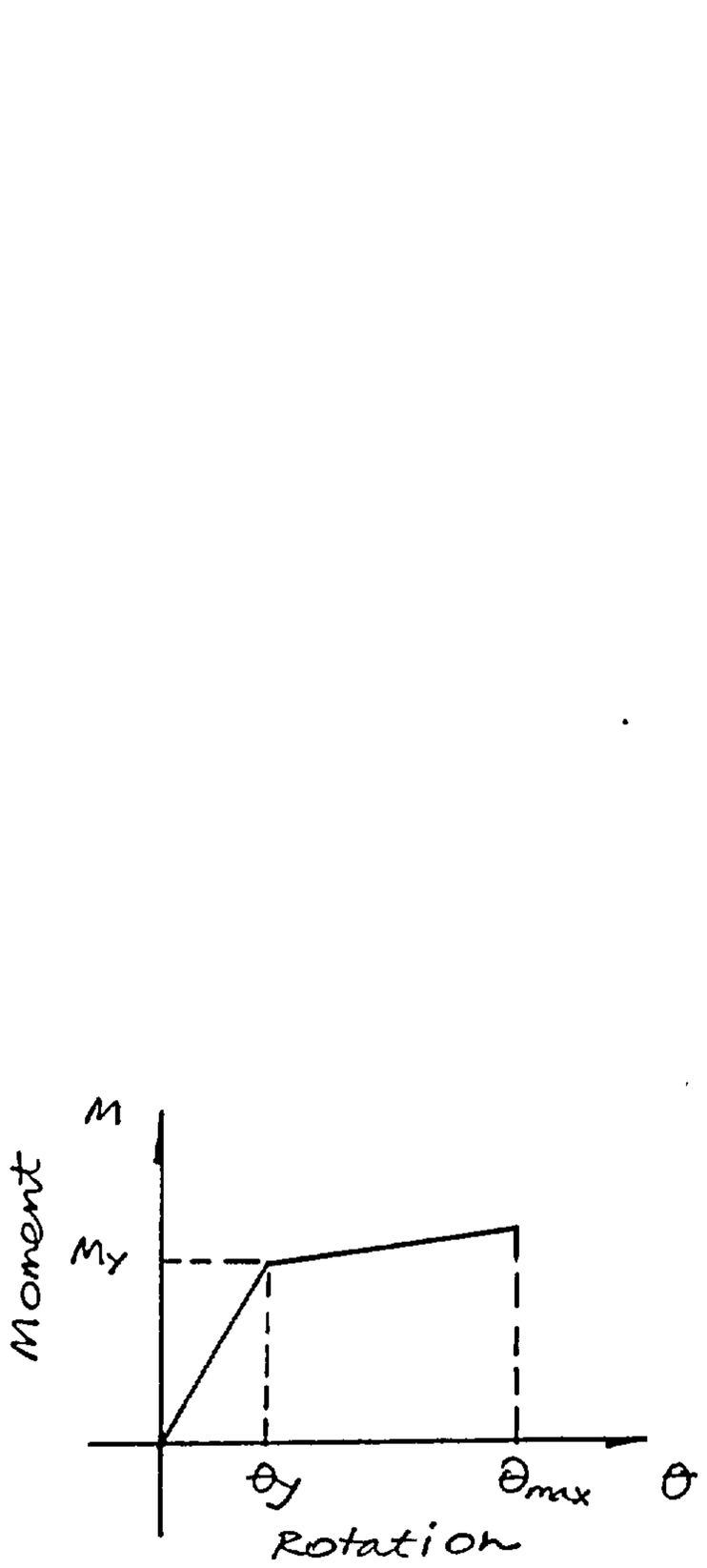

Ductility Demand = $\frac{\theta_{max}}{\theta_y} = \mu$

FIG. 1 DUCTILITY DEMAND

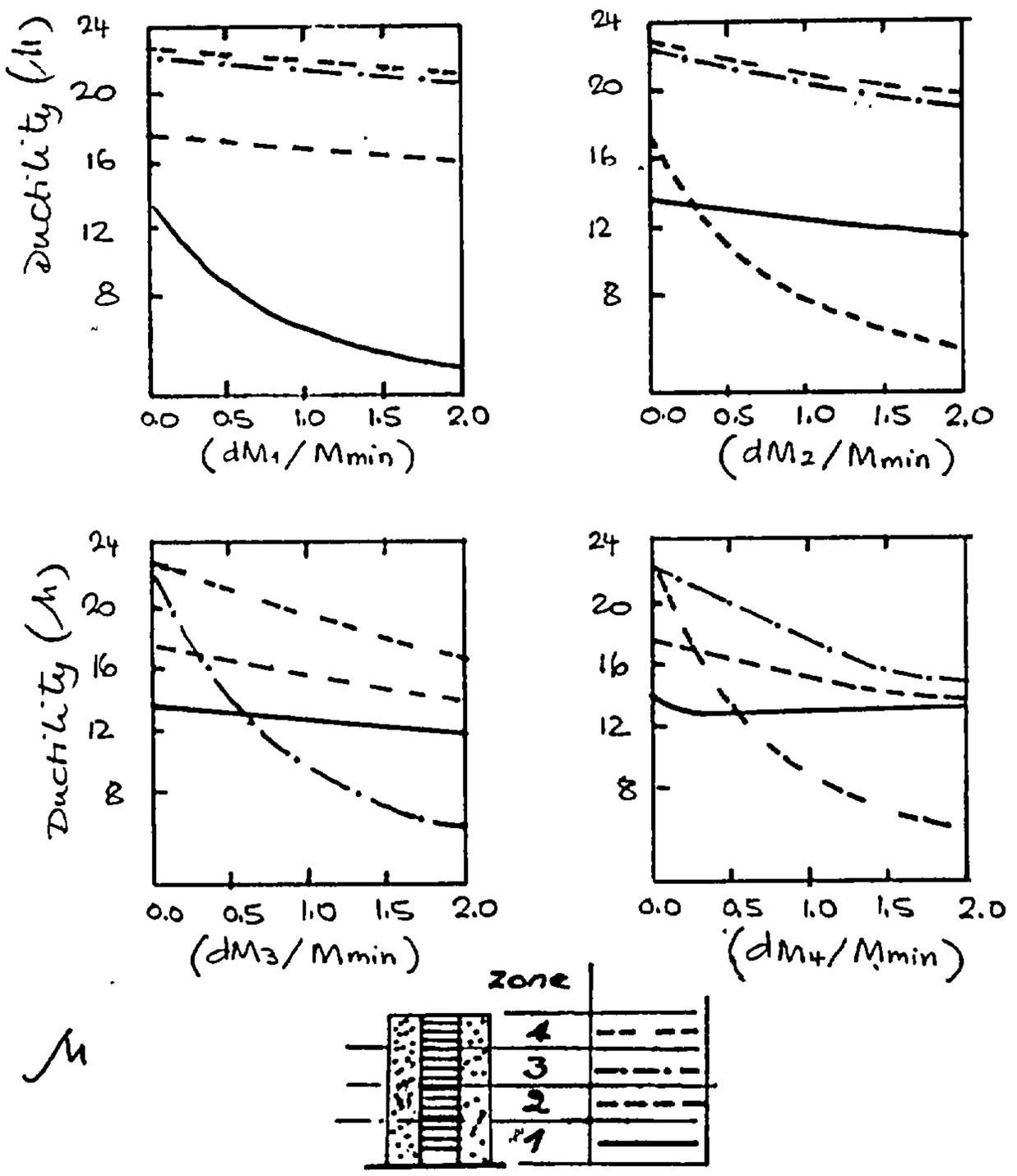

FIG. 2 EFFECT OF YIELD MOMENT ON DUCTILITY DEMAND

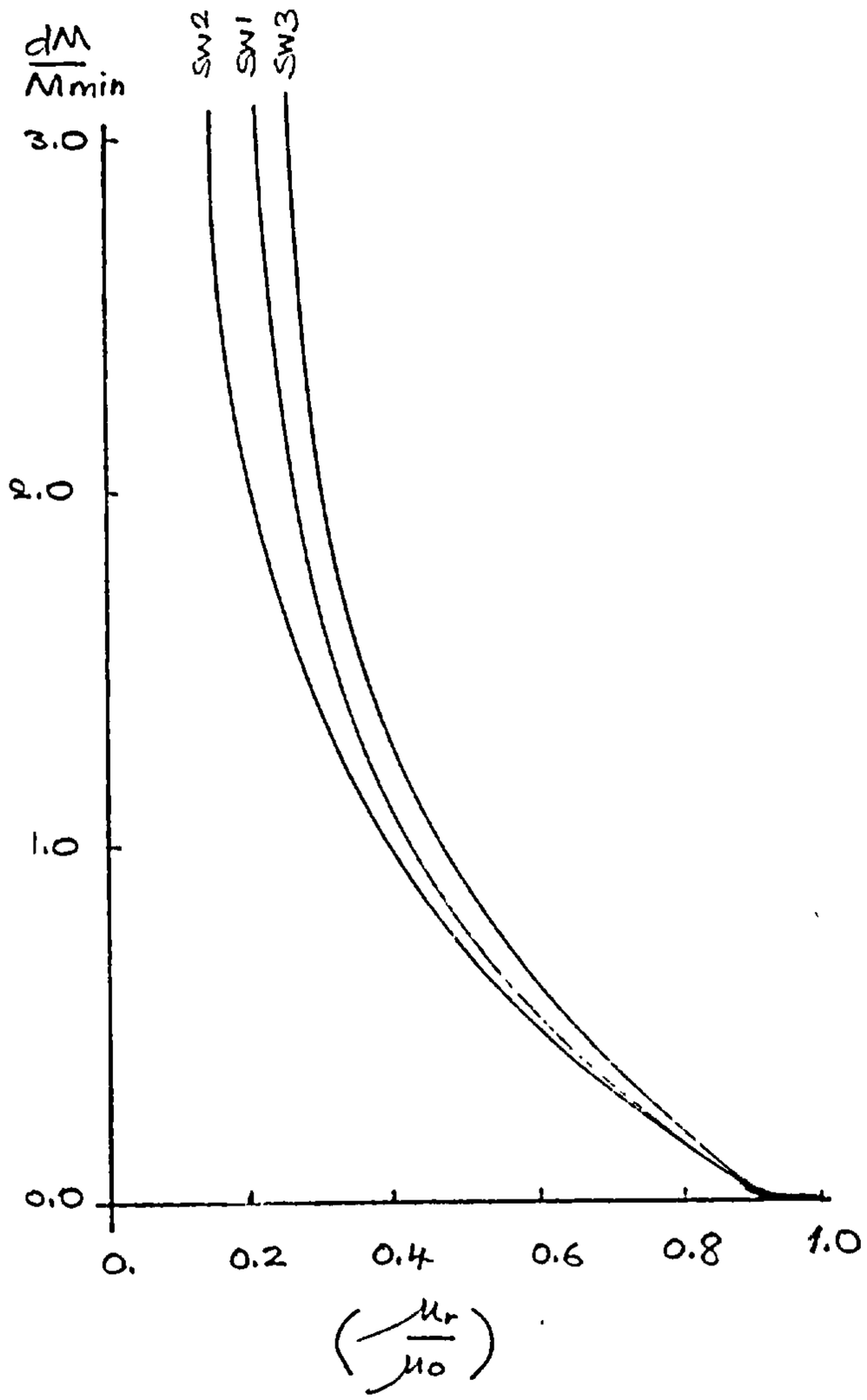

FIG. 3 DUCTILITY DECAY CURVE